

UC Irvine

UC Irvine Electronic Theses and Dissertations

Title

Design, Synthesis and Study of Potent Small Molecule Antifungal Synergizers and Palladium-Carbene Mediated C-C and C-N Bond Formations

Permalink

<https://escholarship.org/uc/item/1hs0h5rp>

Author

Ilandari Dewage, Udara Anulal Premachandra

Publication Date

2016

Peer reviewed|Thesis/dissertation

UNIVERSITY OF CALIFORNIA,
IRVINE

Design, Synthesis and Study of Potent Small Molecule Antifungal Synergizers

and

Palladium-Carbene Mediated C–C and C–N Bond Formations

DISSERTATION

Submitted in partial satisfaction of the requirements
for the degree of

DOCTOR OF PHILOSOPHY

in Chemistry

by

Ilandari Dewage Udara Anulal Premachandra

Dissertation Committee:
Professor David L. Van Vranken, Chair
Professor A. Richard Chamberlin
Professor Kenneth J. Shea

2016

Chapter 2 is reproduced in part with permission from Premachandra, I. D. U. A.; Scott, K. A.; Shen, C.; Wang, F.; Lane, S.; Liu, H.; Van Vranken, D. L. *ChemMedChem*. **2015**, *10*, 1672–1686. Copyright 2016 WILEY-VCH Verlag GmbH & Co. KGaA, Weinheim.
Chapter 6 reproduced in part with permission from Premachandra, I. D. U. A.; Nguyen, T. A.; Shen, C.; Gutman, E. S.; Van Vranken, D. L. *Org. Lett.* **2015**, *17*, 5464–5467.

Copyright 2015 American Chemical Society.

Chapter 7 reproduced in part with permission from Khanna, A.; Premachandra, I. D. U. A.; Sung, P. D.; Van Vranken, D. L. *Org. Lett.* **2013**, *15*, 3694–3697. Copyright 2013 American Chemical Society.

Chapter 8 reproduced in part with permission from Khanna, A.; Premachandra, I. D. U. A.; Sung, P. D.; Van Vranken, D. L. *Org. Lett.* **2013**, *15*, 3158–3161. Copyright 2013 American Chemical Society.

All other materials © 2016 Ilandari Dewage Udara Anulal Premachandra

DEDICATION

To

my grandmother

in recognition of her unconditional love and care

“The only real failure in life is one not learned from.”

- Anthony J. D'Angelo

TABLE OF CONTENTS

	Page
LIST OF FIGURES	viii
LIST OF SCHEMES	xi
LIST OF TABLES	xiv
ACKNOWLEDGMENTS	xv
CURRICULUM VITAE	xviii
ABSTRACT OF THE DISSERTATION	xxi
CHAPTER 1: Azole Synergizers	1
Introduction	1
Role of Ergosterol and Biosynthesis of Ergosterol in Antifungal Drug Discovery	2
Polyenes as Antifungals	3
Allylamines as Antifungal Drugs	4
Antimetabolites as Antifungal Drugs	4
Echinocandins as Antifungal Drugs	5
Azoles as Antifungal Drugs	6
Drug Synergy as a Solution to Drug-Resistance	7
Small Molecules Have Identified as Fluconazole Synergizers	8
Massive Screenings to Identify Small Molecule Fluconazole Synergizers	9
Conclusion	13
CHAPTER 2: Small Molecule Fluconazole Synergizers - Spiroindolinones	14
Introduction	14
Inhibition of Upc2 and Sensitizing Resistant Fungal Strains	14

Initial Results and Attempts to Make Potent Analogues	15
Results and Discussion	20
Chemistry	20
Structure-Activity Relationships	28
Activity Against Resistant Cell Lines	30
Cytotoxicity of Synazo-1 Against Mammalian Cells	32
Drug-Like Parameters for Synazo-1	33
Biological Studies	34
Conclusions	34
Experimental Section	35
Chemistry	35
General Experimental Details	35
Experimental Procedures	36
Biological Evaluations	58
Strains, media, and compounds	58
Dose-Response Curves for Test Compounds Against <i>C. albicans</i> with and without Fluconazole	58
Determination of FIC90s with a Checkerboard Assay	59
Molecular Properties	60
CHAPTER 3: Small Molecule Fluconazole Synergizers - Dihydroisoquinoline	61
Introduction	61
Results and Discussion	64
Synthesis of dihydroisoquinoline acid chloride fragment	65

Synthesis of Amine Fragment	66
Coupling of the dihydroisoquinoline acid chloride and amine fragments and further modifications	67
Structure-Activity Relationships	69
Synthesis and Activity of Functional Biological Probes	71
Conclusions	72
Chemistry	73
Experimental Procedures	73
Biological Evaluations	95
Strains, media, and compounds	95
Dose-Response Curves for Test Compounds Against <i>C. albicans</i> with and without Fluconazole	96
CHAPTER 4: Reactivity of Palladium-Carbene Intermediates	97
Introduction	97
Palladium-carbenes	97
Palladium-Catalyzed Carbenylation	99
Palladium-Carbenes to π -Allylpalladium Intermediates	101
Trapping of π -Allylpalladium Intermediates Generated from Palladium-Carbenes	101
Conclusions	104
CHAPTER 5: Carbenylative Coupling Involving Palladium Alkylidene Intermediates	105
Alkylidene Precursors in Palladium-Catalyzed Carbenylative Coupling Reactions	105
β -Hydride Elimination in Processes Involving Pd-Alkylidene Intermediates	105
β -hydride Elimination With Pd-alkylidenes Generated from Ketone Hydrazones	106

Ketone <i>N</i> -tosylhydrazone and ArPdX from Arylhalides/pseudohalides in Pd-catalyzed carbenylative coupling	106
Ketone <i>N</i> -tosylhydrazones and ArPdX derived from Nucleophiles and Oxidants in Pd-catalyzed Carbenylative Coupling	108
Ketone <i>N</i> -tosylhydrazone and ArPdX or ArCOPdX Derived from Tandem Reactions in Pd-catalyzed Carbenylative Coupling	109
β -hydride Elimination With Pd-alkylidenes Generated from Diazo Compounds	111
β -hydride Elimination With Pd-alkylidenes Generated from Aldehyde Hydrazones	112
Palladium-catalyzed Carbenylative Coupling Processes with Cyclopropyl Ketone <i>N</i> -Tosylhydrazones	112
Carbenylative Couplings Involving β -Hydride Elimination Toward the Alkyl Halide	114
Palladium-Catalyzed Homo-coupling Processes Involving β -hydride Elimination	114
Carbenylative Coupling Processes without β -Elimination	116
Formation of π -allyl/Oxa-Allyl Palladium Intermediates Prior to β -Hydride Elimination	116
Ketene/Ketenamine Formation Prior to β -Hydride Elimination	118
CHAPTER 6: Carbenylative Amination and Alkylation of Vinyl Iodides via Palladium Alkylidene Intermediates	120
Introduction	120
Results and Discussion	121
Conclusions	129
Experimental Section	129
Experimental Procedures	131

CHAPTER 7: Palladium-Catalyzed Bis-cyclization/Dimerization Reactions	152
Introduction	152
Results and Discussion	152
Conclusions	160
Experimental Section	160
Experimental Procedures	160
CHAPTER 8: Palladium-Catalyzed Catellani Aminocyclopropanation	
Reactions with Vinyl Halides	166
Introduction	166
Results and Discussion	167
Conclusions	172
Experimental Section	172
Experimental Procedures	172
APPENDIX A: Chapter 2 – HPLC Traces	204
APPENDIX B: Chapter 2 – NMR Spectra	232
APPENDIX C: Chapter 3 – NMR Spectra	289
APPENDIX D: Chapter 6 – NMR Spectra	356
APPENDIX D: Chapter 7 – NMR Spectra	408
APPENDIX D: Chapter 8 – NMR Spectra	421

LIST OF FIGURES

	Page	
Figure 1-1	Mechanism of Action of Azoles in Ergosterol Biosynthesis	7
Figure 1-2	Summary of the Broad assay	12
Figure 2-1	Transcriptional Regulation of Upc2	15
Figure 2-2	Initial Transcriptional Regulation Results for Spitzer Hits	17
Figure 2-3	Summary of SAR Study of Flufenamic Acid Analogues	17
Figure 2-4	Downregulators Identified in the Initial Screen	18
Figure 2-5	Upregulators Identified in the Initial Screen	19
Figure 2-6	Attempts to Synthesize Analogues of CID 2948951	19
Figure 2-7	Fluconazole synergizer CID 6584729 and diastereomer 1	20
Figure 2-8	Stereochemical Configurations of Azomethine Ylides	24
Figure 2-9	The Structure of Compound 31 , Renamed Synazo-1	32
Figure 2-10	Cytotoxicity of Compounds 1 , 13 and Synazo-1 Against NIH 3T3 Cells	32
Figure 3-1	Representative Examples of Dihydrophthalazine Tested in Broad Screen	62
Figure 3-2	Initial Plan to Synthesize Dihydrophthalazine Core	62
Figure 3-3	Synthesis of Arylhydrazine	63
Figure 3-4	Fluconazole Synergizer CID 22334057 and Dihydroisoquinoline Analogues	63
Figure 3-5	Dihydroisoquinolines Screened in Broad Assay	64
Figure 4-1	Depictions of Fischer and Schrock Carbenes	98
Figure 4-2	Pd(0)-Carbene Catalyzed Cyclopropanations , C–H insertions and Ylide formations	99

Figure 4-3	Comparison of Migratory Insertions	100
Figure 4-4	Pd-Catalyzed Carbenylative Coupling Between Aryl Halides and TMSCHN ₂	100
Figure 4-5	Proposed Mechanism for the Nucleophilic Trapping after Carbenylative Insertion	101
Figure 4-6	Pd-Catalyzed Three-Component Coupling	102
Figure 4-7	Scope of Vinyl Halide in Carbenylative Three-Component Coupling	103
Figure 4-8	Pd-Catalyzed Three-Component Coupling with EDA	104
Figure 5-1	Palladium(II) Alkylidene Leads to β -Hydride Eliminations	106
Figure 5-2	Representative Examples of Pd-Catalyzed Carbenylative Coupling with Ketone <i>N</i> -Tosylhydrazone and ArPdX from Arylhalides/pseudohalides	107
Figure 5-3	Proposed Reaction Mechanism for the Palladium-Catalyzed Carbenylative Coupling with Ketone <i>N</i> -Tosylhydrazone	107
Figure 5-4	Synthesis of <i>iso</i> CA-4 and the Structure of <i>Combretastatin A-4</i> (CA-4)	108
Figure 5-5	Representative Examples of Palladium-Catalyzed Oxidative Carbenylative Couplings	109
Figure 5-6	Pd-Catalyzed Oxidative Coupling of Terminal Alkynes with <i>N</i> -Tosylhydrazone	109
Figure 5-7	Pd-Catalyzed Carbonylative Cross-Coupling with <i>N</i> -Tosylhydrazone and Aryl Halide	110
Figure 5-8	Palladium-Catalyzed Ring Opening of Norbornene	110
Figure 5-9	Palladium-Catalyzed Carbenylative Coupling of α -Diazocarbonyl Compounds with Arylbornic Acids	111

Figure 5-10	Palladium-Catalyzed Carbenylative Coupling of Aldehyde <i>N</i> -Tosylhydrazones with Aryl Halides	112
Figure 5-11	Synthesis of 1,3-Butadiene via Cyclopropylcarbenylpalladium Species	113
Figure 5-12	Proposed Reaction Mechanism for The Synthesis of 1,3-Butadiene via Cyclopropylcarbenylpalladium Species	113
Figure 5-13	Palladium-Catalyzed Homologation of Benzyl Halides with TMSD	114
Figure 5-14	Pd-Catalyzed Oxidative Homo-coupling of <i>N</i> -Tosylhydrazones	115
Figure 5-15	Proposed Mechanism for the Pd-Catalyzed Oxidative Homo-Coupling of <i>N</i> -Tosylhydrazones	115
Figure 5-16	Three-Component Coupling Reaction to Generate γ -Aminoesters	116
Figure 5-17	Proposed Mechanism for the Pd-Catalyzed Three-Component Coupling Reaction to Generate γ -Aminoesters	117
Figure 5-18	Palladium-Catalyzed reaction of Phenyl Iodide and Ketone <i>N</i> -Tosylhydrazone in the presence of CO	117
Figure 5-19	Palladium-Catalyzed Three-Component Coupling of Aniline, CO and Diazo Compounds	118
Figure 5-20	Palladium-Catalyzed Amidation of <i>N</i> -Tosylhydrazones with Isocyanides	119
Figure 6-1	Carbenylative Amination and Alkylation with Alkylidene Carbenes without β -Hydride Elimination	121
Figure 6-2	Acyclic Stereocontrol. a. Nucleophilic Addition to Carbonyls, b. 1,2-Migration to Palladium Carbenes	126
Figure 8-1	Establishing the relative stereochemistry	169

LIST OF SCHEMES

	Page	
Scheme 1-1	Chemical Structures of Representative Antifungal Drugs	2
Scheme 1-2	Cholesterol vs. Ergosterol Biosynthesis	3
Scheme 1-3	Chemical Structures of Cytosine, Flucytosine and 5-Fluorouracil	5
Scheme 1-4	Chemical Structures of Some of the Azole Antifungals	6
Scheme 1-5	LaFleur Assay Summary	10
Scheme 1-6	Best Molecules Identified After SAR Studies of the Probes	13
Scheme 2-1	Synthesis of Substituted <i>N</i> -Phenylmaleimides	20
Scheme 2-2	Synthesis of Substituted Isatins	21
Scheme 2-3	Synthesis of Compound 1 and nOes Used in the Assignment of Relative Configuration	22
Scheme 2-4	Synthesis of Spirocyclic Pyrrolidines Through a Three-Component, 1-Pot [1,3]-Dipolar Cycloaddition with Amino Acids	23
Scheme 2-5	<i>Endo/Exo</i> Selectivity in Dipolar Cycloadditions of Azomethine Ylides	25
Scheme 2-6	Stereoselectivity in the Three-Component, 1-Pot [1,3]-Dipolar Cycloaddition with (2 <i>S</i> , 4 <i>R</i>)-4-Hydroxyproline	26
Scheme 2-7	Synthesis of Pentacyclic Pyrrolidines Through Further Substitutions to Compound 26	27
Scheme 2-8	Biotin and Rhodamine Attached Compound 18	34
Scheme 3-1	Synthesis of Dihydroisoquinoline Acid Chloride Analogues	65
Scheme 3-2	Synthesis of Dihydroisoquinoline Analogue 8d	66

Scheme 3-3	Synthesis of Amines 16a-d	67
Scheme 3-4	Coupling of Dihydroisoquinoline Acid Chloride and Amine Fragments	68
Scheme 3-5	Synthesis of Dihydroisoquinoline Analogue 24	69
Scheme 3-6	Structure-Activity Relationship of Dihydroisoquinoline Analogues	70
Scheme 3-7	Synthesis of Biotinylated Analogue 27	71
Scheme 6-1	β -Hydride Elimination Out-Competes Nucleophilic Trapping	120
Scheme 6-2	Intramolecular Carbenylative Amination with an Alkylidene Precursor	122
Scheme 6-3	Intramolecular Carbenylative Alkylation with an Alkylidene Precursor	123
Scheme 6-4	Intermolecular Carbenylative Amination with Alkylidene Precursors	123
Scheme 6-5	Allylamines Slowly Isomerize Under the Conditions of the Reaction	124
Scheme 6-6	Carbenylative Cross-Coupling with a Hindered Vinyl Iodide	124
Scheme 6-7	Scope of Intermolecular Carbenylative Alkylation and Amination with Alkylidene Precursors	125
Scheme 6-8	Assignment of Relative Stereochemistry by Conversion to Known Bis-Pyrrolidine	128
Scheme 6-9	Sterically Encumbered <i>N</i> -Tosylhydrazone 27 Shown to Give Only the <i>E</i> Product 28	128
Scheme 6-10	Proposed Catalytic Cycle of Carbenylative Amination and Alkylation of Vinyl Iodide	129
Scheme 7-1	Dimerization as a Competing Side Reaction in Carbenylative Amination	152
Scheme 7-2	NMR and X-ray Crystallography Establish the Configuration of the Double Bond and the Relative Configuration	154

Scheme 7-3	The Bis-cyclization/Dimerization Reaction Tolerates a Variety of <i>N</i> -Alkyl Groups	155
Scheme 7-4	One-Step Synthesis of the Hyalbidone Skeleton	155
Scheme 7-5	The Balme Dimerization of Terminal Alkynes is Distinct from Reactions of Vinyl Halides	156
Scheme 7-6	Bis-Cyclization/Dimerization with a Carbon Nucleophile	156
Scheme 7-7	A Variety of Mechanistic Pathways Would Lead to Dimer	158
Scheme 7-8	A Cyclopropanation Experiment	159
Scheme 7-9	A Crossover Experiment	159
Scheme 8-1	Common Reactive Intermediates in Catellani Cyclopropanations can Generate Three Different Products	166
Scheme 8-2	Aminocyclopropanation Reactions	167
Scheme 8-3	Intramolecular Aminocyclopropanation with Variations in the Amine Substituent	169
Scheme 8-4	Scope of Alkene Acceptor	170
Scheme 8-5	Carbon Nucleophiles Generate Carbocyclic Rings in Conjunction with Cyclopropanation	170
Scheme 8-6	Mechanistic Models for Intramolecular Aminocyclopropanation	171

LIST OF TABLES

	Page	
Table 1-1	Antifungal Drugs and Their Targets	2
Table 2-1	Structure-Activity Relationships for Polycyclic Pyrrolidines Against the Susceptible Strain HLY4123 of <i>C. albicans</i> in the Presence of Fluconazole (0.25 µg/mL)	29
Table 2-2	Effect of Compound 31 on the Growth of Resistant Clinical Strains in the Presence of Fluconazole	31
Table 2-3	FIC Indices for Compound 31 and Fluconazole in Different Strains of <i>C. albicans</i>	31
Table 2-4	Calculated Physicochemical Properties of Synazo-1	33
Table 6-1	Stereoselectivity in Carbenylative Amination	127
Table 6-2	Optimization of Conditions for Intramolecular Carbenylative Amination with <i>N</i> -Trisylhydrazone 3	130
Table 6-3	Optimization of Conditions for Intermolecular Carbenylative Amination with <i>N</i> -Tosylhydrazone 2a	130
Table 7-1	Optimization of the Bis-cyclization/Dimerization of Vinyl Iodide 1 to Generate Dimer 3	153
Table 8-1	Optimization of the Aminocyclopropanation of Norbornadiene	168

ACKNOWLEDGMENTS

It's been almost five years since I started grad school and it still feels like yesterday. The time I spent as a grad student is filled with happiness, accomplishments, disappointments and a whole array of different emotions. However, I should say I enjoyed every single moment of it and this is the time to be thankful for everyone who contributed to this life changing learning experience.

I would have never accomplished the things I achieved in my life if it wasn't for my mom. I don't think I ever told you how grateful I am for everything that you have done for me. I understand it was very hard for you to be a single mother with three children and to have a minimum wage job. I want to say, you've done an outstanding job raising us to be productive members of the society and I am eternally grateful for all the sacrifices you've made to make my life a little easier. So thank you and I hope you'll be proud of what I'm going to do in life.

Next, I want to thank my grandmother who practically raised me in Sri Lanka when my mom was working in the United States. All the love and caring you've given me over the years made me the person I am today.

I'd like to credit my two sisters for being the best friends in my life. We always shared what life gave us, regardless of whether it was something good or bad. We never complained about our hard times, because we knew we had each other to share it with. Your love helped me to overcome so many obstacles in life and I know I can always count on you when I need you.

I am grateful to Professor David L. Van Vranken for his invaluable mentoring and being the best advisor that anyone could ever asked for. You taught me to solve problems not only in chemistry, but also in real life. I remember the time we wrote the patent application together. I spent countless hours in your office assisting you with the writing. After numerous hours of

work, when I got totally overwhelmed, I saw you still kept going like you just started working on it. That was one of those countless times I felt your infectious enthusiasm to learn new things and it made me to train myself to keep up with you. Over the past five years, your mentorship, patience and humility have been inspirational. I am extremely grateful to you for teaching me how to be a good scientist and hope I will have your continuous support for my future endeavors.

Professors Richard Chamberlin and Ken Shea, thank you for serving in my thesis committee. You've been extremely helpful and over the years our discussions have been valuable resources to my graduate career. The UCI chemistry department has been an excellent working environment and I will truly miss the entire faculty and staff that are dedicated to help anyone whenever they need it. The UCI is a very special place for me and I was blessed with making life long friendships at this place. Janine, Dan and Mariam thanks for making most of my disappointing days bearable. Thank you for your friendship and being the best people to hang out with. I enjoyed every single second we spent together.

I feel truly privileged to be a member of the Van Vranken group. Throughout this time I've been fortunate to collaborate with a number of co-workers in all my projects. Dr. Avinash Khanna's enormous support during the early years of my graduate career tremendously helped me to excel in later years. Our discussions over the years immensely helped me to think of new avenues in my projects. Thanks for being an exceptional mentor to me. My very motivated two undergraduate co-workers, Kevin and John were great resources for a major portion of my graduate career. I really appreciate you putting up with my demands and always supporting to reach our goals very quickly. I know you will achieve greater things in life and I am very happy I could play a small part of it. I also want to give a special thank to Vanessa for proofreading my thesis several times and being very helpful in all the technical issues I had with my computer

over the years. I am extremely fortunate to work side by side with all the other Van Vranken group members as well. Gene, Stan, Thi, Aaron, Paul, Nancy and Daniel, thanks for all the good times I had in the lab.

Finally, I want to thank the rest of my family who lives in different parts of the world. Your continuous love and support makes everything I do worthwhile.

CURRICULUM VITAE

ILANDARI DEWAGE UDARA ANULAL PREMACHANDRA

EDUCATION

- 2016 May
Cambridge, MA **Postdoctoral Fellow**, *beginning May 2016*, Harvard University
Advisor: Professor Andrew G Myers
- 2011 – 2016
Irvine, CA **Ph.D. in Organic Chemistry**, *in progress*, University of California, Irvine
Advisor: Professor David L. Van Vranken
- Awards:**
Deutsche Forschungsgemeinschaft fellow at 65th Lindau Nobel Laureates Meeting, Germany, June 2015
Regents' Dissertation Fellow 2015-2016
- 2007 – 2011
Northridge, CA **B.S. in Biochemistry**, with Honors, California State University, Northridge
Advisor: Professor Joseph Hajdu
- Awards:**
Hypercube Scholar Award 2011

EXPERIENCE

- 2011 – 2016
Irvine, CA Graduate Teaching Assistant, University of California, Irvine
- Instructed undergraduate courses in General and Organic Chemistry
- 2012 – 2016
Irvine, CA Mentor to Graduate and Undergraduate Researchers, UC Irvine
- Direct mentor to one graduate student and three undergraduates.
- 2013 – 2016
Irvine, CA Van Vranken Laboratory Safety Representative
- Overlook the laboratory safety, SOPs and employee training.

RESEARCH

- Development of new metal-catalyzed carbene reactions
- Development of novel inhibitors of fungal transcription

PUBLICATIONS

1. **Premachandra, I. D. U. A.**; Mood, A. D.; Hiew, S.; Scott, K. A.; Wang, F.; Oldenhuis, N. J.; Liu, H.; Van Vranken, D. L. "Potent Antifungal Synergy of Phthalazinone and Isoquinolones with Azoles Against *C. Albicans*" *manuscript in preparation*.
2. **Premachandra, I. D. U. A.**; Nguyen, T. A.; Shen, C.; Gutman, E. S.; Van Vranken, D. L. "Stereoselectivity in the Aminocarbonylation of Vinyl Iodides involving Palladium Alkylidenes" *Org. Lett.* **2015**, *17*, 5464–5467.
3. **Premachandra, I. D. U. A.**; Scott, K. A.; Shen, C.; Wang, F.; Lane, S.; Liu, H.; Van Vranken, D. L. "Potent Synergy between Spirocyclic Pyrrolidinoindolinones and Fluconazole against *Candida albicans*" *ChemMedChem.* **2015**, *10*, 1672–1686.
4. Van Vranken, D. L.; Liu, H.; **Premachandra, I. D. U. A.**; Wang, F.-Q.; Shen, C.; Scott, K. A.; Lane, S. R.-A. US Application No.62/175,202:"Spiroindolinones and Therapeutic Uses Thereof", filed on 12 June 2015.
5. Khanna, A.[†]; **Premachandra, I. D. U. A.**[†]; Sung, P. D.; Van Vranken, D. L. "Palladium-Catalyzed Catellani Aminocyclopropanation Reactions with Vinyl Halides" *Org. Lett.* **2013**, *15*, 3158–3161. [†] = Contributed equally
6. Khanna, A.; **Premachandra, I. D. U. A.**; Sung, P. D.; Van Vranken, D. L. "Palladium-Catalyzed Bis-cyclization/Dimerization Reactions of ω -Aminovinyl Halides" *Org. Lett.* **2013**, *15*, 3694–3697.

PRESENTATIONS

"Palladium-Catalyzed Cyclodimerization and Cyclopropanation Reactions of Vinyl Halides", **Kyoto University, Japan**, January 2014 – **Presentation**

"Harnessing Palladium-carbenoid reactivity." **Premachandra, I. D. U. A.**; Gutman, E. S.; Arredondo, V.; Van Vranken, D. L. Incoming Graduate Student Recruitment, March 2014 and 2015 (Poster)

"Palladium-Catalyzed Dimerization of Vinyl Halides." Khanna, A.; **Premachandra, I. D. U. A.**; Sung, P. D.; Van Vranken, D. L. Incoming Graduate Student Recruitment, March 2013. (Poster)

OUTREACH

Organizer of Graduate Student and Post-Doctorate Colloquium - Fall 2013 – Fall 2015

- A monthly colloquium that allows graduate students and postdoctoral fellows to present their research in an informal setting.

REFERENCES

Prof. David L. Van Vranken
Department of Chemistry
University of California, Irvine
1102 Natural Sciences II
Irvine, CA 92697
(949) 824-5455
david.vv@uci.edu

Prof. Richard Chamberlin
Department of Chemistry
University of California, Irvine
147 Biol. Sci. Admin.
Irvine, CA 92697
(949) 824-7089
archambe@uci.edu

Prof. Kenneth J. Shea
Department of Chemistry
University of California, Irvine
1102 Natural Sciences II
Irvine, CA 92697
(949) 824-5844
kjshea@uci.edu

ABSTRACT OF THE DISSERTATION

Design, Synthesis and Study of Potent Small Molecule Antifungal Synergizers

and

Palladium-Carbene Mediated C–C and C–N Bond Formations

By

Ilandari Dewage Udara Anulal Premachandra

Doctor of Philosophy in Chemistry

University of California, Irvine, 2016

Professor David L Van Vranken, Chair

The doctoral studies described herein include two distinct aspects. One involves the design, synthesis and study of small molecule antifungal synergizers and the other consists of novel palladium-catalyzed C–C and C–N bond formations.

Spiroindolinones and dihydroisoquinolines were previously reported to enhance the antifungal effect of *Candida albicans*. A different diastereomer of a lead spiroindolinone, CID 6584729 was synthesized and shown to have synergy with fluconazole against *C. albicans*. Various other analogues of spiroindolinones and dihydroisoquinolines were designed, synthesized and studied. Many of the compounds were shown to enhance the antifungal activity of fluconazole against *C. albicans*, some with exquisite potency. One spirocyclic compound, which we have named synazo-1 and one dihydroisoquinoline analogue, compound **3-19** were shown to enhance fluconazole activity against several resistant clinical isolates with low EC₅₀ values. Both of these compounds exhibit true synergy with fluconazole, with FIC indices below

0.5 in both susceptible and resistant strains. Synazo-1 and compound **3-19** also exhibited low intrinsic cytotoxicity in mammalian cells.

In a separate project, vinyl iodide were shown to be useful precursors in palladium-catalyzed transformations to gain access to η^3 -allylpalladium intermediates that resist β -hydride elimination and to generate cyclodimerization and cyclopropanation adducts in synthetically useful yields.

Most palladium-catalyzed reactions involving insertion of alkylidenes with α -hydrogens undergo β -hydride elimination from alkylpalladium(II) intermediates to form alkenes. Vinyl iodides were utilized to generate η^3 -allylpalladium intermediates and preserve the sp^3 center adjacent to the carbene. Acyclic stereocontrol (*syn/anti*) for carbenylative amination and alkylation reactions was found to be low, suggesting lack of control in the migratory insertion step. Highly hindered carbene precursors inexplicably led to formation of *Z*-alkenes with high levels of stereocontrol.

Vinyl iodides were shown to undergo palladium-catalyzed dimerizations and cyclization to generate pyrrolidine and piperidine dimers connected by a *trans*-ethylene bridge. The dimerization generates the skeleton of the alkaloid, hyalbidone in a single step. A crossover experiment is consistent with a Michael-type addition to vinylpalladium cation to generate Pd(0) alkylidene intermediate. A palladium-catalyzed intramolecular aminocyclopropanation of norbornenes with vinyl halides was shown to generate cyclopropylcarbinyl adducts in good yields. Stabilized enolate nucleophiles were also employed in these transformations.

Chapter 1:

Azole Synergizers

Introduction

Species of the yeast *Candida* are the most common cause of fungal infections¹ and account for 80% of major systemic fungal infections.² Among all the *Candida* species, *Candida albicans* is considered to be the most common infectious agent.³ *C. albicans* normally exists within the gastrointestinal microbiome in a commensal relationship, but in immunocompromised patients it can become an invasive pathogen. Candidiasis is an infection of *Candida* and most commonly affects the areas such as skin, genitals, throat, mouth and/or blood. Candidemia, the most common form of invasive candidiasis is responsible for the high rates of morbidity and mortality of immunosuppressed or immunocompromised patients. According to recent United States Centers for Disease Control and Prevention surveillance data, mortality among people with candidemia is approximately 30% and overall fungal infections are responsible for increasing the cost of health care and the length of the hospital stay significantly.⁴

The antifungal drug market continues to be very profitable. Recent data suggest over \$6 billion of annual sales and sales are predicted to grow annually. Several classes of antifungals are currently used to battle fungal infections (Table 1-1 and Scheme 1-1) and numerous other compounds are going through the FDA approval process to make it to the markets.

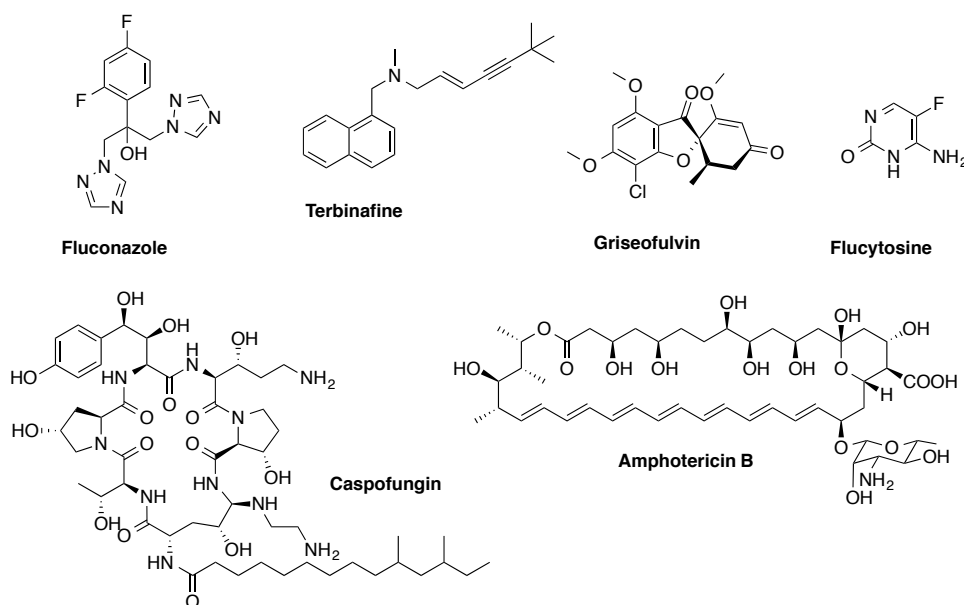
Major classes of antifungal drugs include azoles, polyenes, allylamines, antimetabolites, echinocandins and other compounds such as tolnaftate, cicloprimox, FK506 and ciclosporin. The potency and cytotoxicity of these drugs has significantly improved over the years and have noticeably changed the approach to antifungal therapy.⁵

Table 1-1: Antifungal Drugs and Their Targets

Compound Class	Example Drug	Target
Polyenes	Amphotericin B	Ergosterol
Azoles	Fluconazole	Ergosterol biosynthesis, lanosterol demethylase
Allylamines	Terbinafine	Ergosterol biosynthesis, squalene epoxidase
Antimetabolites	Flucytosine	Fungal nucleic acid (RNA and DNA)
Echinocandins	Caspofungin	Cell wall, β -1,3-glucan synthesis
Other	Griseofulvin	Fungal mitotic apparatus

Source: <http://www.doctorfungus.org>

Scheme 1-1. Chemical Structures of Representative Antifungal Drugs

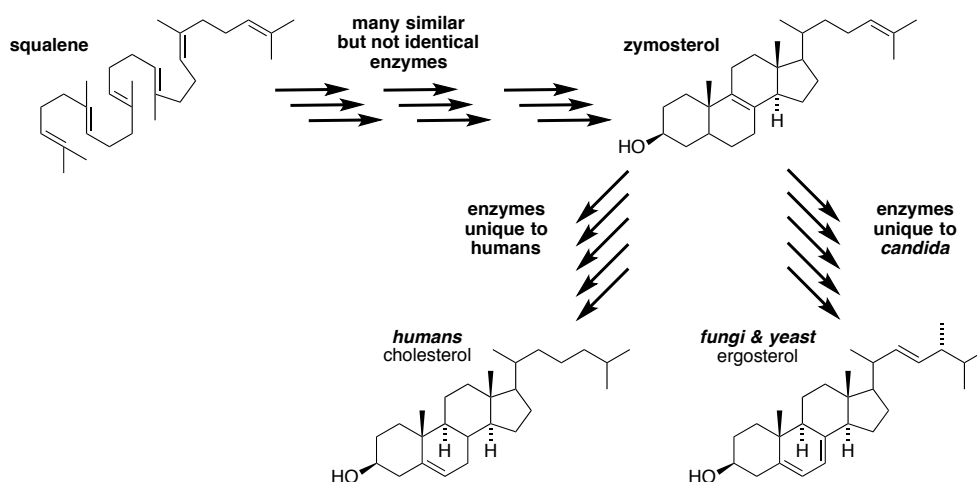


Role of Ergosterol and Biosynthesis of Ergosterol in Antifungal Drug Discovery

Several antifungal drugs' fungicidal or fungistatic activities involve targeting ergosterol or different stages of ergosterol biosynthesis (Table 1-1). Ergosterol, the functional fungal analogue of cholesterol, plays a vital role in maintaining membrane fluidity, nutrient transport and supporting cell wall biosynthesis.²¹ Ergosterol also induces growth and proliferation of

fungal cells due to its hormone-like function.^{21,24} During the biosynthesis of either cholesterol or ergosterol, both humans and *Candida* produce zymosterol, a common intermediate, using homologous enzymes. Humans convert zymosterol into cholesterol using enzymes not found in *Candida* and conversely, *Candida* convert zymosterol into ergosterol using enzymes not found in humans (Scheme 1-2). These differences between fungal enzymes and human enzymes have created opportunities for drug development.

Scheme 1-2: Cholesterol vs. Ergosterol Biosynthesis



Polyenes as Antifungal Drugs

The polyene macrolide amphotericin B (Scheme 1-1) was the first commercially significant antifungal drug and it has been prescribed over 50 years as an effective treatment for most of the systemic fungal infections.⁶ Amphotericin B is fungicidal due to its ability to interact with sterols present in the fungal cell wall, primarily ergosterol. These interactions result in the formation of pores in the cell membrane and subsequent leakage of cellular components. However, the drug's ability to interact with sterols has negative consequences on mammalian cells, since they are a vital part of mammalian cell membranes. In some cases the drug demonstrate significant cytotoxicity. Some adverse effects involve acute infusion reactions, neuropathy, gastrointestinal (GI) upset, renal failure, anemia, thrombophlebitis, hearing loss,

rash, hypokalemia and hypomagnesemia.⁵ In order to alleviate the severe cytotoxicity in patients who do not respond well to the conventional formulation of amphotericin B, lipid-based formulations such as amphotericin B deoxycholate are designed and administered intravenously.⁷

Allylamines as Antifungal Drugs

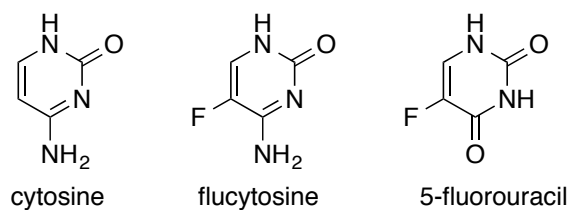
Allylamine antifungals are both orally and topically active drugs and they are found to be fungicidal against most of the dermatophytes, *Aspergillus* species, *Candida parapsilosis*, *Scopulariopsis brevicaulis*, *Blastomyces dermatitidis* and *Histoplasma capsulatum*. Interestingly, it is only fungistatic against *C.albicans*.⁸ Allylamine antifungals inhibit the enzyme squalene epoxidase that catalyzes the epoxidation of squalene to form 2,3-oxidosqualene, a transformation required in the biosynthesis of sterols. However, the potency of the drug towards the fungal enzyme is significantly higher than toward the mammalian squalene epoxidase. Consequently, the potential for the drug to interfere with the host sterol biosynthesis is very low.⁸ Adverse effects of allylamines range from gastrointestinal problems such as diarrhea, constipation, and nausea to central nervous system, psychological problems. Minor side effects such as hair loss (alopecia), anemia, muscle pain and hepatitis were also reported.⁹

Antimetabolites as Antifungal Drugs

The cytosine analogue flucytosine (5-fluorocytosine, 5-FC), a compound that belongs to the general class of antimetabolites was first synthesized in 1957 as a potential anti-tumor agent (Scheme 1-1).¹⁰ However, it was later discovered to be inadequately effective against tumors.¹¹ Flucytosine is a prodrug; once the susceptible fungal cell lines take up the flucytosine, the enzyme cytosine deaminase rapidly transforms the pro-drug to its active compound 5-fluorouracil (Scheme 1-3).¹² The resulting deaminated product is highly effective against fungi, because it inhibits the protein synthesis by incorporating into RNA.¹³ Active intermediate 5-

fluorouracil is also responsible for inhibiting the DNA synthesis of the fungi by inhibiting the enzyme thymidylate synthase.¹² The active metabolite 5-fluorouracil can not be administered directly due to severe toxicity to mammalian cells and poor uptake by fungal cells.¹⁴ Gaining resistance towards the monotherapy of flucytosine is a major drawback for the compound as an antifungal. This leads to administration of high and potentially cytotoxic doses to the patients. Consequently, 5-FC is currently used in combination with other antifungal drugs; mainly with amphotericin B.¹⁵ Flucytosine demonstrates side effects such as nausea, diarrhea, hepatotoxicity and bone marrow depression.¹⁶

Scheme 1-3: Chemical Structures of Cytosine, Flucytosine and 5-Fluorouracil

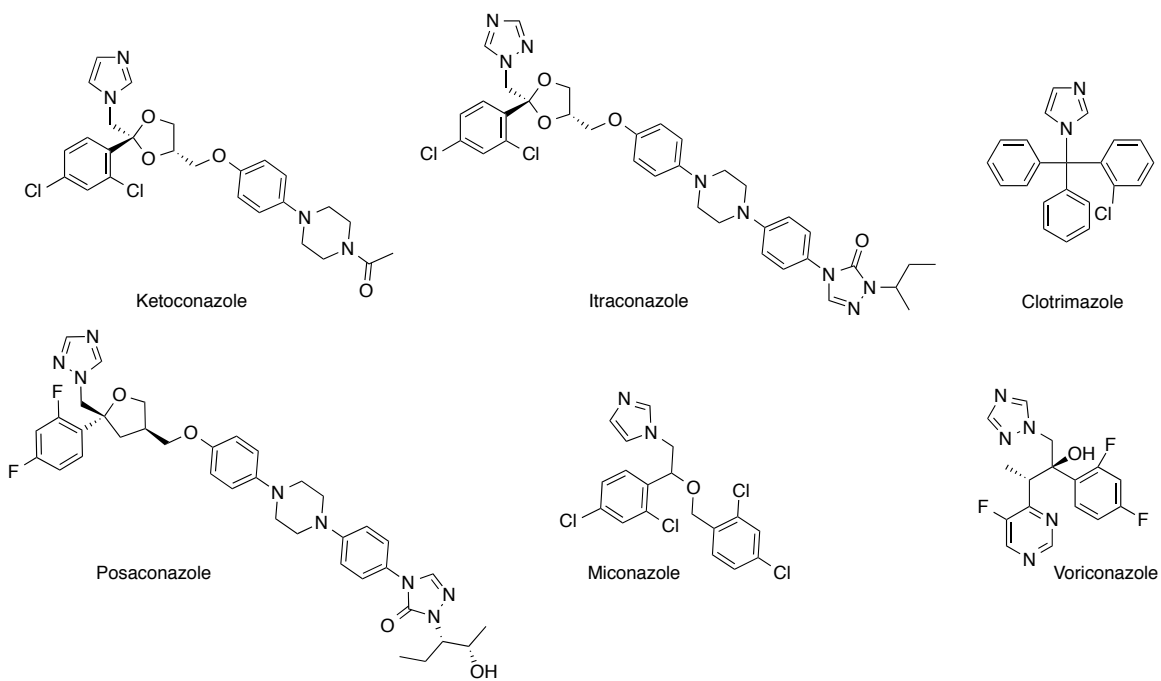


Echinocandins as Antifungal Drugs

Echinocandins are lipopeptides and the latest addition to the growing list of antifungals. Currently, there are three semi-synthetic echinocandins that have been approved for clinical use in the United States: caspofungin, micafungin, and anidulafungin. This is the first class of antifungals that attacks the fungal cell wall by inhibiting the enzyme β -1,3-D-glucan synthase, the key enzyme that is responsible for the synthesis of β -1,3-D-glucan. The combination of β -1,3-D-glucan and chitin is responsible for the integrity and shape of the cell wall.¹⁷ Thus the inhibition of β -1,3-D-glucan synthesis leads to osmotic lysis of the fungal cell. Therefore, echinocandins act as fungicides. Similar to other lipopeptide antibiotics, echinocandins demonstrate limited oral bioavailability and therefore it is administered via intravenous infusion.¹⁸ Echinocandins are now widely prescribed for treatment of systemic fungal infections

due to higher potency against azole-resistant *Candida* species such as *C. glabrata* and *C. krusei*. Also, echinocandins demonstrate significantly low cytotoxicity and drug-drug interactions. Minimal levels of adverse effects are reported including infusion-related reactions, such as rash and swelling and increased levels of hepatic transaminases were also observed.¹⁹ However, one of the down sides to echinocandins is its ineffectiveness against *Cryptococcus* species.²⁰ This makes echinocandins a less attractive option in treating patients with compromised immune systems due to the challenges of identifying the responsible fungal strain in a reasonable time.

Scheme 1-4: Chemical Structures of Some of the Azole Antifungals



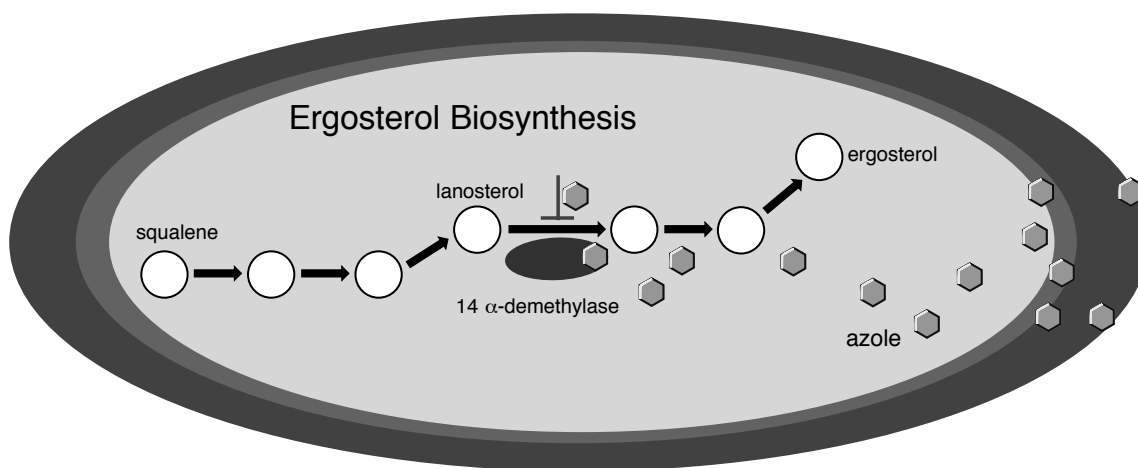
Azoles as Antifungal Drugs

Azole antifungal drugs have evolved over the years, from less potent ketoconazole that exhibits severe adverse effects, to more potent and less cytotoxic fluconazole, itraconazole, posaconazole, and voriconazole (Scheme 1-4). Azole drugs can be further divided into imidazole and triazole based drugs. Some of the imidazole-based antifungals include ketoconazole,

clotrimazole, miconazole and econazole. More effective and less toxic triazoles include fluconazole, itraconazole, posaconazole, and voriconazole.

Azoles are fungistatic and they inhibit fungal cell growth by disrupting the ergosterol biosynthesis pathway. Particularly by inhibiting the cytochrome P-450-dependent enzyme, 14 α -sterol demethylase (P-450_{DM}) (Figure 1-1).^{21,22,23,24} P-450_{DM} has plays a vital role in mammalian cholesterol biosynthesis as well.²³ However, the efficacy of the azole drugs is attributed to their high affinity towards the fungal lanosterol 14 α -sterol demethylase than the corresponding mammalian enzyme.²³ Minimal reported side effects include GI discomfort and rash. Hepatic necrosis, Stevens-Johnson syndrome, anaphylaxis and alopecia were also rarely reported.⁵

Figure 1-1: Mechanism of Action of Azoles in Ergosterol Biosynthesis



There are other antifungal drugs (e.g., griseofulvin, amorolfine) that are not frequently prescribed in the clinics. These drugs become either fungicidal or fungistatic by targeting several key aspects of the fungal cellular structures and mechanisms such as the mitotic apparatus and will not be discussed in this report.

Drug Synergy as a Solution to Drug-Resistance

Evolution of azole-resistant fungal strains is one of the major clinical challenges in the treatment of fungal infections.²⁵ Antifungal resistance has been classified in three different

categories: intrinsic, acquired and “clinical resistance”.²⁶ Intrinsic resistance occurs before the exposure to antifungals, while acquired resistance develops after the exposure to the antifungals. Stable or transient genotypic alterations cause such acquired resistance. Finally, “clinical resistance, which encompasses progression or relapse of an infection by a fungal isolate that seems, in laboratory testing, to be fully susceptible to the antifungal used for the treatment of infection.”²⁶ Clinical resistance is very common in patients with compromised immune systems.

One successful approach to treat patients with antifungal-resistant fungal infections is to utilize drugs that can act in a synergistic fashion. This drug combination approach enhances each drug’s effectiveness more than the effect from the sum of each drug’s individual impact.²⁷ Such a treatment is thought to not only decrease the microorganism’s resistance towards individual drugs but also increase the drug repertoire²⁷ and improve toxicities.²⁸

Small Molecules Have Identified as Fluconazole Synergizers

A large number of studies have been carried out to test the synergy of small molecules with fluconazole against *Candida* spp. Varying levels of synergy were observed and compounds that synergize with fluconazole at low concentrations (e.g., MIC₉₀ <0.1 µg/mL) are unusual. The antifungal agents flucytosine,^{29,30,31,32} and fenpropimorph³³ have been shown to potentially synergize with fluconazole against various strains of *C. albicans*. Micafungin^{34,35,36} and caspofungin³³ are highly potent, but not synergistic with fluconazole, with FIC indices above 1.0. A number of drugs commonly used against non-fungal human diseases have also been shown to synergize with azoles against *C. albicans*. The calcineurin inhibiting drug tacrolimus^{37,38} potentially enhances the activity of fluconazole against *C. albicans*. Quite a few other compounds have been reported to inhibit the growth of *Candida* in synergy with fluconazole, with MIC₉₀s below 1 µg/mL, but not below 0.1 µg/mL: e.g., *T. broussonetii* extract,³⁹ terbinafine,⁴⁰ amlodarone,⁴¹

catechin, quercetin, epigallocatechin,⁴² simvastatin,⁴³ tunicamycin,³³ cationic peptides IJ3, IJ4⁴⁴ and VS3,⁴⁵ ketorolac,⁴⁶ cyclosporin A,^{37,47} nystatin,⁴⁸ sanguinarine,⁴⁹ allicin,⁵⁰ declofenac,⁴⁶ leaf extracts of *Lippia alba*,⁵¹ diphenyldiselenide,⁵² balcalein,⁵³ geldanamycin,⁴⁹ pseudolaric acid B,⁵⁴ and doxycycline.⁵⁵ Hundreds of other compounds have been reported to exhibit antifungal activity in concert with azoles but not below 1 μ M. Chemical synthesis can be used to improve the potency of lead molecules; in a recent study, several analogues of the azole synergizer berberine (MIC₈₀ 1.0 μ g/mL) were identified with up to 8 times higher potency.^{56,57}

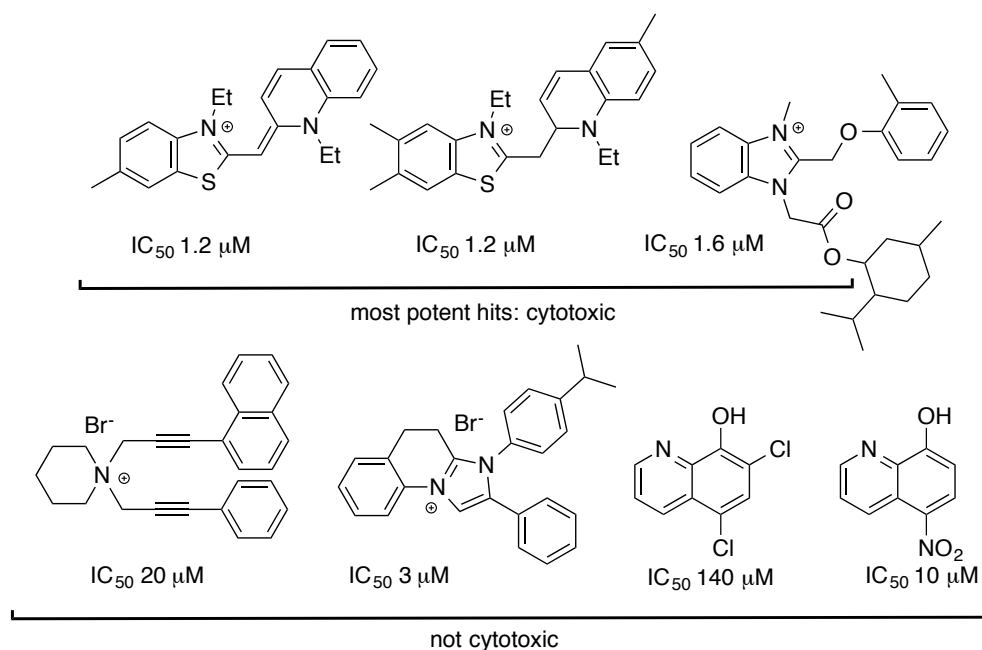
Massive Screenings to Identify Small Molecule Fluconazole Synergizers

Several groups have screened large libraries of compounds in search of small molecules that synergize with azoles. In 2011, Spitzer and co-workers screened the Prestwick library of off-patent drugs.⁵⁸ During the initial high-throughput assay they screened 1120 off-patent drugs (30 μ M [drug]) in the presence and absence of half of the minimal inhibitory concentration (MIC₅₀) of fluconazole. The assay primarily tested the antifungal activity of fluconazole and drug combination against four fungal species: *C.neoformans* (H99), *C.gattii* (R265), *C.albicans* (Caf2-1), *S.cerevisiae* (BY4741). A total of 148 compounds demonstrated to enhance the antifungal activity of fluconazole in at least one of the 4 fungal strains tested. Out of this pool of compounds, 12 compounds were selected to study the synergy with fluconazole depending on commercial availability of the compound, distinct chemical class, therapeutic importance and known mode of action of the compound. Interestingly, sertraline, a potent antidepressant and trifluoperazine, an antipsychotic have shown to synergize with fluconazole in all four strains. In addition, clofazimine, clomiphene, *L*-cycloserine and mitoxantrone synergized with fluconazole in *S.cerevisiae* and other antifungals, ketoconazole and caspofungin synergized with fluconazole in *C. albicans*. None of the compounds synergized with fluconazole in *Cryptococcus* species.

Further analysis of some these drugs in genome-wide chemical–genetic screens revealed potential targets of the off-patent drugs in fungi. In these assays around 1000 deletion strains heterozygous for several essential genes were tested for drug sensitivity. Trifluoperazine, tamoxifen, clomiphene, sertraline and suloctidil were found to be effective due to the perturbation of cell membranes, interruption of the cellular vesicle trafficking and sterol biosynthesis, whereas *L*-cycloserine seems to disrupt the early stages of sphingolipid biosynthesis.⁵⁹ In this study the authors were able to establish the importance of systemic screens in discovering new antifungal drug combinations.

Also in 2011, LaFleur and co-workers screened a library of 120,000 compounds in search of molecules that could act in synergy with clotrimazole against a variant of *C. albicans* CAF2-1 that forms biofilms.⁶⁰ The initial screen identified 19 hits and only 4 of those compounds were non-toxic to mammalian cells and all these compounds exhibit low antifungal activities in the presence of the azole drugs (3-140 μM) (Scheme 1-5).

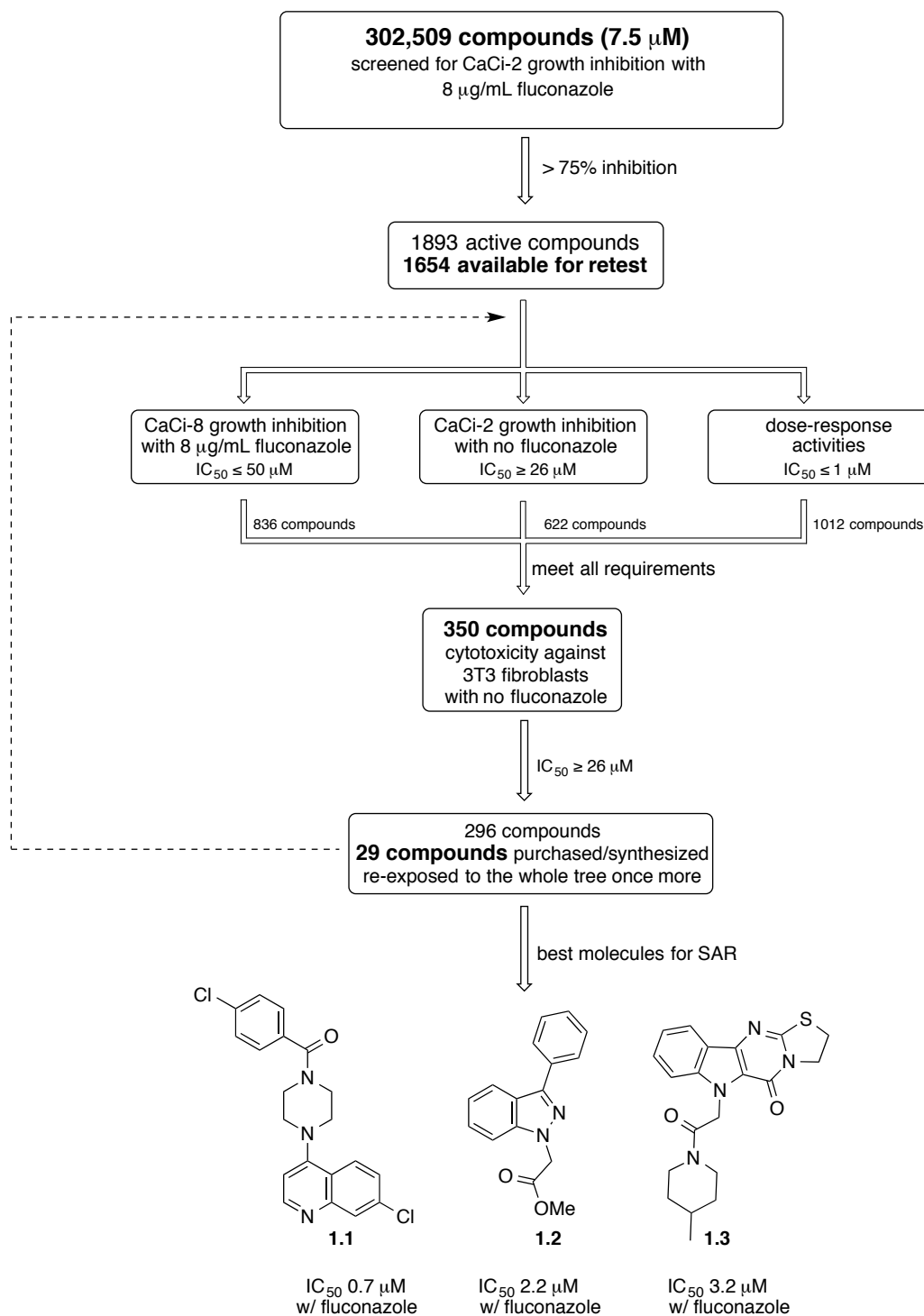
Scheme 1-5: LaFleur Assay Summary



Starting in 2010 Lindquist, Schreiber, and others at the Broad Institute reported a massive screening of NIH's Molecular Libraries Small Molecule Repository (MLSMR)⁶¹ to identify small molecules capable of inhibiting growth of *C. albicans* in synergy with fluconazole with a particular interest in Hsp90 and calcineurin pathways.^{62,63}

Initially 302,509 compounds from MLSMR were screened for the growth inhibition of *C. albicans* clinical isolate CaCi-2 (MIC of fluconazole 2 µg/mL) in the presence of 8 µg/mL fluconazole (Figure 1-2). MIC is the minimum concentration of fluconazole required to completely inhibit the growth of microorganism. Interestingly, the Lindquist and co-workers utilized higher concentrations of fluconazole than its minimum inhibitory concentration against the corresponding clinical isolate, CaCi-2. However, according to the authors, "these strains continue to proliferate steadily (albeit at a reduced rate) when treated with fluconazole at or above the reported MIC. This behavior may contribute to the inability of fluconazole therapy to effectively clear the infection and allows for the further development of resistance."⁶⁴ Out of 1,893 total compounds that demonstrated >75% growth inhibition, 1,654 compounds were selected for further studies on the basis of availability. The selected molecules were subjected to three parallel assays that tested for: 1) growth inhibition of a slightly resistant strain CaCi-8 (MIC of fluconazole 8 µg/mL) in the presence of 8 µg/mL of fluconazole, 2) growth inhibition of CaCi-2 in the absence of fluconazole and 3) potency in a dose-response assay (the cut-off limits are indicated in Figure 1-2). Based on those assays, they identified 350 compounds that satisfied their selection criteria. A subsequent cytotoxicity assay against NIH 3T3 fibroblasts reduced the potential candidates to 296 compounds that did not demonstrate significant cytotoxicity below 26 µM. A total of 29 compounds were selected to be re-exposed to the screening tree once more.

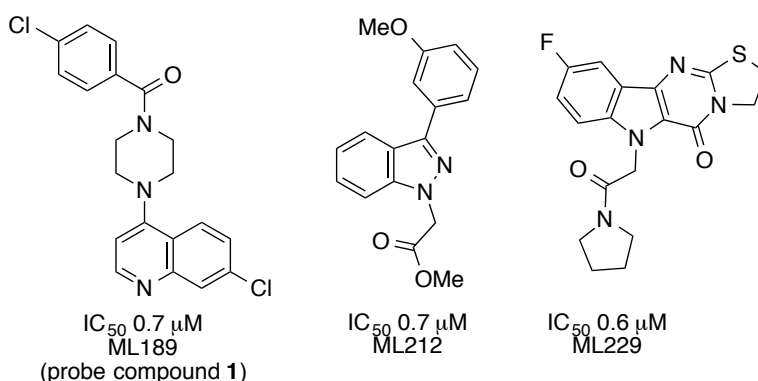
Figure 1-2: Summary of the Broad assay



Three of the most promising compounds^{65,63} (Figure 1-2, compounds **1.1**, **1.2**, **1.3**) were selected for further optimization. However, none of the resulting compounds ML189, ML212,

and ML229 respectively were active below 0.7 μM against CaCi-8 (Scheme 1-6). The many active enhancers of fluconazole identified in this study provide a rich source of lead molecules for further development.

Scheme 1-6: Best Molecules Identified After SAR Studies of the Probes



Conclusion:

Systemic fungal infections are serious and sometimes life threatening conditions that have to be addressed immediately and efficiently. Several classes of antifungals are currently used in the clinics as potent drugs. However, constant evolution of antifungal resistant strains is a major clinical issue. Several groups have conducted massive screenings of small molecules to identify potent compounds that can synergize with fluconazole and some small molecule synergizers are shown to make the existing antifungals more potent against resistant cell lines. These small molecules provide excellent probes for further optimizations to make very effective drugs that can be combined with existing antifungals to combat resistant fungal infections.

Chapter 2

Small Molecule Fluconazole Synergizers - Spiroindolinones

Introduction

Small molecules have been demonstrated to enhance the antifungal activity of fluconazole by synergizing with the azole. Several high-throughput screening campaigns have identified numerous small molecules with the potential to be potent antifungal synergizers, but only with further optimization.^{58,60,62,63,65} Consequently, we have decided to identify and optimize the small molecules that were identified in high-throughput screens, but were not further optimized by the corresponding research groups. Also, we were equally interested in identifying sites on the azole synergizers that can be biotinylated without losing their potency and eventually used for affinity isolation of proteins responsible for the antifungal activity/synergy.

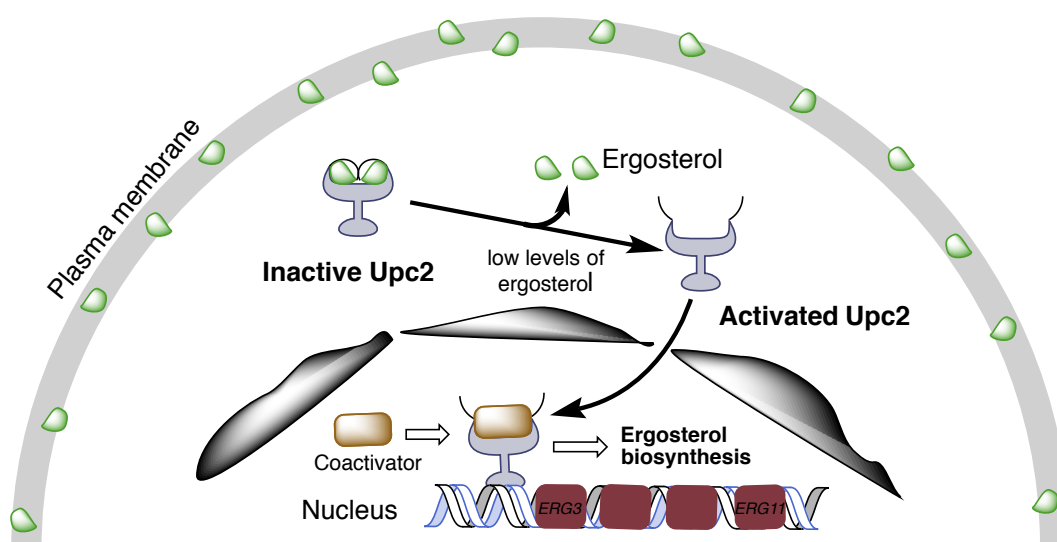
Inhibition of Upc2 and Sensitizing Resistant Fungal Strains

Ergosterol and enzymes responsible of ergosterol biosynthesis are the most common targets of antifungal drugs. Upc2 is a transcriptional regulator that is responsible for controlling the expression of genes that are responsible for the ergosterol biosynthesis in *C. albicans*.⁶⁶ At the outset of this work, the mechanisms for regulation of these genes was poorly understood.⁶⁷ Upc2 is a zinc finger transcription factor. Recently, it was discovered that in Upc2 the ligand-binding domain is the C-terminus domain (CTD) and the nuclear localization domain to be the N-terminus domain.⁶⁷ Additionally, CTD is responsible for sensing ergosterol levels in the cell. According to the current model, ergosterol binding leads to sequestration of Upc2 in the cytosol. When ergosterol levels are low, the ergosterol-free form of Upc2 translocates from the cytosol to the nucleus (Figure 2-1). Once Upc2 enters the nucleus, it binds to DNA and activates transcription; but the downstream coactivators of Upc2 are unknown. The complexation of a co-

activator with Upc2 triggers the signal for the transcription of *ERG* genes that are responsible for ergosterol biosynthesis.

One of the major resistant mechanisms of azole drugs involves overexpression of the enzymes that are inhibited by the antifungals in ergosterol biosynthesis. Therefore, as one strategy to overcome this mode of antifungal resistance, we were interested in small molecules that can potentially inhibit the activity of Upc2 and in turn prevent the upregulation of the genes responsible for the ergosterol biosynthesis. Potently interfering with Upc2 transcription factor binding to the DNA is expected to sensitize the resistant *C. albicans* to the antifungals.

Figure 2-1: Transcriptional Regulation of Upc2



Initial Results and Attempts to Make Potent Analogues

Spitzer and co-workers have screened 1,120 off-patent drugs and identified 30 synthetic compounds that could enhance the activity of fluconazole against *C. albicans* CAF2-1.⁵⁸ We ordered 25 out of 30 compounds that were commercially available. Dr. Fu-Qiang Wang in Professor Haoping Liu's lab in the Department of Biological Chemistry at UC Irvine performed

the initial *ERG* expression and antifungal assays. I later carried the antifungal assays of my synthetic compounds.

ERG genes are responsible for the enzymes that catalyze ergosterol biosynthesis and these genes are under the control of transcription regulator Upc2. Mutations occurring in *ERG3* and *ERG11* are directly related to fluconazole drug resistance.⁶⁸ Therefore, the *C. albicans* strain, HLY4123 that was used as the susceptible laboratory strain in this study carries a GFP reporter for *ERG3* and *ERG11* expression. It was constructed by plasmid transformation of the commonly used laboratory *C. albicans* strain CAI4. Fluorescence-activated cell sorting (FACS) analysis was employed to monitor expression of *ERG* genes.

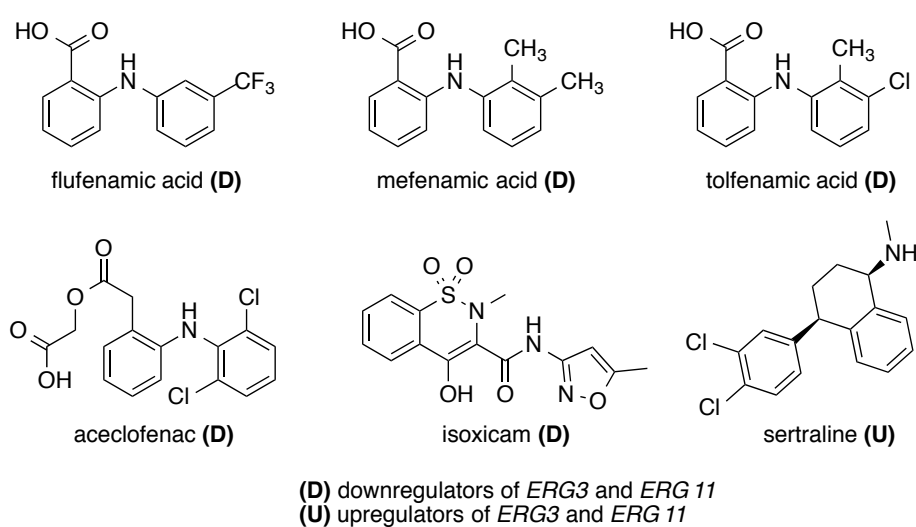
Several NSAIDs based on anthranilic acid such as flufenamic acid, mefenamic acid, tolfenamic acid, aceclofenac and isoxicam, which carried a benzothiazine core, were identified as downregulators of *ERG3* and *ERG11* genes at a single dose of 30 μ M (Figure 2-2) in the presence of fluconazole. A potent selective serotonin reuptake inhibitor (SSRI) sertraline was also found to be an upregulator of *ERG3* and *ERG11* genes at 30 μ M. It was reported by Zhai and co-workers that sertraline potently inhibits the translation of *Cryptococcus neoformans* by an unknown mechanism with EC₅₀ of 1 nM.⁶⁹

Interestingly, all the upregulators in this study inhibited the growth of *C. albicans* whereas all the downregulators except flufenamic acid showed no growth inhibition of *C. albicans* in the presence of fluconazole. Flufenamic acid indicated fungicidal activity even in the absence of fluconazole.

In order to optimize the potency and identify the site(s) for biotinylation, I initiated the synthesis of several different analogues of fenamic acid derivatives. Also I trained two

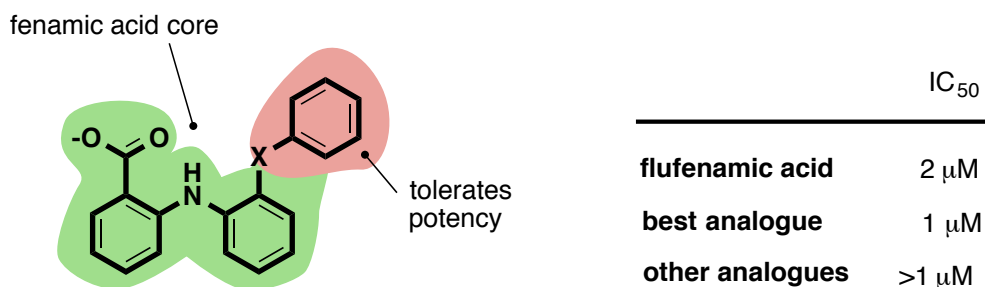
undergraduate researchers (Kevin A. Scott and Chengtian (John) Shen) to assist me with synthesis and antifungal assays.

Figure 2-2: Initial Transcriptional Regulation Results for Spitzer Hits



We synthesized 16 fenamic acid analogues and 8 aceclofenac analogues. Flufenamic acid demonstrated an EC_{50} of 2 μM in the presence of 0.25 $\mu\text{g/mL}$ of fluconazole. Unfortunately, none of our analogs exhibited significantly better activities than the parent flufenamic acid. However, structure-activity relationships revealed that the fenamic acid core is essential for the activity (Figure 2-3). Also the fenamic acid core cannot be readily modified to improve or investigate the potency further.

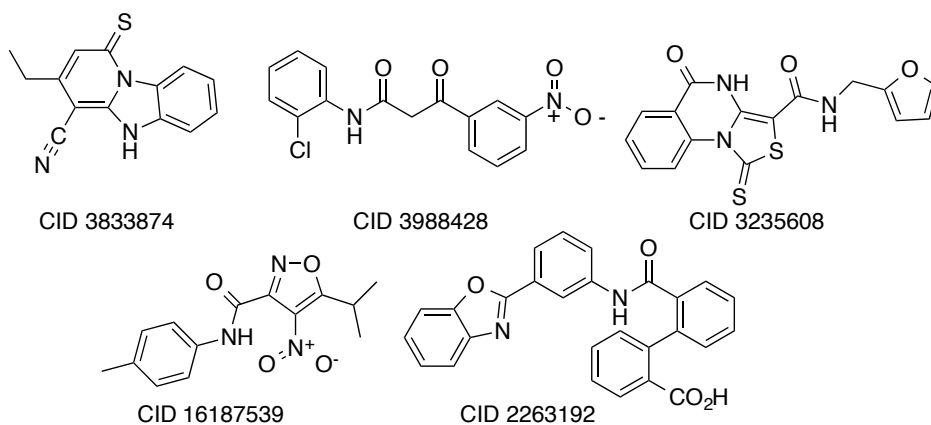
Figure 2-3: Summary of SAR Study of Flufenamic Acid Analogues



In 2010 Lindquist, Schreiber, and others at the Broad Institute reported a screen of 302,509 compounds searching for compounds that could enhance the antifungal activity of

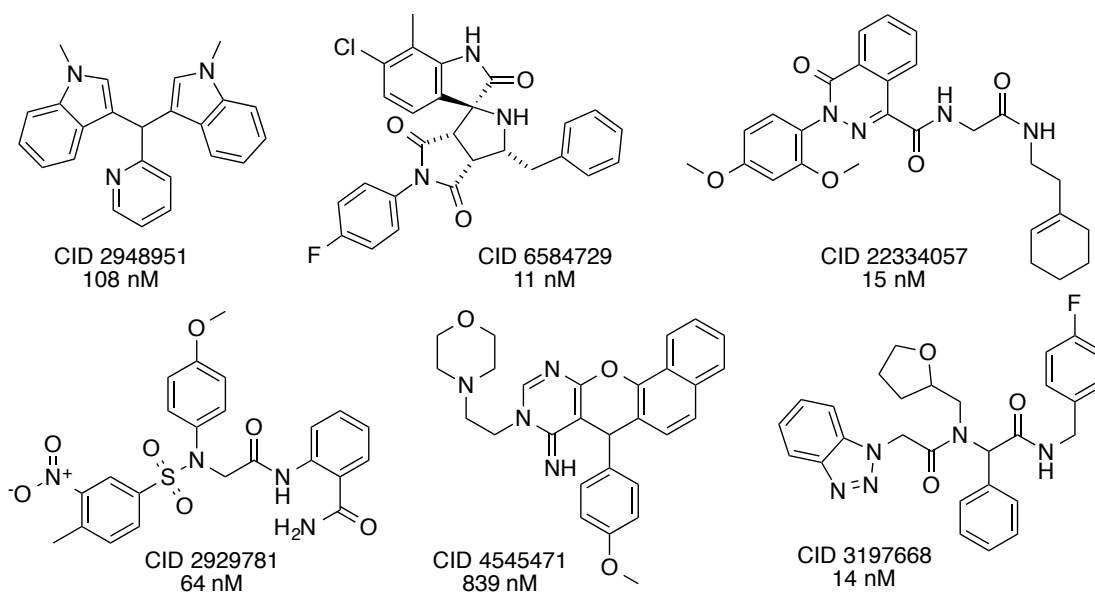
fluconazole against a susceptible *C. albicans* isolate CaCi-2 (Fluconazole MIC 2 $\mu\text{g/mL}$). They identified a subset of 296 compounds that were active against susceptible CaCi-2, slightly resistant isolate CaCi-8 (Fluconazole MIC 8 $\mu\text{g/mL}$) and were non-toxic to NIH 3T3 fibroblasts. We ordered 51 of those 256 compounds that were inactive against Hsp90 or calcineurin from commercial suppliers and screened them for their effect on *ERG3* and *ERG11* transcription and discovered 20 compounds that affected the transcription of *ERG3* and *ERG11* at some level. In a secondary screen Dr. Fu-Qiang Wang discovered 5 compounds as potent downregulators, but none enhanced the antifungal activity of fluconazole against the non-resistant GFP-reporter strain, HLY4123 (Figure 2-4).

Figure 2-4: Downregulators Identified in the Initial Screen



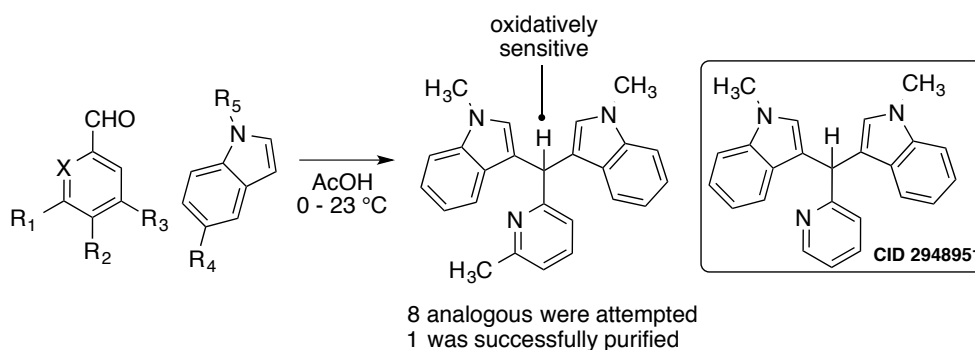
However, 6 of the 20 compounds were potent upregulators at 30 μM in the presence of 0.25 $\mu\text{g/mL}$ fluconazole, and all six enhanced the antifungal effect of fluconazole against the non-resistant GFP-reporter strain (Figure 2-5). Since the upregulators exhibited antifungal activity in the presence of fluconazole, that made them very interesting candidates for further optimization.

Figure 2-5: Upregulators Identified in the Initial Screen



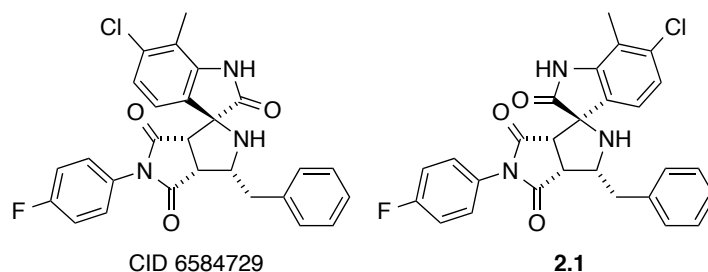
I attempted to synthesize and purify 8 different analogues of bisindolylpicoline, PubChem CID 2948951. Unfortunately, low solubility made chromatographic purification difficult and the oxidative sensitivity of the analogues caused them to readily form colored impurities. Only one minor variant of CID 2948951 was successfully purified and tested as an enhancer of fluconazole antifungal activity. However, it was slightly inferior to CID 2948951 (Scheme 2-6). Analogues of bisindolylpicoline CID 2948951 are unstable and difficult to purify and therefore made them unattractive candidates for further optimizations.

Figure 2-6: Attempts to Synthesize Analogues of CID 2948951



We then focused on the other potential analogs for optimization and were intrigued by the structurally interesting spirocyclic compound (1*S*,3*R*,3*aR*,6*aS*)-1-benzyl-6'-chloro-5-(4-fluorophenyl)-7'-methylspiro[1,2,3*a*,6*a*-tetrahydropyrrolo[3,4-*c*]pyrrole-3,3'-1*H*-indole]-2',4,6-trione (PubChem CID 6584729) and the potential activity of synthetically accessible diastereomer **2.1** and related analogues (Figure 2-7).

Figure 2-7: Fluconazole synergizer CID 6584729 and diastereomer **2.1**

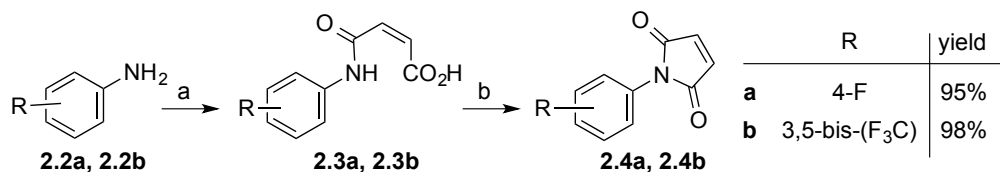


Results and Discussion

Chemistry

As shown in Scheme 2-1 *N*-phenylmaleimides **2.4a** and **2.4b** were synthesized through a two-step condensation of substituted anilines with maleic anhydride.⁷⁰ Anilines **2.2a** and **2.2b** were condensed with maleic anhydride to form the corresponding *N*-phenylmaleamic acids **2.3a** and **2.3b** that were cyclized using acetic anhydride in the presence of sodium acetate to afford the corresponding maleimides.

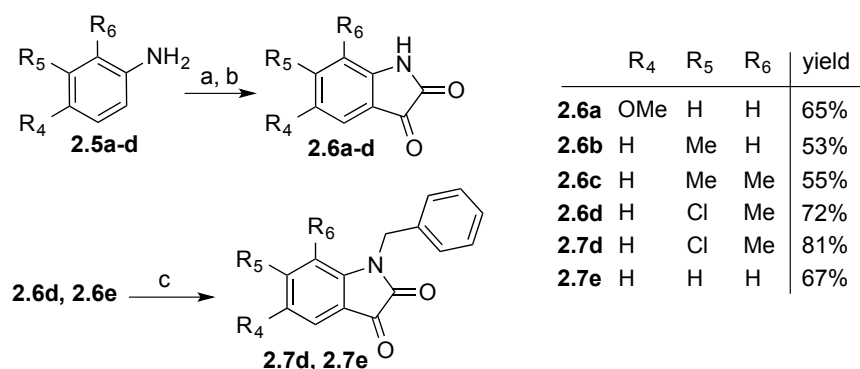
Scheme 2-1: Synthesis of Substituted *N*-Phenylmaleimides



Reagents and conditions: (a) 1.0 equiv maleic anhydride, Et₂O, 23 °C, 15 min; (b) 0.7 equiv sodium acetate, (CH₃CO)₂O, 70 °C, 30 min.

Various substituted isatins were prepared from the corresponding anilines using the two-step Sandmeyer synthesis (Scheme 2-2).⁷¹ Anilines were reacted with the oxime of chloral, generated in situ, to afford isonitrosoacetanilides, which were pure by TLC. The isonitrosoacetanilides were cyclized, without purification, through an intramolecular Friedel-Crafts reaction to afford the corresponding isatins **2.6a-2.6d** in good yield. *N*-Benzylisatins **2.7d** and **2.7e** were prepared by alkylation with benzyl bromide using sodium hydride as a base.⁷²

Scheme 2-2: Synthesis of Substituted Isatins



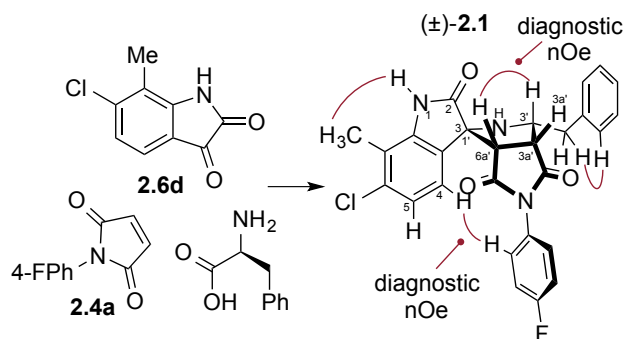
Reagents and conditions: (a) 1.1 equiv chloral hydrate, 3.0 equiv NH₂OH•HCl, 9.0 equiv Na₂SO₄, 1.1 equiv HCl, H₂O, 70 °C, 1 h; (b) H₂SO₄, 23 °C, 5 min, (c) 1.1 equiv benzyl bromide, 1.1 equiv NaH, DMF, 23 °C, 2 h.

Spiroindolinones are readily accessible through one-pot three-component coupling reactions of isatins, amino acids, and maleimides.^{73,74,75} The reaction of isatin **2.6d**, L-phenylalanine and maleimide **2.4a** generated compound **2.1** as a single diastereomer in 74% yield (Scheme 2-3). The optically pure amino acid undergoes decarboxylation during the reaction; unless otherwise stated all spiroindolinones were isolated and tested as racemates.

The relative stereochemistry of compound **2.1** was secured through a NOESY experiment (Scheme 2-3) and shown to match that of related spiroindolinones prepared from isatins and maleimides under the same reaction conditions.⁷⁵ In particular, the strong nOe between protons on C3' and C6a' of the pyrrolidine ring indicate that they are on the same face and conversely

that the benzyl group and succinimide ring are both on the opposing face. Furthermore the strong nOe between the fluorophenyl proton and the proton on C4 of the indolone ring is consistent with the stereochemistry of compound **2.1**. Interestingly, the ^1H NMR spectra, ^{13}C NMR spectra and nOes for the compound sold as CID 6584729 (by Vitas-M) were indistinguishable from those of compound **2.1**. Thus commercial STK580951 is in fact the same as our synthetic compound **2.1** and does not match PubChem CID 6584729.

Scheme 2-3: Synthesis of Compound **2.1** and nOes Used in the Assignment of Relative Configuration



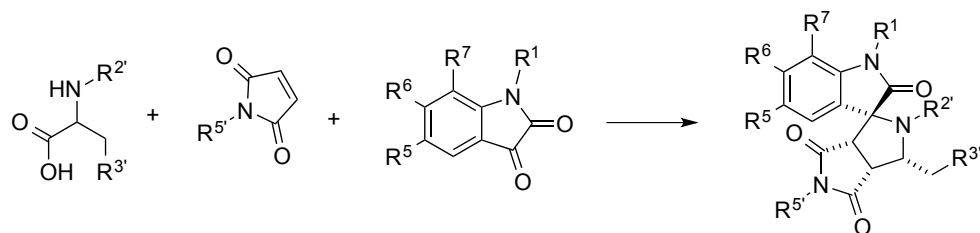
Reagents and conditions: 3:1 MeOH/H₂O, 65 °C, 16 h.

Other analogues of spirocycle **2.1** were synthesized (Scheme 2-4) using phenylalanine, tryptophan, and *N*_ε-Boc-Lysine. In all cases, the limiting reagent, isatin **2.6** or **2.7**, was completely consumed and the reaction gave the desired cycloadduct as a single diastereomer. The reactions of these amino acids were highly stereoselective, affording products with a relative configuration analogous to spiroindolinone **2.1**. We did not observe nor isolate other diastereomers of the spiroindolinones **2.8-2.13**.

The formation of diastereomer **2.1**, and **2.8-2.13** was anticipated based on the work of Pavlovskaya and co-workers,⁷⁴ but is best explained by examining a larger body of work involving reactions of amino acids, enones, and either isatins or phenylglyoxalate derivatives, which are essentially acyclic analogues of isatins. All known reactions of amino acids, isatins,

and enones react to give products consistent with *syn-anti* azomethine ylides (Figure 2-8, configuration A).^{76,77,78,79} However, in the corresponding reactions with phenylglyoxylate, the reactive configuration of the azomethine ylide seems to depend on the type of amino acid: proline gives products consistent with *syn-anti* azomethine ylides (Figure 2-8, configuration A),⁸⁰ whereas acyclic amino acids give products consistent with *anti-anti* azomethine ylides (Figure 2-8, configuration B).^{81,82,83}

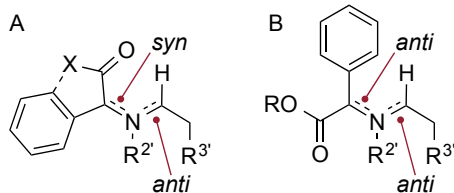
Scheme 2-4: Synthesis of Spirocyclic Pyrrolidines Through a Three-Component, 1-Pot [1,3]-Dipolar Cycloaddition with Amino Acids



Compound	R ^{5'}	R ^{2'}	R ^{3'}	R ⁵	R ⁶	R ⁷	R ¹	Yield
2.1	4-fluorophenyl	H	Ph	H	Cl	CH ₃	H	74%
2.8	Bn	H	Ph	H	H	H	H	60%
2.9	Bn	H	3-indolyl	H	H	H	H	70%
2.10	Bn	H	(CH ₂) ₃ NHBoc	H	H	H	H	33%
2.11	Bn	H	Ph	H	H	H	Bn	46%
2.12	Ph	H	Ph	H	H	H	Bn	57%
2.13	Ph	H	Ph	H	Cl	CH ₃	H	26%
2.14	Ph	CH ₂ CH ₂ N(Boc)		H	Cl	CH ₃	H	60%
2.15	4-fluorophenyl	CH ₂ CH ₂ N(Boc)		H	Cl	CH ₃	H	49%
2.16	3,5-bis(F ₃ C)phenyl	CH ₂ CH ₂ N(Boc)		H	Cl	CH ₃	H	12%
2.17	Ph	CH ₂ CH ₂ N(Boc)		H	Cl	CH ₃	Bn	82%
2.18	Bn	CH ₂ CH ₂ N(Boc)		H	H	H	Bn	56%
2.19	Bn	CH ₂ CH ₂ N(Boc)		H	H	H	H	53%
2.20	Ph	CH ₂ CH ₂ N(Boc)		H	H	H	Bn	71%
2.21	Bn	CH ₂ CH ₂ N(Boc)		MeO	H	H	H	53%
2.22	Ph	CH ₂ CH ₂ N(Boc)		H	H	CH ₃	H	60%
2.23	Ph	CH ₂ CH ₂ N(Boc)		H	CH ₃	CH ₃	H	61%

Reagents and conditions: 3:1 MeOH/H₂O, 65 °C, 4 h - 16 h.

Figure 2-8: Stereochemical Configurations of Azomethine Ylides



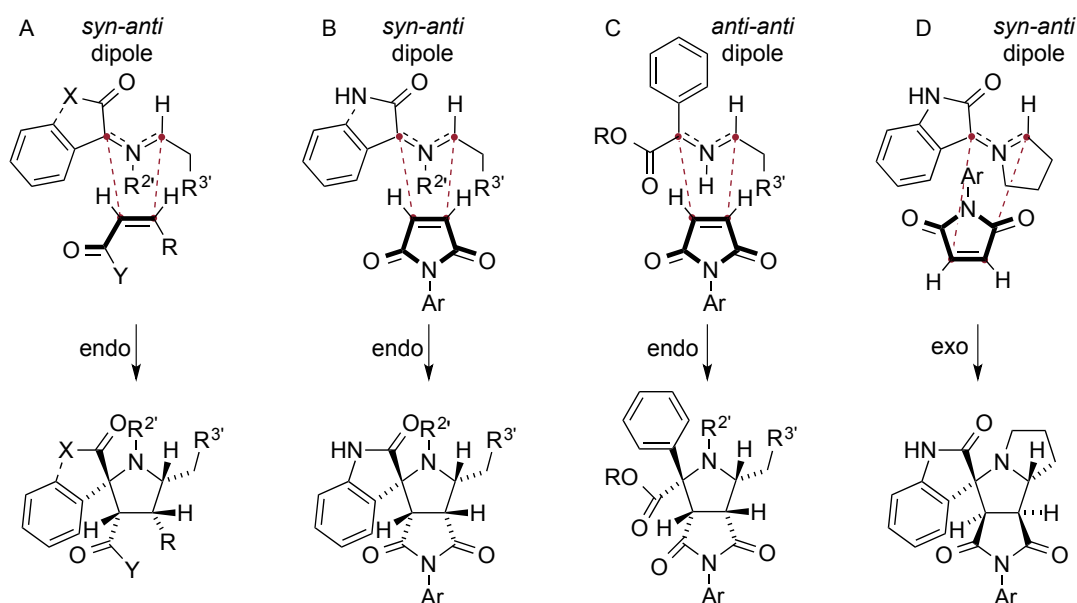
The 1,3-dipolar cycloaddition can proceed through either an *endo* or *exo* transition state. The products derived from all known reactions of amino acids, acyclic enones, and either isatins or phenylglyoxalates can be rationalized to arise through *endo* transition states (Scheme 2-5, path A).^{77,78,79,80,81, 84} In contrast, reactions of amino acids, maleimides and either isatins or phenylglyoxalates can proceed through *endo* or *exo* transition states depending on the structure of the amino acid. Acyclic amino acids give products consistent with *endo* transition states (Scheme 2-5, paths B and C).^{74,77,81,82,83,84} The only known reaction of a cyclic six-membered ring amino acid, pipercolic acid, with isatin and an acyclic dipolarophile also gives products consistent with an *endo* transition state (Scheme 2-5, path B);⁷⁸ however, the stereochemical outcome in the reaction of azomethine ylides with acyclic dipolarophiles cannot be extrapolated to reactions with maleimides.^{75,79a} In contrast, the cyclic five-membered ring amino acid proline gives products consistent with an *exo* transition state (Scheme 2-5, path D).⁷⁵

Similar ylides can be accessed from three-component reactions with amines instead amino acids, but there are cases where the trends in ylide configuration⁸⁵ and *endo/exo* selectivity⁸⁶ no longer hold. Notably, Ardil and co-workers showed that 1,3-dipoles derived from *N*-methylpiperazine aminals and related compounds favor *exo* adducts over *endo* adducts — sometimes exclusively *exo* — in refluxing toluene.⁸⁶

The assumption that isatins would react through path C (Scheme 2-5) may have led to the misassignment of the compound CID 6584729 by the commercial supplier along with over 100

spiroindolinones in the PubChem database. We cannot be sure of the stereochemistry of the compound CID 6584729 that was tested by Lindquist and co-workers since the experimental data for compounds in PubChem assay IDs 1979, 2467, and 2423 were never reported. One cannot rule out the possibility that the compound CID 6584729 tested in those assays was correctly assigned and generated through a more lengthy synthetic route than the one-pot reaction used in this and related work.

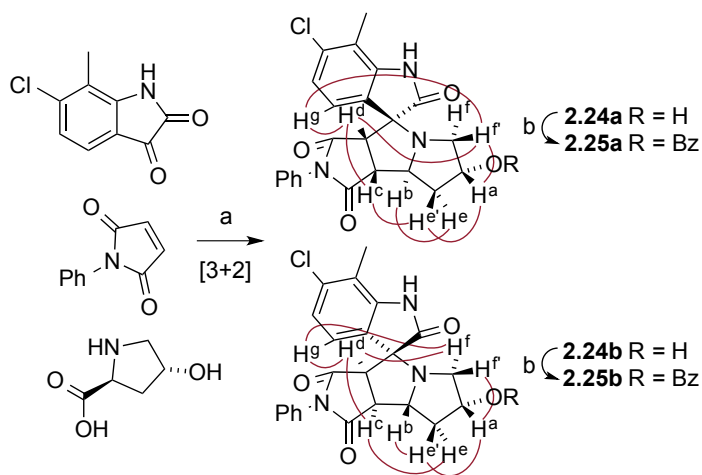
Scheme 2-5: *Endo/Exo* Selectivity in Dipolar Cycloadditions of Azomethine Ylides



To provide access to diastereomeric spiroindolinones with defined absolute stereochemistries we carried out a three-component coupling with isatin **2.6d**, *N*-phenylmaleimide and (2*S*, 4*R*)-4-hydroxyproline (Scheme 2-6). After 16 h, the reaction generated an inseparable mixture of two spiroindolinones, **2.24a** and **2.24b**, in 30% yield along with unreacted isatin. The two optically pure stereoisomers were readily separated by silica gel chromatography after benzylation of the hydroxy groups to afford esters **2.25a** and **2.25b**. The relative stereochemistry was assigned on the basis of diagnostic nOes. In particular, in both spiroindolinones **2.25a** and **2.25b**, there is an nOe between the bridgehead proton H^d and the

arene proton H^g on the indolone ring. In spiroindolinone **2.25a**, protons H^f, H^a, and H^e on the β -face of the proline ring exhibit vicinal nOes between each other. Protons H^e and H^f on the β -face of the proline ring exhibit long-range nOes with protons H^c and H^d on the succinimide ring, respectively; and proton H^f exhibits highly diagnostic long-range nOes to the indolone aryl proton H^g. In spiroindolinone **2.25b**, protons H^f, H^a, H^e and H^b on the β -face of the proline ring exhibit vicinal nOes between each other. Protons H^e and H^f on the α -face of the proline ring exhibit long-range nOes with protons H^c and H^d on the succinimide ring, respectively; and proton H^f exhibits a highly diagnostic long-range nOe to the indolone aryl proton H^g. Thus, the [3+2] cycloaddition of trans-hydroxyproline assemblies proceeds via *exo* addition of maleimide to an azomethine ylide with a *syn-anti* configuration (Scheme 2-5, path D).

Scheme 2-6: Stereoselectivity in the Three-Component, 1-Pot [1,3]-Dipolar Cycloaddition with (2*S*, 4*R*)-4-Hydroxyproline. Stereochemistry was established by nOes (red lines)

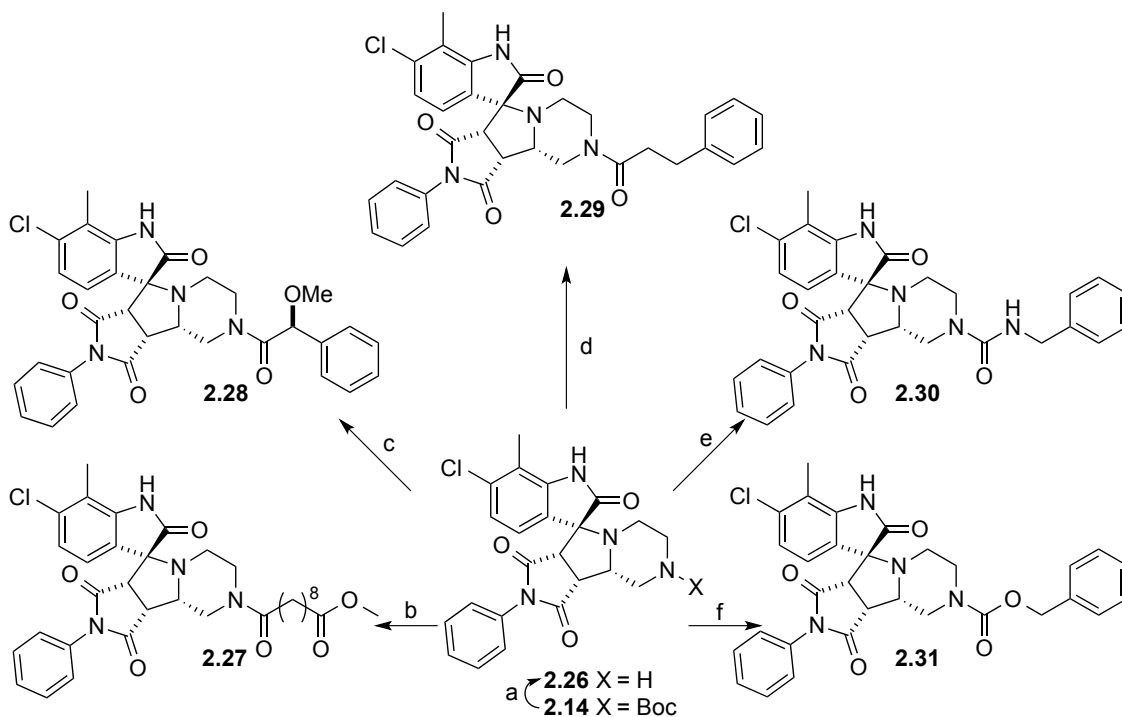


Reagents and conditions: a) 3:1 MeOH/H₂O, 90 °C, 16 h, b) 1.1 equiv BzCl, 1.2 equiv Et₃N, DMF, 23 °C, 20 h.

The reaction of the six-membered ring amino acid *N*_ε-Boc-piperazine-2-carboxylic acid proceeds in manner analogous with pipercolic acid (Scheme 2-5, path B) to afford spirocyclic indolinone **2.14** as a single diastereomer. The relative stereochemistry of spirocyclic piperazine **2.14** was secured with nOes after removal of the Boc and shown to match that of compound **2.1**.

Related spiroindolinones **2.15-2.23** were also prepared stereoselectively from *N*_ε-Boc-piperazine-2-carboxylic acid (Scheme 2-4).

Scheme 2-7: Synthesis of Pentacyclic Pyrrolidines Through Further Substitutions to Compound **2.26**



Reagents and conditions: (a) 1:1 TFA/CH₂Cl₂ 23 °C, 15 min, 90%, (b) 1.04 equiv methyl 10-chloro-10-oxodecanoate, 1.0 equiv Na₂CO₃, CH₂Cl₂, 23 °C, 30 min, 53%, (c) 1.3 equiv (*S*)-2-methoxy-2-phenylacetic acid, 2.1 equiv EDC, 3.5 equiv Et₃N, CH₂Cl₂, 23 °C, 20 min, 45%, (d) 1.05 equiv 3-phenylpropanoyl chloride, 1.1 equiv Et₃N, CH₂Cl₂, 23 °C, 3 h, 64%, (e) 1.1 equiv (isocyanatomethyl)benzene, CH₂Cl₂, 23 °C, 4 h, 75%, (f) 1.1 equiv benzyl chloroformate, 2.1 equiv DIPEA, CH₂Cl₂, 0-23 °C, 2.5 h, 54%.

The Boc group was removed from the spirocyclic piperazine **2.14** using trifluoroacetic acid to give a 90% yield of the piperazine **2.26** (Scheme 2-7). Piperazine **2.26** served as the precursor for various *N*-acyl derivatives **2.27-2.31** in the following reactions (Scheme 2-7). Compound **2.27** was synthesized by acylating **2.26** with methyl 10-chloro-10-oxodecanoate in the presence of sodium carbonate. Carbodiimide mediated coupling of (*S*)-2-methoxy-2-phenylacetic acid with the racemic piperazine **2.26** in the presence of triethylamine resulted in a mixture of diastereomers; only one diastereomer **2.28** was readily purified but the relative

stereochemistry was not assigned. Acylation of **2.26** with hydrocinnamoyl chloride in the presence of triethylamine afforded amide **2.29**. The reaction of piperazine **2.26** with benzyl isocyanate generated the urea **2.30**. Carbamate **2.31** was synthesized by acylation of piperazine **2.26** with benzyl chloroformate.

Structure-Activity Relationships

CID 6584729 was reported to enhance the effect of fluconazole against the partially resistant clinical isolate of *C. albicans* CaCi-8 at EC₅₀ 0.12 μM.⁸⁷ We determined the antifungal potency of the new spiroindolinones in combination with fluconazole against a susceptible strain (HLY4123) derived from a commonly used laboratory strain of *C. albicans*. The activity of compound **2.1** was promising, with an EC₅₀ of 0.011 μM. We then compared the activity of compound **2.1**, derived from phenylalanine with the activity of spiroindolinones derived from other amino acids (Table 2-1, compounds **2.1**, **2.8**, **2.9**, and **2.10**). Neither tryptophan nor *N*_ε-Boc-lysine derivatives were better than the parent compound **2.1** derived from phenylalanine. Regardless of the maleimide substituent, *N*-benzylisatin derivatives exhibited relatively low activity (compounds **2.11** and **2.12**). Compound **2.13** derived from 6-chloro-7-methylisatin but lacking the 4-fluoro substituent was exceedingly potent with an EC₅₀ of 1 nM.

When we employed the non-natural amino acid *N*_ε-Boc-piperazine-2-carboxylic acid, the resulting spirocyclic piperazine **2.14** was still highly active with an EC₅₀ of 5.6 nM. *N*-Benzylsuccinimide derivatives **2.18**, **2.19**, and **2.21** were not highly active. The substituents on the indolone ring were still important, even with the pentacyclic piperazine core (compounds **2.17**, **2.20**, **2.22**, **2.23**). We removed the Boc group from the piperazine ring of compound **2.14**, leading to a loss of potency (compound **2.26**).

Table 2-1: Structure-Activity Relationships for Polycyclic Pyrrolidines Against the Susceptible Strain HLY4123 of *C. albicans* in the Presence of Fluconazole (0.25 $\mu\text{g/mL}$)

Compound	R ^{5'}	R ^{2'}	R ^{3'}	R ⁵	R ⁶	R ⁷	R ¹	EC ₅₀ (μM) ^[a]
2.1	4-fluorophenyl	H	Ph	H	Cl	CH ₃	H	0.011 \pm 0.004
2.8	Bn	H	Ph	H	H	H	H	\sim 10 \pm 1.3
2.9	Bn	H	3-indolyl	H	H	H	H	\sim 10 \pm 1.8
2.10	Bn	H	(CH ₂) ₃ NHBoc	H	H	H	H	>100
2.11	Bn	H	Ph	H	H	H	Bn	>10
2.12	Ph	H	Ph	H	H	H	Bn	>100
2.13	Ph	H	Ph	H	Cl	CH ₃	H	0.001 \pm 0.0005
2.14	Ph	CH ₂ CH ₂ N(Boc)		H	Cl	CH ₃	H	0.0056 \pm 0.003
2.15	4-fluorophenyl	CH ₂ CH ₂ N(Boc)		H	Cl	CH ₃	H	0.037 \pm 0.001
2.16	3,5-bis(F ₃ C)phenyl	CH ₂ CH ₂ N(Boc)		H	Cl	CH ₃	H	0.0237 \pm 0.01
2.17	Ph	CH ₂ CH ₂ N(Boc)		H	Cl	CH ₃	Bn	>100
2.18	Bn	CH ₂ CH ₂ N(Boc)		H	H	H	Bn	0.0318 \pm 0.4
2.19	Bn	CH ₂ CH ₂ N(Boc)		H	H	H	H	>100
2.20	Ph	CH ₂ CH ₂ N(Boc)		H	H	H	Bn	>100
2.21	Bn	CH ₂ CH ₂ N(Boc)		MeO	H	H	H	230 \pm 5.7
2.22	Ph	CH ₂ CH ₂ N(Boc)		H	H	CH ₃	H	0.213 \pm 0.08
2.23	Ph	CH ₂ CH ₂ N(Boc)		H	CH ₃	CH ₃	H	0.0057 \pm 0.006
2.26	Ph	CH ₂ CH ₂ NH		H	Cl	CH ₃	H	\sim 10 \pm 1.5
2.27	Ph	CH ₂ CH ₂ N[CO(CH ₂) ₈ CO ₂ Me]		H	Cl	CH ₃	H	0.0379 \pm 0.009
2.28	Ph	CH ₂ CH ₂ N[COCH(OCH ₃)C ₆ H ₅]		H	Cl	CH ₃	H	0.035 \pm 0.007
2.29	Ph	CH ₂ CH ₂ N[CO(CH ₂) ₂ Ph]		H	Cl	CH ₃	H	0.0181 \pm 0.004
2.30	Ph	CH ₂ CH ₂ N[CONHCH ₂ Ph]		H	Cl	CH ₃	H	0.256 \pm 0.1
2.31	Ph	CH ₂ CH ₂ N(Cbz)		H	Cl	CH ₃	H	0.0003 \pm 0.00001

[a] Each value is the arithmetic mean \pm SD of three independent experiments.

Surprisingly, the carboxyl oxygen of the carbamate moiety appears to be essential for high potency; because carbamates **2.14** and **2.31** were more potent than amides **2.27** and **2.28**. Even more revealing, the isosteric amide **2.29** and urea **2.30** were two and three orders of magnitude less active, respectively, than benzyloxycarbamate **2.31**. Ultimately, benzyloxycarbamate **2.31** proved to be exquisitely active in improving the efficacy of fluconazole with an EC₅₀ of 300 pM. The two hydroxyproline adducts **2.25a** and **2.25b**, exhibited almost no activity under the conditions of the assay; those results are not surprising

given that the relative stereochemistry of those compounds was different from all the other compounds that were tested.

In general, substitution of small, hydrophobic groups on 6 and 7 positions of the indolone ring and benzyl substitution on the 3' position of the central pyrrolidine improves the antifungal activity. Also, a phenyl moiety not benzyl in the succinamide ring enhances the antifungal activity. When the piperazine is present in the polycyclic pyrrolidine, carbamoyl moiety but not the acyl groups on the piperazine ring significantly improves the antifungal activity. On the other hand, fluorinated substituents on the *para* and *meta* positions of the phenyl group in the succinamide ring as well as *N*-substitution of the indolone moiety diminish the activity of the spiroindolinones against *C. albicans*.

Activity Against Resistant Cell Lines

A variety of resistant clinical isolates of *C. albicans* were screened with 64 µg/ml fluconazole and compound **2.31** at a single dose (3 µM) in a broth microdilution assay (Table 2-2).⁸⁸ The strains grow at dramatically different rates. The published fluconazole minimum inhibitory concentrations (MICs) for these isolates convey the level of resistance.

Strains for which growth in the presence of compound **2.31** and fluconazole was less than 25% of growth in the presence of fluconazole alone (Isolates 17, 23, 26, 33, 36, and 45) were selected for determination of EC₅₀s. Compound **2.31** was particularly active against clinical isolates 17, 26 and 36 and exhibited good activity against the highly resistant isolate 45.

A checkerboard assay was used to determine the fractional inhibitory concentrations for compound **2.31** and fluconazole against the fluconazole-susceptible strain (HLY4123) and two fluconazole-resistant clinical isolates 26 and 45 (Table 2-3).⁸⁸

Table 2-2: Effect of Compound **2.31** on the Growth of Resistant Clinical Strains in the Presence of Fluconazole

Isolate ^[a]	Growth (OD ₆₀₀) ^[b]			Potency
	MIC _{Flc} ^[a]	+Fluc ^[c]	+Cpd 2.31 ^[d] +Fluc ^[c]	+Cpd 2.31 EC ₅₀ (nM) ^[c,e]
17	32	3.96	0.76	5 ± 0.011
23	32	6.77	0.60	53 ± 0.005
26	32	6.44	0.83	2 ± 0.002
33	64	7.38	0.88	11 ± 0.008
36	64	5.08	1.07	5 ± 0.251
45	128	9.17	1.03	16 ± 0.002

[a] From reference 88. [b] Growth measured after 16 h in SC at 30°C. [c] [fluconazole]=64 µg/mL. [d] [compound **2.31**]=3 µM. [e] Each value is the arithmetic mean ± SD of three independent experiments.

Table 2-3: FIC Indices for Compound **2.31** and Fluconazole in Different Strains of *C. albicans* (MIC90 measured in µM)^[a]

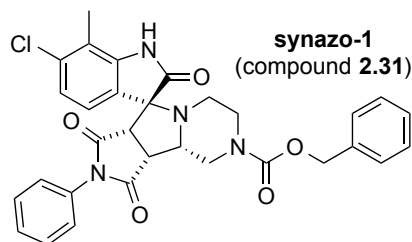
Strain	MIC _{cpd}	MIC _{cpd} (+Flc)	MIC _{Flc}	MIC _{Flc} (+cpd)	FICI
HLY4123	>300	0.03	0.5	0.125	0.25
26	>30	0.3	836	105	0.14
45	>30	0.03	836	105	0.13

[a] MIC data are derived from single replicates of two independent experiments; values were consistent between experiments.

In all of the strains tested, the FIC index was below 0.5, fitting the classical definition of synergy.⁸⁹ Compound **2.31** alone did not have measurable toxicity against any of the strains at the solubility limit (between 30 and 300 µM). In the strains tested, fluconazole dramatically enhances the activity of compound **2.31** against *C. albicans*. Conversely compound **2.31** makes fluconazole more potent against those same strains but the effect is less dramatic. We have named compound **2.31** as synazo-1 (Figure 2-9).

Greater than 90% inhibition of *C. albicans* sterol α -demethylase (a.k.a. Erg11 or CYP51) would be expected at ten times the K_i for fluconazole, which has been determined to be 0.03 μM .^{90,91} When synazo-1 is present at 300 nM in the susceptible strain, the MIC₉₀ for fluconazole is reduced from 0.5 μM to 0.125 μM , consistent with the theoretical limit for fluconazole potency of around 0.3 μM .

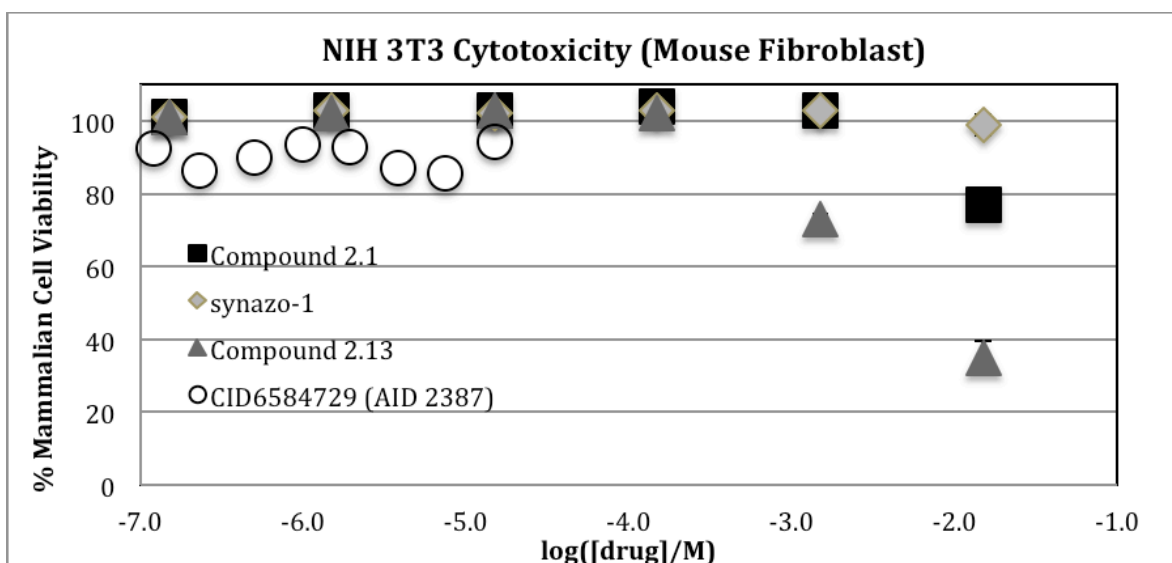
Figure 2-9: The Structure of Compound **2.31**, Renamed Synazo-1



Cytotoxicity of Synazo-1 Against Mammalian Cells

We compared the cytotoxicity of spiroindolinone **2.1**, synazo-1 and compound **2.13** against NIH 3T3 cells at higher concentrations up to 15 mM (Figure 2-10).

Figure 2-10: Cytotoxicity of Compounds **2.1**, **2.13** and Synazo-1 Against NIH 3T3 Cells



Data represent arithmetic means \pm SD of three independent experiments.

All compounds exhibited only weak cytotoxicity. Compound **2.13** was slightly more cytotoxic, but not at the concentrations required for antifungal synergy. According to PubChem, CID 6584729 was previously tested for cytotoxicity against NIH 3T3 cells (PubChem AID 2387) but the EC50 was $\geq 160 \mu\text{M}$, the limit of the assay. It is unclear how the biological activities reported for CID 6584729 should relate to that of the diastereomer **2.1** or whether they were even distinct compounds.

Drug-Like Parameters for Synazo-1

A wide range of readily calculated properties is often used as indicators of oral bioavailability. The calculated physicochemical properties of synazo-1 were compared with typical ranges for lead-like molecules.^{92,93,94} Synazo-1 flags just one of the common warnings for drug lead-like properties (Table 2-4) — molecular weight. For comparison, the orally available azole posaconazole is outside the range on four of the parameters. It is widely recognized that the average molecular weight and complexity of newly approved oral drugs has been increasing with each year.^{95,96}

Table 2-4: Calculated Physicochemical Properties of Synazo-1^[a]

Property	Range	Synazo-1
milogP	-4.0 to 4.2	4.173
TPSA	$\leq 120 \text{ \AA}^2$	99.3 \AA^2
molecular weight	≤ 460	571
N+O	≥ 1	9
H-bond donors	≤ 5	1
rotatable bonds	≤ 10	4
halogens	≤ 7	1
fraction sp^3	0.15-0.80	0.20
H-bond acceptors	≤ 9	5

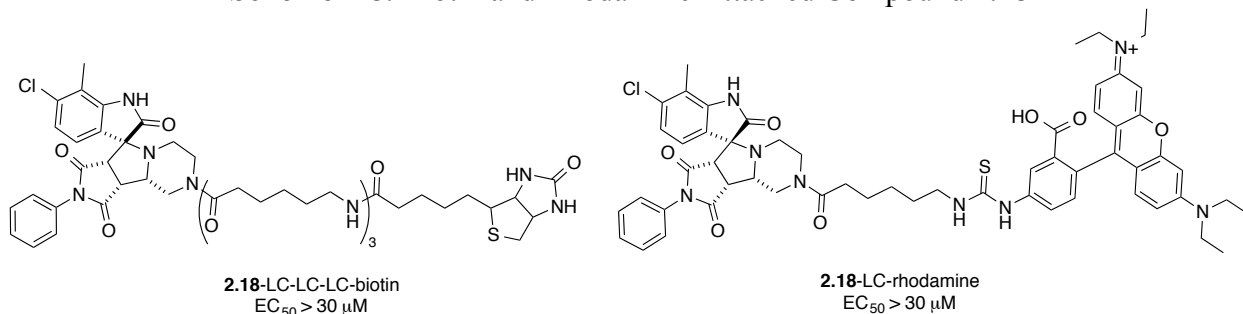
[a] Calculated with Molinspiration property calculation service.
<http://www.molinspiration.com/cgi-bin/properties>.

Both the carbamate and imide moieties are potential liabilities for metabolism, yet when the stability of synazo-1 was tested in 10% FBS/phosphate buffered saline at 37 °C no decomposition was observed over 16 h.

Biological Studies

Inspired by the SAR studies, biological probes containing biotin and rhodamine were synthesized to use in pull-down and small molecule localization assays. Unfortunately, both molecules had no dose-dependent activity within the concentrations tested (30 μ M, solubility limit) (Scheme 2-8). This is probably due to the decreasing cell permeation ability of molecules with the increasing values of molecular weight, rotatable bonds and fraction sp^3 . In order to avoid this issue Shelley Lane in Liu lab carried out the pull-down assay with cell lysates instead of whole cell. However, after MS-MS studies, they were unable to pull-down interesting proteins that might be responsible for the synergistic activity of the synazo-1 and related analogues.

Scheme 2-8: Biotin and Rhodamine Attached Compound **2.18**



Conclusions

In conclusion, we have designed, synthesized and studied spiroindolinones inspired by CID 6584729, a screening hit that was previously reported to exhibit activity against *C. albicans* in combination with fluconazole. The relative stereochemistry of compound **2.1** and analogues was secured through 2D NMR experiments. The three-component, one-pot [3+2] dipolar cycloaddition of isatins, amino acids, and maleimides was found to proceed through *endo*

addition of maleimides to a *syn-anti* azomethine ylide in all cases except for a proline derivative. A number of the new spiroindolinones were substantially more potent against *C. albicans* than the original lead compound **2.1** when used in combination with fluconazole. In particular, synazo-1 was exquisitely potent with an EC₅₀ of 300 pM against a susceptible strain. Synazo-1 also exhibited low nanomolar activity against a number of resistant isolates of *Candida*. When tested in both susceptible and resistant strains of *C. albicans*, synazo-1 was a true synergizer with an FIC index below 0.5. Synazo-1 has many of the calculated parameters associated with orally available drug molecules and represents a promising candidate for development as an antifungal synergizer.

Experimental Section

Chemistry

Analytical High-Performance Liquid Chromatography (HPLC)

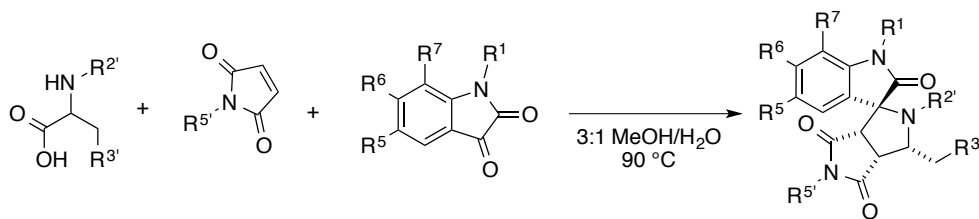
The HPLC instrument consisted of an Agilent Technologies series 1200 autosampler, series 1200 UV/Vis detector, series 1100 pump, using ChemStation software (Agilent Technologies, Santa Clara, CA, USA). The analytical column was a reverse-phase Waters Nova-pak® C18 150 mm × 3.9 mm column. A gradient elution was used (flow rate 0.2 mL/min), starting with 80% water and progressing to 100% acetonitrile over a period of 1 h, with both solvents containing 0.1% formic acid. All compounds have purity ≥95% (254 nm) by HPLC.

General Experimental Procedures

NMR spectral data were recorded at room temperature using a Bruker 500 or 600 MHz spectrometer unless stated otherwise. The NMR data are reported as follows: chemical shifts in ppm from an internal tetramethylsilane standard on the δ scale, multiplicity (br = broad, app = apparent, s = singlet, d = doublet, t = triplet, q = quartet, and m = multiplet), coupling constants

(Hz), and integration. Analytical thin layer chromatography (TLC) was performed using EMD Reagents 0.25 mm silica gel 60-F plates. “Flash” chromatography on silica gel was performed using Silicycle silica gel (40-63 μm). All reactions were carried out under an atmosphere of nitrogen in glassware that was evacuated and back-filled with nitrogen three times. Reactions were carried out at room temperature unless otherwise indicated. Unless otherwise noted, all reagents were commercially obtained and, where appropriate, purified prior to use. THF, Et_2O , DMF and CH_2Cl_2 were dried by filtration through alumina according to the procedure of Grubbs and co-workers.⁹⁷ For final compounds the purity was determined by HPLC (Agilent Technologies series 1200).

General procedure for the synthesis of pyrrolidines through a three-component dipolar cycloaddition (2.1, 2.8-2.23, 2.24a and 2.24b):⁷³

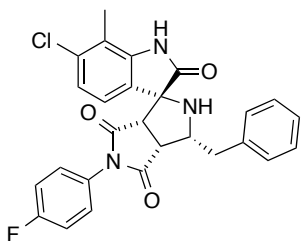


A 100 mL round bottom flask was charged with substituted isatin (1.0 equiv), *N*-substituted maleimide (1.1 equiv), the amino acid (1.1 equiv) and a stir bar. A 3:1 (v/v) mixture of water and methanol was added to the reaction flask such that the concentration of isatin was 0.25 M. The reaction was heated at reflux by immersing the reaction flask in a hot oil bath at 90 °C up to the level of the flask’s contents. Initially a clear solution was obtained and CO_2 evolution was observed. However, after a few hours the reaction mixture became cloudy. The reaction was monitored for consumption of the substituted isatin by TLC (EtOAc/hex).

Upon consumption of the substituted isatin, the reaction was cooled to room temperature. Next, the reaction mixture was quenched by pouring it into a mixture of ice and sat. aq.

NaHCO₃. The resulting solid was filtered and washed thoroughly with water in the Büchner funnel to afford a grey solid. The solid was then dissolved in minimum amount of CH₂Cl₂ and purified by flash chromatography with EtOAc/hex (1:1) to afford the racemic substituted pyrrolidine.

(±)-(3*R*,3'*R*,3*a*'*R*,6*a*'*S*)-3'-benzyl-6-chloro-5'-(4-fluorophenyl)-7-methyl-2',3',3*a*',6*a*'-tetrahydro-4'*H*-spiro[indoline-3,1'-pyrrolo[3,4-*c*]pyrrole]-2,4',6'(5'*H*)-trione, 2.1.

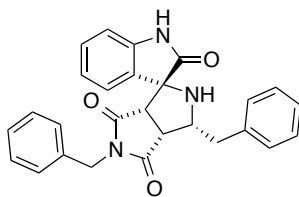


A 100 mL round bottom flask was charged with 1-(4-fluorophenyl)-1*H*-pyrrole-2,5-dione (0.50 g, 2.55 mmol, 1.0 equiv), *p*-fluoro-*N*-phenylmaleimide (0.53 g, 2.8 mmol, 1.1 equiv), L-phenylalanine (0.46 g, 2.8 mmol, 1.1 equiv) and a stir bar. A 3:1 mixture of water and methanol (11 mL) was added to the reaction flask. The content of the reaction flask was heated at reflux by immersing the reaction flask in a hot oil bath up to the level of the flask's contents. Initially a clear solution was obtained and CO₂ was expelled. After few hours a cloudy solution was observed.

Upon consumption of the substituted isatin (16 h), the reaction was allowed to cool to room temperature. Next, the reaction mixture was quenched by pouring it into a mixture of ice and sat. aq. NaHCO₃. The resulting solid was washed thoroughly with water in Büchner funnel to afford a grey solid. The solid was then dissolved in minimum amount of CH₂Cl₂ and purified by flash chromatography with different combinations of EtOAc/hex to afford the pyrrolidine **2.1** as a white solid (0.93 mg, 1.9 mmol, 74%). *R_f* = 0.35 (1:1 EtOAc/hex); mp 212-215. The ¹H NMR chemical shifts were concentration-dependent in CDCl₃, particularly within the range 0.5-2 mM. ¹H NMR (600 MHz, CDCl₃) δ 8.00 (s, 1H), 7.41-7.38 (m, 2H), 7.27-7.16 (m, 6H), 7.02 (d, *J* = 8.0 Hz, 2H), 6.81 (d, *J* = 8.5 Hz, 1H), 4.72-4.71 (m, 1H), 3.75-3.69 (m, 1H), 3.45 (dd, *J* = 14.0, 4.0 Hz, 1H), 2.73 (dd, *J* = 13.8, 10.5 Hz, 1H), 2.16 (s, 1H), 1.99 (s, 3H); ¹³C NMR (500

MHz, CDCl₃) δ 180.4, 175.1, 174.4, 163.4, 161.4, 140.5, 139.1, 136.2, 128.9, 128.8, 128.3, 127.6, 126.7, 124.6, 124.5, 123.5, 118.2, 116.6, 116.4, 68.2, 58.9, 51.6, 47.6, 37.9, 13.5; IR (thin film) 3201, 3065, 1710, 1696, 1623, 1601, 1510; HRMS (ESI): m/z calculated for C₂₈H₂₉ClN₄O₅Na [M+Na]⁺ 559.1724, found 559.1743. HPLC purity: 95.76%.

(±)-(3*R*,3'*R*,3*a*'*R*,6*a*'*S*)-3',5'-Dibenzyl-2',3',3*a*',6*a*'-tetrahydro-4'*H*-spiro[indoline-3,1'-pyrrolo[3,4-*c*]pyrrole]-2,4',6'(5'*H*)-trione, 2.8.

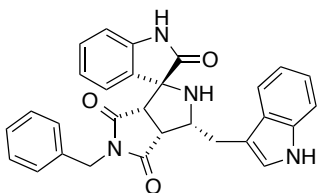


Using the general procedure for the synthesis of pyrrolidines outlined above, indoline-2,3-dione (0.37 g, 2.5 mmol, 1.0 equiv) was used and the product was purified by flash chromatography with EtOAc/hex to afford the pyrrolidine **2.8** as a white solid (0.65

mg, 1.5 mmol, 60%). R_f = 0.50 (1:1 EtOAc/hex); mp 138-142; ¹H NMR (600 MHz, CDCl₃) δ 7.50-7.49 (m, 2H), 7.40-7.38 (m, 3H), 7.29 (br s, 1H), 7.26-7.25 (m, 1H), 7.24-7.22 (m, 3H), 7.18- 7.16 (m, 2H), 6.80 (t, J = 7.5 Hz, 1H), 6.69 (d, J = 7.8 Hz, 1H), 6.50 (d, J = 7.5 Hz, 1H), 4.83 (d, J = 14.0 Hz, 1H), 4.69 (d, J = 14.0 Hz, 1H), 4.68-4.67 (m, 1H), 3.58-3.56 (m, 1H), 3.42 (d, J = 7.6 Hz, 2H), 2.60 (dd, J = 13.8, 10.4 Hz, 1H), 2.01 (br s, 1H); ¹³C NMR (500 MHz, CDCl₃, 313 K) δ 180.1, 175.8, 174.5, 140.3, 139.3, 135.8, 129.8, 129.0, 128.9, 128.8, 128.7, 128.1, 126.9, 126.5, 126.4, 122.6, 109.7, 67.6, 58.5, 51.5, 47.7, 42.7, 38.2; IR (thin film) 3850, 3646, 2971, 2843, 1697, 1619, 1054, 1032; HRMS (ESI): m/z calculated for C₂₇H₂₃N₃O₃Na [M+Na]⁺ 460.1637, found 460.1620. HPLC purity: 100%.

(±)-(3*R*,3'*R*,3*a*'*R*,6*a*'*S*)-3'-((1*H*-Indol-3-yl)methyl)-5'-benzyl-2',3',3*a*',6*a*'-tetrahydro-4'*H*-spiro[indoline-3,1'-pyrrolo[3,4-*c*]pyrrole]-2,4',6'(5'*H*)-trione, 2.9.

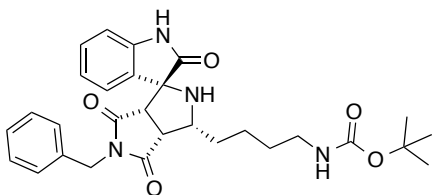
Using the general procedure for the synthesis of pyrrolidines outlined above, indoline-2,3-dione (0.37 g, 2.5 mmol, 1.0 equiv) was used and the product was purified by flash



chromatography with EtOAc/hex to afford the pyrrolidine **2.9** as a yellow solid (0.83 mg, 1.7 mmol, 70%). $R_f = 0.35$ (1:1 EtOAc/hex); mp 130-142; $^1\text{H NMR}$ (600 MHz, CDCl_3) δ 7.96 (br s, 1H), 7.60 (d, $J = 7.9$ Hz, 1H), 7.52 (d, $J = 7.3$ Hz, 2H),

7.42-7.39 (m, 2H), 7.36-7.33 (m, 1H), 7.30- 7.29 (m, 1H), 7.17- 7.11 (m, 2H), 7.09- 7.06 (m, 2H), 6.80- 6.77 (m, 1H), 6.62 (d, $J = 7.7$ Hz, 1H), 6.49 (d, $J = 7.5$ Hz, 1H), 4.86 (d, $J = 14.0$ Hz, 1H), 4.80-4.76 (m, 1H), 4.70 (d, $J = 14.0$ Hz, 1H), 3.60 (t, $J = 7.7$ Hz, 1H), 3.49 (dd, $J = 14.6$, 3.7 Hz, 1H), 3.41 (d, $J = 7.7$ Hz, 1H), 2.82 (dd, $J = 14.6$, 10.3 Hz, 1H), 2.13 (br s, 1H); $^{13}\text{C NMR}$ (500 MHz, CDCl_3 , 313 K) δ 180.3, 176.0, 174.8, 140.4, 136.2, 135.9, 129.6, 129.0, 128.8, 128.2, 127.5, 126.8, 126.5, 122.5, 122.4, 122.1, 119.5, 119.1, 113.6, 111.1, 109.7, 67.7, 58.1, 51.6, 47.7, 42.6, 27.7; IR (thin film) 3679, 2971, 2864, 2843, 1695, 1619, 1054, 1032; HRMS (ESI): m/z calculated for $\text{C}_{29}\text{H}_{24}\text{N}_4\text{O}_3\text{Na}$ $[\text{M}+\text{Na}]^+$ 499.1746, found 499.1739. HPLC purity: 98.81%.

(±)-*tert*-Butyl (4-((3*R*,3'*R*,3*a*'*R*,6*a*'*S*)-5'-benzyl-2,4',6'-trioxo-3',3*a*',4',5',6',6*a*'-hexahydro-2'*H*-spiro[indoline-3,1'-pyrrolo[3,4-*c*]pyrrol]-3'-yl)butyl)carbamate, **2.10.**

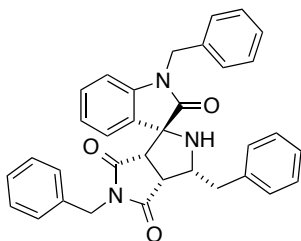


Using the general procedure for the synthesis of pyrrolidines outlined above, indoline-2,3-dione (0.37 g, 2.5 mmol, 1.0 equiv) was used and the product was

purified by flash chromatography with EtOAc/hex to afford the pyrrolidine **2.10** as a white solid (0.42 mg, 0.82 mmol, 33%). $R_f = 0.35$ (4:6 EtOAc/hex); mp 109-113; $^1\text{H NMR}$ (600 MHz, CDCl_3) δ 7.45-7.44 (m, 2H), 7.38-7.33 (m, 3H), 7.29 (br s, 1H), 7.20-7.17 (m, 1H), 6.79-6.76 (m, 2H), 6.36 (d, $J = 7.4$ Hz, 1H), 4.78 (d, $J = 14.0$ Hz, 1H), 4.70-4.63 (m, 1H), 4.61 (d, $J = 14.0$ Hz, 1H), 4.34-4.32 (m, 1H), 3.50 (t, $J = 7.7$ Hz, 1H), 3.42 (d, $J = 7.7$ Hz, 1H), 3.18-3.08 (m, 2H), 2.06-1.91 (m, 2H), 1.57-1.53 (m, 2H), 1.43 (s, 9H); $^{13}\text{C NMR}$ (500 MHz, CDCl_3 , 313 K) δ

180.15, 175.8, 174.5, 140.3, 135.8, 129.8, 129.2, 128.8, 128.2, 126.5, 126.4, 122.7, 109.8, 68.1, 58.3, 51.7, 48.1, 42.7, 40.1, 31.2, 30.0, 28.5, 24.6, 14.3; IR (thin film) 3707, 2971, 2843, 1345, 1054, 1032; HRMS (ESI): m/z calculated for $C_{29}H_{34}N_4O_5Na$ $[M+Na]^+$ 541.2427, found 541.2411. HPLC purity: 97.81%.

(±)-(3*R*,3'*R*,3*a*'*R*,6*a*'*S*)-1,3',5'-Tribenzyl-2',3',3*a*',6*a*'-tetrahydro-4'*H*-spiro[indoline-3,1'-pyrrolo[3,4-*c*]pyrrole]-2,4',6'(5'*H*)-trione, 2.11.

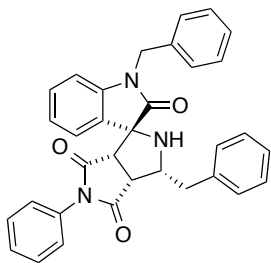


Using the general procedure for the synthesis of pyrrolidines outlined above, 1-benzylindoline-2,3-dione (0.07 g, 0.32 mmol, 1.0 equiv) was used and the product was purified by flash chromatography with EtOAc/hex to afford the pyrrolidine **2.11** as a

white solid (0.08 mg, 0.15 mmol, 46%). R_f = 0.60 (1:1 EtOAc/hex); mp 173-175; 1H NMR (600 MHz, $CDCl_3$) δ 7.50-7.49 (m, 2H), 7.39-7.12 (m, 14H), 6.82-6.79 (m, 1H), 6.64 (d, J = 9.3 Hz, 1H), 6.54 (d, J = 8.7 Hz, 1H), 4.88-4.81 (m, 2H), 4.80-4.72 (m, 1H), 4.71-4.65 (m, 2H), 3.64-3.60 (m, 1H), 3.44-3.39 (m, 2H), 2.61 (dd, J = 16.6, 12.3 Hz, 1H), 2.01 (br s, 1H); ^{13}C NMR (500 MHz, $CDCl_3$, 313 K) δ 178.7, 175.9, 174.4, 142.6, 139.3, 135.8, 135.4, 129.8, 129.0, 128.9, 128.9, 128.8, 128.6, 128.1, 127.8, 127.3, 126.5, 126.4, 125.8, 122.6, 109.1, 67.5, 58.5, 51.8, 47.7, 43.6, 42.7, 38.2; IR (thin film) 3850, 3708, 2971, 2864, 1453, 1054, 1032; HRMS (ESI): m/z calculated for $C_{34}H_{29}N_3O_3Na$ $[M+Na]^+$ 550.2106, found 550.2108. HPLC purity: 98.45%.

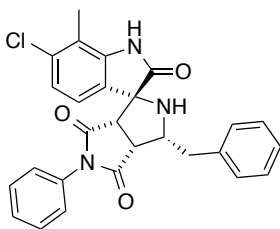
(±)-(3*R*,3'*R*,3*a*'*R*,6*a*'*S*)-1,3'-Dibenzyl-5'-phenyl-2',3',3*a*',6*a*'-tetrahydro-4'*H*-spiro[indoline-3,1'-pyrrolo[3,4-*c*]pyrrole]-2,4',6'(5'*H*)-trione, 2.12.

Using the general procedure for the synthesis of pyrrolidines outlined above, 1-benzylindoline-2,3-dione (0.30 g, 1.3 mmol, 1.0 equiv) was used and the product was purified by flash chromatography with EtOAc/hex to afford the pyrrolidine **2.12** as a yellow solid (0.38



mg, 0.74 mmol, 57%). $R_f = 0.60$ (1:1 EtOAc/hex); mp 183-188; ^1H NMR (600 MHz, $\text{DMSO-}d_6$) δ 7.57-7.52 (m, 2H), 7.46-7.44 (m, 1H), 7.40-7.37 (m, 4H), 7.34-7.33 (m, 3H), 7.31-7.25 (m, 3H), 7.21-7.17 (m, 2H), 7.14 (dd, $J = 7.4, 1.5$ Hz, 1H), 6.97 (t, $J = 7.5$ Hz, 1H), 6.84 (d, $J = 7.8$ Hz, 1H), 4.90 (d, $J = 15.6$ Hz, 1H), 4.76 (d, $J = 15.6$ Hz, 1H), 4.52-4.50 (m, 1H), 3.73 (dd, $J = 7.5, 1.8$ Hz, 1H), 3.63 (dd, $J = 7.8, 2.7$ Hz, 1H), 2.61 (dd, $J = 16.6, 12.3$ Hz, 1H), 3.32 (br s, 1H), 2.82-2.78 (m, 1H); ^{13}C NMR (500 MHz, CDCl_3 , 313 K) δ 178.7, 175.9, 174.4, 142.6, 139.3, 135.8, 135.4, 129.8, 129.0, 128.9, 128.9, 128.8, 128.6, 128.1, 127.8, 127.3, 126.5, 126.4, 125.8, 122.6, 109.1, 67.5, 58.5, 51.8, 47.7, 43.6, 42.7, 38.2; IR (thin film) 3680, 2966, 2865, 1706, 1054, 1032; HRMS (ESI): m/z calculated for $\text{C}_{34}\text{H}_{29}\text{N}_3\text{O}_3\text{Na}$ $[\text{M}+\text{Na}]^+$ 550.2106, found 550.2108. HPLC purity: 95.07%.

(±)-(3*R*,3'*R*,3*a*'*R*,6*a*'*S*)-3'-Benzyl-6-chloro-7-methyl-5'-phenyl-2',3',3*a*',6*a*'-tetrahydro-4'*H*-spiro[indoline-3,1'-pyrrolo[3,4-*c*]pyrrole]-2,4',6'(5'*H*)-trione, 2.13.

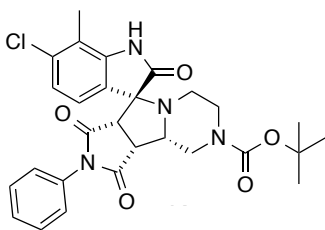


Using the general procedure for the synthesis of pyrrolidines outlined above, 6-chloro-7-methylindoline-2,3-dione (0.30 g, 1.7 mmol, 1.0 equiv) was used and the product was purified by flash chromatography with EtOAc/hex to afford the pyrrolidine **2.13** as a white solid (0.21 g, 0.44 mmol, 26%). $R_f = 0.60$ (1:1 EtOAc/hex); mp 168-171; ^1H NMR (600 MHz, $\text{DMSO-}d_6$) δ 10.12 (s, 1H), 7.54-7.51 (m, 2H), 7.45-7.43 (m, 1H), 7.39-7.35 (m, 4H), 7.29-7.27 (m, 2H), 7.19-7.17 (m, 1H), 6.97 (d, $J = 8.0$ Hz, 1H), 6.90 (d, $J = 8.0$ Hz, 1H), 4.55 (br s, 1H), 3.72 (t, $J = 7.5$ Hz, 1H), 3.53 (d, $J = 7.8$ Hz, 1H), 3.38-3.35 (m, 2H), 2.27 (s, 3H); ^{13}C NMR (500 MHz, $\text{DMSO-}d_6$) δ 142.8, 140.6, 135.1, 134.5, 132.9, 129.4, 129.3, 128.7, 127.6, 127.3, 126.4, 125.0, 121.9, 117.3; IR (thin film) 3850, 3626, 2971, 2864, 1710, 1693, 1014,

1032; HRMS (ESI): m/z calculated for $C_{27}H_{22}ClN_3O_3Na$ $[M+Na]^+$ 494.1247, found 494.1255.

HPLC purity: 95.00%.

(±)-*tert*-Butyl (3*R*,3*a*'*R*,3*b*'*S*,9*a*'*S*)-6-chloro-7-methyl-1',2,3'-trioxo-2'-phenyl-2',3',3*a*',3*b*',4',6',7',9*a*'-octahydrospiro[indoline-3,9'-pyrrolo[3',4':3,4]pyrrolo[1,2-*a*]pyrazine]-5'(1'*H*)-carboxylate, 2.14.

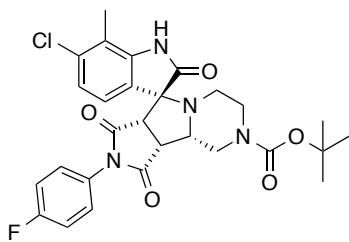


Using the general procedure for the synthesis of pyrrolidines outlined above, 6-chloro-7-methylindoline-2,3-dione (0.81 g, 4.1 mmol, 1.0 equiv) was used and the product was purified by flash chromatography with EtOAc/hex to afford the pyrrolidine **2.14** as

a light pink solid (1.3 g, 2.5 mmol, 60%). R_f = 0.35 (4:6 EtOAc/hexanes); mp 201-205; 1H NMR (600 MHz, DMSO- d_6 , 400 K) δ 10.90 (s, 1H), 7.54-7.51 (m, 2H), 7.47-7.46 (m, 1H), 7.31 (d, J = 7.8 Hz, 2H), 7.06 (d, J = 7.8 Hz, 1H), 6.73 (d, J = 7.8 Hz, 1H), 4.31 (br s, 1H), 3.85 (t, J = 7.5 Hz, 2H), 3.64-3.65 (m, 1H), 3.55 (d, J = 7.8 Hz, 1H), 2.74-2.58 (m, 2H) 2.25 (app s, 4H), 2.13-2.08 (m, 1H), 1.41 (s, 9H); ^{13}C NMR (500 MHz, DMSO- d_6 , 313 K) δ 177.9, 174.7, 173.4, 153.6, 142.8, 134.6, 132.1, 128.9, 128.5, 126.9, 124.6, 123.2, 122.8, 117.3, 79.1, 71.7, 62.3, 58.7, 57.6, 50.4, 45.9, 44.9, 27.9, 13.7; IR (thin film) 3840, 3708, 3626, 2971, 2843, 1713, 1695, 1032; HRMS (ESI): m/z calculated for $C_{28}H_{29}ClN_4O_5Na$ $[M+Na]^+$ 559.1724, found 559.1743. HPLC purity: 96.96%.

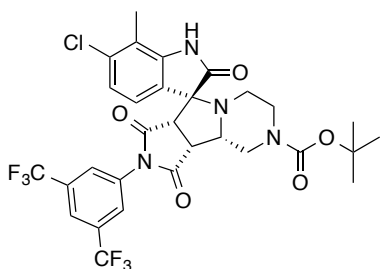
(±)-*tert*-Butyl (3*R*,3*a*'*R*,3*b*'*S*,9*a*'*S*)-6-chloro-2'-(4-fluorophenyl)-7-methyl-1',2,3'-trioxo-2',3',3*a*',3*b*',4',6',7',9*a*'-octahydrospiro[indoline-3,9'-pyrrolo[3',4':3,4]pyrrolo[1,2-*a*]pyrazine]-5'(1'*H*)-carboxylate, 2.15.

Using the general procedure for the synthesis of pyrrolidines outlined above, 6-chloro-7-methylindoline-2,3-dione (0.12 g, 0.63 mmol, 1.0 equiv) was used and the product was purified by flash chromatography with EtOAc/hex to afford the pyrrolidine **2.15** as a white solid (0.17



mg, 0.31 mmol, 49%). $R_f = 0.35$ (4:6 EtOAc/hex); $R_f = 0.35$ (4:6 EtOAc/hexanes); mp 246-248; $^1\text{H NMR}$ (600 MHz, DMSO- d_6 , 400 K) δ 10.42 (s, 1H), 7.39-7.35 (m, 2H), 7.32-7.29 (m, 2H), 7.02 (d, $J = 7.8$ Hz, 2H), 6.75 (d, $J = 7.8$ Hz, 1H), 4.35 (dd, $J = 12.6, 1.8$ Hz, 1H), 3.89-3.83 (m, 2H), 3.74-3.71 (m, 1H), 3.56 (d, $J = 7.8$ Hz, 1H), 2.74-2.58 (m, 2H) 2.77-2.73 (m, 1H), 2.74-2.54 (m, 1H), 2.50 (s, 3H), 2.29-2.09 (M, 1H), 1.44 (s, 9H); $^{13}\text{C NMR}$ (500 MHz, DMSO- d_6 , 313 K) δ 178.5, 175.3, 173.9, 161.0, 154.2, 143.3, 135.1, 129.7, 128.8, 125.1, 123.7, 122.6, 117.9, 116.6, 116.4, 79.6, 72.2, 58.1, 51.0, 46.6, 45.6, 45.9, 28.5, 14.3; IR (thin film) 3850, 3708, 2965, 2866, 1706, 1689, 1032; HRMS (ESI): m/z calculated for $\text{C}_{28}\text{H}_{28}\text{ClFN}_4\text{O}_5\text{Na} [\text{M}+\text{Na}]^+$ 577.1630, found 577.1644. HPLC purity: 100%.

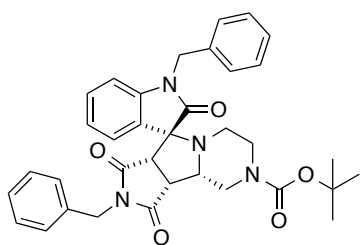
(±)-tert-Butyl (3*R*,3*a'R*,3*b'**S*,9*a'**S*)-2'--(3,5-bis(trifluoromethyl)phenyl)-6-chloro-7-methyl-1',2,3'-trioxo-2',3',3*a'*,3*b'*,4',6',7',9*a'*-octahydrospiro[indoline-3,9'-pyrrolo[3',4':3,4]pyrrolo[1,2-*a*]pyrazine]-5'(1'*H*)-carboxylate, 2.16.**



Using the general procedure for the synthesis of pyrrolidines outlined above, 6-chloro-7-methylindoline-2,3-dione (0.50 g, 2.6 mmol, 1.0 equiv) was used and the product was purified by flash chromatography with EtOAc/hex to afford the pyrrolidine **2.16** as a white solid (0.13 mg, 0.30 mmol, 12%). $R_f = 0.5$ (2:3 EtOAc/hex); mp 199-201; $^1\text{H NMR}$ (600 MHz, CDCl_3 , 320 K) δ 8.51 (s, 1H), 7.93-7.92 (m, 3H), 7.12 (d, $J = 8.1$ Hz, 1H), 6.70 (d, $J = 8.0$ Hz, 1H), 4.59 (br s, 1H), 4.11 (br s, 1H), 3.80-3.82 (m, 1H), 3.81-3.78 (m, 1H), 3.74-3.72 (m, 1H), 2.82-2.89 (m, 1H), 2.65-2.71 (m, 1H), 2.33-2.34 (m, 2H), 2.17 (s, 3H), 1.47 (s, 9H); $^{13}\text{C NMR}$ (500 MHz, DMSO- d_6) δ 177.6, 174.2, 173.0, 154.4, 141.2, 136.8, 133.0, 132.7, 126.2, 124.5, 123.8, 123.7, 122.5, 118.4, 81.0, 72.9, 62.3, 58.3, 57.6, 50.5, 46.17, 45.6, 28.4, 13.8; IR (thin film) 3187, 1724, 1706, 1680,

1599, 1276, 1132; HRMS (ESI): m/z calculated for $C_{30}H_{27}ClF_6N_4O_5Na$ $[M+Na]^+$ 695.1472, found 695.1450. HPLC purity: 98.46%.

(±)-*tert*-Butyl (3*R*,3*a'R*,3*b'**S*,9*a'**S*)-1,2'-dibenzyl-1',2,3'-trioxo-2',3',3*a'*,3*b'*,4',6',7',9*a'*-octahydrospiro[indoline-3,9'-pyrrolo[3',4':3,4]pyrrolo[1,2-*a*]pyrazine]-5'(1'*H*)-carboxylate, 2.18.**

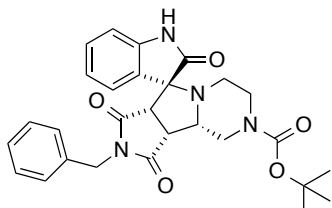


Using the general procedure for the synthesis of pyrrolidines outlined above, 1-benzylindoline-2,3-dione (0.30 g, 1.3 mmol, 1.0 equiv) was used and the product was purified by flash chromatography with EtOAc/hex to afford the pyrrolidine **2.18**

as a white solid (0.39 mg, 0.66 mmol, 56%). $R_f = 0.8$ (1:1 EtOAc/hex); mp 191-192; 1H NMR (600 MHz, DMSO- d_6) δ 7.38-7.37 (m, 4H), 7.36-7.32 (m, 5H), 7.31-7.27 (m, 1H), 7.22-7.20 (m, 1H), 6.87 (d, $J = 7.8$ Hz, 1H), 6.82-6.79 (m, 1H), 6.50 (d, $J = 7.2$ Hz, 1H), 4.87 (s, 2H), 4.65 (AB q, $J = 14.7$ Hz, 2H), 4.36-4.34 (m, 1H), 3.85-3.83 (m, 1H), 3.79-3.76 (m, 1H), 3.72-3.71 (m, 1H), 3.49 (d, $J = 7.8$ Hz, 1H), 2.68-2.64 (m, 1H), 2.51-2.53 (m, 1H), 2.12-2.09 (m, 1H), 1.44 (s, 9H); ^{13}C NMR (500 MHz, DMSO- d_6 , 313 K) δ 176.1, 175.8, 174.5, 155.2, 143.7, 136.6, 136.4, 130.1, 129.2, 129.0, 128.2, 128.1, 127.9, 127.7, 126.7, 124.2, 122.7, 109.7, 79.7, 71.7, 58.2, 50.8, 46.3, 45.5, 43.1, 42.2, 28.5; IR (thin film) 3850, 3626, 2971, 2862, 1707, 1693, 1678, 1032; HRMS (ESI): m/z calculated for $C_{35}H_{36}N_4O_5Na$ $[M+Na]^+$ 615.2584, found 615.2572. HPLC purity: 100%.

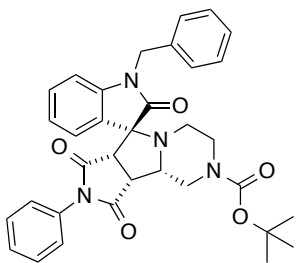
(±)-*tert*-Butyl (3*R*,3*a'R*,3*b'**S*,9*a'**S*)-2'-benzyl-1',2,3'-trioxo-2',3',3*a'*,3*b'*,4',6',7',9*a'*-octahydrospiro[indoline-3,9'-pyrrolo[3',4':3,4]pyrrolo[1,2-*a*]pyrazine]-5'(1'*H*)-carboxylate, 2.19.**

Using the general procedure for the synthesis of pyrrolidines outlined above, indoline-2,3-dione (0.37 g, 2.5 mmol, 1.0 equiv) was used and the product was purified by flash chromatography with EtOAc/hex to afford the pyrrolidine **2.19** as a white solid (0.66 mg, 1.3



mmol, 53%). $R_f = 0.45$ (1:1 EtOAc/hex); mp 207-208; $^1\text{H NMR}$ (600 MHz, CDCl_3) δ 7.46-7.43 (m, 3H), 7.36-7.35 (m, 3H), 7.23-7.20 (m, 1H), 6.83-6.81 (m, 1H), 6.77 (d, $J = 7.7$ Hz, 1H), 6.32 (d, $J = 6.8$ Hz, 1H), 4.80 (d, $J = 14.1$ Hz, 1H), 4.63 (d, $J = 14.1$ Hz, 1H), 4.22-4.12 (m, 1H), 3.80-3.78 (m, 1H), 3.60-3.58 (m, 1H), 3.41 (d, $J = 7.9$ Hz, 1H), 2.79-2.45 (m, 2H), 2.27-2.18 (m, 2H), 1.46 (s, 9H); $^{13}\text{C NMR}$ (500 MHz, $\text{DMSO-}d_6$, 310 K) δ 180.4, 175.8, 174.7, 156.1, 140.5, 135.8, 129.7, 129.2, 128.9, 128.8, 128.2, 126.5, 122.6, 109.9, 68.1, 58.3, 51.6, 48.1, 42.6, 40.1, 31.1, 30.0, 28.5, 24.6; IR (thin film) 3679, 2971, 2864, 1706, 1642, 1054, 1032, 1012; HRMS (ESI): m/z calculated for $\text{C}_{28}\text{H}_{30}\text{N}_4\text{O}_5\text{Na}$ $[\text{M}+\text{Na}]^+$ 525.2114, found 525.2106. HPLC purity: 100%.

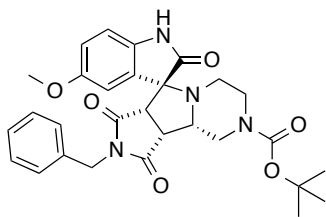
(±)-*tert*-Butyl (3*R*,3*a'R*,3*b'**S*,9*a'**S*)-2'-benzyl-1',2,3'-trioxo-2',3',3*a'*,3*b'*,4',6',7',9*a'*-octahydrospiro[indoline-3,9'-pyrrolo[3',4':3,4]pyrrolo[1,2-*a*]pyrazine]-5'(1'*H*)-carboxylate, 2.20.**



Using the general procedure for the synthesis of pyrrolidines outlined above, 1-benzylindoline-2,3-dione (0.30 g, 1.3 mmol, 1.0 equiv) was used and the product was purified by flash chromatography with EtOAc/hex to afford the pyrrolidine **2.20** as a yellow solid (0.43 mg, 0.75 mmol, 71%). $R_f = 0.75$ (1:1 EtOAc/hex); mp 210-212; $^1\text{H NMR}$ (600 MHz, $\text{DMSO-}d_6$, 400 K) δ 7.54-7.51 (m, 2H), 7.46-7.44 (m, 1H), 7.35-7.34 (m, 6H), 7.29-7.26 (m, 2H), 7.03-7.02 (m, 2H), 6.92 (d, $J = 8.4$ Hz, 1H), 4.91 (s, 2H), 4.40-4.38 (m, 1H), 3.92-3.89 (m, 2H), 3.81-3.77 (m, 1H), 3.61 (d, $J = 7.8$ Hz, 1H), 2.84-2.77 (m, 1H), 2.68-2.63 (m, 1H), 2.24-2.16 (m, 2H), 1.45 (s, 9H); $^{13}\text{C NMR}$ (500 MHz, $\text{DMSO-}d_6$, 310 K) δ 176.7, 175.7, 174.3, 155.2, 144.2, 137.1, 133.1, 130.7, 130.0, 129.7, 129.5, 128.4, 128.1, 127.9, 126.9, 124.8, 123.4, 110.2, 80.1, 72.4, 58.8, 51.7, 47.0, 46.8, 43.6, 28.9; IR (thin film) 3850,

3671, 2972, 2843, 1712, 1690, 1135, 1032; HRMS (ESI): m/z calculated for $C_{34}H_{34}N_4O_5Na$ $[M+Na]^+$ 601.2427, found 601.2415. HPLC purity: 100%.

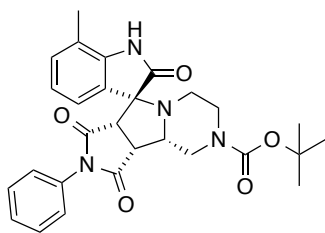
(±)-*tert*-Butyl (3*R*,3*a*'*R*,3*b*'*S*,9*a*'*S*)-2'-benzyl-5-methoxy-1',2,3'-trioxo-2',3',3*a*',3*b*',4',6',7',9*a*'-octahydrospiro[indoline-3,9'-pyrrolo[3',4':3,4]pyrrolo[1,2-*a*]pyrazine]-5'(1'*H*)-carboxylate, 2.21.



Using the general procedure for the synthesis of pyrrolidines outlined above, indoline-2,3-dione (0.45 g, 2.5 mmol, 1.0 equiv) was used and the product was purified by flash chromatography with EtOAc/hex to afford the pyrrolidine **2.21** as a white solid (0.66 mg, 1.3 mmol, 53%). $R_f = 0.35$ (1:1 EtOAc/hex); mp 218-220; 1H NMR (600 MHz, DMSO- d_6) δ 10.43 (s, 1H), 7.38-7.36 (m, 2H), 7.33-7.32 (m, 2H), 7.29-7.27 (m, 1H), 6.77 (dd, $J = 8.7, 2.1$ Hz, 1H), 6.73-6.71 (m, 1H), 6.07 (s, 1H), 4.64 (AB q, $J = 15$ Hz, 2H), 4.31 (br s, 1H), 3.87-3.83 (m, 1H), 3.75-3.73 (m, 1H), 3.68-3.64 (m, 1H), 3.45 (d, $J = 7.8$ Hz, 1H), 2.61-2.59 (m, 2H), 2.18-2.16 (m, 1H), 2.04 (td, $J = 11.2, 3.0$ Hz, 1H), 1.40 (s, 9H); ^{13}C NMR (500 MHz, DMSO- d_6 , 310 K) δ 177.7, 176.1, 174.7, 154.9, 153.8, 136.4, 129.1, 127.9, 127.5, 126.0, 115.4, 113.4, 110.5, 79.7, 72.3, 61.2, 57.9, 55.5, 50.6, 46.3, 45.2, 42.0, 28.5; IR (thin film) 3850, 3648, 2967, 1710, 1641, 1130, 1032; HRMS (ESI): m/z calculated for $C_{28}H_{30}N_4O_5Na$ $[M+Na]^+$ 555.2222, found 555.2239. HPLC purity: 96.22%.

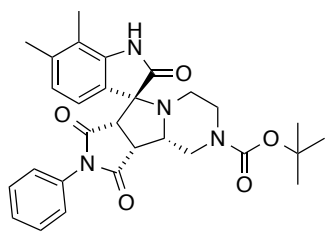
(±)-*tert*-Butyl (3*R*,3*a*'*R*,3*b*'*S*,9*a*'*S*)-7-methyl-1',2,3'-trioxo-2'-phenyl-2',3',3*a*',3*b*',4',6',7',9*a*'-octahydrospiro[indoline-3,9'-pyrrolo[3',4':3,4]pyrrolo[1,2-*a*]pyrazine]-5'(1'*H*)-carboxylate, 2.22.

Using the general procedure for the synthesis of pyrrolidines outlined above, 7-methylindoline-2,3-dione (1.0 g, 6.2 mmol, 1.0 equiv) was used and the product was purified by flash chromatography with EtOAc/hex to afford the pyrrolidine **2.22** as a white solid (2.0 g, 4.0 mmol, 60%). $R_f = 0.3$ (1:1 EtOAc/hex); mp 212-214; 1H NMR (600 MHz, DMSO- d_6 , 398 K) δ



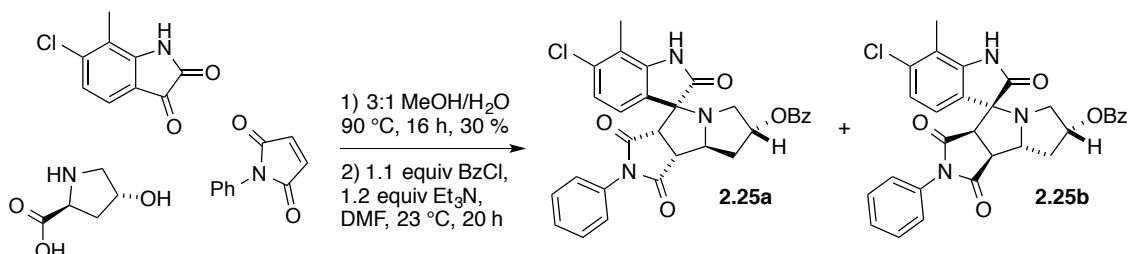
10.1 (s, 1H), 7.53-7.51 (m, 2H), 7.45-7.42 (m, 1H), 7.34-7.33 (m, 2H), 7.05 (d, $J = 7.8$ Hz, 1H), 6.88-6.86 (m, 1H), 6.76 (d, $J = 7.2$ Hz, 1H), 4.37-4.35 (m, 1H), 3.87-3.82 (m, 2H), 3.75-3.73 (m, 1H), 3.55-3.54 (m, 1H), 2.79-2.75 (m, 1H), 2.65-2.61 (m, 1H), 2.31-2.22 (m, 4H), 2.21-2.19 (m, 1H), 1.44 (s, 9H); ^{13}C NMR (500 MHz, DMSO- d_6) δ 178.6, 175.5, 174.1, 154.5, 141.8, 132.7, 131.5, 129.6, 129.0, 127.5, 124.8, 123.9, 122.2, 119.5, 79.6, 72.3, 58.1, 50.9, 49.1, 46.7, 28.5, 16.7, 14.6; IR (thin film) 3229, 2973, 2360, 2340, 1714, 1696, 1391; HRMS (ESI): m/z calculated for $\text{C}_{28}\text{H}_{30}\text{N}_4\text{O}_5\text{Na}$ $[\text{M}+\text{Na}]^+$ 525.2114, found 525.2108. HPLC purity: 99.18%.

(\pm)-*tert*-Butyl (3*R*,3*a'R*,3*b'**S*,9*a'**S*)-6,7-dimethyl-1',2,3'-trioxo-2'-phenyl-2',3',3*a'*,3*b'*,4',6',7',9*a'*-octahydrospiro[indoline-3,9'-pyrrolo[3',4':3,4]pyrrolo[1,2-*a*]pyrazine]-5'(1'*H*)-carboxylate, **2.23**.**



Using the general procedure for the synthesis of pyrrolidines outlined above, 6,7-dimethylindoline-2,3-dione (0.38 g, 2.2 mmol, 1.0 equiv) was used and the product was purified by flash chromatography with EtOAc/hex to afford the pyrrolidine **2.23** as a white solid (0.60 g, 1.20 mmol, 61%). $R_f = 0.3$ (1:1 EtOAc/hex); mp 215-218; ^1H NMR (500 MHz, DMSO- d_6) δ 10.6 (s, 1H), 7.53-7.52 (m, 2H), 7.50-7.44 (m, 1H), 7.29-7.28 (m, 2H), 6.77 (d, $J = 7.5$ Hz, 1H), 6.60 (d, $J = 7.5$ Hz, 1H), 4.29 (br s, 1H), 3.82-3.79 (m, 2H), 3.64-3.65 (m, 1H), 3.47-3.46 (m, 1H), 2.62 (br s, 2H), 2.19-2.17 (m, 4H), 2.09-2.07 (m, 4H), 1.39 (s, 9H); ^{13}C NMR (500 MHz, DMSO- d_6 , 320 K) δ 178.8, 175.5, 174.1, 141.8, 138.7, 132.7, 129.6, 129.0, 127.4, 123.6, 123.5, 122.4, 118.2, 79.6, 72.4, 58.1, 50.9, 46.7, 28.5, 20.1, 13.5; IR (thin film) 3739, 3244, 2976, 1712, 1696, 1417, 1390; HRMS (ESI): m/z calculated for $\text{C}_{29}\text{H}_{32}\text{N}_4\text{O}_5\text{Na}$ $[\text{M}+\text{Na}]^+$ 539.2271, found 539.2268. HPLC purity: 98.24%.

Synthesis of (3*S*,3*a'S*,7*R*,8*a'**S*,8*b'**R*)-6-chloro-7-methyl-1',2,3'-trioxo-2'-phenyl-2',3',3*a'*,6',7',8',8*a'*,8*b'*-octahydro-1'H-spiro[indoline-3,4'-pyrrolo[3,4-*a*]pyrrolizin]-7'-yl benzoate, 2.25a and (3*R*,3*a'**R*,7*R*,8*a'**R*,8*b'**S*)-6-chloro-7-methyl-1',2,3'-trioxo-2'-phenyl-2',3',3*a'*,6',7',8',8*a'*,8*b'*-octahydro-1'H-spiro[indoline-3,4'-pyrrolo[3,4-*a*]pyrrolizin]-7'-yl benzoate, 2.25b.**



Using the general procedure for the synthesis of pyrrolidines outlined above, 6-chloro-7-methylindoline-2,3-dione (0.50 g, 2.6 mmol, 1.0 equiv) was used. The resulting crude reaction mixture was dissolved in cold DCM and the products precipitated as a yellow solid. Then the solid was collected by vacuum filtration and washed with cold DCM until the solid became white. The pyrrolidine products were collected as a mixture of two diastereomers. The resulting products were highly insoluble in most of the organic solvents and this made it very hard to separate the two diastereomers by flash column chromatography.

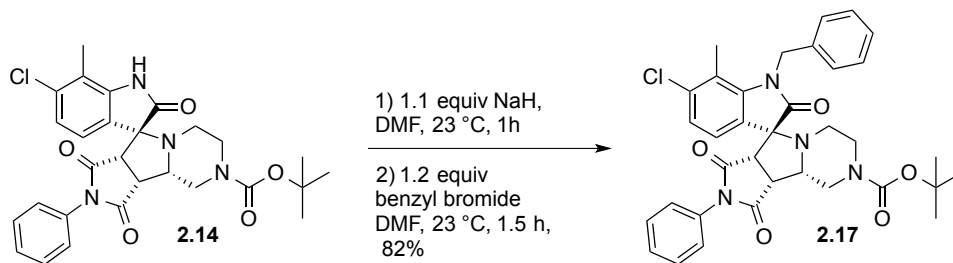
The mixture of two stereoisomers (0.030 g, 0.07 mmol, 1 equiv) from the above procedure was added to a 5 mL oven-dried round-bottom flask. The flask was fitted with a septum and purged with nitrogen. Next, 1.4 mL of DMF was added to the reaction flask such that the concentration of the mixture of two diastereomers was 0.05 M. Next, benzoyl chloride (9.0 mL, 0.075 mmol, 1.1 equiv) and triethylamine (0.01 mL, 0.08 mmol, 1.2 equiv) was added to the reaction flask and the reaction was allowed to stir at room temperature until the consumption of the alcohols as confirmed by TLC (9:1 DCM/MeOH).

Upon consumption of the alcohols, the reaction mixture was concentrated under vacuum to give a yellow solid. The solid was then purified by flash chromatography with DCM/Et₂O (20:1) to afford esters **2.25a** and **2.25b**.

The first stereoisomer **2.25a** (0.012 g, 0.02 mmol, 65%) was isolated as a white solid. R_f = 0.55 (20:1 DCM/Et₂O); mp 236-239; ¹H NMR (600 MHz, Acetone-*d*₆) δ 9.67 (s, 1H), 7.97 (dd, J = 8.4, 1.2 Hz, 2H), 7.61-7.58 (m, 1H), 7.51 (d, J = 7.8 Hz, 1H), 7.48-7.37 (m, 5H), 7.28 (d, J = 7.8 Hz, 2H), 7.16 (d, J = 7.8 Hz, 1H), 5.63-5.61 (m, 1H), 4.71-4.69 (m, 1H), 4.35 (d, J = 9.6 Hz, 1H), 3.82 (dd, J = 10.2, 6.6 Hz, 1H), 3.52 (dd, J = 11.1, 5.1 Hz, 1H), 3.01 (d, J = 10.8 Hz, 1H), 2.76-2.72 (m, 1H), 2.56-2.52 (m, 1H), 2.33 (s, 3H); ¹³C NMR (500 MHz, Acetone-*d*₆) δ 177.4, 176.6, 174.9, 165.6, 135.6, 133.0, 130.2, 129.3, 128.6, 128.4, 128.1, 127.2, 125.6, 124.4, 122.4, 118.1, 74.7, 65.1, 55.3, 53.4, 53.1, 37.7, 13.3; IR (thin film) 3685, 2978, 2851, 1721, 1054, 1032, 1012; HRMS (ESI): m/z calculated for C₃₀H₂₄ClN₃O₅Na [M+Na]⁺ 564.1302, found 564.1302. HPLC purity: 96.63%.

The second stereoisomer **2.25b** (0.015 g, 0.03 mmol, 81%) was also isolated as a white solid. R_f = 0.48 (20:1 DCM/Et₂O); mp 221-224; ¹H NMR (600 MHz, Acetone-*d*₆) δ 9.69 (s, 1H), 8.09 (dd, J = 8.4, 1.2 Hz, 2H), 7.67 (t, J = 7.5 Hz, 1H), 7.54 (t, J = 7.8 Hz, 1H), 7.48-7.37 (m, 3H), 7.28 (d, J = 7.8 Hz, 2H), 7.13 (d, J = 8.4 Hz, 1H), 5.44-5.42 (m, 1H), 4.55-4.52 (m, 1H), 4.39 (d, J = 10.2 Hz, 1H), 4.00 (dd, J = 9.9, 6.9 Hz, 1H), 3.38 (dd, J = 10.2, 6.0 Hz, 1H), 3.28 (dd, J = 9.9, 6.3 Hz, 1H), 2.83-2.78 (m, 1H), 2.39-2.36 (m, 1H), 2.35 (s, 3H); ¹³C NMR (500 MHz, Acetone-*d*₆) δ 177.4, 176.5, 174.8, 165.6, 135.6, 133.3, 133.0, 130.1, 129.5, 128.6, 128.2, 127.3, 125.5, 125.2, 124.6, 122.4, 74.7, 64.9, 54.4, 53.5, 53.3, 36.6, 13.3; IR (thin film) 3686, 2980, 2481, 1720, 1050, 1030, 1014; HRMS (ESI): m/z calculated for C₃₀H₂₄ClN₃O₅Na [M+Na]⁺ 564.1302, found 564.1305. HPLC purity: 95.36%.

Synthesis of (\pm)-*tert*-butyl (3*R*,3*a*'*R*,3*b*'*S*,9*a*'*S*)-1-benzyl-6-chloro-7-methyl-1',2,3'-trioxo-2'-phenyl-2',3',3*a*',3*b*',4',6',7',9*a*'-octahydrospiro[indoline-3,9'-pyrrolo[3',4':3,4]pyrrolo[1,2-*a*]pyrazine]-5'(1'*H*)-carboxylate, **2.17.⁹⁸**

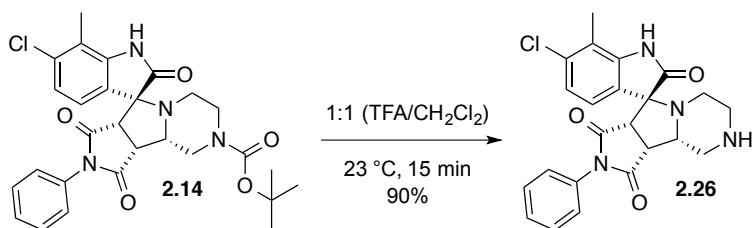


A 5 mL oven-dried round-bottom flask was charged with sodium hydride (60 wt % in mineral oil, 0.01 g, 0.37 mmol, 1.1 equiv) and the mineral oil dispersed in sodium hydride was removed by washing with hexanes (3 \times 2 mL). The resulting white solid of sodium hydride was suspended in 0.2 mL of DMF. The suspension was cooled to 0 °C in an ice bath, after which pyrrolidines **2.14** (0.18 g, 0.34 mmol, 1.0 equiv) was added as a solid over the course of 15 min. After the addition was complete the ice bath was removed and the solution was stirred for 1 h at room temperature. Next, benzyl bromide (48 mL, 0.40 mmol, 1.2 equiv) was added to the reaction flask and the reaction was allowed to stir at room temperature until the consumption of **2.15** confirmed by TLC (2:3 EtOAc/hex).

Upon consumption of the **2.14**, the reaction mixture was concentrated under vacuum to give a yellow solid. The solid was then purified by flash chromatography with EtOAc/hex (4:1) to afford the pyrrolidine **2.17**, a white solid (0.17 g, 0.27 mmol, 82%). R_f = 0.65 (2:3 EtOAc/hex); mp 145-154; ^1H NMR (600 MHz, DMSO- d_6 , 400 K) δ 7.51-7.48 (m, 2H), 7.42-7.41 (m, 1H), 7.34-7.31 (m, 4H), 7.26-7.24 (m, 1H), 7.18-7.17 (m, 2H), 7.13 (d, J = 8.1 Hz, 1H), 6.86 (d, J = 8.1 Hz, 1H), 5.21-5.16 (m, 2H), 4.37-4.35 (m, 1H), 3.87-3.86 (m, 2H), 3.74-3.72 (m, 1H), 3.60 (d, J = 8.1 Hz, 1H), 2.80-2.78 (m, 1H), 2.67-2.65 (m, 1H), 2.34-2.32 (m, 1H), 2.27 (s, 3H), 2.19-2.17 (m, 1H), 1.42 (s, 9H); ^{13}C NMR (500 MHz, DMSO- d_6 , 310 K) δ 177.6, 175.2, 173.8, 154.2, 143.4, 137.8, 136.6, 132.6, 129.6, 129.5, 129.0, 127.7, 127.5, 125.8, 125.1, 124.5,

124.0, 118.6, 79.7, 71.0, 63.9, 58.6, 51.9, 46.5, 45.8, 45.1, 30.7, 28.5, 14.7; IR (thin film) 3680, 2971, 2843, 1713, 1054, 1032, 1012; HRMS (ESI): m/z calculated for $C_{35}H_{35}ClN_4O_5Na$ $[M+Na]^+$ 649.2194, found 649.2194. HPLC purity: 100%.

Synthesis of (\pm)-(3*R*,3*a'R*,3*b'**S*,9*a'**S*)-6-chloro-7-methyl-2'-phenyl-3*a'*,4',5',6',7',9*a'*-hexahydrospiro[indoline-3,9'-pyrrolo[3',4':3,4]pyrrolo[1,2-*a*]pyrazine]-1',2,3'(2'*H*,3*b'**H*)-trione, **2.26**.⁹⁹**

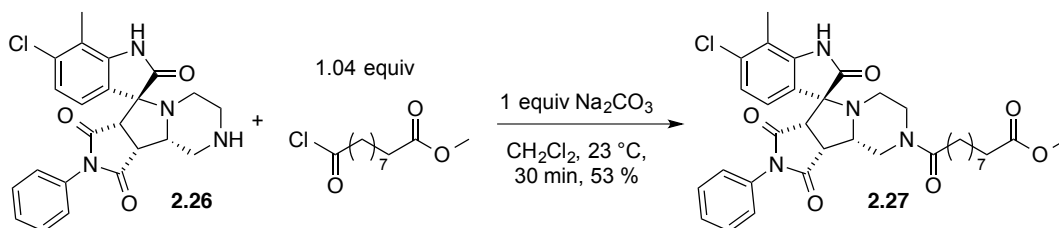


A 10 mL round bottom flask was charged with pyrrolidine **2.14** (0.57 g, 1.1 mmol, 1 equiv) and a stir bar. The flask was fitted with a septum and purged with nitrogen. Next, 3.1 mL CH₂Cl₂ was added to the reaction flask such that the concentration of **2.14** was 0.34 M and stirred for 10 min. A pink color solution resulted. Then 3.1 mL trifluoroacetic acid was slowly added to the reaction mixture by syringe. A dark brown color solution resulted. The deprotection reaction was stirred until TLC indicated complete consumption of the pyrrolidine **2.14**, 15 min.

Upon consumption of the **2.14**, the reaction mixture was concentrated under vacuum to give a brown oil. 5 mL of saturated aqueous NaHCO₃ was added to the oil and the aqueous layer was then extracted with (3 × 5 mL) CH₂Cl₂. The combined organic layers were then washed with brine and dried over Na₂SO₄. The resulting organic solution was concentrated under vacuum to afford **2.26**, a pink solid, (0.42 g, 0.96 mmol, 87%). $R_f = 0.81$ (20:80:5 EtOAc/hex/Et₃N); mp 196-200; ¹H NMR (600 MHz, DMSO-*d*₆) δ 10.89 (s, 1H), 7.58-7.53 (m, 2H), 7.47-7.45 (m, 1H), 7.30 (d, $J = 7.4$ Hz, 2H), 7.06 (d, $J = 8.0$ Hz, 1H), 6.71 (d, $J = 8.0$ Hz, 1H), 3.77-3.76 (m, 2H), 3.51-3.50 (m, 1H), 3.42 (br s, 1H), 3.30 (d, $J = 11.9$ Hz, 1H), 2.79 (app d, $J = 12.1$ Hz, 1H),

2.43-2.41 (m, 1H), 2.25 (s, 3H), 2.24-2.21 (m, 2H); ^{13}C NMR (500 MHz, CDCl_3 , 310 K) δ 178.8, 175.5, 174.2, 143.4, 134.9, 132.7, 129.6, 128.9, 127.4, 125.2, 124.1, 122.5, 117.7, 72.6, 58.7, 50.7, 48.7, 47.1, 46.7, 44.9, 14.3; IR (thin film) 3850, 3671, 2971, 2864, 1709, 1054, 1032, 1013; HRMS (ESI): m/z calculated for $\text{C}_{23}\text{H}_{21}\text{ClN}_4\text{O}_3\text{Na}$ $[\text{M}+\text{Na}]^+$ 459.1200, found 459.1190. HPLC purity: 100%.

Synthesis of (\pm)-methyl 10-((3*R*,3*a'R*,3*b'**S*,9*a'**S*)-6-chloro-7-methyl-1',2,3'-trioxo-2'-phenyl-2',3',3*a'*,3*b'*,4',6',7',9*a'*-octahydrospiro[indoline-3,9'-pyrrolo[3',4':3,4]pyrrolo[1,2-*a*]pyrazin]-5'(1'*H*)-yl)-10-oxodecanoate, **2.27**.¹⁰⁰**

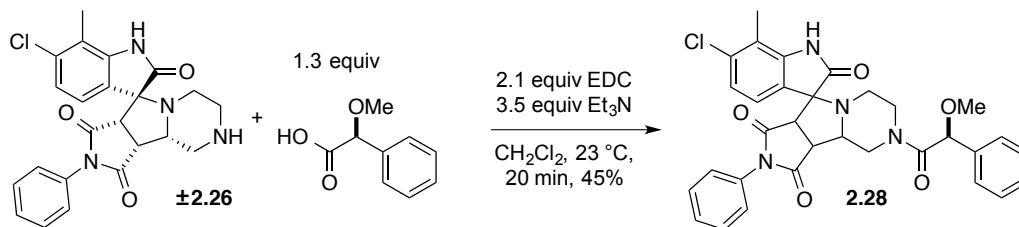


A 15 mL round bottom flask was charged with pyrrolidine **2.26** (0.13 g, 0.30 mmol, 1 equiv), Na_2CO_3 (0.03 g, 0.30 mmol, 1.0 equiv) and a stir bar. The flask was fitted with a septum and purged with nitrogen. Then 6 mL of CH_2Cl_2 was added to the reaction flask such that the concentration of **2.26** was 0.05 M. Next, methyl 10-chloro-10-oxodecanoate (0.07 mL, 0.31 mmol, 1.04 equiv) was added drop-wise to the reaction mixture by syringe. The reaction was allowed to stir at room temperature until the consumption of **2.26** confirmed by TLC (20:80:5 EtOAc/hex/ Et_3N).

Upon consumption of **2.26**, the reaction mixture was concentrated under vacuum to give a yellow oil. The oil was then purified by flash chromatography with EtOAc/hex/ Et_3N (80:20:5) to afford the pyrrolidine **2.27**, a yellow solid, (0.10 g, 0.16 mmol, 53%). $R_f = 0.75$ (20:80:5 EtOAc/hex/ Et_3N); mp 110-115; ^1H NMR (600 MHz, $\text{DMSO}-d_6$, 400 K) δ 10.42 (s, 1H), 7.53-7.51 (m, 2H), 7.45-7.43 (m, 1H), 7.33 (d, $J = 7.8$ Hz, 2H), 7.03 (d, $J = 8.4$ Hz, 1H), 6.78 (d, $J =$

7.8 Hz, 1H), 4.58 (br s, 1H), 4.08 (br s, 1H), 3.86 (t, $J = 7.8$ Hz, 1H), 3.73-3.72 (m, 1H), 3.61-3.58 (m, 4H), 2.61-2.82 (m, 4H), 2.34-2.27 (m, 5H), 2.22-2.18 (m, 1H), 1.59-1.53 (m, 4H), 1.22-1.42 (m, 9H); ^{13}C NMR (500 MHz, CDCl_3 , 313 K) δ 178.2, 174.6, 174.3, 172.2, 171.7, 141.8, 136.6, 131.7, 129.4, 128.9, 126.3, 124.4, 123.5, 122.3, 118.7, 72.7, 58.7, 51.4, 50.4, 48.7, 46.2, 45.3, 44.5, 41.1, 34.1, 33.4, 29.7, 29.3, 29.2, 25.3, 24.9, 13.6; IR (thin film) 3817, 3671, 2921, 2863, 1710, 1617, 1054, 1032; HRMS (ESI): m/z calculated for $\text{C}_{34}\text{H}_{39}\text{ClN}_4\text{O}_6\text{Na}$ $[\text{M}+\text{Na}]^+$ 657.2456, found 657.2435. HPLC purity: 97.45%.

Synthesis of (\pm)-(3*R*,3*a'R*,3*b'**S*,9*a'**S*)-6-chloro-5'-((*S*)-2-methoxy-2-phenylacetyl)-7-methyl-2'-phenyl-3*a'*,4',5',6',7',9*a'*-hexahydrospiro[indoline-3,9'-pyrrolo[3',4':3,4]pyrrolo[1,2-*a*]pyrazine]-1',2,3'(2'*H*,3*b'**H*)-trione, **2.28**.¹⁰¹**

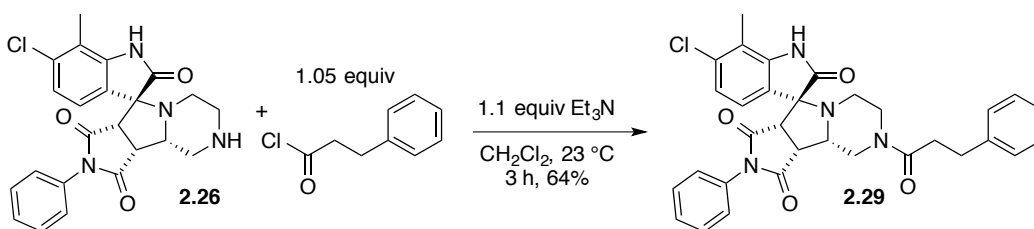


A 15 mL round bottom flask was charged with pyrrolidine **2.26** (0.20 g, 0.46 mmol, 1.0 equiv), (*S*)-2-methoxy-2-phenylacetic acid (0.10 g, 0.60 mmol, 1.3 equiv), *N*-(3-dimethylaminopropyl)-*N'*-ethylcarbodiimide hydrochloride (0.18 g, 0.96 mmol, 2.1 equiv) and a stir bar. The flask was fitted with a septum and purged with nitrogen. Then 6 mL of CH_2Cl_2 was added to the reaction flask such that the concentration of **2.26** was 0.07 M. Next triethylamine (0.22 mL, 1.6 mmol, 3.5 equiv) was added to the reaction mixture and the reaction was allowed to stir at room temperature until the consumption of **2.26** confirmed by TLC (20:80:5 EtOAc/hex/ Et_3N).

Upon consumption of the **2.26**, the reaction mixture was quenched with 5 mL of 1 N aq. HCl and the aqueous layer was then extracted with (3×5 mL) CH_2Cl_2 . The combined organic

layers were then washed with brine and dried over Na₂SO₄. The resulting organic solution was concentrated under vacuum to give a yellow oil. The oil was then purified by flash chromatography with EtOAc/hex/Et₃N (80:20:5) to afford the pyrrolidine **2.28**, a white solid, (0.12 g, 0.21 mmol, 45%). *R_f* = 0.65 (1:1 EtOAc/hex); ¹H NMR (600 MHz, DMSO-*d*₆, 400 K) δ 10.42 (s, 1H), 7.51-7.49 (m, 2H), 7.44-7.41 (m, 1H), 7.39-7.35 (m, 4H), 7.32-7.31 (m, 3H), 7.01 (d, *J* = 8.0 Hz, 1H), 6.74 (d, *J* = 8.0 Hz, 1H), 5.17-5.16 (m, 1H), 4.71-4.70 (m, 1H), 4.19-4.17 (m, 1H), 3.79-3.75 (m, 1H), 3.64-3.60 (m, 1H), 3.54 (app dd, *J* = 8.0, 2.9 Hz, 1H), 3.39-3.37 (m, 3H), 2.73-2.64 (m, 2H), 2.27-2.22 (m, 4H), 2.07-2.05 (m, 1H); ¹³C NMR (500 MHz, DMSO-*d*₆, 310 K) (2 rotamers observed) δ 178.5, 175.3, 173.9, 154.9, 137.4, 135.2, 132.6, 129.5, 129.0, 128.9, 128.6, 127.6, 127.5, 127.3, 125.2, 123.6, 122.6, 117.8, 81.8, 81.0, 72.1, 68.9, 63.9, 58.6, 58.2, 57.3, 56.3, 50.9, 46.5, 45.3, 44.5, 41.7, 32.5, 30.6, 30.1, 21.8, 19.0, 17.1; IR (thin film) 3850, 3708, 2971, 2921, 1712, 1643, 1054, 1032, 1012; HRMS (ESI): *m/z* calculated for C₃₂H₂₉ClN₄O₅Na [M+Na]⁺ 607.1724, found 607.1736. HPLC purity: 97.04%.

Synthesis of (±)-(3*R*,3*a'R*,3*b'**S*,9*a'**S*)-6-chloro-7-methyl-2'-phenyl-5'-(3-phenylpropanoyl)-3*a'*,4',5',6',7',9*a'*-hexahydrospiro[indoline-3,9'-pyrrolo[3',4':3,4]pyrrolo[1,2-*a*]pyrazine]-1',2,3'(2'*H*,3*b'**H*)-trione, **2.29**.**

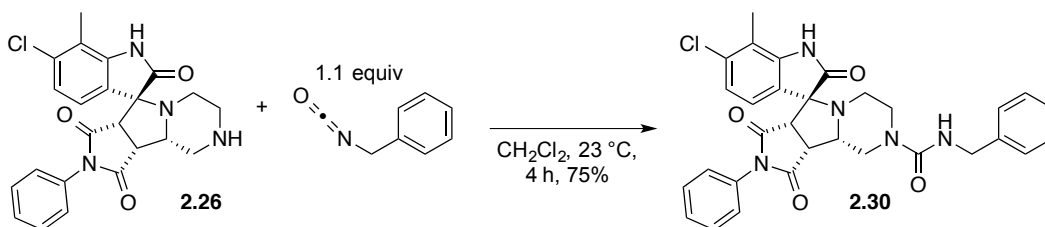


A 10 mL round bottom flask was charged with pyrrolidine **2.26** (0.05 g, 0.11 mmol, 1.0 equiv), triethylamine (18.0 mL, 0.13 mmol, 1.1 equiv) and a stir bar. The flask was fitted with a septum and purged with nitrogen. Then 2.0 mL of CH₂Cl₂ was added to the round bottom flask by syringe. Then hydrocinnamoyl chloride (18.0 mL, 0.12 mmol, 1.05 equiv) was added to the

reaction flask with a syringe. The reaction mixture was allowed to stir for 3 h at room temperature. The reaction was monitored for consumption of **2.26** by TLC (100:5 EtOAc/Et₃N).

Upon consumption of **2.26**, the reaction mixture was quenched with 5 mL of saturated aqueous NaHCO₃ and the aqueous layer was then extracted with (3 × 5 mL) CH₂Cl₂. The combined organic layers were then washed with brine and dried over Na₂SO₄. The resulting organic solution was concentrated under vacuum to give a yellow oil. The oil was then purified by flash chromatography with EtOAc/hex/Et₃N (60:40:5) to afford the pyrrolidine **2.29**, a white solid, (0.04 g, 0.07 mmol, 64%). R_f = 0.2 (60:40:5 EtOAc/hex/ Et₃N); mp 236-239; ¹H NMR (600 MHz, DMSO-*d*₆, 400 K) δ 10.40 (s, 1H), 7.53-7.51 (m, 2H), 7.45-7.42 (m, 1H), 7.34-7.33 (m, 2H), 7.27-7.23 (m, 4H), 7.17-7.15 (m, 1H), 7.03 (d, *J* = 7.8 Hz, 1H), 6.78 (d, *J* = 8.4 Hz, 1H), 4.59 (s, 1H), 7.09-7.06 (m, 1H), 3.87-3.84 (m, 1H), 3.73-3.69 (m, 1H), 3.59-3.57 (m, 1H), 2.90-2.88 (m, 2H), 2.84-2.82 (m, 2H), 2.78-2.74 (m, 2H), 2.31-2.28 (m, 4H), 2.19-2.15 (m, 1H); ¹³C NMR (500 MHz, DMSO-*d*₆, 310 K) δ 178.6, 178.5, 175.4, 175.3, 174.0, 170.6, 143.4, 141.9, 135.2, 132.7, 129.6, 129.0, 128.8, 128.7, 127.5, 126.3, 125.2, 123.9, 122.6, 117.9, 72.2, 60.2, 58.9, 51.2, 48.5, 45.5, 44.9, 34.5, 31.2, 14.3; IR (thin film) 3423, 2917, 1708, 1633, 1620, 1384, 1204; HRMS (ESI): *m/z* calculated for C₃₂H₂₉ClN₄O₄Na [M+Na]⁺ 591.1775, found 591.1763. HPLC purity: 98.20%.

Synthesis of (3R,3a'R,3b'S,9a'S)-N-benzyl-6-chloro-7-methyl-1',2,3'-trioxo-2'-phenyl-2',3',3a',3b',4',6',7',9a'-octahydrospiro[indoline-3,9'-pyrrolo[3',4':3,4]pyrrolo[1,2-a]pyrazine]-5'(1'H)-carboxamide, 2.30.



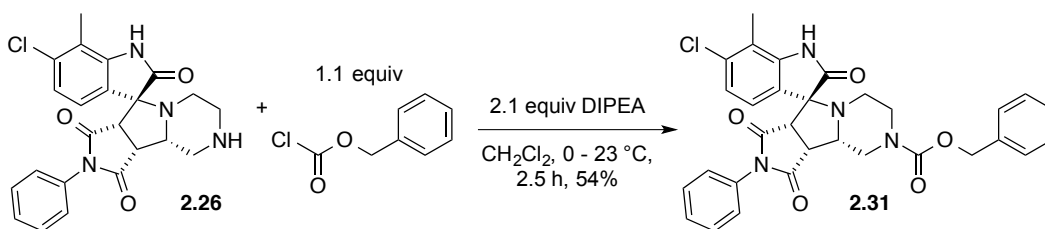
A 10 mL round bottom flask was charged with pyrrolidine **2.26** (0.06 g, 0.15 mmol, 1.0 equiv) and a stir bar. The flask was fitted with a septum and purged with nitrogen. Then 3.0 mL of CH₂Cl₂ was added to the round bottom flask by syringe. Next, (isocyanatomethyl)benzene (0.02 mL, 0.16 mmol, 1.1 equiv) was added to the reaction flask by syringe. Then the reaction mixture was allowed to stir for 4 h at room temperature. The reaction was monitored for consumption of **2.26** by TLC (50:50:5 EtOAc/Hex/Et₃N).

Upon consumption of **2.26**, the resulting organic solution was concentrated under vacuum to give a yellow oil. The oil was then purified by flash chromatography with EtOAc/hex/Et₃N (60:40:5) to afford the pyrrolidine **2.30**, a white solid, (0.63 g, 0.11 mmol, 75%). *R_f* = 0.24 (50:50:5 EtOAc/Hex/Et₃N); mp 258-259; ¹H NMR (600 MHz, DMSO-*d*₆, 400 K) δ 10.44 (s, 1H), 7.53-7.51 (m, 2H), 7.45-7.44 (m, 1H), 7.33-7.32 (m, 2H), 7.29-7.28 (m, 4H), 7.20 (m, 1H), 7.03 (d, *J* = 8.0 Hz, 1H), 6.76 (d, *J* = 8.0 Hz, 1H), 4.47-4.45 (m, 1H), 4.29-4.27 (m, 2H), 3.95 (d, *J* = 14.1 Hz, 1H), 3.82-3.77 (m, 2H), 3.56 (d, *J* = 7.9 Hz, 1H), 2.75-2.71 (m, 1H), 2.64-2.58 (m, 1H), 2.28 (s, 3H), 2.25-2.23 (m, 2H); ¹³C NMR (500 MHz, DMSO-*d*₆) δ 178.7, 175.4, 174.1, 157.6, 143.4, 141.4, 135.1, 132.7, 129.6, 129.1, 128.6, 127.5, 126.9, 125.1, 123.9, 122.6, 117.9, 72.3, 58.3, 51.1, 47.5, 46.7, 45.7, 44.1, 43.6 ; IR (thin film) 3618, 2922, 2360, 2340, 1712, 1616, 1536, 1387; HRMS (ESI): *m/z* calculated for C₃₁H₂₈ClN₅O₄Na [M+Na]⁺ 592.1727, found 592.1724. HPLC purity: 97.18%.

Synthesis of (±)-benzyl (3*R*,3*a'R*,3*b'**S*,9*a'**S*)-6-chloro-7-methyl-1',2,3'-trioxo-2'-phenyl-2',3',3*a'*,3*b'*,4',6',7',9*a'*-octahydrospiro[indoline-3,9'-pyrrolo[3',4':3,4]pyrrolo[1,2-*a*]pyrazine]-5'(1'*H*)-carboxylate, **2.31**.¹⁰²**

A 5 mL round bottom flask was charged with pyrrolidine **2.26** (0.20 g, 0.45 mmol, 1.0 equiv), *N,N*-Diisopropylethylamine (0.17 mL, 0.96 mmol, 2.1 equiv) and a stir bar. The flask was fitted with a septum and purged with nitrogen. Then 0.92 mL of CH₂Cl₂ was added to the

round bottom flask by syringe. The reaction mixture was cooled to 0 °C with an ice bath. Meanwhile another 5 mL pear-shaped flask was charged with benzyl chloroformate (0.07 mL, 0.50 mmol, 1.1 equiv) and the flask was fitted with a septum and purged with nitrogen. Then 0.34 mL of CH₂Cl₂ was added to the pear shaped vial containing the benzyl chloroformate and stirred for 10 min. Next the contents of the 5 mL pear shaped vial was slowly added to the 5 mL round bottom flask containing **2.26**. Ice bath was removed and the reaction mixture was allowed to stir for 2.5 h at room temperature. The reaction was monitored for consumption of **2.26** by TLC (50:50:5 EtOAc/Hex/Et₃N).



Upon consumption of **2.26**, the reaction mixture was quenched with 5 mL of saturated aqueous NaHCO₃ and the aqueous layer was then extracted with (3 × 5 mL) CH₂Cl₂. The combined organic layers were then washed with brine and dried over Na₂SO₄. The resulting organic solution was concentrated under vacuum to give a yellow oil. The oil was then purified by flash chromatography with EtOAc/hex/Et₃N (60:40:5) to afford the pyrrolidine **2.31**, a white solid, (0.14 g, 0.25 mmol, 54%). R_f = 0.81 (1:1 EtOAc/hex); mp 209-211; ¹H NMR (600 MHz, DMSO-*d*₆, 400 K) δ 10.40 (s, 1H), 7.53-7.51 (m, 2H), 7.45-7.42 (m, 1H), 7.37-7.35 (m, 6H), 7.32-7.31 (m, 1H), 7.03 (d, *J* = 8.0 Hz, 1H), 6.80 (d, *J* = 8.0 Hz, 1H), 5.16 (s, 2H), 4.48 (d, *J* = 12.7 Hz, 1H), 3.99 (d, *J* = 13.1 Hz, 1H), 3.89-3.87 (m, 1H), 3.82-3.79 (m, 1H), 3.61 (d, *J* = 8.0 Hz, 1H), 2.91-2.86 (m, 2H), 2.78-2.75 (m, 1H), 2.34-2.25 (m, 5H); ¹³C NMR (500 MHz, DMSO-*d*₆) δ 178.5, 175.3, 173.9, 154.9, 143.4, 137.3, 135.2, 132.6, 129.5, 129.0, 128.9, 128.3, 128.1, 127.4, 72.3, 66.9, 58.2, 51.0, 47.2, 43.5, 30.9, 21.1, 14.3 ; IR (thin film) 3850, 3678, 3262, 2966,

2864, 1715, 1694, 1032; HRMS (ESI): m/z calculated for $C_{31}H_{27}ClN_4O_5Na$ $[M+Na]^+$ 593.1567, found 593.1584. HPLC purity: 97.60%.

Biological Evaluation

Strains, media, and compounds

The *C. albicans* strain HLY4123 was used as the susceptible laboratory strain for the antifungal evaluation in this study. HLY4123 carries a GFP reporter for ERG3 expression and was constructed by plasmid transformation of the commonly used laboratory *C. albicans* strain CAI4. Selected resistant *C. albicans* strains with different mechanisms of becoming drug resistance were obtained from Dr. David Rogers.⁸⁸ The strains were cultured at 30 °C under constant shaking (200 rpm) in synthetic complete (SC) medium containing 2% glucose. The stock solution of fluconazole (Sigma-Aldrich, USA) was prepared in sterile water (0.1 mg/mL), whereas the other test compounds were prepared in DMSO. The commercial sample sold as CID 6584729 was obtained from Vitas-M (supplier number STK 580951).

Dose-Response Curves for Test Compounds Against *C. albicans* with and without Fluconazole:

C. albicans was grown in SC medium overnight and then diluted to an effective OD₆₀₀ of 0.0625. Serial ten-fold dilutions of the test compounds (0.15-1500 μ M) were prepared in DMSO in 1.5 mL Eppendorf tubes. To each well in columns B-D (triplicate analysis) of a 24-well Falcon plate was added 2.5 μ L of fluconazole solution. To each well in all four columns of the plate was added 1 mL of cells in SC medium such that the column A served as a control to assess the EC₅₀ of the compound in the absence of fluconazole. Then to each well in rows 2-5 was added a solution of the compound in DMSO (2 μ L each) such that the final solution fluconazole in columns 2-4 was 0.25 μ g/mL and the concentration of compound in each row varied from 0.003 μ M to 30 μ M. The plates were incubated in a rotary shaker/incubator at 30 °C

for 16 h. The contents of each well were re-suspended with a micropipettor and a 20 μL aliquot was added to a polystyrene cuvette and diluted with 680 μL of deionized water. The suspension was triturated again immediately before measuring the absorbance at 600 nm (OD600) for cell densities. EC_{50} values were determined by fitting to a standard curve using the Excel-based tool ED50PLUS v1.0 (Mario H. Vargas).

Determination of FIC90s with a Checkerboard Assay:

Checkerboard assays were carried out using four 24-well plates. The results on each plate were normalized by duplication of one row and one column with a row and column on another plate. *C. albicans* was grown in SC medium overnight and then diluted to an effective OD600 of 0.0625. Serial ten-fold dilutions of the test compounds (150 mM) were prepared in DMSO in 1.5 mL Eppendorf tubes. Serial two-fold dilutions of the fluconazole (6.53 μM) were prepared in sterile water in 1.5 mL Eppendorf tubes. To each well was added 2 mL of a stock solution of compound in DMSO and 2.5 μL of a stock solution of fluconazole in water. Concentrations of compound in rows 1-11 varied from 300 μM to 0.0003 nM; the last row 12 contained no compound. Concentrations of fluconazole in each column B-H varied from 0.0625 to 2 μM ; the first column A contained no fluconazole. The plates were incubated in a rotary shaker/incubator at 30 °C for 16 h. The contents of each well was resuspended with a micropipettor and a 20 μL aliquot was added to a polystyrene cuvette and diluted with 680 μL of deionized water. The suspension was triturated again immediately before measuring the absorbance at 600 nm. The MIC90 values were determined as the lowest concentrations of the drugs (alone or in combination) that inhibited fungal growth by 90% compared with that of the drug-free wells.

Molecular Properties

Physicochemical properties were calculated from the SMILES representation of synazo-1 using the Molinspiration Property Calculation Service at www.molinspiration.com.

Chapter 3

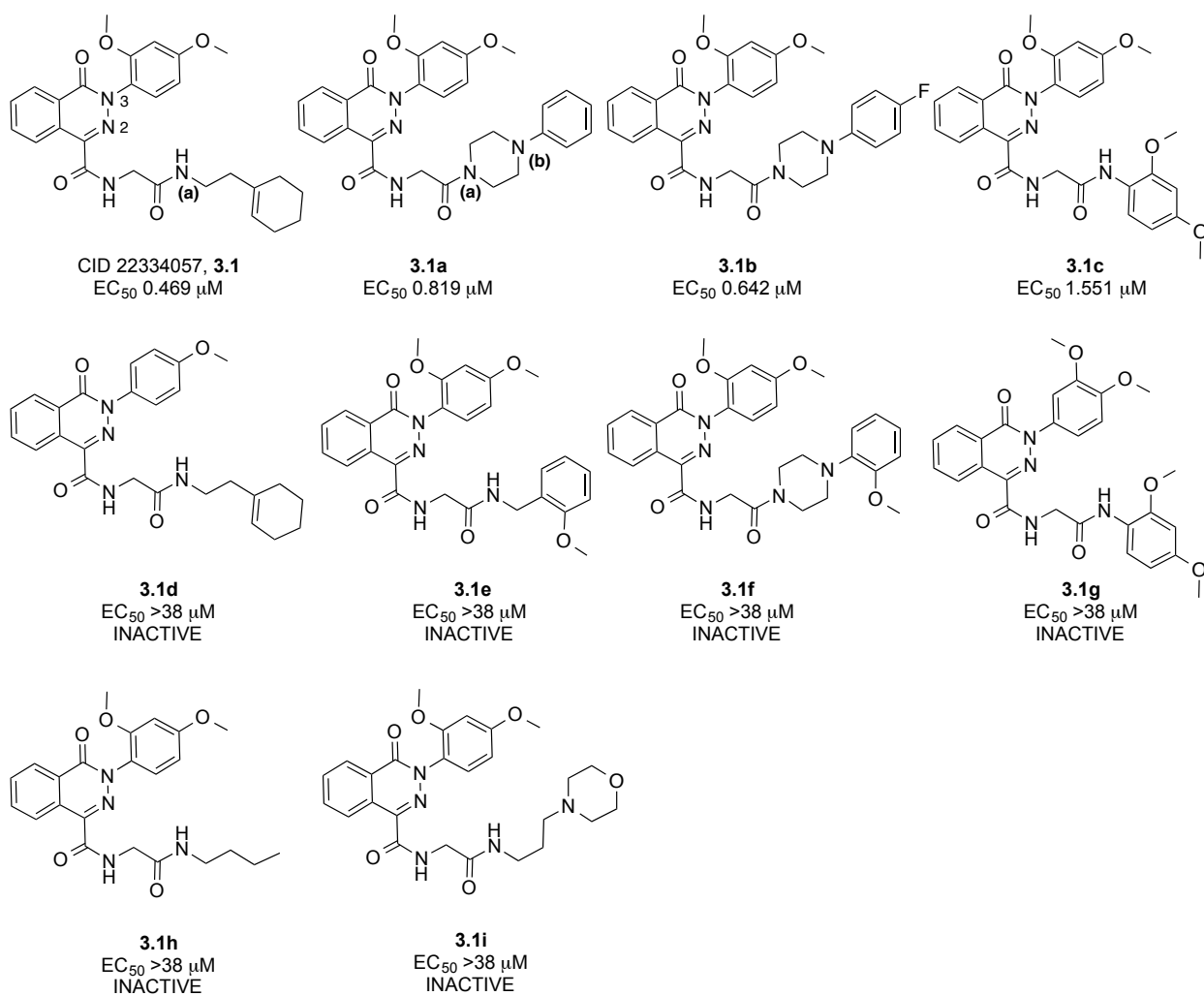
Small Molecule Fluconazole Synergizers - Dihydroisoquinolines

Introduction

Inspired by the highly potent analogues of spiroindolinone CID 6584729 (Scheme 2-5), we set out to optimize another molecule, dihydrophthalazine CID 22334057 from the Broad screening⁶² that is also an active hit in our initial assays. I trained a first year graduate student Aaron Mood to work with me on this project. With my initial planning and designing of the analogues, my co-worker Aaron performed the major portion of the synthesis.

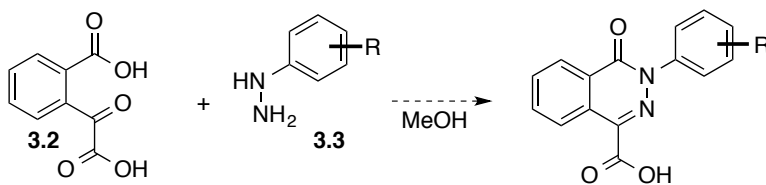
Schreiber and others at the Broad institute screened over 60 dihydrophthalazine analogues.¹⁰³ Yet only 4 analogues exhibited measurable antifungal activities against a susceptible *C.albicans* clinical isolate, CaCi-2 (fluconazole MIC 2 $\mu\text{g/mL}$) in the presence of 8 $\mu\text{g/mL}$ fluconazole (Figure 3-1). However, some of the inactive molecules provide valuable insights of the structure activity relationships. Substitution pattern on the arene ring fused to the N3 of the dihydrophthalazine core seems to play a key role in the activity. Especially the *ortho*-substitution that provides a rotational barrier to the arene ring is vital to the potency of the molecule (compounds **3.1** and **3.1d** and compounds **3.1c** and **3.1g**). When atoms N_a and N_b are part of a piperazine ring and N_b is part of an aniline, the arrangement of aniline substituents plays an important role in synergistic activity. Groups on the *ortho*- position are detrimental to the activity (compounds **3.1a**, **3.1b** and **3.1f**). Substitution on the amide N_a is also key to the antifungal enhancement activity of these molecules. It is evident that not every non-polar alkyl chain provides the required activity to the molecule. The cyclohexenethyl group on N_a is specifically important for the activity and substituting it with other groups diminish the antifungal enhancement activity (compounds **3.1**, **3.1e**, **3.1h** and **3.1i**).

Figure 3-1: Representative Examples of Dihydrophthalazine Tested in Broad Screen (Activities against *C.albicans*, CaCi-2 in the presence of 8 $\mu\text{g/mL}$ fluconazole)



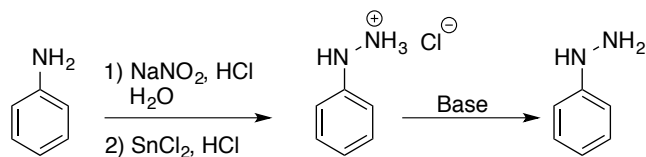
Early attempts to synthesize analogues of CID 22334057 by my undergraduate co-worker Kevin Scott resulted in unsuccessful condensation of dicarboxylic acid **3.2** and phenylhydrazine **3.3** (Figure 3-2).

Figure 3-2: Initial Plan to Synthesize Dihydrophthalazine Core



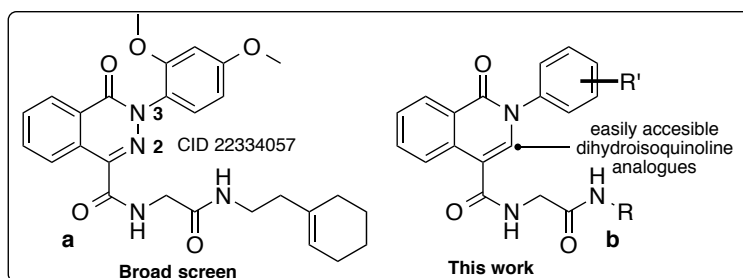
Handling of free base of the electron-rich arylhydrazine was also problematic. The synthesis was carried out with the initial diazotization of the aniline derivative by nitrous acid (Figure 3-3). Then subsequent reduction of the diazonium ion by tin(II) chloride in the presence of hydrochloric acid resulted in the HCl salt of the corresponding arylhydrazine product.¹⁰⁴ The diazotation and reduction steps were carried out successfully and the resulting arylhydrazine•HCl salt was characterized by ¹H NMR. However, the attempts to prepare the free base of the phenylhydrazine analogues were hampered by the instability of the electron-rich arylhydrazine.¹⁰⁵ Therefore, the condensation of dicarboxylic acid **3.2** and the arylhydrazine•HCl was attempted in the presence of various bases (Na₂CO₃, NaHCO₃, Et₃N and K₃PO₄). Yet, none of the combinations resulted in the expected dihydrophthalazine adduct and we only observed the starting material by TLC during the reaction and by ¹HNMR.

Figure 3-3: Synthesis of Arylhydrazine



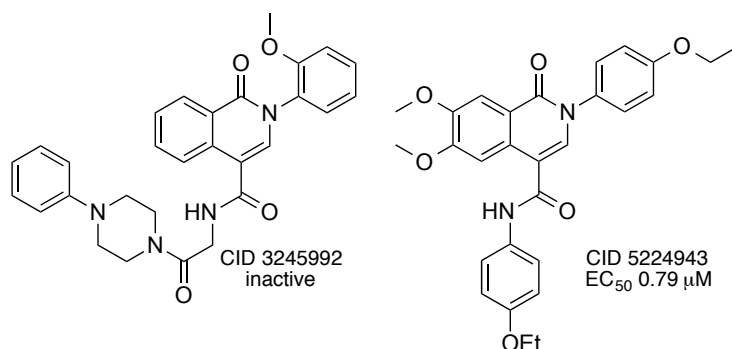
The difficulties arising while designing a convenient and efficient synthetic route to make the dihydrophthalazine core led us to focus on synthesizing the dihydroisoquinoline core containing isosteric methine moiety at the N2 position (Figure 3-4).

Figure 3-4: Fluconazole Synergizer CID 22334057 and Dihydroisoquinoline Analogues



During the massive screening for antifungal synergizers Schreiber and others at the Broad Institute tested 10 other analogues of dihydroisoquinolines that bears the core depicted in Figure 3-4 (structure **b**). Interestingly, structurally similar compound dihydrophthalazine **3.1a** (Figure 3-1) and dihydroisoquinolines, CID 3245992 (Figure 3-5) displayed significantly different results. Compound **3.1a** had antifungal activity at EC_{50} 0.819 μ M in the presence of fluconazole whereas CID 3245992 demonstrated no antifungal enhancer activity in the initial high throughput assay. Instead, compound CID 5224943 that lacks the glycine moiety of the parent compound **3.1b** displayed a comparable EC_{50} value of 0.79 μ M.⁸⁷

Figure 3-5: Dihydroisoquinolines Screened in Broad Assay



With this information in hand, we set out to optimize the antifungal enhancer activity of lead compound CID 22334057 in the presence of fluconazole and also to identify the sites for attachment of biological tags.

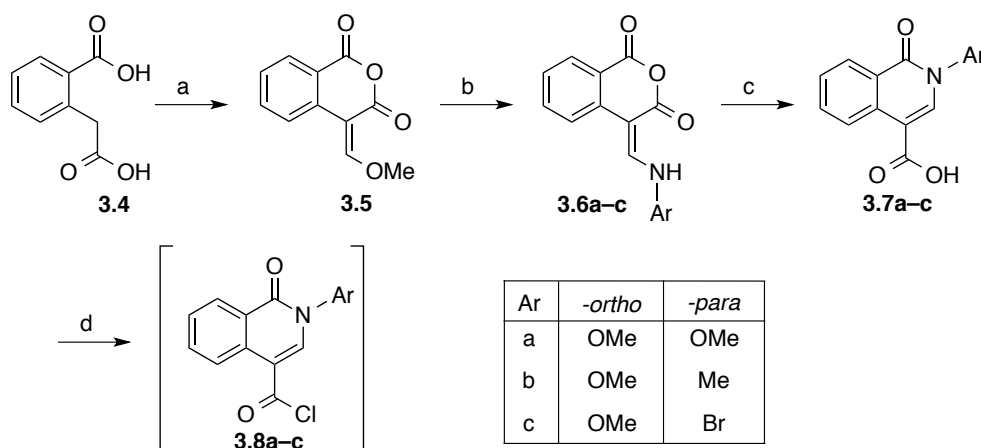
Results and Discussion

The overall synthesis strategy of isosteric dihydroisoquinoline analogues of CID 22334057 involved two aspects: dihydroisoquinoline acid chlorides and various amines. Final coupling was expected to result in different combinations of two fragments and therefore new analogues of the parent compound.

Synthesis of dihydroisoquinoline acid chloride fragment

As shown in Scheme 3-1, dihydroisoquinoline acid chlorides were synthesized by initial formylative condensation followed by cyclization of homophthalic acid **3.4** to afford enol ether **3.5** (Scheme 3-1).¹⁰⁶ Then conjugate substitution of the methoxy group with an aniline resulted in enamine adduct **3.6**. The presence of ethanol under basic conditions facilitated the final rearrangement of **3.6** to afford dihydroisoquinoline **3.7**.¹⁰⁷ Under Vilsmeier conditions acid chloride **3.8** was synthesized from the corresponding carboxylic acid.¹⁰⁸

Scheme 3-1: Synthesis of Dihydroisoquinoline Acid Chloride Analogues*



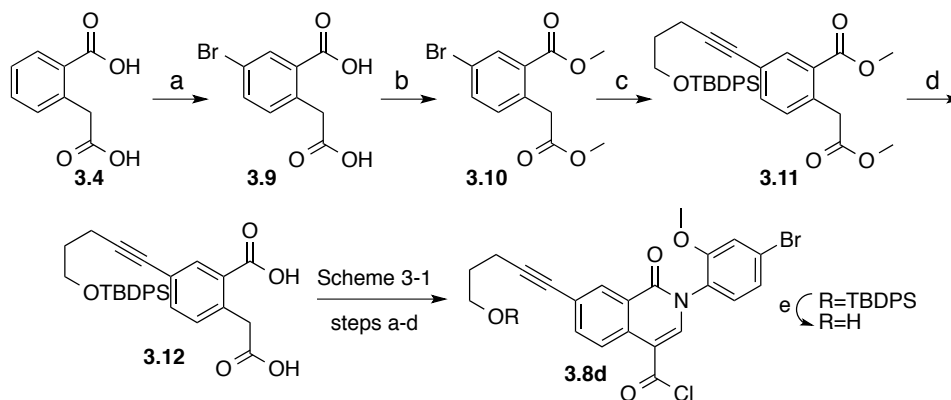
Reagents and conditions: (a) 1.0 equiv $\text{CH}(\text{OCH}_3)_3$, Ac_2O , $140\text{ }^\circ\text{C}$, 1 h, 65%, (b) 1.0 equiv ArNH_2 , 1,4-dioxane, $23\text{ }^\circ\text{C}$, 1-4 h, 35-70%, (c) 5.0 equiv NaOH , EtOH , $80\text{ }^\circ\text{C}$, 1-4 h, 47-77%, (d) 1.5 equiv oxalyl chloride, 10 mol% DMF , CH_2Cl_2 , $0\text{ }^\circ\text{C}$, 2 h, 64%. *Performed by Aaron Mood.

In order to evaluate the electronic effects on overall antifungal enhancement, three analogues of dihydroisoquinoline acid chlorides (**3.8a-c**) were synthesized. Compound **3.8c** allowed further derivatization of the aryl ring via various cross coupling reactions in later stages.

We were able to successfully attach an alkynyl substituent to the benzo ring of the bicyclic dihydroisoquinoline. This modification allowed us to determine the substituent tolerance of the benzo ring. Overall synthesis includes an initial bromination of homophthalic acid **3.4** to

result in 5-bromo-2-(carboxymethyl)benzoic acid adduct **3.9**.¹⁰⁹ Subsequent Presser esterification of **3.9** with trimethylsilyldiazomethane afforded the dimethyl ester **3.10** in excellent yield.¹¹⁰ Sonogashira coupling with TBDPS-protected 4-pentyn-1-ol was carried out before the introduction of bromoaniline.¹¹¹ Diester **3.11** was saponified to afford the carboxylic acid **3.12**.¹¹² Final cyclization to form the dihydroisoquinoline core was successfully achieved by following the same methods as in Scheme 3-1, steps a-d. Deprotection of the TBDPS group with tetrabutylammonium fluoride afforded dihydroisoquinoline analogue **3.8d**. However, earlier attempts to synthesize **3.8d** by eliminating protection/deprotection steps of the alcohol was unsuccessful due to the inability of the corresponding TBDPS free alcohol analogue of **3.12** to take part in the formylation/cyclization step to form the enol ether (Scheme 3-1, step a).

Scheme 3-2: Synthesis of Dihydroisoquinoline Analogue 3.8d*



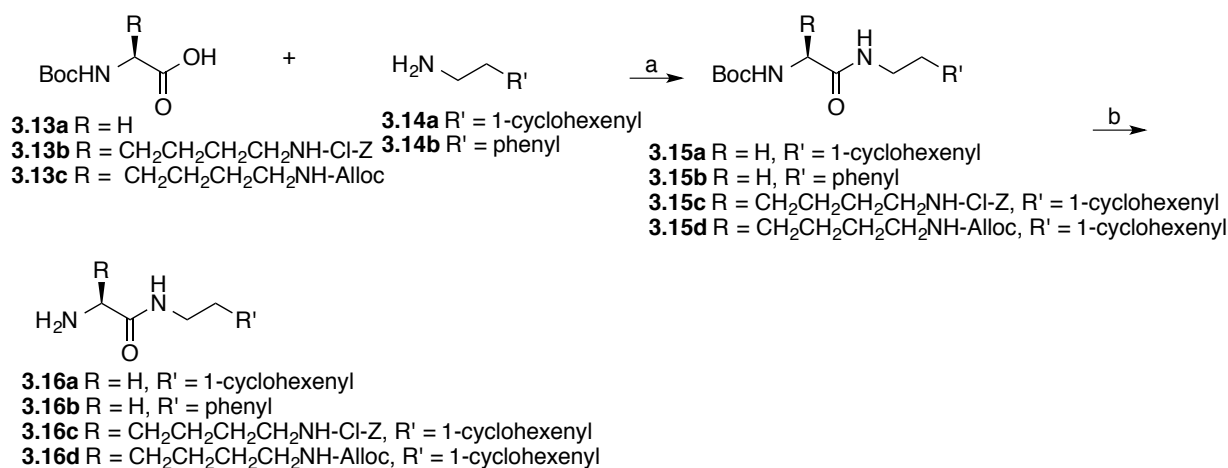
Reagents and conditions: (a) 1.5 equiv KBrO_3 , $\text{H}_2\text{O}/\text{H}_2\text{SO}_4$, $90\text{ }^\circ\text{C}$, 4 h, 39%, (b) 2.8 equiv TMSCHN_2 , 2:1 benzene/MeOH, $23\text{ }^\circ\text{C}$, 2 h, 99%, (c) 5 mol% $\text{Pd}_2\text{Cl}_2(\text{PPh}_3)_2$, 5 mol% CuI , 3:2 DMF/ Et_3N , $100\text{ }^\circ\text{C}$, 45 min, 85%, (d) 3.8 equiv LiOH , 3:1 THF/ H_2O , $23\text{ }^\circ\text{C}$, 16 h, 90%.
*Conducted by Aaron Mood.

Synthesis of Amine Fragment

Amines, **3.16a-d** were synthesized for subsequent coupling with dihydroisoquinoline acid chlorides **3.8a-d** (Scheme 3-3). *N*-Boc amino acids, **3.13a-c** were coupled with amines **3.14a-b** through carbodiimide coupling reactions to afford amides **3.15a-d** in good yields.¹¹³ However,

deprotection of the Boc group in the presence of the acid-sensitive cyclohexenyl group was found to be challenging. Common reagents such as trifluoroacetic acid resulted in complete degradation of the starting material due to protonation of the alkene. Consequently, thermal deprotection strategy was employed to generate the amines **3.16a-d**. Compounds such as **3.15a** and **3.15b** were heated under reflux in water to remove the Boc group.¹¹⁴ However, compounds with very limited solubility in water such as **3.15c** and **3.15d** were heated under reflux in the presence of ethylene glycol.¹¹⁵

Scheme 3-3: Synthesis of Amines 3.16a-d*



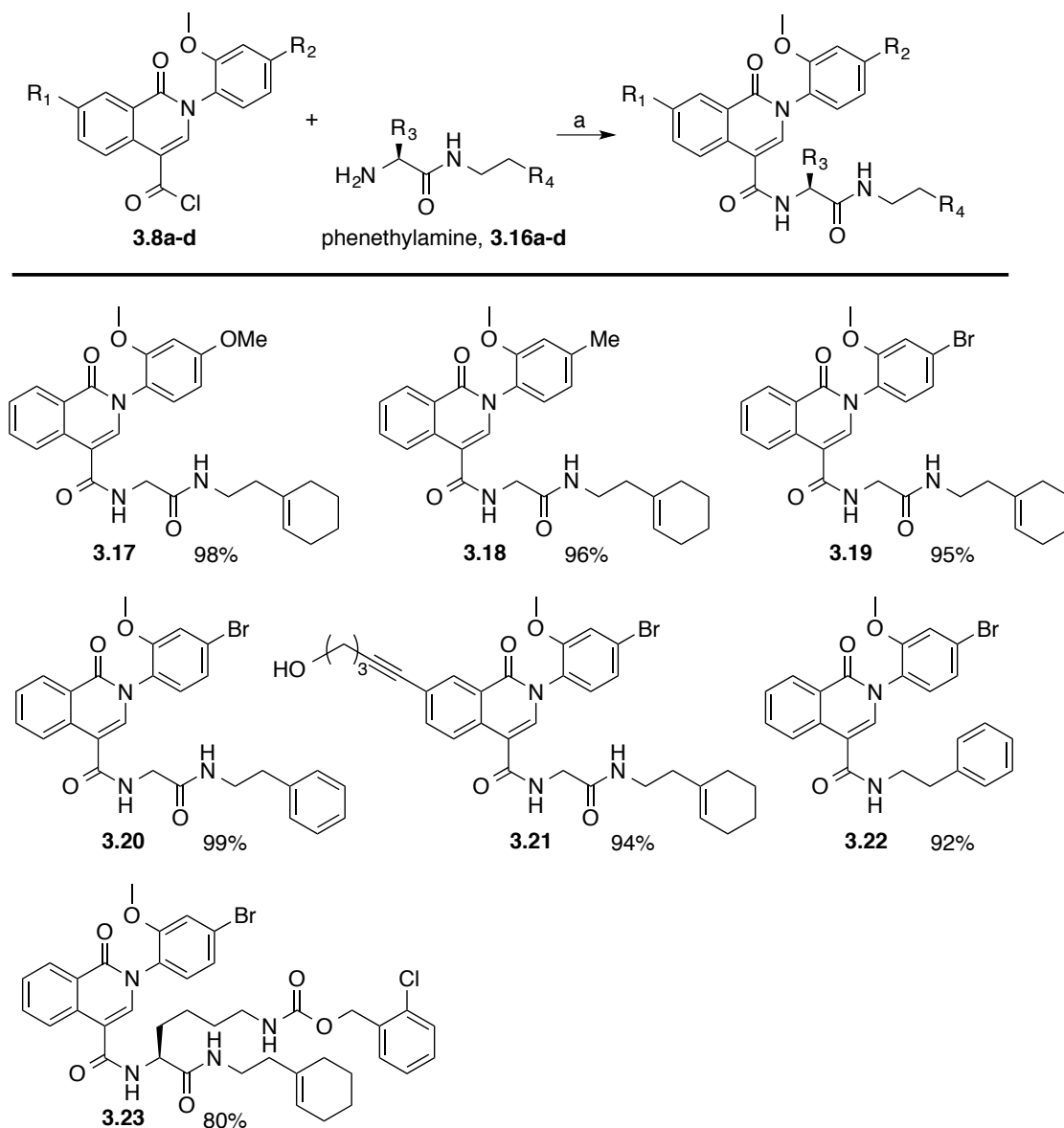
Reagents and conditions: (a) 1.2 equiv HOBt, 1.2 equiv EDC•HCl, 1.5 equiv DIPEA, CH₂Cl₂, 0-23 °C, 4 h, 71-74%, (b) H₂O, 100 °C or ethylene glycol, 200 °C, 74-99%. *Aaron Mood performed all steps leading to **3.16b** and **3.16d**.

Coupling of the dihydroisoquinoline acid chloride and amine fragments and further modifications:

Dihydroisoquinoline acid chlorides **3.8a**, **3.8b** and **3.8d** were coupled with amine **3.16a**. Acid chloride **3.8c** was coupled with phenethylamine and amines **3.16a-d**. The reactions afforded carbon analogues of the lead dihydrophthalazine CID 22334057 in good yields (Scheme 3-4).¹¹⁶

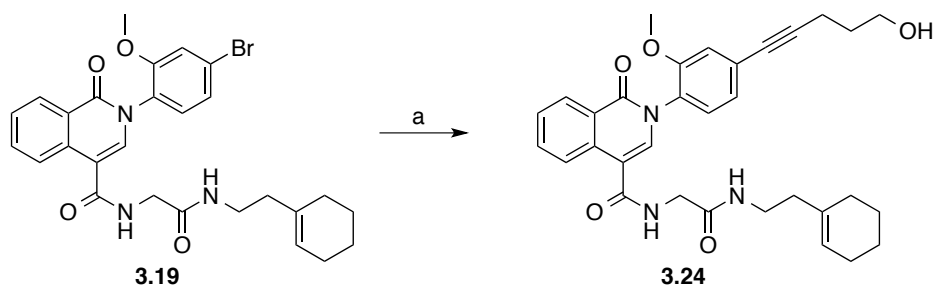
Dihydroisoquinoline **3.19** was further functionalized by utilizing the Sonogashira coupling to form compound **3.24** with another rigid linker to test the SAR and also to explore a possible site for the attachment of biological tags (Scheme 3-5).

Scheme 3-4: Coupling of Dihydroisoquinoline Acid Chloride and Amine Fragments*



Reagents and conditions: (a) 1.2 equiv Et₃N, CH₂Cl₂, 0-23 °C, 30 min. * Performed by Aaron Mood.

Scheme 3-5: Synthesis of Dihydroisoquinoline Analogue 3.24



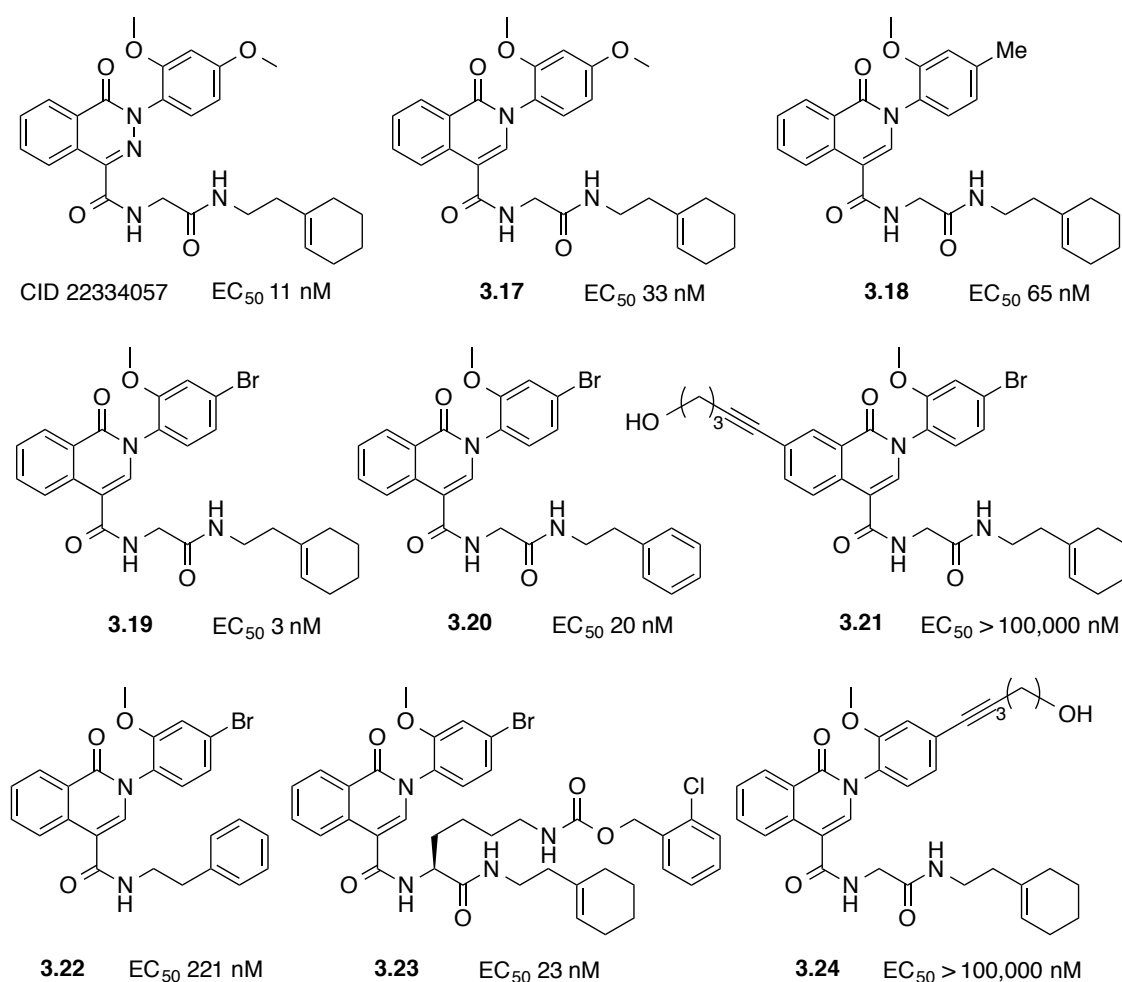
Reagents and conditions: (a) 1.2 equiv 4-pentyn-1-ol, 5 mol% Pd₂Cl₂(PPh₃)₂, 5 mol% CuI, 3:2 DMF/Et₃N, 100 °C, 45 min, 68%.

Structure-Activity Relationships

Lead molecule CID 22334057 was reported to synergize with fluconazole in a partially resistant clinical isolate of *C. albicans* CaCi-8 at EC₅₀ 0.23 μM.⁸⁷ We tested our compounds against a susceptible strain (HLY4123) derived from a commonly used *C. albicans* strain. CID 22334057 demonstrated better and promising activity in the cell line that we used in our study (Scheme 3-6). Replacing the imino nitrogen of the dihydropthalazine core with a methine group did not affect the synergistic activity of the analogues significantly (CID 22334057 and compound 3.17). Substitution on the phenyl moiety proved to be essential to the biological activity of the molecules (molecules 3.17, 3.18 and 3.19). Specifically, replacing the 4-position with a bromo substituent showed the para bromo group to be superior to both methoxy and methyl substituents. As mentioned above deprotection of the Boc group from the amine moiety was problematic due to the presence of cyclohexene group. Therefore, we synthesized phenethyl homologue 3.20 by replacing the cyclohexene with a phenyl group. Interestingly, the substitution of cyclohexene with a phenyl moiety did not affect the synergistic activity significantly (Compound 3.19 and 3.20). In addition, the inactivity of alkynyl analogues 3.21 and 3.24 show that the *N*-phenyl substituent and the benzo fragment of the dihydroisoquinoline cannot tolerate bulky groups, suggesting that these two sites play important roles in binding to the biological

target. Attempting to bypass the glycine moiety in the amine fragment negatively affected the antifungal synergistic activity of the molecules (Compound **3.19** and **3.22**). Finally, the potent activity of ClCbz-lysine derivative **3.23** revealed a site where a large functional tag could be affixed without compromising antifungal activity. This short list of structure-activity relationship data allowed us to not only identify molecules that demonstrate comparable antifungal activities to the lead molecule but also to locate a site that can tolerate a bulky substituent and allow the attachment of a biological tag. However, additional work is required to make analogues that display sub-nanomolar potent antifungal activity in the presence of azole drugs.

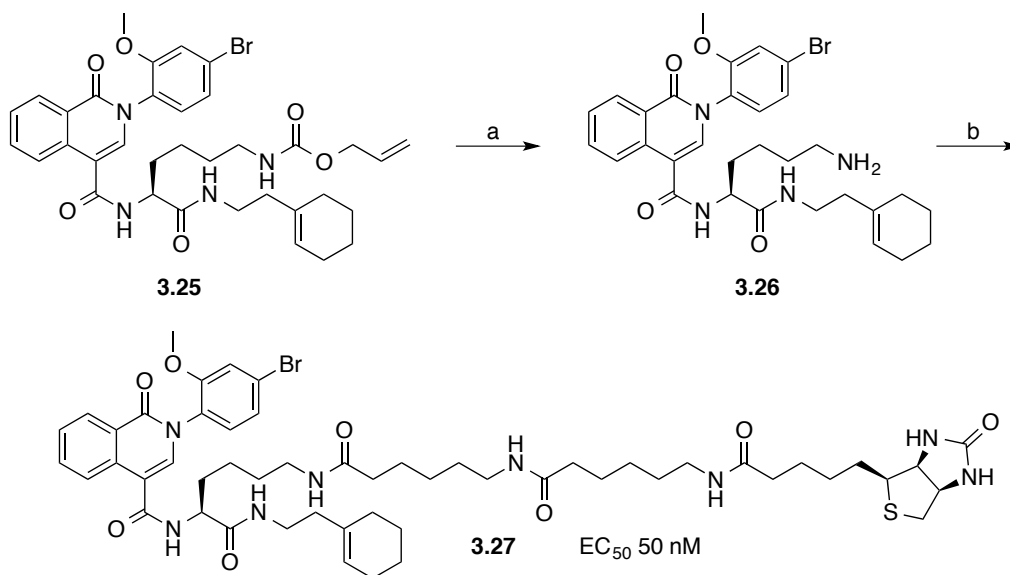
Scheme 3-6: Structure-Activity Relationship of Dihydroisoquinoline Analogues



Synthesis and Activity of Functional Biological Probes:

Taking advantage of the information revealed during the SAR studies we set out to synthesize compounds that carry biological probes such as biotin. Deprotection of 2-ClCbz in compound **3.23** requires acidic conditions, which can lead to the complications with the cyclohexene moiety. Therefore, we decided to synthesize an analogue that contains an alloc-protecting group that could be removed without affecting the acid-sensitive and hydrogenation prone cyclohexene ring (Scheme 3-7, compound **3.25**).¹¹⁷ Dihydroisoquinoline **3.25** was synthesized by utilizing the same steps described in Schemes 3-2, 3 and 4. Alloc group was deprotected with phenylsilane and catalytic palladium.

Scheme 3-7: Synthesis of Biotinylated Analogue **3.27**



Reagents and conditions: (a) 100 equiv PhSiH₃, 20 mol% Pd(PPh)₃, 3:1 CH₂Cl₂/DMF, 23 °C, 1 h, 70%, (b) 1.1 equiv NHS-LC-LC-Biotin, 2.0 equiv DIPEA, DMF, 23 °C, 24 h, 53%.

The resulting amine **3.26** was biotinylated with a longer spacer to afford biotinylated dihydroisoquinoline **3.27**.¹¹⁸ The space between the pharmacophore and the biological tag is important for the binding and potency of the compound. Longer linkers correlate with better binding due to the less interference of the tag. Biotin analogue **3.27** had an EC₅₀ value of 50 nM,

suggesting that the biotin does not significantly affect binding to the target. Shelley Lane at Liu lab has conducted the pull-down assay with *C.albicans* cell lysates. However, they did not pursue the results of the MS-MS results to identify a potential target that is responsible for the antifungal activity in the presence of fluconazole.

A checkerboard assay was used to determine the fractional inhibitory concentration for the synergistic activity of compound **3.19** and fluconazole against the fluconazole-susceptible strain (HLY4123). Compound **3.19** proved to be synergistic with fluconazole with the FIC index of 0.06.

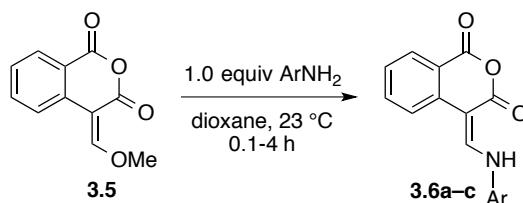
Conclusions:

In conclusion, we have designed, synthesized and studied dihydroisoquinolines inspired by CID 22334057 that was previously reported to exhibit activity against *C. albicans* in combination with fluconazole. Substituting imino N2 in the dihydrophthalazine with a methine group did not significantly affect the antifungal activity and replacement of a 4-methoxy group with a bromine atom in the aniline moiety increased the activity. Ultimately, the best analogue compound **3.19** (EC₅₀ 3 nM) demonstrated more potent activity than the lead compound CID 22334057 (EC₅₀ 11 nM). A biotinylated dihydroisoquinoline analogue **3.27** was synthesized and hopefully the Liu lab will be able to identify a potential target that is responsible for the antifungal activity in the presence of fluconazole. Also, compound **3.19** was found to be a true synergizer of fluconazole with the FIC index of 0.06.

Experimental Section

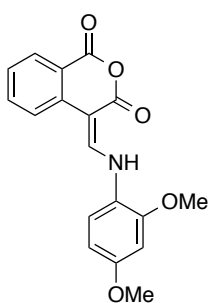
Chemistry

General procedure for the synthesis of enamines, **3.6a–c**.¹¹⁹



An oven-dried round bottom flask was charged with anhydride **3.5** (1.0 equiv) and a stir bar. Next, dioxane (0.50 M with respect to **3.5**) was added to the reaction flask. The resulting mixture turned into a cloudy white solution. Meanwhile, a separate oven-dried round bottom flask was charged with the substituted aniline (1.0 equiv) and a stir bar. Addition of dioxane (0.50 M with respect to the aniline) to the flask containing the aniline resulted in a deep red solution. Then, the contents of the flask with the aniline were transferred to the flask containing **3.5** via syringe. The reaction mixture gradually became a heterogenous green solution. The reaction was monitored until **3.5** was no longer detected by TLC. Upon consumption of **3.5**, the resulting green solid was filtered in a Büchner funnel. Then, the solid was washed with cold dioxane (3 x 15 mL) and dried under vacuum to obtain the corresponding pure enamine adduct, **3.6a–c**.

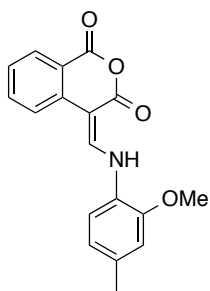
4-(((2,4-Dimethoxyphenyl)amino)methylene)isochromane-1,3-dione, **3.6a**.



An oven-dried round bottom flask was charged with enol ether **3.5** (0.50 g, 2.5 mmol, 1.0 equiv) and a stir bar. Next, dioxane (5.0 mL) was added to the reaction flask. The resulting mixture turned into a cloudy white solution. Meanwhile, a separate oven-dried round bottom flask was charged with 2,4-dimethoxyaniline (0.38 g, 2.5 mmol, 1.0 equiv) and a stir

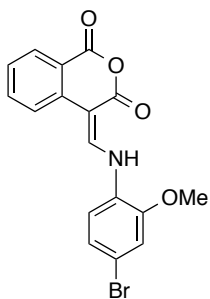
bar. Addition of dioxane (5.0 mL) to the flask containing the aniline resulted in a deep red solution. Immediately after, the contents of the flask with the aniline were transferred to the flask containing **3.5** via syringe. The reaction mixture gradually became a heterogeneous green solution. The reaction was monitored until **3.5** was no longer detected by TLC (10 min). Upon consumption of **3.5**, the resulting green solid was filtered in a Büchner funnel. Then, the green solid was washed with cold dioxane (3 x 15 mL) to give enamine **3.6a** (0.53 g, 1.6 mmol, 70%). $R_f = 0.44$ (1:1:0.05 EtOAc:hex:Et₃N). ¹H NMR (500 MHz, CDCl₃) δ 11.64 (d, $J = 13.2$ Hz, 1H), 8.41 (d, $J = 13.8$ Hz, 1H), 8.20 (d, $J = 8.1$ Hz, 1H), 7.61 (t, $J = 7.3$ Hz, 1H), 7.55 (d, $J = 8.1$ Hz, 1H), 7.27–7.21 (m, 2H), 6.56–6.54 (m, 2H), 3.94 (s, 3H), 3.84 (s, 3H); ¹³C NMR (500 MHz, CDCl₃) δ 163.5, 161.9, 158.6, 150.7, 144.2, 137.5, 135.0, 131.0, 124.9, 121.9, 117.7, 117.3, 116.3, 104.8, 99.5, 91.1, 56.1, 55.7; HRMS (ESI): m/z calculated for C₁₈H₁₅NO₅Na [M+Na]⁺ 348.0848, found 348.0854.

4-(((2-Methoxy-4-methylphenyl)amino)methylene)isochromane-1,3-dione, **3.6b**.



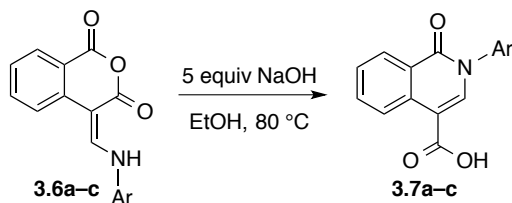
Using the general procedure for enamine formation outlined above, enol ether **5** (0.50 g, 2.5 mmol, 1.0 equiv) was used to give enamine **3.6b** (0.27 g, 0.86 mmol, 35%) as a green solid. $R_f = 0.52$ (1:1 EtOAc:hex). ¹H NMR (500 MHz, CDCl₃) δ 11.68 (d, $J = 13.5$ Hz, 1H), 8.46 (d, $J = 13.6$, 1H), 8.20 (d, $J = 8.0$ Hz, 1H), 7.62 (t, $J = 8.1$ Hz, 1H), 7.57 (d, $J = 8.2$ Hz, 1H), 7.26 (t, $J = 7.6$ Hz, 1H), 7.19 (d, $J = 8.0$ Hz, 1H), 6.84 (d, $J = 8.3$ Hz, 1H), 6.80 (s, 1H), 3.95 (s, 3H), 2.38 (s, 3H); ¹³C NMR (500 MHz, CDCl₃) δ 163.5, 161.8, 149.3, 143.9, 137.4, 136.5, 135.0, 131.1, 125.7, 125.0, 121.7, 117.8, 117.4, 114.9, 112.5, 91.5, 56.0, 21.5; HRMS (ESI): m/z calculated for C₁₈H₁₅NO₄Na [M+Na]⁺ 332.0899, found 348.0907.

4-(((4-Bromo-2-methoxyphenyl)amino)methylene)isochromane-1,3-dione, **3.6c**.



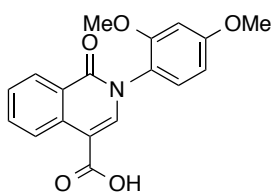
Using the general procedure for enamine formation outlined above, enol ether **3.5** (0.50 g, 2.5 mmol, 1.0 equiv) was used to give enamine **3.6c** (0.97 g, 2.6 mmol, 70%) as a green solid. $R_f = 0.53$ (1:1:0.05 EtOAc:hex:Et₃N). ¹H NMR (500 MHz, CDCl₃) δ 11.65 (d, $J = 13.3$ Hz, 1H), 8.43 (d, $J = 13.5$ Hz, 1H), 8.21 (d, $J = 8.4$ Hz, 1H), 7.64 (td, $J = 7.5$ Hz, 1.3, 1H), 7.58 (d, $J = 8.0$ Hz, 1H) 7.30 (t, $J = 7.8$ Hz, 1H), 7.18 (br s, 2H), 7.11 (s, 1H), 3.98 (s, 3H); ¹³C NMR (500 MHz, CDCl₃) δ 163.5, 161.5, 149.8, 143.1, 136.9, 135.2, 131.2, 127.5, 125.5, 124.2, 118.4, 118.0, 117.6, 115.8, 115.2, 92.7, 56.4; HRMS (ESI): m/z calculated for C₁₇H₁₂BrNO₄Na [M+Na]⁺ 395.9847, found 395.9850

General procedure for the synthesis of dihydroisoquinolines, **3.7a–c**.¹²⁰



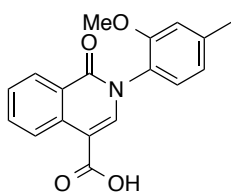
An oven-dried round bottom flask was charged with the corresponding enamine **3.6a–c** (1.0 equiv), anhydrous NaOH (5.0 equiv), and a stir bar. Next, EtOH (0.26 M with respect to **3.6**) was added to the flask and the flask was fitted with a reflux condenser. The reaction mixture was heated at reflux for 1.5 h. The reaction was monitored by TLC for disappearance of the enamine. Upon consumption of the enamine, the reaction mixture was cooled to room temperature. Then, the resulting mixture was treated with 3 N HCl to afford a solution with a pH of 1–2. The resulting solid was filtered with cold water (3 x 20 mL) in a Büchner funnel and dried under vacuum to obtain the corresponding pure dihydroisoquinoline adduct, **3.7a–c**.

2-(2,4-Dimethoxyphenyl)-1-oxo-1,2-dihydroisoquinoline-4-carboxylic acid, **3.7a**.



An oven-dried round bottom flask was charged with enamine **3.6a** (1.5 g, 4.6 mmol, 1.0 equiv), anhydrous NaOH (0.91 g, 23 mmol, 5.0 equiv), and a stir bar. Next, EtOH (18 mL) was added to the flask and the flask was fitted with a reflux condenser. The reaction mixture was heated at reflux for 1.5 h. The reaction was monitored by TLC for disappearance of the enamine. Upon consumption of the enamine, the reaction mixture was cooled to room temperature. Then, the resulting mixture was treated with 3 N HCl to afford a solution with a pH of 1–2. The resulting solid was filtered with cold water (3 x 20 mL) in a Büchner funnel to give dihydroisoquinoline **3.7a** (1.1 g, 3.5 mmol, 75%) as a purple solid. $R_f = 0.60$ (4:1 CH_2Cl_2 :MeOH). $^1\text{H NMR}$ (500 MHz, DMSO) δ 12.86 (s, 1H), 8.86 (d, $J = 8.4$ Hz, 1H), 8.28 (d, $J = 7.2$ Hz, 1H), 8.02 (s, 1H), 7.85 (td, $J = 7.7$ Hz, 1.3, 1H), 7.60 (t, $J = 7.7$ Hz, 1H), 7.35 (d, $J = 8.7$ Hz, 1H), 6.78 (d, $J = 2.6$ Hz, 1H) 6.66 (d, $J = 2.6$ Hz, 1H), 6.64 (d, $J = 2.7$ Hz, 1H), 3.84 (s, 3H) 3.75 (s, 3H); $^{13}\text{C NMR}$ (500 MHz, DMSO) δ 166.3, 161.0, 160.9, 155.1, 142.0, 134.5, 133.2, 129.3, 127.7, 127.2, 125.2, 125.2, 122.0, 105.7, 105.1, 99.4, 56.0, 55.6; HRMS (ESI): m/z calculated for $\text{C}_{18}\text{H}_{15}\text{NO}_5\text{Na}$ $[\text{M}+\text{Na}]^+$ 348.0848, found 348.0858.

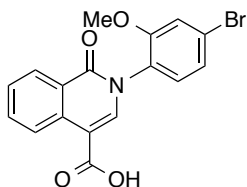
2-(2-Methoxy-4-methylphenyl)-1-oxo-1,2-dihydroisoquinoline-4-carboxylic acid, **3.7b**.



Using the general procedure for dihydroisoquinoline formation outlined above, enamine **3.6b** (0.20 g, 0.81 mmol, 1.0 equiv) was used to give dihydroisoquinoline **3.7b** (0.12 g, 0.38 mmol, 47%) as a brown solid. $R_f = 0.57$ (17:3 CH_2Cl_2 :MeOH). $^1\text{H NMR}$ (500 MHz, DMSO) δ 12.86 (br s, 1H), 8.86 (d, $J = 8.3$ Hz, 1H), 8.29 (d, $J = 8.0$ Hz, 1H), 8.02 (s, 1H), 7.85 (t, $J = 7.8$ Hz, 1H), 7.61 (t, $J = 7.6$ Hz, 1H), 7.31 (d, $J = 7.8$ Hz, 1H), 7.08 (s, 1H), 6.91 (d, $J = 7.9$ Hz, 1H), 3.75 (s,

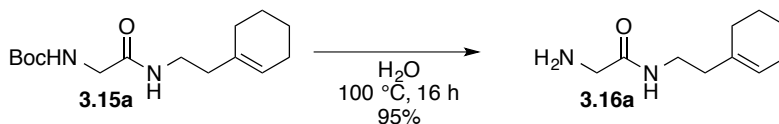
3H), 2.41 (s, 3H); ^{13}C NMR (500 MHz, DMSO) δ 166.3, 160.9, 153.8, 141.7, 140.5, 134.5, 133.3, 128.4, 127.7, 127.3, 126.4, 125.2, 125.16, 121.1, 113.2, 105.7, 55.8, 21.3; HRMS (ESI): m/z calculated for $\text{C}_{18}\text{H}_{15}\text{NO}_4\text{Na}$ $[\text{M}+\text{Na}]^+$ 332.0899, found 348.0904.

2-(4-Bromo-2-methoxyphenyl)-1-oxo-1,2-dihydroisoquinoline-4-carboxylic acid, 3.7c.



Using the general procedure for dihydroisoquinoline formation outlined above, enamine **3.6c** (0.23 g, 0.61 mmol, 1.0 equiv) was used to give dihydroisoquinoline **3.7c** (0.18 g, 0.47 mmol, 77% yield) as a brown solid. $R_f = 0.35$ (17:3 CH_2Cl_2 :MeOH). ^1H NMR (500 MHz, DMSO) δ 12.90 (s, 1H), 8.85 (d, $J = 8.4$ Hz, 1H), 8.28 (d, $J = 8.0$ Hz, 1H), 8.06 (s, 1H), 7.86 (t, $J = 7.7$ Hz, 1H), 7.61 (t, $J = 7.7$ Hz, 1H), 7.47–7.43 (m, 2H), 7.31 (dd, $J = 8.2, 1.6$ Hz, 1H), 3.79 (s, 3H); ^{13}C NMR (500 MHz, DMSO) δ 166.2, 160.7, 155.1, 141.1, 134.5, 133.4, 133.4, 130.6, 128.2, 127.7, 127.4, 125.3, 125.0, 123.6, 123.0, 116.0, 106.1, 56.6; HRMS (ESI): m/z calculated for $\text{C}_{17}\text{H}_{12}\text{BrNO}_4\text{Na}$ $[\text{M}+\text{Na}]^+$ 395.9847, found 395.9842.

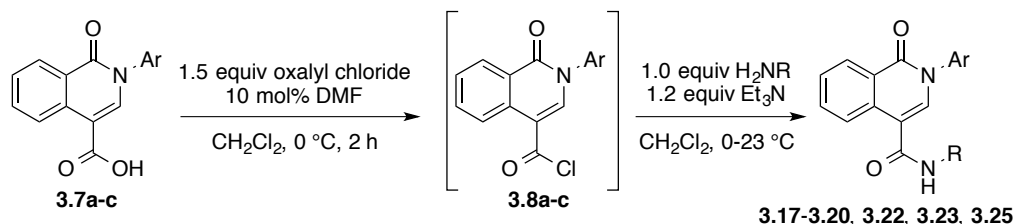
2-Amino-N-(2-(cyclohex-1-en-1-yl)ethyl)acetamide, 3.16a.¹²¹



A round bottom flask was charged with Boc-protected amine **3.15a** (1.5 g, 5.3 mmol, 1.0 equiv) and a stir bar. Next, water (110 mL, 0.048 M with respect to **3.15a**) was added to the flask and the flask was fitted with a reflux condenser. The reaction mixture was heated at reflux for 16 h and monitored by TLC for disappearance of **3.15a**. Upon consumption of **3.15a**, the reaction mixture was cooled to room temperature. The aqueous layer was extracted with CH_2Cl_2 (3 x 100 mL). Then, the combined organic layers were concentrated *in vacuo* to give amine **3.16a** (0.91 g, 5.0 mmol, 95%) as a yellow oil. $R_f = 0$ (6:4 EtOAc:hex). ^1H NMR (500 MHz, CDCl_3) δ 7.21 (br

s, 1H), 5.48 (s, 1H), 3.38–3.34 (m, 4H), 2.15 (t, $J = 6.7$ Hz, 2H), 2.0–1.94 (m, 4H), 1.65–1.51 (m, 4H), 1.42 (br s, 2H); ^{13}C NMR (500 MHz, CDCl_3) δ 172.5, 134.7, 123.4, 44.8, 37.7, 36.8, 28.0, 25.3, 22.9, 22.4; HRMS (ESI): m/z calculated for $\text{C}_{10}\text{H}_{18}\text{N}_2\text{ONa}$ $[\text{M}+\text{Na}]^+$ 205.1317, found 205.1312.

General procedure for synthesis of amides via acid chlorides, 3.17–3.20, 3.22, 3.23, 3.25.^{122,123}

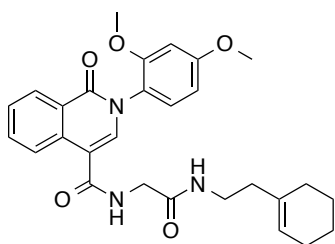


A flame-dried round bottom flask was charged with the corresponding carboxylic acid **3.7a–c** (1.0 equiv) and a stir bar. Next, CH_2Cl_2 (0.077 M with respect to the carboxylic acid) was added to the flask and the reaction mixture was cooled to $0\text{ }^\circ\text{C}$ with an ice bath. Subsequently, oxalyl chloride (1.5 equiv) and DMF (10 mol%) were added sequentially. The reaction mixture was stirred at $0\text{ }^\circ\text{C}$ for 2 h. The resulting solution was clear. Next, the reaction mixture was concentrated *in vacuo* to yield the corresponding acid chloride, **3.8a–c**.

A separate flame-dried round bottom flask was charged with the corresponding amine (**3.15aa–3.15ca** and phenethylamine) (1.0 equiv) and a stir bar. Next, CH_2Cl_2 (0.040 M with respect to amine) and Et_3N (1.2 equiv) were added to the flask via syringe and the flask was cooled to $0\text{ }^\circ\text{C}$ with an ice bath. Next, the acid chloride was dissolved in CH_2Cl_2 (0.036 M with respect to acid chloride) and transferred dropwise to the reaction mixture via syringe over 10 min. Afterwards, the reaction vessel was warmed to room temperature. The reaction mixture was stirred until the acid chloride was no longer detected by TLC (30 min). Upon consumption of the acid chloride, the reaction mixture was washed with 10% K_2CO_3 and extracted with CH_2Cl_2 (3 x 20 mL). The combined organic layers were washed with brine and dried over Na_2SO_4 . The

resulting organic solution was concentrated *in vacuo*. The crude material was purified by flash chromatography to afford the amide.

***N*-(2-((2-(cyclohex-1-en-1-yl)ethyl)amino)-2-oxoethyl)-2-(2,4-dimethoxyphenyl)-1-oxo-1,2-dihydroisoquinoline-4-carboxamide, 3.17.**

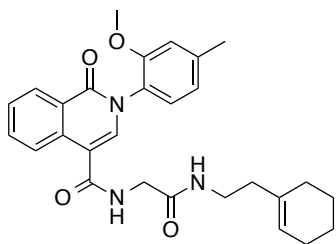


A flame-dried round bottom flask was charged with carboxylic acid **3.7a** (0.050 g, 0.15 mmol, 1.0 equiv) and a stir bar. Next, CH₂Cl₂ (2.0 mL) was added to the flask and the reaction mixture was cooled to 0 °C with an ice bath. Subsequently, oxalyl chloride (20 μL, 0.23 mmol, 1.5 equiv) and DMF (1.2 μL, 0.015 mmol, 10 mol%) were added sequentially. The reaction mixture was stirred at 0 °C for 2 h. The resulting solution was clear. Next, the reaction mixture was concentrated *in vacuo* to yield the acid chloride **3.8a**.

A separate flame-dried round bottom flask was charged with amine **3.16a** (0.028 g, 0.15 mmol, 1.0 equiv) and a stir bar. Next, CH₂Cl₂ (4.0 mL) and Et₃N (0.025 mL, 0.18 mmol 1.2 equiv) were added to the flask via syringe and the flask was cooled to 0 °C with an ice bath. Afterwards, the acid chloride was dissolved in CH₂Cl₂ (6.0 mL) and transferred drop-wise to the reaction mixture via syringe over 10 min. Then, the reaction vessel was warmed to room temperature. The reaction mixture was stirred until the acid chloride was no longer detected by TLC (30 min). Upon consumption of the acid chloride, the reaction mixture was washed with 10% K₂CO₃ and extracted with CH₂Cl₂ (3 x 20 mL). The combined organic layers were washed with brine and dried over Na₂SO₄. The resulting organic solution was concentrated *in vacuo* to afford a purple solid. The crude material was purified by flash chromatography (CH₂Cl₂/Et₂O) to afford amide **3.17** (0.074 g, 0.15 mmol, 98%) as a white solid. *R_f* = 0.17 (6:4 EtOAc:hex). ¹H NMR (500 MHz, CDCl₃) δ 8.47 (d, *J* = 7.9 Hz, 1H), 8.23 (d, *J* = 8.3 Hz, 1H), 7.72 (t, *J* = 7.5 Hz,

1H), 7.54 (t, $J = 7.8$ Hz, 1H), 7.51 (s, 1H), 7.17 (d, $J = 8.7$ Hz, 1H), 6.84 (t, $J = 4.9$ Hz, 1H), 6.57 (d, $J = 2.6$ Hz, 1H), 6.53 (dd, $J = 9.6, 2.5$ Hz, 1H), 6.06 (t, $J = 5.3$ Hz, 1H), 5.46 (s, 1H), 4.08 (d, $J = 5.0$ Hz, 2H), 3.85 (s, 3H), 3.75 (s, 3H), 3.56 (q, $J = 5.6$ Hz, 2H), 2.14 (t, $J = 7.0$ Hz, 2H), 1.96–1.90 (m, 4H), 1.62–1.50 (m, 4H); ^{13}C NMR (500 MHz, CDCl_3) δ 168.4, 168.8, 162.0, 161.4, 155.5, 135.7, 134.4, 134.2, 133.1, 129.3, 128.8, 127.6, 126.3, 124.8, 124.0, 122.4, 112.8, 104.7, 99.8, 56.0, 55.8, 43.6, 37.6, 37.5, 28.0, 25.3, 22.9, 22.4; HRMS (ESI): m/z calculated for $\text{C}_{28}\text{H}_{31}\text{N}_3\text{O}_5\text{Na}$ $[\text{M}+\text{Na}]^+$ 512.2161, found 512.2150

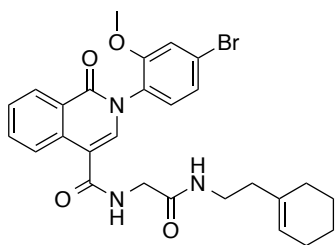
***N*-(2-((2-(cyclohex-1-en-1-yl)ethyl)amino)-2-oxoethyl)-2-(2-methoxy-4-methylphenyl)-1-oxo-1,2-dihydroisoquinoline-4-carboxamide, 3.18.**



Using the general procedure for the formation of amides via acid chlorides outlined above, carboxylic acid 6b (0.051 g, 0.17 mmol, 1.0 equiv) and amine **3.16a** (0.031 g, 0.17 mmol, 1.0 equiv) were used. The crude material was purified by flash chromatography using $\text{CH}_2\text{Cl}_2:\text{Et}_2\text{O}$ to give amide **3.18** (0.075 g, 0.16 mmol, 96%)

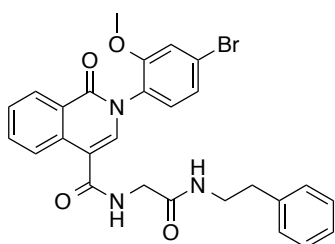
as a white solid. $R_f = 0.18$ (6:4 EtOAc:hex). ^1H NMR (500 MHz, CDCl_3) δ 8.47 (d, $J = 8.0$ Hz, 1H), 8.23 (d, $J = 8.2$ Hz, 1H), 7.72 (t, $J = 7.1$ Hz, 1H), 7.53 (t, $J = 8.0$ Hz, 1H), 7.51 (s, 1H), 7.13 (d, $J = 8.3$ Hz, 1H), 6.86 – 6.83 (m, 3H), 6.08 (br s, 1H), 5.45 (s, 1H), 4.07 (d, $J = 5.0$ Hz, 2H), 3.77 (s, 3H), 3.35 (q, $J = 6.7$ Hz, 2H), 2.41 (s, 3H), 2.13 (t, $J = 6.8$ Hz, 2H), 1.97 – 1.86 (m, 4H), 1.62 – 1.49 (m, 4H); ^{13}C NMR (500 MHz, CDCl_3) δ 168.4, 166.8, 161.9, 154.3, 141.0, 135.5, 134.4, 134.2, 133.1, 128.8, 128.4, 127.6, 126.6, 126.3, 124.8, 124.0, 121.7, 113.1, 112.8, 55.9, 43.6, 37.6, 37.5, 28.0, 25.3, 22.9, 22.4, 21.9; HRMS (ESI): m/z calculated for $\text{C}_{28}\text{H}_{31}\text{N}_3\text{O}_4\text{Na}$ $[\text{M}+\text{Na}]^+$ 496.2212, found 496.2229.

2-(4-Bromo-2-methoxyphenyl)-N-(2-((2-(cyclohex-1-en-1-yl)ethyl)amino)-2-oxoethyl)-1-oxo-1,2-dihydroisoquinoline-4-carboxamide, 3.19.



Using the general procedure for the formation of amides via acid chlorides outlined above, carboxylic acid 6c (0.059 g, 0.15 mmol, 1.0 equiv) and amine **3.16a** (0.029 g, 0.16 mmol, 1.0 equiv) were used. The crude material was purified by flash chromatography using CH₂Cl₂:Et₂O to give amide **3.19** (0.078 g, 0.14 mmol, 95%) as a white solid. $R_f = 0.16$ (6:4 EtOAc:hex). ¹H NMR (500 MHz, CDCl₃) δ 8.46 (d, $J = 8.1$ Hz, 1H), 8.22 (d, $J = 8.1$ Hz, 1H), 7.73 (t, $J = 7.6$ Hz, 1H), 7.55 (t, $J = 7.5$ Hz, 1H), 7.46 (s, 1H), 7.19–7.14 (m, 3H), 6.89 (br s, 1H), 6.05 (br s, 1H), 5.46 (s, 1H), 4.08 (d, $J = 4.8$ Hz, 2H), 3.79 (s, 3H), 3.35 (q, $J = 6.2$ Hz, 2H), 2.14 (t, $J = 6.72$ Hz, 2H), 1.97–1.90 (m, 4H), 1.62–1.50 (m, 4H); ¹³C NMR (500 MHz, CDCl₃) δ 168.4, 166.6, 161.6, 155.3, 134.7, 134.4, 134.2, 133.3, 130.1, 128.8, 128.3, 127.9, 126.2, 124.9, 124.2, 124.1, 123.9, 116.1, 113.3, 56.4, 43.5, 37.57, 37.56, 28.0, 25.3, 22.9, 22.4; HRMS (ESI): m/z calculated for C₂₇H₂₈BrN₃O₄Na [M+Na]⁺ 560.1161, found 560.1158.

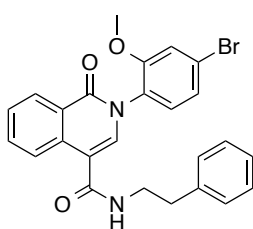
2-(4-Bromo-2-methoxyphenyl)-1-oxo-N-(2-oxo-2-(phenethylamino)ethyl)-1,2-dihydroisoquinoline-4-carboxamide, 3.20.



Using the general procedure for the formation of amides via acid chlorides outlined above, carboxylic acid 6c (0.059 g, 0.16 mmol, 1.0 equiv) and amine **3.16b** (0.029 g, 0.16 mmol, 1.0 equiv) were used. The crude material was purified by flash chromatography using EtOAc:hex to give amide **3.20** (0.087 g, 0.16 mmol, >99%) as a white solid. $R_f = 0.28$ (6:4 EtOAc:hex). ¹H NMR (500 MHz, DMSO) δ 8.58 (t, $J = 5.6$ Hz, 1H), 8.33 (d, $J = 8.8$ Hz, 1H), 8.27 (d, $J = 8.1$ Hz, 1H), 8.05 (t, $J = 5.5$ Hz, 1H), 7.81 (t, $J = 8.1$ Hz, 1H), 7.71 (s, 1H), 7.60 (t, $J = 7.5$ Hz, 1H), 7.48 (d, $J = 1.6$ Hz, 1H), 7.40 (d, $J = 8.2$ Hz, 1H),

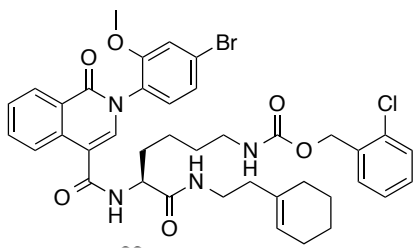
7.35 (dd, $J = 8.2$ Hz, 1.8, 1H), 7.26 (t, $J = 7.6$ Hz, 2H), 7.22–7.16 (m, 3H), 3.82–3.78 (m, 5H), 3.3 (q, $J = 7.0$ Hz, 2H), 2.72 (t, $J = 7.6$ Hz, 2H); ^{13}C NMR (500 MHz, DMSO δ 168.8, 165.8, 160.2, 155.4, 139.4, 135.3, 134.6, 133.0, 130.6, 128.7, 128.3, 127.5, 127.4, 126.1, 125.3, 125.1, 123.6, 122.8, 115.9, 112.0, 79.2, 56.5, 42.4, 40.3, 35.2 HRMS (ESI): m/z calculated for $\text{C}_{27}\text{H}_{24}\text{BrN}_3\text{O}_4\text{Na}$ $[\text{M}+\text{Na}]^+$ 556.0848, found 556.0844.

2-(4-Bromo-2-methoxyphenyl)-1-oxo-N-phenethyl-1,2-dihydroisoquinoline-4-carboxamide, 3.22.



Using the general procedure for the formation of amides via acid chlorides outlined above, carboxylic acid **3.7c** (0.058 g, 0.16 mmol, 1.0 equiv) and phenethylamine (0.019 g, 0.16 mmol, 1.0 equiv) were used. The crude material was purified by flash chromatography using EtOAc:hex to give amide **3.22** (0.067 g, 0.14 mmol, 92%) as a white solid. $R_f = 0.75$ (6:4 EtOAc:hex). ^1H NMR (500 MHz, CDCl_3) δ 8.42 (d, $J = 8.1$, 1H), 8.0 (d, $J = 8.2$, 1H), 7.7 (t, $J = 7.3$, 1H), 7.52 (t, $J = 7.8$, 1H), 7.30–7.25 (m, 3H), 7.25–7.15 (m, 5H), 7.11 (d, $J = 8.3$, 1H), 5.94 (t, $J = 5.5$, 1H), 3.76–3.70 (m, 5H), 2.95 (t, 6.9, 2H); ^{13}C NMR (500 MHz, CDCl_3) δ 166.3, 161.4, 155.2, 138.7, 134.1, 133.9, 133.2, 130.0, 128.9, 128.8, 128.6, 128.3, 127.7, 126.7, 126.1, 124.7, 124.1, 123.8, 116.0, 114.4, 56.2, 41.0, 35.5; HRMS (ESI): m/z calculated for $\text{C}_{25}\text{H}_{21}\text{BrN}_2\text{O}_3\text{Na}$ $[\text{M}+\text{Na}]^+$ 499.0633, found 499.0637.

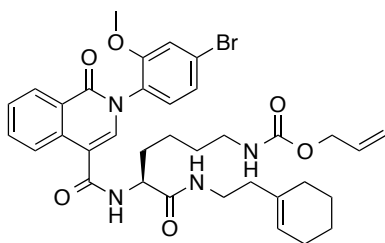
2-Chlorobenzyl (S)-(5-(2-(4-bromo-2-methoxyphenyl)-1-oxo-1,2-dihydroisoquinoline-4-carboxamido)-6-((2-(cyclohex-1-en-1-yl)ethyl)amino)-6-oxohexyl)carbamate, 3.23.



Using the general procedure for the formation of amides via acid chlorides outlined above, carboxylic acid **3.7c** (0.058 g, 0.16 mmol, 1.0 equiv) and amine **3.16c** (0.068 g, 0.16 mmol, 1.0 equiv) were used. The crude material was

purified by flash chromatography using EtOAc:hex to give amide **3.23** (0.097 g, 0.12 mmol, 80%) as a white solid. $R_f = 0.57$ (6:4 EtOAc:hex). $^1\text{H NMR}$ (500 MHz, CDCl_3) δ 8.44 (d, $J = 7.9$ Hz, 1H), 8.17 (d, $J = 8.1$ Hz, 1H), 7.72 (t, $J = 7.3$ Hz, 1H), 7.53 (t, $J = 7.7$ Hz, 1H), 7.41 (s, 1H), 7.35–7.32 (m, 2H), 7.26–7.13 (m, 5H), 6.80 (d, $J = 7.8$ Hz, 1H), 6.15 (t, $J = 5.6$ Hz, 1H), 5.44 (s, 1H), 5.12 (q, $J = 9.3$ Hz, 2H), 4.95 (s, $J = 5.1$ Hz, 1H), 4.57 (q, $J = 6.5$ Hz, 1H), 3.78 (s, 3H), 3.42–3.34 (m, 1H), 3.31–3.25 (m, 1H), 3.20 (q, $J = 6.5$ Hz, 2H), 2.13 (t, $J = 6.5$ Hz, 2H), 1.98–1.86 (m, 5H), 1.88–1.70 (m, 1H), 1.62–1.39 (m, 8H); $^{13}\text{C NMR}$ (500 MHz, CDCl_3) δ 171.3, 166.3, 161.5, 156.5, 155.3, 134.43, 134.37, 134.27, 134.17, 133.6, 133.3, 130.1, 129.8, 129.6, 129.5, 128.8, 128.3, 127.8, 127.0, 126.1, 124.8, 124.2, 124.0, 116.1, 113.6, 64.1, 56.3, 53.4, 40.5, 37.6, 37.5, 32.7, 29.7, 28.0, 25.4, 22.9, 22.7, 22.4; HRMS (ESI): m/z calculated for $\text{C}_{39}\text{H}_{42}\text{BrClN}_4\text{O}_6\text{Na}$ $[\text{M}+\text{Na}]^+$ 799.1874, found 799.1873.

Allyl (S)-(5-(2-(4-bromo-2-methoxyphenyl)-1-oxo-1,2-dihydroisoquinoline-4-carboxamido)-6-((2-(cyclohex-1-en-1-yl)ethyl)amino)-6-oxohexyl)carbamate, 3.25.

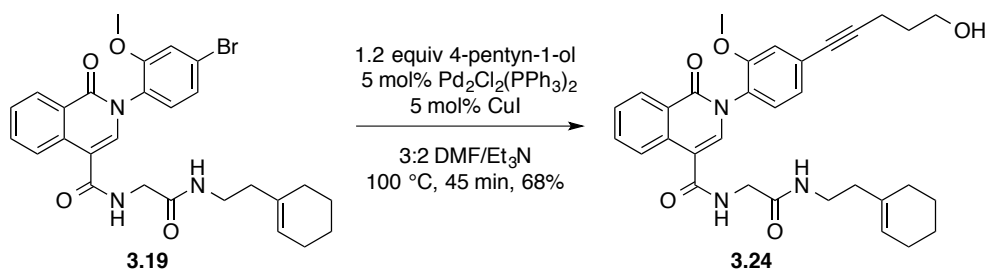


Using the general procedure for the formation of amides via acid chlorides outlined above, carboxylic acid **3.7c** (0.21 g, 0.55 mmol, 1.0 equiv) and amine **3.16d** (0.18 g, 0.55 mmol, 1.0 equiv) were used. The crude material was purified by flash chromatography using EtOAc:hex to give amide **3.25**

(0.37 g, 0.53 mmol, 97%) as a white solid. $R_f = 0.44$ (6:4 EtOAc:hex). $^1\text{H NMR}$ (500 MHz, CDCl_3) δ 8.46 (d, $J = 7.8$ Hz, 1H), 8.17 (d, $J = 8.4$ Hz, 1H), 7.74 (t, $J = 7.2$ Hz, 1H), 7.55 (t, $J = 7.7$ Hz, 1H), 7.41 (s, 1H), 7.22–7.15 (m, 3H), 6.83 (d, $J = 7.6$ Hz, 1H), 6.19 (br s, 1H), 5.87 – 5.78 (m, 1H), 5.45 (s, 1H), 5.23 (d, $J = 17.0$ Hz, 1H), 5.15 (d, $J = 10.6$ Hz, 1H), 4.86 (br s, 1H), 4.57 (q, $J = 6.1$ Hz, 1H), 4.49–4.39 (m, 2H), 3.80 (s, 3H), 3.45–3.35 (m, 1H), 3.31–3.25 (m, 1H), 3.20–3.14 (m, 2H), 2.13 (t, $J = 6.6$ Hz, 2H), 1.98–1.86 (m, 5H), 1.78–1.70 (m, 1H), 1.63–1.36

(m, 8H); ^{13}C 171.3, 166.3, 161.5, 156.6, 155.3, 134.42, 134.37, 134.2, 133.3, 132.9, 130.1, 128.8, 128.3, 127.8, 126.1, 124.8, 124.2, 124.0, 117.7, 116.1, 113.6, 65.6, 56.4, 53.4, 40.4, 37.6, 37.5, 32.6, 29.7, 27.9, 25.3, 22.9, 22.6, 22.4; NMR (500 MHz, CDCl_3) δ HRMS (ESI): m/z calculated for $\text{C}_{35}\text{H}_{41}\text{BrN}_4\text{O}_6\text{Na}$ $[\text{M}+\text{Na}]^+$ 715.2107, found 715.2101.

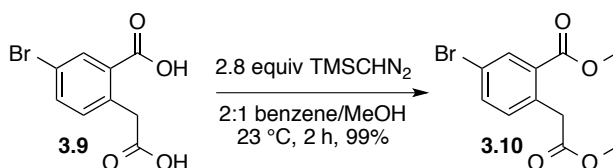
***N*-(2-((2-(cyclohex-1-en-1-yl)ethyl)amino)-2-oxoethyl)-2-(4-(5-hydroxypent-1-yn-1-yl)-2-methoxyphenyl)-1-oxo-1,2-dihydroisoquinoline-4-carboxamide, 3.24**¹²⁴



A flame-dried round bottom flask was charged with aryl bromide **3.19** (0.051 g, 0.095 mmol, 1.0 equiv). Next, 3:2 DMF/ Et_3N (1 mL, 0.095 M with respect to **3.19**) and 4-pentyn-1-ol (0.010 mL, 0.11 mmol, 1.2 equiv) were added to the reaction flask via syringe and the reaction mixture was stirred for 3 min. Afterwards, CuI (0.90 mg, 0.0046 mmol, 5 mol%) and $\text{Pd}_2\text{Cl}_2(\text{PPh}_3)_2$ (3.3 mg, 0.0046 mmol, 5 mol%) were added quickly by lifting up the septum. Next, the flask was fitted with a reflux condenser and heated at reflux for 45 min. The reaction was monitored by TLC for disappearance of the aryl bromide. Upon consumption of **3.19**, the reaction mixture was cooled to room temperature and diluted with CH_2Cl_2 (10 mL). The organic layer was washed with water (5 x 10 mL) followed by brine and dried over Na_2SO_4 . The resulting solution was concentrated *in vacuo* to give a red solid. The crude material was purified by flash chromatography (EtOAc:hex) to yield carboxamide **3.24** (0.035 g, 0.065 mmol, 68%) as a white solid. R_f = 0.23 (4:1 EtOAc:hex). ^1H NMR (500 MHz, CDCl_3) δ 8.46 (d, J = 8.3 Hz, 1H), 8.22 (d, J = 8.2 Hz, 1H), 7.73 (t, J = 7.8 Hz, 1H), 7.54 (t, J = 8.1 Hz, 1H), 7.49 (s, 1H), 7.18 (d, J = 7.8 Hz, 1H), 7.06–7.04 (m, 2H), 6.93 (t, J = 5.0 Hz, 1H), 6.12 (t, J = 5.1 Hz, 1H), 5.45 (s,

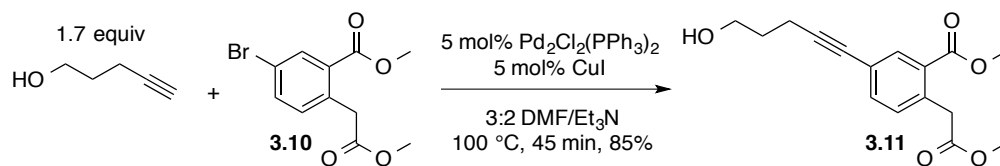
1H), 4.07 (d, $J = 5.4$ Hz, 2H), 3.82 (t, $J = 6.6$ Hz, 2H), 3.77 (s, 3H), 3.35 (q, $J = 5.9$ Hz, 2H), 2.56 (t, 7.2, 2H), 2.14 (t, $J = 6.9$ Hz, 2H), 1.98–1.70 (m, 7H), 1.63–1.49 (m, 4H); ^{13}C 168.4, 166.7, 161.6, 154.3, 135.0, 134.4, 134.2, 133.2, 128.8, 128.73, 128.67, 127.8, 126.24, 126.18, 124.9, 124.4, 124.0, 115.4, 113.1, 91.0, 80.6, 61.8, 56.1, 43.6, 37.55, 37.53, 31.40, 28.0, 25.3, 22.9, 22.4, 16.1; NMR (500 MHz, CDCl_3) δ HRMS (ESI): m/z calculated for $\text{C}_{32}\text{H}_{35}\text{N}_3\text{O}_5\text{Na}$ $[\text{M}+\text{Na}]^+$ 564.2474, found 564.2480.

Methyl 5-bromo-2-(2-methoxy-2-oxoethyl)benzoate, 3.10.¹²⁵



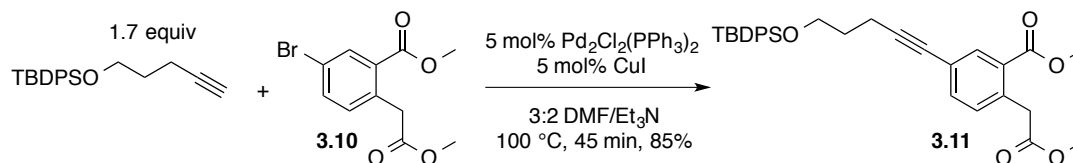
An oven-dried round bottom flask was charged with dicarboxylic acid **3.9** (0.99 g, 3.9 mmol, 1.0 equiv) and a stir bar. Next, 2:1 Benzene/MeOH (29 mL, 0.13 M with respect to **3.9**) was added to the reaction flask via syringe. Afterwards, TMSCHN_2 (2.0 M in Et_2O , 5.5 mL, 11 mmol, 2.8 equiv) was added drop wise to the reaction flask via syringe over 2 h. The reaction was monitored by TLC for disappearance of **3.9**. Upon consumption of the dicarboxylic acid, the reaction mixture was concentrated *in vacuo* to afford a pale yellow oil. The crude material was purified by flash chromatography (EtOAc:hex) to yield diester **3.10** (1.1 g, 3.8 mmol, >99%) as a clear oil. $R_f = 0.86$ (9:1 CH_2Cl_2 :MeOH). ^1H NMR (500 MHz, CDCl_3) δ 8.15 (s, 1H), 7.61 (d, $J = 8.2$ Hz, 1H), 7.14 (d, $J = 8.2$ Hz, 1H), 3.97 (s, 2H), 3.88 (s, 3H), 3.70 (s, 3H); ^{13}C NMR (500 MHz, CDCl_3) δ 171.6, 166.3, 135.4, 135.1, 134.1, 134.0, 131.4, 121.3, 52.5, 52.2, 40.0; HRMS (ESI): m/z calculated for $\text{C}_{11}\text{H}_{11}\text{O}_4\text{Na}$ $[\text{M}+\text{Na}]^+$ 308.9738, found 308.9739.

Methyl 5-(5-hydroxypent-1-yn-1-yl)-2-(2-methoxy-2-oxoethyl)benzoate.¹²⁶



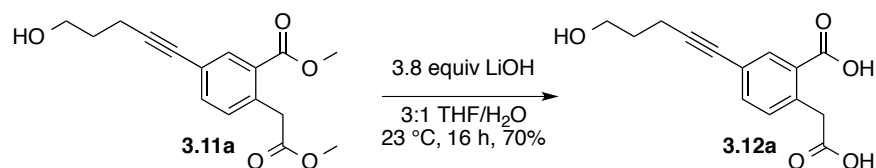
A flame-dried round bottom flask was charged with diester **3.10** (0.050 g, .17 mmol, 1.0 equiv) and a stir bar. Next, 3:2 DMF/Et₃N (1.9 mL, 0.095 M with respect to **3.9**) and 4-pentyn-1-ol (0.019 mL, 0.21 mmol, 1.2 equiv) were added to the reaction flask via syringe. Then, the reaction mixture was stirred for 3 min. Afterwards, CuI (0.017 g, 0.0087 mmol, 5 mol%) and Pd₂Cl₂(PPh₃)₂ (0.0061 g, 0.0087 mmol, 5 mol%) were added quickly by lifting up the septum. Next, the flask was fitted with a reflux condenser and heated at reflux for 45 min. The reaction mixture was monitored by TLC for disappearance of **3.10**. Upon consumption of **3.10**, the reaction mixture was cooled to room temperature and diluted with CH₂Cl₂ (10 mL). The organic layer was washed with water (5 x 10 mL) followed by brine and dried over Na₂SO₄. The resulting solution was concentrated *in vacuo* to afford a red oil. The crude material was purified by flash chromatography (EtOAc:hex) to yield alkyne product (0.041 g, 0.14 mmol, 81%) as a red oil. $R_f = 0.43$ (1:1 EtOAc:hex). ¹H NMR (500 MHz, CDCl₃) δ 8.04 (d, $J = 1.7$ Hz, 1H), 7.48 (dd, $J = 6.0, 1.8$ Hz, 1H), 7.18 (d, $J = 7.8$ Hz, 1H), 3.99 (s, 2H), 3.87 (s, 3H), 3.82 (br s, 2H), 3.69 (s, 3H), 2.55 (t, $J = 7.0$ Hz, 2H), 1.87 (quin, $J = 6.5$ Hz, 2H), 1.57 (br s, 1H); ¹³C NMR (500 MHz, CDCl₃) δ 171.9, 167.1, 135.4, 135.2, 134.3, 132.4, 129.8, 123.4, 90.7, 80.0, 61.8, 52.3, 52.2, 40.41, 31.4, 16.1; HRMS (ESI): m/z calculated for C₁₆H₁₈O₅Na [M+Na]⁺ 313.1052, found 313.1060.

Methyl 5-(5-((tert-butyl dimethylsilyl)oxy)pent-1-yn-1-yl)-2-(2-methoxy-2-oxoethyl)benzoate, 3.11.



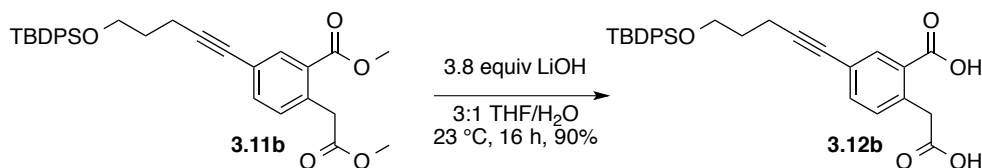
A flame-dried round bottom flask was charged with diester **3.10** (0.75 g, 2.6 mmol, 1.0 equiv) and a stir bar. Next, 3:2 DMF/Et₃N (28 mL, 0.095 M with respect to **3.10**) and tert-butylpent-4-ynoxydiphenylsilane (1.4 g, 4.3 mmol, 1.7 equiv) were added to the reaction flask via syringe. Then, the reaction mixture was stirred for 3 min. Afterwards, CuI (0.025 g, 0.13 mmol, 5 mol%) and Pd₂Cl₂(PPh₃)₂ (0.092 g, 0.13 mmol, 5 mol%) were added quickly by lifting up the septum. Next, the flask was fitted with a reflux condenser and heated at reflux for 45 min. The reaction mixture was monitored by TLC for disappearance of **3.10**. Upon consumption of **3.10**, the reaction mixture was cooled to room temperature and diluted with CH₂Cl₂ (50 mL). The organic layer was washed with water (5 x 50 mL) followed by brine and dried over Na₂SO₄. The resulting solution was concentrated *in vacuo* to afford a red oil. The crude material was purified by flash chromatography (EtOAc:hex) to yield alkyne **3.11** (1.2 g, 2.2 mmol, 85%) as a red oil. $R_f = 0.49$ (1:4 EtOAc:hex). ¹H NMR (500 MHz, CDCl₃) δ 8.02 (d, $J = 1.7$ Hz, 1H), 8.03–8.00 (m, 4H), 7.45–7.35 (m, 7H), 7.2 (d, $J = 8.1$ Hz, 1H), 3.99 (s, 2H), 3.87 (s, 3H), 3.81 (t, $J = 6.1$ Hz, 2H), 3.70 (s, 3H), 2.57 (t, $J = 7.2$ Hz, 2H), 1.85 (quin, $J = 7.2$ Hz, 2H), 1.06 (s, 9H); ¹³C NMR (500 MHz, CDCl₃) δ 171.9, 167.1, 135.7, 135.24, 135.22, 134.3, 133.9, 132.4, 129.74, 129.71, 127.8, 123.7, 91.3, 79.7, 62.5, 52.3, 52.2, 40.4, 31.6, 27.0, 19.4, 16.1; HRMS (ESI): m/z calculated for C₃₂H₃₆O₅SiNa [M+Na]⁺ 551.2230, found 551.2228.

2-(Carboxymethyl)-5-(5-hydroxypent-1-yn-1-yl)benzoic acid, **3.12a**.¹²⁷



A round bottom flask was charged with alkyne **3.11a** (0.040 g, 0.14 mmol, 1.0 equiv) and a stir bar. Next, THF (1.3 mL, 0.11 M with respect to **3.10a**) and LiOH (1.4 M in water, 0.39 mL, 0.53 mmol, 3.8 equiv) was added to the flask via syringe. The reaction mixture was monitored by TLC for disappearance of **3.11a**. After consumption of **3.11a** overnight, 4 mL of 1 N HCl and 6.5 mL of EtOAc were added to the reaction mixture. The mixture was extracted with EtOAc (3 x 10 mL). The combined organic layers were washed with brine and dried with Na₂SO₄. The resulting solution was concentrated *in vacuo* to yield dicarboxylic acid **3.12a** (0.025 g, 0.098 mmol, 70 %) as a brown solid. $R_f = 0.30$ (8:2:1 CH₂Cl₂:MeOH:AcOH). ¹H NMR (500 MHz, DMSO) δ 12.64 (br s, 2H), 7.86 (d, $J = 1.7$ Hz, 1H), 7.52 (dd, $J = 7.8, 1.8$ Hz, 1H), 7.33 (d, $J = 8.1$ Hz, 1H), 4.58 (s, 1H), 3.95 (s, 2H), 3.54 (t, $J = 6.2$ Hz, 2H), 2.50 (t, $J = 7.1$ Hz, 2H), 1.71 (quin, $J = 6.6$ Hz, 2H); ¹³C NMR (500 MHz, DMSO) δ 172.2, 167.6, 136.2, 134.1, 133.0, 132.8, 131.0, 122.1, 91.4, 79.4, 59.4, 31.5, 15.3; HRMS (ESI): m/z calculated for C₁₄H₁₃O₅ [M – H][–] 261.0763, found 261.0769.

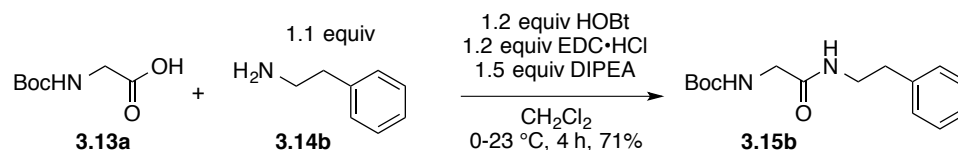
5-(5-((*Tert*-butyldimethylsilyloxy)pent-1-yn-1-yl)-2-(carboxymethyl)benzoic acid, **3.12b**.



A round bottom flask was charged with alkyne **3.11b** (0.73 g, 1.4 mmol, 1.0 equiv) and a stir bar. Next, THF (13 mL, 0.11 M with respect to **3.11b**) and LiOH (1.4 M in water, 3.9 mL,

5.3 mmol, 3.8 equiv) was added to the flask via syringe. The reaction mixture was monitored by TLC for disappearance of **3.11b**. After consumption of **3.11b** overnight, 40 mL of 1 N HCl and 65 mL of EtOAc were added to the reaction mixture. The mixture was extracted with EtOAc (3 x 100 mL). The combined organic layers were washed with brine and dried with Na₂SO₄. The resulting solution was concentrated *in vacuo* to yield dicarboxylic acid **3.12b** (0.62 g, 1.2 mmol, 90%) as a brown solid. *R_f* = 0.46 (17:3 CH₂Cl₂:MeOH). ¹H NMR (500 MHz, DMSO) δ 13.2–12.0 (br s, 2H), 7.82 (s, 1H), 7.66–7.61 (m, 4H), 7.46–7.36 (m, 7H), 7.30 (d, *J* = 7.8 Hz, 1H), 3.93 (s, 2H), 3.79 (t, *J* = 6.0 Hz, 2H), 2.57 (t, *J* = 7.0 Hz, 2H), 1.81 (quin, *J* = 6.6 Hz, 2H), 1.01 (s, 9H); ¹³C NMR (500 MHz, DMSO) δ 172.2, 167.6, 136.3, 135.0, 134.5, 134.1, 133.1, 133.0, 132.8, 129.9, 127.9, 121.9, 90.7, 79.7, 62.0, 30.9, 26.7, 18.8, 15.2; HRMS (ESI): *m/z* calculated for C₃₀H₃₁O₅Si [M – H][–] 499.1941, found 499.1953.

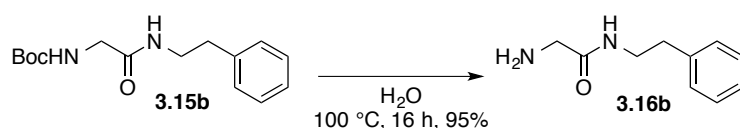
***Tert*-butyl (2-oxo-2-(phenethylamino)ethyl)carbamate, **3.15b**.**¹²⁸



An oven-dried round bottom flask was charged with Boc-glycine **3.13a** (0.64 g, 3.7 mmol, 1.0 equiv), HOBt (0.59 g, 4.3 mmol, 1.2 equiv) and a stir bar. Next, CH₂Cl₂ (90 mL, 0.41 M with respect to **3.13a**) was added to the reaction vessel followed by phenethylamine (0.50 mL, 3.97 mmol, 1.1 equiv). The reaction vessel was cooled to 0 °C with an ice bath and then EDC·HCl (0.83 g, 4.33 mmol, 1.2 equiv) was added by lifting the septum. Next, DIPEA (0.95 mL, 5.6 mmol, 1.5 equiv) was added to the reaction vessel via syringe and the reaction mixture was stirred for 1 h. Afterwards, the reaction vessel was warmed to room temperature. The reaction was monitored for disappearance of **3.13a** by TLC (4 h). Upon consumption of **3.13a**, the reaction mixture was washed with saturated NaHCO₃ and extracted with CH₂Cl₂ (3 x 100

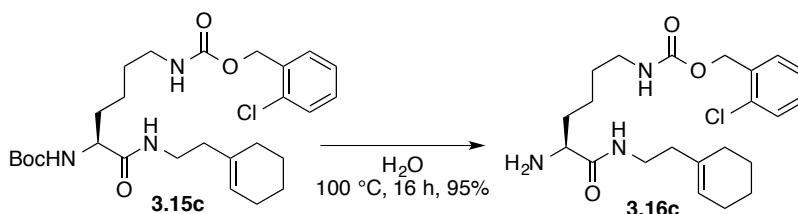
mL). The combined organic layers were washed with brine and dried with Na₂SO₄. The resulting solution was concentrated *in vacuo* to afford a yellow oil and purified with flash chromatography (EtOAc/hex) to yield amide **3.15b** (0.11 g 71%) as a yellow oil. $R_f = 0.57$ (17:3 CH₂Cl₂:MeOH). ¹H NMR (500 MHz, CDCl₃) δ 7.31 (t, $J = 7.3$ Hz, 2H), 7.25–7.18 (m, 3H), 6.12 (s, 1H), 5.09 (s, 1H), 3.74 (d, $J = 5.7$ Hz, 2H), 3.54 (q, $J = 6.6$ Hz, 2H), 2.82 (t, $J = 7.1$ Hz, 2H), 1.43 (s, 9H); HRMS (ESI): m/z calculated for C₁₅H₂₂N₂O₃Na [M+Na]⁺ 301.1528, found 301.1531.

2-Amino-*N*-phenethylacetamide, **3.16b**.



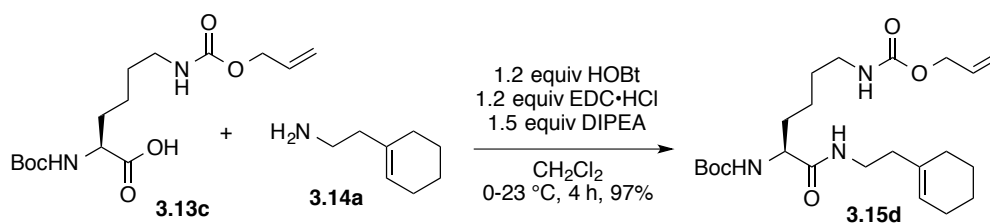
A round bottom flask was charged with Boc-protected amine **3.15b** (0.25 g, 0.89 mmol, 1 equiv) and a stir bar. Next, water (20 mL, 0.045 M with respect to **3.15b**) was added to the flask and the flask was fitted with a reflux condenser. The reaction mixture was heated at reflux for 16 h and monitored by TLC for disappearance of **3.15b**. Upon consumption of **3.15b**, the reaction mixture was cooled to room temperature. Next, the aqueous layer was extracted with CH₂Cl₂ (3 x 20 mL) and the combined organic layers were concentrated *in vacuo* to give amine **3.16b** (0.91 g, 0.85 mmol, 95%) as a yellow oil. $R_f = 0$ (6:4 EtOAc:hex). ¹H NMR (500 MHz, CDCl₃) δ 7.34–7.18 (m, 6H), 3.55 (q, $J = 6.7$ Hz, 2H), 3.32 (s, 2H), 2.84 (t, $J = 7.1$ Hz, 2H), 1.40 (s, 2H); HRMS (ESI): m/z calculated for C₁₀H₁₄N₂ONa [M+Na]⁺ 201.1004, found 201.1002.

2-Chlorobenzyl (S)-(5-amino-6-((2-(cyclohex-1-en-1-yl)ethyl)amino)-6-oxohexyl)carbamate, **3.16c**.¹²⁹



An oven-dried round bottom flask was charged with the Boc-protected amine **3.15c** (0.66 g, 1.3 mmol, 1 equiv) and a stir bar. Next, ethylene glycol (28 mL, 0.046 M with respect to **3.15c**) was added to the flask and the flask was fitted with a reflux condenser. The reaction mixture was heated at reflux for 16 h and monitored by TLC for disappearance of the Boc-protected amine. Upon consumption of the Boc-protected amine (20 min), the reaction mixture was cooled to room temperature and diluted with CH₂Cl₂ (50 mL). Next, the organic layer was washed with water (5x100 mL) followed by brine and dried over Na₂SO₄. The resulting solution was concentrated *in vacuo* to give amine **3.16c** (0.39 g, 0.96 mmol, 74%) as a yellow oil. *R_f* = 0 (6:4 EtOAc:hex). ¹H NMR (500 MHz, CDCl₃) δ 7.43–7.35 (m, 2H), 7.26–2.20 (m, 3H), 5.45 (s, 1H), 5.25–5.17 (m, 3H), 4.92 (br s, 1H), 3.34–3.29 (m, 2H), 3.21 (q, *J* = 6.5 Hz, 2H), 2.13 (t, *J* = 6.8 Hz, 2H), 2.02–1.90 (m, 4H), 1.85–1.78 (m, 1H), 1.64–1.39 (m, 11H); ¹³C NMR (500 MHz, CDCl₃) δ 174.8, 156.4, 134.8, 134.5, 133.6, 129.8, 129.6, 129.4, 127.0, 123.6, 64.0, 55.2, 40.9, 37.9, 37.0, 34.8, 29.9, 28.0, 25.4, 23.0, 22.9, 22.5; HRMS (ESI): *m/z* calculated for C₂₂H₃₂ClN₃O₃H [M + H]⁺ 422.2210, found 422.2216.

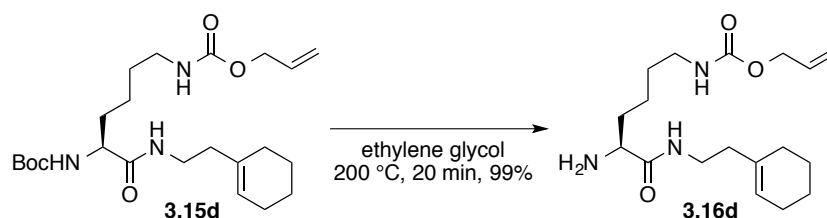
Allyl tert-butyl (6-((2-(cyclohex-1-en-1-yl)ethyl)amino)-6-oxohexane-1,5-diyl) (S)-dicarbamate, 3.15d.



Following the same procedure for the amide synthesis of **3.16b**, carboxylic acid **3.13c** (1.0 g, 3.0 mmol, 1.0 equiv) and amine **3.14a** (0.42 g, 3.32 mmol, 1.1 equiv) were used. The crude material was purified by flash chromatography using EtOAc:hex to give amide **3.15d** (1.17 g, 2.9 mmol, 97%) as a yellow oil. *R_f* = 0.76 (7:3 EtOAc:hex). ¹H NMR (500 MHz, CDCl₃) δ

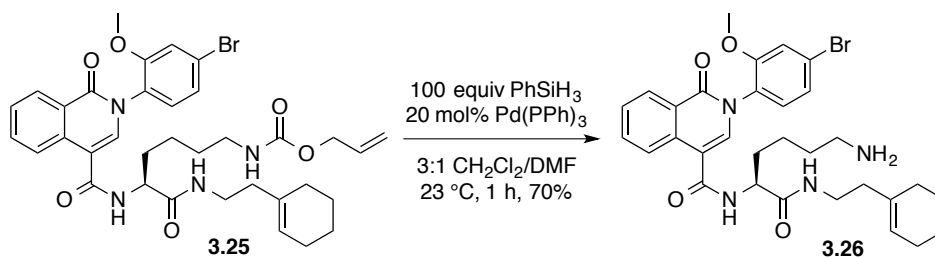
6.03 (br s, 1H), 5.96–5.87 (m, 1H), 5.46 (s, 1H), 5.30 (dd, $J = 17.2, 1.6$ Hz, 1H), 5.25 (dd, $J = 10.3, 1.1$, 1H), 5.09 (s, 1H), 4.81 (s, 1H), 4.55 (d, $J = 4.7$ Hz, 2H), 4.01 (s, 1H), 3.38–3.24 (m, 2H), 3.18 (d, $J = 6.1$ Hz, 2H), 2.12 (t, 7.0, 2H), 2.01–1.88 (m, 4H), 1.86–1.78 (m, 1H), 1.64–1.48 (m, 7H), 1.44 (s, 9H), 1.40–1.33 (m, 2H); ^{13}C NMR (500 MHz, CDCl_3) δ 171.9, 156.6, 155.9, 134.6, 133.1, 123.8, 117.8, 80.16, 65.6, 54.5, 40.5, 37.7, 37.3, 32.2, 29.7, 28.5, 28.0, 25.4, 22.9, 22.6, 22.5; HRMS (ESI): m/z calculated for $\text{C}_{23}\text{H}_{39}\text{N}_3\text{O}_5\text{Na}$ $[\text{M}+\text{Na}]^+$ 460.2787, found 460.2790.

Allyl (S)–(5-amino-6-((2-(cyclohex-1-en-1-yl)ethyl)amino)-6-oxohexyl)carbamate, 3.16d.



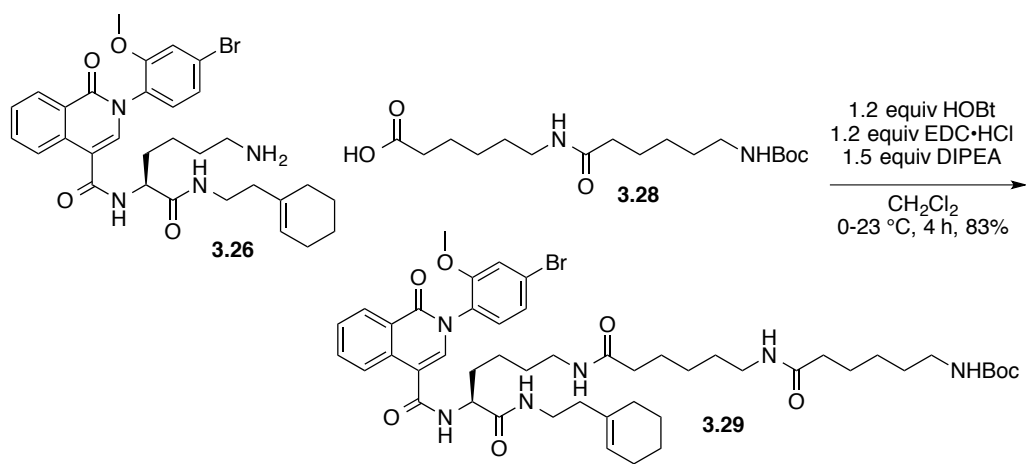
Following the same procedure for the amine synthesis of **3.16c**, Boc-protected amine **3.15d** (0.69 g, 1.6 mmol, 1.0 equiv) and ethylene glycol (27 mL, 0.046 M with respect to **3.15d**) were used. The amine product **3.16d** (0.43 g, 1.6 mmol, 99%) was isolated as a yellow oil. $R_f = 0.36$ (1:1 EtOAc:hex). ^1H NMR (500 MHz, CDCl_3) δ 7.22 (br s, 1H), 5.94–5.89 (m, 1H), 5.46 (s, 1H), 5.30 (d, $J = 17.2$ Hz, 1H), 5.21 (d, $J = 10.4$ Hz, 1H), 4.90 (s, 1H), 4.55 (d, $J = 5.3$ Hz, 2H), 3.36–3.28 (m, 3H), 3.19 (q, $J = 6.4$ Hz, 2H), 2.13 (t, $J = 6.4$ Hz, 2H), 2.01–1.90 (m, 4H), 1.85–1.78 (m, 1H), 1.65–1.35 (m, 11H); ^{13}C NMR (500 MHz, CDCl_3) δ 174.8, 156.5, 134.8, 133.1, 123.5, 117.7, 65.5, 55.2, 40.7, 37.8, 36.9, 34.8, 29.9, 28.0, 25.4, 22.94, 22.92, 22.5; HRMS (ESI): m/z calculated for $\text{C}_{18}\text{H}_{31}\text{N}_3\text{O}_3\text{Na}$ $[\text{M}+\text{Na}]^+$ 360.2263, found 360.2259.

(S)-N-(6-amino-1-((2-(cyclohex-1-en-1-yl)ethyl)amino)-1-oxohexan-2-yl)-2-(4-bromo-2-methoxyphenyl)-1-oxo-1,2-dihydroisoquinoline-4-carboxamide, 3.26.¹³⁰



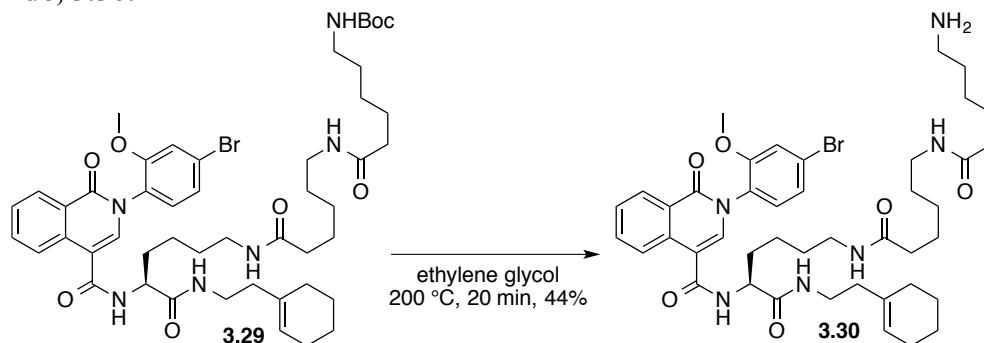
A flame-dried round bottom flask was charged with alloc protected amine **3.25** (0.20 g, 0.29 mmol, 1.0 equiv) and a stir bar. Next, 3:1 CH₂Cl₂/DMF (40 mL, 0.0073 M with respect to **3.25**) was added to the flask via syringe. Afterwards, phenylsilane (3.6 mL, 2.9 mmol, 100 equiv) was added to the flask drop wise via syringe over 3 min. After 15 min, Pd(PPh₃)₄ (0.067 g, 0.060 mmol, 20 mol%) was added by lifting up the septum. The reaction was monitored by TLC for disappearance of **3.25**. Upon consumption of the **3.25** (1 h), the reaction mixture was cooled to room temperature. Next, the organic layer was washed with water (5x100 mL) followed by brine and dried over Na₂SO₄. The resulting solution was concentrated *in vacuo* and purified with flash chromatography (CH₂Cl₂:MeOH) to yield amine **3.26** (0.12g, 0.20 mmol, 70%) as a brown solid. R_f = 0.75 (5:1 Acetone: CH₂Cl₂). ¹H NMR (500 MHz, CDCl₃) δ 8.42 (d, *J* = 8.0 Hz, 1H), 8.12 (d, *J* = 8.1 Hz, 1H), 7.70, (t, *J* = 7.7 Hz, 1H), 7.54–7.32 (m, 4H), 7.25–7.11 (m, 3H), 5.40 (s, 1H), 4.70 (q, *J* = 5.8 Hz, 1H), 3.77 (s, 3H), 3.35–3.16 (m, 2H), 2.95 (br s, 3H), 2.64 (d, *J* = 14.4 Hz, 1H), (br s, 2H), 1.94–1.43 (m, 14H); ¹³C NMR (500 MHz, CDCl₃) δ 171.5, 166.8, 161.5, 155.3, 134.8, 134.6, 134.1, 133.3, 130.2, 128.8, 128.3, 127.8, 2.10 126.0, 124.7, 124.3, 124.0, 123.4, 116.1, 113.0, 56.4, 53.2, 39.4, 38.0, 37.7, 32.6, 28.1, 26.9, 25.4, 23.0, 22.6, 22.4; HRMS (ESI): *m/z* calculated for C₃₁H₃₇BrN₄O₄H [M + H]⁺ 609.2076, found 609.2076.

***Tert*-butyl (*S*)-6-(((6-((5-(2-(4-bromo-2-methoxyphenyl)-1-oxo-1,2-dihydroisoquinoline-4-carboxamido)-6-((2-(cyclohex-1-en-1-yl)ethyl)amino)-6-oxohexyl)amino)-6-oxohexyl)amino)-6-oxohexyl)carbamate, **3.29**.**



Following the same procedure for the synthesis of amide **3.16b**, amine **3.26** (0.050 g, 0.082 mmol, 1.0 equiv) and carboxylic acid **3.28** (0.026 g, 0.075 mmol, 1.0 equiv), were used. The crude material was purified by flash chromatography using CH₂Cl₂:MeOH to give amide **3.29** (0.058 g, 0.068 mmol, 83%) as a yellow solid. $R_f = 0.37$ (9:1 CH₂Cl₂:MeOH). ¹H NMR (500 MHz, CDCl₃) δ 8.44 (d, $J = 8.2$ Hz, 1H), 8.20 (br s, 1H), 7.73 (t, $J = 8.0$ Hz, 1H), 7.55 (t, $J = 8.0$ Hz, 1H), 7.46 (s, 1H), 7.25–7.15 (m, 3H), 6.73 (br s, 1H), 6.19 (br s, 1H), 6.02 (br s, 1H), 5.42 (s, 1H), 4.70 (s, 1H), 4.57 (s, 1H), 3.79 (s, 3H), 3.41 – 3.03 (m, 8H), 2.15–1.12 (m, 42); ¹³C NMR (500 MHz, CDCl₃) δ 173.5, 173.2, 171.6, 165.5, 161.6, 156.2, 155.3, 134.6, 134.3, 133.3, 130.0, 128.6, 128.4, 127.9, 127.8, 126.0, 124.9, 124.2, 123.9, 123.6, 116.1, 114.0, 133.6, 79.2, 56.3, 53.5, 40.5, 39.1, 37.7, 37.6, 36.6, 36.4, 29.9, 29.8, 29.2, 29.1, 28.5, 28.0, 26.5, 26.3, 25.5, 25.3, 25.2, 22.9, 22.7, 22.5; NMR (500 MHz, CDCl₃) δ HRMS (ESI): m/z calculated for C₄₈H₆₇BrN₆O₈Na [M+Na]⁺ 957.4102, found 957.4105.

(S)-N-(6-(6-(6-aminohexanamido)hexanamido)-1-((2-(cyclohex-1-en-1-yl)ethyl)amino)-1-oxohexan-2-yl)-2-(4-bromo-2-methoxyphenyl)-1-oxo-1,2-dihydroisoquinoline-4-carboxamide, 3.30.



Following the same procedure for the synthesis of amine **3.15ba**, Boc-protected amine **3.29** (0.050 g, 0.053 mmol, 1.0 equiv) and ethylene glycol (1.2 mL, 0.044 M with respect to **3.29**) were used. The amine product **3.30** (0.019 g, 0.023 mmol, 44%) was isolated as a yellow solid. $R_f = 0.32$ (47:3 CH₂Cl₂:MeOH). ¹H NMR (500 MHz, CDCl₃) δ 8.45 (d, $J = 7.6$ Hz, 1H), 8.2 (br s, 1H), 7.74 (br s, 1H), 7.55 (br s, 1H), 7.46 (s, 1H), 7.26–7.10 (m, 3H), 6.81 (br s, 1H), 6.72 (br s, 1H), 6.07 (br s, 1H), 5.98 (br s, 1H), 5.44 (s, 1H), 4.57 (br s, 1H), 4.10 (br s, 1H), 3.80 (s, 1H), 3.80–3.10 (m, 8H), 2.70–1.10 (m, 33); ¹³C NMR (500 MHz, CDCl₃) δ 174.3, 171.6, 168.8, 161.6, 155.4, 153.4, 134.6, 134.3, 133.3, 130.1, 128.7, 128.4, 127.9, 127.8, 124.9, 124.3, 124.0, 123.7, 116.1, 114.0, 56.4, 53.4, 39.1, 37.7, 37.6, 36.7, 36.5, 32.1, 31.1, 29.84, 29.80, 29.3, 28.0, 26.5, 26.3, 25.5, 25.3, 25.2, 22.9, 22.8, 22.4; HRMS (ESI): m/z calculated for C₄₃H₅₉BrN₆O₆H [M + H]⁺ 835.3758, found 835.3785.

Biological evaluations

Strains, media, and compounds: The *C. albicans* strain HLY4123 was used as the susceptible laboratory strain for the antifungal evaluation in this study. HLY4123 carries a GFP reporter for ERG3 expression and was constructed by plasmid transformation of the commonly used laboratory *C. albicans* strain CAI4. The strains were cultured at 30 °C under constant shaking (200rpm) in synthetic complete (SC) medium containing 2% glucose. The stock solution

of fluconazole (Sigma–Aldrich, USA) was prepared in sterile H₂O (0.1 mg/mL), whereas the other test compounds were prepared in DMSO.

Dose–response curves for test compounds against *C. albicans* with and without fluconazole:

C. albicans was grown in SC medium overnight and then diluted to an effective OD₆₀₀ of 0.0625. Serial ten- fold dilutions of the test compounds (0.15–1500 µM) were prepared in DMSO in 1.5 mL Eppendorf tubes. To each well in columns B–D (triplicate analysis) of a 24- well Falcon plate was added 2.5 µL of fluconazole solution. To each well in all four columns of the plate was added 1 mL of cells in SC medium such that column A served as a control to assess the EC₅₀ value of the compound in the absence of fluconazole. Then to each well in rows 2–5 was added a solution of the compound in DMSO (2 µL each) such that the final fluconazole concentration in columns 2–4 was 0.25 µg/mL, and the concentration of compound in each row varied from 0.003 to 30 µM. The plates were incubated in a rotary shaker/incubator at 30 °C for 16 h. The contents of each well were re-suspended with a micropipettor and a 20 µL aliquot was added to a polystyrene cuvette and diluted with 680 µL deionized water. The suspension was triturated again immediately before measuring the absorbance at $\lambda = 600$ nm (OD₆₀₀) for cell densities. EC₅₀ values were determined by fitting to a standard curve using the Excel- based tool ED50PLUS v. 1.0 (Mario H. Vargas).

Chapter 4

Reactivity of Palladium-Carbene Intermediates

Introduction

Transition metal-catalyzed reactions play a vital role in synthetic organic chemistry as one of the most powerful and direct ways to access complex molecules. Among many transition metals, palladium catalysts and reagents have proved to be more useful and versatile in organic synthesis.¹³¹ The facility of oxidative addition under mild reaction conditions, the tolerance of many polar functional groups and the high degree of chemo-, regio- and stereoselectivity makes Pd-catalysis uniquely suitable for an array of organic transformations.¹³¹ Therefore, novel reactive intermediates involving palladium catalysis allow unique bond disconnections that will be enormously useful in complex molecule synthesis.¹³² In this regard, palladium-carbene intermediates provide a very interesting starting point to explore.

Palladium-carbenes can potentially be coupled with a variety of other reactions accessible to Pd, such as oxidative addition, reductive elimination, and migratory insertion.¹³¹ This provides an opportunity to incorporate the carbene units, during other palladium mediated transformations in modular synthesis of complex molecules.¹³² Recent work in this research area utilizes such transient carbene units in multi-component coupling reactions as cross-coupling partners.¹³³

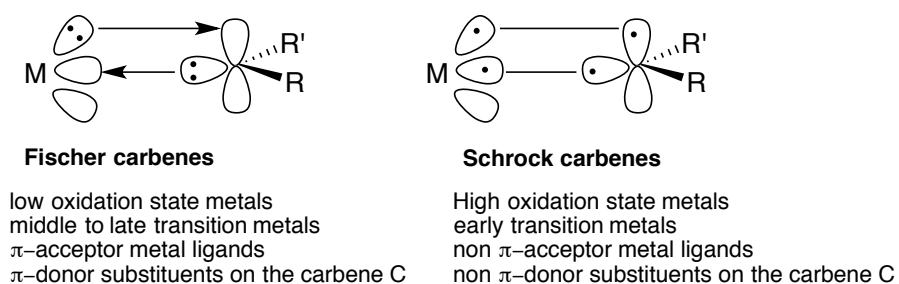
This chapter discusses the synthetic methods and reactivity of palladium-carbenes and their utility in organic synthesis.

Palladium-Carbenes

Metal-carbenes are organometallic complexes that consist of divalent carbon ligands. There are two extremes of metal-carbenes: Fischer carbenes and Schrock carbenes (Figure 4-1). Fischer carbenes arise from two different bonding interactions. One interaction is between a filled

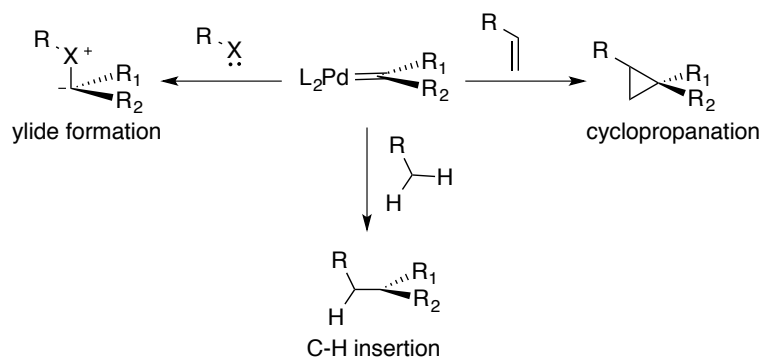
d_{yz} orbital of the metal and an empty p-orbital of the carbon and the second interaction occurs between a filled sp^2 orbital of the carbon and an empty d_z^2 orbital of the metal. Middle to late transition metals with low oxidation states prefer to make Fischer carbenes and they are generally electrophilic in the carbene carbon. The π -donor substituents on the carbene carbon generally stabilize the metal-carbene complex in Fischer carbenes. Conversely, Schrock carbenes are nucleophilic in the carbene center.

Figure 4-1: Depictions of Fischer and Schrock Carbenes



Palladium carbenes are classified as a Fischer carbene because palladium is a late transition metal and exhibit electrophilic character at the carbene carbon. Carbenes arising from palladium(0) intermediates show distinct reactivities from alkylpalladium(II) carbenes. Palladium(0) carbene intermediates efficiently participate in cyclopropanation reactions,¹³⁴ ylide formations,¹³⁵ and C–H insertions (Figure 4-2).¹³⁶ Palladium-catalyzed cyclopropanation reactions that proceed via carbene intermediates involve an initial palladacyclobutane formation followed by a reductive elimination to generate a cyclopropane. The cyclopropanation reaction is generally stereospecific. Unlike rhodium(II) acetate-catalyzed cyclopropanation reactions palladium-catalyzed reactions go through unimolecular migratory insertion. Therefore the efficiency of the reaction depends on the ligand's ability to ligate to palladium(0).

Figure 4-2: Pd(0)-Carbene Catalyze Cyclopropanations , C–H insertions and Ylide Formations

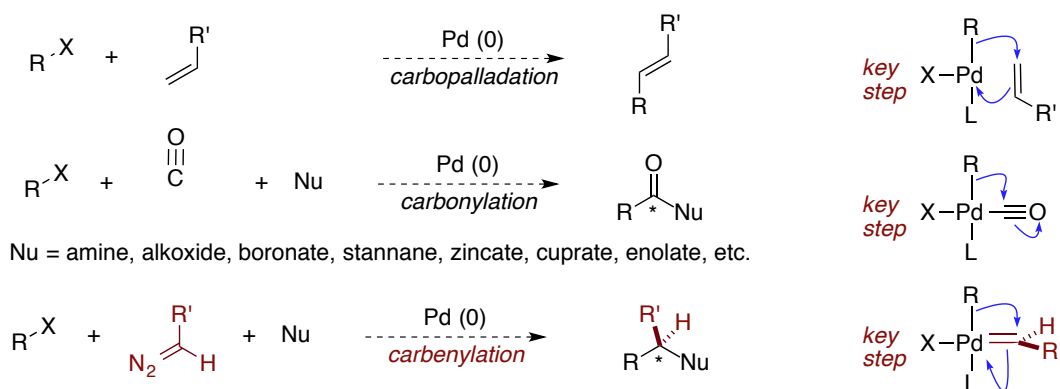


Palladium(II) carbene intermediates comprise of a more electrophilic carbene carbon than the carbene carbon in a palladium(0) carbene intermediates. Additionally, palladium(II)-carbene complexes generally contain anionic ligands that rapidly migrate to the electron-deficient carbene carbon. The resulting alkylpalladium complex can be trapped with nucleophiles or undergo β -hydride elimination. For the past ten years reactions exploiting the migratory insertions in alkylpalladium(II) complexes have become a very exciting field of exploration.¹³⁷

Palladium-Catalyzed Carbenylation

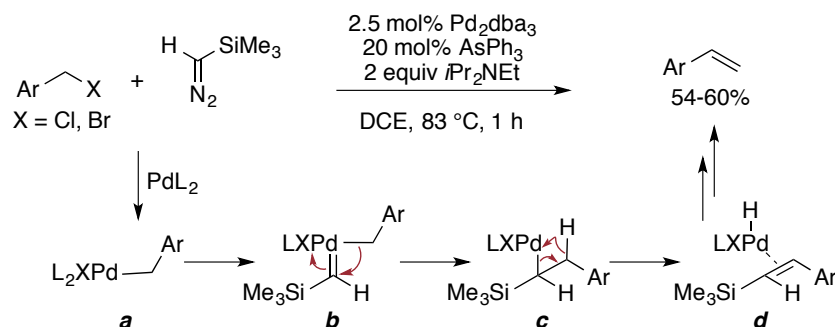
Migratory insertion is one of the most important elementary reactions in organometallic chemistry, especially in Pd-catalyzed transformations. In carbopalladation, the key step in Heck reaction, a two-carbon unit inserts into a Pd–C bond, whereas in carbonylation with CO and carbenylation a one-carbon unit inserts into a Pd–C bond (Figure 4-3). Carbonylation is utilized as a powerful tool for inserting an sp^2 carbon during related transformations. Carbenylation also offers a way to insert an sp^3 carbon; unlike carbonylation, carbenylation provides a new and powerful mode of enantioselective insertion of the one-carbon unit. Therefore, exploiting new methods of carbenylation that leads to C–C bond formation would tremendously benefit synthetic organic chemistry.¹³⁸

Figure 4-3: Comparison of Migratory Insertions



In 2001, Van Vranken and co-workers demonstrated the first example of catalytic cross-coupling reaction involving Pd-carbenes (Figure 4-4).¹³⁹ It is hypothesized that the formation of benzylpalladium(II) carbene intermediate **b** is initiated by the oxidative addition of the benzyl halide to form **a** followed by the trapping by trimethylsilyldiazomethane. Intermediate **b** undergoes migratory insertion to give alkylpalladium **c**, which readily undergoes β -hydride elimination to form the palladium•olefin complex **d**. subsequent hydride transfer and protodesilylation leads to the styrene adduct. Although the reaction has a few limitations with the scope and the efficiency, it provided an excellent avenue to explore effective transformations involving migratory insertions into palladium-carbenes.¹³³

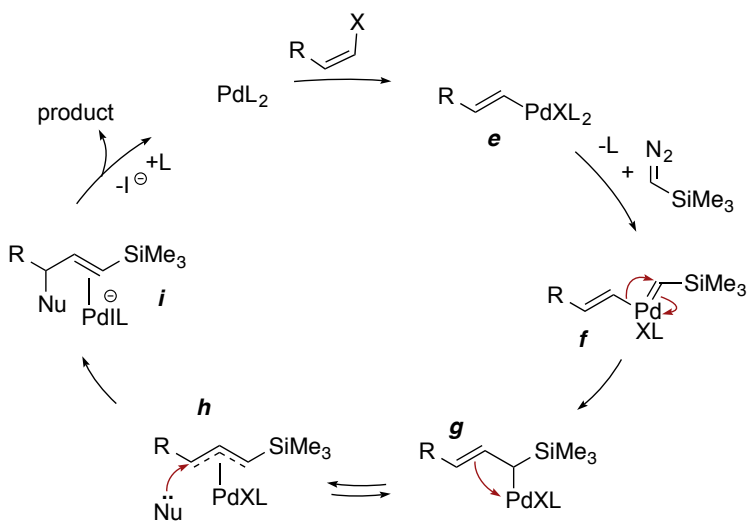
Figure 4-4: Pd-Catalyzed Carbenylative Coupling Between Aryl Halides and TMSCHN₂



Palladium-Carbenes to π -Allylpalladium Intermediates

The Van Vranken group has discovered that when a vinyl moiety migrates to a carbene center (intermediate **f**) it gives rise to an η^1 -allylpalladium intermediate (intermediate **g**). Upon isomerizing to η^3 -allylpalladium intermediate (intermediate **h**) it can be trapped with nucleophiles to afford chiral vinylsilane adducts in a single step.^{140,141}

Figure 4-5: Proposed Mechanism for the Nucleophilic Trapping after Carbenylative Insertion

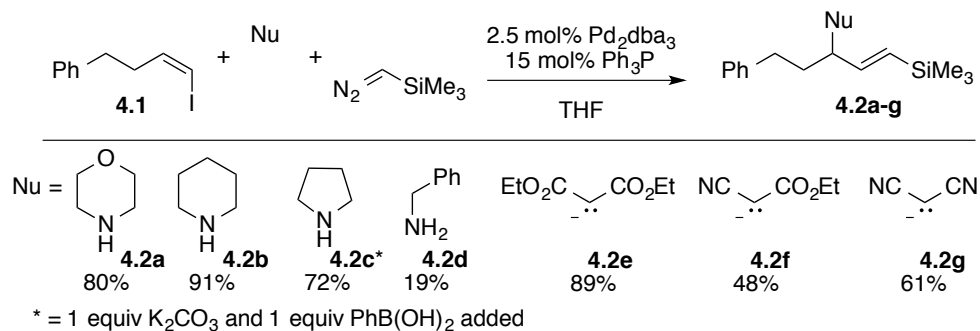


Trapping of π -Allylpalladium Intermediates Generated from Palladium-Carbenes

The nucleophilic trapping of η^3 -allylpalladium intermediates generated from palladium carbenes was successfully utilized to synthesize a variety of vinylsilanes from different nucleophiles (Figure 4-6). During the initial optimization, when *E*-styrylbromide and arylstannane were used as coupling partners, palladium catalyzed homocoupling of *E*-styrylbromide was observed. This was attributed to the carbapalladation of the styryl bromide by the vinylpalladium bromide, followed by β -elimination of PdBr_2 , which is reduced back to palladium(0) by the arylstannane. Therefore, to avoid this competitive Heck-dimerization Van Vranken group utilized vinyl halides with aliphatic substituents and enolate nucleophiles instead of aryl-substituted alkenes and arylstannane nucleophiles.

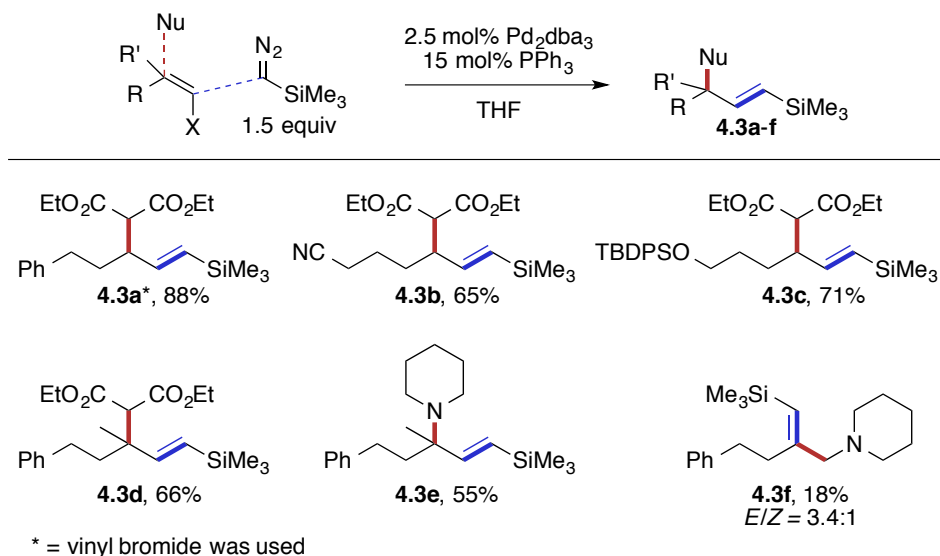
Cyclic amine nucleophiles were superior to the acyclic amines such as benzylamine (compounds **4.2a-d**). When pyrrolidine was included as the nucleophile, formation of catalytically inactive palladium(II) salts were noted. Addition of phenylboronic acid effectively regenerated active palladium(0) catalyst and afforded the corresponding vinylsilane adduct, **4.2c** in good yield. Utilizing (*E*)- **4.1** resulted in reduced 11% yield, probably due to the decreased rate of migratory insertion in a sterically unnumbered environment. Stabilized carbon nucleophiles required larger amounts of the corresponding nucleophile (4 equiv of amines vs. 12 equiv of malonates) and elevated temperatures (46 °C for amines vs. 66 °C for malonates) to afford products in reasonable yields.

Figure 4-6: Pd-Catalyzed Three-Component Coupling



The scope of the vinyl iodide was analyzed in the Pd-catalyzed carbonylative coupling reaction. Under the optimized reaction conditions both vinyl iodides and vinyl bromides resulted in comparable yields suggesting similar efficiencies (Figure 4-6, compound **4.2e** and Figure 4-7, compound **4.3a**). Cyano substituents and silyl protected hydroxyl groups were tolerated under the reaction conditions (compounds **4.3b** and **4.3c**). Both stabilized carbon nucleophiles and amines participated in the three-component coupling with geminally-substituted vinyl iodides to afford **4.3d** and **4.3e** in slightly lower efficiencies. Finally a reaction with an internal vinyl iodide resulted in a sluggish reaction to afford vinyl silane **4.3f** in 18% yield.

Figure 4-7: Scope of Vinyl Halide in Carbenylative Three-Component Coupling

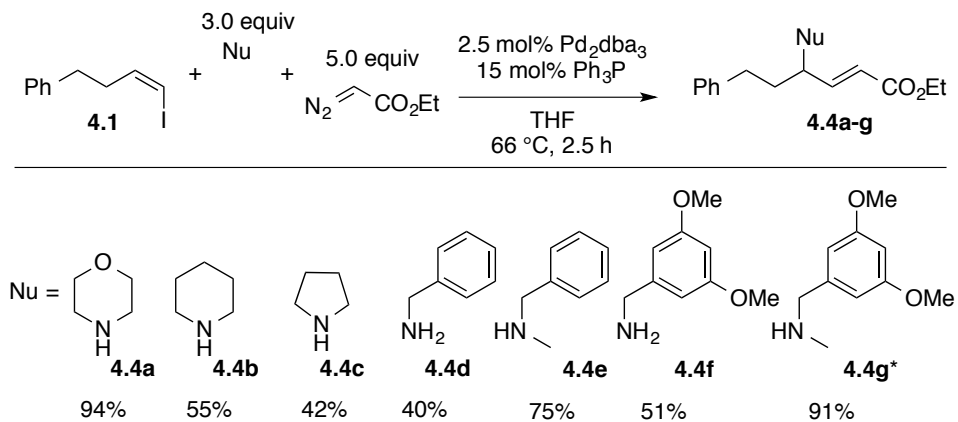


Next, trimethylsilyldiazomethane was replaced with ethyl diazoacetate (EDA) as the carbene precursor to gain access to α,β -unsaturated γ -amino esters, common pharmacophores in covalent cysteine protease inhibitors (Figure 4-8).¹⁴² Morpholine reacted more efficiently compared to the other cyclic amines to afford **4.4a** in 94% yield (compounds **4.4a-c**). Secondary amines were superior to the primary amine counterparts, probably due to the more nucleophilic character on N atom in secondary amines (compounds **4.4d-g**). Addition of triethylamine as a sacrificial amine increased the yields from 42% to 62% in formation of **4.4c**. In subsequent reactions that are not described in this report, Kudrika and co-workers discovered that *Z*-vinyl iodides participate in the more efficient coupling reactions compared to *E*-vinyl iodides.

Overall, the pioneering work by the Van Vranken group paved the way to understanding the utility of palladium-catalyzed carbenylation in useful transformation. Followed by these initial findings, the Van Vranken group and several other groups have reported new transformations that resulted from trapping carbene insertion intermediates arising from diazo compounds with nucleophiles other than amines and stabilized anions. These reactions include

incorporating carbenylation with a heck reaction to form indenenes and indenyl amines.¹⁴³ Also, Wang and co-workers were able to trap the intermediates of their carbenylation reaction with aryl boronic acids.¹⁴⁴

Figure 4-8: Pd-Catalyzed Three-Component Coupling with EDA



* = 5 mol% Pd₂dba₃ was added

Conclusion

In this chapter I described the general reactivity of metal-carbenes with emphasis on Pd-carbenes. Mechanistically, palladium(0)-carbenes show distinct reactivities compared to Pd(II)-carbenes. Migration of anionic ligands in palladium(II) to the carbene center opens up a new avenue to explore new C–C and C–heteroatom bond formations. During the past 10 years, the carbenylation process was exploited successfully and as a future prospect, controlling the migration to form enantioenriched adducts will provide a powerful tool in organic synthesis.

Chapter 5

Carbenylative Coupling Involving Palladium Alkylidene Intermediates

Alkylidene Precursors in Palladium-Catalyzed Carbenylative Coupling Reactions

Metal-carbene intermediates are involved in a wide variety of transformations.¹⁴⁵ During the early work, diazo compounds served as the sole carbene precursors. Generally, diazo compounds are stabilized anions and the π -acceptor groups such as carbonyl or phenyl moieties are present to stabilize the anion. Therefore, compounds that do not present π -acceptor groups such as diazoalkanes (alkylidines) are highly unattractive starting materials due to their explosive nature and toxicity.¹⁴⁶

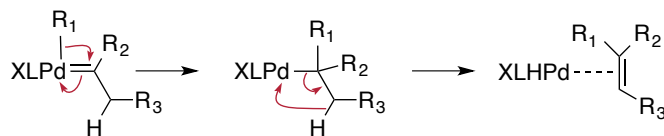
The discovery of the utility of *N*-tosylhydrazone as carbene precursors tremendously increased the substrate scope of the carbenylative coupling reactions. In the presence of base, *N*-tosylhydrazones undergo Bamford-Stevens reaction to form corresponding diazo compounds *in situ*.¹⁴⁷ Aggarwal and co-workers successfully utilized *N*-tosylhydrazones to deliver unstabilized diazo compounds in iron- and rhodium-catalyzed cyclopropanations and olefination reactions.¹⁴⁸ In 2007, Barluenga and co-workers efficaciously implemented *N*-tosylhydrazones in Pd-catalyzed carbenylations to synthesize poly-substituted olefins.¹⁴⁹ Several other less common classes of compound such as tethered alkynes,¹⁵⁰ diazirines,¹⁵¹ Fischer carbenes,¹⁵² and chloroform¹⁵³ were also employed as carbene precursors in several other transformations.

β -Hydride Elimination in Processes Involving Pd-Alkylidene Intermediates

Palladium(II) alkylidenes that possess hydrogens adjacent to the carbene center rapidly undergo β -hydride elimination causing the carbene center to end up as an sp^2 center (Figure 5-1). Such a process can be exploited as a way to regenerate active Pd(0) catalyst upon reductively eliminating HX. However, β -hydride elimination takes away the opportunity to preserve the

stereochemical information gained from the migratory insertion of anionic ligand to the carbene center.

Figure 5-1: Palladium(II) Alkylidene Leads to β -Hydride Eliminations



β -hydride Elimination With Pd-alkylidenes Generated from Ketone Hydrazones

Ketone *N*-tosylhydrazone and ArPdX from Arylhalides/pseudohalides in Pd-catalyzed carbenylative coupling

Barluenga and co-workers reported the first example of a palladium-catalyzed carbenylative coupling with *N*-tosylhydrazones (Scheme 5-2).¹⁴⁹ The scope of the alkylidienes was previously limited by the stability of the diazo precursor. However, employing *N*-tosylhydrazones as carbene precursors greatly increased the scope of carbenylative coupling reactions. Many groups have demonstrated the ability to utilize several R-X functional groups such as aryl halides¹⁵⁴ and pseudohalides such as nonaflates¹⁵⁵ as well as alkenyl pseudohalides such as alkenyl tosylates¹⁵⁶ as coupling partners in such transformations.

The proposed mechanism for the palladium-catalyzed carbenylative coupling with ketone *N*-tosylhydrazone involves an initial oxidative addition of an aryl/alkyl halide to palladium(0) to form RPdX intermediate **b**. *N*-tosylhydrazone reacts with the base to form the corresponding diazo compound *in situ*. Incorporation of the diazo moiety results in palladium alkylidene intermediate **c**. Migration of the aryl/alkyl group to the carbene center generates alkylpalladium halide intermediate **d**, which then undergoes rapid β -hydride elimination to yield alkene product. Reductive elimination of HX from palladium(II) hydride regenerates the active palladium(0) catalyst.

Figure 5-2: Representative Examples of Pd-Catalyzed Carbenylative Coupling with Ketone *N*-Tosylhydrazone and ArPdX from Arylhalides/pseudohalides

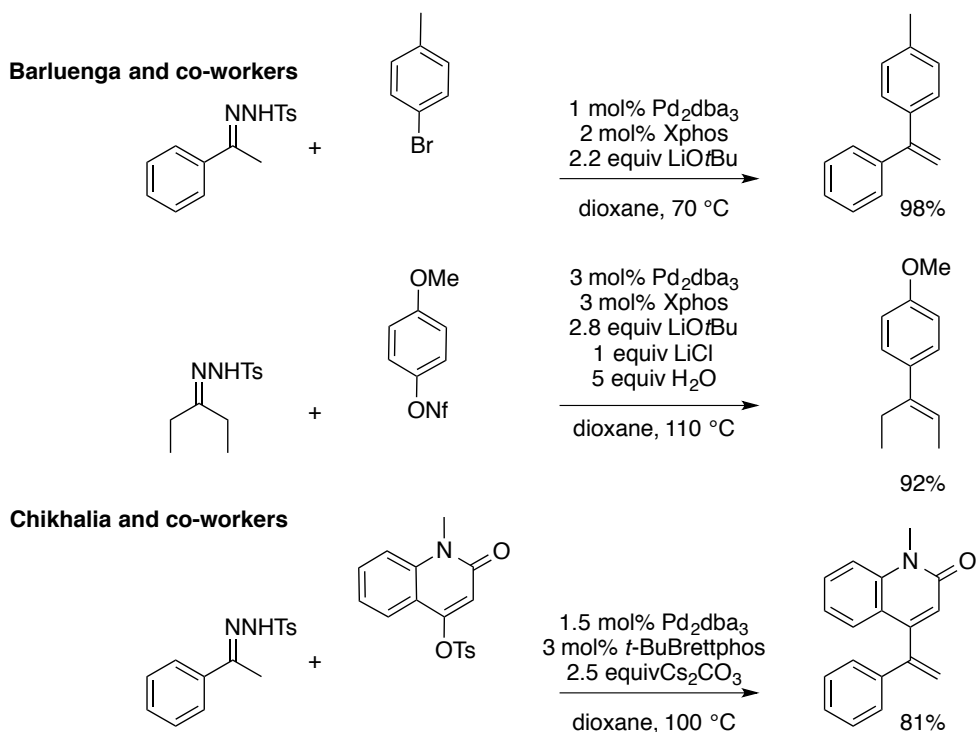
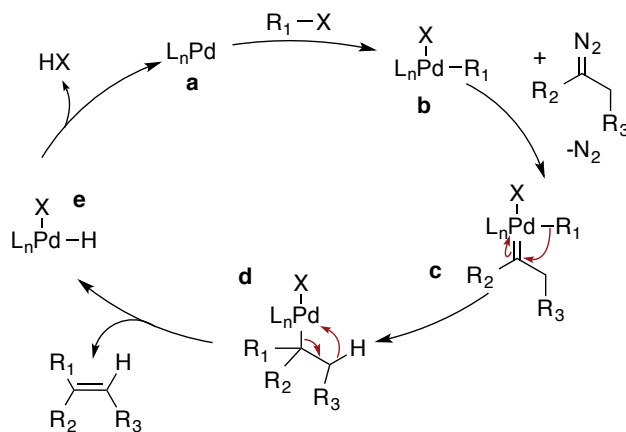


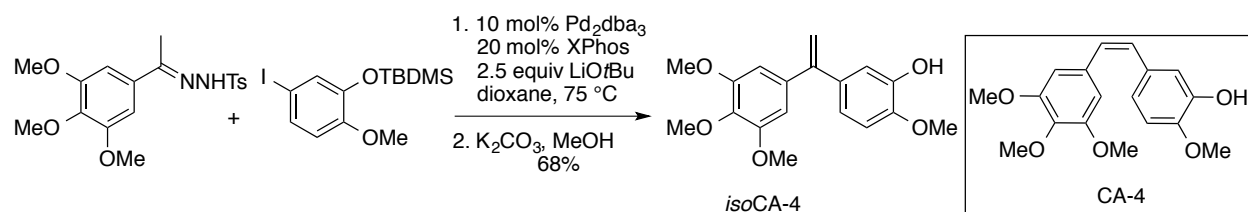
Figure 5-3: Proposed Reaction Mechanism for the Palladium-Catalyzed Carbenylative Coupling with Ketone *N*-Tosylhydrazone



Synthesis of combrestatin A-4 (CA-4), a potent cytotoxic agent and its analogues have been readily accessed by palladium-catalyzed carbenylative coupling reactions (Figure 5-4). Petit and co-workers isolated combrestatin A-4, a *Z*-stilbene from an Eastern Cape South African bushwillow tree, *Combretum caffrum*.¹⁵⁷ It has been shown that combrestatin A-4 is potently

cytotoxic to a variety of cancer cells and it is the most studied example of vascular disrupting agents that bind on β -tubulin at the colchicine binding site.¹⁵⁸ However, over time combrestatin A-4 isomerizes into its less cytotoxic (*E*)-isomer. Several analogues of CA-4, such as *isocombretastatin A-4*, (*isoCA-4*), *isoNH₂CA-4*, *isoFCA-4* have been shown to be active in nanomolar concentrations against several cancer cell lines. The palladium-catalyzed carbenylative coupling reactions have been utilized to readily access the 1,1-diarylethylene motifs in CA-4 and its analogues.¹⁵⁹

Figure 5-4: Synthesis of *isoCA-4* and the Structure of *Combretastatin A-4* (CA-4)



Ketone *N*-tosylhydrazones and ArPdX derived from Nucleophiles and Oxidants in Pd-catalyzed Carbenylative Coupling

Under oxidative conditions palladium-alkylidene intermediates react with boronic acids^{144,160} and indoles and other nitrogen-containing heterocycles such as carbazole, 1,2,3,4-tetrahydrocarbazole, pyrrole, 1,5,6,7-tetrahydro-4H-indol-4-one, benzimidazole, and imidazole¹⁶¹ to afford corresponding substituted olefin products (Figure 5-5). Mechanistically, these transformations are similar to the reactions shown in Figure 5-2, except palladium(II) intermediates were accessed via oxidation of palladium(0) by utilizing various different oxidants such as molecular oxygen,^{146b,d,147a} benzoquinone,^{144,146b} and iodobenzene.^{147b,c}

Terminal alkynes were also used in palladium-catalyzed coupling reactions under oxidative conditions (Figure 5-6).¹⁶² Weak electron-rich tris-(2-furyl)phosphine ligands were used to facilitate the formation of alkynylpalladium(II) intermediate. The reaction tolerates a

wide variety of *N*-tosylhydrazones and terminal alkynes. Conjugated enynes were also synthesized with high >20:1 *Z/E* selectivity.

Figure 5-5: Representative Examples of Palladium-Catalyzed Oxidative Carbenylative Couplings

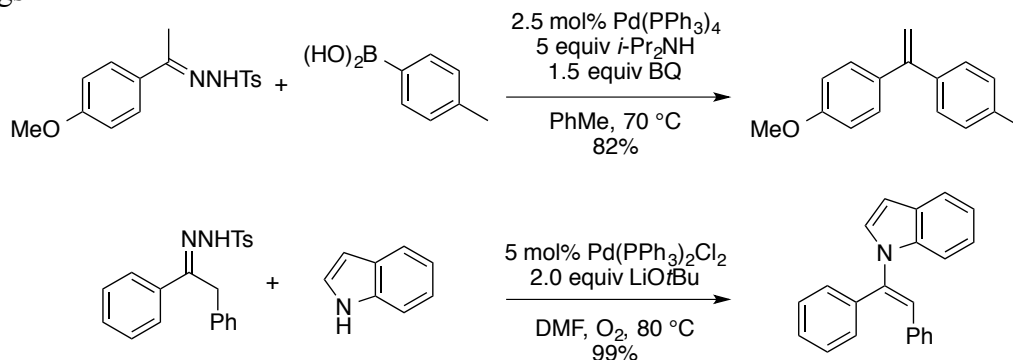
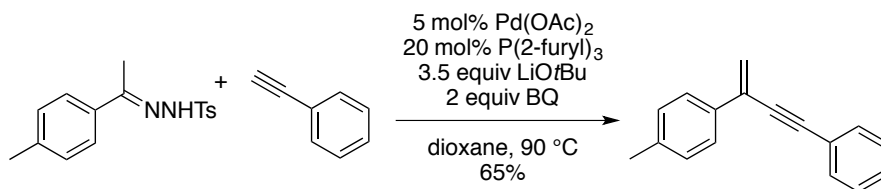


Figure 5-6: Pd-Catalyzed Oxidative Coupling of Terminal Alkynes with *N*-Tosylhydrazone



Ketone *N*-tosylhydrazone and ArPdX or ArCOPdX Derived from Tandem Reactions in Pd-catalyzed Carbenylative Coupling

In 2010, Wang and co-workers demonstrated that *N*-tosylhydrazones could participate in tandem carbonylative cross-coupling reactions.¹⁶³ Upon oxidative addition of the aryl iodide the aryl group on the palladium intermediate migrates to a carbon monoxide ligand to result in a benzoyl group. The benzoyl group can then migrate to the alkylidene moiety to form an alkylpalladium intermediate (Figure 5-7). Consequent β -hydride elimination results in the enone product **5.1**. Also the alkylpalladium intermediate can be trapped with Et_3SiH to give the ketone adduct **5.2**. The reaction can also be tuned to afford either the enone **5.1** or the ketone **5.2** products by changing the palladium pre-catalyst and the ligand.

Figure 5-7: Pd-Catalyzed Carbonylative Cross-Coupling with *N*-Tosylhydrazone and Aryl Halide

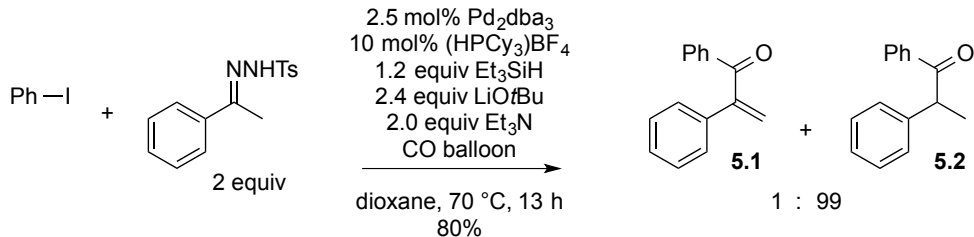
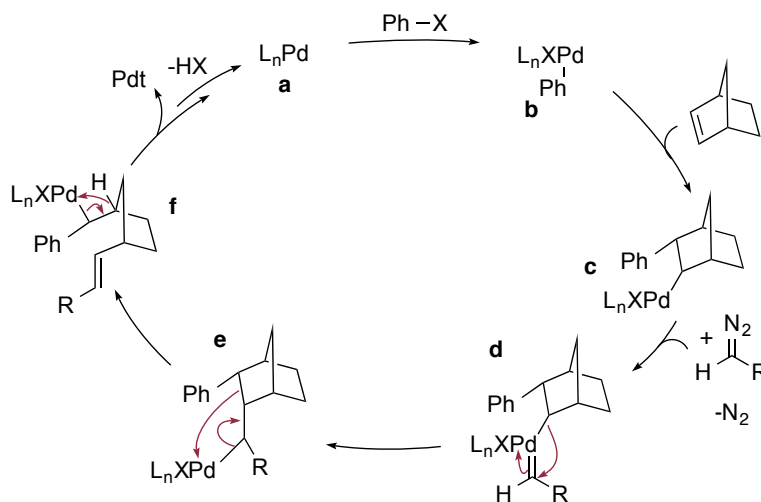
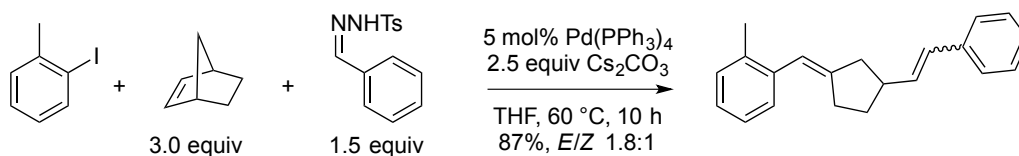


Figure 5-8: Palladium-Catalyzed Ring Opening of Norbornene



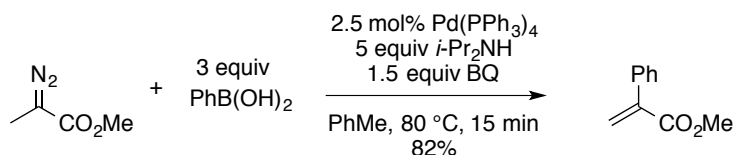
Recently, Liang and co-workers have established that *N*-tosylhydrazone could be involved in palladium-catalyzed ring opening of norbornene to synthesize methylenecyclopentane derivatives (Scheme 5-8).¹⁶⁴ This multi-step domino reaction involves the oxidative addition of aryl halide to afford arylpalladium halide intermediate **b**. Carbopalladation across aryl palladium results in intermediate **c**. Palladium(II) benzyldiene intermediate **d** forms upon incorporation of the diazo compound and alkyl migration to the carbene carbon yields alkyl palladium adduct **e**. C–C bond cleavage followed by β -hydride elimination affords the desired methylenecyclopentane product. A wide range of aryl iodides and

aryl aldehyde *N*-tosylhydrazones tolerated the reaction conditions. Ketone *N*-tosylhydrazones gave lower yields. The authors attributed the lower yields to the less reactive nature of the ketone *N*-tosylhydrazones compared to the corresponding aldehyde substrates and the formation of undesired β -hydride eliminating byproducts.

β -hydride Elimination With Pd-alkylidenes Generated from Diazo Compounds

Diazo compounds are not an ideal carbene precursor in carbenylative couplings due to their high reactivity. However, in 2008, Wang and co-workers reported the first example of α -diazocarbonyl compounds with arylboronic acids to access α -aryl substituted α,β -unsaturated carbonyl compounds (Figure 5-9).¹⁴⁴ The reaction tolerates a wide variety of α -diazocarbonyl compounds such as α -alkyl substituted diazocarbonyl compounds and cyclic and acyclic α -diazoketones. Electron rich aryl groups on the aryl boronic acid facilitate product formation in good yields where electron deficient groups afforded the products in lower yields. Also, a tetra-substituted olefin, which is difficult to access, can be obtained in moderate yields. The same group has shown the utility of palladium-catalyzed carbenylative cross coupling of cyclic α -diazoketones with vinyl boronic acids to synthesize 1,3-diene compounds bearing a ring structure in good yields.^{146b} The reaction with β -substituted vinyl boronic acids proceeded smoothly and α -aryl vinyl boronic acid gave the corresponding products in diminished yields.

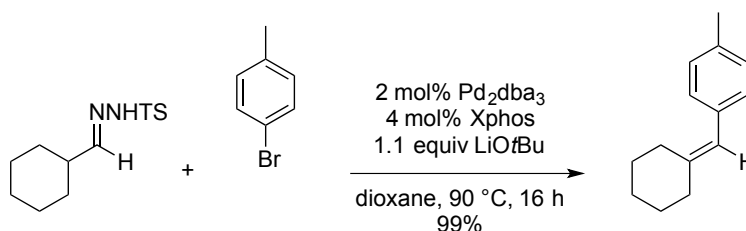
Figure 5-9: Palladium-Catalyzed Carbenylative Coupling of α -Diazocarbonyl Compounds with Arylboronic Acids



β -hydride Elimination With Pd-alkylidenes Generated from Aldehyde Hydrazones

Aldehyde *N*-tosylhydrazones are shown to be more reactive than ketone substrates and aldehyde *N*-tosylhydrazones are very rarely used in carbenylative coupling processes compared to the corresponding ketone *N*-tosylhydrazones.¹⁶⁵ Barluenga and co-workers have demonstrated that aldehyde *N*-tosylhydrazones can engage in palladium-catalyzed carbenylative coupling reactions with aryl halides to afford the corresponding elimination products in high efficiency (Figure 5-10). Aldehyde *N*-tosylhydrazones have shown to give coupling products with both aryl halides and pseudohalides such as triflates and nonaflates with similar efficiencies as their ketone counterparts.

Figure 5-10: Palladium-Catalyzed Carbenylative Coupling of Aldehyde *N*-Tosylhydrazones with Aryl Halides

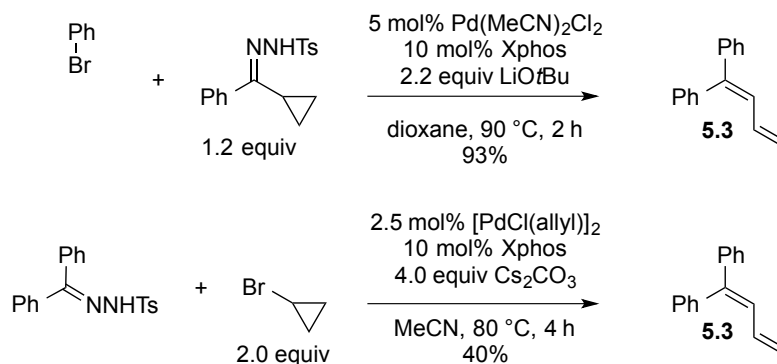


Palladium-catalyzed Carbenylative Coupling Processes with Cyclopropyl Ketone *N*-Tosylhydrazones

Methods to synthesize 1,3-butadiene adducts via cyclopropylmethyl palladium species have been reported. Wang and Yu have independently shown that cyclopropyl *N*-tosylhydrazone with aryl/alkyl halide or ketone *N*-tosylhydrazone with cyclopropyl halide can afford the corresponding 1,3-butadiene products in good to moderate yields (Figure 5-11).¹⁶⁶ When bromocyclopropane was used as the coupling partner the elimination product **5.3** gave significantly lower yields. The transformation demonstrates that when a cyclopropyl group and hydrogen occupy the beta position of the cyclopropylmethyl palladium species the β -alkyl

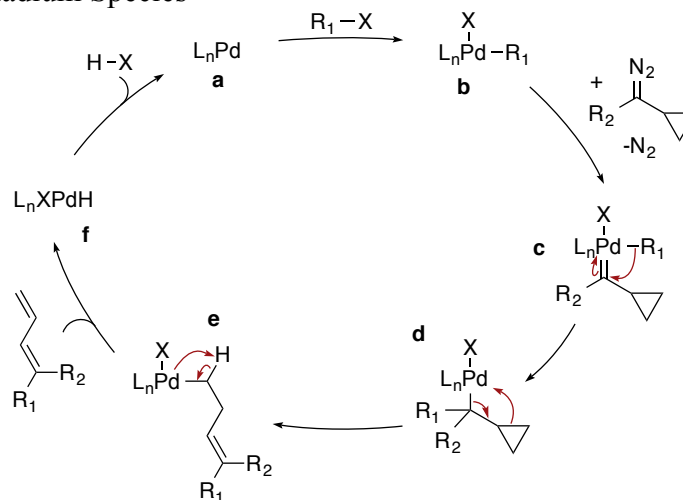
elimination of a strained C–C bond in the 3-membered ring is much faster than the β -hydride elimination.

Figure 5-11: Synthesis of 1,3-Butadiene via Cyclopropylcarbenylpalladium Species



Mechanistically, the initial oxidative addition of aryl halide forms allylpalladium(II) halide intermediate **b**. In the presence of a base *N*-tosylhydrazone decomposes to diazo compound *in situ* and the diazo compound reacts with **b** to afford cyclopropylcarbenylpalladium intermediate **c**. Migratory insertion of the aryl moiety generates cyclopropylcarbinylpalladium intermediate **d**. Upon β -alkyl elimination, homoallylpalladium intermediate **e** undergoes β -hydride elimination to form 1,3 diene product. Final reductive elimination of HX regenerates the active palladium(0) catalyst.

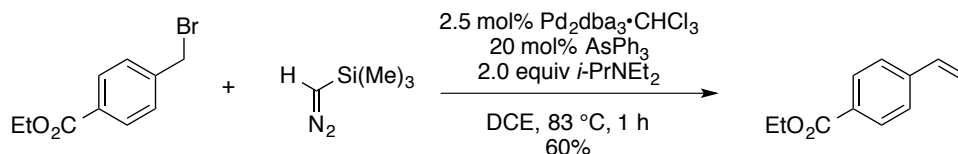
Figure 5-12: Proposed Reaction Mechanism for The Synthesis of 1,3-Butadiene via Cyclopropylcarbenylpalladium Species



Carbenylative Couplings Involving β -Hydride Elimination Toward the Alkyl Halide

Benzyl and allyl halides have been shown to engage in carbenylative coupling processes. Such electrophiles had been utilized in several palladium-catalyzed reactions¹⁶⁷ and in carbenylative coupling reactions the β -hydride elimination occurs on the electrophile in the absence of hydrogens adjacent to the carbene carbon. In 2001, Van Vranken and co-workers have reported the first example of synthesizing styrene derivatives by using (trimethylsilyl)diazomethane (TMSD), benzyl halides and catalytic palladium.¹⁶⁸ Nucleophilic phosphine ligands were avoided in order to prevent substitutions on benzyl bromides.¹⁶⁹ Allyl halides were also shown to participate in the homologation processes with β -hydride elimination on the electrophile.¹⁷⁰

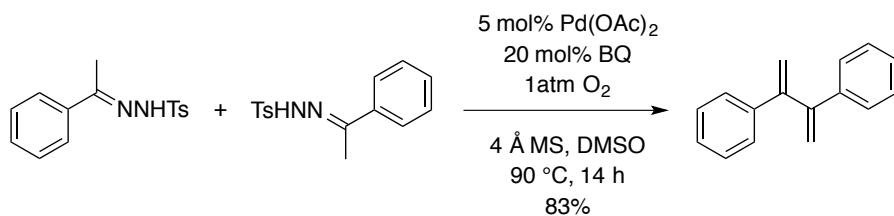
Figure 5-13: Palladium-Catalyzed Homologation of Benzyl Halides with TMSD



Palladium-Catalyzed Homo-coupling Processes Involving β -hydride Elimination

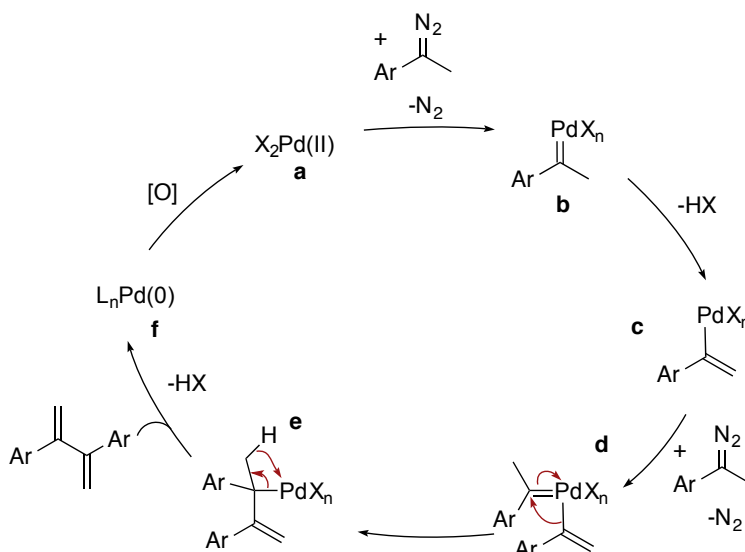
In 2013, both Jiang and Prabhu independently showed that ketone *N*-tosylhydrazone can undergo oxidative homo-coupling in the presence of a palladium catalyst to form 2,3-substituted-1,3-butadiene adducts (Figure 5-14).^{171,172} The reaction tolerated a wide variety of substitutions on both the aryl ring and the α -carbon. Electron donating moieties on the aryl ring tended to give relatively higher yields and *vice versa*. Also α -substitution showed good levels of *E/Z* selectivities on the resulting branched dienes.

Figure 5-14: Pd-Catalyzed Oxidative Homo-coupling of *N*-Tosylhydrazones



A plausible mechanism for the palladium-catalyzed oxidative homo-coupling of *N*-tosylhydrazones is proposed in Figure 5-15. Diazo compounds that formed via Bamford-Stevens reaction of *N*-tosylhydrazone reacted with the palladium(II) active catalyst to form palladium-carbene intermediate **b**. Elimination of the α -proton affords vinylpalladium adduct **c** that combines with another diazo compound to form vinylpalladium alkylidene intermediate **d**. Upon migration of the vinyl group to the carbene carbon, allylpalladium intermediate **e** undergoes β -hydride elimination to generate the branched alkene product. Finally the resulting palladium(0) intermediate is oxidized by molecular oxygen into the active palladium(II) in the reaction.

Figure 5-15: Proposed Mechanism for the Palladium-Catalyzed Oxidative Homo-coupling of *N*-Tosylhydrazones.



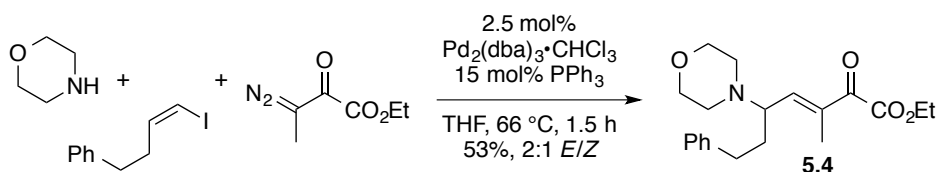
Carbenylative Coupling Processes without β -Elimination

A few reports have demonstrated that other processes could avoid competitive β -hydride elimination. These reports can be categorized into two general classes of reactions that occur prior to β -hydride elimination; formation of π -allyl/oxa-allyl palladium intermediate and formation of ketene/ketenamine formation.

Formation of π -allyl/Oxa-Allyl Palladium Intermediates Prior to β -Hydride Elimination

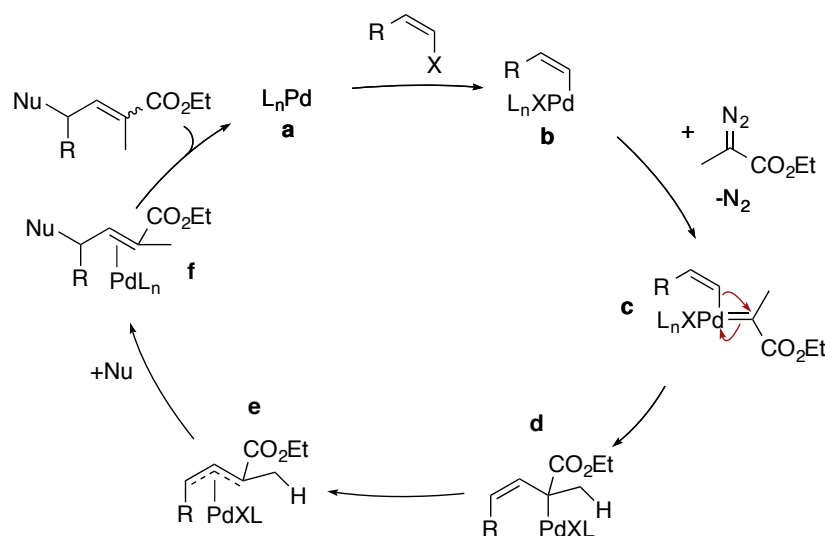
In 2009, Van Vranken and co-workers reported the first example of bypassing β -hydride elimination to form η^1 -allylpalladium intermediates that can be trapped with various nucleophiles upon isomerization to η^3 -allylpalladium intermediates.¹⁷³ Palladium-catalyzed three-component coupling of ethyl α -diazopropionate, morpholine and vinyl iodide was used to generate γ -aminoester, **5.4** in 2:1 *E/Z* selectivity (Figure 5-16).

Figure 5-16: Three-Component Coupling Reaction to Generate γ -Aminoesters



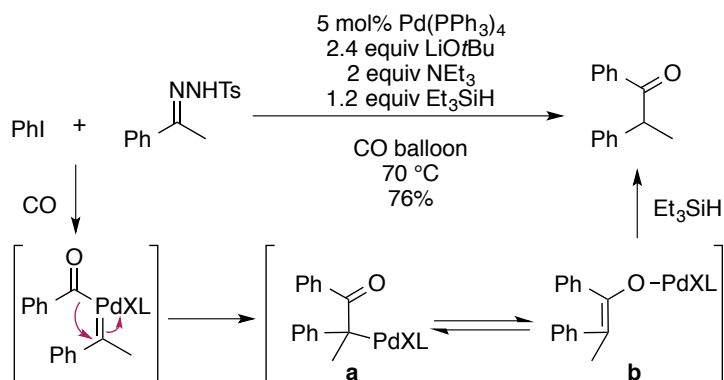
The reaction is expected to start with oxidative addition of palladium to the vinyl iodide to generate vinylpalladium halide **b** (Figure 5-17). Subsequent incorporation of the diazo compound formed vinylpalladium carbene intermediate **c**. Vinyl group migration to the carbene ligand generates η^1 -allylpalladium complex **d** that isomerizes to an η^3 -allylpalladium intermediate **e**. The η^3 -allylpalladium intermediate can be trapped with nucleophiles to afford γ -aminoesters without β -hydride elimination.

Figure 5-17: Proposed Mechanism for the Pd-Catalyzed Three-Component Coupling Reaction to Generate γ -Aminoesters



In a similar transformation Wang and co-workers¹⁶³ and Zhou and co-workers¹⁷⁴ have independently reported that oxa-allyl intermediates can also outcompete the β -hydride elimination. In their seminal work Wang and co-workers reported the first example of palladium-catalyzed tandem migratory insertion with both CO and a carbene (Figure 5-18). In this example, formation of O-palladium enolate **b** prior to the β -hydride elimination from the C- palladium enolate **a**, generates the expected ketone products in high yields.

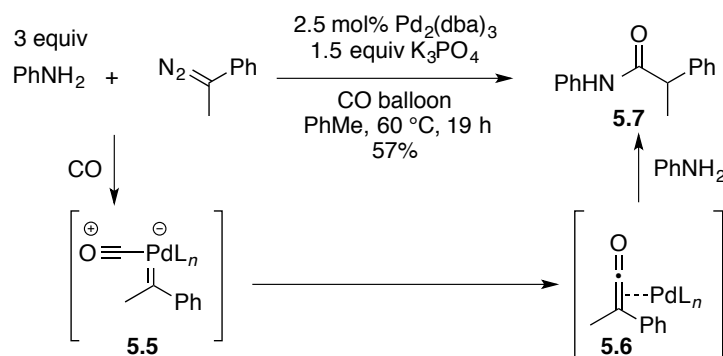
Figure 5-18: Palladium-Catalyzed reaction of Phenyl Iodide and Ketone *N*-Tosylhydrazone in the presence of CO



Ketene/Ketenamine Formation Prior To β -Hydride Elimination

In palladium-catalyzed carbonylation, insertion of a CO ligand to Pd–C bond results in acyl-palladium intermediate. However, CO insertion into a palladium-carbene ligand generates ketene intermediates that can be trapped by different nucleophiles in subsequent steps. Wang and co-workers have reported that when (1-diazoethyl)benzene is reacted with aniline in a CO atmosphere it generates the corresponding amide product **5.7** in moderate efficiency (Figure 5-19). Mechanistically, CO ligand in intermediate **5.5** migrates to the carbene center and generates the ketene intermediate **5.6**. Migration of CO is expected to be faster than the competitive β -hydride elimination.

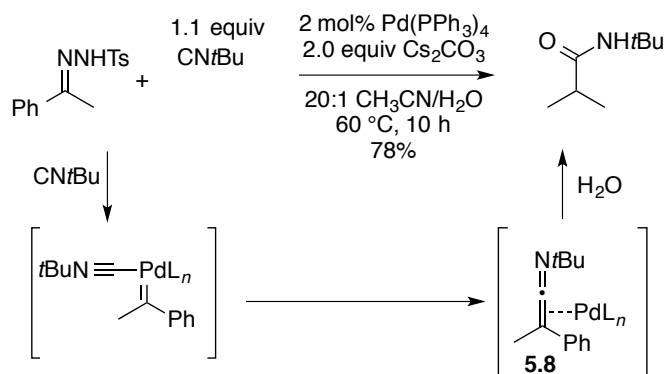
Figure 5-19: Palladium-Catalyzed Three-Component Coupling of Aniline, CO and Diazo Compounds



Similarly, Zhou and co-workers used isocyanides that are isoelectronic to carbon monoxides in similar carbenylative coupling reactions to generate ketenimine intermediates.¹⁷⁵ Isocyanide insertion is analogous to the previously described CO insertion and in the presence of hydrogens next to the carbene reactions leading to amides are faster than the β -hydride elimination (Figure 5-20). The resulting ketenimine intermediate **5.8** was trapped with water to afford amide products. The reaction tolerated a variety of aldehydes and ketones derived *N*-tosylhydrazones. However, *N*-tosylhydrazones derived from alkyl aldehydes resulted in reduced

yields. Authors have attributed this to the weaker stabilizing ability of the alkyl groups of the resulting carbene intermediates.

Figure 5-20: Palladium-Catalyzed Amidation of *N*-Tosylhydrazones with Isocyanides



As a result, they speculated that palladium-carbene species are more reactive and decompose faster under the reaction conditions. Optimal conditions for the amidation reaction with aryl aldehydes/ketones derived *N*-tosylhydrazones resulted in lower yields of reactions with *N*-tosylhydrazones derived from alkyl ketones. By switching the solvent, CH₃CN with less polar 1,4-dioxane generated the desired products from alkyl ketones in moderate yields.

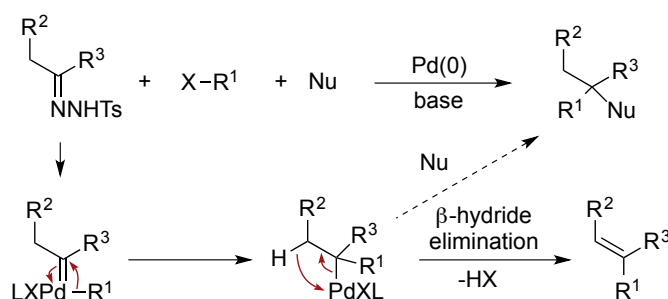
Chapter 6

Carbenylative Amination and Alkylation of Vinyl Iodides via Palladium Alkylidene Intermediates

Introduction

Palladium-catalyzed carbenylative insertion processes are gaining increasing attention, as they are analogous to widely used carbonylative insertion processes. Three-component carbenylative cross-coupling reactions offer a powerful method for joining molecular fragments through one-carbon units, similar to three-component carbonylative cross-coupling reactions. In initial applications, diazo compounds served as the major carbene precursors, but more recently *N*-tosylhydrazone anions have been used to expand the scope of carbene precursors to include benzyldiene and alkylidene derivatives.^{149,141c,176} When there are hydrogens adjacent to the carbene center, carbene insertion is usually followed by β -hydride elimination which out-competes nucleophilic trapping and erases any stereochemical information created in the carbene insertion step (Scheme 6-1).

Scheme 6-1: β -Hydride Elimination Out-Competes Nucleophilic Trapping



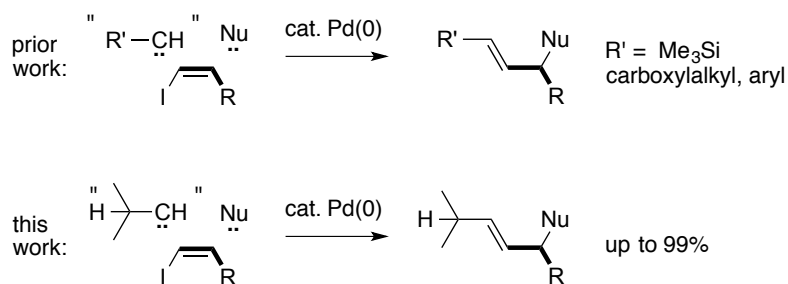
Most palladium-catalyzed carbene insertion processes involve $RPdX$ complexes derived from oxidative addition of aryl (pseudo)halides,¹⁷⁷ benzylic and allylic halides.¹⁷⁸ In other processes, $RPdX$ complexes arise from addition of nucleophiles to palladium(II).¹⁷⁹ Regardless of how the migratable group ends up on the palladium(II) intermediate, migration to the

alkylidene ligand ultimately results in substituted olefins due to the susceptibility to β -hydride eliminations. Two-component reactions of palladium(0) alkylidenes with carbon monoxide or isonitriles lead to ketenes or ketenimines, respectively, without β -hydride elimination.^{180,181}

In rare instances, three-component carbenylative insertions have been observed to out-compete β -hydride elimination using η^1 -to η^3 -allyl or oxa-allyl transitions,^{142,182,183} but the generality of this approach has not previously been demonstrated. Palladium catalysts have been used to unite vinyl iodides with nucleophiles and carbene precursors incapable of undergoing hydride elimination: trimethylsilyl, carboxyalkyl, aryl, and vinyl (Figure 6-1).^{142,184} In this work, we demonstrate that simple alkylidene groups can efficiently engage in three-component carbenylative cross-coupling reactions of vinyl iodides without β -hydride elimination. Furthermore, we demonstrate the utility of *N*-trisyldrazones as alkylidene precursors that react faster than the corresponding *N*-tosylhydrazones.

Results and Discussion

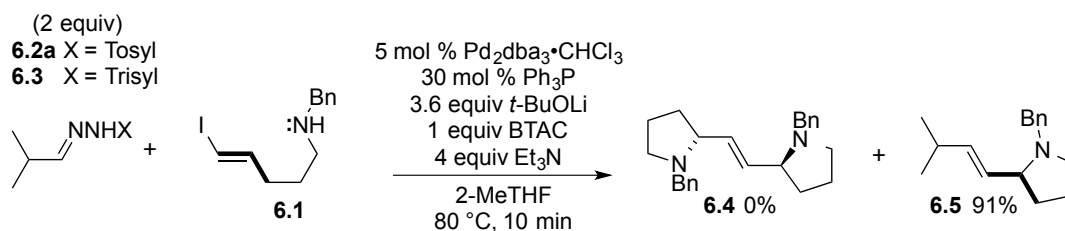
Figure 6-1: Carbenylative Amination and Alkylation with Alkylidene Carbenes without β -Hydride Elimination



We initiated the investigation of carbenylative insertion reactions of ω -aminovinyl iodide **6.1** and isobutyraldehyde *N*-tosylhydrazone **6.2a** using conditions similar to our previous work on carbenylative amination of benzaldehyde tosylhydrazones.^{171b} The only product isolated from the reaction was known dimer **6.4** (31%)^{171b,185} and a large amount of unreacted vinyl iodide **6.1**

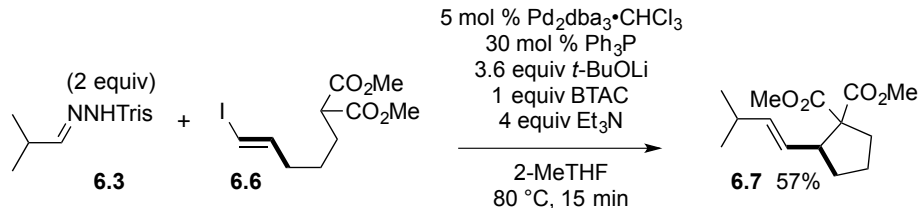
(68%) was recovered. We speculated that the low solubility of the lithiated *N*-tosylhydrazone was responsible for its failure to engage in the reaction. When the corresponding *N*-trisylhydrazone **6.3** was employed as the alkyldiene precursor, the lithiated *N*-trisylhydrazone exhibited better solubility in the reaction and afforded the desired pyrrolidine **6.5** in 15% yield. From there the conditions were optimized to afford pyrrolidine **6.5** in 91% yield, and no evidence of dimer **6.4** or products resulting from elimination of the alkyldiene α proton (Scheme 6-2).

Scheme 6-2: Intramolecular Carbenylative Amination with an Alkyldiene Precursor



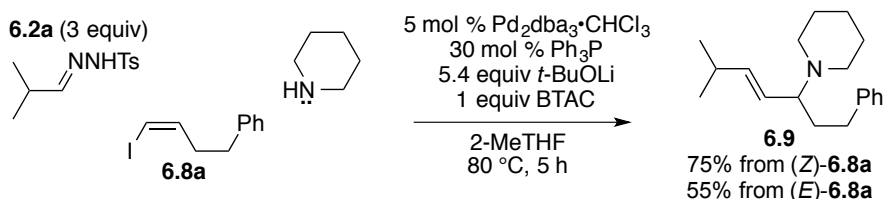
Alkenylcyclopentanes are found in a variety of natural products, such as brefeldin C, doproston B, isopulo'upone and amaminol A. To test the potential for carbon nucleophiles in the intramolecular carbenylative insertion reaction, substrate **6.6** was synthesized and subjected to the optimized reaction conditions (Scheme 6-3). The lithium enolate of malonate **6.6**, produces the corresponding alkenylcyclopentane **6.7** in 57% yield. The low yield is probably attributable to the sensitivity of the substrate. Srivastava and co-workers have previously shown related ϵ -iodovinylmalonates to be highly sensitive to alkoxides.¹⁸⁶ When malonate **6.6** was exposed to potassium carbonate, lithium *tert*-butoxide, or potassium *tert*-butoxide at 80 °C for 1 h, increasing levels of decomposition (17%, 52%, and 100%, respectively) were observed.

Scheme 6-3: Intramolecular Carbenylative Alkylation with an Alkylidene Precursor



A three-component version of the reaction was tested using piperidine as the external nucleophile and *Z*-vinyl iodide **6.8a** (Scheme 6-4). Under the conditions optimized for intramolecular trapping with vinyl iodide **6.1**, none of the desired allylamine **6.9** was observed. Under these conditions trisylhydrazone **6.3** was too reactive as a carbene source. When *N*-tosylhydrazone **6.2a** was used along with four equivalents of piperidine, the desired allylamine **6.9** was obtained in 44% yield. The triethylamine additive can be omitted from the reaction conditions. Under optimized conditions, 5 equiv of piperidine was used and the amount of *N*-tosylhydrazone and lithium *tert*-butoxide was increased, leading to a 75% isolated yield of the carbenylative amination product **6.9**. When the *E* isomer of vinyl iodide **6.8a** was employed in the reaction, the product was obtained in lower yield (55%). Previously, it had been shown that *Z*-vinyl iodides and *E*-vinyl iodides give comparable yields in intramolecular carbenylative aminations.^{184b}

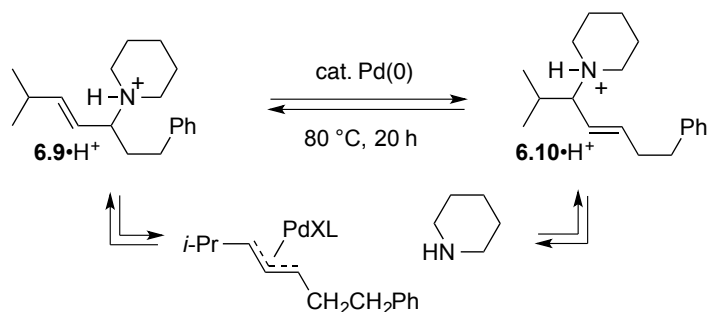
Scheme 6-4: Intermolecular Carbenylative Amination with Alkylidene Precursors



The reaction is believed to involve intermolecular attack of piperidine on an η^3 -allylpalladium intermediate on the least hindered side of the allyl fragment.¹⁸⁷ When fewer equivalents of lithium *tert*-butoxide were used, allylamine **6.9** (55%) was accompanied by the

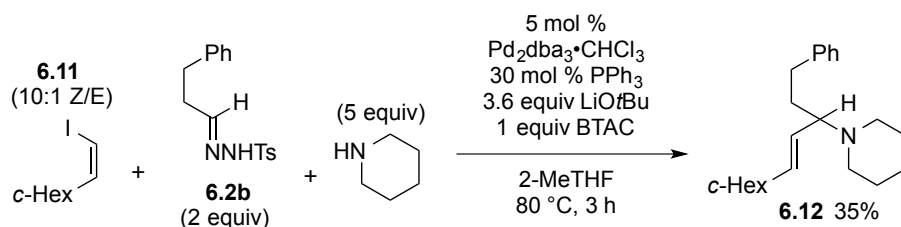
allylic regioisomer **6.10** (25%). The poor regioselectivity is probably attributable to the faster palladium-catalyzed equilibration of the protonated forms of allylic amines **6.9** and **6.10** (Scheme 6-5).¹⁸⁸ To test this hypothesis, we exposed product **6.9** to the less basic conditions, without the vinyl iodide starting material, for 20 h and found it to produce an 80:20 mixture of allylamines **6.9** and **6.10**.

Scheme 6-5: Allylamines Slowly Isomerize Under the Conditions of the Reaction



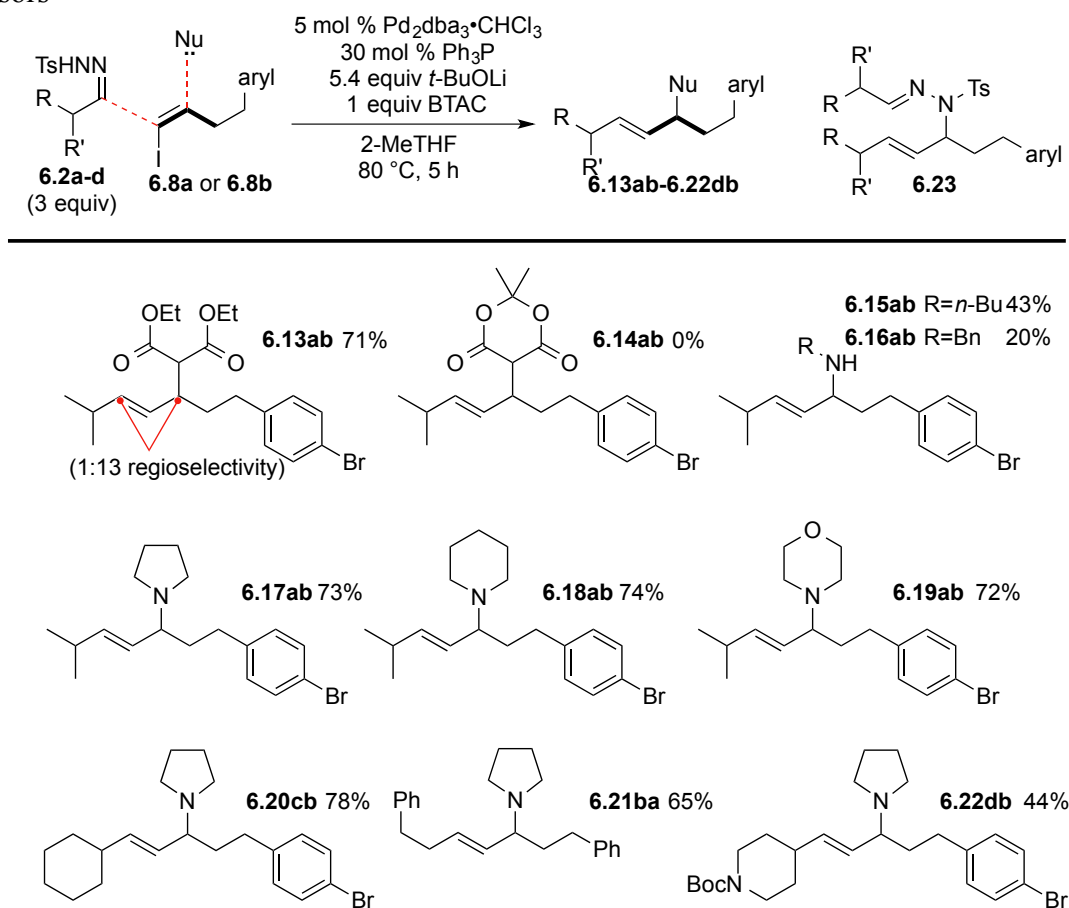
In theory, regioisomer **6.9** should be highly favored under kinetic conditions regardless of how one accesses the η^3 -allylpalladium intermediate. When the vinyl iodide, rather than the *N*-tosylhydrazone, is substituted with a secondary alkyl group, the amine still prefers to attack at the least hindered side of the allylic system. Reaction of vinyl iodide **6.11** with *N*-tosylhydrazone **6.2b** generated allylamine **6.12** (Scheme 6-6), analogous to the preferred formation of regioisomer **6.9** over **6.10**. The net transformation is a carbenylative cross-coupling, similar to a carbonylative cross-coupling reaction with carbon monoxide.

Scheme 6-6: Carbenylative Cross-Coupling with a Hindered Vinyl Iodide



With optimized conditions for the intermolecular carbenylative cross coupling reaction in hand, we next set out to explore variations in the alkylidene precursor **6.2a-d**, the vinyl iodide, **6.8a** and **6.8b**, and the nucleophile (Scheme 6-7). The sulfonylhydrazone anions compete with other nucleophiles in the reaction by attacking the η^3 -allylpalladium intermediate;¹⁸⁹ and formation of *N*-allylated hydrazone **6.23** accounts for 20-30% of the mass balance based on NMR of the crude reaction mixtures.

Scheme 6-7: Scope of Intermolecular Carbenylative Alkylation and Amination with Alkylidene Precursors

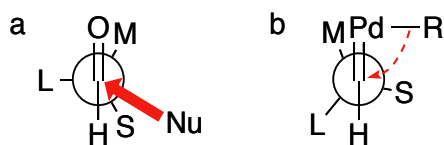


In the absence of a nucleophile a mixture of diene products, resulting from β -hydride elimination, was observed along with adduct **6.23** (22%). Diethyl malonate afforded comparable yields and resulted in a 13:1 regioisomeric mixture of allylic alkylation products (**6.13ab**). Not surprisingly, when Meldrum's acid was utilized as the nucleophile, none of the desired adduct

6.14ab was obtained, probably due to the weaker nucleophilicity of the conjugate base ($pK_a' = 4.97$). Butylamine and benzylamine gave modest yields of the desired coupling products **6.15ab** and **6.16ab** respectively. The cyclic secondary amines, pyrrolidine, piperidine and morpholine gave good yields (**6.17ab-6.19ab**). The superiority of cyclic amines in three-component carbenylative amination reactions was demonstrated in previous studies.^{142,184a} The carbenylative amination and alkylation reactions proceed with high chemoselectivity; oxidative addition across the Ar–Br bond was not observed. We next explored the tolerance of different alkyltosylhydrazones, and the coupling reactions furnished yields up to 78% (**6.20cb**, **6.21ba**, **6.22db**).

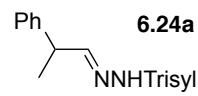
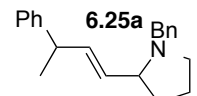
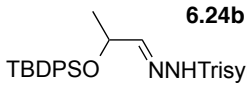
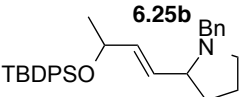
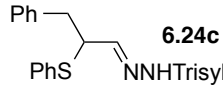
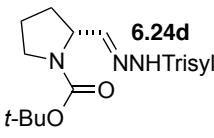
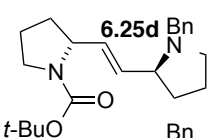
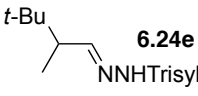
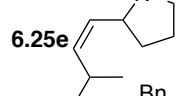
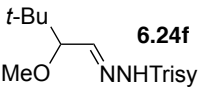
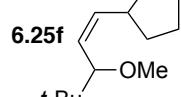
Valdés and co-workers have previously shown that palladium-catalyzed reactions of *N*-tosylhydrazones derived from α -chiral ketones proceed with preservation of stereochemistry.^{154c} Since carbenylative amination reactions create new stereogenic centers it is possible to assess the potential for acyclic stereocontrol. The Felkin-Anh model reliably predicts the acyclic stereocontrol in nucleophilic additions to carbonyls with α -chiral centers (Figure 6-2a). Chiral centers might also affect 1,2-migration reactions in alkylpalladium carbene complexes, but it has never been studied. There have been surprisingly few studies of asymmetric 1,2-migrations to discrete acyclic carbocations, which are structurally analogues to late metal carbenes; none involve an adjacent stereogenic center.¹⁹⁰

Figure 6-2: Acyclic Stereocontrol. a. Nucleophilic Addition to Carbonyls, b. 1,2-Migration to Palladium Carbenes



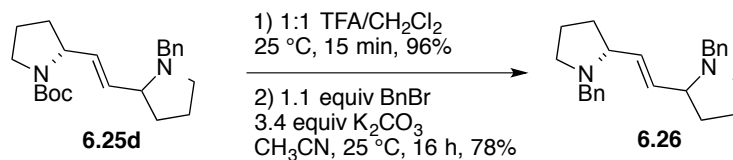
The effect of adjacent stereogenic centers in migratory carbene insertions was evaluated by utilizing chiral alkyl *N*-trisylhydrazones **6.24a-f** in intramolecular carbenylative aminations (Table 6-1). Unfortunately, the products were obtained as nearly equal mixtures of *syn* and *anti* diastereomers. *N*-Trisylhydrazones **6.24a** and **6.24b** afforded pyrrolidines **6.25a** and **6.25b**, respectively, in good yields but thioether **6.24c** gave none of the desired product, and 85% of the vinyl iodide was recovered. *N*-Boc-pyrrolidine **6.24d** gave a slight preference for the one diastereomer of **6.25d**.

Table 6-1: Stereoselectivity in Carbenylative Amination

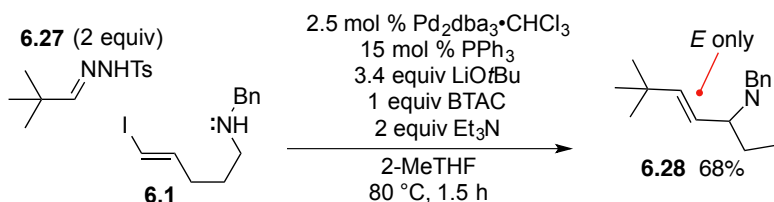
entry	starting material	product	yield (%)	dr
1	 6.24a	 6.25a	72	55:45
2	 6.24b	 6.25b	77	58:42
3	 6.24c	—	0	—
4	 6.24d	 6.25d	75	65:35 anti:syn
5	 6.24e	 6.25e	72	56:44
6	 6.24f	 6.25f	99	50:50

The stereochemistry of the major diastereomer of **6.25d** was assigned as *anti* by converting the inseparable mixture to the corresponding bis-*N*-benzyl-bis-pyrrolidines; the major diastereomer was shown to be identical to the known *meso* (*anti*) isomer **6.26** (Scheme 6-8).¹⁸⁵ To our surprise, when sterically encumbered *N*-trisylylhydrazones **6.24e** and **6.24f** were employed the products were obtained as the *Z* alkenes ($J \leq 7.9$ Hz) with none of the expected *E* alkene products (Table 6-1, entries 5 and 6). To test the effect of steric encumbrance on alkene geometry, the hindered *N*-tosylhydrazone **6.27** was tested and shown to give only the *E* product **6.28** (Scheme 6-9). Thus sterics alone is not sufficient to explain formation of *Z* products **6.25e** and **6.25f**.

Scheme 6-8: Assignment of Relative Stereochemistry by Conversion to Known Bis-Pyrrolidine



Scheme 6-9: Sterically Encumbered *N*-Tosylhydrazone **6.27** Shown to Give Only the *E* Product **6.28**



Adjacent stereogenic centers seem to exert much less influence in migration to palladium carbenes than they do in corresponding nucleophilic addition to carbonyls. This may be due to the elevated temperatures used for the palladium reactions and/or the difference in preferred angles for 1,2-migration processes versus carbonyl additions.

Conclusions

In conclusion, unstabilized alkylidene groups are shown to participate in palladium-catalyzed carbenylative amination and carbenylative alkylation reactions in high efficiency for both intramolecular and intermolecular processes. Good yields are obtained under conditions that minimize a number of competing processes such as palladium-catalyzed ionization of allylic amines, competing addition of metalated hydrazones to η^3 -allylpalladium complexes, and base-promoted decomposition of vinyl iodides with pendant malonate groups. *N*-Trisylhydrazones are shown to give superior results relative to *N*-tosylhydrazones when faster rates of participation are needed from the alkylidene precursor. When there is a stereogenic center adjacent to the metal carbene carbon, the resulting products are obtained with low levels of *syn/anti* stereocontrol but high levels of *E* or *Z* selectivity.

Experimental Section

Scheme 6-10. Proposed Catalytic Cycle of Carbenylative Amination and Alkylation of Vinyl Iodide.

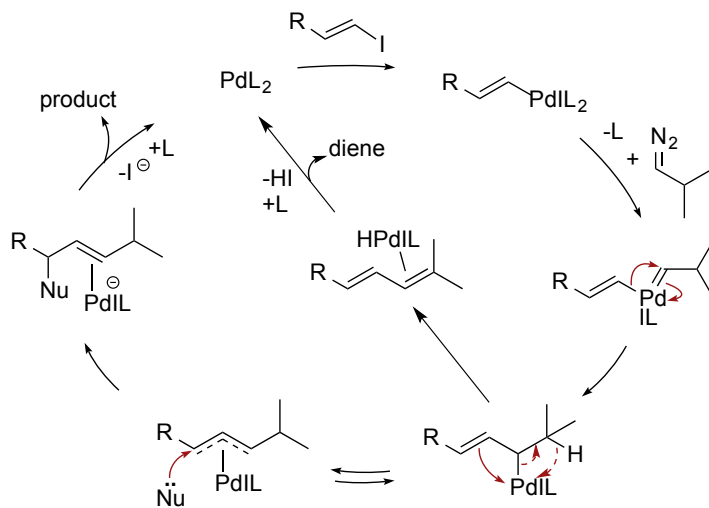
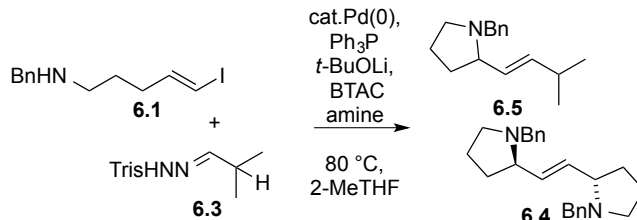


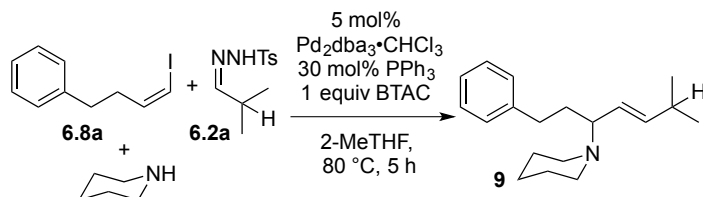
Table 6-2. Optimization of Conditions for Intramolecular Carbenylative Amination with *N*-Trisylhydrazone **6.3**^a



entry	equiv of BTAC	amine	equiv of amine	yield of 6.5
1 ^b	1	Et ₃ N	2	31% 6.4 + 68% 6.1
2	1	Et ₃ N	2	15%
3	1	Et ₃ N	4	46%
4	1	Et ₃ N	6	30%
5 ^c	1	Et ₃ N	4	33%
6	1	<i>i</i> PrNH ₂	4	36%
7	1	Et ₂ NH	4	30%
8	0	Et ₃ N	4	26%
9	2	Et ₃ N	4	48%
10 ^d	1	Et ₃ N	4	91%

^a Conditions: 2.5 mol% Pd₂dba₃CHCl₃, 15 mol% Ph₃P, 2 equiv of **6.3**, 3.6 equiv *t*-BuOLi. ^b 2 equiv of tosylhydrazone instead of trisylhydrazone. ^c 20 equiv H₂O. ^d 5 mol Pd₂dba₃CHCl₃, 30 mol% Ph₃P.

Table 6-3. Optimization of Conditions for Intermolecular Carbenylative Amination with *N*-Tosylhydrazone **6.2a**

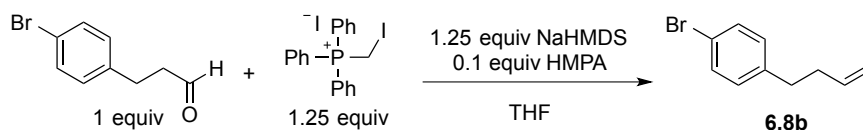


entry	equiv of 6.2a	equiv of LiOtBu	equiv of piperidine	yield of 9
1 ^a	2	3.6	4	0%
2 ^b	2	3.6	4	44%
3	2	3.6	4	56%
4	2	3.6	5	66%
5	2	3.6	10	68%
6 ^c	2	3.6	5	29%
7 ^d	2	3.6	5	41%
8 ^e	2	3.6	5	54%
9	3	5.4	5	75%
10	4	7.2	5	60%

Conditions: ^a 2 equiv isobutyraldehyde trisylhydrazone and 4 equiv Et₃N was utilized. ^b 4 equiv Et₃N added. ^c no BTAC used, ^d temperature 60 °C, ^e 20 equiv of H₂O added

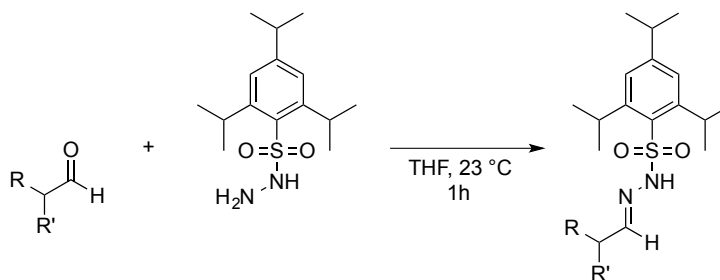
Experimental

Synthesis of (*Z*)-1-bromo-4-(4-iodobut-3-en-1-yl)benzene, **6.8b**.¹⁹¹



An oven-dried 200 mL round-bottom flask was charged with iodomethylphosphonium iodide (5.07 g, 9.56 mmol, 1.25 equiv) and a stir bar. The flask was fitted with a septum and purged with nitrogen. Tetrahydrofuran (30 mL) was added and the yellow slurry was stirred at room temperature. A solution of NaHMDS (1.0 M in THF) (9.56 mL, 9.56 mmol, 1.25 equiv) was slowly added to the slurry. The reaction mixture was cooled to -60 °C, and then HMPA (133 μ L, 0.765 mmol, 0.1 equiv) was added. The reaction mixture was cooled to -78 °C, and then 3-(4-bromophenyl)propanal (1.63 g, 7.65 mmol, 1.0 equiv) was added drop-wise via a syringe. The reaction was stirred at -78 °C for 30 min and let warm to room temperature over an hour. The reaction mixture was poured into brine (12 mL) and extracted with pentane (3x30 mL). The combined organic layers were dried with Na₂SO₄ and concentrated *in vacuo* to give orange oil. The oil was purified by flash chromatography with hexanes to afford *Z*-isomer **6.8b** as a colorless liquid with 10:1 *Z/E* isomer (1.63 g, 4.32 mmol, 56 %). R_f = 0.59 (hexanes); ¹H NMR (500 MHz, CDCl₃) δ 7.41 (d, J = 8.4 Hz, 2H), 7.08 (d, J = 8.4 Hz, 2H), 6.25 (d, J = 7.4 Hz, 1H), 6.17 (q, J = 7.0 Hz, 1H), 2.69 (t, J = 7.5 Hz, 2H), 2.44 (q, J = 7.3 Hz, 2H); ¹³C NMR (125 MHz, CDCl₃) δ 140.0, 139.8, 131.5, 130.3, 119.9, 83.6, 36.2, 33.5; IR (thin film) 2925, 1608, 1487, 1283, 1071, 1011 cm⁻¹; HRMS (ESI): m/z calculated for C₁₀H₁₀BrI [M]⁺ 335.9011, found 335.9022.

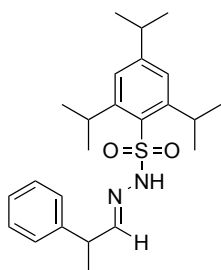
General procedure for the synthesis of *N*-sulfonylhydrazones:



A 50 mL round-bottom flask was charged with 2,4,6-triisopropylbenzenesulfonyl hydrazide (1.0 equiv) and a stir bar. The flask was fitted with a septum and purged with nitrogen. THF (0.5 M) was added and the reaction flask was cooled to 0 °C. The corresponding aldehyde (1.0 equiv) was added drop-wise to the flask containing the trisyl hydrazide and THF. Reaction mixture was stirred at 23 °C and was monitored for consumption of the starting material by TLC (10:90 EtOAc/hex).

Upon consumption of the starting materials, the crude reaction mixture was concentrated *in vacuo* to give a white solid. The solid was then purified by flash chromatography with EtOAc/hex to afford the corresponding hydrazones.

(*E*)-2,4,6-triisopropyl-*N'*-(2-phenylpropylidene)benzenesulfonohydrazide, 6.24a.

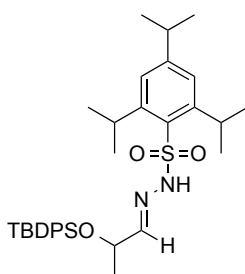


A 50 mL round-bottom flask was charged with 2,4,6-triisopropylbenzenesulfonyl hydrazide (2.22 g, 7.48 mmol, 1.0 equiv) and a stir bar. The flask was fitted with a septum and purged with nitrogen. Next, 14 mL of THF was added and the reaction flask was cooled to 0 °C.

Then 2-phenylpropanal (0.15 mL, 7.45 mmol, 1.0 equiv) was added drop-wise to the flask containing the trisyl hydrazide and THF. Reaction mixture was stirred at 23 °C and was monitored for consumption of the starting material by TLC (10:90 EtOAc/hex).

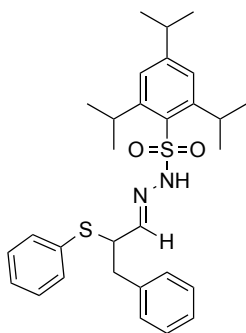
Upon consumption of the starting materials, the crude reaction mixture was concentrated *in vacuo* to give a white solid. The crude mixture was then purified by flash chromatography with EtOAc/hex to afford the hydrazone **6.24a** (2.94 g, 7.09 mmol, 95%) as a white solid, mp: 109-112 °C. $R_f = 0.48$ (1:9 EtOAc/hex); $^1\text{H NMR}$ (600 MHz, CDCl_3) δ 7.46 (s, 1H), 7.24-7.19 (m, 4H), 7.16 (d, $J = 5.0$ Hz, 1H), 6.99 (d, $J = 7.1$ Hz, 2H), 4.19 (sep, $J = 6.7$ Hz, 2H), 3.60-3.56 (m, 1H), 2.93 (sep, $J = 6.8$ Hz, 1H), 1.33 (d, $J = 7.0$ Hz, 3H), 1.28 (d, $J = 6.9$ Hz, 6H), 1.25 (dd, $J = 6.7, 1.4$ Hz, 12H); $^{13}\text{C NMR}$ (125 MHz, CDCl_3) δ 153.4, 152.8, 151.3, 141.5, 131.2, 128.8, 127.5, 127.0, 123.8, 42.6, 34.2, 30.0, 24.9, 24.8, 23.6, 18.3; IR (thin film) 3185, 2954, 1598, 1450, 1322, 1165, 1024 cm^{-1} ; HRMS (ESI): m/z calculated for $\text{C}_{24}\text{H}_{34}\text{N}_2\text{O}_2\text{SNa}$ $[\text{M}+\text{Na}]^+$ 437.2239, found 437.2238.

**(*E*)-*N'*-(2-((*tert*-butyldiphenylsilyl)oxy)propylidene)-2,4,6-triisopropylbenzenesulfonohydr-
-azide, **6.24b**.**



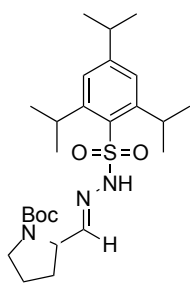
Using the general procedure for condensation outlined above, 2-((*tert*-butyldiphenylsilyl)oxy)propanal (0.50 g, 1.60 mmol, 1.0 equiv) was used and the product was purified by flash chromatography with EtOAc/hex (1:9) to afford the trisylhydrazone **6.24b** (0.87 g, 1.47 mmol, 92%) as a white solid, mp: 61-63 °C. $R_f = 0.55$ (1:9 EtOAc/hex); $^1\text{H NMR}$ (600 MHz, CDCl_3) δ 7.59-7.52 (m, 4H), 7.40-7.24 (m, 8H), 4.32-4.30 (m, 1H), 4.13-4.10 (m, 2H), 2.91-2.89 (m, 1H), 1.26 (d, $J = 6.5$ Hz, 6H), 1.20 (d, $J = 5.5$ Hz, 12H), 1.14 (d, $J = 6.2$ Hz, 3H), 0.97 (s, 9H); $^{13}\text{C NMR}$ (125 MHz, CDCl_3) δ 153.4, 151.6, 151.4, 135.7, 134.8, 133.7, 133.3, 131.1, 129.8, 129.7, 127.7, 127.6, 123.8, 69.1, 34.2, 29.9, 26.8, 24.8, 24.7, 23.6, 21.6, 19.1; IR (thin film) 2982, 1634, 1383 cm^{-1} ; HRMS (ESI): m/z calculated for $\text{C}_{34}\text{H}_{48}\text{N}_2\text{O}_3\text{SSiNa}$ $[\text{M}+\text{Na}]^+$ 615.3052, found 615.3053.

(E)-2,4,6-triisopropyl-N'-(3-phenyl-2-(phenylthio)propylidene)benzenesulfonohydrazide, 6.24c.



Using the general procedure for condensation outlined above, 3-phenyl-2-(phenylthio)propanal (0.12 g, 0.50 mmol, 1.0 equiv) was used and the product was purified by flash chromatography with EtOAc/hex (1:9) to afford the trisylhydrazone **6.24c** (0.23 g, 0.44 mmol, 88%) as a white solid, mp: 48-50 °C. $R_f = 0.35$ (2:8 EtOAc/hex); $^1\text{H NMR}$ (600 MHz, CDCl_3) δ 8.18 (s, 1H), 7.17-7.14 (m, 7H), 7.07-6.97 (m, 6H), 4.11-4.05 (m, 2H), 3.89 (q, $J = 3.9$ Hz, 1H), 3.06 (dd, $J = 14.1, 7.5$ Hz, 1H), 2.96-2.89 (m, 2H), 1.29 (d, $J = 6.9$ Hz, 6H), 1.19 (d, $J = 6.7$ Hz, 6H), 1.13 (d, $J = 6.7$ Hz, 6H); $^{13}\text{C NMR}$ (125 MHz, CDCl_3) δ 153.4, 151.5, 147.5, 137.5, 132.7, 132.2, 131.2, 129.3, 128.8, 128.4, 127.3, 126.7, 123.9, 50.5, 37.8, 34.3, 29.9, 24.9, 24.8, 23.8, 23.7; IR (thin film) 3193, 2958, 1599, 1455, 1316, 1151 cm^{-1} ; HRMS (ESI): m/z calculated for $\text{C}_{30}\text{H}_{38}\text{N}_2\text{O}_2\text{S}_2\text{Na}$ $[\text{M}+\text{Na}]^+$ 545.2272, found 545.2258.

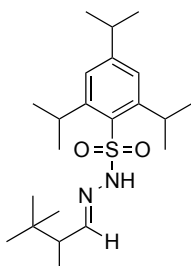
***tert*-Butyl (E)-2-((2-((2,4,6-triisopropylphenyl)sulfonyl)hydrazono)methyl)pyrrolidine-1-carboxylate, 6.24d.**



Using the general procedure for condensation outlined above, *tert*-butyl 2-formylpyrrolidine-1-carboxylate (0.50 g, 2.51 mmol, 1.0 equiv) was used and the product was purified by flash chromatography with EtOAc/hex (1:9) to afford the trisylhydrazone **6.24d** (1.14 g, 2.38 mmol, 95%) as a white solid, mp: 72-75 °C. $R_f = 0.31$ (2:8 EtOAc/hex); $^1\text{H NMR}$ (600 MHz, $\text{DMSO-}d_6$, 380 K) δ 10.8 (s, 1H), 7.26 (d, $J = 4.5$ Hz, 1H), 7.20 (br s, 2H), 4.26-4.21 (m, 2H), 4.19-4.17 (m, 1H), 3.27-3.23 (m, 1H), 3.17-3.13 (m, 1H), 2.95-2.91 (m, 3H), 1.93-1.87 (m, 1H), 1.82-1.77 (m, 1H), 1.70-1.66 (m, 1H), 1.60-1.52 (m, 1H), 1.29 (br s, 8H), 1.23-1.19 (m, 18H); $^{13}\text{C NMR}$ (125 MHz, CDCl_3) δ 151.3, 123.9, 34.3, 29.9, 28.4, 28.3, 24.9, 24.8, 23.6; IR (thin

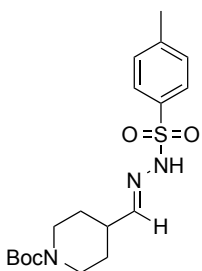
film) 2959, 1667, 1392, 1163 cm^{-1} ; HRMS (ESI): m/z calculated for $\text{C}_{25}\text{H}_{41}\text{N}_3\text{O}_4\text{SNa}$ $[\text{M}+\text{Na}]^+$ 502.2715, found 502.2705.

(E)-2,4,6-Triisopropyl-*N'*-(2,3,3-trimethylbutylidene)benzenesulfonohydraziden, 6.24e.



Using the general procedure for condensation outlined above, 2,3,3-trimethylbutanal (2.23 g mL, 7.48 mmol, 1.0 equiv) was used and the product was purified by flash chromatography with EtOAc/hex (1:9) to afford the trisylhydrazone **6.24e** (2.81 g, 7.12 mmol, 95%) as a white solid, mp: 118-121 $^{\circ}\text{C}$. $R_f = 0.42$ (1:9 EtOAc/hex); ^1H NMR (600 MHz, CDCl_3) δ 7.28 (s, 1H), 7.15 (s, 1H), 7.05 (d, $J = 7.0$ Hz, 1H), 4.20-4.16 (m, 2H), 2.91-2.87 (m, 1H), 2.09-2.05 (m, 1H), 1.27 (d, $J = 2.9$ Hz, 12H), 1.25 (d, $J = 2.9$ Hz, 6H), 0.92 (d, $J = 7.0$ Hz, 3H), 0.71 (s, 1H); ^{13}C NMR (125 MHz, CDCl_3) δ 154.4, 153.4, 151.0, 131.1, 123.8, 123.7, 46.4, 34.2, 33.0, 29.9, 27.2, 24.9, 24.8, 23.6, 12.6; IR (thin film) 3209, 2958, 1599, 1460, 1321, 1163 cm^{-1} ; HRMS (ESI): m/z calculated for $\text{C}_{22}\text{H}_{38}\text{N}_2\text{O}_2\text{SNa}$ $[\text{M}+\text{Na}]^+$ 417.2552, found 417.2539.

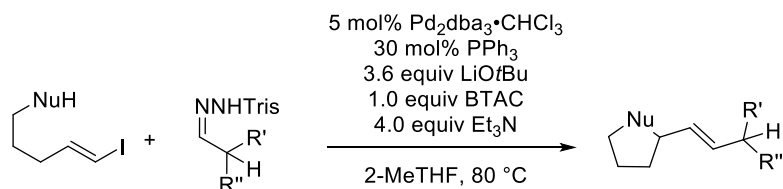
***tert*-Butyl (E)-4-((2-tosylhydrazono)methyl)piperidine-1-carboxylate, 6.2d.**



Using the general procedure for condensation outlined above, *tert*-butyl 4-formylpiperidine-1-carboxylate (0.97 g, 4.55 mmol, 1.1 equiv) and tosyl hydrazide (0.77 g, 4.14 mmol, 1.0 equiv) were used to afford the tosylhydrazone **6.2d** (1.48 g, 3.89 mmol, 94%) as a white solid, mp: 48-49 $^{\circ}\text{C}$. $R_f = 0.48$ (1:9 EtOAc/hex); ^1H NMR (600 MHz, $\text{DMSO}-d_6$, 380 K) δ 8.32 (s, 1H), 7.78 (d, $J = 9.8$ Hz, 2H), 7.31 (d, $J = 9.8$ Hz, 2H), 7.11 (d, $J = 5.9$ Hz, 1H), 3.98 (br s, 3H), 2.91-2.67 (m, 3H), 2.43 (s, 3H), 2.34-2.30 (m, 1H), 1.69-1.65 (m, 2H), 1.45-1.43 (m, 9H); ^{13}C NMR (125 MHz, CDCl_3) δ 178.2, 154.8, 154.0, 144.2, 136.2, 129.6, 127.9, 79.7, 38.8, 28.8,

28.4, 21.7; IR (thin film) 2975, 1658, 1426, 1365, 1234, 1158 cm^{-1} ; HRMS (ESI): m/z calculated for $\text{C}_{18}\text{H}_{27}\text{N}_3\text{O}_4\text{SNa}$ $[\text{M}+\text{Na}]^+$ 404.1620, found 404.1618.

General procedure for intramolecular carbonylation:



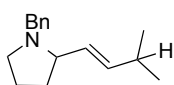
An oven-dried 5 mL pear-shaped flask was charged with $\text{Pd}_2\text{dba}_3\cdot\text{CHCl}_3$ (5.0 mol%), PPh_3 (30 mol%), and a stir bar. The flask was fitted with a septum and purged with nitrogen. 2-Methyltetrahydrofuran (2-MeTHF) was added to make a 0.01 M solution, and the brown slurry was then stirred for 20 min at room temperature to give a clear yellow catalyst solution.

Meanwhile, a separate oven-dried 5 mL round-bottom flask containing of *N*- trisylhydrazone (2.0 equiv), benzyltriethylammonium chloride (1.0 equiv), lithium *tert*-butoxide base (3.6 equiv), and a stir bar. The reaction vessel was evacuated and back-filled with N_2 three times, and then capped with a septum. A solution of the vinyl iodide (1.0 equiv, 0.5 M in 2-MeTHF) was transferred from a pear-shaped flask by syringe to the dry reagents in the round-bottom flask. The residual vinyl iodide in the pear-shaped flask was transferred to the reaction vessel using 2-MeTHF (2 x 0.15 mL). Triethylamine (4.0 equiv) was added to the round-bottom flask.

Finally, the catalyst solution was transferred to the reaction vessel via syringe, the remaining catalyst solution was transferred 2-MeTHF (2 x 0.2 mL). The reaction vessel was fitted with a reflux condenser and capped with a septum. The reaction vessel was immersed in an 80 °C oil bath up to the level of the flask contents, and the stirred slurry rapidly reached reflux temperature.

The reaction was monitored by thin layer chromatography (20:79:1 EtOAc/hex/Et₃N) to check for depletion of the vinyl iodide. The reactions reached completion between ca. 5 and 30 min depending on *N*-trisylhydrazone. Upon consumption of the vinyl iodide, the reaction was allowed to cool to room temperature and 1% (w/v) aq. NaOH was added to the reaction vessel. The mixture was extracted with EtOAc three times and the combined organic extracts were washed with brine, dried with Na₂SO₄, and concentrated *in vacuo*. The pyrrolidine was purified by silica gel chromatography.

(*E*)-1-benzyl-2-(3-methylbut-1-en-1-yl)pyrrolidine, 6.5.



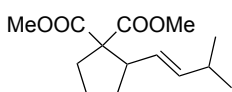
An oven-dried 5 mL pear-shaped flask was charged with Pd₂dba₃•CHCl₃ (5.4 mg, 0.0071 mmol), PPh₃ (11.0 mg, 0.042 mmol), and a stir bar. The flask was fitted with a septum and purged with nitrogen. 2-MeTHF (0.2 mL) was added, and the brown slurry was then stirred for 20 min at room temperature to give a clear yellow catalyst solution.

Meanwhile, a separate oven-dried 5 mL round-bottom flask containing of *N*-trisylhydrazone (98.6 mg, 0.280 mmol), benzyltriethylammonium chloride (31.9 mg, 0.140 mmol), lithium *tert*-butoxide base (40.4 mg, 0.504 mmol), and a stir bar. The reaction vessel was evacuated and back-filled with N₂ three times, and then capped with a septum. A solution of the vinyl iodide **6.1** (42.1 mg, 0.140 mmol) in 0.2 mL of 2-MeTHF was transferred from a pear-shaped flask by syringe to the dry reagents in the round-bottom flask. The residual vinyl iodide in the pear-shaped flask was transferred to the reaction vessel using 2-MeTHF (2 x 0.15 mL). Triethylamine (78 mL, 0.560 mmol) was added to the round-bottom flask.

Finally, the catalyst solution was transferred to the reaction vessel via syringe, the remaining catalyst solution was transferred 2-MeTHF (2 x 0.2 mL). The reaction vessel was fitted with a reflux condenser and capped with a septum. The reaction vessel was immersed in a

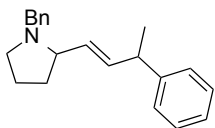
80 °C oil bath up to the level of the flask contents, and the stirred slurry rapidly reached reflux temperature. The reaction reached completion within 10 min and was allowed to cool to room temperature; then 2 mL 1% (w/v) aq. NaOH was added to the reaction vessel. The mixture was extracted with 3x5 mL EtOAc and the combined organic extracts were washed with brine, dried with Na₂SO₄, and concentrated *in vacuo*. The crude reaction mixture was purified by silica gel chromatography (10:85:5 EtOAc/Hex/Et₃N) to provide pyrrolidine **6.5** (29.0 mg, 91%), as a brown oil. $R_f = 0.6$ (20:79:1 EtOAc/Hexanes/Et₃N). ¹H NMR (600 MHz, CDCl₃) δ 7.43-7.07 (m, 5H), 5.59 (dd, $J = 15.3, 6.4$ Hz, 1H), 5.33 (dd, $J = 15.3, 8.3$ Hz, 1H), 4.01 (d, $J = 13$ Hz, 1H), 3.04 (d, $J = 12.9$ Hz, 1H), 2.93 (t, $J = 8.4$, 1H), 2.70 (dd, $J = 16.0, 8.0$ Hz, 1H), 2.32-2.29 (m, 1H), 2.09-2.06 (m, 1H), 1.92-1.89 (m, 1H), 1.76-1.60 (m, 3H), 1.00-0.99 (m, 6H); ¹³C NMR (125 MHz, CDCl₃) δ 132.5, 129.3, 129.0, 128.7, 128.2, 128.1, 127.0, 67.8, 57.7, 53.1, 31.6, 30.9, 22.6, 22.5, 21.8; IR (thin film) 2959, 1681, 1455, 1364 cm⁻¹; HRMS (ESI): m/z calc'd for C₁₆H₂₃NH (M+H)⁺ 230.1909, found 230.1902.

Dimethyl (*E*)-2-(3-methylbut-1-en-1-yl)cyclopentane-1,1-dicarboxylate, **6.7.**



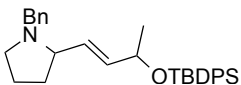
Following the general procedure for intramolecular carbonylation, vinyl iodide, dimethyl (*E*)-2-(5-iodopent-4-en-1-yl)malonate **6.6** (40.8 mg, 0.125 mmol) gave compound **6.7** (18.1 mg, 57%) as a brown oil. $R_f = 0.5$ (5:95 EtOAc/Hex). ¹H NMR (500 MHz, CDCl₃) δ 5.46 (dd, $J = 15.4, 6.7$ Hz, 1H), 5.30 (dd, $J = 15.4, 8.2$ Hz, 1H), 3.72 (s, 3H), 3.63 (s, 3H), 3.21 (q, $J = 7.5$ Hz, 1H), 2.57-2.33 (m, 1H), 2.31-2.15 (m, 1H), 2.12-2.00 (m, 1H), 2.00-1.90 (m, 1H), 1.90-1.77 (m, 1H), 1.71-1.49 (m, 1H), 0.94 (dd, $J = 6.7, 1.0$ Hz, 6H); ¹³C NMR (125 MHz, CDCl₃) δ 172.9, 171.3, 139.3, 126.1, 64.6, 52.5, 52.0, 48.8, 33.8, 31.3, 31.0, 29.7, 23.2, 22.6, 22.5; IR (thin film) 2954, 1729, 1433, 1264, 1212 cm⁻¹; HRMS (ESI): m/z calc'd for C₁₄H₂₂O₄Na (M+Na)⁺ 277.1416, found 277.1413.

(E)-1-benzyl-2-(3-phenylbut-1-en-1-yl)pyrrolidine, 6.25a.



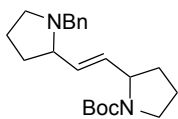
Following the general procedure for intramolecular carbenylation, vinyl iodide **6.1** (44.3 mg, 0.147 mmol) gave pyrrolidine **6.25a** (30.9 mg, 72%) as a brown oil and a mixture of 2 diastereomers that were inseparable by flash column chromatography. $R_f = 0.8$ (20:79:1 EtOAc/Hex/Et₃N). ¹H NMR (500 MHz, CDCl₃) δ 7.31-7.11 (m, 10H), 5.84-5.76 (m, 1H), 5.50-5.40 (m, 1H), 4.04 (d, $J = 13.0$ Hz, 1H), 3.57-3.43 (m, 1H), 3.07 (d, $J = 12.9$ Hz, 1H), 2.95-2.90 (m, 1H), 2.77 (q, $J = 8.2$ Hz, 1H), 2.10 (q, $J = 8.8$ Hz, 1H), 1.99-1.86 (m, 1H), 1.83-1.59 (m, 3H), 1.37 (dd, $J = 7.0, 3.0$ Hz, 3H); ¹³C NMR (125 MHz, CDCl₃) δ 146.1, 139.7, 137.9, 131.4, 129.2, 128.5, 128.2, 127.3, 126.8, 126.1, 67.7, 58.3, 53.4, 42.2, 31.8, 22.0, 21.6; IR (thin film) 3026, 2964, 2787, 1601, 1493, 1452, 1370 cm⁻¹; HRMS (ESI): m/z calc'd for C₂₁H₂₅NH (M+H)⁺ 292.2065, found 292.2057.

(E)-1-benzyl-2-(3-((tert-butyldiphenylsilyl)oxy)but-1-en-1-yl)pyrrolidine, 6.25b.



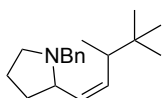
Following the general procedure for intramolecular carbenylation, vinyl iodide **6.1** (34.5 mg, 0.115 mmol) gave pyrrolidine **6.25b** (41.5 mg, 77%) as a brown oil. $R_f = 0.9$ (20:79:1 EtOAc/Hex/Et₃N). ¹H NMR (600 MHz, CDCl₃) δ 7.71-7.64 (m, 4H), 7.46-7.17 (m, 11H), 5.69 (dd, $J = 15.5, 6.3$ Hz, 1H), 5.44 (dd, $J = 15.4, 8.3$ Hz, 1H), 4.42-4.27 (m, 1H), 3.93 (d, $J = 13.0$ Hz, 1H), 3.01 (d, $J = 13.0$ Hz, 1H), 2.91-2.85 (m, 1H), 2.74-2.65 (m, 1H), 2.12-2.01 (m, 1H), 1.94-1.79 (m, 1H), 1.77-1.62 (m, 1H), 1.57-1.43 (m, 1H), 1.16 (d, $J = 6.3$ Hz, 3H), 1.08-1.04 (m, 9H); ¹³C NMR (125 MHz, CDCl₃) δ 139.8, 136.8, 132.4, 130.2, 129.7, 129.3, 72.7, 67.8, 58.1, 53.1, 31.0, 32.1, 30.6, 27.5, 26.8; IR (thin film) 2982, 1734, 1373 cm⁻¹; HRMS (ESI): m/z calc'd for C₃₁H₄₀NOSiH (M+H)⁺ 470.2879, found 470.2881.

***tert*-butyl (*E*)-2-(2-(1-benzylpyrrolidin-2-yl)vinyl)pyrrolidine-1-carboxylate, 6.25d.**



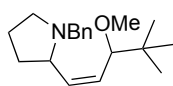
Following the general procedure for intramolecular carbonylation, vinyl iodide **6.1** (41.4 mg, 0.138 mmol) gave pyrrolidine **6.25d** (36.8 mg, 75%) as a brown oil. $R_f = 0.8$ (20:79:1 EtOAc/Hex/Et₃N). ¹H NMR (600 MHz, DMSO-*d*₆, 400 K) δ 7.31-7.23 (m, 4H), 7.21-7.18 (m, 1H), 5.58 (dd, $J = 15.3, 6.0$ Hz, 1H), 5.41 (m, 1H), 4.35-4.14 (m, 1H), 3.93 (d, $J = 13.6$ Hz, 1H), 3.47-3.24 (m, 2H), 3.21 (d, $J = 13.4$ Hz, 1H), 3.10-2.72 (m, 2H), 2.19 (q, $J = 8.5$ Hz, 1H), 2.07-1.86 (m, 2H), 1.94-1.79 (m, 1H), 1.78-1.76 (m, 2H), 1.73-1.59 (m, 3H), 1.55-1.52 (m, 1H), 1.43-1.34 (m, 9H); ¹³C NMR (125 MHz, DMSO-*d*₆) δ 139.4, 132.9, 131.7, 128.2, 128.1, 127.9, 126.4, 77.9, 66.2, 57.6, 57.0, 52.5, 45.8, 31.4, 28.0, 21.6; IR (thin film) 2970, 1692, 1392, 1249, 1167, 1112 cm⁻¹; HRMS (ESI): m/z calc'd for C₂₂H₃₂N₂O₂Na (M+Na)⁺ 379.2361, found 379.2360.

(*Z*)-1-benzyl-2-(3,4,4-trimethylpent-1-en-1-yl)pyrrolidine, 6.25e.



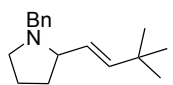
Following the general procedure for intramolecular carbonylation, vinyl iodide **6.1** (39.7 mg, 0.132 mmol) gave pyrrolidine **6.25e** (25.8 mg, 72%) as a brown oil. $R_f = 0.8$ (20:79:1 EtOAc/Hex/Et₃N). Two diastereomers were observed. ¹H NMR (600 MHz, CDCl₃) δ 7.34-7.27 (m, 4H), 7.23 (dd, $J = 13.0, 4.1$ Hz, 1H), 5.59-5.54 (m, 1H), 5.34 (dd, $J = 8.4, 4.1$ Hz, 1H), 4.05 (dd, $J = 20.1, 12.8$ Hz, 1H), 3.03 (dd, $J = 12.7, 9.7$, 1H), 2.96-2.85 (m, 1H), 2.75-2.71 (m, 1H), 2.09-2.07 (m, 1H) 1.99-1.87 (m, 1H), 1.85-1.51 (m, 1H), 1.03-0.92 (m, 4H), 0.87 (d, $J = 9.9, 9H$); ¹³C NMR (125 MHz, CDCl₃) δ 139.7, 139.6, 136.8, 136.6, 132.2, 132.0, 129.2, 129.1, 128.3, 128.2, 126.8, 126.7, 68.1, 67.9, 58.2, 58.1, 53.4, 53.3, 47.1, 46.9, 32.9, 32.8, 31.8, 31.7, 27.6, 27.5, 22.0, 21.9, 15.8, 15.7; IR (thin film) 2960, 1685, 1454, 1364 cm⁻¹; HRMS (ESI): m/z calc'd for C₁₉H₂₉NH (M+H)⁺ 272.2378, found 272.2369.

(Z)-1-benzyl-2-(3-methoxy-4,4-dimethylpent-1-en-1-yl)pyrrolidine, 6.25f.



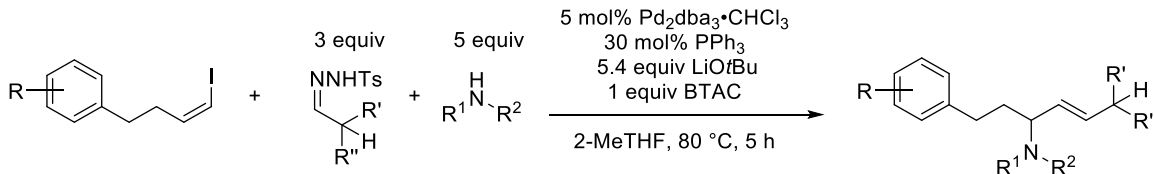
Following the general procedure for intramolecular carbenylation, vinyl iodide **6.1** (45.9 mg, 0.152 mmol) gave pyrrolidine **6.25f** (43.4 mg, 99%) as a brown oil. $R_f = 0.7$ (20:79:1 EtOAc/Hex/Et₃N). Two diastereomers were observed. ¹H NMR (600 MHz, CDCl₃) δ 7.30-7.29 (m, 4H), 7.23-7.22 (m, 1H), 5.64 (dd, $J = 7.9, 3.5$ Hz, 1H), 5.60 (d, $J = 8.1$ Hz, 1H), 4.05 (dd, $J = 20.1, 12.8$ Hz, 1H), 3.03 (dd, $J = 12.7, 9.7$, 1H), 2.96-2.85 (m, 1H), 2.75-2.71 (m, 1H), 2.09-2.07 (m, 1H) 1.99-1.87 (m, 1H), 1.85-1.51 (m, 1H), 1.03-0.92 (m, 4H), 0.87 (d, $J = 9.9, 9\text{H}$); ¹³C NMR (125 MHz, CDCl₃) δ 139.7, 139.6, 136.8, 136.6, 132.2, 132.0, 129.2, 129.1, 128.3, 128.2, 126.8, 126.7, 68.1, 67.9, 58.2, 58.1, 53.4, 53.3, 47.1, 46.9, 32.9, 32.8, 31.8, 31.7, 27.6, 27.5, 22.0, 21.9, 15.8, 15.7; IR (thin film) 2954, 1695, 1454, 1362, 1179, 1092 cm⁻¹; HRMS (ESI): m/z calc'd for C₁₉H₂₉NOH (M+H)⁺ 288.2327, found 288.2324.

(E)-1-Benzyl-2-(3,3-dimethylbut-1-en-1-yl)pyrrolidine, 6.28.



Following the procedure for intramolecular carbenylation by Khanna, *et al.*,³ vinyl iodide **6.1** (45.2 mg, 0.150 mmol) and *N*-tosylhydrazone of pivalaldehyde (0.130 g, 0.420 mmol) were used to give pyrrolidine **6.28** (24.9 mg, 68%) as a yellow oil. $R_f = 0.24$ (10:90 EtOAc/Hex). ¹H NMR (600 MHz, CDCl₃) δ 7.62 (app d, $J = 4.4$ Hz, 3H), 7.23 (sext, $J = 4$ Hz, 1H), 5.63 (d, $J = 15.6$ Hz, 1H), 5.28 (dd, $J = 15.6, 8.4$ Hz, 1H), 3.98 (d, $J = 12.9$ Hz, 1H), 3.04 (d, $J = 12.9$ Hz, 1H), 2.93 (dt, $J = 9.2, 2.2$ Hz, 1H), 2.69 (q, $J = 8.4$ Hz, 1H), 2.09 (q, $J = 8.85$ Hz, 1H), 1.95-1.90 (m, 1H), 1.80-1.72 (m, 1H), 1.71-1.58 (m, 3H), 1.02 (s, 9H); ¹³C NMR (125 MHz) δ 144.6, 139.8, 129.1, 128.2, 127.1, 126.7, 67.9, 58.1, 53.4, 32.9, 31.8, 29.8, 21.9; IR (thin film) 2957, 2786, 1454, 1362 cm⁻¹; HRMS (ESI): m/z calc'd for C₁₇H₂₅NH (M+H)⁺ 244.2065, found 244.2074.

General procedure for intermolecular carbonylation:



An oven-dried 5 mL pear-shaped flask was charged with Pd₂dba₃•CHCl₃ (5.0 mol%), PPh₃ (30 mol%), and a stir bar. The flask was fitted with a septum and purged with nitrogen. 2-MeTHF was added to make a 0.01 M solution, and the brown slurry was then stirred for 20 min at room temperature to give a clear yellow catalyst solution.

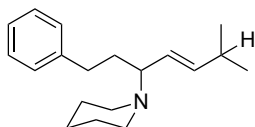
Meanwhile, a separate oven-dried 5 mL round-bottom flask containing of *N*-tosylhydrazone (3.0 equiv), benzyltriethylammonium chloride (1.0 equiv), lithium *tert*-butoxide base (5.4 equiv), and a stir bar was evacuated and back-filled with N₂ three times, and then capped with a septum. A solution of the vinyl iodide (1.0 equiv, 0.5 M in 2-MeTHF) was transferred from a pear-shaped flask by syringe to the dry reagents in the round-bottom flask. The residual vinyl iodide in the pear-shaped flask was transferred to the reaction vessel using 2-MeTHF (2 x 0.15 mL). Next, amine (5.0 equiv) was added to the round-bottom flask.

Finally, the catalyst solution was transferred to the reaction vessel via syringe, the remaining catalyst solution was transferred using 2-MeTHF (2 x 0.2 mL). The reaction vessel was fitted with a reflux condenser and capped with a septum. The reaction vessel was immersed in an 80 °C oil bath up to the level of the flask contents, and the stirred slurry rapidly reached reflux temperature.

The reaction was monitored by thin layer chromatography (20:79:1 EtOAc/hex/Et₃N) to check for depletion of the vinyl iodide. The reactions reached completion between ca. 3 and 5 h depending on *N*-tosylhydrazone. Upon consumption of the vinyl iodide, the reaction was allowed

to cool to room temperature and 1% (w/v) aq. NaOH was added to the reaction vessel. The mixture was extracted with EtOAc three times and the combined organic extracts were washed with brine, dried with Na₂SO₄, and concentrated *in vacuo*. The pyrrolidine was purified by silica gel chromatography.

(E)-1-(6-methyl-1-phenylhept-4-en-3-yl)piperidine, 6.9.



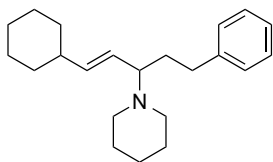
An oven-dried 5 mL pear-shaped flask was charged with Pd₂dba₃•CHCl₃ (8.6 mg, 0.008 mmol), PPh₃ (13.1 mg, 0.050 mmol), and a stir bar. The flask was fitted with a septum and purged with nitrogen. 2-MeTHF (0.2 mL) was added, and the brown slurry was then stirred for 20 min at room temperature to give a clear yellow catalyst solution.

Meanwhile, a separate oven-dried 5 mL round-bottom flask containing of *N*-tosylhydrazone (0.12 g, 0.499 mmol), benzyltriethylammonium chloride (46.2 mg, 0.166 mmol), lithium *tert*-butoxide base (72.2 mg, 0.899 mmol), and a stir bar was evacuated and back-filled with N₂ three times, and then capped with a septum. A solution of the (*Z*)-(4-iodobut-3-en-1-yl)benzene **6.8a** (43.0 mg, 0.167 mmol) in 0.2 mL of 2-MeTHF was transferred from a pear-shaped flask by syringe to the dry reagents in the round-bottom flask. The residual vinyl iodide in the pear-shaped flask was transferred to the reaction vessel using 2-MeTHF (2 x 0.15 mL). Next, piperidine (82 mL, 0.833 mmol) was added to the round-bottom flask.

Finally, the catalyst solution was transferred to the reaction vessel via syringe, the remaining catalyst solution was transferred 2-MeTHF (2 x 0.2 mL). The reaction vessel was fitted with a reflux condenser and capped with a septum. The reaction vessel was immersed in a 80 °C oil bath up to the level of the flask contents, and the stirred slurry rapidly reached reflux temperature. The reaction reached completion within 10 min and was allowed to cool to room

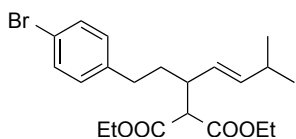
temperature; then 2 mL 1% (w/v) aq. NaOH was added to the reaction vessel. The mixture was extracted with 3x10 mL EtOAc and the combined organic extracts were washed with brine, dried with Na₂SO₄, and concentrated *in vacuo*. The pyrrolidine was purified by silica gel chromatography (10:85:5 EtOAc/Hex/Et₃N) to provide of pyrrolidine **6.9** (29.0 mg, 91%), as a yellow oil. *R_f* = 0.45 (10:90:5 EtOAc/Hexanes/Et₃N). ¹H NMR (600 MHz, CDCl₃) δ 7.37-7.21 (m, 2H), 7.20-7.08 (m, 3H), 5.47 (dd, *J* = 15.4, 6.6 Hz, 1H), 5.30 (dd, *J* = 15.4, 8.9 Hz, 1H), 2.73-2.69 (m, 1H), 2.65-2.59 (m, 1H), 2.56-2.45 (m, 3H), 2.42-2.26 (m, 3H), 2.07-1.82 (m, 1H), 1.83-1.64 (m, 1H), 1.64-1.47 (m, 4H), 1.46-1.33 (m, 2H), 1.02 (d, *J* = 6.7 Hz, 6H); ¹³C NMR (125 MHz, CDCl₃) δ 142.8, 141.5, 128.5, 128.3, 125.6, 125.5, 67.5, 50.6, 34.4, 33.0, 31.2, 26.4, 24.9, 22.9, 22.8; IR (thin film) 2929, 2856, 2791, 1495, 1453, 1101 cm⁻¹; HRMS (ESI): *m/z* calc'd for C₁₉H₂₉NH (M+H)⁺ 272.2378, found 272.2384.

(E)-1-(1-cyclohexyl-5-phenylpent-1-en-3-yl)piperidine, 6.12.



Following the general procedure for intermolecular carbonylation, vinyl iodide **6.11** (38.5 mg, 0.163 mmol) gave **6.12** (14.5 mg, 35%) as a yellow oil. *R_f* = 0.45 (10:90:5 EtOAc/Hex/Et₃N). ¹H NMR (500 MHz, CDCl₃) δ 7.27-7.24 (m, 2H), 7.17-7.14 (m, 3H), 5.44 (dd, *J* = 15.5, 6.6 Hz, 1H), 5.30 (ddd, *J* = 15.5, 9.0, 0.9 Hz, 1H), 2.71-2.59 (m, 2H), 2.54-2.48 (m, 3H), 2.38-2.96 (m, 2H), 2.03-1.92 (m, 2H), 1.76-1.53 (m, 7H), 1.60-1.50 (m, 4H), 1.43-1.39 (m, 2H), 1.33-1.24 (m, 3H), 1.22-1.07 (m, 3H); ¹³C NMR (125 MHz, CDCl₃) δ 142.8, 140.3, 128.5, 128.3, 126.1, 125.6, 67.6, 50.6, 40.8, 34.4, 33.4, 33.3, 33.0, 26.5, 26.3, 26.1, 24.9; IR (thin film) 2922, 2850, 1730, 1495, 1449, 1271, 1116 cm⁻¹; HRMS (ESI): *m/z* calc'd for C₂₂H₃₃NH (M+H)⁺ 312.2691, found 312.2698.

Diethyl (*E*)-2-(1-(4-bromophenyl)-6-methylhept-4-en-3-yl)malonate, 6.13ab.



Diethyl malonate (0.23 mL, 1.52 mmol, 12 equiv) was slowly added to a suspension of NaH (0.055 g, 1.38 mmol, 11 equiv) in THF (1.0 mL) at 0 °C. The mixture was stirred at room temperature for 10 min and set aside.

An oven-dried 5 mL pear-shaped flask was charged with Pd₂dba₃•CHCl₃ (6.5 mg, 0.006 mmol, 0.05 equiv), PPh₃ (9.4 mg, 0.038 mmol, 0.3 equiv), and a stir bar. The flask was fitted with a septum and purged with nitrogen. 2-MeTHF (0.3 mL) was added, and the brown slurry was then stirred for 20 min at room temperature to give a clear orange catalyst solution.

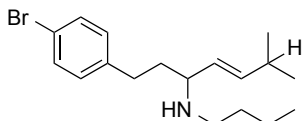
Meanwhile, a separate oven-dried 5 mL round-bottom flask containing of *N*-tosylhydrazine (91.2 mg, 0.380 mmol, 3.0 equiv), benzyltriethylammonium chloride (35.1 mg, 0.126 mmol, 1.0 equiv), lithium *tert*-butoxide base (54.8 mg, 0.683 mmol, 5.4 equiv), and a stir bar. The reaction vessel was evacuated and back-filled with N₂ three times, and then capped with a septum. A solution of the vinyl iodide **6.8b** (47.7 mg, 0.126 mmol, 1.0 equiv) in 0.2 mL of 2-MeTHF was transferred from a pear-shaped flask by syringe to the dry reagents in the round-bottom flask. The residual vinyl iodide in the pear-shaped flask was transferred to the reaction vessel using 2-MeTHF (2 x 0.15 mL). Sodium malonate solution was added via syringe to the round-bottom flask.

Finally, the catalyst solution was transferred to the reaction vessel via syringe, the remaining catalyst solution was transferred 2-MeTHF (2 x 0.2 mL). The reaction vessel was fitted with a reflux condenser and capped with a septum. The reaction vessel was immersed in a 80 °C oil bath up to the level of the flask contents, and the stirred slurry rapidly reached reflux temperature. The reaction reached completion within 3 h. The resulting orange mixture was cooled to room temperature and quenched with a saturated NH₄Cl solution. The resulting

solution was extracted three times with EtOAc. The combined organic extracts were washed with brine, dried over Na₂SO₄ and concentrated by rotary evaporation to give an orange oil.

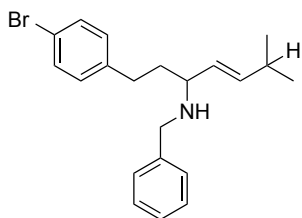
The crude reaction mixture was purified by silica gel chromatography (1:9 EtOAc/Hex) to afford **6.13ab** (24.3 mg, 71%), as a colorless oil. $R_f = 0.56$ (10:90 EtOAc/Hex). Isolated as a mixture of 2 regioisomers, 13% of the minor regioisomer was inseparable by column chromatography. ¹H NMR (600 MHz, CDCl₃) δ 7.38 (d, $J = 7.8$ Hz, 2H), 7.02 (d, $J = 7.9$ Hz, 1H), 5.48 (dd, $J = 15.3, 6.7$ Hz, 1H), 5.21 (dd, $J = 15.3, 9.6$ Hz, 1H), 4.22-4.04 (m, 4H), 3.30 (d, $J = 8.9$, 1H), 2.76-2.39 (m, 2H), 2.27 (dq, $J = 13.5, 6.6$ Hz, 1H), 1.83-1.48 (m, 1H), 1.29-1.20 (m, 6H), 0.97 (dd, $J = 10.9, 6.8$ Hz, 6H), ¹³C NMR (125 MHz, CDCl₃) δ 168.4, 168.2, 141.8, 140.9, 131.4, 131.3, 130.3, 130.2, 125.9, 119.5, 61.3, 61.2, 57.5, 42.6, 34.2, 32.9, 31.2, 25.8, 22.6, 22.5, 14.2, 14.2; IR (thin film) 2958, 1731, 1488, 1367, 1242, 1149 cm⁻¹; HRMS (ESI): m/z calc'd for C₂₁H₂₉BrO₄Na (M+Na)⁺ 447.1147, found 447.1154.

(E)-1-(4-bromophenyl)-N-butyl-6-methylhept-4-en-3-amine, 6.15ab.



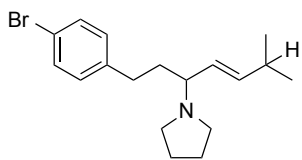
Following the general procedure for intermolecular carbonylation, vinyl iodide **6.8b** (53.9 mg, 0.143 mmol) gave **6.15ab** (20.9 mg, 43%) as a yellow oil. $R_f = 0.41$ (10:90:5 EtOAc/Hex/Et₃N). ¹H NMR (500 MHz, CDCl₃) δ 7.38 (d, $J = 8.0$ Hz, 2H), 7.04 (d, $J = 7.9$ Hz, 1H), 5.49 (dd, $J = 15.4, 6.6$ Hz, 1H), 5.14 (dd, $J = 15.4, 8.4$ Hz, 1H), 2.93-2.88 (m, 1H), 2.67-2.49 (m, 2H), 2.46-2.41 (m, 2H), 2.36-2.27 (m, 1H), 1.81-1.74 (m, 1H), 1.68-1.60 (m, 1H), 1.47-1.38 (m, 2H), 1.35-1.29 (m, 2H), 1.01 (d, $J = 6.6$ Hz, 6H), 0.9 (t, $J = 7.2$ Hz, 4H); ¹³C NMR (125 MHz, CDCl₃) δ 141.2, 131.4, 130.3, 119.4, 66.9, 60.6, 46.7, 31.8, 31.0, 22.69, 22.64, 20.5, 14.0; IR (thin film) 2956, 2926, 2867, 1488, 1464, 1072, 1012 cm⁻¹; HRMS (ESI): m/z calc'd for C₁₈H₂₈NBrH (M+H)⁺ 338.1483, found 338.1496.

(E)-N-benzyl-1-(4-bromophenyl)-6-methylhept-4-en-3-amine, 6.16ab.



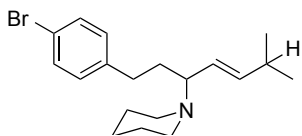
Following the general procedure for intermolecular carbonylation, vinyl iodide **6.8b** (148 mg, 0.440 mmol) gave **6.16ab** (33.7 mg, 21%) as a colorless oil. $R_f = 0.9$ (20:79:1 EtOAc/Hex/Et₃N). ¹H NMR (500 MHz, CDCl₃) δ 7.36 (d, $J = 8.4$ Hz, 2H), 7.32-7.22 (m, 5H), 7.23 (d, $J = 8.4$ Hz, 2H), 5.50 (dd, $J = 15.4, 6.7$ Hz, 1H), 5.19 (ddd, $J = 15.4, 8.5, 1$ Hz, 1H), 3.80 (d, $J = 13.2$ Hz, 1H), 3.62 (d, $J = 13.2$, 1H), 2.96 (m, 1H), 2.57 (m, 2H), 2.37-2.30 (m, 1H), 1.81-1.74 (m, 1H), 1.71-1.64 (m, 1H), 1.02 (dd, $J = 6.8, 3.2$ Hz, 6H); ¹³C NMR (125 MHz, CDCl₃) δ 141.4, 140.8, 140.7, 131.4, 130.2, 129.2, 128.4, 128.3, 126.9, 119.4, 59.7, 51.2, 37.5, 31.8, 31.0, 22.74, 22.70; IR (thin film) 2923, 1727, 1488, 1454, 1288, 1105, 1072, 1011 cm⁻¹; HRMS (ESI): m/z calc'd for C₂₁H₂₆BrNH (M+H)⁺ 372.1327, found 372.1328.

(E)-1-(1-(4-bromophenyl)-6-methylhept-4-en-3-yl)pyrrolidine, 6.17ab.



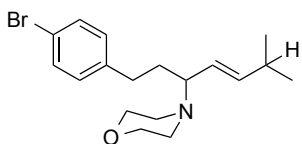
Following the general procedure for intermolecular carbonylation, vinyl iodide **6.8b** (51.2 mg, 0.136 mmol) gave **6.17ab** (32.0 mg, 70 %) as a yellow oil. $R_f = 0.43$ (10:90:5 EtOAc/Hex/Et₃N). ¹H NMR (500 MHz, CDCl₃) δ 7.38 (d, $J = 8.3$ Hz, 2H), 7.04 (d, $J = 8.3$ Hz, 2H), 5.50 (dd, $J = 15.4, 6.6$ Hz, 1H), 5.31 (ddd, $J = 15.4, 8.9, 0.6$ Hz, 1H), 2.64-2.41 (m, 6H), 2.35-2.29 (m, 1H), 2.01-1.94 (m, 1H), 1.75-1.65 (m, 6H), 1.01 (dd, $J = 6.8, 3.3$ Hz, 6H); ¹³C NMR (125 MHz, CDCl₃) δ 141.6, 140.7, 131.3, 130.3, 127.9, 119.4, 67.1, 51.6, 35.7, 31.9, 31.0, 23.2, 22.7; IR (thin film) 2957, 2867, 2782, 1487, 1458, 1361, 1121, 1071, 1011 cm⁻¹; HRMS (ESI): m/z calc'd for C₁₈H₂₆BrNH (M+H)⁺ 336.1327, found 336.1330.

(E)-1-(1-(4-bromophenyl)-6-methylhept-4-en-3-yl)piperidine, 6.18ab.



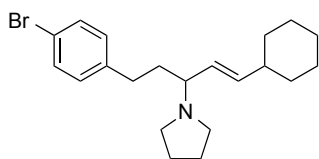
Following the general procedure for intermolecular carbonylation, vinyl iodide **6.8b** (49.7 mg, 0.132 mmol) gave **6.18ab** (34.0 mg, 74%) as a yellow oil. $R_f = 0.45$ (10:90:5 EtOAc/Hex/Et₃N). ¹H NMR (600 MHz, CDCl₃) δ 7.42-7.33 (m, 2H), 7.04 (d, $J = 8.3$ Hz, 2H), 5.44 (dd, $J = 15.4, 6.6$ Hz, 1H), 5.31-5.25 (m, 1H), 2.68-2.65 (m, 1H), 2.61-2.56 (m, 1H), 2.50-2.45 (m, 3H), 2.33-2.29 (m, 3H), 1.94-1.86 (m, 1H), 1.71-1.61 (m, 1H), 1.61-1.48 (m, 4H), 1.43-1.35 (m, 2H), 1.01 (dd, $J = 6.7, 2.1$ Hz, 6H); ¹³C NMR (125 MHz, CDCl₃) δ 141.7, 141.6, 131.3, 130.3, 125.4, 119.3, 67.2, 50.6, 34.2, 32.4, 31.2, 26.5, 24.9, 22.9, 22.8; IR (thin film) 2929, 2855, 2791, 1660, 1487, 1452, 1095, 1071, 1011 cm⁻¹; HRMS (ESI): m/z calc'd for C₁₉H₂₈BrNH (M+H)⁺ 350.1483, found 350.1482.

(E)-4-(1-(4-bromophenyl)-6-methylhept-4-en-3-yl)morpholine, 6.19ab.



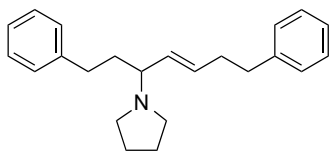
Following the general procedure for intermolecular carbonylation, vinyl iodide **6.14** (47.6 mg, 0.126 mmol) gave **6.19ab** (31.9 mg, 72%) as a colorless oil. $R_f = 0.41$ (10:90:5 EtOAc/Hex/Et₃N). ¹H NMR (600 MHz, CDCl₃) δ 7.40-7.36 (m, 2H), 7.04 (d, $J = 8.3$ Hz, 2H), 5.44 (dd, $J = 15.5, 6.6$ Hz, 1H), 5.31-5.25 (ddd, $J = 15.5, 6.6, 1.2$ Hz, 1H), 3.76-3.62 (m, 4H), 2.68-2.58 (m, 2H), 2.58-2.46 (m, 3H), 2.43-2.37 (m, 2H), 2.36-2.29 (m, 1H), 1.97-1.87 (m, 1H), 1.70-1.61 (m, 1H), 1.01 (dd, $J = 6.8, 1.1$ Hz, 6H); ¹³C NMR (125 MHz, CDCl₃) δ 142.4, 141.4, 131.4, 130.3, 125.0, 119.4, 67.4, 67.0, 50.1, 33.6, 32.0, 31.2, 22.8, 22.7; IR (thin film) 2954, 2853, 2810, 1487, 1452, 1117, 1071, 1011 cm⁻¹; HRMS (ESI): m/z calc'd for C₁₈H₂₆BrNOH (M+H)⁺ 352.1276, found 352.1278.

(E)-1-(5-(4-bromophenyl)-1-cyclohexylpent-1-en-3-yl)piperidine, 6.20cb.



Following the general procedure for intermolecular carbenylation, vinyl iodide **6.8b** (53.9 mg, 0.160 mmol) gave **6.20cb** (47.0 mg, 78%) as a yellow oil. $R_f = 0.59$ (5:95:3 EtOAc/Hex/Et₃N). ¹H NMR (500 MHz, CDCl₃) δ 7.37 (d, $J = 8.2$ Hz, 2H), 7.33-7.24 (d, $J = 8.1$ Hz, 2H), 5.48 (dd, $J = 15.5, 6.6$ Hz, 1H), 5.31 (dd, $J = 15.4, 8.9$ Hz, 1H), 2.70-2.31 (m, 8H), 1.99-1.94 (m, 2H), 1.80-1.60 (m, 9H), 1.35-1.00 (m, 6H); ¹³C NMR (125 MHz, CDCl₃) δ 141.6, 139.6, 131.3, 130.3, 128.3, 119.3, 67.2, 51.6, 40.6, 35.7, 33.2, 33.3, 31.9, 26.2, 26.1, 23.2; IR (thin film) 2921, 1652, 1487, 1447, 1122, 1072, 1011 cm⁻¹; HRMS (ESI): m/z calc'd for C₂₁H₃₀BrNH (M+H)⁺ 376.1640, found 376.1637.

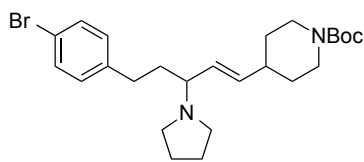
(E)-1-(1,8-diphenyloct-4-en-3-yl)piperidine, 6.21ba.



Following the general procedure for intermolecular carbenylation, vinyl iodide **6.8a** (49.0 mg, 0.190 mmol) gave **6.21ba** (34.3 mg, 57%) as a yellow oil. $R_f = 0.39$ (10:90:5 EtOAc/Hex/Et₃N). ¹H NMR (500 MHz, CDCl₃) δ 7.28-7.25 (m, 4H), 7.20-7.13 (m, 6H), 5.56 (dt, $J = 15.4, 6.7$ Hz, 1H), 5.41-5.37 (m, 1H), 2.75-2.72 (m, 2H), 2.62-2.56 (m, 2H), 2.48-2.39 (m, 5H), 2.00-1.94 (m, 1H), 1.73-1.67 (m, 4H), 1.63 (s, 3H); ¹³C NMR (125 MHz, CDCl₃) δ 142.7, 141.8, 132.2, 128.5, 128.4, 128.33, 128.30, 125.8, 125.6, 67.3, 51.6, 35.83, 35.80, 34.1, 32.4, 23.2; IR (thin film) 2925, 2782, 1603, 1495, 1454 cm⁻¹; HRMS (ESI): m/z calc'd for C₂₃H₂₉NH (M+H)⁺ 320.2378, found 320.2379.

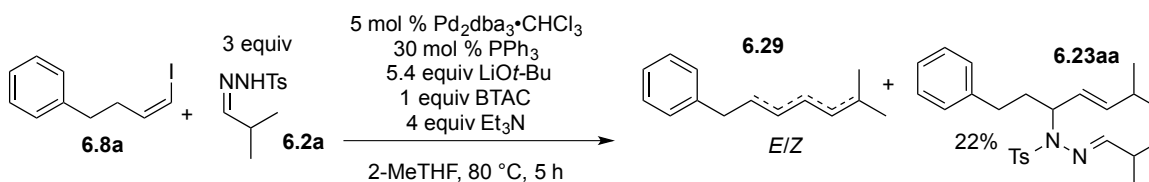
tert-Butyl (E)-4-(5-(4-bromophenyl)-3-(piperidin-1-yl)pent-1-en-1-yl)piperidine-1-carboxylate, 6.22db.

Following the general procedure for intermolecular carbenylation, vinyl iodide **6.8b** (49.9 mg, 0.148 mmol) gave **6.22db** (35.3 mg, 50%) as a yellow oil. $R_f = 0.27$ (10:90:5



EtOAc/Hex/Et₃N). ¹H NMR (500 MHz, CDCl₃) δ 7.37 (d, *J* = 8.4 Hz, 2H), 7.03 (d, *J* = 8.4 Hz, 2H), 5.49 (dd, *J* = 15.5, 6.4 Hz, 1H), 5.38 (dd, *J* = 15.7, 8.7 Hz, 1H), 4.10 (m, 2H), 2.82-2.69 (m, 2H), 2.63-2.40 (m, 7H), 2.19-2.12 (m, 1H), 2.02-1.96 (m, 1H), 1.75-1.67 (m, 6H), 1.46 (s, 9H), 1.35-1.27 (m, 3H); ¹³C NMR (125 MHz, CDCl₃) δ 154.9, 141.3, 137.5, 131.4, 130.2, 129.6, 119.4, 79.4, 67.0, 51.6, 38.8, 35.4, 32.0, 31.8, 29.8, 28.5, 23.2; IR (thin film) 2927, 2853, 1689, 1422, 1364, 1274, 1231, 1162 cm⁻¹; HRMS (ESI): *m/z* calc'd for C₂₅H₃₇BrN₂O₂H (M+H)⁺ 477.2117, found 477.2126.

Control experiment: Carbenylation in the absence of the amine nucleophile.



An oven-dried 5 mL pear-shaped flask was charged with Pd₂dba₃•CHCl₃ (7.6 mg, 0.007 mmol), PPh₃ (11.5 mg, 0.044 mmol), and a stir bar. The flask was fitted with a septum and purged with nitrogen. 2-MeTHF (0.2 mL) was added, and the brown slurry was then stirred for 20 min at room temperature to give a clear yellow catalyst solution.

Meanwhile, a separate oven-dried 5 mL round-bottom flask containing of *N*-tosylhydrazone **6.2a** (0.11 g, 0.441 mmol), benzyltriethylammonium chloride (40.8 mg, 0.147 mmol), lithium *tert*-butoxide base (63.6 mg, 0.793 mmol), and a stir bar was evacuated and back-filled with N₂ three times, and then capped with a septum. A solution of the (*Z*)-(4-iodobut-3-en-1-yl)benzene **6.8a** (37.9 mg, 0.147 mmol) in 0.2 mL of 2-MeTHF was transferred from a pear-shaped flask by syringe to the dry reagents in the round-bottom flask. The residual vinyl iodide

in the pear-shaped flask was transferred to the reaction vessel using 2-MeTHF (2 x 0.15 mL). Next, triethylamine (78 mL, 0.587 mmol) was added to the round-bottom flask.

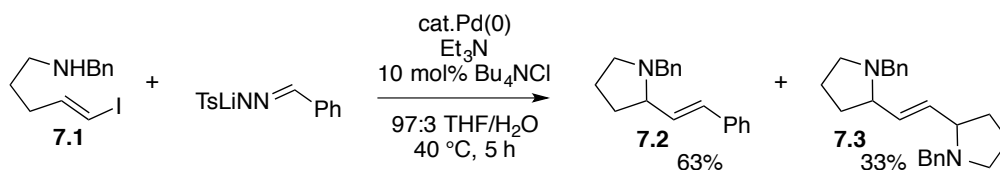
Finally, the catalyst solution was transferred to the reaction vessel via syringe, the remaining catalyst solution was transferred using 2-MeTHF (2 x 0.2 mL). The reaction vessel was fitted with a reflux condenser and capped with a septum. The reaction vessel was immersed in a 80 °C oil bath up to the level of the flask contents, and the stirred slurry rapidly reached reflux temperature. The reaction reached completion within 3 h and was allowed to cool to room temperature; then 2 mL 1% (w/v) aq. NaOH was added to the reaction vessel. The mixture was extracted with 3x10 mL EtOAc and the combined organic extracts were washed with brine, dried with Na₂SO₄, and concentrated *in vacuo*. The crude reaction mixture was analyzed by GC/MS (EI). In the absence of an amine nucleophile, the reaction conditions resulted in 43% of β-hydride eliminated diene **6.29**, 22% of **6.23aa** and 10% of remaining starting vinyl iodide **6.8a**.

Chapter 7

Palladium-Catalyzed Bis-cyclization/Dimerization Reactions

In 2012, we reported an intramolecular carbenylative amination reaction that employed *N*-tosylhydrazones as carbene precursors to generate 2-substituted pyrrolidines **7.2**.^{184b} During optimization of the carbenylative amination, we noted that dimerization of the vinyl halide was competing with the desired carbenylation reaction to form bis-pyrrolidine **7.3** (Scheme 7-1). When the *N*-tosylhydrazone was omitted from the reaction, the bis-pyrrolidine dimer **7.3** was formed in 67% yield. Intrigued by this unprecedented dimerization, my coworker Avinash Khanna and I set out to explore the scope and potential applications of the reaction.

Scheme 7-1: Dimerization as a Competing Side Reaction in Carbenylative Amination

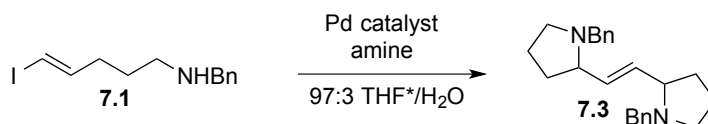


First we sought to identify which components of the heavily optimized carbenylative insertion were necessary for the dimerization reaction and to improve the yield of the dimer (Table 7-1). Among the catalyst precursors that we examined (Ph₃P)₄Pd proved to be more efficient than Pd₂dba₃•CHCl₃ or palladium(II) pre-catalysts (entries 1-5). Reducing the amount of lithium *tert*-butoxide to just 1.1 equivalents was beneficial (entries 1, 6 and 7), but surprisingly, lithium hydroxide was less efficient than lithium *tert*-butoxide, even though water is a cosolvent. Other metal alkoxides were less efficient (entries 7, 10 and 11). Substitution of lithium *tert*-butoxide with silver salts as bases led to a dramatic acceleration of the reaction rate, reducing the half-life to under an hour (entries 12-15). The triethylamine additive proved to be

dispensable (entries 18 and 20). Ultimately, the best yields with silver phosphate were obtained at 55 °C (entries 18 and 20).

Other experiments not shown in Table 1 revealed that the added water was essential for good yields and that other solvents were less efficient. Surprisingly, doubling the amount of palladium catalyst to 10 mol % reduced the yield of dimer **7.3**.

Table 7-1: Optimization of the Bis-cyclization/Dimerization of Vinyl Iodide **7.1** to Generate Dimer **7.3**



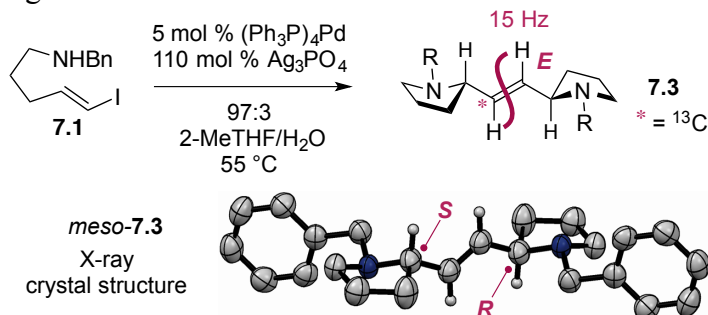
entry	Pd source (mol %)	phosphine (mol %)	base (equiv)	equiv Et ₃ N	temp	time	yield
1	Pd ₂ dba ₃ •CHCl ₃ (2.5%)	Ph ₃ P (15%)	<i>t</i> -BuOLi (2.2)	2	23 °C	24 h	61%
2	(Ph ₃ P) ₄ Pd (5.0%)	-	<i>t</i> -BuOLi (2.2)	2	23 °C	24 h	65%
3	(Ph ₃ P) ₂ PdCl ₂ (5.0%)	-	<i>t</i> -BuOLi (2.2)	2	23 °C	24 h	47%
4	Pd ₂ dba ₃ •CHCl ₃ (2.5%)	dppe (5%)	<i>t</i> -BuOLi (2.2)	2	23 °C	24 h	50%
5	Pd(OAc) ₂ (5.0%)	Ph ₃ P (10%)	<i>t</i> -BuOLi (2.2)	2	23 °C	24 h	18%
6	Pd ₂ dba ₃ •CHCl ₃ (2.5%)	Ph ₃ P (15%)	<i>t</i> -BuOLi (4.4)	2	23 °C	24 h	33%
7	Pd ₂ dba ₃ •CHCl ₃ (2.5%)	Ph ₃ P (15%)	<i>t</i> -BuOLi (1.1)	2	23 °C	24 h	67%
8	Pd ₂ dba ₃ •CHCl ₃ (2.5%)	Ph ₃ P (15%)	-	2	23 °C	24 h	10%
9	Pd ₂ dba ₃ •CHCl ₃ (2.5%)	Ph ₃ P (15%)	LiOH (1.1)	2	23 °C	24 h	48%
10	Pd ₂ dba ₃ •CHCl ₃ (2.5%)	Ph ₃ P (15%)	<i>t</i> -BuONa (1.1)	2	23 °C	24 h	<20%
11	Pd ₂ dba ₃ •CHCl ₃ (2.5%)	Ph ₃ P (15%)	<i>t</i> -BuOK (1.1)	2	23 °C	24 h	55%
12	Pd ₂ dba ₃ •CHCl ₃ (2.5%)	Ph ₃ P (15%)	Ag ₂ CO ₃ (1.1)	2	23 °C	3 h	51%
13	Pd ₂ dba ₃ •CHCl ₃ (2.5%)	Ph ₃ P (15%)	Ag ₃ PO ₄ (1.1)	2	23 °C	3 h	61%
14	Pd ₂ dba ₃ •CHCl ₃ (2.5%)	Ph ₃ P (15%)	Ag ₃ PO ₄ (0.37)	2	23 °C	3 h	65%
15	Pd ₂ dba ₃ •CHCl ₃ (2.5%)	Ph ₃ P (15%)	Ag ₃ PO ₄ (0.11)	2	23 °C	3 h	49%
16	(Ph ₃ P) ₄ Pd (5.0%)	-	Ag ₃ PO ₄ (1.1)	2	23 °C	3 h	71%
17	(Ph ₃ P) ₄ Pd (5.0%)	-	Ag ₃ PO ₄ (0.37)	2	23 °C	3 h	50%
18	(Ph ₃ P) ₄ Pd (5.0%)	-	Ag ₃ PO ₄ (1.1)	2	55 °C	1 h	72%
19	(Ph ₃ P) ₄ Pd (5.0%)	-	Ag ₃ PO ₄ (1.1)	2	80 °C	0.16 h	65%
20	(Ph ₃ P) ₄ Pd (5.0%)	-	Ag ₃ PO ₄ (1.1)	0	55 °C	1 h	75%

* temperature dependence studies were carried out in 2-methyltetrahydrofuran

The optimized dimerization reaction generates only the *trans* alkene. The configuration of the double bond in **7.3** was established rigorously as *E* by the 15 Hz coupling constants in the ¹³C satellites for the olefinic protons (Scheme 7-2). With alkoxide bases, dimer (*E*)-**7.3** was present as a mixture of two different stereoisomers in about 95:5 ratio, differing in configuration at the

stereogenic centers. With silver phosphate a single stereoisomer was obtained. The stereochemistry of the dimer **7.3** was rigorously established as *meso* by a crystal structure (Scheme 7-2). Of note, *meso* dimers of this kind cannot be efficiently made through olefin metathesis.

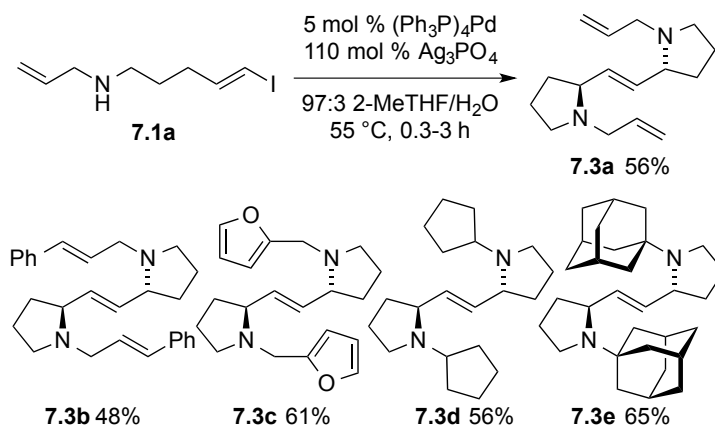
Scheme 7-2: NMR and X-ray Crystallography Establish the Configuration of the Double Bond and the Relative Configuration



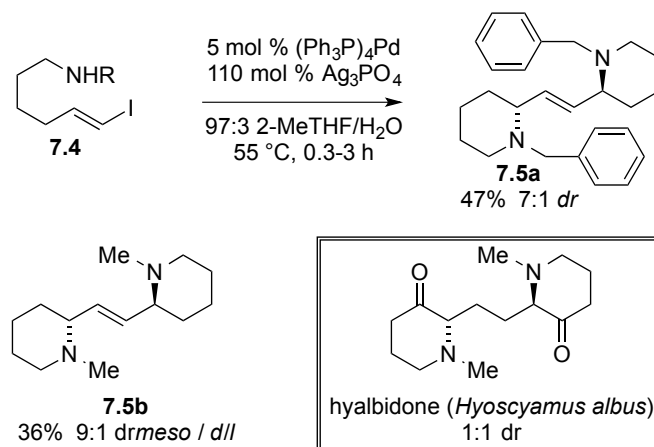
With optimized conditions for stereoselective formation of the dimer **7.3** we next assessed the tolerance of the reaction to variations of the *N*-alkyl substituent (Scheme 7-3). The reaction was chemoselective, tolerating terminal olefins and styryl groups to give **7.3a** and **7.3b** in 56% and 48% yield, respectively. The reaction tolerated electron rich furans to give dimer **7.3c** in good yield. Surprisingly, cyclopentyl, and even 1-adamantyl substituents were well tolerated on the amino group. However, the *N*-adamantyl substrate required a slightly longer reaction time (3 h) to generate **7.3e**.

The bis-piperidines are formed less efficiently than bis-pyrrolidines under the optimized reaction conditions (Scheme 7-4). However the dimerization of **7.4** directly generates the skeleton of the bis-piperidine alkaloid hyalbidone in a single step. The natural product hyalbidone was isolated as mixture of *meso* and *d/l* isomers from the roots of *H. albus*.¹⁹² It is not clear whether the mixture of stereoisomers occurs in Nature or was the result of epimerization during isolation.

Scheme 7-3: The Bis-cyclization/Dimerization Reaction Tolerates a Variety of *N*-Alkyl Groups

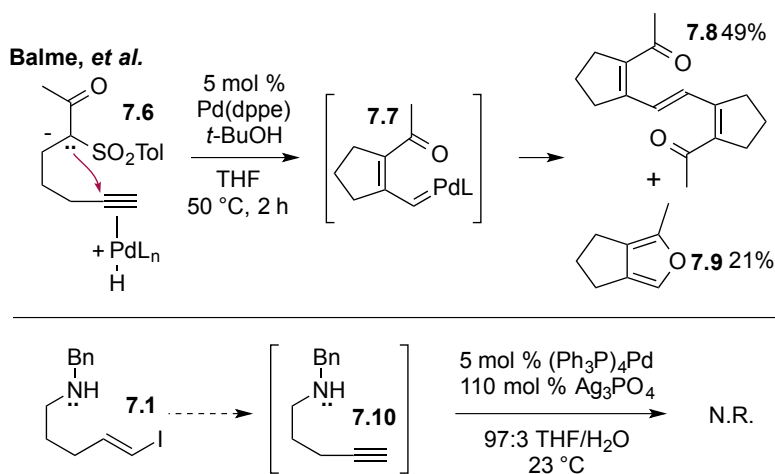


Scheme 7-4: One-Step Synthesis of the Hyalbidone Skeleton



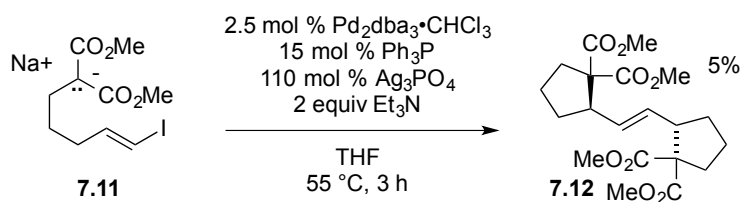
The dimeric products accessed by our reaction bear a remarkable resemblance to the dimeric products noted by Balme and co-workers in the palladium-catalyzed reactions of terminal ω -sulfonylalkyne **7.6** (Scheme 7-5). The products observed by Balme¹⁹³ were rationalized to arise from carbopalladation of a terminal alkyne by a hydridopalladium species leading to Pd(0) alkylidene intermediate **7.7**.¹⁹⁴

Scheme 7-5: The Balme Dimerization of Terminal Alkynes is Distinct from Reactions of Vinyl Halides



We do not observe alkyne intermediates in our dimerization reactions. To test whether our reaction was occurring through a *syn* elimination to form a terminal alkyne intermediate, we synthesized the terminal alkyne **7.10** and subjected it to the bis-cyclization/dimerization reaction conditions. No dimer was formed and the alkyne starting material **7.10** was recovered. Thus, the bis-cyclization/dimerization reaction reported in this work is complementary to, yet distinct from, the desulfonylative dimerization of alkynes reported by Balme.

Scheme 7-6: Bis-Cyclization/Dimerization with a Carbon Nucleophile



The Balme system exploited a carbon-centered nucleophile to forge the cyclodimer **7.8**. To test the potential for carbon nucleophiles in our cyclodimerization, substrate **7.11** was synthesized and subjected to the optimized conditions from Scheme 7-3. None of the desired dimer was formed even when water was omitted to prevent hydrolysis of the malonate ester.

Using slightly modified conditions, the hindered bis-cyclopentane **7.12** was formed in a modest 5% yield, representing a single turnover (Scheme 7-6).

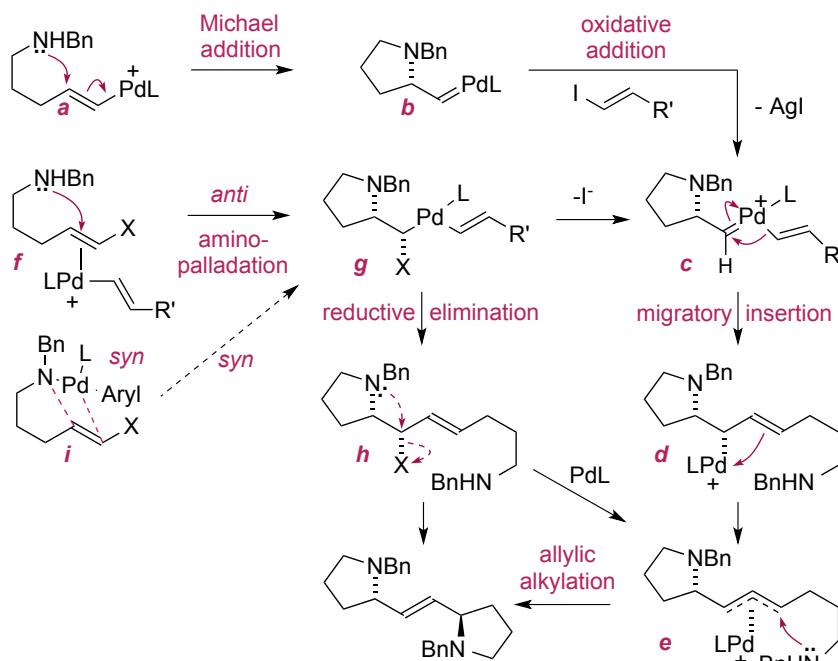
The beneficial effect of silver is consistent with the involvement of a vinylpalladium(II) cation (Scheme 7-7). Inspired by the palladium carbenes proposed for the Balme reaction, we hypothesized that the ω -amino group on intermediate **a** might be poised to add to the vinylpalladium cation in a process resembling a Michael addition.¹⁹⁵ The resulting palladium(0) carbene **b** could then undergo oxidative addition, much like palladium(0) complexes with *N*-heterocyclic carbene ligands, to generate vinylpalladium carbene **c**. Migratory insertion would generate an η^1 -allylpalladium intermediate **d** which could undergo an allylic alkylation through the η^3 -allylpalladium intermediate **e**.

Alternatively, the first C–N bond might arise through an intramolecular aminopalladation reaction of **f** or **i** to generate α -iodopalladium carbenoid intermediate **g**. α -Elimination of the halide would produce the same palladium carbene intermediate **c** that was invoked for the Michael-type addition mechanism. Palladium carbenoid **g** is also set up for reductive elimination to generate an allyl iodide **h**, that could undergo substitution through an S_N2' reaction or a palladium-catalyzed allylic alkylation.

The starting materials in this bis-cyclization reaction bear a striking resemblance to *N*-Boc and *N*-aryl substrates used in the Wolfe reaction and related processes.¹⁹⁶ However, both Balme¹⁹⁷ and Wolfe¹⁹⁸ have independently noted the failure of *N*-alkylamines (and specifically *N*-benzylpent-4-en-1-amine) to engage in intramolecular *syn* aminopalladation reactions, presumably due to the difficulty in forming the amidopalladium intermediate **i** (X = H). Given the lack of precedence for Wolfe reactions of *N*-alkylamines, we are reluctant to invoke *syn* aminopalladation. Complexes such as **f** would be well-suited for an *anti* aminopalladation –

analogues to a Wacker reaction – leading to the palladium carbenoid **g**.¹⁹⁹ Given the potential for vicinal amino groups to promote substitution with double inversion,²⁰⁰ the stereospecificity of the aminopalladation can not be used to rationalize formation of the *meso* bis-pyrrolidine **3** from either diastereomer of intermediate **g**.

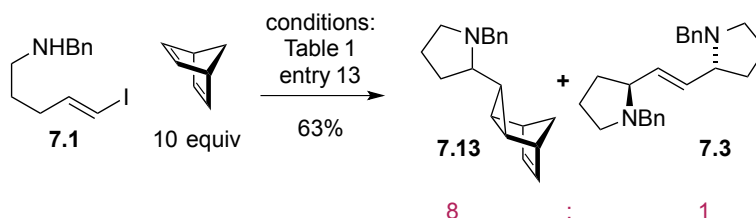
Scheme 7-7: A Variety of Mechanistic Pathways Would Lead to Dimer



When vinyl iodide **7.1** was subjected to the dimerization reaction in the presence of norbornadiene, an 8:1 mixture of cyclopropane **7.13** and dimer **7.3** was obtained. The formation of cyclopropanes is consistent with Pd(0) alkylidene intermediates. We showed that vinyl iodide **7.1** and related compounds **7.1a-7.1e** could cyclopropanate norbornadiene (Scheme 7-8) consistent with a palladium-alkylidene intermediate **b** in Scheme 7-7.^{201,193} Unfortunately, cyclopropanation of norbornenes is also consistent with a double carbopalladation sequence proposed by Catellani and co-workers or a carbopalladation/aminopalladation/reductive elimination sequence.^{202, 203} When styrene was added to the reaction mixture, no cyclopropanation was observed. Thus, it is unclear whether formation of cyclopropanes from

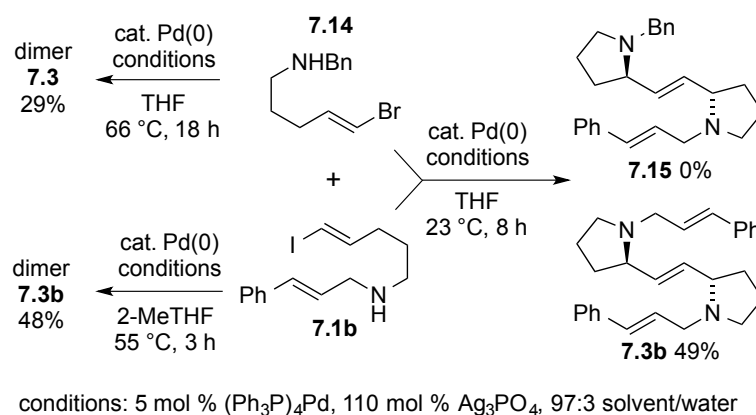
vinyl iodide **7.1** and norbornadiene is evidence for a Pd(0) alkylidene intermediate or merely symptomatic of the unique reactivity of norbornenes.

Scheme 7-8: A Cyclopropanation Experiment



In order to gather mechanistic insight we set up a crossover experiment, taking advantage of the sluggish oxidative addition of vinyl bromides relative to vinyl iodides (Scheme 7-9). Vinyl bromide **7.14** gives little reaction at 55 °C over 3 h, conditions where vinyl iodide **7.1b** generates dimer **7.3b** in 48% yield. The vinyl bromide can be coaxed to form dimer **7.3** in 29% yield at higher temperature and with an extended reaction time. When 50 mol % of vinyl iodide **7.1b** and 50 mol % of vinyl bromide **7.14** were subjected to the reaction, the only dimer that formed was the bis-cinnamylamine dimer **7.3b**, isolated in 49% yield. None of the bis-benzylamine dimer **7.3** and none of the mixed dimer **7.15** were observed during the reaction or after workup. Some of the vinyl bromide (35%) starting material was recovered whereas the vinyl iodide was completely consumed.

Scheme 7-9: A Crossover Experiment



Based on the result of this crossover experiment, the aminopalladation pathway in Scheme 7-7 is untenable because the intermediate cationic Pd(II)•olefin complex **f** would be expected to undergo intramolecular aminopalladation at comparable rates regardless of whether the halide substituent X was bromide or iodide. The intermediate **g** (X=Br) would either generate mixed dimer **7.15**, or if unreactive, would reduce the catalytic turnover and yield; and neither of these results was observed. In contrast, the exclusive formation of dimer **7.3b** is consistent with the Michael-type addition/oxidative addition pathway in which both of the vinyl halides that are incorporated into the dimer participate through successive oxidative additions. The ability to access palladium(0) alkylidene intermediates such as **b** in Scheme 7-7 from vinyl halides would offer immense potential for construction of complex molecules.²⁰⁴

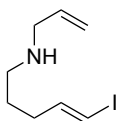
In conclusion we have described the first example of a bis-cyclization/dimerization reaction of vinyl iodides that generates *meso* bis-pyrrolidines and bis-piperidines. The reaction tolerates a range of *N*-alkyl substituents and was used to synthesize the skeleton of the alkaloid hyalbidone in a single step. A crossover experiment is consistent with a novel Michael-type addition of an amine to a vinylpalladium cation giving rise to a palladium(0) alkylidene intermediate.

Experimental Section

Vinyl iodides **7.1a-e** and **7.11** were synthesized by the method of Khanna and co-workers.²⁰¹

Experimental

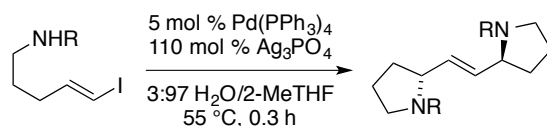
(*E*)-*N*-Allyl-5-iodopent-4-en-1-amine, **7.1a**.



A flame dried 5 mL round bottom flask was charged with the (*E*)-5-iodopent-4-en-1-yl methanesulfonate²⁰¹ (0.29 g, 1.0 mmol, 1.0 equiv). Next, allyl amine (0.75 mL, 10 mmol, 10 equiv) and 0.8 mL DMSO were added by syringe. Then sodium

iodide (8.2 mg, 0.055 mmol, 0.055 equiv) was added to the reaction flask by quickly opening the septum. This mixture was heated at 55 °C until the mesylate starting material was no longer detectable by TLC (EtOAc/hex 50:50), 3 h. Upon consumption of the mesylate, the reaction mixture was added to 1% (w/v) aq. NaOH (3 mL) and then extracted with (3 x 5 mL) Et₂O. The combined organic extracts were dried with Na₂SO₄ and concentrated *in vacuo* to give a yellow oil. The oil was purified by flash chromatography with EtOAc/hex/Et₃N (20:80:5) to afford the monoalkylated amine **7.1a** as a brown oil (0.24 g, 0.97 mmol, 97%). *R_f* = 0.35 (20:80:5 EtOAc/hex/Et₃N); ¹H NMR (500 MHz, CDCl₃) δ 6.51 (dt, *J* = 14.0, 7.5 Hz, 1H), 5.99 (d, *J* = 14.9 Hz, 1H), 5.88 (m, 1H), 5.18 (dd, *J* = 17.0, 1.5 Hz, 1H), 5.08 (d, *J* = 10.0 Hz, 1H), 3.23 (d, *J* = 6.0 Hz, 2H), 2.60 (t, *J* = 7.2 Hz, 2H), 2.09-2.13 (m, 2H), 1.56-1.61 (m, 2H), 1.20 (br s, 1H); ¹³C NMR (125 MHz, CDCl₃) δ 146.1, 136.9, 115.9, 74.9, 52.5, 48.5, 33.9, 28.8; IR (thin film) 2935, 2853, 2250, 1667, 1551; HRMS (ESI): *m/z* calculated for C₈H₁₃IN [M-H]⁻ 250.0094, found 250.0093.

General procedure for the dimerization of ω-aminovinyl iodides, 7.3, 7.3a-e:

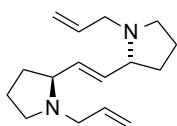


A 10 mL pear-shaped flask was charged with tetrakis(triphenylphosphine)palladium (0.050 equiv), silver(I) phosphate (1.1 equiv) and a stir bar. The flask was fitted with a septum and purged with nitrogen. Meanwhile, a separate 5 mL pear-shaped flask was charged with the ω-aminovinyl iodide (1.0 equiv). Under a stream of nitrogen, the pear-shaped flask was fitted with a septum and 2-MeTHF (0.07 M with respect to the vinyl iodide) was added. The solution of vinyl iodide was added to the flask containing the tetrakis(triphenylphosphine)palladium and inorganic base, followed sequentially by water (20 equiv). Reaction mixture was heated to 55 °C

by immersing the reaction flask in a hot oil bath up to the level of the flask's contents. The reaction was monitored for consumption of the vinyl iodide by TLC (10:90:5 EtOAc/hex/Et₃N).

Upon consumption of the vinyl iodide, the reaction was cooled to room temperature, the crude reaction mixture was washed with 1% (w/v) aq. NaOH. The aqueous layer was then extracted with (3 x 10 mL) Et₂O. The combined organic layers were then washed with brine and dried over Na₂SO₄. The resulting organic solution was concentrated *in vacuo* to give dark brown oil. The oil was then purified by flash chromatography with EtOAc/hex/Et₃N (10:90:5) to afford the bis-pyrrolidine dimer.

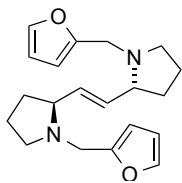
(*E*)-1-((*R*)-1-Allylpyrrolidin-2-yl)-2-((*S*)-1-allylpyrrolidin-2-yl)ethane, 7.3a.



Using the general procedure for dimerization outlined above, (*E*)-*N*-allyl-5-iodopent-4-en-1-amine **7.1a** (29 mg, 0.11 mmol, 1.0 equiv) was used and the product was purified by flash chromatography with EtOAc/hex/Et₃N (10:90:5) to afford the bis-pyrrolidine dimer **7.3a** as a dark brown oil (7.8 mg, 0.032 mmol, 56%). *R_f* = 0.78 (10:90:5 EtOAc/hex/Et₃N); ¹H NMR (500 MHz, CDCl₃) δ 5.94-5.86 (m, 2H), 5.49-5.48 (m, 2H), 5.19-5.16 (m, 2H), 5.11-5.09 (m, 2H), 3.45-3.39 (m, 2H), 3.18-3.09 (m, 4H), 2.66-2.62 (m, 2H), 2.18-2.13 (m, 2H), 1.97-1.82 (m, 4H), 1.76-1.71 (m, 2H), 1.61-1.54 (m, 2H); ¹³C NMR (125 MHz, CDCl₃) δ 136.1, 136.0, 134.9, 134.6, 117.1, 117.0, 61.2, 62.0, 57.0, 56.8, 53.4, 53.3, 31.7, 31.4, 22.0, 21.9; IR (thin film) 2968, 2792, 1683, 1386 cm⁻¹; HRMS (ESI): *m/z* calculated for C₁₆H₂₇N₂ [M+H]⁺ 247.2174, found 247.2172.

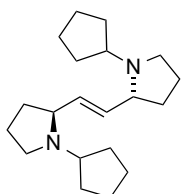
(*E*)-1-((*R*)-1-(Furan-2-ylmethyl)pyrrolidin-2-yl)-2-((*S*)-1-(furan-2-ylmethyl)pyrrolidin-2-yl)ethane, 7.3c.

Using the general procedure for dimerization outlined above, (*E*)-*N*-(furan-2-ylmethyl)-5-iodopent-4-en-1-amine **7.1c** (29 mg, 0.10 mmol, 1.0 equiv) was used and the product was purified by flash chromatography with EtOAc/hex/Et₃N (10:90:5) to afford the bis-pyrrolidine



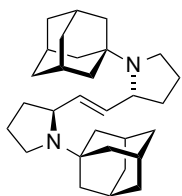
dimer **7.3c** as a dark brown oil (9.8 mg, 0.030 mmol, 61%). $R_f = 0.78$ (10:90:5 EtOAc/hex/Et₃N); ¹H NMR (500 MHz, CDCl₃) δ 7.34 (app s, 2H), 6.28 (dd, $J = 6.1, 1.9$ Hz, 2H), 6.14 (d, $J = 3.0$ Hz, 2H), 5.57-5.51 (m, 2H), 3.87 (d, $J = 14.1$ Hz, 2H), 3.30 (d, $J = 14.1$ Hz, 2H), 3.04-3.00 (m, 2H), 2.82-2.78 (m, 2H), 2.27-2.23 (m, 2H), 1.99-1.91 (m, 2H), 1.84-1.77 (m, 2H), 1.66-1.62 (m, 4H); ¹³C NMR (125 MHz, CDCl₃) δ 152.9, 141.9, 134.9, 110.0, 108.0, 66.6, 53.4, 49.4, 31.9, 21.9; IR (thin film) 2982, 1734, 1373 cm⁻¹; HRMS (ESI): m/z calculated for C₂₀H₂₆N₂O₂Na [M+Na]⁺ 349.1892, found 349.1898.

(E)-1-((R)-1-Cyclopentylpyrrolidin-2-yl)-2-((S)-1-cyclopentylpyrrolidin-2-yl)ethane, 7.3d.



Using the general procedure for dimerization outlined above, (while obtaining TLC samples extra care was taken to prevent exposure to air), (*E*)-*N*-(5-iodopent-4-en-1-yl)cyclopentanamine **7.1d** (50 mg, 0.18 mmol, 1.0 equiv) and the product was purified by flash chromatography with EtOAc/hex/Et₃N (10:90:5) to afford the bis-pyrrolidine dimer **7.3d** as a dark brown oil (15 mg, 0.050 mmol, 56%). $R_f = 0.75$ (10:90:5 EtOAc/hex/Et₃N); ¹H NMR (500 MHz, CDCl₃) δ 5.49-5.47 (m, 2H), 3.02-2.96 (m, 4H), 2.79-2.77 (m, 2H), 2.51-2.49 (m, 2H), 1.96-1.94 (m, 2H), 1.93-1.90 (m, 4H), 1.81-1.77 (m, 4H), 1.76-1.67 (m, 6H), 1.65-1.40 (m, 8H); ¹³C NMR (125 MHz, CDCl₃) δ 133.2, 66.3, 64.2, 51.2, 32.4, 32.2, 29.4, 24.3, 23.8, 22.5; IR (thin film) 2970, 1771, 1394, 1299 cm⁻¹; HRMS (ESI): m/z calculated for C₂₀H₃₄N₂Na [M+Na]⁺ 325.2620, found 325.2608.

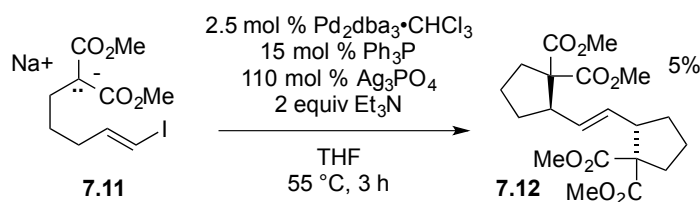
(E)-1-((R)-1-Adamantylpyrrolidin-2-yl)-2-((S)-1-adamantylpyrrolidin-2-yl)ethane, 7.3e.



Using the general procedure for dimerization outlined above, (3*s*,5*s*,7*s*)-*N*-((*E*)-5-iodopent-4-en-1-yl)adamantan-1-amine **7.1e** (37 mg, 0.11 mmol, 1.0 equiv) was used and the product was purified by flash chromatography with

EtOAc/hex/Et₃N (10:90:5) to afford the bis-pyrrolidine dimer **7.3e** as a dark brown oil (15 mg, 0.035 mmol, 66%). The reaction required slightly longer reaction time (3 h). R_f = 0.88 (10:90:5 EtOAc/hex/ Et₃N); ¹H NMR (500 MHz, CDCl₃) δ 5.36-5.48 (m, 2H), 3.46-3.55 (m, 2H), 2.87-2.96 (m, 2H), 2.74-2.69 (m, 2H), 2.02 (br s, 6H), 1.78-1.76 (m, 10H), 1.66-1.54 (m, 22H); ¹³C NMR (125 MHz, CDCl₃) δ 134.7, 57.9, 54.3, 46.0, 40.1, 37.0, 33.4, 29.7, 23.7; IR (thin film) 2956, 2924, 2873, 2860, 1540, 1373 cm⁻¹; HRMS (ESI): *m/z* calculated for C₃₀H₄₇N₂ [M+H]⁺ 435.3739, found 435.3737.

(2*R*,2*S*)-Tetramethyl 2,2'-((*E*)-ethene-1,2-diyl)bis(cyclopentane-1,1-dicarboxylate), 7.12.

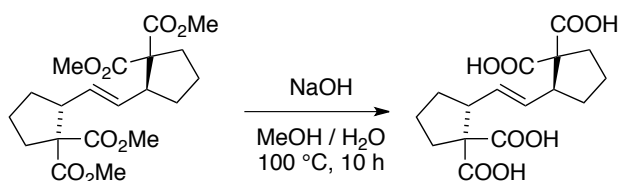


Sodium hydride (95 wt%, 6.7 mg, 0.26 mmol) was added to a 10 mL round bottom flask and suspended in 0.1 mL of THF. The suspension was cooled to 0 °C with an ice bath, after which dimethyl malonate vinyl iodide **7.11**²⁰¹ (82 mg, 0.25 mmol) was added via syringe over 15 min. After the addition was complete, the ice bath was removed and the solution was stirred for 75 min at room temperature.

A 5 mL pear-shaped flask was and charged with Pd₂dba₃·CHCl₃ (13 mg, 2.5 mol %) and Ph₃P (9.9 mg, 15 mol %), meanwhile another 5 mL round bottom flask was charged with silver(I) phosphate (0.12 g, 1.1 equiv) and a stir bar. 1.0 mL of THF was added to the pear-shaped flask containing Pd₂dba₃·CHCl₃ and Ph₃P and stirred (approximately 5 min). The solution of sodiomalonate vinyl iodide was added to the flask containing the silver(I) phosphate, followed by Et₃N (70 mL, 2.0 equiv). Lastly, the catalyst solution of Pd₂dba₃·CHCl₃ and Ph₃P in THF was added to the round bottom flask. The round bottom flask was heated to 55 °C by

immersing the reaction flask in a hot oil bath up to the level of the flask's contents. The reaction was monitored for consumption of the vinyl iodide by TLC (20:80 EtOAc/Hex).

The reaction reached completion at 4 h, and was then cooled to room temperature. The crude reaction mixture was washed with 1% (w/v) aq. NaOH. The aqueous layer was then extracted with (3 x 10 mL) Et₂O. The combined organic layers were then washed with brine and dried over Na₂SO₄. The resulting organic solution was concentrated *in vacuo* to give dark brown oil. Standard flash chromatography was unsuccessful for purification of cyclopentyl dimer **7.12**. Therefore, **7.12** was hydrolyzed and purified by extraction via the following procedure:²⁰⁵



A solution of cyclopentyl dimer **7.12** (25 mg, 0.06 mmol, 1 equiv), sodium hydroxide (35 mg, 0.88 mmol, 15 equiv) in 0.2 mL of ethanol and 0.7 mL of water was heated at reflux for 10 h. The reaction was cooled to room temperature, and the crude reaction mixture was extracted with (3 x 2 mL) Et₂O. The aqueous layer was treated with 1N HCl to obtain a pH 3 solution. The resulting mixture was extracted again with (3 x 2 mL) Et₂O. The resulting organic solution was concentrated *in vacuo* to yield the pure diacid derivative of **7.12** as a white solid. (20 mg, 0.060 mmol, 5% from vinyl iodide **7.11**). $R_f = 0.70$ (20:80 MeOH/CHCl₃); ¹H NMR (500 MHz, CDCl₃) δ 12.5 (s, 4H), 5.36 (dd, $J = 5.1, 2.3$ Hz, 2H), 2.91-3.03 (m, 2H), 2.20-2.29 (m, 2H), 1.90-1.98 (m, 2H), 1.87-1.75 (m, 2H), 1.77-1.65 (m, 2H), 1.49-1.44 (m, 4H); ¹³C NMR (125 MHz, CDCl₃) δ 174.1, 172.1, 131.1, 64.1, 48.1, 33.5, 31.8, 22.9; IR (thin film) 3354, 1645, 1635, 1046 cm⁻¹; HRMS (ESI): m/z calculated for C₁₆H₁₉O₈ [M-H]⁻ 339.1080, found 339.1084.

Chapter 8

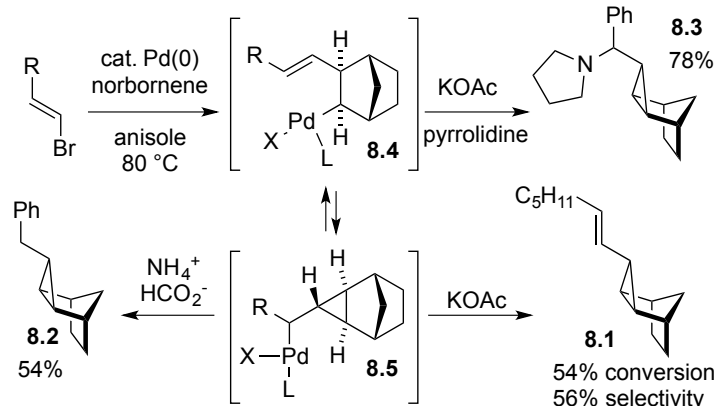
Palladium-Catalyzed Catellani Aminocyclopropanation Reactions with Vinyl Halides

Norbornenes are gaining increasing attention for their participation in metal-catalyzed reactions, for example as traceless participants in C–H activation reactions²⁰⁶ and as ligands for asymmetric catalysis.²⁰⁷ Norbornenes are also exceptional substrates for cyclopropanation. Palladium(0) can catalyze the cyclopropanation of norbornenes using traditional carbene precursors such as α -diazo esters²⁰⁸ and various carbenoid precursors.²⁰⁹

Vinyl halides have received scant attention as reagents for cyclopropanation. In the 1980s Catellani and co-workers reported that tandem Heck reactions of vinyl bromides with norbornene generate three types of cyclopropane products (Scheme 8-1). In the presence of potassium acetate, 1-bromo-1-octene reacts via β -hydride elimination to generate vinylcyclopropane **8.1**.²¹⁰ β -Styryl bromide generates intermediates that can be trapped with hydride donors or secondary amines such as benzylcyclopropane **8.2** and cyclopropylcarbinylamine **8.3**.²¹¹ It was proposed that all three products arise from a tandem reaction involving intermolecular carbopalladation of norbornene to give vinylnorbornane **8.4**, followed by intramolecular carbopalladation to give cyclopropylcarbinylpalladium intermediate **8.5**.²¹²

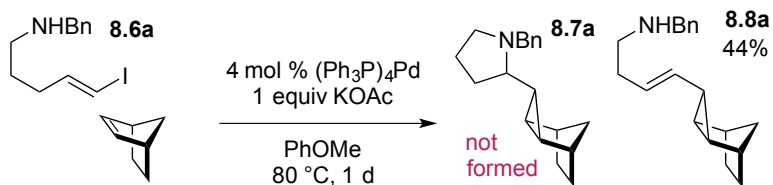
Other than styryl bromide, no other vinyl halides have been shown to generate cyclopropylcarbinylamines, presumably due to facile β -hydride elimination that leads to formation of vinylcyclopropanes analogues to **8.1**. Together with my coworker Avinash Khanna we set out to explore this distinctive aminocyclopropanation reaction using vinyl halides other than styryl bromides.

Scheme 8-1: Common Reactive Intermediates in Catellani Cyclopropanations can Generate Three Different Products



In order to favor this unique aminocyclopropanation reaction, we turned to a vinyl iodide substrate **8.6a** with a pendant secondary amine. Under the conditions reported for styryl bromide, none of the cyclopropylcarbinylamine **8.7a** was observed and we isolated only (*E*)-vinylcyclopropane **8.8a**, resulting from β -hydride elimination (Scheme 8-2).

Scheme 8-2: Aminocyclopropanation Reactions

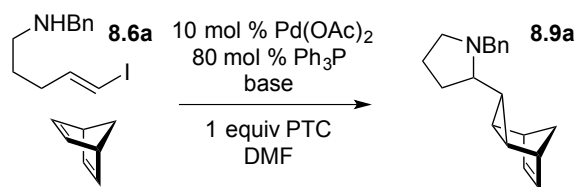


In order to promote the formation of pyrrolidine **8.7a**, we changed both the alkene acceptor and the reaction conditions. We substituted norbornadiene for norbornene since it has been reported to provide higher yields in palladium-catalyzed cyclopropanation reactions with diazo compounds.^{208a} We also changed the reaction conditions to those reported by Torii for reductive trapping of a putative cyclopropylcarbinylpalladium intermediate using formic acid as a hydride source.²¹³ In a footnote, Torii and co-workers reported the isolation of a cyclopropane in 84% yield by reacting a vinyl iodide, norbornene, Ph₃P, Pd(OAc)₂, and Et₃N in DMF.

Therefore, we set out to optimize the aminocyclopropanation of norbornadiene under the Torii conditions (Table 8-1).

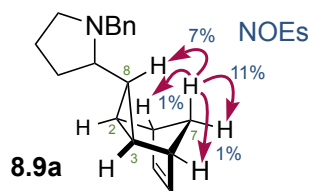
The reaction is complete in less than one hour with a large excess of norbornadiene and additional phosphine (Table 1, entries 1-3). The yields slightly improved in the presence of the phase transfer catalyst tetra-*n*-butylammonium chloride (entry 2 and 4), and the optimal temperature was 80 °C (entries 4-6). Unfortunately, the reaction was less efficient when the amount of triphenylphosphine was reduced (entries 5 and 7). Two equivalents of diethylamine were optimal over other stoichiometries, and secondary amine additives were superior to tertiary or primary amines (entries 8-15). To better accommodate the volatile reaction components, the reaction was carried out in sealed tubes, ultimately providing yields over 80% (entries 12 and 13). The optimized conditions (entry 12) favor the participation of an amine nucleophile in the cyclopropanation reaction as opposed to β -hydride elimination.

Table 8-1: Optimization of the Aminocyclopropanation of Norbornadiene



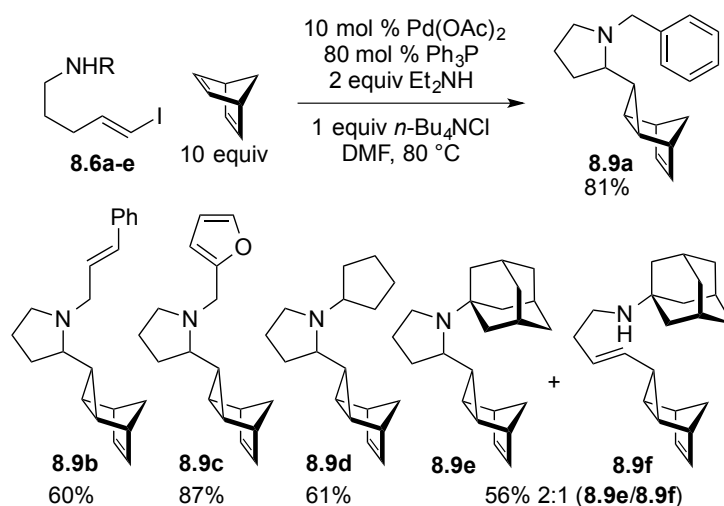
entry	equiv Ph ₃ P	equiv amine	equiv nbd	PTC	temp	vessel	yield
1	0.4	2 Et ₃ N	2		80 °C		39%
2	0.8	2 Et ₂ NH	5		80 °C		52%
3	0.8	2 Et ₂ NH	10		80 °C		64%
4	0.8	2 Et ₂ NH	10	Bu ₄ NCl	66 °C		73%
5	0.8	2 Et ₂ NH	10	Bu ₄ NCl	80 °C		79%
6	0.8	2 Et ₂ NH	10	Bu ₄ NCl	100 °C		57%
7	0.4	2 Et ₂ NH	10	Bu ₄ NCl	80 °C		56%
8	0.8	-	10	Bu ₄ NCl	80 °C		21%
9	0.8	2 Bu ₃ N	10	Bu ₄ NCl	80 °C		36%
10	0.8	2 Et ₃ N	10	Bu ₄ NCl	80 °C		56%
11	0.8	2 Et ₂ NH	10		80 °C	sealed	66%
12	0.8	2 Et ₂ NH	10	Bu ₄ NCl	80 °C	sealed	81%
13	0.8	3 Et ₂ NH	10	Bu ₄ NCl	80 °C	sealed	82%
14	0.8	1 Et ₂ NH	10	Bu ₄ NCl	80 °C	sealed	70%
15	0.8	2 <i>n</i> -PrNH ₂	10	Bu ₄ NCl	80 °C	sealed	72%

Figure 8-1: Establishing the relative stereochemistry



The relative stereochemistry of the amine product **8.9a** was established by the presence of a positive steady state nOe from one of the protons on the norbornene bridge C7 to one of the cyclopropane protons and an absence of nOes between the proton at C8 and the protons at C2 and C3 (Figure 8-1).

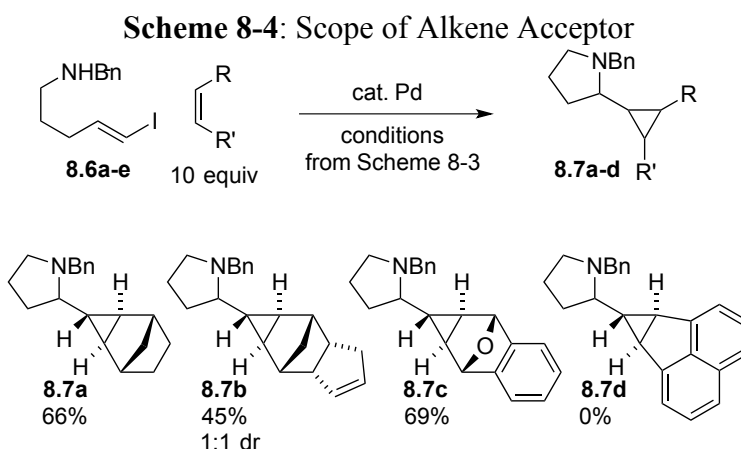
Scheme 8-3: Intramolecular Aminocyclopropanation with Variations in the Amine Substituent



With optimized conditions in hand, we next explored the tolerance of the amine nitrogen substituent to varying degrees of steric hindrance (Scheme 8-3). The reaction conditions led to chemoselective cyclopropanation of the norbornadiene acceptor without a competing reaction of a pendant cinnamyl group in **8.9b**. The reaction furnished cyclopropanes in yields up to 87%. As expected, the bulky *N*-cyclopentylamine **8.9d** was formed in lower yield. The exceedingly hindered adamantyl group of adamantylamine **8.6e** led to a slower reaction and an inseparable

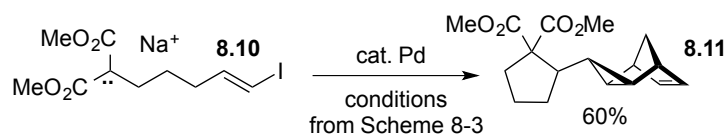
2:1 mixture of pyrrolidine **8.9e** and vinylcyclopropane **8.9f** in 56% yield. The *N*-benzyl vinyl bromide corresponding to **8.6a** also provided the cyclopropylcarbinylamine **8.9a** in 53% yield.

We next set out to explore variations in the alkene acceptor. Norbornene and dicyclopentadiene were slightly less efficient than norbornadiene (Scheme 8-4). The adduct of dicyclopentadiene **8.7b** was obtained as an inseparable 1:1 mixture of diastereomers. An oxabicyclic [2.2.1] substrate generated the aminocyclopropane **8.7c** in 69% yield.²¹⁴ The cyclic alkene acenaphthylene, which has been shown to resist β -hydride elimination, generated none of the cyclopropane **8.7d**.²¹⁵



We set out to test carbon nucleophiles in the Catellani cyclopropanation. The malonate anion **8.10**, generated with sodium hydride, produces the corresponding cyclopropane adduct **8.11** in 60% yield under the optimized conditions (Scheme 8-5).

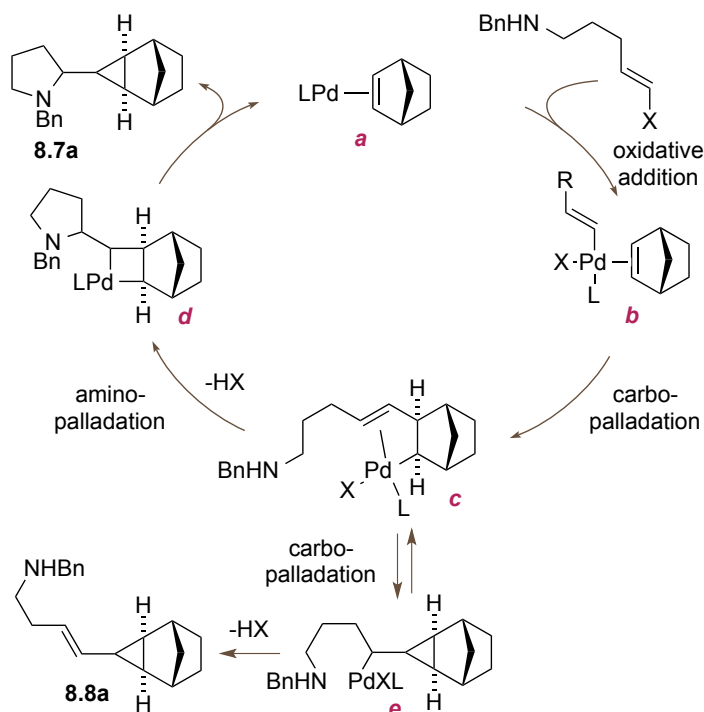
Scheme 8-5: Carbon Nucleophiles Generate Carbocyclic Rings in Conjunction with Cyclopropanation



The mechanism of these unique cyclizations and cyclopropanations is still unclear. In their seminal report Catellani and co-workers proposed the intermediacy of

cyclopropylcarbinylpalladium intermediate **8.5** (Scheme 8-1) in the aminocyclopropanation reaction.²⁰² The first step involves an oxidative addition to form vinylpalladium halide **b** (Scheme 8-6), followed by intermolecular carbopalladation across the norbornene double bond to give *exo*-norbornylpalladium intermediate **c**. The *exo* palladium atom can not undergo *syn* β -hydride elimination but is poised to carbopalladate across the *exo* vinyl group to produce cyclopropylcarbinylpalladium intermediate **e**. Carbon-nitrogen bond formation could occur via a reductive elimination²⁰² or ionization of XPd^- to give a cyclopropylcarbinyl cation, both of which would generate the aminocyclopropane product. Reductive elimination seems less likely as a mechanism for C-N bond formation given the challenges that have been documented²¹⁶ with Buchwald-Hartwig aminations.

Scheme 8-6: Mechanistic Models for Intramolecular Aminocyclopropanation



However, the olefin and palladium groups in norbornylpalladium intermediate **c** are poised for an aminopalladation to give palladacyclobutane **d**. Palladacyclobutanes have

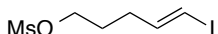
previously been invoked in the mechanisms for palladium catalyzed cyclopropanation.^{217, 209b} In previous studies of aminopalladations, *N*-alkylamines have been shown to aminopalladate *anti*²¹⁸ whereas *N*-aryl and *N*-sulfonyl amines have been shown to aminopalladate *syn*.²¹⁹ Moreover, the participation of malonate anions is consistent with the well-accepted *anti*-carbopalladation mechanism.²²⁰

In summary, we show for the first time that the Catellani reaction can be applied to aliphatic vinyl halides – not just styryl bromide – and can even engage stabilized enolates as well as amine nucleophiles. The reaction is selective for norbornenes over other alkenes, even acenaphthylene, which, like norbornenes should generate palladium intermediates that resist β -hydride elimination. Ultimately, the mechanism of the reaction is unclear, but given the participation of both alkylamines and stabilized enolates as nucleophiles, we favor a mechanism involving palladacyclobutanes such as *d* in Scheme 8-6.

Experimental Section

Experimental

(*E*)-5-Iodopent-4-en-1-yl methanesulfonate, 8.12.²²¹



An oven-dried 50 mL round-bottom flask was charged with a stir bar, (*E*)-5-iodopent-4-en-1-ol²²² (0.514 g, 2.44 mmol), and dichloromethane (12 mL). Et₃N (0.540 mL, 3.90 mmol) was added to the solution of alcohol and then the reaction mixture was cooled to -10 °C. Subsequently, methanesulfonyl chloride (0.230 mL, 2.93 mmol) was added dropwise to the reaction flask. Soon after the addition of methanesulfonyl chloride, the reaction turned from a colorless clear to a pale yellow solution. Upon completion of the reaction, as observed by TLC (10 min), the crude mixture was washed with water (15 mL), saturated aq. NaHCO₃ (15 mL) and brine (15 mL) respectively. The organic phase was then

dried over Na₂SO₄ and concentrated *in vacuo* to furnish pale yellow oil. The oil was then purified by flash column chromatography (10:90 EtOAc/hex) to yield mesylate **8.12** as a yellow oil (0.64 g, 90% yield). $R_f = 0.8$ (1:1 EtOAc /hex); ¹H NMR (500 MHz, CDCl₃) δ 6.49 (dt, $J = 14.4, 7.2$ Hz, 1H), 6.11 (d, $J = 14.5$ Hz, 1H), 4.22 (t, $J = 6.0$ Hz, 2H), 3.01 (s, 3H), 2.21 (app q, $J = 7.3$ Hz, 2H), 1.86 (app p, $J = 6.2$ Hz, 2H); ¹³C NMR (125 MHz, CDCl₃) δ 144.9, 76.4, 68.6, 37.5, 32.0, 27.8; IR (thin film) 1606, 1350, 1332, 1172 cm⁻¹; HRMS (ESI): m/z calculated for C₆H₁₁IO₃SNa [M+Na]⁺ 312.9371, found 312.9361.

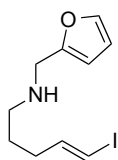
General procedure for alkylation of an amine with mesylate **8.12, **8.6b-e**:**



A flame dried 5 mL round bottom flask was charged with the (*E*)-5-iodopent-4-en-1-yl methanesulfonate **8.12** (1.0 equiv). Subsequently, the primary amine (10 equiv) and DMSO (0.8 M in vinyl iodide) were added by syringe. Lastly, sodium iodide (0.055 equiv) was added to the reaction flask by temporarily removing the septum. The reaction mixture was heated at 55 °C until mesylate **8.12** was no longer detectable by thin layer chromatography (2-5 h). The reaction mixture was added to 1% (w/v) aq. NaOH and then extracted with (3 × 5 mL) Et₂O. The combined organic extracts were dried with Na₂SO₄ and concentrated under vacuum to give yellow oil. The oil was then purified by flash chromatography with EtOAc/hex/Et₃N (20:80:5) to afford the monoalkylated amine.

(*E*)-*N*-(Furan-2-ylmethyl)-5-iodopent-4-en-1-amine, **8.6c.**

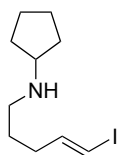
Using the general procedure for alkylation, furfurylamine was alkylated with mesylate **8.12** (29 mg, 0.11 mmol, 1.0 equiv) and the product was purified by flash chromatography with EtOAc/hex/Et₃N (20:80:5) to afford monoalkylated amine **8.6c** as a brown oil (29 mg, 0.10



mmol, 98%). $R_f = 0.54$ (20:80:5 EtOAc/hex/Et₃N); ¹H NMR (500 MHz, CDCl₃) δ 7.36 (dd, $J = 13.4, 1.0$ Hz, 1H), 6.49 (dt, $J = 14.3, 7.2$ Hz, 1H), 6.31 (dd, $J = 3.0, 1.9$ Hz, 1H), 6.16 (app d, $J = 3.0$ Hz, 1H), 6.00 (dt, $J = 14.4, 1.2$ Hz, 1H), 3.77 (s, 2H), 2.60 (t, $J = 7.0$ Hz, 2H), 2.08-2.12 (m, 2H), 1.56-1.60 (m, 2H), 1.36 (s, 1H);

¹³C NMR (125 MHz, CDCl₃) δ 153.9, 146.0, 141.9, 110.2, 106.9, 74.9, 48.2, 46.2, 33.8, 28.7; IR (thin film) 2938, 1669, 1456 cm⁻¹; HRMS (ESI): m/z calculated for C₁₀H₁₃INO [M-H]⁺ 290.0042, found 290.0042.

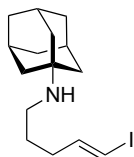
(*E*)-*N*-(5-Iodopent-4-en-1-yl)cyclopentanamine, 8.6d.



Using the general procedure for alkylation, cyclopentylamine was alkylated with mesylate **8.12** (29 mg, 0.11 mmol, 1.0 equiv) and the product was purified by flash chromatography with EtOAc/hex/Et₃N (20:80:5) to afford monoalkylated amine

8.6d as a brown oil (0.27 mg, 0.11 mmol, 98%). $R_f = 0.55$ (20:80:5 EtOAc/hex/Et₃N); ¹H NMR (500 MHz, CDCl₃) δ 6.51 (dt, $J = 14.3, 7.2$ Hz, 1H), 6.00 (d, $J = 14.3$ Hz, 1H), 3.04 (quintet, $J = 6.8$ Hz, 1H), 2.58 (t, $J = 7.2$ Hz, 2H), 2.12-2.08 (m, 2H), 1.84-1.82 (m, 2H), 1.62-1.71 (m, 2H), 1.60-1.52 (m, 4H), 1.30-1.27 (m, 3H); ¹³C NMR (125 MHz, CDCl₃) δ 146.2, 74.8, 59.9, 47.9, 34.0, 33.3, 29.1, 24.1; IR (thin film) 2983, 1653, 1236 cm⁻¹; HRMS (ESI): m/z calculated for C₁₀H₁₇IN [M-H]⁺ 278.0406, found 278.0411.

(3*s*,5*s*,7*s*)-*N*-((*E*)-5-Iodopent-4-en-1-yl)adamantan-1-amine, 8.6e.

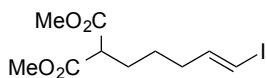


Using the general procedure for alkylation, 1-adamantylamine was alkylated with mesylate **8.12** (29 mg, 0.11 mmol, 1.0 equiv) and the product was purified by flash chromatography with EtOAc/hex/Et₃N (20:80:5) to afford monoalkylated

amine **8.6e** as a white solid (0.16 mg, 0.10 mmol, 94%). $R_f = 0.67$ (20:80:5 EtOAc/hex/Et₃N); ¹H NMR (500 MHz, CDCl₃) δ 6.50 (dt, $J = 14.3, 7.2$ Hz, 1H), 6.00 (d, $J = 14.3$ Hz, 1H), 2.57 (t, $J =$

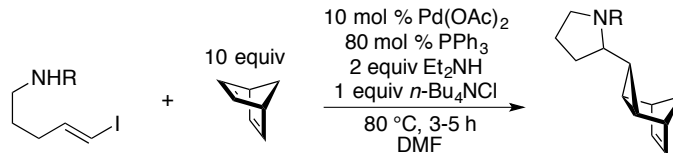
7.2 Hz, 2H), 2.09-2.12 (m, 2H), 1.98 (app s, 3H), 1.68-1.59 (m, 12H), 1.56-1.53 (m, 3H); ^{13}C NMR (125 MHz, CDCl_3) δ 146.2, 74.8, 50.8, 42.8, 39.6, 36.8, 34.1, 29.8, 29.6; IR (thin film) 2980, 1660 cm^{-1} ; HRMS (ESI): m/z calculated for $\text{C}_{15}\text{H}_{24}\text{IN}$ $[\text{M}+\text{H}]^+$ 346.1032, found 346.1041.

(E)-Dimethyl 2-(5-iodopent-4-en-1-yl)malonate, 8.10.



A 100 mL oven-dried round-bottom flask was charged with sodium hydride (60 wt % in mineral oil, 0.43 g, 10.8 mmol) and the mineral oil was removed by washing with hexanes (3×2 mL). The sodium hydride was suspended in DMF (54 mL). The suspension was cooled to 0 °C on an ice bath, after which dimethyl malonate (1.42 g, 10.8 mmol) was added via syringe over the course of 15 min. After the addition was complete, the ice bath was removed and the solution was stirred for 30 min at room temperature. Meanwhile, a solution of mesylate **8.12** (1.25 g, 4.31 mmol) was prepared by dissolving it in THF (22 mL). The solution of **8.12** was added to the reaction flask by a syringe followed by potassium iodide (0.716 g, 4.31 mmol). The reaction mixture was then allowed to stir at 80 °C for 11 h. Subsequently, saturated NH_4Cl solution (30 mL) was added to the reaction mixture, which was then extracted with EtOAc (3×30 mL). The combined organic layers were then washed with H_2O (5×30 mL). The resulting organic layer was then over MgSO_4 and concentrated *in vacuo* to deliver a pale yellow oil. The oil was purified by flash chromatography (10:90 EtOAc/hex) to yield the monoalkylated malonate, as a colorless oil (1.1 g, 79% yield). R_f = 0.30 (10:90 EtOAc/hex); ^1H NMR (500 MHz, CDCl_3) δ 6.47 (dt, J = 14.3, 7.1 Hz, 1H), 6.02 (dt, J = 14.4, 1.2 Hz, 1H), 3.74 (s, 6H), 3.35 (t, J = 7.5 Hz, 1H), 2.08 (br, 2H), 1.91 (dt, J = 8.1, 7.7, 2H), 1.42 (br, 2H); ^{13}C NMR (125 MHz, CDCl_3) δ 169.7, 145.5, 75.4, 52.6, 51.5, 35.6, 28.1, 26.1; IR (thin film) 3021, 2954, 1732, 1435 cm^{-1} ; HRMS (ESI): m/z calculated for $\text{C}_{10}\text{H}_{15}\text{IO}_4\text{Na}$ $[\text{M}+\text{Na}]^+$ 348.9913, found 348.9911.

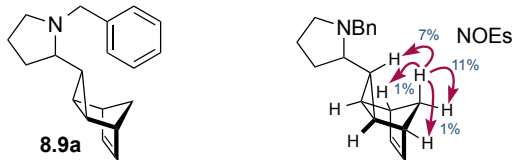
General procedure for cyclopropanation:



An oven-dried 10 mL conical vial with a stir bar was charged with tetra-*n*-butylammonium chloride (1.0 equiv). Then the conical vial was sealed and purged with nitrogen. A separate 5 mL pear-shaped flask with a stir bar was charged with palladium(II) acetate (0.10 equiv), Ph₃P (0.80 equiv) and DMF (0.10 M solution with respect to palladium). The catalyst mixture was stirred for 20-30 min resulting an orange solution. Meanwhile, a separate oven-dried 5 mL pear-shaped flask containing ω -aminovinyl iodide (1.0 equiv) and DMF (0.3 M with respect to vinyl iodide) was prepared. The solution of vinyl iodide was added to the 10 mL conical vial, followed by addition of diethylamine (2.0 equiv) and norbornadiene (10 equiv). Finally, the palladium catalyst solution was transferred to the reaction flask by syringe. Additional DMF was added to the conical vial by syringe, resulting in a 0.17 M reaction with respect to the ω -aminovinyl iodide. The reaction mixture was heated to 80 °C by immersing the reaction flask in a hot oil bath up to the level of the flask contents. The stirred reaction was then monitored by TLC (10:90:5 EtOAc/hex/Et₃N) to check for depletion of the vinyl iodide.

After cooling to ambient temperature, the crude reaction mixture was washed with 1% (w/v) aq. NaOH. The aqueous layer was then extracted with (3 × 10 mL) Et₂O. The combined organic layers were then washed with brine and dried over Na₂SO₄. The resulting organic solution was concentrated under vacuum to give dark brown oil. The oil was then purified by flash chromatography with EtOAc/hex/Et₃N (10:90:5) to afford the aminocyclopropanated product.

Sample procedure for cyclopropanation: 1-benzyl-2-((1*R*,2*R*,4*S*,5*S*)-tricyclo[3.2.1.0^{2,4}]oct-6-en-3-yl)pyrimidine, **8.9a.**

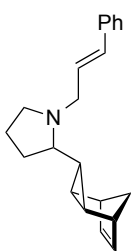


An oven-dried 10 mL conical vial with a stir bar was charged with tetra-*n*-butylammonium chloride (34 mg, 0.12 mmol, 1.0 equiv). Then the conical vial was sealed and purged with nitrogen. A separate 5 mL pear-shaped flask with a stir bar was charged with palladium(II) acetate and DMF (0.2 mL) was added to the pear-shaped flask and stirred for 20 min resulting an orange solution of the catalyst. Meanwhile, a separate oven-dried 5 mL pear-shaped flask containing reported ω -aminovinyl iodide **8.6a**²²³ (37 mg, 0.12 mmol, 1.0 equiv) and DMF (0.1 mL) was prepared. The solution of vinyl iodide was added to the 10 mL conical vial, followed by diethylamine (25 mL, 0.25 mmol, 2.0 equiv), norbornadiene (0.12 mL, 1.2 mmol, 10 equiv). Finally, the palladium catalyst solution was transferred to the reaction flask by syringe. Additional DMF (0.6 mL) was added to the conical vial by syringe. The Reaction mixture was heated to 80 °C by immersing the reaction flask in a hot oil bath up to the level of the flask contents. The stirred reaction was monitored by TLC (10:90:5 EtOAc/hex/Et₃N) to check for depletion of the vinyl iodide.

After cooling to ambient temperature, the crude reaction mixture was washed with 1% (w/v) aq. NaOH. The aqueous layer was then extracted with (3 × 10 mL) Et₂O. The combined organic layers were then washed with brine and dried over Na₂SO₄. The resulting organic solution was concentrated under vacuum to give dark brown oil. The oil was then purified by flash chromatography with EtOAc/hex/Et₃N (10:90:5) to afford the aminocyclopropanated product **8.9a** as a dark brown oil (26 mg, 0.098 mmol, 81% (95% purity)). This product contained an impurity (< 5 mol%) that was difficult to remove by column chromatography. $R_f =$

0.81 (10:90:5 EtOAc/hex/Et₃N); ¹H NMR (500 MHz, CDCl₃) δ 7.36 (d, *J* = 6.1 Hz, 2H), 7.31 (t, *J* = 6.2 Hz, 2H), 7.23 (t, *J* = 6.1 Hz, 1H), 6.38 (dd, *J* = 2.4, 4.7 Hz, 1H), 6.36 (dd, *J* = 2.4, 4.7 Hz, 1H), 4.29 (d, *J* = 10.7 Hz, 1H), 3.11 (d, *J* = 10.8 Hz, 1H), 2.88 (t, *J* = 7.5 Hz, 1H), 2.80 (s, 1H), 2.75 (s, 1H), 2.05 (q, 8.5 Hz, 1H), 1.94-1.88 (m, 2H), 1.78-1.60 (m, 4H), 1.17 (d, *J* = 9.0 Hz, 1H), 0.94 (d, *J* = 7.5 Hz, 1H), 0.85 (d, *J* = 9.0 Hz, 1H), 0.79 (d, *J* = 7.5 Hz, 1H); ¹³C NMR (125 MHz, CDCl₃) δ 141.0, 140.8, 140.2, 129.0, 128.9, 126.7, 68.0, 59.1, 54.1, 41.8, 41.6, 39.1, 36.4, 30.8, 30.1, 25.3, 21.6; IR (thin film) 2906, 1736, 1457, 1371, 1239, 1041 cm⁻¹; HRMS (ESI): *m/z* calculated for C₁₉H₂₄N [M+H]⁺ 266.1909, found 266.1904.

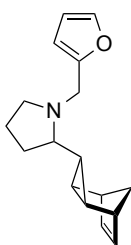
1-Cinnamyl-2-((1*R*,2*R*,4*S*,5*S*)-tricyclo[3.2.1.0^{2,4}]oct-6-en-3-yl)pyrrolidine, **8.9b.**



Using the general procedure for cyclopropanation, (*E*)-*N*-cinnamyl-5-iodopent-4-en-1-amine **8.6b** (89 mg, 0.27 mmol, 1.0 equiv) was reacted with norbornadiene and the product was purified by flash chromatography with EtOAc/hex/Et₃N (10:90:5) to afford the cyclopropane **8.9b** as a light brown solid (48 mg, 0.16 mmol, 60%). *R_f* = 0.84 (10:90:5 EtOAc/hex/Et₃N); ¹H NMR (500 MHz, CDCl₃)

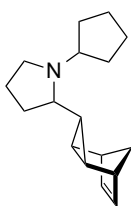
δ 7.38 (d, *J* = 7.5 Hz, 2H), 7.30 (t, *J* = 7.5 Hz, 2H), 7.21 (t, *J* = 7.0 Hz, 1H), 6.53 (d, *J* = 16.0 Hz, 1H), 6.41-6.35 (m, 3H), 3.88 (dd, *J* = 4.5, 13.0 Hz, 1H), 3.11 (t, *J* = 7.0 Hz, 1H), 2.88 (dd, *J* = 8.0, 13.0 Hz, 1H), 2.82 (s, 1H), 2.80 (s, 1H), 2.15 (q, *J* = 9.0 Hz, 1H), 1.93-1.89 (m, 1H), 1.86 (2.5, 6.0 Hz, 1 H), 1.82-1.75 (m, 1H), 1.71 (q, *J* = 7.5 Hz, 1H), 1.67-1.59 (m, 2H), 1.19 (d, *J* = 9.0 Hz, 1H), 0.96 (d, *J* = 7.0 Hz, 1H), 0.86 (d, *J* = 9.5 Hz, 1H), 0.78 (d, *J* = 7.0 Hz, 1H); ¹³C NMR (125 MHz, CDCl₃) δ 141.0, 140.8, 137.3, 131.8, 128.6, 128.2, 127.3, 126.3, 67.4, 56.8, 54.1, 41.8, 41.6, 39.1, 36.2, 30.9, 29.9, 25.4, 21.6; IR (thin film) 2970, 2908, 2786, 2359, 2336, 1494, 1314, 1153 cm⁻¹; HRMS (ESI): *m/z* calculated for C₂₁H₂₆N (M+H⁺) 292.2065, found 292.2064.

1-(Furan-2-ylmethyl)-2-((1R,2R,4S,5S)-tricyclo[3.2.1.0^{2,4}]oct-6-en-3-yl)pyrrolidine, 8.9c.



Using the general procedure for cyclopropanation, (*E*)-*N*-(furan-2-ylmethyl)-5-iodopent-4-en-1-amine **8.6c** (37 mg, 0.12 mmol, 1.0 equiv) was reacted with norbornadiene and the product was purified by flash chromatography with EtOAc/hex/Et₃N (10:90:5) to afford the cyclopropane **8.9c** as a dark brown oil (15 mg, 0.050 mmol, 87%). *R_f* = 0.82 (10:90:5 EtOAc/hex/Et₃N); ¹H NMR (500 MHz, CDCl₃) δ 7.34 (app s, 1H), 6.38-6.34 (m, 1H), 6.28 (d, *J* = 1.0 Hz, 2H), 6.29-6.28 (m, 1H), 4.14 (d, *J* = 14.0 Hz, 1H), 3.37 (d, *J* = 14.0 Hz, 1H), 2.95-2.91 (m, 1H), 2.81 (s, 1H), 2.79 (s, 1H), 2.19 (q, *J* = 7.2 Hz, 1H), 1.91-1.84 (m, 2H), 1.78-1.70 (m, 2H), 1.67-1.55 (m, 2H), 1.17 (d, *J* = 9.5 Hz, 1H), 0.97 (d, *J* = 7.5 Hz, 1H), 0.85 (d, *J* = 9.0 Hz, 1H), 0.76 (d, *J* = 7.5 Hz, 1H); ¹³C NMR (125 MHz, CDCl₃) δ 153.1, 141.8, 141.0, 140.9, 140.8, 140.8, 110.0, 107.9, 66.8, 53.8, 50.0, 41.8, 41.6, 39.1, 36.1, 30.8, 29.7, 25.2, 21.6; IR (thin film) 3498, 2997, 2919, 2363, 1352, 1224 cm⁻¹; HRMS (ESI): *m/z* calculated for C₁₇H₂₂NO [M+H]⁺ 256.1701, found 256.1708.

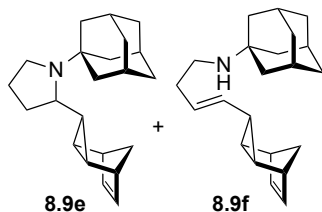
1-Cyclopentyl-2-((1R,2R,4S,5S)-tricyclo[3.2.1.0^{2,4}]oct-6-en-3-yl)pyrrolidine, 8.9d.



Using the general procedure for cyclopropanation, ((*E*)-*N*-(5-iodopent-4-en-1-yl)cyclopentanamine **8.6d** (50 mg, 0.18 mmol, 1.0 equiv) was reacted with norbornadiene and the product **8.9d** was purified by flash chromatography with EtOAc/hex/Et₃N (10:90:5) to afford the cyclopropane as a dark brown oil (27 mg, 0.11 mmol, 61%). *R_f* = 0.84 (10:90:5 EtOAc/hex/Et₃N); ¹H NMR (500 MHz, CDCl₃) δ 6.40-6.34 (m, 2H), 3.26-3.24 (m, 1H), 3.00-2.92 (m, 1H), 2.80 (s, 1H), 2.77 (s, 1H), 2.44 (q, 7.1 Hz, 1H), 2.03-1.97 (m, 2H), 1.88-1.83 (m, 2H), 1.77-1.74 (m, 2H), 1.67-1.61 (m, 5H), 1.49-1.43 (m, 3H), 1.16 (d, *J* = 8.8 Hz, 1H), 0.95 (d, *J* = 7.5 Hz, 1H), 0.83 (d, *J* = 9.3 Hz, 1H), 0.74 (d, *J* = 7.6 Hz, 1H); ¹³C NMR (125 MHz, CDCl₃) δ 140.9, 140.8, 62.3, 49.6, 41.8, 41.7, 39.0, 31.7, 31.1,

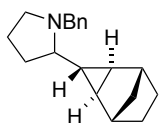
30.3, 27.5, 26.2, 24.6, 24.5, 21.9; IR (thin film) 3029, 2939, 2785, 1702, 1452, 907 cm^{-1} ; HRMS (ESI): m/z calculated for $\text{C}_{17}\text{H}_{26}\text{N}$ $[\text{M}+\text{H}]^+$ 244.2065, found 244.2070.

1-((3*S*,5*S*,7*S*)-Adamantan-1-yl)-2-((1*R*,2*R*,4*S*,5*S*)-tricyclo[3.2.1.0^{2,4}]oct-6-en-3-yl)pyrrolidines, **8.9e.**



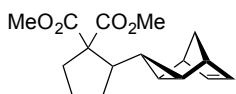
Using the general procedure for cyclopropanation, *N*-((*E*)-5-iodopent-4-en-1-yl)adamantan-1-amine **8.6e** (49 mg, 0.14 mmol, 1.0 equiv) was reacted with norbornadiene and the product **8.9e** and the product was purified by flash chromatography with EtOAc/hex/Et₃N (2:98:5) to afford an inseparable 2:1 mixture of aminocyclopropanated product **8.9e** and the vinylcyclopropane **8.9f** (25 mg, 56%). An analytical sample (3 mg) of pyrrolidine **8.9e** was isolated after three more rounds of flash chromatography: ¹H NMR (600 MHz, CDCl₃) δ 6.35 (br s, 2H), 2.91 (t, $J = 7.8$, 1H), 2.79-2.75 (m, 3H), 2.56 (t, $J = 7.8$ Hz, 1H), 2.06 (br s, 3H), 1.96 (d, $J = 7.8$ Hz, 1H), 1.88-1.80 (m, 1H), 1.74-1.60 (m, 11H), 1.53-1.48 (m, 1H), 1.17 (d, $J = 9.6$ Hz, 1H), 0.98 (d, $J = 6.6$ Hz, 1H), 0.79 (d, $J = 9.0$ Hz, 2H); ¹³C NMR (125 MHz, CDCl₃) δ 140.9, 140.8, 58.0, 53.5, 46.4, 42.1, 41.8, 41.0, 40.1, 39.0, 37.0, 32.1, 30.3, 29.6, 28.2, 24.5; IR (thin film) 2902, 2848, 2363, 2328, 1451, 1312, 1096 cm^{-1} ; HRMS (ESI): m/z calculated for $\text{C}_{22}\text{H}_{32}\text{N}$ ($\text{M}+\text{H}^+$) 310.2535, found 310.2534. The residual signals in the ¹H NMR spectrum of the 2:1 mixture are consistent with vinylcyclopropane **8.9f**: ¹H NMR (500 MHz, CDCl₃) δ 5.41-5.36 (m, 1H), 5.13-5.11 (m, 1H), 2.83-2.75 (m, 1H), 2.65-2.57 (m, 1H), 2.41-2.40 (m, 1H), 2.38-2.30 (m, 1H), 2.24-2.20 (m, 1H), 2.11-2.01 (m, 4H), 1.99-1.96 (m, 1H), 1.75-1.73 (m, 1H), 1.75-1.72 (m, 3H), 1.63-1.56 (m, 15H), 1.40-1.35 (m, 1H), 1.32-1.28 (m, 1H); $R_f = 0.84$ (2:98:5 EtOAc/hex/Et₃N).

1-Benzyl-2-((1*R*,2*S*,3*r*,4*R*,5*S*)-tricyclo[3.2.1.0^{2,4}]octan-3-yl)pyrrolidine, **8.7a**.



Using the general procedure for cyclopropanation, (*E*)-*N*-benzyl-5-iodopent-4-en-1-amine **8.6a** (36 mg, 0.14 mmol, 1.0 equiv) was reacted with norbornene (126 mg, 1.34 mmol, 10.0 equiv) and the product was purified by flash chromatography with EtOAc/hex/Et₃N (10:90:5) to afford the cyclopropane **8.7a** as a dark brown oil (24 mg, 0.089 mmol, 66%). $R_f = 0.84$ (10:90:5 EtOAc/hex/Et₃N); ¹H NMR (500 MHz, CDCl₃) δ 7.35 (d, $J = 7.3$ Hz, 2H), 7.30 (t, $J = 7.6$ Hz, 2H), 7.23 (t, $J = 7.0$ Hz, 1H), 4.31 (d, $J = 12.8$ Hz, 1H), 3.06 (d, $J = 12.6$ Hz, 1H), 2.86 (t, $J = 7.8$ Hz, 1H), 2.27 (s, 1H), 2.24 (s, 1H), 2.03 (q, 8.6 Hz, 1H), 1.92-1.85 (m, 1H), 1.71-1.54 (m, 4H), 1.46-1.38 (m, 2H), 1.23-1.19 (m, 2H), 0.98 (d, $J = 10.5$ Hz, 1H), 0.73 (d, $J = 8.3$ Hz, 1H), 0.63-0.60 (m, 2H), 0.46 (d, $J = 5.6$ Hz, 1H); ¹³C NMR (125 MHz, CDCl₃) δ 140.2, 129.0, 128.2, 126.7, 68.0, 59.1, 54.1, 36.0, 35.8, 31.0, 29.8, 29.7, 28.7, 23.5, 21.5, 18.7, 17.6; IR (thin film) 2938, 1736, 1469, 1371, 1233, 1044 cm⁻¹; HRMS (ESI): m/z calculated for C₁₉H₂₆N [M+H]⁺ 268.2065, found 268.2060.

Dimethyl 2-((2*S*,3*R*)-tricyclo[3.2.1.0_{2,4}]octan-3-yl)cyclopentane-1,1-dicarboxylate, **8.11**.



A 10 mL oven-dried round-bottom flask was charged with sodium hydride (95 wt%, 6.7 mg, 0.26 mmol) sodium hydride was suspended in 0.1 mL of DMF. The suspension was cooled to 0 °C with an ice bath, after which malonate derivative **8.10** (82 mg, 0.25 mmol) was added via syringe over 15 min. after the addition was done, ice bath was removed and the solution was stirred for 75 min at room temperature.

Using the general procedure for cyclopropanation, (*E*)-dimethyl 2-(5-iodopent-4-en-1-yl)sodiomalonate (82 mg, 0.25 mmol, 1.0 equiv) and the product was purified by flash chromatography with EtOAc/hex (10:90) to afford the cyclopropane **8.11** as a pale yellow oil (44 mg, 0.15 mmol, 60%). $R_f = 0.64$ (10:90 EtOAc/hex); ¹H NMR (500 MHz, CDCl₃) δ 6.32-6.29

(m, 2H), 4.10 (s, 3H), 3.72 (s, 3H), 2.72 (s, 1H), 2.65 (s, 1H), 2.51-2.46 (m, 1H), 2.21-2.17 (m, 1H), 2.07-2.03 (m, 1H), 1.91-1.86 (m, 1H), 1.81-1.76 (m, 1H), 1.69-1.67 (m, 1H), 1.54-1.48 (m, 1H), 1.46-1.41 (m, 1H), 1.08 (d, $J = 9.2$ Hz, 1H), 0.95 (d, $J = 7.2$ Hz, 1H), 0.82 (d, $J = 6.6$ Hz, 1H), 0.79 (d, $J = 9.1$ Hz, 1H); ^{13}C NMR (125 MHz, CDCl_3) δ 173.2, 171.7, 140.7, 140.6, 63.7, 52.6, 52.1, 48.3, 41.7, 38.8, 34.4, 34.3, 31.6, 29.7, 28.2, 23.3; IR (thin film) 2943, 2904, 1729, 1435, 1263 cm^{-1} ; HRMS (ESI): m/z calculated for $\text{C}_{17}\text{H}_{22}\text{O}_4\text{Na}$ $[\text{M}+\text{Na}]^+$ 313.1416, found 313.1419.

References:

- ¹ Richards, M. J.; Edwards, J. R.; Culver, D. H.; Gaynes, R. P. “Nosocomial infections in combined medical-surgical intensive care units in the United States” *Infect. Control Hosp. Epidemiol.* **2000**, *21*, 510–515.
- ² Revankar, S. G.; Sobel, J. D. Eds. *Candidiasis (Invasive)*. Merck Manual, **2014**. http://www.merckmanuals.com/professional/infectious_diseases/fungi/candidiasis_invasive.html
- ³ Achkar, J. M.; Fries, B. C. “*Candida* Infections of the Genitourinary Tract” *Clin. Microbiol Rev.* **2010**, *23*, 253–273.
- ⁴ Cleveland, A. A.; Farley, M. M.; Harrison, L. H.; Stein, B.; Hollick, R.; Lockhart, S. R.; Magill, S. S.; Derado, G.; Park, B. J.; Chiller, T. M. “Changes in incidence and antifungal drug resistance in candidemia: results from population-based laboratory surveillance in Atlanta and Baltimore, 2008-2011” *Clin Infect Dis.* **2012**, *55*, 1352–1361.
- ⁵ Revankar, S. G.; Sobel, J. D. Eds. *Antifungal Drugs*. Merck Manual, **2014**. <http://www.merckmanuals.com/professional/infectious-diseases/fungi/antifungal-drugs>.
- ⁶ Gallism, H. A.; Drew, R. H.; Pickard, W. W. “Amphotericin B: 30 years of clinical experience” *Rev. Infect. Dis.* **1990**, *12*, 2, 308–329.
- ⁷ Abelcet, (Amphotericin B Lipid Complex Injection). Sigma-Tau PharmaSource, Inc., Indianapolis, IN. Available at: http://www.sigmatau.com/products/Abe_PI2col_I10141USN_F_102513_20140203161706_545762.pdf. Accessed January 9, 2016.
- ⁸ Balfour, J. A.; Faulds, D. “Terbinafine. A review of its pharmacodynamic and pharmacokinetic properties, and therapeutic potential in superficial mycoses” *Drugs*, **1992**, *43*, 2, 259–284.
- ⁹ “Lamisil (terbinafine): Side Effects”. Doublecheckmd.com. 2010-06-16. Accessed January 11, 2016.
- ¹⁰ Duschinsky, R.; Plevin, E.; Heidelberger, C. “The Synthesis of 5-Fluoropyrimidines” *J. Am. Chem. Soc.* **1957**, *79*, 16, 4559–4560.
- ¹¹ Heidelberger, C.; Griesbach, L.; Montag, B. J.; Mooren, D.; Cruz, O.; Schnitzer, R.J.; Grunberg, E. “Studies on fluorinated pyrimidines. II. Effects on transplanted tumors” *Cancer Res.* **1958**, *18*, 3, 305–317.
- ¹² Polak, A.; Scholer, H. J. “Mode of action of 5-fluorocytosine and mechanisms of resistance” *Chemotherapy* **1975**, *21*, 113–130.
- ¹³ Waldorf, A. R.; Polak, A. “Mechanisms of action of 5-fluorocytosine” *Antimicrob. Agents Chemother.* **1983**, *23*, 79–85.
- ¹⁴ Polak, A.; Grenson, M. “Evidence for a common transport system for cytosine, adenine and hypoxanthine in *Saccharomyces cerevisiae* and *Candida albicans*” *Eur. J. Biochem.* **1973**, *32*, 276–282.
- ¹⁵ (a) Medoff, G.; Comfort, M.; Kobayashi, G. S. “Synergistic action of amphotericin B and 5-fluorocytosine against yeast-like organisms” *Proc. Soc. Exp. Biol. Med.* **1971**, *138*, 571–574. (b) Montgomerie, J. Z.; Edwards, J. E. Jr.; Guze, L. B. “Synergism of amphotericin B and 5-fluorocytosine for candida species” *J. Infect. Dis.* **1975**, *132*, 82–86.
- ¹⁶ Vermees, A.; Guchelaar, H. J.; Dankert, J. “Flucytosine: a review of its pharmacology, clinical indications, pharmacokinetics, toxicity and drug interactions” *J. Antimicrob. Chemother.* **2000**, *46*, 171–179.
- ¹⁷ Cappelletty, D.; Eiselstein-McKittrick, K. “The Echinocandins” *Pharmacotherapy*, **2007**, *27*, 369–388.

- ¹⁸ Lewis, R. E. Pharmacology of echinocandins. *UpToDate* (Eds.: Kauffman, C. A. and Thorner, A. R.) May 05, 2015.
- ¹⁹ (a) Vasquez J. “Anidulafungin: a new echinocandin with a novel profile” *Clin. Ther.* **2005**, *27*, 657–673. (b) Caspofungin package insert. Whitehouse Station, NJ: Merck & Co.; 2005 Feb. (c) Micafungin package insert. Deerfield, IL: Astellas Pharma US; 2005 Apr. (d) Morris, M. I.; Villmann, M. “Echinocandins in the management of invasive fungal infections, part 1” *Am. J. Health Syst. Pharm.* **2006**, *63*, 18, 1693–1703.
- ²⁰ Maligie, M. A.; Selitrennikoff, C. P. “*Cryptococcus neoformans* Resistance to Echinocandins: (1,3) β -Glucan Synthase Activity Is Sensitive to Echinocandins” *Antimicrob. Agents Chemother.* **2005**, *49*, 2851–2856.
- ²¹ Georgopapadakou, N. H.; Walsh, T. J. “Antifungal agents: chemotherapeutic targets and immunologic strategies” *Antimicrob. Agents Chemother.* **1996**, *40*, 279–291.
- ²² Ghannoum, M. A. “Future of antimycotic therapy” *Dermatol. Ther.* **1997**, *3*, 104–111.
- ²³ Koltin, Y.; Hitchcock, C. A.; “Progress in the search for new triazole antifungal agents” *Curr. Opin. Chem. Biol.* **1997**, *1*, 176–182.
- ²⁴ White, T. C.; Marr, K. A.; Bowden, R. A. “Clinical, cellular, and molecular factors that contribute to antifungal drug resistance” *Clin. Microbiol. Rev.* **1998**, *11*, 382–402.
- ²⁵ (a) Anderson, J. B. “Evolution of antifungal-drug resistance: mechanisms and pathogen fitness” *Nat. Rev. Microbiol.* **2005**, *3*, 547–556. (b) Cantas, L.; Shah, S. Q. A.; Cavaco, L. M.; Manaia, C. M.; Walsh, F.; Popowska, M.; Garelick, H.; Bürgmann, H.; Sørum, H. “A brief multi-disciplinary review on antimicrobial resistance in medicine and its linkage to the global environmental microbiota” *Front Microbiol* **2013**, *4*, 96.
- ²⁶ Kontoyiannis, D. P.; Lewis, R. E. “Antifungal drug resistance of pathogenic fungi” *Lancet* **2002**, *359*, 9312, 1135–1144.
- ²⁷ (a) Brown, J. C.; Nelson, J.; VanderSluis, B.; Deshpande, R.; Butts, A.; Kagan, S.; Polacheck, I.; Krysan, D. J.; Myers, C. L.; Madhani, H. D. *Cell* **2014**, *159*, 5, 1168–1187. (b) Kalan, L.; Wright, G. D. “Antibiotic adjuvants: multicomponent anti- infective strategies” *Expert Rev. Mol. Med.* **2011**, *13*, e5.
- ²⁸ (a) Kathiravan, M. K.; Salake, A. B.; Chothe, A. S.; Dudhe, P. B.; Watode, R. P.; Mukta, M. S.; Gadhwane, S. “The biology and chemistry of antifungal agents: a review” *Bioorg. Med. Chem.* **2012**, *20*, 5678–5698. (b) Lehár, J.; Krueger, A. S.; Avery, W.; Heilbut, A. M.; Johansen, L. M.; Price, E. R.; Rickles, R. J.; Short, G. F. 3rd; Staunton, J. E.; Jin, X.; Lee, M. S.; Zimmermann, G. R.; Borisy, A. A. “Synergistic drug combinations tend to improve therapeutically relevant selectivity” *Nat. Biotechnol.* **2009**, *27*, 659–666.
- ²⁹ Scalapone, G. M.; Mikami, Y.; Kurita, N.; Yazawa, K.; Uno, J.; Miyaji, M. “In vitro comparative evaluations of the postantifungal effect: synergistic interaction between flucytosine and fluconazole against *Candida albicans*” *Mycoses* **1991**, *34*, 405–410.
- ³⁰ Sekine, Y.; Kamiyama, T.; Sakurai, C.; Arisawa, M. In vitro and in vivo effects on *Candida* spp. of flucytosine combined with fluconazole. *Chemotherapy* **1994**, *42*, 164–171.
- ³¹ Te Dorsthorst, D. T.; Verweij, P. E.; Meletiadis, J.; Bergervoet, M.; Punt, N. C.; Meis, J. F.; Mouton, J. W. “In vitro interaction of flucytosine combined with amphotericin B or fluconazole against thirty-five yeast isolates determined by both the fractional inhibitory concentration index and the response surface approach” *Antimicrob. Agents Chemother.* **2002**, *46*, 2982–2589.
- ³² Pfaller, M. A.; Messer, S. A.; Boyken, L.; Huynh, H.; Hollis, R. J.; Diekema, D. J. “In vitro activities of 5-fluorocytosine against 8,803 clinical isolates of *Candida* spp.: global assessment of

primary resistance using National Committee for Clinical Laboratory Standards susceptibility testing methods” *Antimicrob. Agents Chemother.* **2002**, *46*, 3518–3521.

³³ Jansen, G.; Lee, A. Y.; Epp, E.; Fredette, A.; Surprenant, J.; Marcus, D.; Scott, M.; Tan, E.; Nishimura, T.; Whiteway, M.; Hallett, M.; Thomas, D. Y. Chemogenomic profiling predicts antifungal synergies. *Mol. Syst. Biol.* **2009**, *5*, 1–13.

³⁴ Nishi, I.; Sunada, A.; Toyokawa, M.; Asari, S.; Iwatani, Y. “In vitro antifungal combination effects of micafungin with fluconazole, voriconazole, amphotericin B, and flucytosine against clinical isolates of *Candida* species” *J. Infect Chemother.* **2009**; *15*, 1–5.

³⁵ Messer, S. A.; Diekema, D. J.; Boyken, L.; Tendolkar, S.; Hollis, R. J.; Pfaller, M. A. “Activities of micafungin against 315 invasive clinical isolates of fluconazole-resistant *Candida* spp.” *J. Clin. Microbiol.* **2006**, *44*, 324–326.

³⁶ Rodríguez, M. M.; Ruiz, M.; Pastor, F. J.; Quindós, G.; Carrillo, A.; Guarro, J. “In vitro interaction of micafungin and fluconazole against *Candida*” *J. Antimicrob. Chemother.* **2007**, *60*, 188–190.

³⁷ Cruz, M. C.; Goldstein, A. L.; Blankenship, J. R.; Del Poeta, M.; Davis, D.; Cardenas, M. E.; Perfect, J. R.; McCusker, J. H.; Heitman, J. “Calcineurin is essential for survival during membrane stress in *Candida albicans*” *EMBO J.* **2002**, *21*, 546–559.

³⁸ Sun, S.; Li, Y.; Guo, Q.; Shi, C.; Yu, J.; Ma, L. “In vitro interactions between tacrolimus and azoles against *Candida albicans* determined by different methods” *Antimicrob. Agents Chemother.* **2008**, *52*, 409–417.

³⁹ Saad, A.; Fadli, M.; Bouaziz, M.; Benharref, A.; Mezrioui, N.E.; Hassani, L. “Anticandidal activity of the essential oils of *Thymus maroccanus* and *Thymus broussonetii* and their synergism with amphotericin B and fluconazole” *Phytomedicine* **2010**, *17*, 1057–1060.

⁴⁰ Barchiesi, F.; Falconi Di Francesco, L.; Scalise, G. “In vitro activities of terbinafine in combination with fluconazole and itraconazole against isolates of *Candida albicans* with reduced susceptibility to azole” *Antimicrob. Agents Chemother.* **1997**, *41*, 1812–1814.

⁴¹ da Silva, C. R.; de Andrade Neto, J. B.; Sidrim, J. J.; Angelo, M. R.; Magalhães, H. I.; Cavalcanti, B. C.; Brilhante, R. S.; Macedo, D. S.; de Moraes, M. O.; Lobo, M. D.; Grangeiro, T. B.; Nobre Júnior, H. V. “Synergistic effects of amiodarone and fluconazole on *Candida tropicalis* resistant to fluconazole” *Antimicrob. Agents Chemother.* **2013**, *57*, 1691–1700.

⁴² da Silva, C. R.; de Andrade Neto, J. B.; de Sousa Campos, R.; Figueiredo, N. S.; Sampaio, L. S.; Magalhães, H. I.; Cavalcanti, B. C.; Gaspar, D. M.; de Andrade, G. M.; Lima, I. S.; de Barros Viana, G. S.; de Moraes, M. O.; Lobo, M. D.; Grangeiro, T. B.; Nobre Júnior, H. V. “Synergistic effect of the flavonoid catechin, quercetin, or epigallocatechin gallate with fluconazole induces apoptosis in *Candida tropicalis* resistant to fluconazole” *Antimicrob. Agents Chemother.* **2014**, *58*, 1468–1478.

⁴³ Menezes, E. A.; Vasconcelos Júnior, A.A.; Silva, C. L.; Plutarco, F. X.; Cunha Mda, C.; Cunha, F. A. “In vitro synergism of simvastatin and fluconazole against *Candida* species” *Rev. Inst. Med. Trop. Sao Paulo* **2012**, *54*, 197–199.

⁴⁴ Maurya, I. K.; Thota, C. K.; Sharma, J.; Tupe, S. G.; Chaudhary, P.; Singh, M. K.; Thakur, I. S.; Deshpande, M.; Prasad, R.; Chauhan, V. S. “Mechanism of action of novel synthetic dodecapeptides against *Candida albicans*” *Biochim. Biophys. Acta.* **2013**, *1830*, 5193–5203.

⁴⁵ Maurya, I. K.; Pathak, S.; Sharma, M.; Sanwal, H.; Chaudhary, P.; Tupe, S.; Deshpande, M.; Chauhan, V. S.; Prasad, R. Antifungal activity of novel synthetic peptides by accumulation of

reactive oxygen species (ROS) and disruption of cell wall against *Candida albicans*. *Peptides* **2011**, *32*, 1732–1740.

⁴⁶ Abdelmegeed, E.; Shaaban, M. I. “Cyclooxygenase inhibitors reduce biofilm formation and yeast-hypha conversion of fluconazole resistant *Candida albicans*” *J. Microbiol.* **2013**, *51*, 598–604.

⁴⁷ Marchetti, O.; Moreillon, P.; Glauser, M. P.; Bille, J.; Sanglard, D. “Potent synergism of the combination of fluconazole and cyclosporine in *Candida albicans*” *Antimicrob. Agents Chemother.* **2000**, *44*, 2373–2381.

⁴⁸ Guo, X.-J.; Lu, Y.-Y.; Jia, L.-P. “The study of combination of fluconazole with nystatin against isolates of vaginal *Candida albicans* in Vitro” *The Chinese Journal of Dermatovenereology* **2007**, *21*, 277–279.

⁴⁹ Zhang, J.; Liu, W.; Tan, J.; Sun, Y.; Wan, Z.; Li, R. “Antifungal activity of geldanamycin alone or in combination with fluconazole against *Candida* species” *Mycopathologia* **2013**, *175*, 273–279.

⁵⁰ Ahodavandi, A.; Alizadeh, F.; Aala, F.; Sekawi, Z.; Chong, P. P. “In vitro investigation of antifungal activity of allicin alone and in combination with azoles against *Candida* species” *Mycopathologia* **2010**, *169*, 287–295.

⁵¹ Oliveira, G. T.; Ferreira, J. M.; Rosa, L. H.; Siqueira, E. P.; Johann, S.; Lima, L. A. “In vitro antifungal activities of leaf extracts of *Lippia alba* (Verbenaceae) against clinically important yeast species” *Rev. Soc. Bras. Med. Trop.* **2014**, *47*, 247–250.

⁵² Denardi, L. B.; Mario, D. A.; de Loreto, E. S.; Nogueira, C. W.; Santurio, J. M.; Alves, S. H. “Antifungal activities of diphenyl diselenide alone and in combination with fluconazole or amphotericin B against *Candida glabrata*” *Mycopathologia* **2013**, *176*, 165–169.

⁵³ Serpa, R.; França, E. J.; Furlaneto-Maia, L.; Andrade, C. G.; Diniz, A.; Furlaneto, M. C. “In vitro antifungal activity of the flavonoid baicalein against *Candida* species” *J. Med. Microbiol.* **2012**, *61*, 1704–1708.

⁵⁴ Guo, N.; Ling, G.; Liang, X.; Jin, J.; Fan, J.; Qiu, J.; Song, Y.; Huang, N.; Wu, X.; Wang, X.; Deng, X.; Yu, L. “In vitro synergy of pseudolaric acid B and fluconazole against clinical isolates of *Candida albicans*” *Mycoses* **2011**, *54*, e400–e406.

⁵⁵ Gao, Y.; Zhang, C.; Lu, C.; Liu, P.; Li, Y.; Li, H.; Sun, S. “Synergistic effect of doxycycline and fluconazole against *Candida albicans* biofilms and the impact of calcium channel blockers” *FEMS Yeast Res.* **2013**, *13*, 453–462.

⁵⁶ (a) Quan, H.; Cao, Y. -Y.; Xu, Z.; Zhao, J. -X.; Gao, P. H.; Qin, X. -F; Jiang, Y. -Y. “Potent in vitro synergism of fluconazole and berberine chloride against clinical isolates of *Candida albicans* resistant to fluconazole” *Antimicrob. Agents Chemother.* **2006**, *50*, 1096–1099. (b) Xu, Y.; Wang, Y.; Yan, L.; Liang, R. M.; Dai, B. D.; Tang, R. J.; Gao P. H.; Jiang, Y. -Y. “Proteomic analysis reveals a synergistic mechanism of fluconazole and berberine against fluconazole-resistant *Candida albicans*: endogenous ROS augmentation” *J. Proteome Res.* **2009**, *8*, 5296–5304. (c) Iwazaki, R. S.; Endo, E. H.; Ueda-Nakamura, T.; Nakamura, C. V.; Garcia, L. B.; Filho, B. P. “In vitro antifungal activity of the berberine and its synergism with fluconazole” *Antonie Van Leeuwenhoek* **2010**, *97*, 201–205. (d) Wei, G. X.; Xu, X.; Wu, C. D. “In vitro synergism between berberine and miconazole against planktonic and biofilm *Candida* cultures” *Arch. Oral Biol.* **2011**, *56*, 565–572.

⁵⁷ Liu, H.; Wang, L.; Li, Y.; Liu, J.; An, M.; Zhu, S.; Cao, Y.; Jiang, Z.; Zhao, M.; Cai, Z.; Dai, L.; Ni, T.; Liu, W.; Chen, S.; Wei, C.; Zang, C.; Tian, S.; Yang, J.; Wu, C.; Zhang, D.; Liu, H.;

- Jiang, Y. “Structural optimization of berberine as a synergist to restore antifungal activity of fluconazole against drug-resistant *Candida albicans*” *ChemMedChem* **2014**, *9*, 207–216.
- ⁵⁸ Spitzer, M.; Griffiths, E.; Blakely, K. M.; Wildenhain, J.; Ejim, L.; Rossi, L.; De Pascale, G.; Curak, J.; Brown, E.; Tyers, M.; Wright, G. D. “Cross-species discovery of syncretic drug combinations that potentiate the antifungal fluconazole” *Mol. Syst. Biol.* **2011**, *21*, 1–14.
- ⁵⁹ Pinto, W. J.; Wells, G. W.; Lester, R. L. “Characterization of enzymatic synthesis of sphingolipid long-chain bases in *Saccharomyces cerevisiae*: mutant strains exhibiting long-chain-base auxotrophy are deficient in serine palmitoyltransferase activity” *J. Bacteriol.* **1992**, *174*, 2575–2581.
- ⁶⁰ LaFleur, M. D.; Lucumi, E.; Napper, A. D.; Diamond, S. L.; Lewis, K. “Novel high-throughput screen against *Candida albicans* identifies antifungal potentiators and agents effective against biofilms” *J. Antimicrob. Chemother.* **2011**, *66*, 820–826.
- ⁶¹ Additional information about the MLSMR can be found online at <http://mli.nih.gov/mli/secondary-menu/mlscn/ml-small-molecule-repository/>
- ⁶² National Center for Biotechnology Information. PubChem BioAssay Database; AID=2007, Source= Broad Institute. <https://pubchem.ncbi.nlm.nih.gov/assay/assay.cgi?aid=2007> (accessed Mar. 11, 2015).
- ⁶³ Youngsaye, W.; Hartland, C. L.; Morgan, B. J.; Ting, A.; Nag, P. P.; Vincent, B.; Mosher, C. A.; Bittker, J. A.; Dandapani, S.; Palmer, M.; Whitesell, L.; Lindquist, S.; Schreiber, S. L.; Munoz, B. ML212: A small-molecule probe for investigating fluconazole resistance mechanisms in *Candida albicans*. *Beilstein J. Org. Chem.* **2013**, *9*, 1501–1507.
- ⁶⁴ Redding, S.; Smith, J.; Farinacci, G.; Rinaldi, M.; Fothergill, A.; Rhine-Chalberg, J.; Pfaller, M. “Resistance of *Candida albicans* to Fluconazole During Treatment of Oropharyngeal Candidiasis in a Patient with AIDS: Documentation by In Vitro Susceptibility Testing and DNA Subtype Analysis” *Clin. Infect. Dis.* **1994**, *18*, 240–242.
- ⁶⁵ Youngsaye, W.; Dockendorff, C.; Vincent, B.; Hartland, C. L.; Bittker, J. A.; Dandapani, S.; Palmer, M.; Whitesell, L.; Lindquist, S.; Schreiber, S. L.; Munoz, B. Overcoming fluconazole resistance in *Candida albicans* clinical isolates with tetracyclic indoles. *Bioorg. Med. Chem. Lett.* **2012**, *22*, 3362–3365.
- ⁶⁶ Hoot, S. J.; Oliver, B. G.; White, T. C. “*Candida albicans* UPC2 is transcriptionally induced in response to antifungal drugs and anaerobicity through Upc2p-dependent and -independent mechanisms” *Microbiology* **2008**, *154*, 2748–2756.
- ⁶⁷ Yang, H.; Tong, J.; Lee, C. W.; Ha, S.; Eom, S.H.; Im, Y. J. “Structural mechanism of ergosterol regulation by fungal sterol transcription factor Upc2” *Nat. Commun.* **2015**, *6*, 6129.
- ⁶⁸ Sanglard D1, Ischer F, Parkinson T, Falconer D, Bille J. “*Candida albicans* mutations in the ergosterol biosynthetic pathway and resistance to several antifungal agents” *Antimicrob Agents Chemother.* **2003**, *47*, 2404–2412.
- ⁶⁹ Zhai, B.; Wu, C.; Wang, L.; Sachs, M. S.; Lin, X. “The antidepressant sertraline provides a promising therapeutic option for neurotropic cryptococcal infections” *Antimicrob. Agents Chemother.* **2012**, *56*, 3758–3766.
- ⁷⁰ Nascimento-Júnior, N. M.; Mendes, T. C. F.; Leal, D. M.; Corrêa, C. M. N.; Sudo, R. T.; Zapata-Sudo, G.; Barreiro, E. J.; Fraga, C. A. M. “Microwave-assisted synthesis and structure–activity relationships of neuroactive pyrazolo[3,4-b]pyrrolo[3,4-d]pyridine derivatives” *Bioorg. Med. Chem. Lett.* **2010**, *20*, 74–77.

- ⁷¹ (a) Marvel, C. S.; Hiers, G. S. "Isatin" *Org. Syntheses Coll. Vol. I*, **1941**, 327. (b) Marvel, C. S.; Hiers, G. S. "Isatin" *Org. Synth.* **1925**, 5, 71. (c) Sandmeyer, T. "Über Isonitrosoacetanilide und deren Kondensation zu Isatinen" *Helvetica Chim. Acta* **1919**, 2, 234–242.
- ⁷² Overman, L. E.; Peterson, E. A. "Enantioselective synthesis of (–)-idiospermuline" *Tetrahedron*, **2003**, 59, 6905–6919.
- ⁷³ Rehn, S.; Bergman, J.; Stensland, B. "The three-component reaction between isatin, α -amino acids, and dipolarophiles" *Eur. J. Org. Chem.* **2004**, 413–418.
- ⁷⁴ Pavlovskaya, T. L.; Red'kin, R. G.; Yaremenko, F. G.; Shishkina, S. V.; Shishkin, O. V.; Musatov, V. I.; Lipson, V. V. "Synthesis and chemical properties of new derivatives of 3a',6a'-Dihydro-2'H-Spiro-[Indole-3,1'-Pyrrolo[3,4-c]Pyrrole]-2,4',6'(1H,3'H,5'H)-Trione" *Chem. Heterocycl. Compd.* **2013**, 49, 882–896.
- ⁷⁵ Azizian, J.; Asadi, A.; Jadidi, K. "One-pot highly diastereo-selective synthesis of new 2-substituted 8-(spiro-3'-indolino-2'-one)-pyrrolo[3,4-a]-pyrrolizine-1,3-diones mediated by azomethine ylide induced by microwave irradiation" *Synth. Commun.* **2001**, 31, 2727–2733.
- ⁷⁶(a) Rao, J. N. S.; Raghunathan, R. "An expedient diastereoselective synthesis of pyrrolidiny spirooxindoles fused to sugar lactone via [3+2] cycloaddition of azomethine ylides" *Tetrahedron Lett.* **2012**, 53, 854–858. (b) Pavlovskaya, T. L.; Lipson, V. V.; Yaremenko, F. G.; Musatov, V. I. "Acryl- and methacrylamides. New dipolarophiles in reactions of [2+3]-dipolar cycloaddition to 2-oxindolazomethine ylides" *Russ. J. Org. Chem.* **2013**, 49, 1712–1714.
- ⁷⁷ Fokas, D.; Ryan, W.; Casebier, D. S.; Coffen, D. L. "Solution phase synthesis of a spiro[pyrrolidine-2,3'-oxindole] library via a three-component 1,3-dipolar cycloaddition reaction" *Tetrahedron Lett.* **1998**, 39, 2235–2238.
- ⁷⁸ Elboray, E. E.; Gao, C.; Grigg, R. "Skeletal diversity via Pd(0) catalyzed three-component cascades of allene and halides or triflates with protected hydroxylamines and formamide" *Tetrahedron* **2012**, 68, 3103–3111.
- ⁷⁹ (a) Ganguly, A. K.; Seah, N.; Popov, V.; Wang, C. H.; Kuang, R.; Saksena, A. K.; Pramanik, B. N.; Chanb, T. M.; McPhailc, A. T. "Solution- and solid-phase synthesis of enantiomerically pure spiro oxindoles" *Tetrahedron Lett.* **2002**, 43, 8981–8983. (b) Sarrafi, Y.; Sadatshahabia, M.; Hamzehloueianb, M.; Alimohammadic, K.; Tajbakhsha, M. "Synthesis of functionalized pyrrolizidines/pyrrolidines incorporating a spirooxindole motif through [3+2] cycloaddition" *Synthesis* **2013**, 45, 2294–2304. (c) Pavlovskaya, T. L.; Yaremenko, F. G.; Lipson, V. V.; Shishkina, S. V.; Shishkin, O. V.; Musatov, V. I.; Karpenko, A. S. "The regioselective synthesis of spirooxindolo pyrrolidines and pyrrolizidines via three-component reactions of acrylamides and aroylacrylic acids with isatins and α -amino acids" *Beilstein J. Org. Chem.* **2014**, 10, 117–126. (d) Kumar, R. R.; Perumal, S.; Senthilkumar, P.; Yogeewari, P.; Sriram, D. "Discovery of antimycobacterial spiro-piperidin-4-ones: an atom economic, stereoselective synthesis, and biological intervention" *J. Med. Chem.* **2008**, 51, 5731–5735. (e) Kumar, R. R.; Perumal, S.; Senthilkumar, P.; Yogeewari, P.; Sriram, D. "A facile synthesis and antimycobacterial evaluation of novel spiro-pyrido-pyrrolizines and pyrrolidines" *Eur. J. Med. Chem.* **2009**, 44, 3821–3829. (f) Maheswari, S. U.; Perumal, S.; Almansour, A. I. "A facile regio- and stereoselective synthesis of novel dispirooxindolyl-[acridine-20,3-pyrrolidine/thiapyrrolizidine]-10-ones via 1,3-dipolar cycloaddition of azomethine ylides" *Tetrahedron Lett.* **2012**, 53, 349–353. (g) Laihia, K.; Valkonen, A.; Kolehmainen, E.; Antonov, A.; Zhukov, D.; Fedosov, I.; Nikiforov, V. "¹H, ¹³C, ¹⁵N NMR, ESI mass spectral and single crystal X-ray structural characterization of three spiro[pyrrolidine-2,30-oxindoles]" *J. Mol. Struct.* **2006**, 800, 100–105.

(h) Taghizadeh, M. J.; Arvinnezhad, H.; Samadi, S.; Jadidi, K.; Javidan, A.; Notash, B. "Synthesis of new enantiomerically pure spirooxindolopyrrolizidines via a three-component asymmetric 1,3-dipolar cycloaddition reaction of azomethine ylides derived from isatin" *Tetrahedron Lett.* **2012**, *53*, 5148–5150. (i) Kia, Y.; Osman, H.; Kumar, R. S.; Murugaiyah, V.; Basiri, A.; Perumal, S.; Wahab, H. A.; Bing, C. S. "Synthesis and discovery of novel piperidone-grafted mono- and bis-spirooxindole-hexahydropyrrolizines as potent cholinesterase inhibitors" *Bioorg. Med. Chem.* **2013**, *21*, 1696–1707. (j) Li, J.; Wang, J.; Xu, Z.; Zhu, S. "Combinatorial synthesis of functionalized spirooxindole-pyrrolidine/pyrrolizidine/pyrrolothiazole derivatives via three-component 1,3-dipolar cycloaddition reactions" *ACS Comb. Sci.* **2014**, *16*, 506–512. (k) Klochkova, N.; Shchekina, M. P.; Anis'kov, A. A. "Synthesis of spiropyrrrolidines and spiropyrrrolizidines from azomethine ylides" *Chem. Heterocycl. Compd.* **2014**, *50*, 479–488. (l) Salahi, F.; Taghizadeh, M. J.; Arvinnezhad, H.; Moemeni, M.; Jadidi, K.; Notash, K. "An efficient, one-pot, three-component procedure for the synthesis of chiral spirooxindolopyrrolizidines via catalytic highly enantioselective 1,3-dipolar cycloaddition" *Tetrahedron Lett.* **2014**, *55*, 1515–1518. (m) Revathy, K.; Lalitha, A. "An efficient green chemistry protocol for the synthesis of novel spiropyrrrolizidine compounds" *RSC Adv.*, **2014**, 279–285. (n) Murugan, R.; Raghunathan, R.; Narayanan, S. S. "Synthesis of novel spiroheterocycles through 1,3-dipolar cycloaddition of azomethine ylides with triarylidenacetone through decarboxylation" *Synth. Commun.* **2010**, *40*, 3135–3151. (o) Ponnala, S.; Kumar, R.; Maulik, P. R.; Sahu, D. P. "One pot synthesis of novel dirpiro[oxindole-thiazolidinedione/thioxo-thiazolidinone /dihydro pyrazolone]-pyrrolidines via 1,3-dipolar cycloaddition reaction of azomethine ylides" *J. Heterocycl. Chem.* **2006**, *43*, 1635–1640. (p) Purushothaman, S.; Prasanna, R.; Raghunathan, R. "Regioselective synthesis of spiropyrrrolidine/spiropyrrrolizidine/spirothiazolidine-grafted macrocycles through 1,3-dipolar cycloaddition methodology" *Tetrahedron* **2013**, *69*, 9742–9750. (q) Arumugam, N.; Periyasami, G.; Raghunathan, R.; Kamalraj, S.; Muthumary, J. "Synthesis and antimicrobial activity of highly functionalised novel β -lactam grafted spiropyrrrolidines and pyrrolizidines" *Eur. J. Med. Chem.* **2011**, *46*, 600–607. (r) Coulter, T.; Grigg, R.; Malone, J. F.; Sridharan, V. "Chiral induction in cycloaddition reactions of azomethine ylides derived from secondary α -amino acids by the decarboxylative route" *Tetrahedron Lett.* **1991**, *39*, 5417–5420. (s) Powers, D. G.; Casebier, D. S.; Fokas, D.; Ryan, W. J.; Troth, J. R.; Coffen, D. L. "Automated parallel synthesis of chalcone-based screening libraries" *Tetrahedron* **1998**, *54*, 4085–4096. (t) Javidan, A.; Taghizadeh, M. J.; Jadidi, K.; Notash, B. "Synthesis of new spiro-oxindolo-(pyrrolizidines/pyrrolidines) via cycloaddition reactions of azomethine ylides and dibenzylideneacetone" *Monatsh. Chem.* **2014**, *145*, 341–348. (u) Chen, G.; He, H.-P.; Ding, J.; Hao, X.-J. "Synthesis and antitumor activity evaluation of regioselective spiro[pyrrolidine-2,3'-oxindole] compounds" *Heterocycl. Commun.* **2009**, *15*, 355–360.

⁸⁰ Felluga, F.; Forzato, C.; Nitti, P.; Pitacco, G.; Valentin, E.; Zangrando, E. "Application of 1,3-azomethine ylides derived from α -dicarbonyl compounds and L-proline to the synthesis of pyrrolizidines" *J. Heterocycl. Chem.* **2010**, *47*, 664–670.

⁸¹ Grigg, R.; Kemp, J.; Sheldrick, G.; Trotter, J. "1,3-Dipolar cycloaddition reactions of imines of α -amino-acid esters: x-ray crystal and molecular structure of methyl 4-(2-furyl)-2,7-diphenyl-6,8-dioxo-3,7-diazabicyclo[3.3.0]octane-2-carboxylate" *J. Chem. Soc., Chem. Commun.* **1978**, 109–111.

- ⁸² Amornraksa, K.; Grigg, R.; Gunaratne, H. Q. N.; Kemp, J.; Sridharan, V. "X=Y-ZY systems as potential 1,3-dipoles. Part 8. Pyrrolidines and Δ^5 pyrrolines (3,7-diazabicyclo[3.3.0]octenes) from the reaction of imines of α -amino acids and their esters with cyclic dipolarophiles. Mechanism of racemisation of α -amino acids and their esters in the presence of aldehydes" *J. Chem. Soc., Perkin Trans. 1* **1987**, 2285–2296.
- ⁸³ Grigg, R.; Thianpatanagul, S.; Kemp, "J. X=Y-ZH systems as potential 1,3-dipoles. Part 22. Cycloaddition reactions of pyridoxal imines. Relevance to α -amino acid racemases and transaminases" *Tetrahedron*, **1988**, 23, 7283–7292.
- ⁸⁴ Almansour, A. I.; Kumar, R. S.; Arumugam, N.; Basiri, A.; Kia, Y.; Ali, M. A.; Farooq, M.; Murugaiyah, V. "A facile ionic liquid promoted synthesis, cholinesterase inhibitory activity and molecular modeling study of novel highly functionalized spiropyrrrolidines" *Molecules* **2015**, 20, 2296–2309.
- ⁸⁵ Dondas, H. A.; Fishwick, C. W. G.; Grigg, R.; Kilner, C. "1,3-Dipolar cycloaddition of stabilised and non-stabilised azomethine ylides derived from uracil polyoxin C (UPoC): access to nikkomycin analogues" *Tetrahedron*, **2004**, 60, 3473–3485.
- ⁸⁶ Ardill, H.; Dorrity, M.J.R.; Grigg, R.; Leon-Ling, M-S.; Malone, J. F.; Sridharan, V.; Thianpatanagul, S. "X=Y-ZH compounds as potential 1,3-dipoles. part 28. The iminium ion route to azomethine ylides. Background and reaction of amines with bifunctional ketones" *Tetrahedron*, **1990**, 46, 6433–6448.
- ⁸⁷ National Center for Biotechnology Information. PubChem BioAssay Database; AID=2423, Source= Broad Institute. <https://pubchem.ncbi.nlm.nih.gov/assay/assay.cgi?aid=2423> (accessed Mar. 31, 2015).
- ⁸⁸ Flowers, S. A.; Barker, K. S.; Berkow, E. L.; Toner, G.; Chadwick, S. G.; Gygax, S. E.; Morschhäuser, J.; Rogers, P.D. "Gain-of-function mutations in *UPC2* are a frequent cause of *ERG11* upregulation in azole-resistant clinical isolates of *Candida albicans*" *Eukaryotic Cell* **2012**, 11, 1289–1299.
- ⁸⁹ Cuenca-Estrella, M. "Combinations of antifungal agents in therapy—what value are they?" *J. Antimicrob. Chemother.* **2004**, 54, 854–869.
- ⁹⁰ Lamb, D. C., Kelly, D. E.; Schunck, W. H.; Shyadehi, A. Z.; Akhtar, M.; Lowe, D. J.; Baldwin, B. C.; Kelly, S. L. "The mutation T315A in *Candida albicans* sterol 14 α -demethylase causes reduced enzyme activity and fluconazole resistance through reduced affinity" *J. Biol. Chem.* **1997**, 272, 5682–5688.
- ⁹¹ Warrilow, A. G.; Parker, J. E.; Kelly, D. E.; Kelly, S. L. "Azole affinity of sterol 14 α -demethylase (CYP51) enzymes from *Candida albicans* and *Homo sapiens*" *Antimicrob. Agents Chemother.* **2013**, 57, 1352–1360.
- ⁹² Monge, A.; Arrault, A.; Marot, C.; Morin-allory, L. "Managing, profiling and analyzing a library of 2.6 million compounds gathered from 32 chemical providers" *Mol. Div.* **2006**, 10, 389–1403.
- ⁹³ Molinspiration property calculation service. <http://www.molinspiration.com/cgi-bin/properties>.
- ⁹⁴ Li, J.; Zhang, J.; Chen, J.; Luo, X.; Zhu, W.; Shen, J.; Liu, H.; Shen, X.; Jiang, H. "Strategy for discovering chemical inhibitors of human cyclophilin a: focused library design, virtual screening, chemical synthesis and bioassay" *J. Comb. Chem.* **2006**, 8, 326–337.
- ⁹⁵ Proudfoot, J. R. "The evolution of synthetic oral drug properties" *Bioorg. Med. Chem. Lett.* **2005**, 15, 1087–1090.

- ⁹⁶ Leeson, P. D.; Springthorpe, B. “The influence of drug-like concepts on decision-making in medicinal chemistry” *Nat. Rev. Drug Discovery* **2007**, *6*, 881–890.
- ⁹⁷ Pangborn, A. B.; Giardello, M. A.; Grubbs, R. H.; Rosen, R. K.; Timmers, F. J. “Safe and convenient procedure for solvent purification” *Organometallics* **1996**, *15*, 1518–1520.
- ⁹⁸ Peterson, E. A.; Overman, L. E. “Enantioselective synthesis of (–)-idiospermuline” *Tetrahedron* **2003**, *59*, 6905–6919.
- ⁹⁹ Perez, M.; Lamothe, M.; Maraval, C.; Mirabel, E.; Loubat, C.; Planty, B.; Horn, C.; Michaux, J.; Marrot, S.; Letienne, R.; Pignier, C.; Bocquet, A.; Nadal-Wollbold, F.; Cussac, D.; de Vries, L.; Le Grand, B. “Discovery of novel protease activated receptors 1 antagonists with potent antithrombotic activity *in vivo*” *J. Med. Chem.* **2009**, *52*, 5826–5836.
- ¹⁰⁰ Fujirebio Inc. European Patent EP421441 A2, Jan 25, 1995.
- ¹⁰¹ Komatsu, T.; Kikuchi, K.; Takakusa, H.; Hanaoka, K.; Ueno, T.; Kamiya, M.; Urano, Y.; Nagano, T. “Design and synthesis of an enzyme activity-based labeling molecule with fluorescence spectral change” *J. Am. Chem. Soc.* **2006**, *128*, 15946–15947.
- ¹⁰² Binanzer, M.; Hsieh, S. -Y.; Bode, J. W. “Catalytic kinetic resolution of cyclic secondary amines” *J. Am. Chem. Soc.* **2011**, *133*, 19698–19701.
- ¹⁰³ National Center for Biotechnology Information. PubChem BioAssay Database; AID=1979, Source= Broad Institute. <https://pubchem.ncbi.nlm.nih.gov/assay/assay.cgi?aid=1979> (accessed Feb. 18, 2016).
- ¹⁰⁴ Gu, W.; Wang, S. “Synthesis and antimicrobial activities of novel 1*H*-dibenzo[*a,c*]carbazoles from dehydroabiatic acid” *Eur. J. Med. Chem.* **2010**, *45*, 4692–4696.
- ¹⁰⁵ Jankowiak, A.; Kaszynski, P. “Synthesis of oleophilic electron-rich phenylhydrazines” *Beilstein J. Org. Chem.* **2012**, *8*, 275–282.
- ¹⁰⁶ (a) Wolfbeis, O. *Liebigs Ann. Chem.* “Synthesen von Fluoreszenzfarbstoffen, 11 über die Umlagerung von Alkoxymethylen- und Aminomethylenhomophthalsäureanhydriden zu Isocumarinen bzw. Isochinolinonen” **1981**, *5*, 819–827.
- ¹⁰⁷ Hoechst GmbH “Antiarrhythmic and cardioprotective substituted -1(2*H*)isoquinolines, medicament containing them, and their use for combating heart failures” US Patent US5416094 A1, Sep 24, 1993.
- ¹⁰⁸ Berghausen, J.; Buschmann, N.; Furet, P.; Gessier, F.; Hergovich Lisztwan, J.; Holzer, P.; Jacoby, E.; Kallen, J.; Masuya, K.; Pissot Soldermann, C.; Ren, H.; Stutz, S. “*Isoquinolinone and quinazolinone derivatives as MDM2 and MDM4 inhibitors and their preparation and use for the treatment of diseases*” PCT Int. Appl., 2 011 076 786, 2011.
- ¹⁰⁹ Reddy, T.; Reddy, G.; Reddy, L.; Jammula, S.; Lingappa, Y.; Kapavarapu, R.; Meda, C.; Parsa, K.; Pal, M. “Montmorillonite K-10 mediated green synthesis of cyano pyridines: Their evaluation as potential inhibitors of PDE4” *Eur. J. Med. Chem.* **2012**, *48*, 265–274.
- ¹¹⁰ Presser, A.; Hufner, A. “Trimethylsilyldiazomethane – A Mild and Efficient Reagent for the Methylation of Carboxylic Acids and Alcohols in Natural Products” *Monatsh. Chem.* **2004**, *135*, 1015 – 1022.
- ¹¹¹ Delioemeroglu, M. K.; Balci, M.; Ozcan, S. “A short and efficient construction of the dibenzo[*c,h*]chromen-6-one skeleton” *Arkivoc.* **2010**, *2*, 148–160.
- ¹¹² Selwood, D. “Benzamide derivatives useful in the treatment of muscular disorders and pain and for controlling spasticity and tremors.” WO Patent 201 582 938, 2015.
- ¹¹³ Liu, B.; Yi, W.; Zhang, J.; Liu, Q.; Liu, Y.; Fan, S.; Yu, X. *Org. Biomol. Chem.* **2014**, *12*, 3484 – 3492.

- ¹¹⁴ Zinelaabidine, C.; Souad, O.; Zoubir, J.; Malika, B.; Nour-Eddine, A. "A Simple and Efficient Green Method for the Deprotection of N-Boc in Various Structurally Diverse Amines under Water-mediated Catalyst-free Conditions" *Int. J. Chem.* **2012**, *4*, 73–79.
- ¹¹⁵ Martin, L.; Coello, M.; Reyes, B.; Rodriguez, V.; Garranzo, G.; Murcia, P.; Francesch, S.; Sanchez, S.; Fernandez, R. "Antitumoral dihydropyran-2-one compounds." WO Patent 2007 144 423, 2007.
- ¹¹⁶ Liu, Z., Wang, R.; Guo, R.; Hu, J.; Li, R.; Zhao, Y.; Gong, P. "Design, synthesis and biological evaluation of novel 6,7-disubstituted-4-phenoxyquinoline derivatives bearing 4-oxo-3,4-dihydrophthalazine-1-carboxamide moieties as c-Met kinase inhibitors" *Bioorg. Med. Chem.* **2014**, *22*, 3642–3653.
- ¹¹⁷ Galibert, M.; Dumy, P.; Boturyn, D. "One-Pot Approach to Well-Defined Biomolecular Assemblies by Orthogonal Chemoselective Ligations" *Angew. Chem.* **2009**, *121*, 2614–2617.
- ¹¹⁸ Taldone, T.; Rodina, A.; Gomes, E.; Riolo, M.; Patel, H.; Alonso-Sabadell, R.; Zatorska, D.; Patel, M.; Kishinevsky, S.; Chiosis, G. "Synthesis and evaluation of cell-permeable biotinylated PU-H71 derivatives as tumor Hsp90 probes" *Beilstein J. Org. Chem.* **2013**, *9*, 544–556.
- ¹¹⁹ Wolfbeis, O. "Synthesen von Fluoreszenzfarbstoffen, 11 über die Umlagerung von Alkoxymethylen- und Aminomethylenhomophthalsäureanhydriden zu Isocumarinen bzw. Isochinolinonen" *Liebigs Annalen der Chemie* **1981**, *5*, 819–827.
- ¹²⁰ Patil, C. D.; Sadana, A.; Deodhar, S. "Syntheses of 2-substituted-1,2-dihydro-1-oxo-4-isoquinoline-carboxamides and 4-amidoximino-2-substituted-1,2-dihydro-1-oxoisoquinolines as antimicrobial agents." *J. Indian Chem. Soc.* **1990**, *67*, 654–656.
- ¹²¹ Zinelaabidine, C.; Souad, O.; Zoubir, J.; Malika, B.; Nour-Eddine, A. "A Simple and Efficient Green Method for the Deprotection of N-Boc in Various Structurally Diverse Amines under Water-mediated Catalyst-free Conditions." *Int. J. Chem.* **2012**, *4*, 73–79.
- ¹²² Berghausen, J.; Buschmann, N.; Furet, P.; Gessier, F.; Hergovich Lisztwan, J.; Holzer, P.; Jacoby, E.; Kallen, J.; Masuya, K.; Pissot Soldermann, C.; Ren, H.; Stutz, S. "Isoquinolinone and quinazolinone derivatives as MDM2 and MDM4 inhibitors and their preparation and use for the treatment of diseases." PCT Int. Appl. 2 011 076 786, 2011.
- ¹²³ Reddy, T.; Reddy, G.; Reddy, L.; Jammula, S.; Lingappa, Y.; Kapavarapu, R.; Meda, C.; Parsa, K.; Pal, M. "Montmorillonite K-10 mediated green synthesis of cyano pyridines: Their evaluation as potential inhibitors of PDE4." *Eur. J. Med. Chem.* **2012**, *48*, 265–274.
- ¹²⁴ Ochoa-Puentes, C.; Bauer, S.; Kuhnle, M.; Bernhardt, G.; Buschauer, A.; König, B. "Benzanilide–Biphenyl Replacement: A Bioisosteric Approach to Quinoline Carboxamide-Type ABCG2 Modulators." *ACS Med. Chem. Lett.* **2013**, *4*, 393–396.
- ¹²⁵ Selwood, D. "Benzamide derivatives useful in the treatment of muscular disorders and pain and for controlling spasticity and tremors." WO Patent 201 582 938, 2015.
- ¹²⁶ Liu, B.; Yi, W.; Zhang, J.; Liu, Q.; Liu, Y.; Fan, S.; Yu, X. "Synthesis and gene transfection activity of cyclen-based cationic lipids with asymmetric acyl-cholesteryl hydrophobic tails." *Org. Biomol. Chem.* **2014**, *12*, 3484–3492.
- ¹²⁷ Martin, L.; Coello, M.; Reyes, B.; Rodriguez, V.; Garranzo, G.; Murcia, P.; Francesch, S.; Sanchez, S.; Fernandez, R. "Antitumoral dihydropyran-2-one compounds." WO Patent 2 007 144 423, 2007.
- ¹²⁸ Azagarsamy, M.; Kristi, A. S. "Wavelength-Controlled Photocleavage for the Orthogonal and Sequential Release of Multiple Proteins." *Angew. Chem. Int. Ed.* **2013**, *52*, 13803–13807.

- ¹²⁹ Martin, L.; Coello, M.; Reyes, B.; Rodriguez, V.; Garranzo, G.; Murcia, P.; Francesch, S.; Sanchez, S.; Fernandez, R. "Antitumoral dihydropyran-2-one compounds." WO Patent 2 007 144 423, 2007.
- ¹³⁰ Galibert, M.; Dumy, P.; Boturyn, D. "One-Pot Approach to Well-Defined Biomolecular Assemblies by Orthogonal Chemoselective Ligations." *Angew. Chem.* **2009**, *121*, 2614–2617.
- ¹³¹ Tsuji, J. *Palladium Reagents and Catalysts, New Perspectives for the 21st Century*; John Wiley & Sons Ltd: Chichester, U. K. 2003.
- ¹³² Yuan, C.; Du, B.; Yang, L.; Liu, B. "Bioinspired total synthesis of bolivianine: a Diels-Alder/intramolecular hetero-Diels-Alder cascade approach" *J. Am. Chem. Soc.* **2013**, *135*, 9291–9294.
- ¹³³ Xiao, Q.; Zhang, Y.; Wang, J. "Diazo compounds and *N*-tosylhydrazones: novel cross-coupling partners in transition-metal-catalyzed reactions" *Acc. Chem. Res.* **2013**, *46*, 236–247.
- ¹³⁴ (a) Armstrong, R. K. "Decomposition of ethyl diazoacetate by a π -allylic palladium chloride complex" *J. Org. Chem.* **1966**, *31*, 618–620. (b) Nakamura, A; Koyama, T; Otsuka, S. "Some aspects on mechanism of palladium-complex-catalyzed decomposition of and cyclopropanation with ethyl diazoacetate." *Bull. Chem. Soc. Jpn.* **1978**, *51*, 593–595. (c) Bernardi, F.; Bottoni, A.; Miscione, G.P. "DFT study of the palladium-catalyzed cyclopropanation reaction." *Organometallics* **2001**, *20*, 2751–2758. (d) Rodriguez-Garcia, C.; Oliva, A.; Ortuño, R. M.; Branchadell, V. "Mechanism of olefin cyclopropanation by diazomethane catalyzed by palladium dicarboxylates. A density functional study." *J. Am. Chem. Soc.* **2001**, *123*, 6157–6163. (e) Rodriguez-Garcia, C; González-Blanco, O; Oliva, A; Ortuño, R. M.; Branchadell, V. "Density functional study of possible intermediates in the mechanism of olefin cyclopropanation catalyzed by metal carboxylates" *Eur. J. Inorg. Chem.* **2000**, 1073–1078. (f) Illa, O.; Rodriguez-Garcia, C.; Acosta-Silva, C.; Faviere, I.; Picurelli, D.; Oliva, A.; Gómez, M.; Branchadell, V.; Ortuño, R. M. "Cyclopropanation of cyclohexenone by diazomethane catalyzed by palladium diacetate: Evidence for the formation of palladium(0) nanoparticles" *Organometallics* **2007**, *26*, 3306–3314. (g) Berthon-Gelloz, G.; Marchant, M.; Straub, B. F.; Marko, I. E. "Palladium-Catalyzed Cyclopropanation of Alkenyl Silanes by Diazoalkanes: Evidence for a Pd(0) Mechanism" *Chem. Eur. J.* **2009**, *15*, 2923–2931. (h) Straub, B. F. "Pd(0) mechanism of palladium-catalyzed cyclopropanation of alkenes by CH₂N₂: A DFT study" *J. Am. Chem. Soc.* **2002**, *124*, 14195–14201. (i) Illa, O.; Rodriguez-Garcia, C.; Acosta-Silva, C.; Faviere, I.; Picurelli, D.; Oliva, A.; Gómez, M.; Branchadell, V.; Ortuño, R. M. "Cyclopropanation of cyclohexenone by diazomethane catalyzed by palladium diacetate: Evidence for the formation of palladium(0) nanoparticles" *Organometallics* **2007**, *26*, 3306–3314. (j) A. J. Anciaux, A.J. Hubert, A. F. Noels, N. Petiniot, P. Teysie "Transition-metal-catalyzed reactions of diazo compounds. 1. Cyclopropanation of double bonds" *J. Org. Chem.* **1980**, *45*, 695–702. (k) Martin, C.; Molina, F.; Alvarez, E.; Belderrain, T. R. "Stable N-Heterocyclic Carbene (NHC)–Palladium(0) Complexes as Active Catalysts for Olefin Cyclopropanation Reactions with Ethyl Diazoacetate" *Chem. Eur. J.* **2011**, *17*, 14885–14895. (l) Yang, F.; Zhang, Y.M.; Qiu, W.W.; Tang, J.; He, M.-Y. "Immobilization of Pd(II) catalysts for cyclopropanation in ionic liquid" *Chin. J. Chem.* **2002**, *20*, 114–116. (m) Kantam, M. L.; Haritha, Y.; Reddy, N. M.; Choudary, B. M.; Figueras, F. "Cyclopropanation of olefins using a silica gel anchored palladium phosphine complex" *Catalysis Lett.* **2002**, *83*, 187–190. (n) Lautens, M.; Klute, W.; Tam, W. "Transition metal-mediated cycloaddition reactions" *Chem. Rev.* **1996**, *96*, 49–92. (o) Kurek-Tyrlik, A.; Michalak, K.; Urbanczyk-Lipkowska, Z.; Wicha, J. "A synthesis of 17-epi-calcidiol"

Tetrahedron Lett. (2004), 45, 7479–7482. This manuscript referred back to both the Anciaux and Majchrzak procedure paper: Majchrzak, M. W.; Kotelko, A.; Lambert, J. B. *Synthesis* 1983, 469–470. In a 2011 paper, the authors used 10 mol% copper and syringe pump addition for the same transformation on a C-D ring system model. Michalak, K.; Wicha, J. *J. Org. Chem.* 2011, 76, 6906–6911. (p) Majchrzak, M. W.; Kotelko, A.; Lambert, J. B. “Palladium(II) Acetate, an Efficient Catalyst for Cyclopropanation Reactions with Ethyl Diazoacetate.” *Synthesis* 1983, 469–470. (q) Shimamoto, K.; Ishida, M.; Shinozaki, H.; Ohfuné, Y. “Synthesis Of 4 Diastereomeric L-2-(Carboxycyclopropyl)Glycines - Conformationally Constrained L-Glutamate Analogs” *J. Org. Chem.* 1991, 56, 4167–4176. (r) Maas, G. “Transition-metal catalyzed decomposition of aliphatic diazo-compounds - new results and applications in organic synthesis.” *Topics Curr. Chem.* 1987, 137, 75–253. (s) Tomilov, Yu V.; Dokichev, V. A.; Dzhemilev, U. M.; Nefedov, O. M. “Catalytic decomposition of diazomethane as general-method of methylenation of chemical-compounds” *Russ. Chem. Rev.* 1993, 62, 799–838. (t) Tomilov, Y.V.; Bordakov, V.G.; Dolgii, I.E., Nefedov, O.M. “Reaction of Diazoalkanes with Unsaturated-Compounds. 2. Cyclopropanation of Olefins By Diazomethane in the Presence of Palladium Compounds” *Bull. Acad. Sci. USSR Div. Chem. Sci.* 1984, 33, 533–538. (u) Berthon-Gelloz, G.; Marchant, M.; Straub, B. F.; Marko, I. E. “Palladium-Catalyzed Cyclopropanation of Alkenyl Silanes by Diazoalkanes: Evidence for a Pd-0 Mechanism” *Chem. Eur. J.* 2009, 15, 2923–2931.

¹³⁵ (a) Sierra, M. A.; del Amo, J. C.; Mancheno, M. J.; Gomez-Gallego, M. “Pd-Catalyzed Inter- and Intramolecular Carbene Transfer from Group 6 Metal-Carbene Complexes” *J. Am. Chem. Soc.* 2001, 123, 851–861. (b) Albeniz, A. C.; Espinet, P.; Manrique, R.; Perez-Mateo, A. “Observation of the direct products of migratory insertion in aryl palladium carbene complexes and their subsequent hydrolysis” *Angew. Chem. Int. Ed. Engl.* 2002, 41, 2363–2366. (c) Bien, S.; Gillon, A.; Kohen, S. “Dependence of product on catalyst in the transition-metal-catalysed decomposition of ethyl 2-allyl-4-diazoacetate” *J. Chem. Soc., Perkin Trans. 1* 1976, 489–492. (d) Wanat, R. A.; Collum, D. B. “Approaches to the synthesis and detection of a transient palladium(0) alkylidene.” *Organometallics* 1986, 5, 120–127. (e) Kirmse, W.; Kapps, M. “Reaktionen des Diazomethans mit Diallylsulfid und Allylthern unter Kupfersalz-Katalyse.” *Chem. Ber.* 1968, 101, 994–1003. W. Ando. “Ylide formation and rearrangement in the reaction of carbene with divalent sulfur compounds” *Acc. Chem. Res.* 1977, 19, 179. (f) Tamblyn, W.H.; Hoffmann, S.R.; Doyle, M.P. “Correlation between catalytic cyclopropanation and ylide generation” *J. Organomet. Chem.* 1981, 216, C64–C68. (g) Carter, D. S., Van Vranken, D. L. “Metal-Catalyzed Ylide Formation and [2,3] Sigmatropic Rearrangement of Allyl Sulfides with Trimethylsilyldiazomethane.” *Tetrahedron Lett.* 1999, 40, 1617. (h) Aggarwal, V. K.; Ferrara, M.; Hainz, R.; Spey, S. E. “[2,3]-Sigmatropic rearrangement of allylic sulfur ylides derived from trimethylsilyldiazomethane (TMSD)” *Tetrahedron Lett.* 1999, 40, 8923–8927.

¹³⁶ (a) A thorough review on diazo compounds as metal carbene precursors: Ye, T.; McKervery, M. A. “Organic Synthesis with α -Diazocarbonyl Compounds” *Chem. Rev.* 1994, 94, 1091–1160. (b) Trost, B. M.; Self, C. R. “ α -Elimination of α -acetoxysilanes induced by palladium – evidence for the intermediacy of a vinylcarbene palladium complex” *J. Am. Chem. Soc.* 1983, 105, 5942–5944. (c) Fillion, E.; Taylor, N. “Cine-Substitution in the Stille Coupling: Evidence for the Carbenoid Reactivity of sp^3 -gem-Organodimetallic Iodopalladio-trialkylstannylalkane Intermediates” *J. Am. Chem. Soc.* 2003, 125, 12700–12701. (d) Trépanier, V. É.; Fillion, E.

“Ambiphilic Vinylcarbenoid Reactivity of $\text{-(Tributylstannyl)-allyl}$ palladium(II) Species” *Organometallics* **2007**, *26*, 30–32.

¹³⁷ Zhang, Yan; Wang, Jianbo “Recent Developments in Pd-Catalyzed Reactions of Diazo Compounds” *Eur. J. Org. Chem.* **2011**, 1015–1026.

¹³⁸ Jellema, E.; Jongerius, A. L.; Reek, J. N. H.; de Bruin, B. “C1 Polymerisation and Related C–C Bond Forming ‘Carbene Insertion’ Reactions” *Chem. Soc. Rev.* **2010**, *39*, 1706–1723.

¹³⁹ Greenman, K. L.; Carter, D. S.; Van Vranken, D. L. “Palladium-Catalyzed Insertion Reactions of Trimethylsilyldiazomethane” *Tetrahedron* **2001**, *57*, 5219–5225.

¹⁴⁰ Devine, S. K. J.; Van Vranken, D. L. “Palladium-Catalyzed Carbene Insertion into Vinyl Halides and Trapping with Amines” *Org. Lett.* **2007**, *9*, 2047–2049.

¹⁴¹ Devine, S. K. J.; Van Vranken, D. L. “Palladium-Catalyzed Carbene Insertion and Trapping with Carbon Nucleophiles” *Org. Lett.* **2008**, *10*, 1909–1911.

¹⁴² Kudirka, R.; Devine, S. K. J.; Adams, C. S.; Van Vranken, D. L. “Palladium-Catalyzed Insertion of α -Diazoesters into Vinyl Halides To Generate α,β -Unsaturated γ -Amino Esters” *Angew. Chem. Int. Ed.* **2009**, *48*, 3677–3680.

¹⁴³ Kudirka, R.; Van Vranken, D. L. “Cyclization Reactions Involving Palladium-Catalyzed Carbene Insertion into Aryl Halides” *J. Org. Chem.* **2008**, *73*, 3585–3588.

¹⁴⁴ Peng, C.; Wang, Y.; Wang, J. “Palladium-Catalyzed Cross-Coupling of α -Diazocarbonyl Compounds with Arylboronic Acids” *J. Am. Chem. Soc.* **2008**, *130*, 1566–1567.

¹⁴⁵ (a) Ye, T.; McKervey, M. A. “Organic Synthesis with α -Diazo Carbonyl Compounds” *Chem. Rev.* **1994**, *94*, 1091–1160. (b) Doyle, M. P.; McKervey, M. A.; Ye, T. *Modern Catalytic Methods for Organic Synthesis with Diazo Compounds*, Wiley: New York, 1998. (c) Zhang, Z.; Wang, J. “Recent Studies on the Reactions of α -Diazocarbonyl Compounds” *Tetrahedron* **2008**, *64*, 6577–6605.

¹⁴⁶ T. J. de Boer; H. J. Backer, “Diazomethane” *Org. Synth. Coll. Vol. 4* **1963**, *36*, 16

¹⁴⁷ Creary, X. “Tosylhydrazone salt pyrolyses: phenyldiazomethanes”. *Org. Synth.* **1986**, *64*, 207.

¹⁴⁸ (a) Aggarwal, V. K.; de Vicente, J.; Bonnert, R. V. “Catalytic Cyclopropanation of Alkenes Using Diazo Compounds Generated in Situ. A Novel Route to 2-Arylcyclopropylamines” *Org. Lett.* **2001**, *3*, 2785–2788. (b) Aggarwal, V. K.; Fulton, J. R.; Sheldon, C. G.; de Vicente, J. “Generation of Phosphoranes Derived from Phosphites. A New Class of Phosphorus Ylides Leading to High E Selectivity with Semi-stabilizing Groups in Wittig Olefinations” *J. Am. Chem. Soc.* **2003**, *125*, 6034–6035.

¹⁴⁹ Barluenga, J.; Moriel, P.; Valdés, C.; Aznar, F. “*N*-Tosylhydrazones as Reagents for Cross-Coupling Reactions: A Route to Polysubstituted Olefins” *Angew. Chem. Int. Ed.* **2007**, *46*, 5587–5590.

¹⁵⁰ Nevado, C.; Charruault, L.; Michelet, V.; Nieto-Oberhuber, C.; Muñoz, M. P.; Méndez, M.; Rager, M. -N.; Genêt, J. P.; Echavarren, A. M. “On the Mechanism of Carbohydroxypalladation of Enynes. Additional Insights on the Cyclization of Enynes with Electrophilic Metal Complexes” *Eur. J. Org. Chem.* **2003**, 706–713.

¹⁵¹ Amrich, M. J.; Bell, J. A. “Photoisomerization of Diazirine” *J. Am. Chem. Soc.* **1964**, *86*, 292–293.

¹⁵² Sierra, M. A.; Mancheño, M. J.; Sáez, E.; del Amo, J. C. “Chromium(0)–Carbene Complexes as Carbene Sources: Self-Dimerization and Inter- and Intramolecular C–H Insertion Reactions Catalyzed by $\text{Pd}(\text{OAc})_2$ ” *J. Am. Chem. Soc.* **1998**, *120*, 6812–6813.

- ¹⁵³ Hine, J. “Carbon Dichloride as an Intermediate in the Basic Hydrolysis of Chloroform. A Mechanism for Substitution Reactions at a Saturated Carbon Atom” *J. Am. Chem. Soc.* **1950**, *72*, 2438–2445.
- ¹⁵⁴ (a) Barluenga, J.; Escribano, M.; Moriel, P.; Aznar, F.; Valdés, C. “Synthesis of Enol Ethers and Enamines by Pd-Catalyzed Tosylhydrazide-Promoted Cross-Coupling Reactions” *Chem. Eur. J.* **2009**, *15*, 13291–13294. (b) Barluenga, J.; Tomás-Gamasa, M.; Aznar, F.; Valdés, C. “Synthesis of 2-Arylacrylates from Pyruvate by Tosylhydrazide-Promoted Pd-Catalyzed Coupling with Aryl Halides” *Chem. Eur. J.* **2010**, *16*, 12801–12803. (c) Barluenga, J.; Escribano, M.; Aznar, F.; Valdés, C. “Arylation of α -Chiral Ketones by Palladium-Catalyzed Cross-Coupling Reactions of Tosylhydrazones with Aryl Halides” *Angew. Chem. Int. Ed.* **2010**, *49*, 6856–6859. (d) Ojha, D. P.; Prabhu, K. R. “Heteroaryl Halides in the Absence of External Ligands: Synthesis of Substituted Olefins” *J. Org. Chem.* **2012**, *77*, 11027–11033. (e) Roche, M.; Hamze, A.; Brion, J.-D.; Alami, M. “Catalytic Three-Component One-Pot Reaction of Hydrazones, Dihaloarenes, and Amines” *Org. Lett.* **2013**, *15*, 148–151. (f) Roche, M.; Hamze, A.; Provot, O.; Brion, J.-D.; Alami, M. “Synthesis of Ortho/Ortho’-Substituted 1,1-Diarylethylenes through Cross-Coupling Reactions of Sterically Encumbered Hydrazones and Aryl Halides” *J. Org. Chem.* **2013**, *78*, 445–454. (g) Jimenéz-Aquino, A.; Vega, J. A.; Trabanco, A. A.; Valdés, C. “A General Synthesis of α -Trifluoromethylstyrenes through Palladium-Catalyzed Cross-Couplings with 1,1,1-Trifluoroacetone Tosylhydrazone” *Adv. Synth. Catal.* **2014**, *356*, 1079–1084.
- ¹⁵⁵ (a) Barluenga, J.; Florentino, L.; Aznar, F.; Valdés, C. “Synthesis of Polysubstituted Olefins by Pd-Catalyzed Cross-Coupling Reaction of Tosylhydrazones and Aryl Nonaflates” *Org. Lett.* **2011**, *13*, 510–513. (b) Florentino, L.; Aznar, F.; Valdés, C. “Synthesis of Polysubstituted Isoquinolines through Cross-Coupling Reactions with α -Alkoxytosylhydrazones” *Org. Lett.* **2012**, *14*, 2323–2325. (c) Florentino, L.; Aznar, F.; Valdés, C. “Synthesis of (Z)-N-Alkenylazoles and Pyrroloisoquinolines from α -N-Azoleketones through Pd-Catalyzed Tosylhydrazone Cross-Couplings” *Chem. Eur. J.* **2013**, *19*, 10506–10510.
- ¹⁵⁶ Patel, P. K.; Dalvadi, J. P.; Chikhaliya, K. H. “Pd-Catalyzed Cross-Coupling Reactions of less Activated Alkenyl Electrophiles (for Tosylates and Mesylates) with Tosylhydrazones: Synthesis of Various 1,3-Dienes” *RSC Adv.* **2014**, *4*, 55354–55361.
- ¹⁵⁷ (a) Pettit, G. R.; Cragg, G. M.; Herald, D. L.; Schmidt, J. M.; Lohavanijaya, P. “Isolation and Structure of Combretastatin” *Can. J. Chem.* **1982**, *60*, 1374–1376. (b) Pettit, G. R.; Singh, S. B.; Boyd, M. R.; Hamel, E.; Pettit, R. K.; Schmidt, J. M.; Hogan, F. “Antineoplastic Agents. 291. Isolation and Synthesis of Combretastatins A-4, A-5, and A-6” *J. Med. Chem.* **1995**, *38*, 1666–1672.
- ¹⁵⁸ (a) Siemann, D. W.; Chaplin, D. J.; Walicke, P. A. “A Review and Update of the Current Status of the Vasculature-Disabling Agent Combretastatin-A4 Phosphate (CA4P)” *Expert Opin. Invest. Drugs* **2009**, *18*, 189–197. (b) Rajak, H.; Kumar Dewangan, P.; Patel, V.; Kumar Jain, D.; Singh, A.; Veerasamy, R.; Chander Sharma, P.; Dixit, A. “Design of Combretastatin A-4 Analogs as Tubulin Targeted 17 Vascular Disrupting Agent with Special Emphasis on Their cis-Restricted Isomers” *Curr. Pharm. Des.* **2013**, *19*, 1923–1955. (c) Tron, G. C.; Piralì, T.; Sorba, G.; Pagliai, F.; Busacca, S.; Genazzani, A. A. “Medicinal Chemistry of Combretastatin A4: Present and Future Directions” *J. Med. Chem.* **2006**, *49*, 3033–3044.
- ¹⁵⁹ (a) Messaoudi, S.; Tréguier, B.; Hamze, A.; Provot, O.; Peyrat, J.-F.; Losada, J. R. D.; Liu, J.-M.; Bignon, J.; Wdzieczak-Bakala, J.; Thoret, S.; Dubois, J.; Brion, J.-D.; Alami, M.

“Isocombretastatins A versus Combretastatins A: The Forgotten *isoCA-4* Isomer as a Highly Promising Cytotoxic and Antitubulin Agent” *J. Med. Chem.* **2009**, *52*, 4538–4542. (b) Tréguier, B.; Hamze, A.; Provot, O.; Brion, J.-D.; Alami, M. “Expeditious Synthesis of 1,1-Diarylethylenes Related to Isocombretastatin A-4 (*isoCA-4*) via Palladium-Catalyzed Arylation of N-Tosylhydrazones with Aryl Triflates” *Tetrahedron Lett.* **2009**, *50*, 6549–6552. (c) Soussi, M. A.; Aprile, S.; Messaoudi, S.; Provot, O.; Grosso, E. D.; Bignon, J.; Dubois, J.; Brion, J. D.; Grosa, G.; Alami, M. “The Metabolic Fate of *isoCombretastatin A-4* in Human Liver Microsomes: Identification, Synthesis and Biological Evaluation of Metabolites” *ChemMedChem* **2011**, *6*, 1781–1788. (d) Messaoudi, S.; Hamze, A.; Provot, O.; Tréguier, B.; Losada, J. R. D.; Bignon, J.; Liu, J.-M.; Wdzieczak-Bakala, J.; Thoret, S.; Dubois, J.; Brion, J.-D.; Alami, M. “Discovery of Isoerianin Analogues as Promising Anticancer Agents” *ChemMedChem* **2011**, *6*, 488–497. (e) Rasolofonjatovo, E.; Tréguier, B.; Provot, O.; Hamze, A.; Morvan, E.; Brion, J.-D.; Alami, M. “Palladium-Catalyzed Coupling of N-Tosylhydrazones with Ortho Substituted Aryl Halides: Synthesis of 4-Arylchromenes and Related Heterocycles” *Tetrahedron Lett.* **2011**, *52*, 1036–1040. (f) Rasolofonjatovo, E.; Tréguier, B.; Provot, O.; Hamze, A.; Brion, J.-D.; Alami, M. “A One-Pot Three-Step Synthesis of Z-Trisubstituted Olefins from Arylalkynes and Their Cyclization into 4-Aryl-2H-chromenes” *Eur. J. Org. Chem.* **2012**, 1603–1615. (g) Lawson, M.; Hamze, A.; Peyrat, J.-F.; Bignon, J.; Dubois, J.; Brion, J.-D.; Alami, M. “An Efficient Coupling of N-Tosylhydrazones with 2-Halopyridines: Synthesis of 2- α -Styrylpyridines Endowed with Antitumor Activity” *Org. Biomol. Chem.* **2013**, *11*, 3664–3673. (h) Tréguier, B.; Lawson, M.; Bernadat, G.; Bignon, J.; Dubois, J.; Brion, J.-D.; Alami, M.; Hamze, A. “Synthesis of a 3-(α -Styryl)benzo[b]-thiophene Library via Bromocyclization of Alkynes and Palladium-Catalyzed Tosylhydrazones Cross-Couplings: Evaluation as Antitubulin Agents” *ACS Comb. Sci.* **2014**, *16*, 702–710. (i) Ganapathy, D.; Sekar, G. “Efficient Synthesis of Polysubstituted Olefins Using Stable Palladium Nanocatalyst: Applications in Synthesis of Tamoxifen and Isocombretastatin A4” *Org. Lett.* **2014**, *16*, 3856–3859.

¹⁶⁰ (a) Tsoi, Y.-T.; Zhou, Z.; Chan, A. S. C.; Yu, W., -Y. “Palladium-Catalyzed Oxidative Cross-Coupling Reaction of Arylboronic Acids with Diazoesters for Stereoselective Synthesis of (*E*)- α , β -Diarylacrylates” *Org. Lett.* **2010**, *12*, 4506–4509. (b) Xia, Y.; Xia, Y.; Lin, Z.; Zhang, Y.; Wang, J. “Palladium-Catalyzed Cross-Coupling Reaction of Diazo Compounds and Vinyl Boronic Acids: An Approach to 1,3-Diene Compounds” *J. Org. Chem.* **2014**, *79*, 7711–7717. (c) Zhao, X.; Jing, J.; Lu, K.; Zhang, Y.; Wang, J. “Pd-Catalyzed Oxidative Cross-Coupling of N-Tosylhydrazones with Arylboronic Acids” *Chem. Commun.* **2010**, *46*, 1724–1726.

¹⁶¹ (a) Zeng, X.; Cheng, G.; Shen, J.; Cui, X. “Palladium-Catalyzed Oxidative Cross-Coupling of N-Tosylhydrazones with Indoles: Synthesis of *N*-Vinylindoles” *Org. Lett.* **2013**, *15*, 3022–3025. (b) Roche, M.; Bignon, J.; Brion, J.-D.; Hamze, A.; Alami, M. “Tandem One-Pot Palladium-Catalyzed Coupling of Hydrazones, Haloindoles, and Amines: Synthesis of Amino-*N*-vinylindoles and Their Effect on Human Colon Carcinoma Cells” *J. Org. Chem.* **2014**, *79*, 7583–7592. (c) Roche, M.; Frison, G.; Brion, J.-D.; Provot, O.; Hamze, A.; Alami, M. “Csp²-N Bond Formation via Ligand-Free Pd-Catalyzed Oxidative Coupling Reaction of *N*-Tosylhydrazones and Indole Derivatives” *J. Org. Chem.* **2013**, *78*, 8485–8495.

¹⁶² Zhou, L.; Ye, F.; Ma, J.; Zhang, Y.; Wang, J. “Palladium-Catalyzed Oxidative Cross-Coupling of N-Tosylhydrazones or Diazoesters with Terminal Alkynes: A Route to Conjugated Enynes” *Angew. Chem. Int. Ed.* **2011**, *50*, 3510–3514.

- ¹⁶³ Zhang, Z.; Liu, Y.; Gong, M.; Zhao, X.; Zhang, Y.; Wang, J. "Palladium-Catalyzed Carbonylation/Acyl Migratory Insertion Sequence" *Angew. Chem. Int. Ed.* **2010**, *49*, 1139–1142.
- ¹⁶⁴ Wu, X. -X.; Shen, Y.; Chen, W. -C.; Chen, S.; Hao, X. -H.; Xia, Y.; Xu, P. -F.; Liang, Y. -M. "Palladium-Catalyzed Ring Opening of Norbornene: Efficient Synthesis of Methylene-cyclopentane Derivatives" *Chem. Commun.* **2015**, *51*, 8031–8033.
- ¹⁶⁵ (a) Barluenga, J.; Escribano, M.; Moriel, P.; Aznar, F.; Valdés, C. "Synthesis of Enol Ethers and Enamines by Pd-Catalyzed Tosylhydrazide-Promoted Cross-Coupling Reactions" *Chem. Eur. J.* **2009**, *15*, 13291–13294. (b) Roche, M.; Frison, G.; Brion, J. -D.; Provot, O.; Hamze, A.; Alami, M. "Csp²-N Bond Formation via Ligand-Free Pd-Catalyzed Oxidative Coupling Reaction of *N*-Tosylhydrazones and Indole Derivatives" *J. Org. Chem.* **2013**, *78*, 8485–8495. (c) Barluenga, J.; Florentino, L.; Aznar, F.; Valdés, C. "Synthesis of Polysubstituted Olefins by Pd-Catalyzed Cross-Coupling Reaction of Tosylhydrazones and Aryl Nonaflates" *Org. Lett.* **2011**, *13*, 510–513. (d) Barluenga, J.; Moriel, P.; Valdés, C.; Aznar, F. "*N*-Tosylhydrazones as Reagents for Cross-Coupling Reactions: A Route to Polysubstituted Olefin" *Angew. Chem., Int. Ed.* **2007**, *46*, 5587–5590. (e) Barluenga, J.; Tomas-Gamasa, M.; Moriel, P.; Aznar, F.; Valdés, C. "Pd-Catalyzed Cross-Coupling Reactions with Carbonyls: Application in a Very Efficient Synthesis of 4-Aryltetrahydropyridines" *Chem. Eur. J.* **2008**, *14*, 4792–4795.
- ¹⁶⁶ (a) Zhou, L.; Ye, F.; Zhang, Y.; Wang, J. "Cyclopropylmethyl Palladium Species from Carbene Migratory Insertion: New Routes to 1,3-Butadienes" *Org. Lett.* **2012**, *14*, 922–925. (b) Yang, Q.; Chai, H.; Liu, T.; Yu, Z. "Palladium-Catalyzed Cross-Coupling of Cyclopropylmethyl *N*-Tosylhydrazones with Aromatic Bromides: an Easy Access to Multisubstituted 1,3-Butadienes" *Tetrahedron Lett.* **2013**, *54*, 6485–6489.
- ¹⁶⁷ Kambe, N.; Iwasaki, T.; Terao, J. "Pd-Catalyzed Cross-Coupling Reactions of Alkyl Halides" *Chem. Soc. Rev.* **2011**, *40*, 4937–4947.
- ¹⁶⁸ Greenman, K. L.; Carter, D. S.; Van Vranken, D. L. "Palladium-Catalyzed Insertion Reactions of Trimethylsilyldiazomethane" *Tetrahedron* **2001**, *57*, 5219–5225.
- ¹⁶⁹ Cevasco, G.; Thea, S. "Mechanism of Alkaline Hydrolysis of Some HO- π -COOAr Acyl Derivatives" *J. Org. Chem.* **1999**, *64*, 5422–5426.
- ¹⁷⁰ Zhou, Y.; Ye, F.; Wang, X.; Xu, S.; Zhang, Y.; Wang, J. "Synthesis of Alkenylphosphonates through Palladium-Catalyzed Coupling of α -Diazo Phosphonates with Benzyl or Allyl Halides" *J. Org. Chem.* **2015**, *80*, 6109–6118.
- ¹⁷¹ Jiang, H.; He, L.; Li, X.; Chen, H.; Wu, W.; Fu, W. "Facile Synthesis of Dibranching Conjugated Dienes via Palladium-Catalyzed Oxidative Coupling of *N*-Tosylhydrazones" *Chem. Commun.* **2013**, *49*, 9218–9220.
- ¹⁷² Ojha, D. P.; Prabhu, K. R. "Pd-Catalyzed Cross-Coupling Reactions of Hydrazones: Regioselective Synthesis of Highly Branched Dienes" *J. Org. Chem.* **2013**, *78*, 12136–12143.
- ¹⁷³ Kudirka, R.; Devine, S. K. J.; Adams, C. S.; Van Vranken, D. L. "Palladium-Catalyzed Insertion of α -Diazoesters into Vinyl Halides To Generate α,β -Unsaturated γ -Amino Esters" *Angew. Chem. Int. Ed.* **2009**, *48*, 3677–3680.
- ¹⁷⁴ Xie, X. -L.; Zhu, S. -F.; Guo, J. -X.; Cai, Y.; Zhou, Q. -L. "Enantioselective Palladium-Catalyzed Insertion of α -Aryl-diazoacetates into the O–H Bonds of Phenols" *Angew. Chem. Int. Ed.* **2014**, *53*, 2978–2981.
- ¹⁷⁵ Zhou, F.; Ding, K.; Cai, Q. "Palladium-Catalyzed Amidation of *N*-Tosylhydrazones with Isocyanides" *Chem. Eur. J.* **2011**, *17*, 12268–12271.

¹⁷⁶ Barluenga, J.; Valdés, C. “Tosylhydrazones: New Uses for Classic Reagents in Palladium-Catalyzed Cross-Coupling and Metal-Free Reactions” *Angew. Chem., Int. Ed.* **2011**, *50*, 7486–7500.

¹⁷⁷ (a) Zhao, X.; Wu, G.; Yan, C.; Lu, K.; Li, H.; Zhang, Y.; Wang, J. “Microwave-Assisted, Pd(0)-Catalyzed Cross-Coupling of Diazirines with Aryl Halides” *Org. Lett.* **2010**, *12*, 5580–5583. (b) Shu, Z.; Zhang, J.; Zhang, Y.; Wang, J. “Palladium-catalyzed Cross-coupling of Aryl Iodides with β -Trimethylsiloxy- α -diazoesters: A Novel Approach toward β -Keto- α -arylesters” *Chem. Lett.* **2011**, *40*, 1009–1011. (c) Ojha, D. P.; Prabhu, K. R. “Palladium Catalyzed Coupling of Tosylhydrazones with Aryl and Heteroaryl Halides in the Absence of External Ligands: Synthesis of Substituted Olefins” *J. Org. Chem.* **2012**, *77*, 11027–11033. (d) Rasolofonjatovo, E.; Provot, O.; Hamze, A.; Rodrigo, J.; Bignon, J.; Wdzieczak-Bakala, J.; Lenoir, C.; Desravines, D.; Dubois, J.; Brion, J.-D.; Alami, M. “Conformationally Restricted Naphthalene Derivatives Type Isocombretastatin A-4 and Isoerianin Analogues: Synthesis, Cytotoxicity and Antitubulin Activity” *Eur. J. Med. Chem.* **2012**, *52*, 22–32 and reference therein. (e) Xia, Y.; Zhang, Y.; Wang, J. “Catalytic Cascade Reactions Involving Metal Carbene Migratory Insertion” *ACS Catal.* **2013**, *3*, 2586–2598 and references therein. (f) Ganapathy, D.; Sekar, G. “Efficient Synthesis of Polysubstituted Olefins Using Stable Palladium Nanocatalyst: Applications in Synthesis of Tamoxifen and Isocombretastatin A4” *Org. Lett.* **2014**, *16*, 3856–3859. (g) Jimenéz-Aquino, A.; Vega, J. A.; Trabanco, A. A.; Valdés, C. “A General Synthesis of α -Trifluoromethylstyrenes through Palladium-Catalyzed Cross-Couplings with 1,1,1-Trifluoroacetone Tosylhydrazone” *Adv. Synth. Catal.* **2014**, *356*, 1079–1084 and reference therein. (h) Zhou, P.-X.; Ye, Y.-Y.; Ma, J.-W.; Zheng, L.; Tang, Q.; Qiu, Y.-F.; Song, B.; Qiu, Z.-H.; Xu, P.-F.; Liang, Y.-M. “Palladium-Catalyzed/Norbornene-Mediated ortho-Amination/N-Tosylhydrazone Insertion Reaction: An Approach to the Synthesis of ortho-Aminated Vinylarenes” *J. Org. Chem.* **2014**, *79*, 6627–6633 and reference therein. (i) Renko, D.; Provot, O.; Rasolofonjatovo, E.; Bignon, J.; Rodrigo, J.; Dubois, J.; Brion, J.-D.; Hamze, A.; Alami, M. “Rapid Synthesis of 4-Arylchromenes from Ortho-Substituted Alkynols: A Versatile Access to Restricted Isocombretastatin A-4 Analogues as Antitumor Agents” *Eur. J. Med. Chem.* **2015**, *90*, 834–844 and references therein. (j) Florentino, L.; Aznar, F.; Valdés, C. “Synthesis of Polysubstituted Isoquinolines through Cross-Coupling Reactions with α -Alkoxytosylhydrazones” *Org. Lett.* **2012**, *14*, 2323–2325.

¹⁷⁸ (a) Greenman, K. L.; Van Vranken, D. L. “Palladium-Catalyzed Carbene Insertion into Benzyl Bromides” *Tetrahedron* **2005**, *61*, 6438–6441. (b) Xiao, Q.; Ma, J.; Yang, Y.; Zhang, Y.; Wang, J. “Pd-Catalyzed C=C Double-Bond Formation by Coupling of N-Tosylhydrazones with Benzyl Halides” *Org. Lett.* **2009**, *11*, 4732–4735. (c) Zhou, Y.; Ye, F.; Wang, X.; Xu, S.; Zhang, Y.; Wang, J. “Synthesis of Alkenylphosphonates through Palladium-Catalyzed Coupling of α -Diazo Phosphonates with Benzyl or Allyl Halides” *J. Org. Chem.* **2015**, *80*, 6109–6118. (d) Wu, X.-X.; Shen, Y.; Chen, W.-L.; Chen, S.; Hao, X.-H.; Xia, Y.; Xu, P.-F.; Liang, Y.-M. “Palladium-Catalyzed Ring Opening of Norbornene: Efficient Synthesis of Methylene-cyclopentane Derivatives” *Chem. Commun.* **2015**, *51*, 8031–8033.

¹⁷⁹ (a) Peng, C.; Wang, Y.; Wang, J. “Palladium-Catalyzed Cross-Coupling of α -Diazocarbonyl Compounds with Arylboronic Acids” *J. Am. Chem. Soc.* **2008**, *130*, 1566–1567. (b) Tsoi, Y.-T.; Zhou, Z.; Chan, A. S. C.; Yu, W.-Y. “Palladium-Catalyzed Oxidative Cross-Coupling Reaction of Arylboronic Acids with Diazoesters for Stereoselective Synthesis of (*E*)- α,β -Diarylacrylates” *Org. Lett.* **2010**, *12*, 4506–4509. (c) Zhao, X.; Jing, J.; Lu, K.; Zhang, Y.; Wang, J. “Pd-

Catalyzed Oxidative Cross-Coupling of *N*-Tosylhydrazones with Arylboronic Acids” *Chem. Commun.* **2010**, *46*, 1724–1726. (d) Zhou, L.; Ye, F.; Ma, J.; Zhang, Y.; Wang, J. “Palladium-Catalyzed Oxidative Cross-Coupling of *N*-Tosylhydrazones or Diazoesters with Terminal Alkynes: A Route to Conjugated Enynes” *Angew. Chem., Int. Ed.* **2011**, *50*, 3510–3514. (e) Roche, M.; Frison, G.; Brion, J.-D.; Provot, O.; Hamze, A.; Alami, M. “C_{sp}²-N Bond Formation via Ligand-Free Pd-Catalyzed Oxidative Coupling Reaction of *N*-Tosylhydrazones and Indole Derivatives” *J. Org. Chem.* **2013**, *78*, 8485–8495. (f) Zeng, X.; Cheng, G.; Shen, J.; Cui, X. “Palladium-Catalyzed Oxidative Cross-Coupling of *N*-Tosylhydrazones with Indoles: Synthesis of *N*-Vinylindoles” *Org. Lett.* **2013**, *15*, 3022–3025. (g) Roche, M.; Bignon, J.; Brion, J.-D.; Hamze, A.; Alami, M. “Tandem One-Pot Palladium-Catalyzed Coupling of Hydrazones, Haloindoles, and Amines: Synthesis of Amino-*N*-vinylindoles and Their Effect on Human Colon Carcinoma Cells” *J. Org. Chem.* **2014**, *79*, 7583–7592. (h) Xia, Y.; Xia, Y.; Lin, Z.; Zhang, Y.; Wang, J. “Palladium-Catalyzed Cross-Coupling Reaction of Diazo Compounds and Vinyl Boronic Acids: An Approach to 1,3-Diene Compounds” *J. Org. Chem.* **2014**, *79*, 7711–7717.

¹⁸⁰ Zhang, Z.; Liu, Y.; Ling, L.; Li, Y.; Dong, Y.; Gong, M.; Zhao, X.; Zhang, Y.; Wang, J. “Pd-Catalyzed Carbonylation of Diazo Compounds at Atmospheric Pressure: A Catalytic Approach to Ketenes” *J. Am. Chem. Soc.* **2011**, *133*, 4330–4341.

¹⁸¹ Zhou, F.; Ding, K.; Cai, Q. “Palladium-Catalyzed Amidation of *N*-Tosylhydrazones with Isocyanides” *Chem. Eur. J.* **2011**, *17*, 12268–12271.

¹⁸² Zhang, Z.; Liu, Y.; Gong, M.; Zhao, X.; Zhang, Y.; Wang, J. “Palladium-Catalyzed Carbonylation/Acyl Migratory Insertion Sequence” *Angew. Chem., Int. Ed.* **2010**, *49*, 1139–1142.

¹⁸³ Xie, X.-L.; Zhu, S.-F.; Guo, J.-X.; Cai, Y.; Zhou, Q.-L. “Enantioselective Palladium-Catalyzed Insertion of α -Aryl- α -diazoacetates into the O–H Bonds of Phenols” *Angew. Chem., Int. Ed.* **2014**, *53*, 2978–2981.

¹⁸⁴ (a) Devine, S. K. J.; Van Vranken, D. L. “Palladium-Catalyzed Carbene Insertion into Vinyl Halides and Trapping with Amines” *Org. Lett.* **2007**, *9*, 2047–2049. (b) Khanna, A., Maung, C., Johnson, K. R., Luong, T. T., Van Vranken, D. L. “Carbenylative Amination with *N*-Tosylhydrazones” *Org. Lett.* **2012**, *14*, 3233–3235. (c) Zhou, P.-X.; Ye, Y.-Y.; Zhao, H.; Hou, J.-Y.; Kang, X.; Chen, D.-Q.; Tang, Q.; Zhang, J.-Y.; Huang, Q.-X.; Zheng, L.; Ma, J.-W.; Xu, P.-F.; Liang, Y.-M. “Using *N*-Tosylhydrazone as a Double Nucleophile in the Palladium-Catalyzed Cross-Coupling Reaction To Synthesize Allylic Sulfones” *Chem. Eur. J.* **2014**, *20*, 16093–16096.

¹⁸⁵ Khanna, A.; Premachandra, I. D. U. A.; Sung, P. D.; Van Vranken, D. L. “Pd-Catalyzed Biscyclization/Dimerization Reactions of ω -Aminovinyl Halides” *Org. Lett.* **2013**, *15*, 3694–3697.

¹⁸⁶ Srivastava, P. C.; Callahan, A. P.; Cunningham, E. B.; Knapp, F. F., Jr. “Potential Cerebral Perfusion Agents: Synthesis and Evaluation of A Radioiodinated Vinylalkylbarbituric Acid Analog” *J. Med. Chem.* **1983**, *26*, 742–746.

¹⁸⁷ (a) Keinan, E.; Sahai, M. “Regioselectivity in Organo-Transition-Metal Chemistry. A Remarkable Steric Effect in π -Allyl Palladium Chemistry” *J. Chem. Soc., Chem. Commun.* **1984**, 648–650. (b) Trost, B. M.; Schmuff, N. R. “On The Mechanism of Allylic Alkylations Catalyzed by Palladium” *Tetrahedron Lett.* **1981**, *22*, 2999–3000.

¹⁸⁸ Watson, I. D. G.; Yudin, A. K. “New Insights into the Mechanism of Palladium-Catalyzed Allylic Amination” *J. Am. Chem. Soc.* **2005**, *127*, 17516–17529.

¹⁸⁹ (a) Nun, P.; Martin, P.; Martinez, J.; Lamaty, F. “Solvent-Free Synthesis of Hydrazones and Their Subsequent *N*-Alkylation in a Ball-Mill” *Tetrahedron* **2011**, *67*, 8187–8194. (b) Kong, Y.;

Zhang, W.; Tang, M.; Wang, H. “N-Alkylation of Tosylhydrazones in the Presence of Triphenylphosphine” *Tetrahedron* **2013**, *69*, 7487–7491.

¹⁹⁰ (a) Nemoto, H.; Ishibashi, H.; Nagamochi, M.; Fukumoto, K. “A Concise and Enantioselective Approach to Cyclobutanones by Tandem Asymmetric Epoxidation and Enantiospecific Ring Expansion of Cyclopropylidene Alcohols. An Enantiocontrolled Synthesis of (+)- And (-)-.Alpha.-Cuparenones” *J. Org. Chem.* **1992**, *57*, 1707–1712. (b) Liang, T.; Zhang, Z.; Antilla, J. C. “Chiral Brønsted Acid Catalyzed Pinacol Rearrangement” *Angew. Chem., Int. Ed.* **2010**, *49*, 9734–9736. (c) Zhang, Q.-W.; Fan, C.-A.; Zhang, H.-J.; Tu, Y.-Q.; Zhao, Y.-M.; Gu, P.; Chen, Z.-M. “Brønsted Acid Catalyzed Enantioselective Semipinacol Rearrangement for the Synthesis of Chiral Spiroethers” *Angew. Chem., Int. Ed.* **2009**, *48*, 8572–8574.

¹⁹¹ Menzel, K.; Fu, G. C. “Room-Temperature Stille Cross-Couplings of Alkenyltin Reagents and Functionalized Alkyl Bromides that Possess β Hydrogens” *J. Am. Chem. Soc.* **2003**, *125*, 3718–3719.

¹⁹² (a) Sauerwein, M.; Ishimaru, K.; Shimomura, K. “A Piperidone Alkaloid from *Hyoscyamus Albus* Roots Transformed with *Agrobacterium rhizogenes*” *Phytochem.* **1991**, *30*, 2977–2978. (b) Sauerwein, M.; Shimomura, K.; Wink, M. “Alkaloid Formation in Hairy Roots of *Hyoscyamus albus*” *BIOforum.* **1994**, *17*, 462–463.

¹⁹³ (a) Monteiro, N.; Goré, J.; Van Hemelryck, B.; Balme, G. “Palladium Carbenoids from Enolates of α -Sulfonyl ε -Acetylenic Esters, Nitriles or Ketones: Evidence for the Existence of these Intermediates” *Synlett* **1994**, 447–449. (b) Monteiro, N.; Balme, G. “Palladium-Catalyzed Reaction of Propargyl Nucleophiles with α -Sulfonyl α,β -Unsaturated Ketones: A Single-Step Synthesis of Furo[3,4-*c*] Heterocyclic Derivatives” *J. Org. Chem.* **2000**, *65*, 3223–3226.

¹⁹⁴ Hoye, T. R.; Dinsmore, C. J.; Johnson, D. S.; Korkowski, P. F. *J.* “Alkyne Insertion Reactions of Metal-Carbenes Derived from Enynyl- α -Diazoketones [R'CN₂COCR₂CH₂C.tplbond.C(CH₂)_n-2CH:CH₂]” *Org. Chem.* **1990**, *55*, 4518–4520.

¹⁹⁵ Tsuji and co-workers have speculated that Michael-type addition of an enolate to an allenylpalladium species might produce a palladium carbene. Tsuji, J.; Watanabe, H.; Minami, I.; Shimizu, I. “Novel Palladium-Catalyzed Reactions of Propargyl Carbonates with Carbonucleophiles under Neutral Conditions” *J. Am. Chem. Soc.* **1985**, *107*, 2196–2198.

¹⁹⁶ Minatti, A.; Muñiz, K. “Intramolecular Aminopalladation of Alkenes as a Key Step to Pyrrolidines and Related Heterocycles” *Chem. Soc. Rev.* **2007**, *36*, 1142–1152.

¹⁹⁷ Fournet, G.; Balme, G.; Gore, J. “Formation de Cyclopentanes lors de Réactions de Heck” *Tetrahedron* **1990**, *46*, 7763–7774.

¹⁹⁸ Beaudoin, M.; Wolfe, J. P. “Stereoselective Synthesis of N-Protected Pyrrolidines via Pd-Catalyzed Reactions of γ -(N-acylamino) Alkenes and γ -(N-Boc-Amino) Alkenes with Aryl Bromides” *Tetrahedron* **2005**, *61*, 6447–6459.

¹⁹⁹ Åkermark, B.; Bäckvall, J. E. Siirala-Hansén, K.; Sjöberg, K.; Zetterberg, K. “The Steric Course of the Palladium Promoted Amination of Simple Olefins” *Tetrahedron Lett.* **1974**, *15*, 1363–1366.

²⁰⁰ Kondo, Y.; Suzuki, N.; Takahashi, M.; Kumamoto, T.; Masu, H.; Ishikawa, T. “Enantioselective Construction of a Polyhydroxylated Pyrrolidine Skeleton from 3-Vinylaziridine-2-carboxylates: Synthesis of (+)-DMDP and a Potential Common Intermediate for (+)-Hyacinthacine A₁ and (+)-1-*epi*-Australine” *J. Org. Chem.* **2012**, *77*, 7988–7999.

- ²⁰¹ Khanna, A.; Premachandra, I. D. U. A.; Sung, P. D.; Van Vranken, D. L. "Palladium-Catalyzed Catellani Aminocyclopropanation Reactions with Vinyl Halides" *Org. Lett.* **2013**, *15*, 3158–3161.
- ²⁰² Catellani, M.; Chiusoli, G. P. "Oxidative Addition, Insertion, Cyclization and Amination in a Palladium-Catalyzed Sequence" *J. Organomet. Chem.* **1984**, *275*, 257–262.
- ²⁰³ (a) Catellani, M.; Chiusoli, G. P.; Giroladini, W.; Salerno, G. "New Transition Metal-Catalyzed C–C Coupling Reactions Initiated By C–X Bond Cleavage And Terminated By H-Transfer" *J. Organomet. Chem.* **1980**, *199*, C21–C23. (b) Arcadi, A.; Marinelli, F.; Bernocchi, E.; Cacchi, S.; Ortar, G. "Palladium-Catalyzed Preparation of Exo-Aryl Derivatives of the Norbornane Skeleton" *J. Organomet. Chem.* **1989**, *368*, 249–256.
- ²⁰⁴ (a) Schweizer, S.; Song, Z.-Z.; Meyer, F. E.; Parsons, P. J.; de Meijere, A. "Two New Modes of Pd-Catalyzed Domino-Tetracyclization of Bromodienynes—5-exo-trig Cyclization Wins over β -Hydride Elimination" *Angew. Chem. Int. Ed.* **1999**, *38*, 1452–1454. (b) Fillion, E.; Taylor, N. J. "Cine-Substitution in the Stille Coupling: Evidence for the Carbenoid Reactivity of sp^3 -gem-Organodimetallic Iodopalladio-trialkylstannylalkane Intermediates" *J. Am. Chem. Soc.* **2003**, *125*, 12700–12701. (c) Busacca, C. A.; Swestock, J.; Johnson, R. E.; Bailey, T. R.; Musza, L.; Rodger, C. A. "The Anomalous Stille Reactions of Methyl α -(Tributylstannyl)acrylate: Evidence for a Palladium Carbene Intermediate" *J. Org. Chem.* **1994**, *59*, 7553–7556. (d) Hashmi, A. S. K.; Ruppert, T. L.; Knöfel, T.; Bats, J. W. "C–C-Bond Formation by the Palladium-Catalyzed Cycloisomerization/Dimerization of Terminal Allenyl Ketones: Selectivity and Mechanistic Aspects" *J. Org. Chem.* **1997**, *62*, 7295–7304. (e) Farina, V.; Hossain, M. A. "On The Mechanism of Cine Substitution in the Stille Reaction: New Evidence for the Intermediacy of Pd(0) Carbenes" *Tetrahedron Lett.* **1996**, *37*, 6997–7000. (f) Hashmi, A. S. K.; Choi, J.-H.; Bats, J. W. "Synthesis of Allenyl Ketones and Their Palladium-Catalyzed Cycloisomerization/Dimerization: Approaching the Limits" *J. Prakt. Chem.* **1999**, *341*, 342–357.
- ²⁰⁵ Kagan, F.; Cope, A. C. *J. Am. Chem. Soc.* **1958**, *80*, 5499 – 5502.
- ²⁰⁶ (a) Catellani, M.; Motti, N.; Della Ca', N. *Acc. Chem. Res.* **2008**, *41*, 1512 – 1522. (b) Martins, A.; Mariampillai, B.; Lautens, M. *Top. Curr. Chem.* **2010**, *292*, 1 – 33. (c) Faccini, F.; Motti, E.; Catellani, M. *J. Am. Chem. Soc.* **2004**, *126*, 78 – 79. (d) Jiao, L.; Herdtweck, E.; Bach, T. *J. Am. Chem. Soc.* **2012**, *134*, 14563 – 14572. (e) Sehnal, P.; Taylor, R. J. K.; Fairlamb, I. J. S. *Chem. Rev.* **2010**, *110*, 824 – 889. (f) Elena Motti, E.; Della Ca', N.; Xu, D.; Armani, S.; Aresta, B. M.; Catellani, M. *Tetrahedron* **2013**, *69*, 4421 – 4428.
- ²⁰⁷ Hayashi, T.; Ueyama, K.; Tokunaga, N.; Yoshida, K. *J. Am. Chem. Soc.* **2003**, *125*, 11508 – 11509.
- ²⁰⁸ (a) Anciaux, A. J.; Hubert, A. J.; Noels, A. F.; Petiniot, N.; Teyssié, P. *J. Org. Chem.* **1980**, *45*, 695 – 702. (b) Tomilov, Y. V.; Bordakov, V. G.; Dolgii, I. E.; Nefedov, O. *Bull. Acad. Sci. USSR Div. Chem. Sci.* **1984**, *33*, 533 – 538. (c) Straub, B. F. *J. Am. Chem. Soc.* **2002**, *124*, 14195 – 14201.
- ²⁰⁹ (a) Trost, B. M.; Schneider, S. *J. Am. Chem. Soc.* **1989**, *111*, 4430 – 4433. (b) Trost, B. M.; Urabe, H. *Tetrahedron Lett.* **1990**, *31*, 615 – 618. (c) Ohe, K.; Matsuda, H.; Ishihara, T.; Ogoshi, S.; Chatani, N.; Murai, S. *J. Org. Chem.* **1993**, *58*, 1173 – 1177. (d) Ogoshi, S.; Morimoto, T.; Nishio, K.; Ohe, K.; Murai, S. *J. Org. Chem.* **1993**, *58*, 9 – 10. (e) Fillion, E.; Taylor, N. J. *J. Am. Chem. Soc.* **2003**, *125*, 12700 – 12701. (f) Trépanier, V. É.; Fillion, E. *Organometallics* **2007**, *26*, 30 – 32. (g) Horino, Y.; Homura, N.; Inoue, K.; Yoshikawa, S. *Adv. Synth. Catal.* **2012**, *354*, 828 – 834.

- ²¹⁰ Catellani, M.; Chiusoli, G. P. *J. Organomet. Chem.* **1982**, *233*, C21 – C24.
- ²¹¹ Catellani, M.; Chiusoli, G. P. *J. Organomet. Chem.* **1984**, *275*, 257 – 262.
- ²¹² (a) Catellani, M.; Chiusoli, G. P.; Giroladini, W.; Salerno, G. *J. Organomet. Chem.* **1980**, *199*, C21 – C23. (b) Arcadi, A.; Marinelli, F.; Bernocchi, E.; Cacchi, S.; Ortar, G. *J. Organomet. Chem.* **1989**, *368*, 249 – 256.
- ²¹³ Torii, S.; Okumoto, H.; Ozaki, H.; Nakayasu, S.; Tadokoro, T.; Kotani, T. *Tetrahedron Lett.* **1992**, *33*, 3499 – 3502. The cyclopropanation reaction was mentioned in Footnote 8 without a full description of the reaction conditions. (b) Torii, S.; Okumoto, H.; Ozaki, H.; Nakayasu, S.; Kotani, T. *Tetrahedron Lett.* **1990**, *31*, 5319-5322.
- ²¹⁴ The substrate is known to undergo cyclopropanation reactions with high *exo* selectivity: Tenaglia, A.; Marc, S. *J. Org. Chem.* **2006**, *71*, 3569 – 3575.
- ²¹⁵ Dyker, G. *J. Org. Chem.* **1993**, *58*, 234 – 238.
- ²¹⁶ Hartwig, J. F.; Richards, S.; Barañano, D.; Paul, F. *J. Am. Chem. Soc.* **1996**, *118*, 3626 – 3633.
- ²¹⁷ Straub, B. F. *J. Am. Chem. Soc.* **2002**, *124*, 14195 – 14201.
- ²¹⁸ (a) Åkermark, B.; Bäckvall, J. E.; Siirala-Hansén, K.; Sjöberg, K.; Zetterberg, K. *Tetrahedron Lett.* **1974**, *15*, 1363 – 1366. (b) Arnek, R.; Zetterberg, K. *Organometallics* **1987**, *6*, 1230 – 1235.
- ²¹⁹ (a) Ney, J. E.; Wolfe, J. P. *J. Am. Chem. Soc.* **2005**, *127*, 8644 – 8651. (c) Liu, G.; Stahl, S. S. *J. Am. Chem. Soc.* **2007**, *129*, 6328 – 6335. (c) Minatti, A.; Muniz, K. *Chem. Soc. Rev.* **2007**, *36*, 1142 – 1152.
- ²²⁰ (a) Dénès, F.; Pérez-Luna, A.; Chemla, F. *Chem. Rev.* **2010**, *110*, 2366 – 2447. (b) Holton, R. A.; Zoeller, J. R. *J. Am. Chem. Soc.* **1985**, *107*, 2124 – 2131.
- ²²¹ Han, J.; Xu, B.; Hammond, G. B. *J. Am. Chem. Soc.* **2010**, *132*, 916 – 917.
- ²²² Reich, H. J.; Eisenhart, E. K.; Olson, R. E. *J. Am. Chem. Soc.* **1986**, *108*, 7791 – 7800.
- ²²³ Khanna, A.; Maung, C.; Johnson, K. R.; Luong, T. T.; Van Vranken, D. L. *Org. Lett.* **2012**, *14*, 3233 – 3235.

Appendix A: Chapter 2 – HPLC Traces

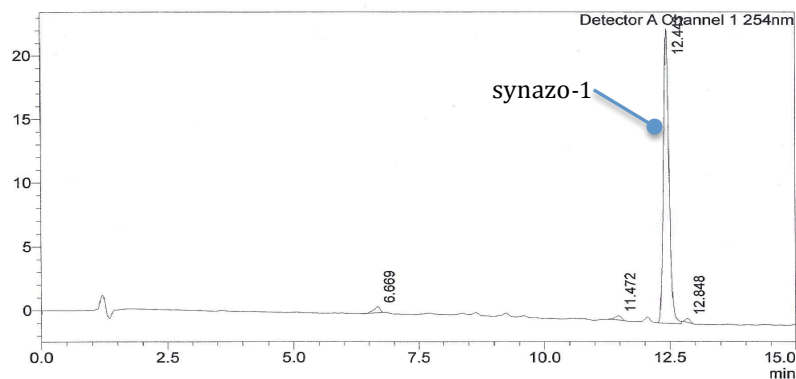
Test of Chemical Stability

HPLC:

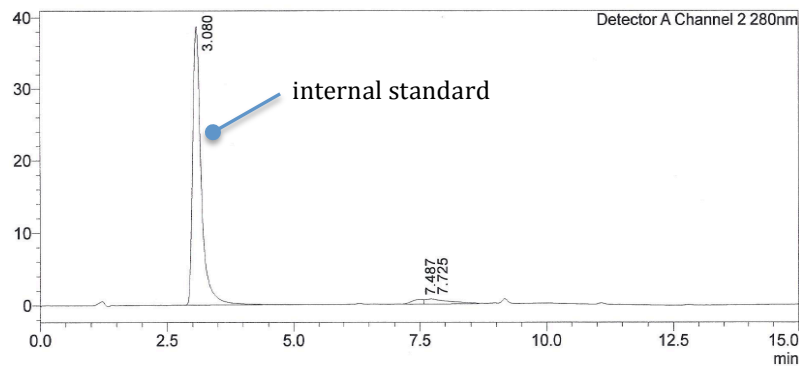
Stationary phase: reverse phase C18

Mobile phase: A: 0.1% aq. trifluoroacetic acid; B: acetonitrile

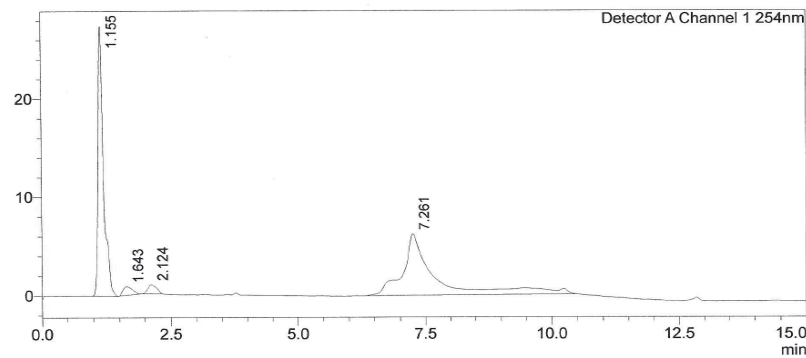
Synazo-1 (30 μ M)



Internal Standard: 1-naphthylmethylamine (30 μ M)

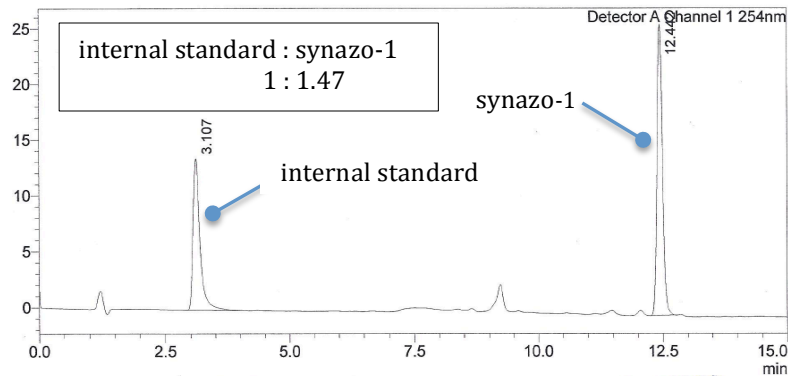


Test Medium: 10:90 FBS/10 mM phosphate, 100 mM NaCl, pH 7.2

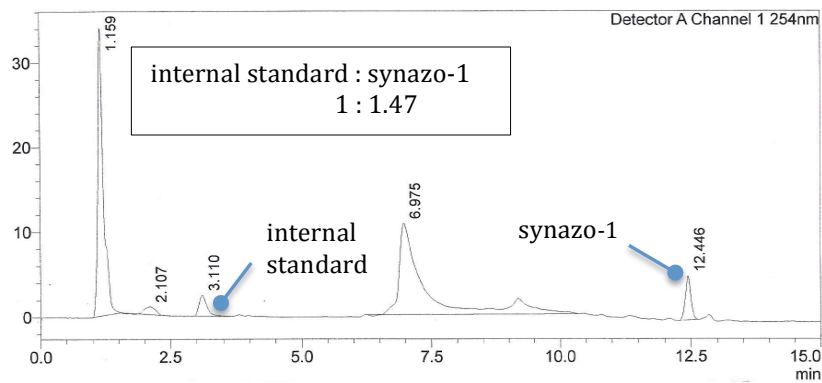


(The compounds in this chromatogram are present in the FBS.)

Synazo-1 (30 μ M) + Internal Standard (30 μ M):



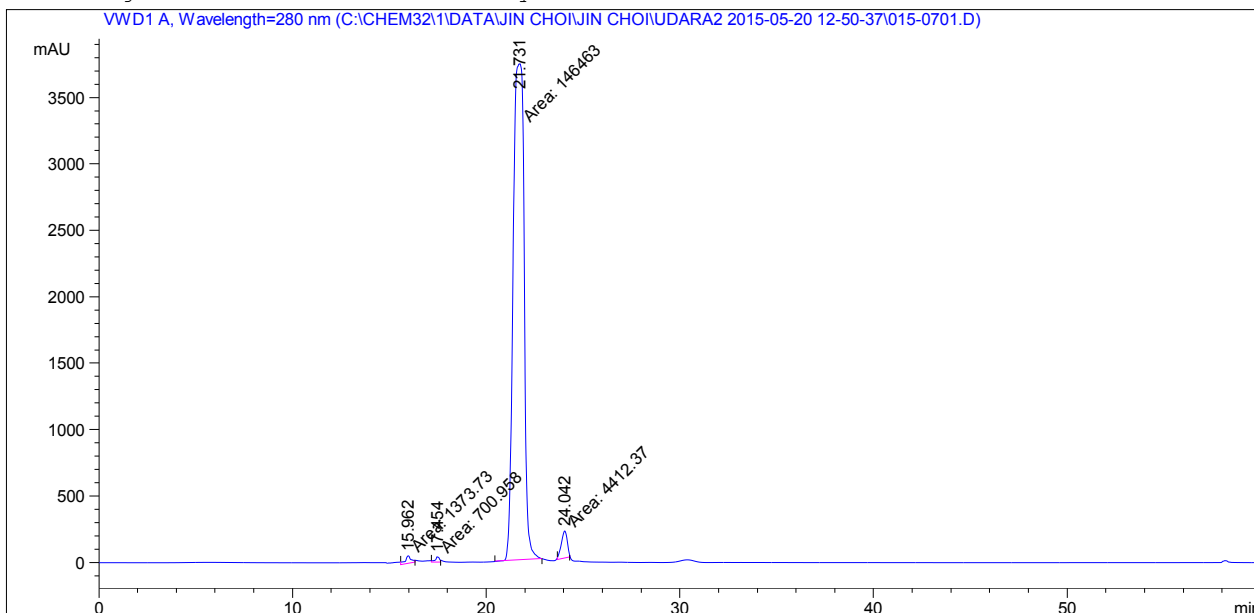
Synazo-1 (30 μ M) + Internal Standard (30 μ M) in 10:90 FBS/10 mM phosphate, 100 mM NaCl, pH 7.2 at 16 h:



```

=====
Acq. Operator   : UDARA                               Seq. Line :    7
Acq. Instrument : Instrument 1                         Location  : Vial 15
Injection Date  : 5/20/2015 7:04:56 PM                Inj       :    1
                                                    Inj Volume: 20 µl

Acq. Method     : C:\Chem32\1\DATA\Jin Choi\JIN CHOI\UDARA2 2015-05-20 12-50-37\UDARA.M
Last changed    : 5/19/2015 6:12:26 PM by UDARA
Analysis Method : C:\CHEM32\1\DATA\JIN CHOI\JIN CHOI\UDARA2 2015-05-20 12-50-37\015-0701.D\DA.M
                (UDARA.M)
Last changed    : 5/21/2015 7:00:40 PM by UDARA
  
```



=====
 Area Percent Report
 =====

```

Sorted By      :      Signal
Multiplier     :      1.0000
Dilution      :      1.0000
Use Multiplier & Dilution Factor with ISTDs
  
```

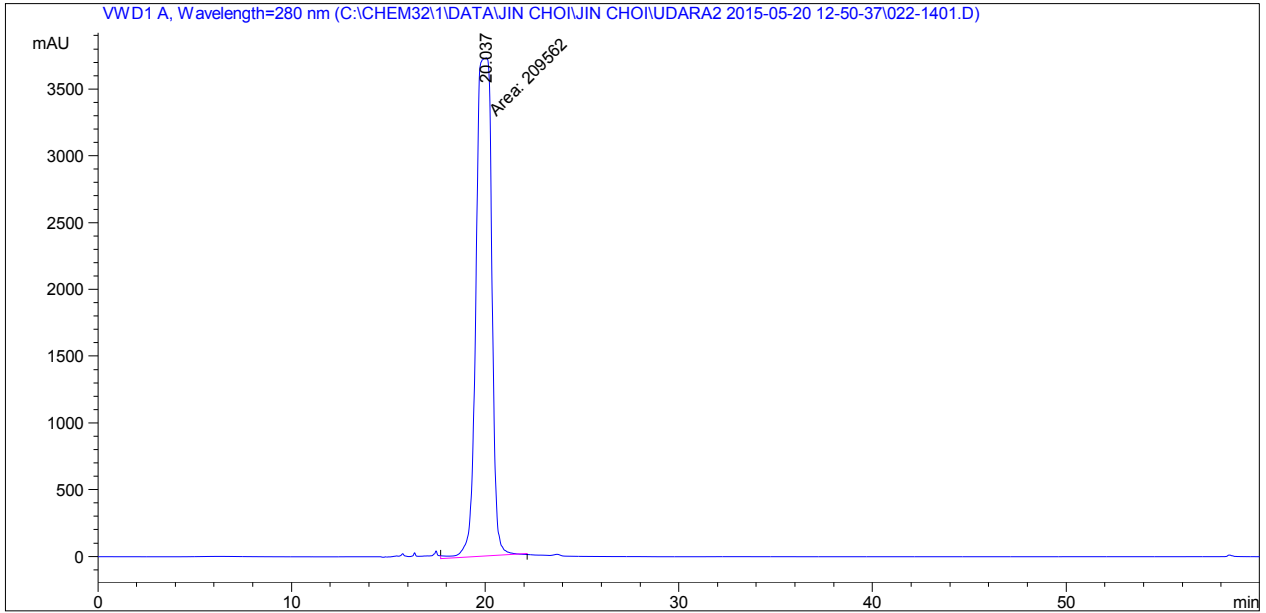
Signal 1: VWD1 A, Wavelength=280 nm

Peak #	RetTime [min]	Type	Width [min]	Area mAU *s	Height [mAU]	Area %
1	15.962	MM	0.3841	1373.73389	59.60886	0.8982
2	17.454	MM	0.2723	700.95770	42.89745	0.4583
3	21.731	MM	0.6536	1.46463e5	3735.03833	95.7587
4	24.042	MM	0.3563	4412.36914	206.39709	2.8849

```

=====
Acq. Operator   : UDARA                               Seq. Line :   14
Acq. Instrument : Instrument 1                       Location  : Vial 22
Injection Date  : 5/21/2015 2:19:28 AM              Inj       :    1
                                                    Inj Volume: 20 µl

Acq. Method    : C:\Chem32\1\DATA\Jin Choi\JIN CHOI\UDARA2 2015-05-20 12-50-37\UDARA.M
Last changed   : 5/19/2015 6:12:26 PM by UDARA
Analysis Method: C:\CHEM32\1\DATA\JIN CHOI\JIN CHOI\UDARA2 2015-05-20 12-50-37\022-1401.D\DA.M
              (UDARA.M)
Last changed   : 5/21/2015 9:41:38 AM by UDARA
  
```



=====
 Area Percent Report
 =====

```

Sorted By      :      Signal
Multiplier     :      1.0000
Dilution      :      1.0000
Use Multiplier & Dilution Factor with ISTDs
  
```

Signal 1: VWD1 A, Wavelength=280 nm

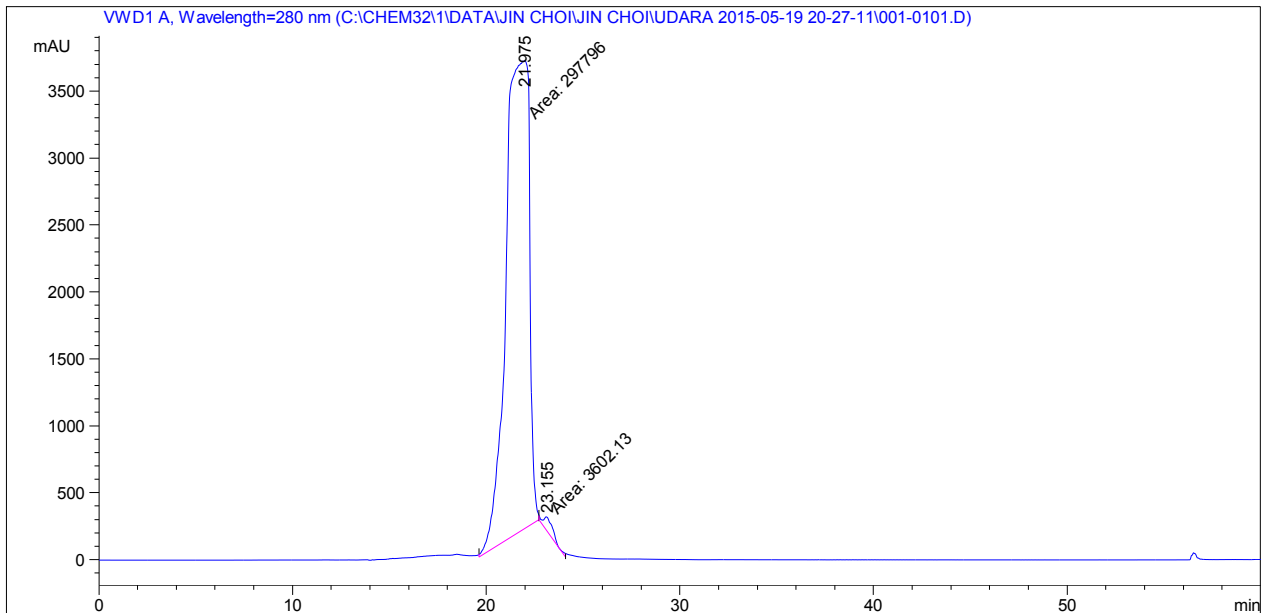
Peak #	RetTime [min]	Type	Width [min]	Area mAU *s	Height [mAU]	Area %
1	20.037	MM	0.9354	2.09562e5	3733.92871	100.0000

Totals : 2.09562e5 3733.92871


```

=====
Acq. Operator   : UDARA                               Seq. Line :    1
Acq. Instrument : Instrument 1                         Location  : Vial 1
Injection Date  : 5/19/2015 8:32:38 PM                Inj       :    1
                                                    Inj Volume: 20 µl

Acq. Method     : C:\Chem32\1\DATA\Jin Choi\JIN CHOI\UDARA 2015-05-19 20-27-11\UDARA.M
Last changed    : 5/19/2015 6:12:26 PM by UDARA
Analysis Method : C:\CHEM32\1\DATA\JIN CHOI\JIN CHOI\UDARA 2015-05-19 20-27-11\001-0101.D\DA.M (
                  UDARA.M)
Last changed    : 5/20/2015 10:07:18 AM by UDARA
                  (modified after loading)
  
```



=====
 Area Percent Report
 =====

```

Sorted By      :      Signal
Multiplier     :      1.0000
Dilution      :      1.0000
Use Multiplier & Dilution Factor with ISTDs
  
```

Signal 1: VWD1 A, Wavelength=280 nm

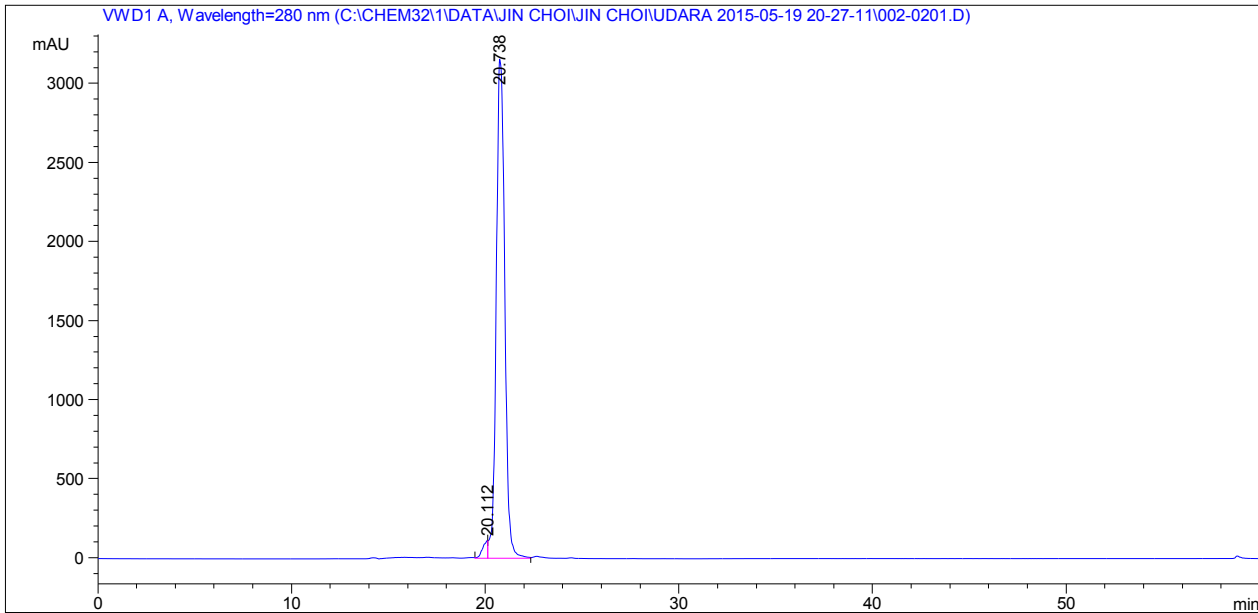
Peak #	RetTime [min]	Type	Width [min]	Area mAU*s	Height [mAU]	Area %
1	21.975	MM	1.4194	2.97796e5	3496.66187	98.8049
2	23.155	MM	0.5826	3602.12891	103.05294	1.1951

Totals : 3.01398e5 3599.71481

```

=====
Acq. Operator   : UDARA                      Seq. Line :    2
Acq. Instrument : Instrument 1                Location  : Vial 2
Injection Date  : 5/19/2015 9:34:36 PM      Inj       :    1
                                           Inj Volume: 20 µl

Acq. Method     : C:\Chem32\1\DATA\Jin Choi\JIN CHOI\UDARA 2015-05-19 20-27-11\UDARA.M
Last changed    : 5/19/2015 6:12:26 PM by UDARA
Analysis Method : C:\CHEM32\1\DATA\JIN CHOI\JIN CHOI\UDARA 2015-05-19 20-27-11\002-0201.D\DA.M (
                  UDARA.M)
Last changed    : 5/20/2015 10:11:16 AM by UDARA
                  (modified after loading)
  
```



=====
 Area Percent Report
 =====

```

Sorted By      :      Signal
Multiplier     :      1.0000
Dilution      :      1.0000
Use Multiplier & Dilution Factor with ISTDs
  
```

Signal 1: VWD1 A, Wavelength=280 nm

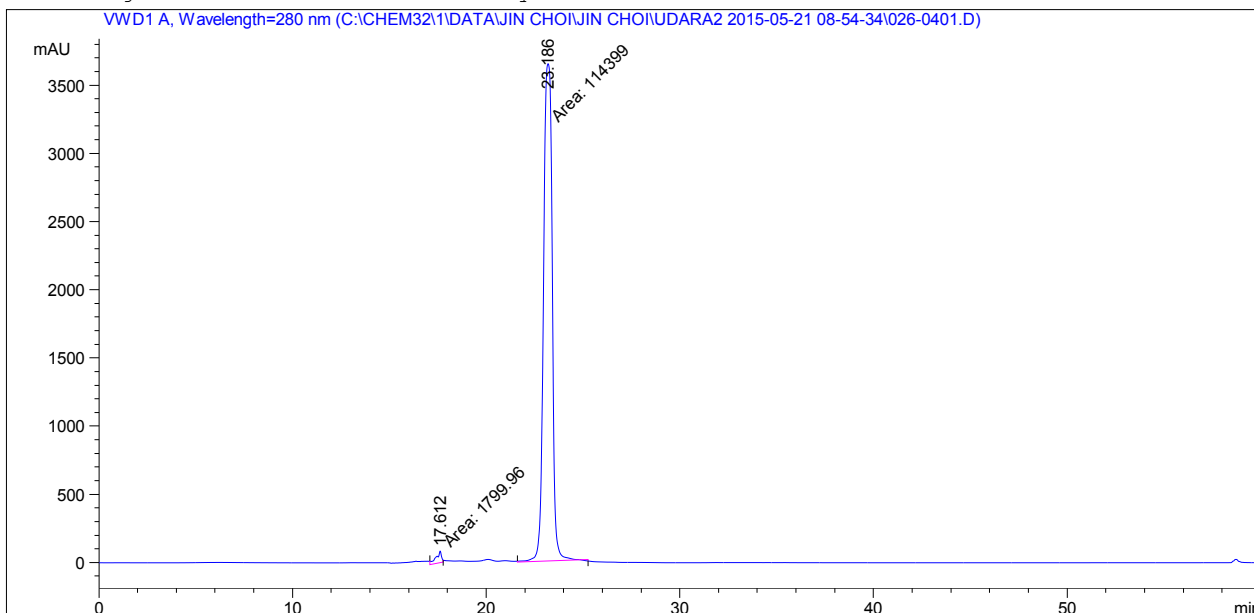
Peak #	RetTime [min]	Type	Width [min]	Area mAU*s	Height [mAU]	Area %
1	20.112	VV	0.2418	2156.25171	115.13561	2.1874
2	20.738	VV	0.4232	9.64191e4	3158.04980	97.8126

Totals : 9.85753e4 3273.18542

```

=====
Acq. Operator   : UDARA                               Seq. Line :    4
Acq. Instrument : Instrument 1                         Location  : Vial 26
Injection Date  : 5/21/2015 12:02:30 PM              Inj       :    1
                                                    Inj Volume: 20 µl

Acq. Method     : C:\Chem32\1\DATA\Jin Choi\JIN CHOI\UDARA2 2015-05-21 08-54-34\UDARA.M
Last changed    : 5/19/2015 6:12:26 PM by UDARA
Analysis Method : C:\CHEM32\1\DATA\JIN CHOI\JIN CHOI\UDARA2 2015-05-21 08-54-34\026-0401.D\DA.M
                (UDARA.M)
Last changed    : 5/21/2015 1:09:43 PM by UDARA
  
```



=====
 Area Percent Report
 =====

```

Sorted By      :      Signal
Multiplier     :      1.0000
Dilution       :      1.0000
Use Multiplier & Dilution Factor with ISTDs
  
```

Signal 1: VWD1 A, Wavelength=280 nm

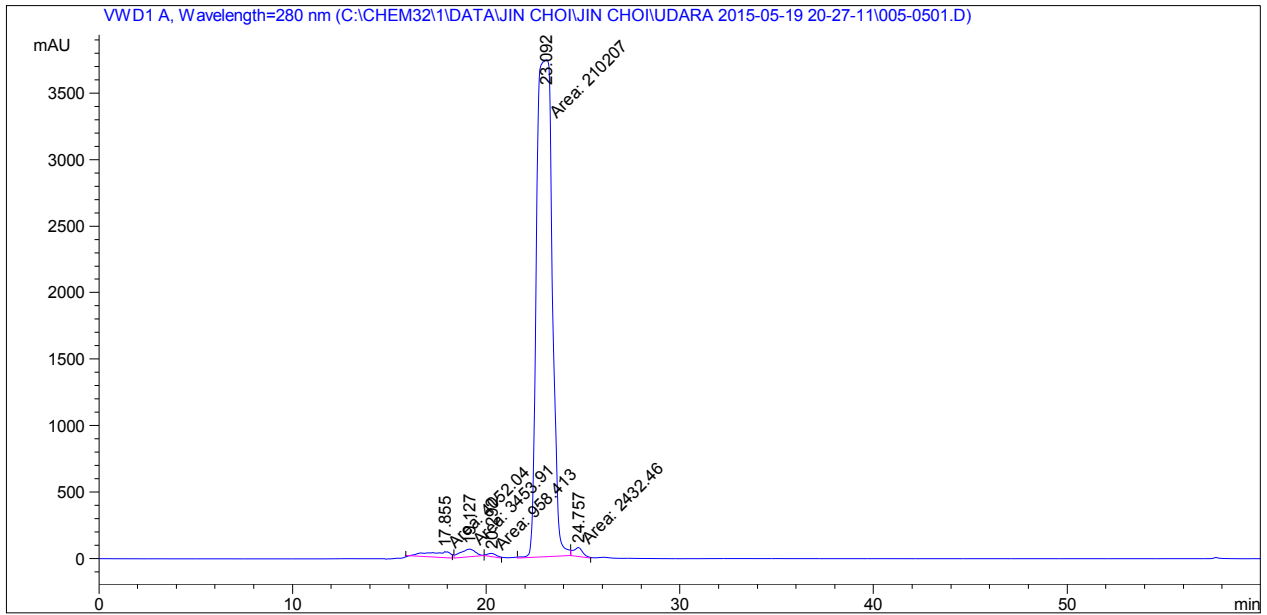
Peak #	RetTime [min]	Type	Width [min]	Area [mAU*s]	Height [mAU]	Area %
1	17.612	MM	0.3397	1799.95520	88.31090	1.5490
2	23.186	MM	0.5225	1.14399e5	3649.06860	98.4510

Totals : 1.16199e5 3737.37950

```

=====
Acq. Operator   : UDARA                               Seq. Line :    5
Acq. Instrument : Instrument 1                         Location  : Vial 5
Injection Date  : 5/20/2015 6:53:16 AM                Inj       :    1
                                                    Inj Volume: 20 µl

Acq. Method     : C:\Chem32\1\DATA\Jin Choi\JIN CHOI\UDARA 2015-05-19 20-27-11\UDARA.M
Last changed    : 5/19/2015 6:12:26 PM by UDARA
Analysis Method : C:\CHEM32\1\DATA\JIN CHOI\JIN CHOI\UDARA 2015-05-19 20-27-11\005-0501.D\DA.M (
                  UDARA.M)
Last changed    : 5/21/2015 7:35:13 PM by UDARA
  
```



Area Percent Report

```

Sorted By      :      Signal
Multiplier     :      1.0000
Dilution       :      1.0000
Use Multiplier & Dilution Factor with ISTDs
  
```

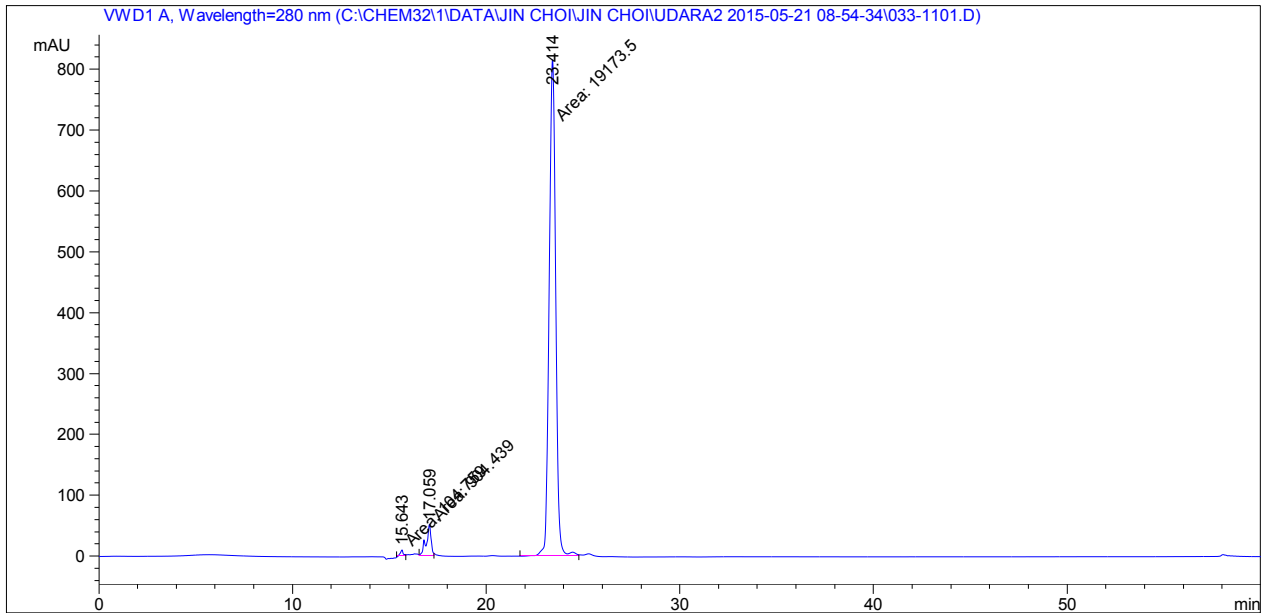
Signal 1: VWD1 A, Wavelength=280 nm

Peak #	RetTime [min]	Type	Width [min]	Area mAU *s	Height [mAU]	Area %
1	17.855	MM	1.3946	4052.03711	48.42530	1.8326
2	19.127	MM	0.9442	3453.91431	60.96648	1.5621
3	20.292	MM	0.5955	958.41284	26.82559	0.4335
4	23.092	MM	0.9361	2.10207e5	3742.41382	95.0716
5	24.757	MM	0.5780	2432.46143	70.13708	1.1001

```

=====
Acq. Operator   : UDARA                               Seq. Line :   11
Acq. Instrument : Instrument 1                         Location  : Vial 33
Injection Date  : 5/21/2015 7:17:01 PM              Inj       :    1
                                                    Inj Volume: 20 µl

Acq. Method     : C:\Chem32\1\DATA\Jin Choi\JIN CHOI\UDARA2 2015-05-21 08-54-34\UDARA.M
Last changed    : 5/19/2015 6:12:26 PM by UDARA
Analysis Method : C:\CHEM32\1\DATA\JIN CHOI\JIN CHOI\UDARA2 2015-05-21 08-54-34\033-1101.D\DA.M
                (UDARA.M)
Last changed    : 5/19/2015 6:12:26 PM by UDARA
  
```



=====
 Area Percent Report
 =====

```

Sorted By      :      Signal
Multiplier     :      1.0000
Dilution      :      1.0000
Use Multiplier & Dilution Factor with ISTDs
  
```

Signal 1: VWD1 A, Wavelength=280 nm

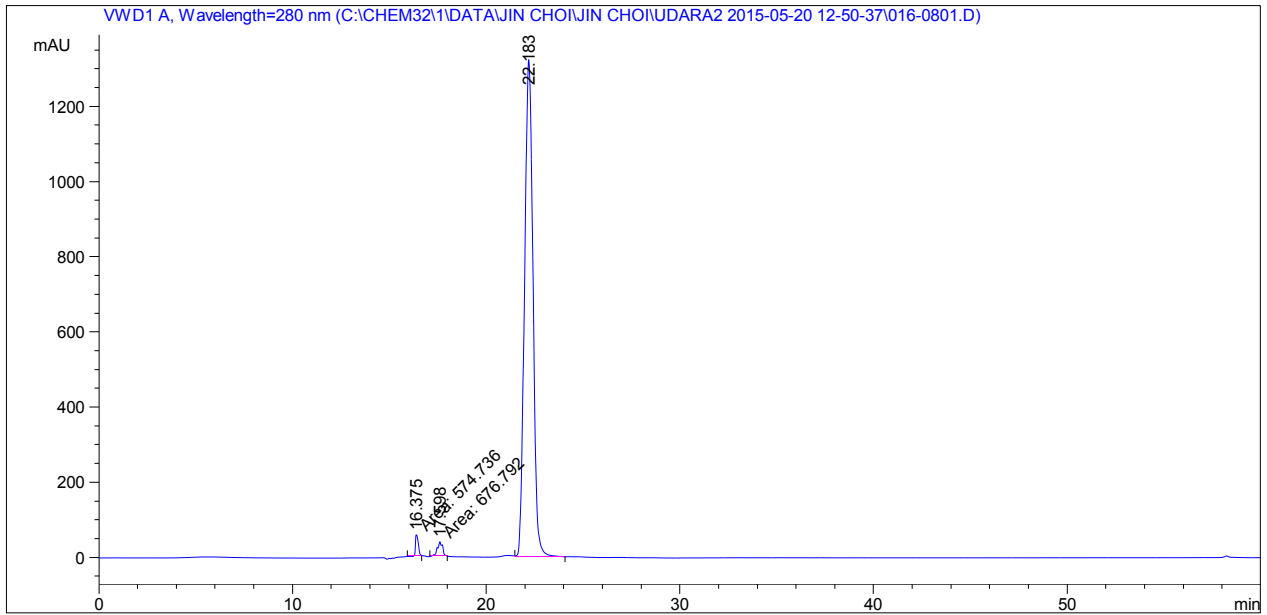
Peak #	RetTime [min]	Type	Width [min]	Area mAU *s	Height [mAU]	Area %
1	15.643	MM	0.1787	104.75854	9.77096	0.5191
2	17.059	MM	0.2919	904.43872	51.63951	4.4813
3	23.414	MM	0.3919	1.91735e4	815.45270	94.9997

Totals : 2.01827e4 876.86317

```

=====
Acq. Operator   : UDARA                               Seq. Line :    8
Acq. Instrument : Instrument 1                         Location  : Vial 16
Injection Date  : 5/20/2015 8:07:01 PM                Inj       :    1
                                                    Inj Volume: 20 µl

Acq. Method     : C:\Chem32\1\DATA\Jin Choi\JIN CHOI\UDARA2 2015-05-20 12-50-37\UDARA.M
Last changed    : 5/19/2015 6:12:26 PM by UDARA
Analysis Method : C:\CHEM32\1\DATA\JIN CHOI\JIN CHOI\UDARA2 2015-05-20 12-50-37\016-0801.D\DA.M
                (UDARA.M)
Last changed    : 5/21/2015 9:31:21 AM by UDARA
  
```



=====
 Area Percent Report
 =====

```

Sorted By      :      Signal
Multiplier     :      1.0000
Dilution      :      1.0000
Use Multiplier & Dilution Factor with ISTDs
  
```

Signal 1: VWD1 A, Wavelength=280 nm

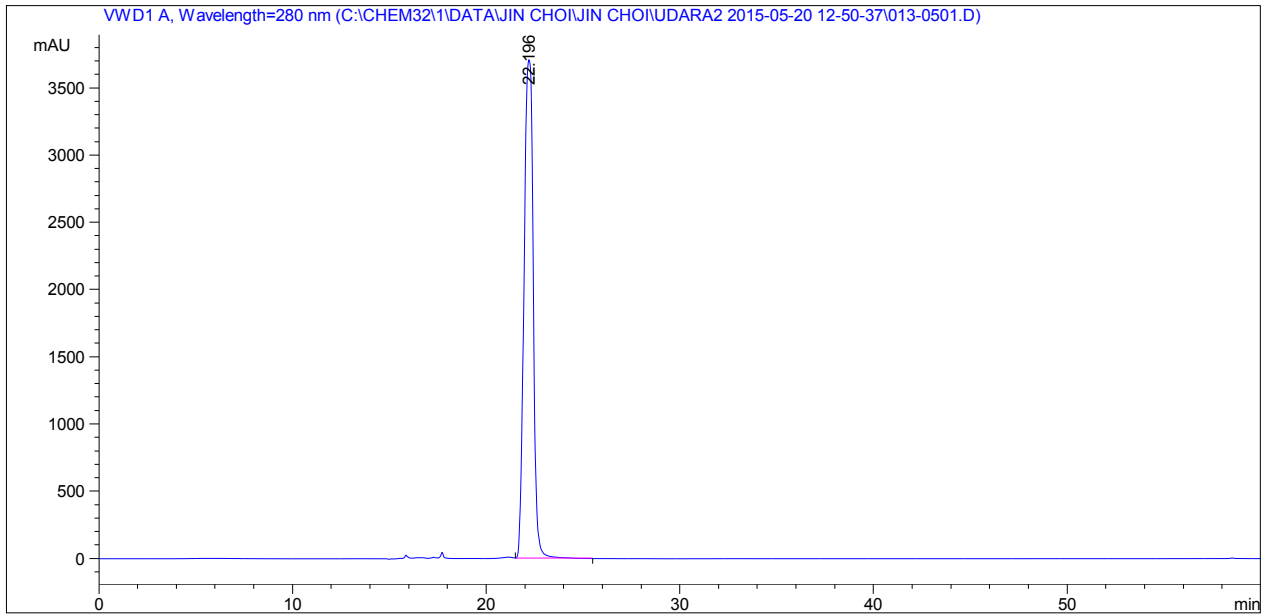
Peak #	RetTime [min]	Type	Width [min]	Area mAU *s	Height [mAU]	Area %
1	16.375	MM	0.1710	574.73639	56.00963	1.3931
2	17.598	MM	0.2990	676.79230	37.72561	1.6405
3	22.183	VB	0.4242	4.00043e4	1322.52563	96.9664

Totals : 4.12558e4 1416.26087

```

=====
Acq. Operator   : UDARA                               Seq. Line :    5
Acq. Instrument : Instrument 1                         Location  : Vial 13
Injection Date  : 5/20/2015 5:00:52 PM              Inj       :    1
                                                    Inj Volume: 20 µl

Acq. Method     : C:\Chem32\1\DATA\Jin Choi\JIN CHOI\UDARA2 2015-05-20 12-50-37\UDARA.M
Last changed    : 5/19/2015 6:12:26 PM by UDARA
Analysis Method : C:\CHEM32\1\DATA\JIN CHOI\JIN CHOI\UDARA2 2015-05-20 12-50-37\013-0501.D\DA.M
                (UDARA.M)
Last changed    : 5/21/2015 9:26:49 AM by UDARA
  
```



=====
 Area Percent Report
 =====

```

Sorted By      :      Signal
Multiplier     :      1.0000
Dilution       :      1.0000
Use Multiplier & Dilution Factor with ISTDs
  
```

Signal 1: VWD1 A, Wavelength=280 nm

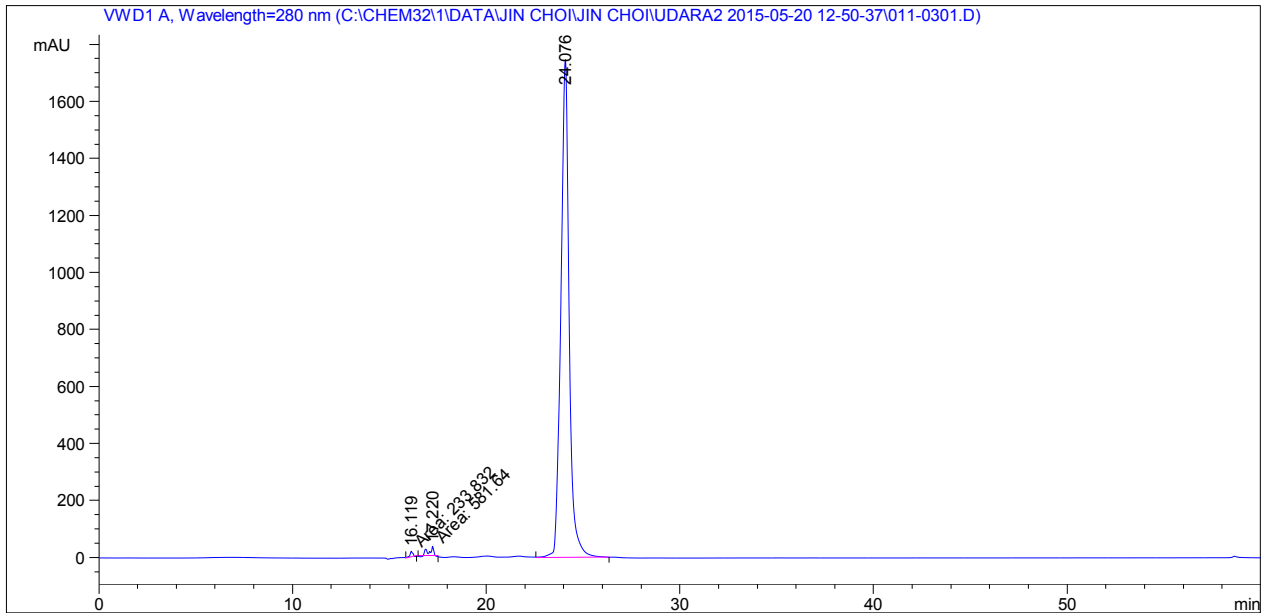
Peak #	RetTime [min]	Type	Width [min]	Area mAU *s	Height [mAU]	Area %
1	22.196	VB	0.5143	1.22338e5	3709.80981	100.0000

Totals : 1.22338e5 3709.80981

```

=====
Acq. Operator   : UDARA                               Seq. Line :    3
Acq. Instrument : Instrument 1                         Location  : Vial 11
Injection Date  : 5/20/2015 2:56:33 PM                Inj       :    1
                                                    Inj Volume: 20 µl

Acq. Method     : C:\Chem32\1\DATA\Jin Choi\JIN CHOI\UDARA2 2015-05-20 12-50-37\UDARA.M
Last changed    : 5/19/2015 6:12:26 PM by UDARA
Analysis Method : C:\CHEM32\1\DATA\JIN CHOI\JIN CHOI\UDARA2 2015-05-20 12-50-37\011-0301.D\DA.M
                (UDARA.M)
Last changed    : 5/21/2015 9:24:50 AM by UDARA
  
```



=====
 Area Percent Report
 =====

```

Sorted By      :      Signal
Multiplier     :      1.0000
Dilution      :      1.0000
Use Multiplier & Dilution Factor with ISTDs
  
```

Signal 1: VWD1 A, Wavelength=280 nm

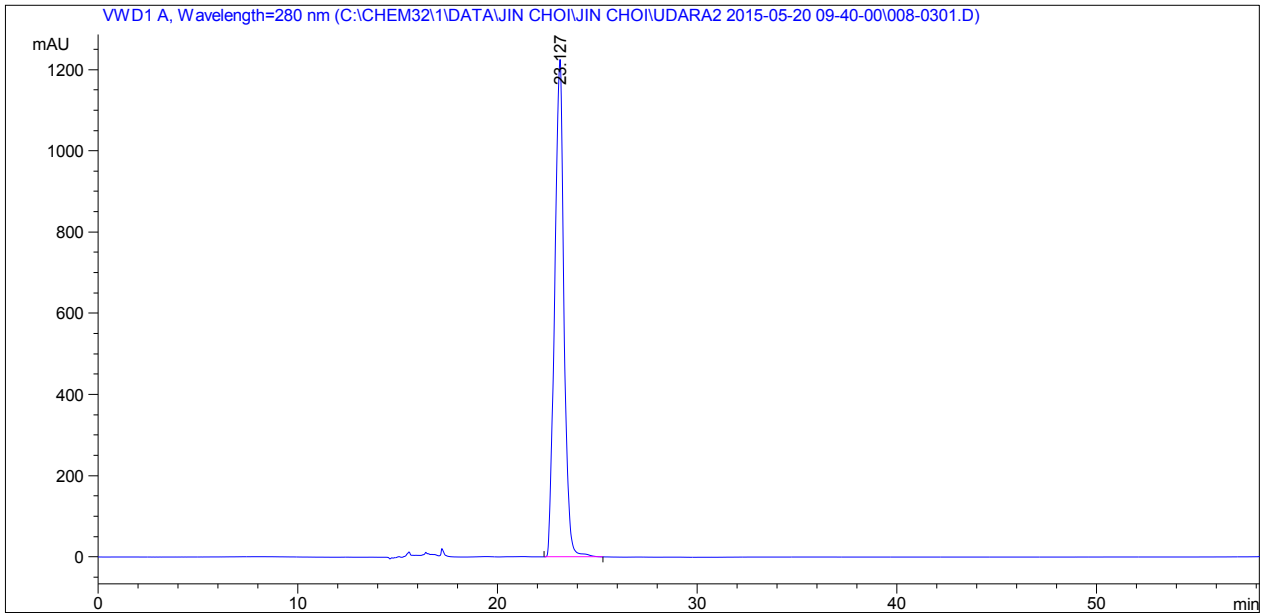
Peak #	RetTime [min]	Type	Width [min]	Area mAU *s	Height [mAU]	Area %
1	16.119	MM	0.1864	233.83177	20.90388	0.4420
2	17.220	MM	0.2918	581.64020	33.21647	1.0995
3	24.076	VB	0.4178	5.20829e4	1746.68005	98.4584

Totals : 5.28984e4 1800.80040


```

=====
Acq. Operator   : UDARA                               Seq. Line :    3
Acq. Instrument : Instrument 1                         Location  : Vial 8
Injection Date  : 5/20/2015 11:45:57 AM              Inj       :    1
                                                    Inj Volume: 20 µl

Acq. Method     : C:\Chem32\1\DATA\Jin Choi\JIN CHOI\UDARA2 2015-05-20 09-40-00\UDARA.M
Last changed    : 5/19/2015 6:12:26 PM by UDARA
Analysis Method : C:\CHEM32\1\DATA\JIN CHOI\JIN CHOI\UDARA2 2015-05-20 09-40-00\008-0301.D\DA.M
                (UDARA.M)
Last changed    : 5/20/2015 12:56:06 PM by UDARA
                (modified after loading)
  
```



=====
 Area Percent Report
 =====

```

Sorted By      :      Signal
Multiplier     :      1.0000
Dilution      :      1.0000
Use Multiplier & Dilution Factor with ISTDs
  
```

Signal 1: VWD1 A, Wavelength=280 nm

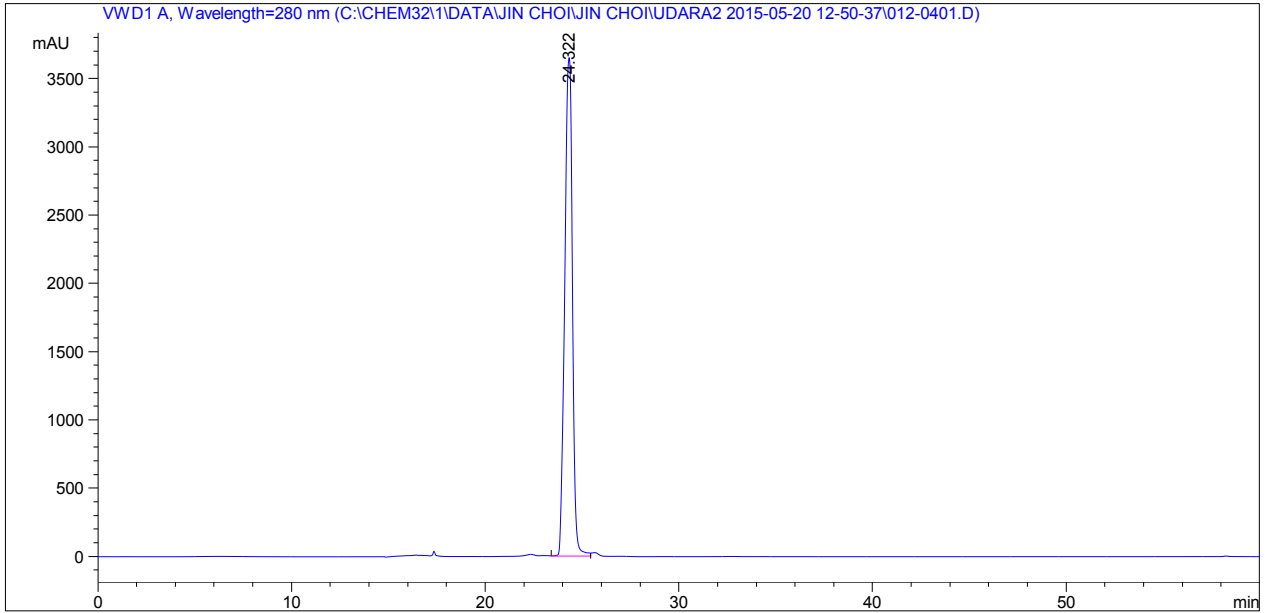
Peak #	RetTime [min]	Type	Width [min]	Area mAU *s	Height [mAU]	Area %
1	23.127	BB	0.4578	3.93470e4	1224.74646	100.0000

Totals : 3.93470e4 1224.74646

```

=====
Acq. Operator   : UDARA                               Seq. Line :    4
Acq. Instrument : Instrument 1                         Location  : Vial 12
Injection Date  : 5/20/2015 3:58:38 PM                Inj       :    1
                                                    Inj Volume: 20 µl

Acq. Method     : C:\Chem32\1\DATA\Jin Choi\JIN CHOI\UDARA2 2015-05-20 12-50-37\UDARA.M
Last changed    : 5/19/2015 6:12:26 PM by UDARA
Analysis Method : C:\CHEM32\1\DATA\JIN CHOI\JIN CHOI\UDARA2 2015-05-20 12-50-37\012-0401.D\DA.M
                (UDARA.M)
Last changed    : 5/21/2015 9:25:55 AM by UDARA
  
```



=====
 Area Percent Report
 =====

```

Sorted By      :      Signal
Multiplier     :      1.0000
Dilution      :      1.0000
Use Multiplier & Dilution Factor with ISTDs
  
```

Signal 1: VWD1 A, Wavelength=280 nm

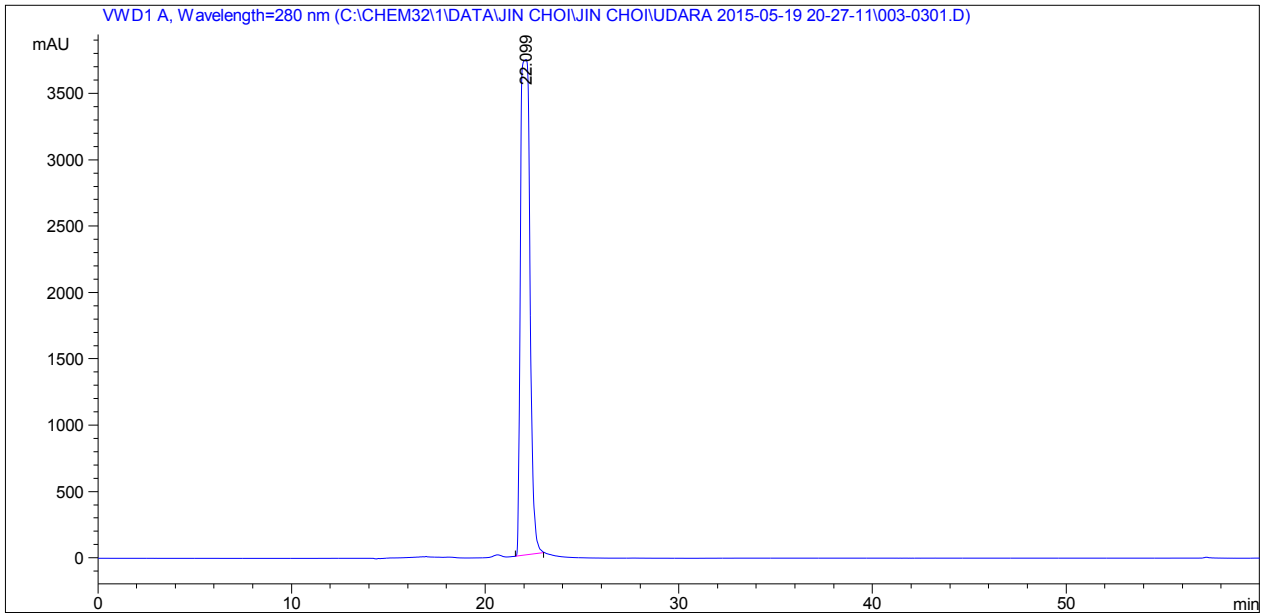
Peak #	RetTime [min]	Type	Width [min]	Area mAU *s	Height [mAU]	Area %
1	24.322	VV	0.4236	1.00716e5	3652.29980	100.0000

Totals : 1.00716e5 3652.29980

```

=====
Acq. Operator   : UDARA                               Seq. Line :    3
Acq. Instrument : Instrument 1                         Location  : Vial 3
Injection Date  : 5/19/2015 11:38:51 PM              Inj       :    1
                                                    Inj Volume: 20 µl

Acq. Method     : C:\Chem32\1\DATA\Jin Choi\JIN CHOI\UDARA 2015-05-19 20-27-11\UDARA.M
Last changed    : 5/19/2015 6:12:26 PM by UDARA
Analysis Method : C:\CHEM32\1\DATA\JIN CHOI\JIN CHOI\UDARA 2015-05-19 20-27-11\003-0301.D\DA.M (
                UDARA.M)
Last changed    : 5/20/2015 10:12:14 AM by UDARA
                (modified after loading)
  
```



=====
 Area Percent Report
 =====

```

Sorted By      :      Signal
Multiplier     :      1.0000
Dilution      :      1.0000
Use Multiplier & Dilution Factor with ISTDs
  
```

Signal 1: VWD1 A, Wavelength=280 nm

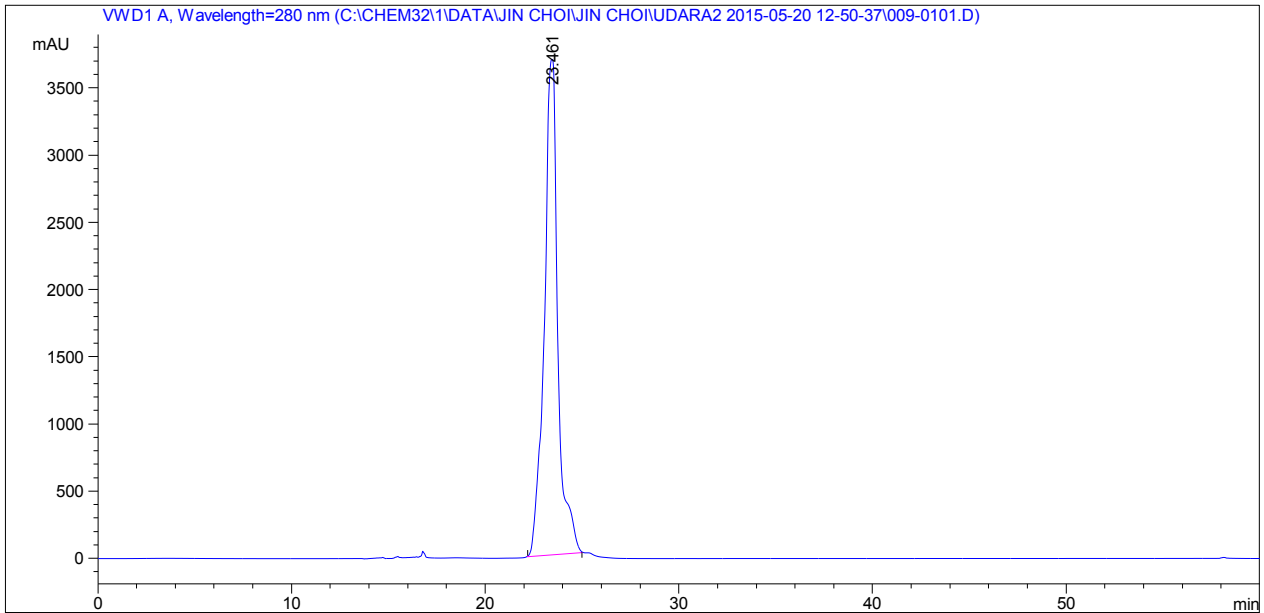
Peak #	RetTime [min]	Type	Width [min]	Area mAU *s	Height [mAU]	Area %
1	22.099	BB	0.4564	1.27038e5	3735.68188	100.0000

Totals : 1.27038e5 3735.68188

```

=====
Acq. Operator   : UDARA                               Seq. Line :    1
Acq. Instrument : Instrument 1                         Location  : Vial 9
Injection Date  : 5/20/2015 12:52:35 PM              Inj       :    1
                                                    Inj Volume: 20 µl

Acq. Method     : C:\Chem32\1\DATA\Jin Choi\JIN CHOI\UDARA2 2015-05-20 12-50-37\UDARA.M
Last changed    : 5/19/2015 6:12:26 PM by UDARA
Analysis Method : C:\CHEM32\1\DATA\JIN CHOI\JIN CHOI\UDARA2 2015-05-20 12-50-37\009-0101.D\DA.M
                (UDARA.M)
Last changed    : 5/21/2015 9:21:48 AM by UDARA
                (modified after loading)
  
```



=====
 Area Percent Report
 =====

```

Sorted By      :      Signal
Multiplier     :      1.0000
Dilution      :      1.0000
Use Multiplier & Dilution Factor with ISTDs
  
```

Signal 1: VWD1 A, Wavelength=280 nm

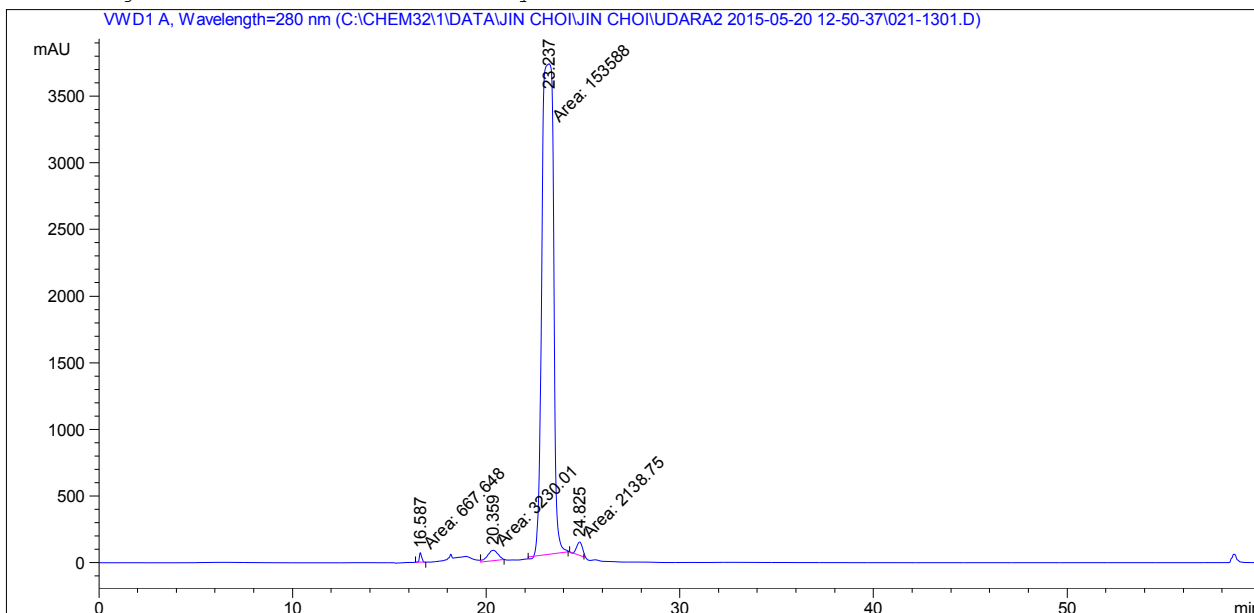
Peak #	RetTime [min]	Type	Width [min]	Area mAU *s	Height [mAU]	Area %
1	23.461	BB	0.6200	1.78877e5	3686.57007	100.0000

Totals : 1.78877e5 3686.57007

```

=====
Acq. Operator   : UDARA                               Seq. Line :   13
Acq. Instrument : Instrument 1                         Location  : Vial 21
Injection Date  : 5/21/2015 1:17:27 AM                Inj       :    1
                                                    Inj Volume: 20 µl

Acq. Method     : C:\Chem32\1\DATA\Jin Choi\JIN CHOI\UDARA2 2015-05-20 12-50-37\UDARA.M
Last changed    : 5/19/2015 6:12:26 PM by UDARA
Analysis Method : C:\CHEM32\1\DATA\JIN CHOI\JIN CHOI\UDARA2 2015-05-20 12-50-37\021-1301.D\DA.M
                (UDARA.M)
Last changed    : 5/21/2015 9:39:45 AM by UDARA
  
```



=====
 Area Percent Report
 =====

```

Sorted By      :      Signal
Multiplier     :      1.0000
Dilution      :      1.0000
Use Multiplier & Dilution Factor with ISTDs
  
```

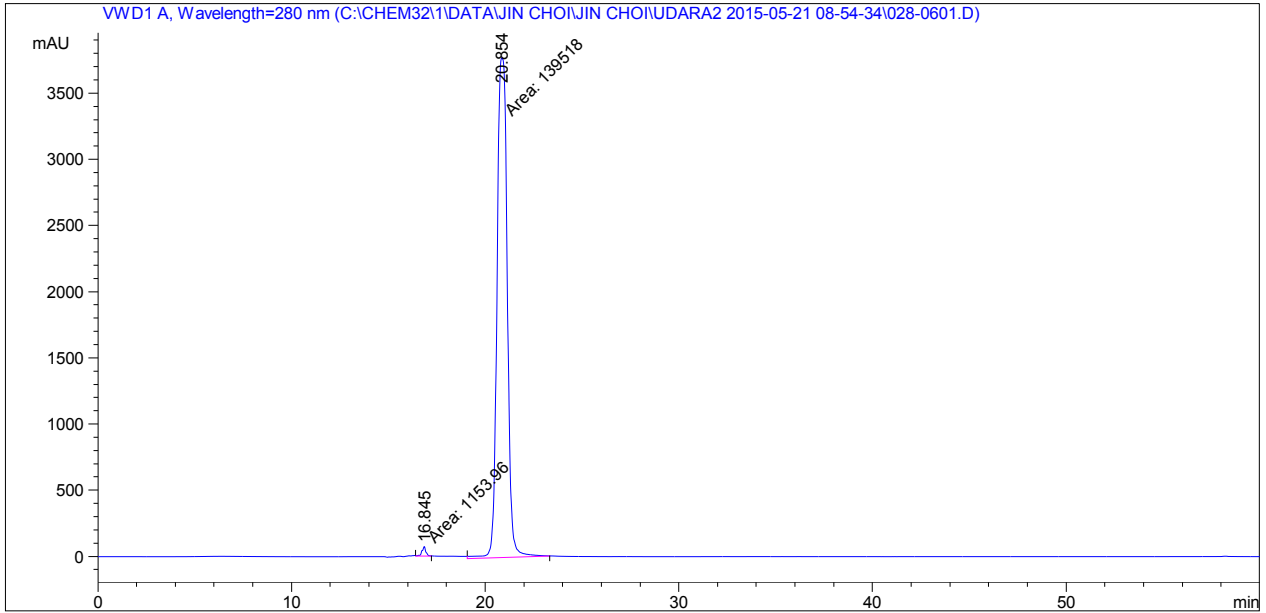
Signal 1: VWD1 A, Wavelength=280 nm

Peak #	RetTime [min]	Type	Width [min]	Area mAU *s	Height [mAU]	Area %
1	16.587	MM	0.1514	667.64807	73.47980	0.4183
2	20.359	MM	0.6603	3230.01245	81.52984	2.0235
3	23.237	MM	0.6943	1.53588e5	3687.11255	96.2184
4	24.825	MM	0.3466	2138.75195	102.85317	1.3399

```

=====
Acq. Operator   : UDARA                               Seq. Line :    6
Acq. Instrument : Instrument 1                         Location  : Vial 28
Injection Date  : 5/21/2015 2:06:33 PM                Inj       :    1
                                                    Inj Volume: 20 µl

Acq. Method     : C:\Chem32\1\DATA\Jin Choi\JIN CHOI\UDARA2 2015-05-21 08-54-34\UDARA.M
Last changed    : 5/19/2015 6:12:26 PM by UDARA
Analysis Method : C:\CHEM32\1\DATA\JIN CHOI\JIN CHOI\UDARA2 2015-05-21 08-54-34\028-0601.D\DA.M
                (UDARA.M)
Last changed    : 5/21/2015 3:10:16 PM by UDARA
  
```



=====
 Area Percent Report
 =====

```

Sorted By      :      Signal
Multiplier     :      1.0000
Dilution       :      1.0000
Use Multiplier & Dilution Factor with ISTDs
  
```

Signal 1: VWD1 A, Wavelength=280 nm

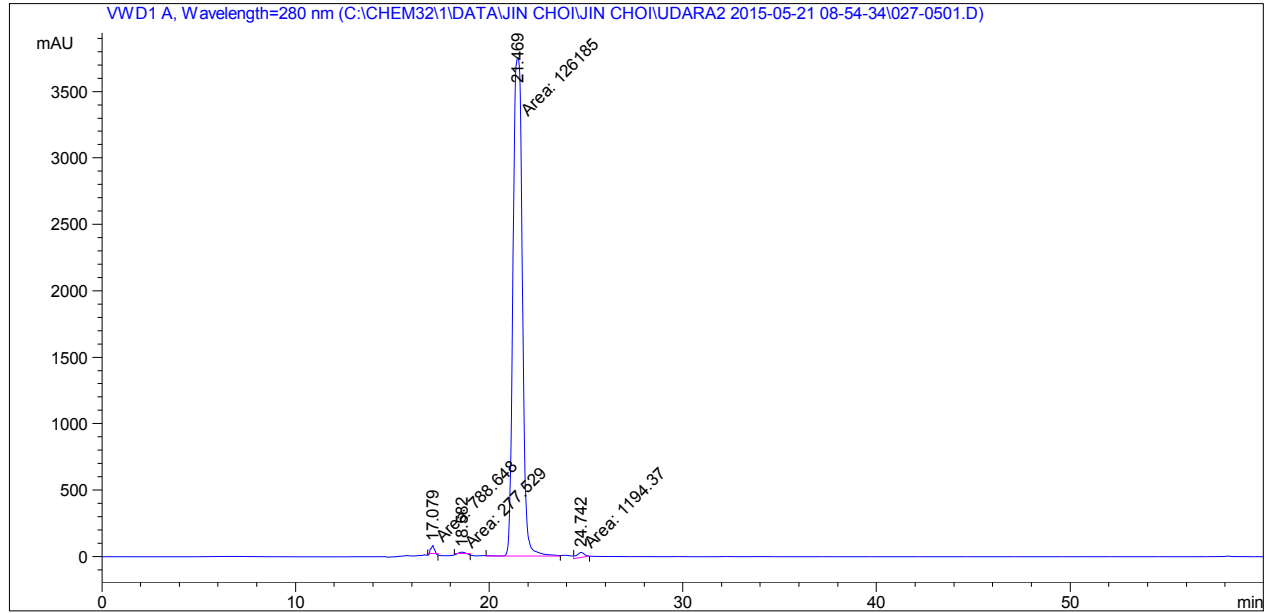
Peak #	RetTime [min]	Type	Width [min]	Area mAU *s	Height [mAU]	Area %
1	16.845	MM	0.2568	1153.96167	74.88272	0.8203
2	20.854	MM	0.6152	1.39518e5	3779.73755	99.1797

Totals : 1.40672e5 3854.62027

```

=====
Acq. Operator   : UDARA                               Seq. Line :    5
Acq. Instrument : Instrument 1                       Location  : Vial 27
Injection Date  : 5/21/2015 1:04:30 PM              Inj       :    1
                                                    Inj Volume: 20 µl

Acq. Method     : C:\Chem32\1\DATA\Jin Choi\JIN CHOI\UDARA2 2015-05-21 08-54-34\UDARA.M
Last changed    : 5/19/2015 6:12:26 PM by UDARA
Analysis Method : C:\CHEM32\1\DATA\JIN CHOI\JIN CHOI\UDARA2 2015-05-21 08-54-34\027-0501.D\DA.M
                (UDARA.M)
Last changed    : 5/19/2015 6:12:26 PM by UDARA
  
```



Area Percent Report

```

Sorted By      :      Signal
Multiplier     :      1.0000
Dilution       :      1.0000
Use Multiplier & Dilution Factor with ISTDs
  
```

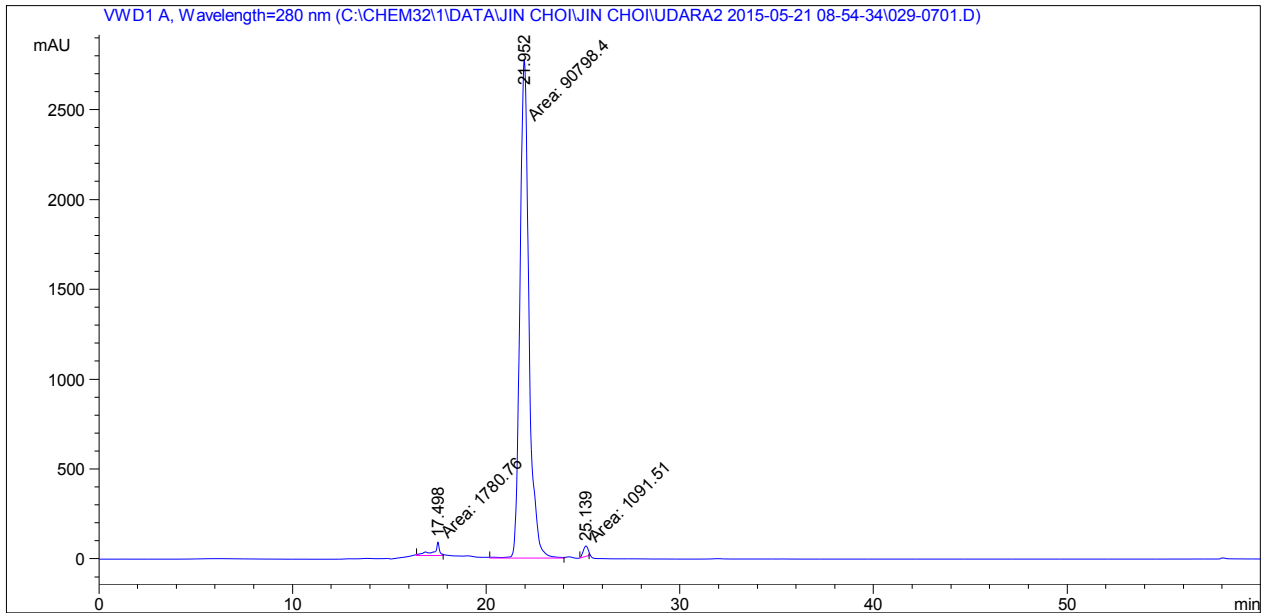
Signal 1: VWD1 A, Wavelength=280 nm

Peak #	RetTime [min]	Type	Width [min]	Area mAU *s	Height [mAU]	Area %
1	17.079	MM	0.2093	788.64758	62.79678	0.6140
2	18.582	MM	0.3490	277.52902	13.25263	0.2161
3	21.469	MM	0.5601	1.26185e5	3754.53735	98.2401
4	24.742	MM	0.4811	1194.37280	41.37428	0.9299

```

=====
Acq. Operator   : UDARA                               Seq. Line :    7
Acq. Instrument : Instrument 1                         Location  : Vial 29
Injection Date  : 5/21/2015 3:08:37 PM                Inj       :    1
                                                    Inj Volume: 20 µl

Acq. Method     : C:\Chem32\1\DATA\Jin Choi\JIN CHOI\UDARA2 2015-05-21 08-54-34\UDARA.M
Last changed    : 5/19/2015 6:12:26 PM by UDARA
Analysis Method : C:\CHEM32\1\DATA\JIN CHOI\JIN CHOI\UDARA2 2015-05-21 08-54-34\029-0701.D\DA.M
                (UDARA.M)
Last changed    : 5/21/2015 4:09:12 PM by UDARA
  
```



=====
 Area Percent Report
 =====

```

Sorted By      :      Signal
Multiplier     :      1.0000
Dilution      :      1.0000
Use Multiplier & Dilution Factor with ISTDs
  
```

Signal 1: VWD1 A, Wavelength=280 nm

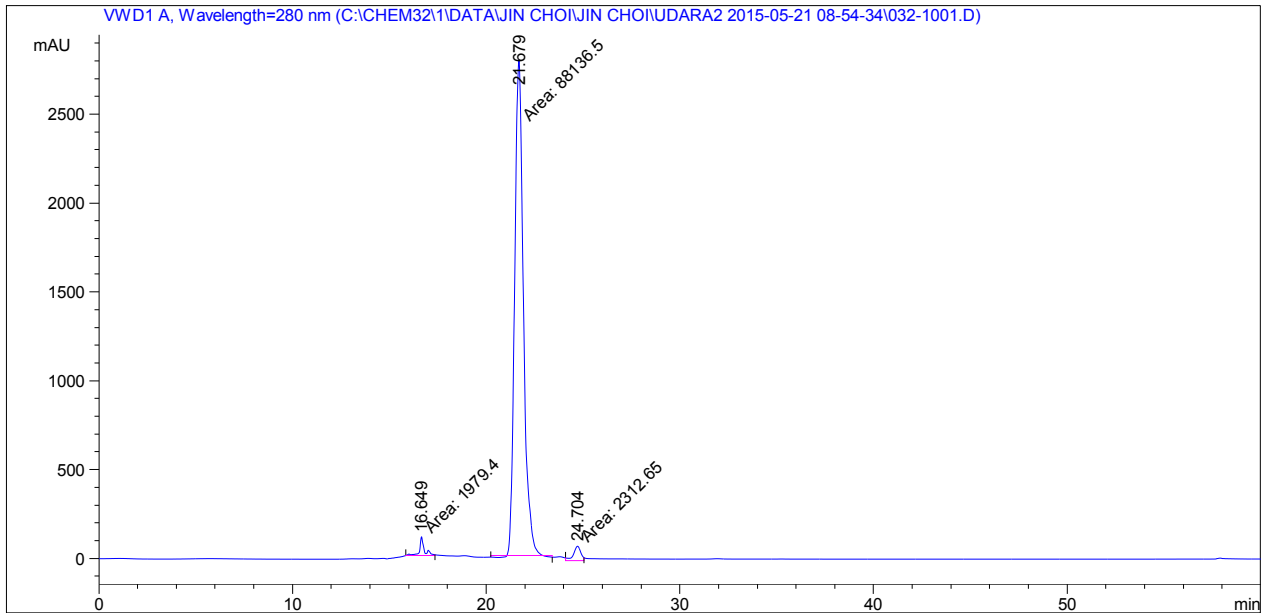
Peak #	RetTime [min]	Type	Width [min]	Area mAU *s	Height [mAU]	Area %
1	17.498	MM	0.3853	1780.76465	77.02604	1.9011
2	21.952	MM	0.5452	9.07984e4	2775.51880	96.9337
3	25.139	MM	0.2988	1091.50671	60.89183	1.1653

Totals : 9.36707e4 2913.43666


```

=====
Acq. Operator   : UDARA                               Seq. Line : 10
Acq. Instrument : Instrument 1                         Location  : Vial 32
Injection Date  : 5/21/2015 6:14:52 PM                Inj       : 1
                                                    Inj Volume: 20 µl

Acq. Method     : C:\Chem32\1\DATA\Jin Choi\JIN CHOI\UDARA2 2015-05-21 08-54-34\UDARA.M
Last changed    : 5/19/2015 6:12:26 PM by UDARA
Analysis Method : C:\CHEM32\1\DATA\JIN CHOI\JIN CHOI\UDARA2 2015-05-21 08-54-34\032-1001.D\DA.M
                (UDARA.M)
Last changed    : 5/19/2015 6:12:26 PM by UDARA
  
```



=====
 Area Percent Report
 =====

```

Sorted By      :      Signal
Multiplier     :      1.0000
Dilution       :      1.0000
Use Multiplier & Dilution Factor with ISTDs
  
```

Signal 1: VWD1 A, Wavelength=280 nm

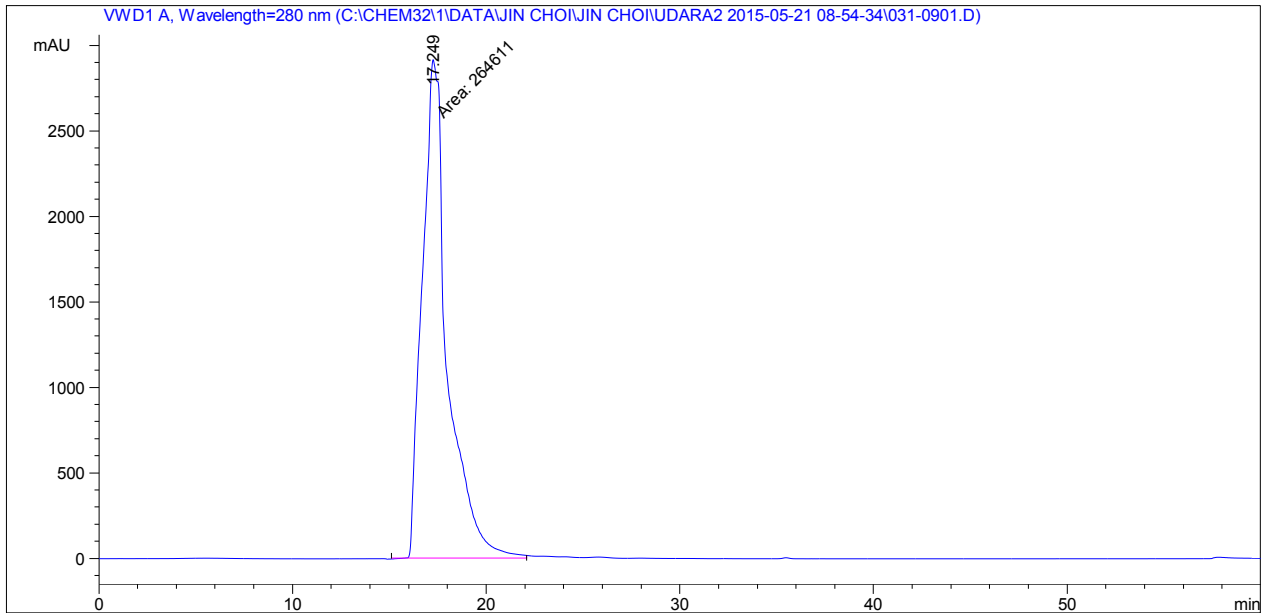
Peak #	RetTime [min]	Type	Width [min]	Area mAU *s	Height [mAU]	Area %
1	16.649	MM	0.3074	1979.40442	107.31641	2.1415
2	21.679	MM	0.5260	8.81365e4	2792.54321	95.3564
3	24.704	MM	0.4618	2312.64844	83.45880	2.5021

Totals : 9.24286e4 2983.31842

```

=====
Acq. Operator   : UDARA                               Seq. Line :    9
Acq. Instrument : Instrument 1                         Location  : Vial 31
Injection Date  : 5/21/2015 5:12:47 PM                Inj       :    1
                                                    Inj Volume: 20 µl

Acq. Method     : C:\Chem32\1\DATA\Jin Choi\JIN CHOI\UDARA2 2015-05-21 08-54-34\UDARA.M
Last changed    : 5/19/2015 6:12:26 PM by UDARA
Analysis Method : C:\CHEM32\1\DATA\JIN CHOI\JIN CHOI\UDARA2 2015-05-21 08-54-34\031-0901.D\DA.M
                (UDARA.M)
Last changed    : 5/21/2015 6:19:47 PM by UDARA
  
```



=====
 Area Percent Report
 =====

```

Sorted By      :      Signal
Multiplier     :      1.0000
Dilution       :      1.0000
Use Multiplier & Dilution Factor with ISTDs
  
```

Signal 1: VWD1 A, Wavelength=280 nm

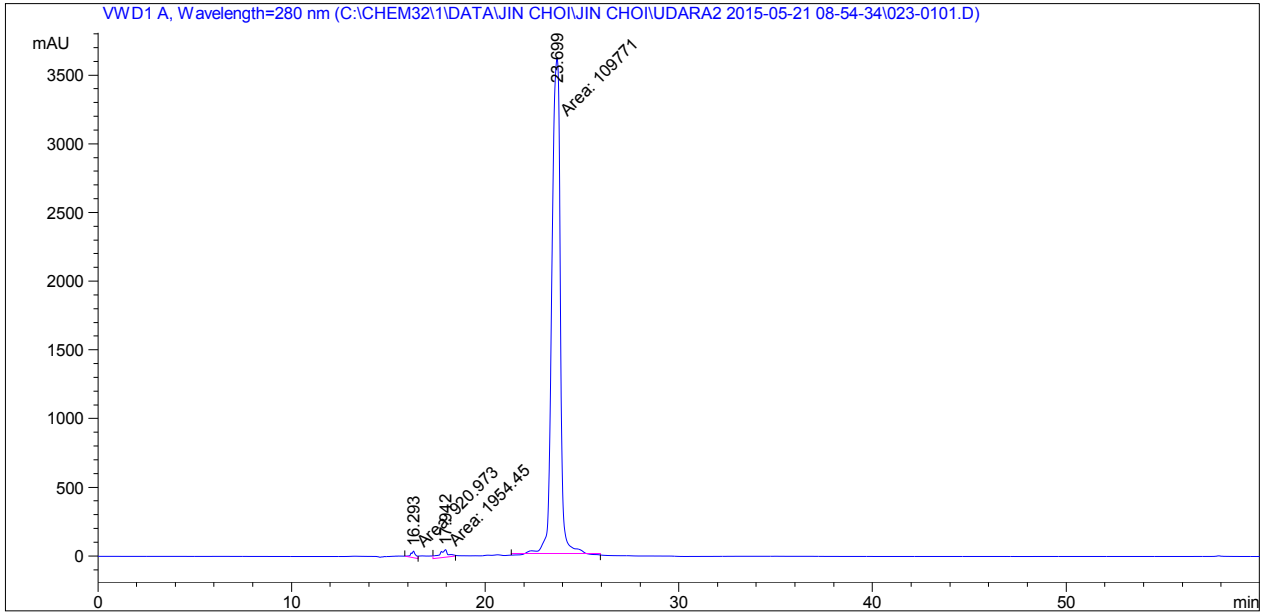
Peak #	RetTime [min]	Type	Width [min]	Area mAU *s	Height [mAU]	Area %
1	17.249	MM	1.5123	2.64611e5	2916.28052	100.0000

Totals : 2.64611e5 2916.28052

```

=====
Acq. Operator   : UDARA                               Seq. Line :    1
Acq. Instrument : Instrument 1                         Location  : Vial 23
Injection Date  : 5/21/2015 8:56:53 AM                Inj       :    1
                                                    Inj Volume: 20 µl

Acq. Method     : C:\Chem32\1\DATA\Jin Choi\JIN CHOI\UDARA2 2015-05-21 08-54-34\UDARA.M
Last changed    : 5/19/2015 6:12:26 PM by UDARA
Analysis Method : C:\CHEM32\1\DATA\JIN CHOI\JIN CHOI\UDARA2 2015-05-21 08-54-34\023-0101.D\DA.M
                (UDARA.M)
Last changed    : 5/19/2015 6:12:26 PM by UDARA
  
```



Area Percent Report

```

Sorted By      :      Signal
Multiplier     :      1.0000
Dilution      :      1.0000
Use Multiplier & Dilution Factor with ISTDs
  
```

Signal 1: VWD1 A, Wavelength=280 nm

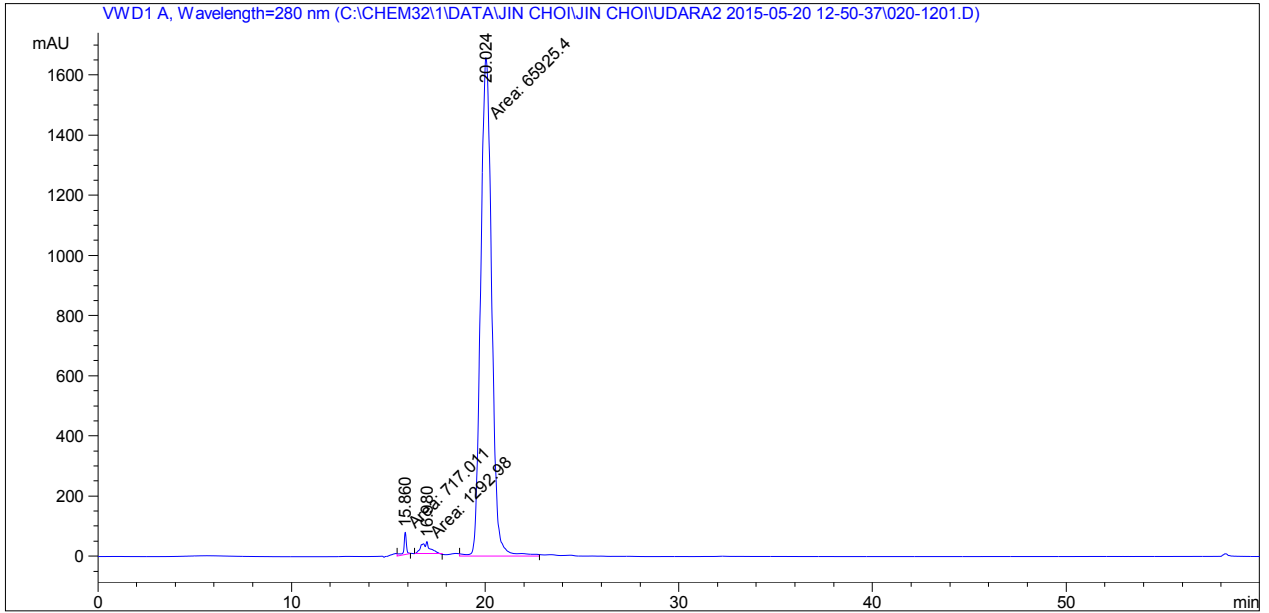
Peak #	RetTime [min]	Type	Width [min]	Area mAU *s	Height [mAU]	Area %
1	16.293	MM	0.3038	920.97321	50.52233	0.8176
2	17.942	MM	0.5627	1954.45496	57.89123	1.7350
3	23.699	MM	0.5066	1.09771e5	3611.09277	97.4474

Totals : 1.12647e5 3719.50634

```

=====
Acq. Operator   : UDARA                               Seq. Line : 12
Acq. Instrument : Instrument 1                         Location  : Vial 20
Injection Date  : 5/21/2015 12:15:26 AM              Inj       : 1
                                                    Inj Volume: 20 µl

Acq. Method     : C:\Chem32\1\DATA\Jin Choi\JIN CHOI\UDARA2 2015-05-20 12-50-37\UDARA.M
Last changed    : 5/19/2015 6:12:26 PM by UDARA
Analysis Method : C:\CHEM32\1\DATA\JIN CHOI\JIN CHOI\UDARA2 2015-05-20 12-50-37\020-1201.D\DA.M
                (UDARA.M)
Last changed    : 5/21/2015 9:38:20 AM by UDARA
  
```



=====
 Area Percent Report
 =====

```

Sorted By      :      Signal
Multiplier     :      1.0000
Dilution       :      1.0000
Use Multiplier & Dilution Factor with ISTDs
  
```

Signal 1: VWD1 A, Wavelength=280 nm

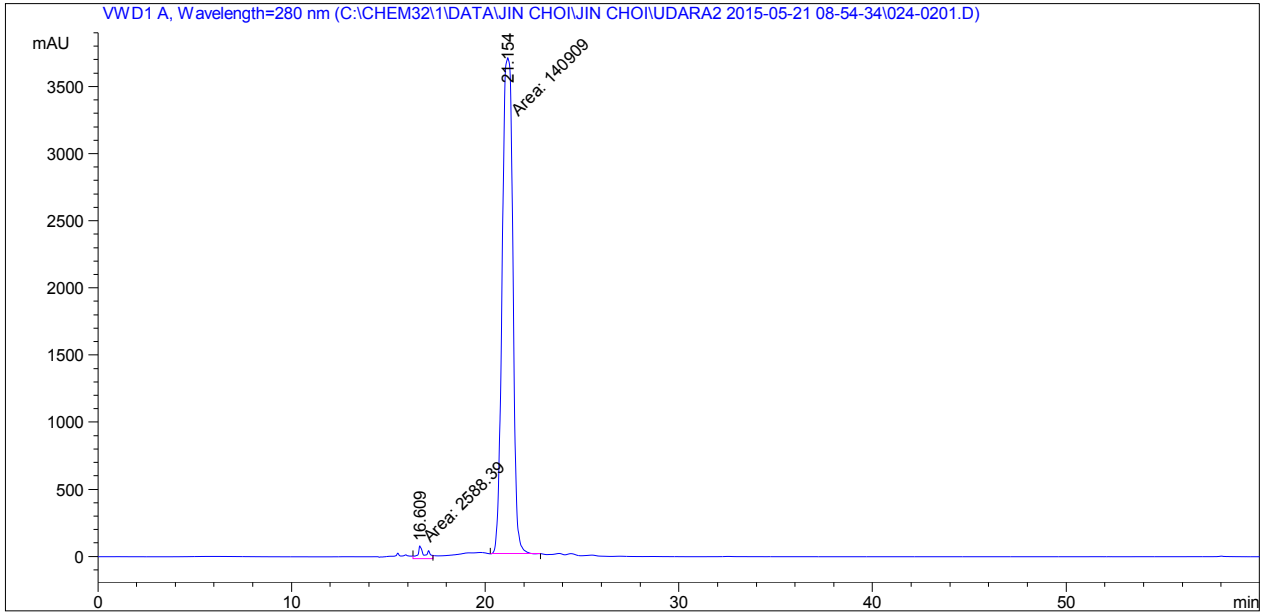
Peak #	RetTime [min]	Type	Width [min]	Area mAU *s	Height [mAU]	Area %
1	15.860	MM	0.1591	717.01111	75.10148	1.0554
2	16.980	MM	0.5235	1292.97766	41.16173	1.9032
3	20.024	MM	0.6626	6.59254e4	1658.29358	97.0413

Totals : 6.79354e4 1774.55679

```

=====
Acq. Operator   : UDARA                               Seq. Line :    2
Acq. Instrument : Instrument 1                         Location  : Vial 24
Injection Date  : 5/21/2015 9:58:22 AM                Inj       :    1
                                                    Inj Volume: 20 µl

Acq. Method     : C:\Chem32\1\DATA\Jin Choi\JIN CHOI\UDARA2 2015-05-21 08-54-34\UDARA.M
Last changed    : 5/19/2015 6:12:26 PM by UDARA
Analysis Method : C:\CHEM32\1\DATA\JIN CHOI\JIN CHOI\UDARA2 2015-05-21 08-54-34\024-0201.D\DA.M
                (UDARA.M)
Last changed    : 5/21/2015 11:30:01 AM by UDARA
  
```



=====
 Area Percent Report
 =====

```

Sorted By      :      Signal
Multiplier     :      1.0000
Dilution       :      1.0000
Use Multiplier & Dilution Factor with ISTDs
  
```

Signal 1: VWD1 A, Wavelength=280 nm

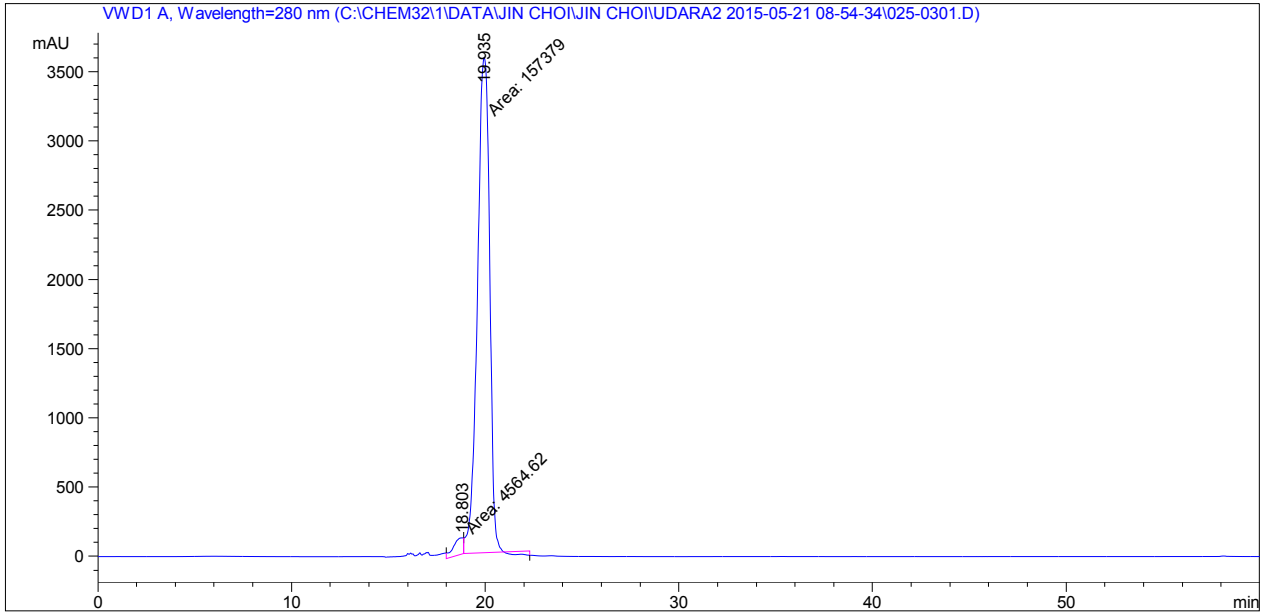
Peak #	RetTime [min]	Type	Width [min]	Area mAU *s	Height [mAU]	Area %
1	16.609	MM	0.4414	2588.38770	97.73698	1.8038
2	21.154	MM	0.6355	1.40909e5	3695.72412	98.1962

Totals : 1.43497e5 3793.46110

```

=====
Acq. Operator   : UDARA                               Seq. Line :    3
Acq. Instrument : Instrument 1                       Location  : Vial 25
Injection Date  : 5/21/2015 11:00:29 AM             Inj       :    1
                                                    Inj Volume: 20 µl

Acq. Method     : C:\Chem32\1\DATA\Jin Choi\JIN CHOI\UDARA2 2015-05-21 08-54-34\UDARA.M
Last changed    : 5/19/2015 6:12:26 PM by UDARA
Analysis Method : C:\CHEM32\1\DATA\JIN CHOI\JIN CHOI\UDARA2 2015-05-21 08-54-34\025-0301.D\DA.M
                (UDARA.M)
Last changed    : 5/21/2015 12:43:42 PM by UDARA
  
```



=====
 Area Percent Report
 =====

```

Sorted By      :      Signal
Multiplier     :      1.0000
Dilution       :      1.0000
Use Multiplier & Dilution Factor with ISTDs
  
```

Signal 1: VWD1 A, Wavelength=280 nm

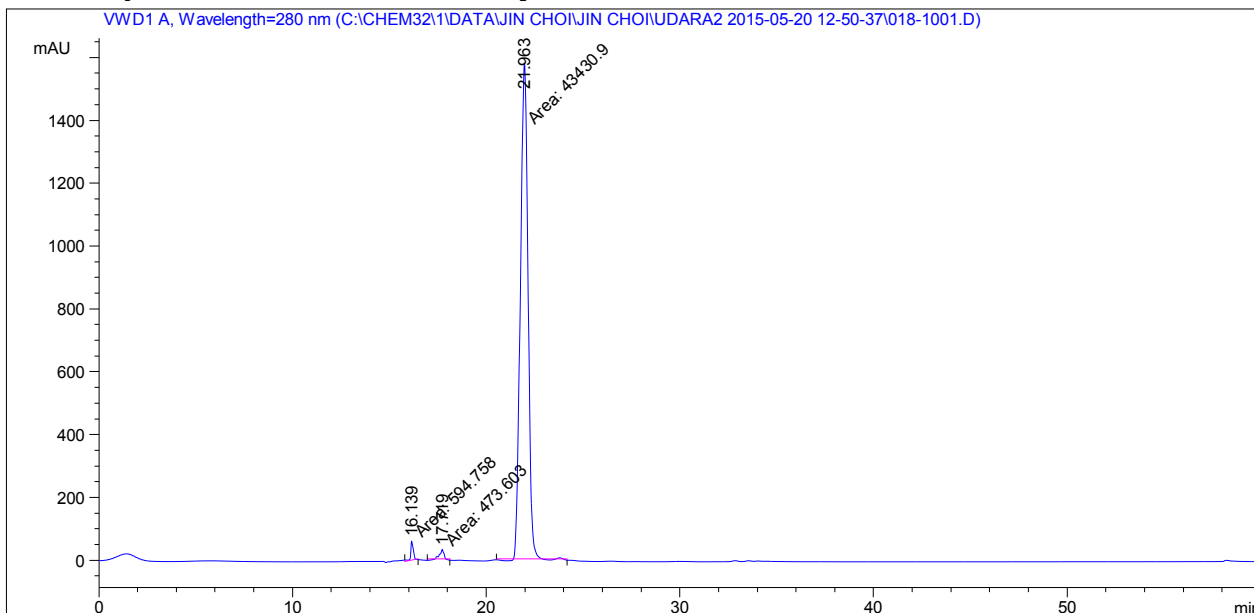
Peak #	RetTime [min]	Type	Width [min]	Area mAU*s	Height [mAU]	Area %
1	18.803	MM	0.4683	4564.62256	119.39576	2.8186
2	19.935	MM	0.7331	1.57379e5	3577.96289	97.1814

Totals : 1.61944e5 3697.35865

```

=====
Acq. Operator   : UDARA                               Seq. Line :   10
Acq. Instrument : Instrument 1                         Location  : Vial 18
Injection Date  : 5/20/2015 10:11:08 PM              Inj       :    1
                                                    Inj Volume: 20 µl

Acq. Method     : C:\Chem32\1\DATA\Jin Choi\JIN CHOI\UDARA2 2015-05-20 12-50-37\UDARA.M
Last changed    : 5/19/2015 6:12:26 PM by UDARA
Analysis Method : C:\CHEM32\1\DATA\JIN CHOI\JIN CHOI\UDARA2 2015-05-20 12-50-37\018-1001.D\DA.M
                (UDARA.M)
Last changed    : 5/19/2015 6:12:26 PM by UDARA
  
```



=====
 Area Percent Report
 =====

```

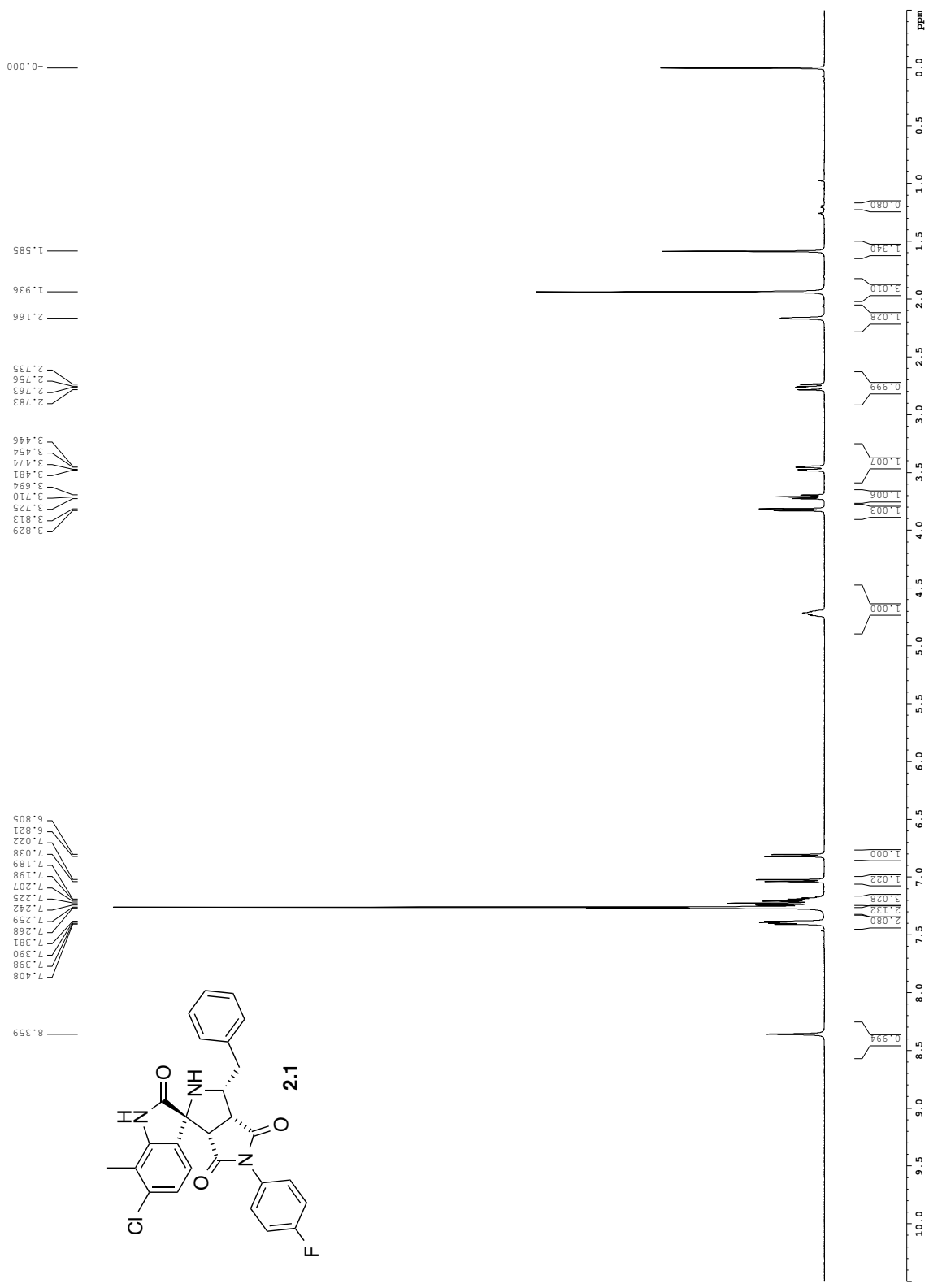
Sorted By      :      Signal
Multiplier     :      1.0000
Dilution      :      1.0000
Use Multiplier & Dilution Factor with ISTDs
  
```

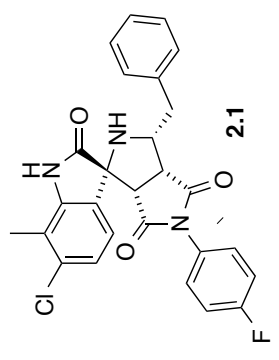
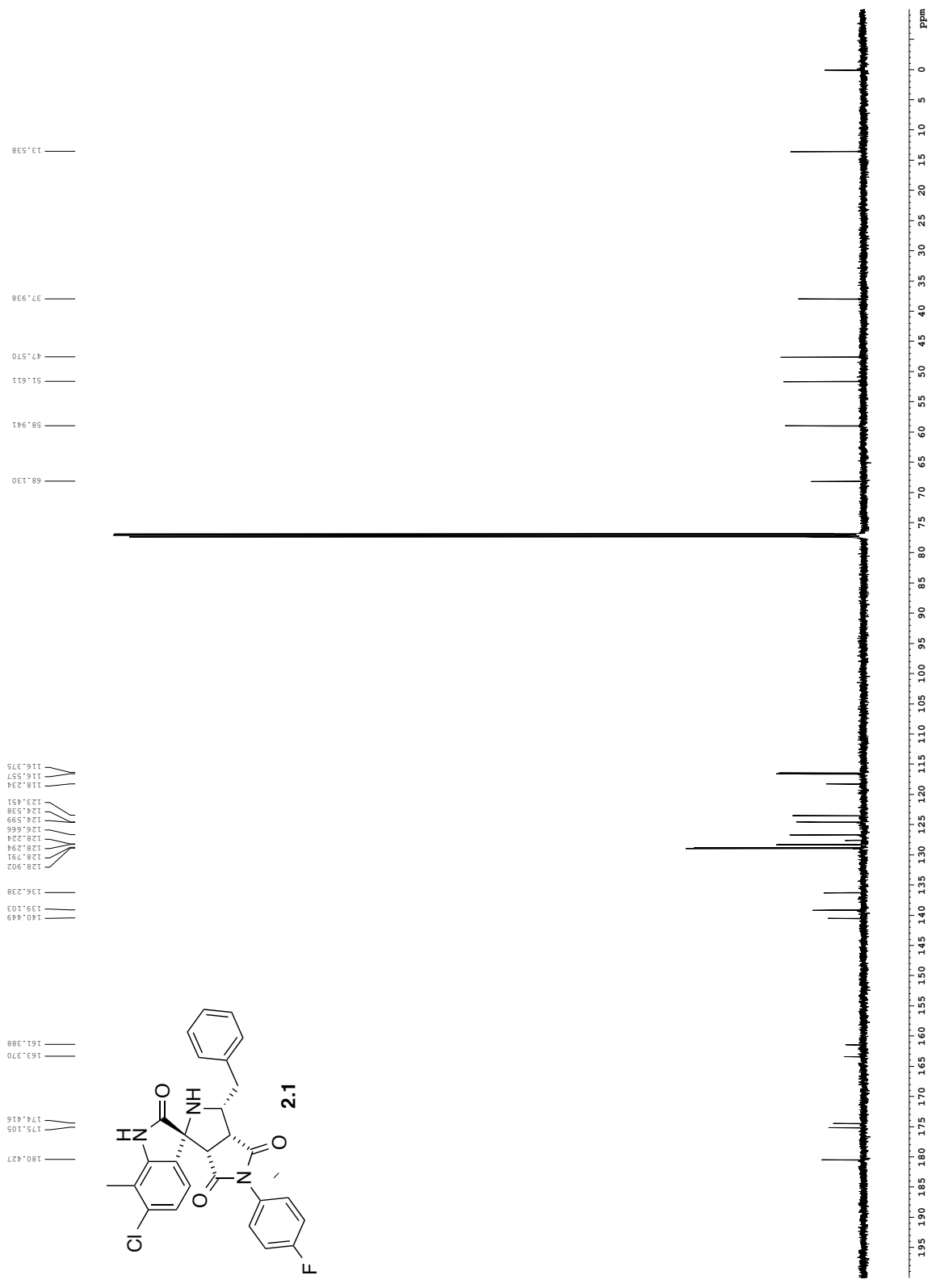
Signal 1: VWD1 A, Wavelength=280 nm

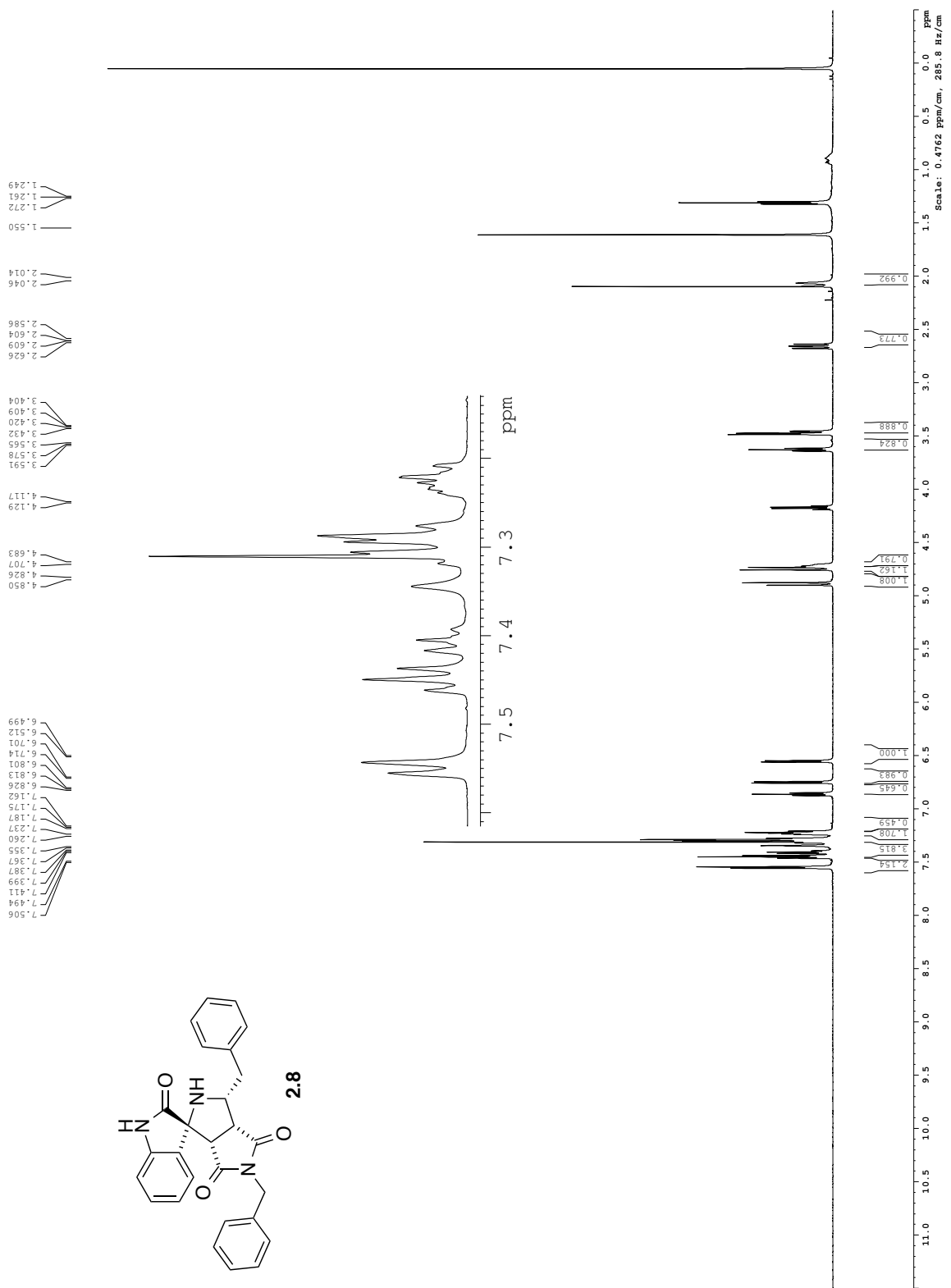
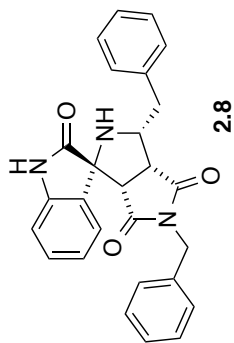
Peak #	RetTime [min]	Type	Width [min]	Area mAU *s	Height [mAU]	Area %
1	16.139	MM	0.1613	594.75769	61.46890	1.3366
2	17.719	MM	0.2505	473.60257	31.51163	1.0643
3	21.963	MM	0.4584	4.34309e4	1579.18811	97.5992

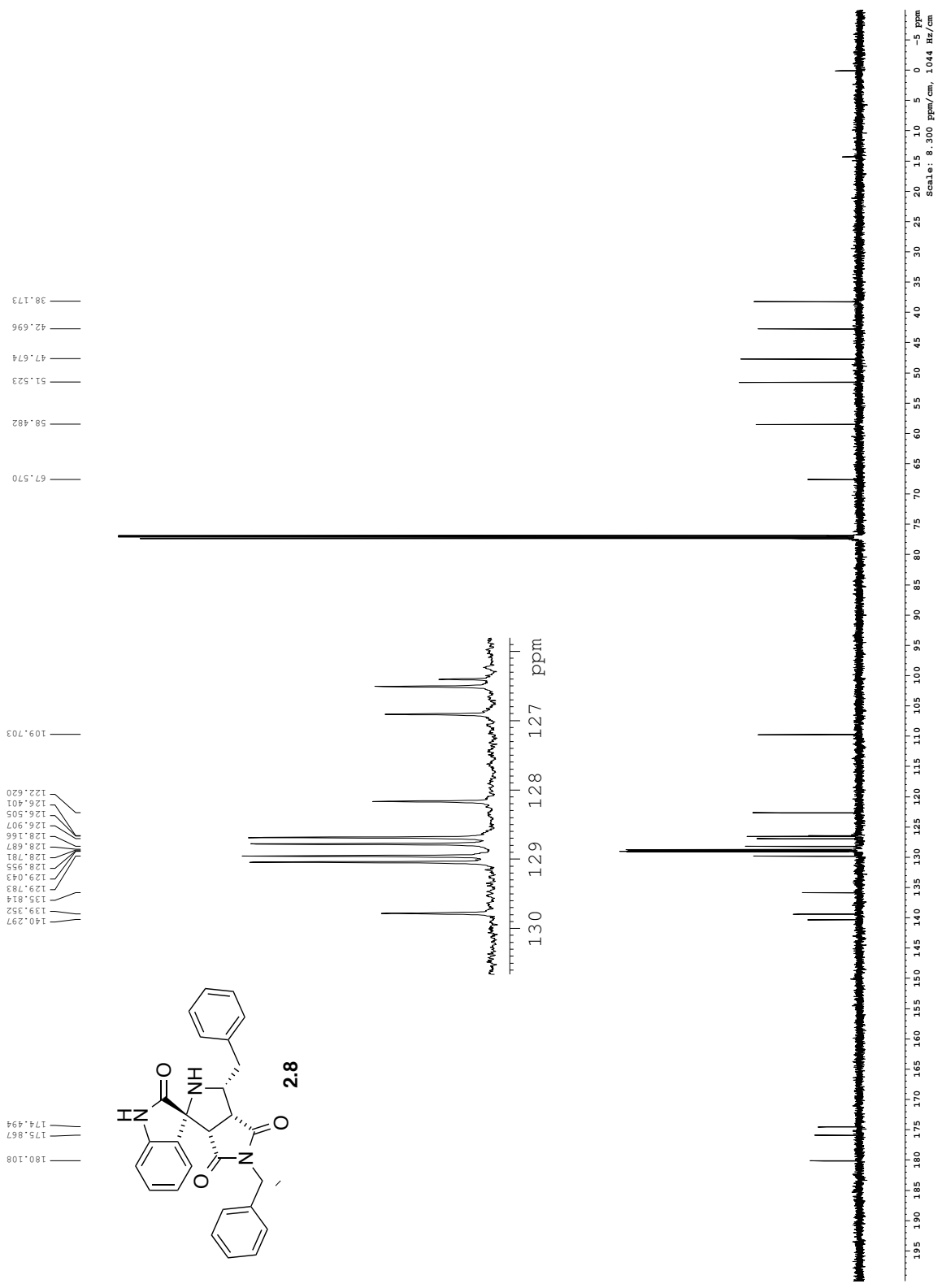
Totals : 4.44993e4 1672.16865

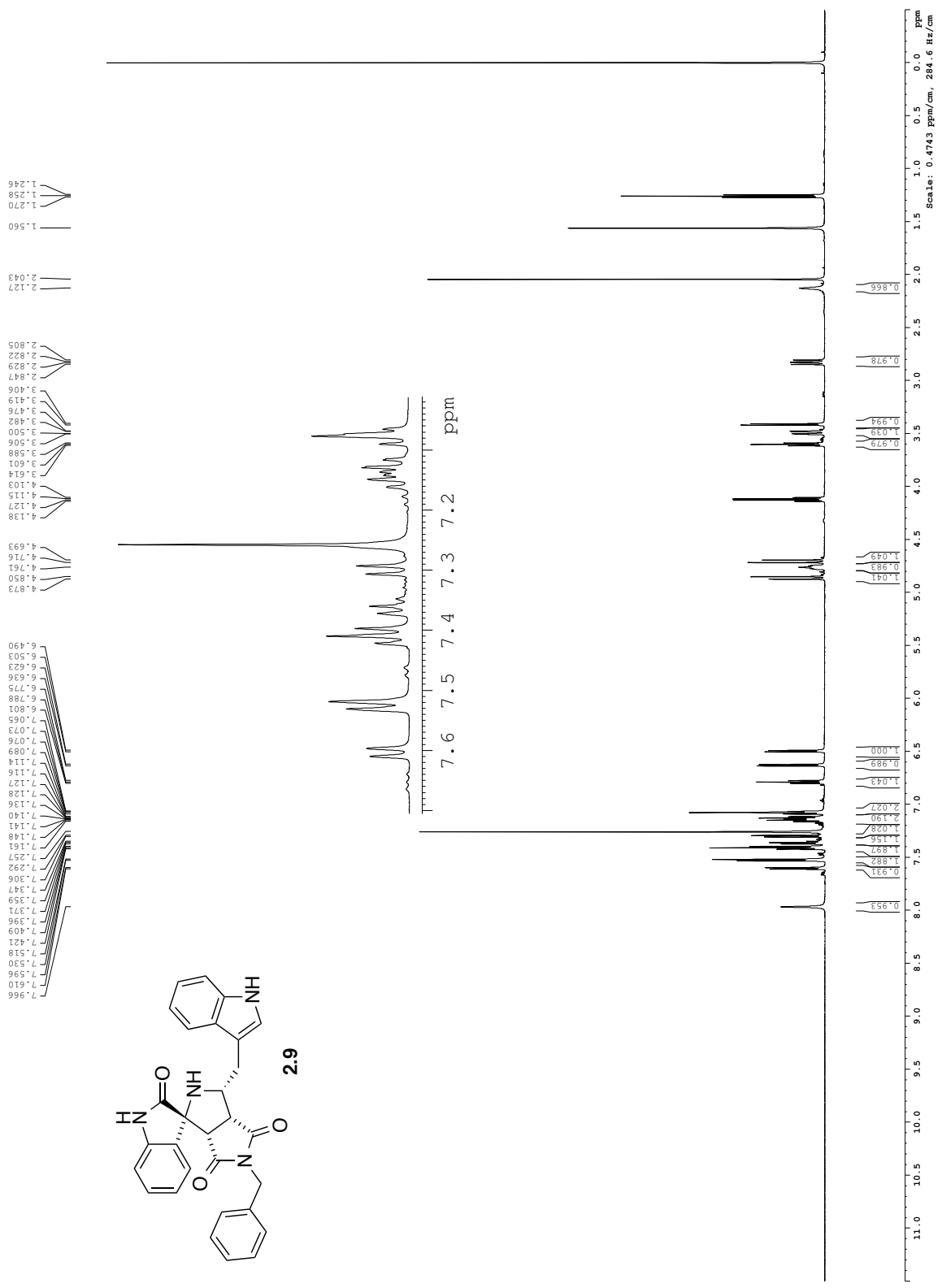
Appendix B: Chapter 2 – NMR Spectra

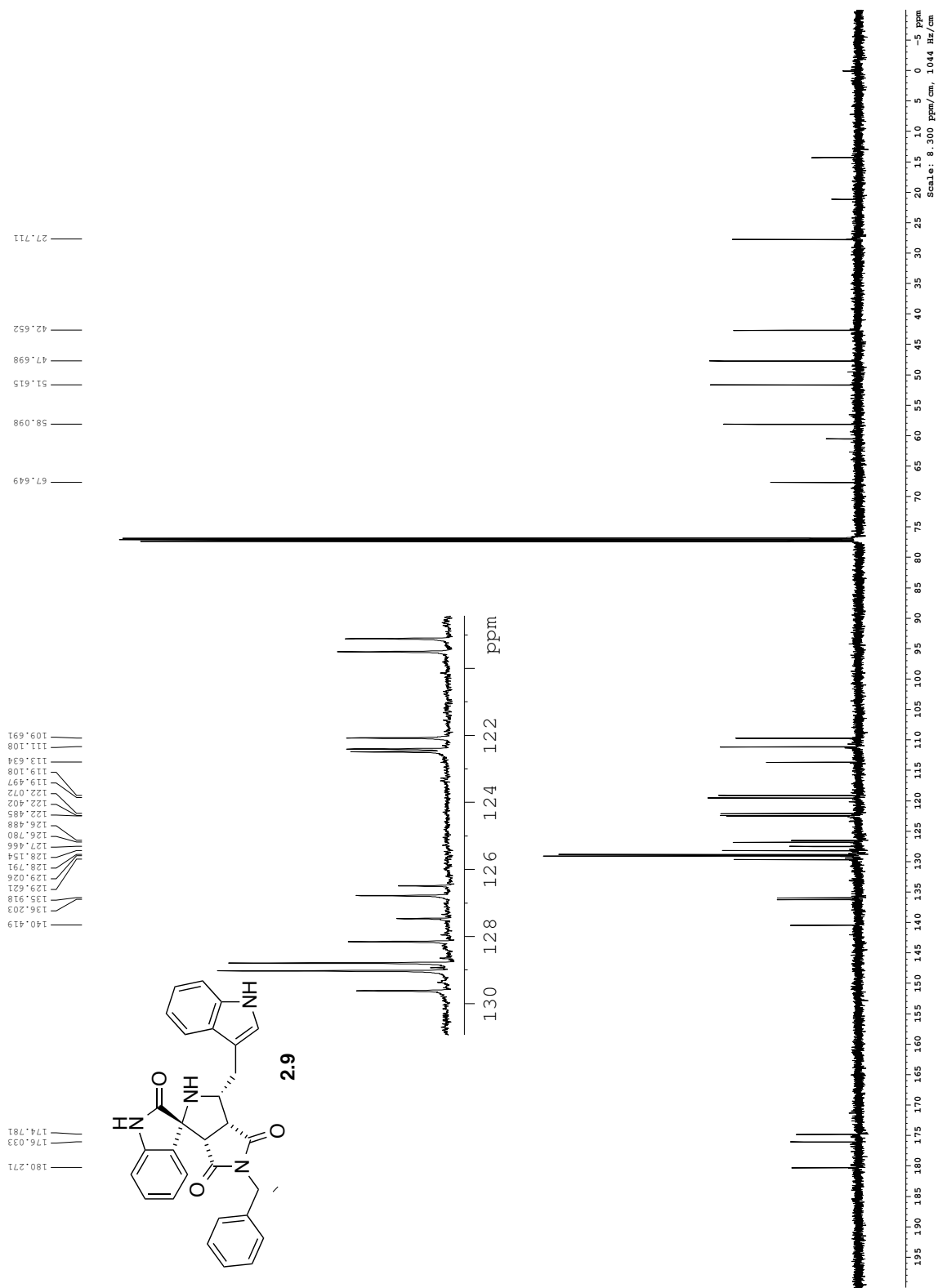


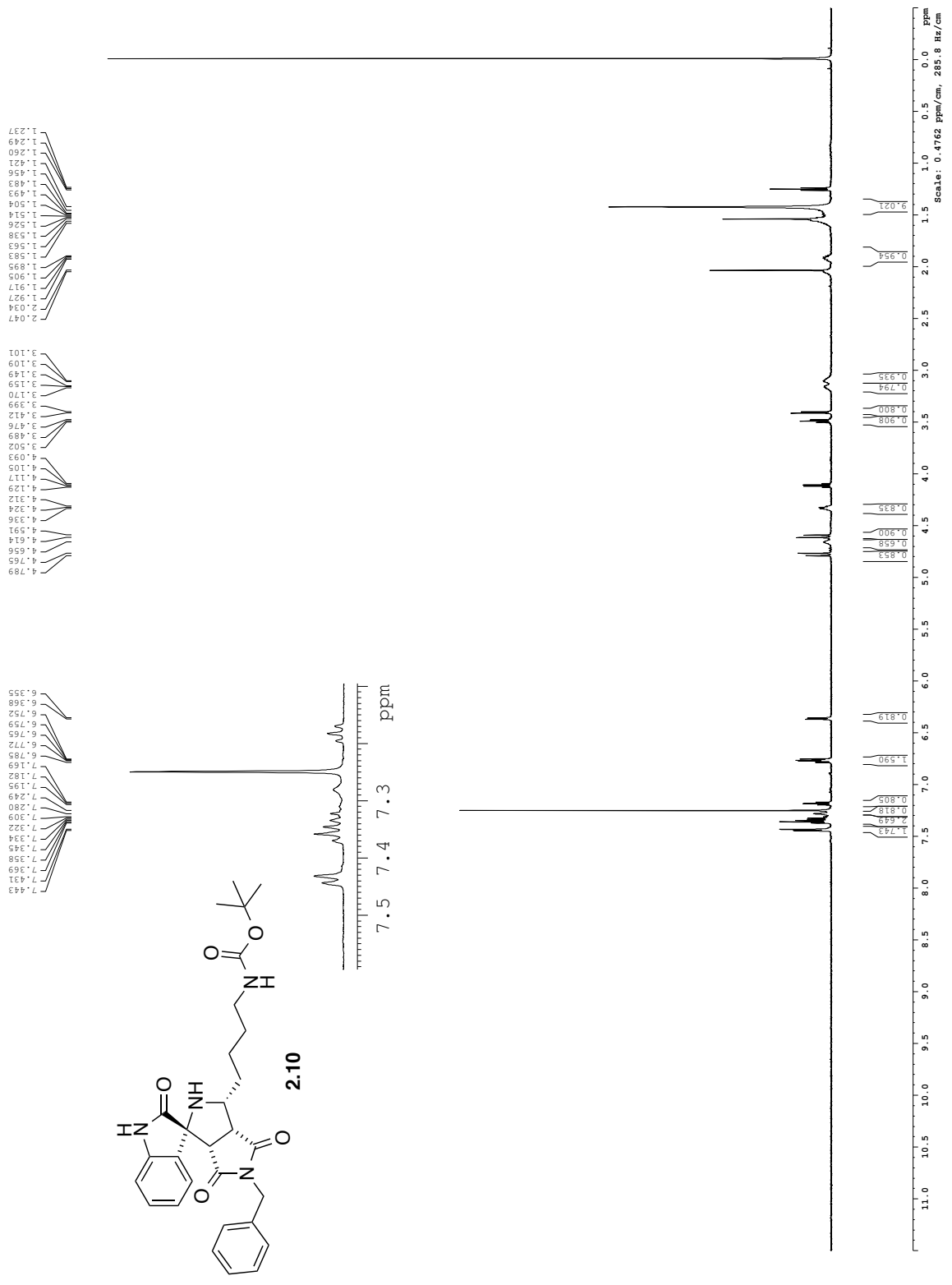


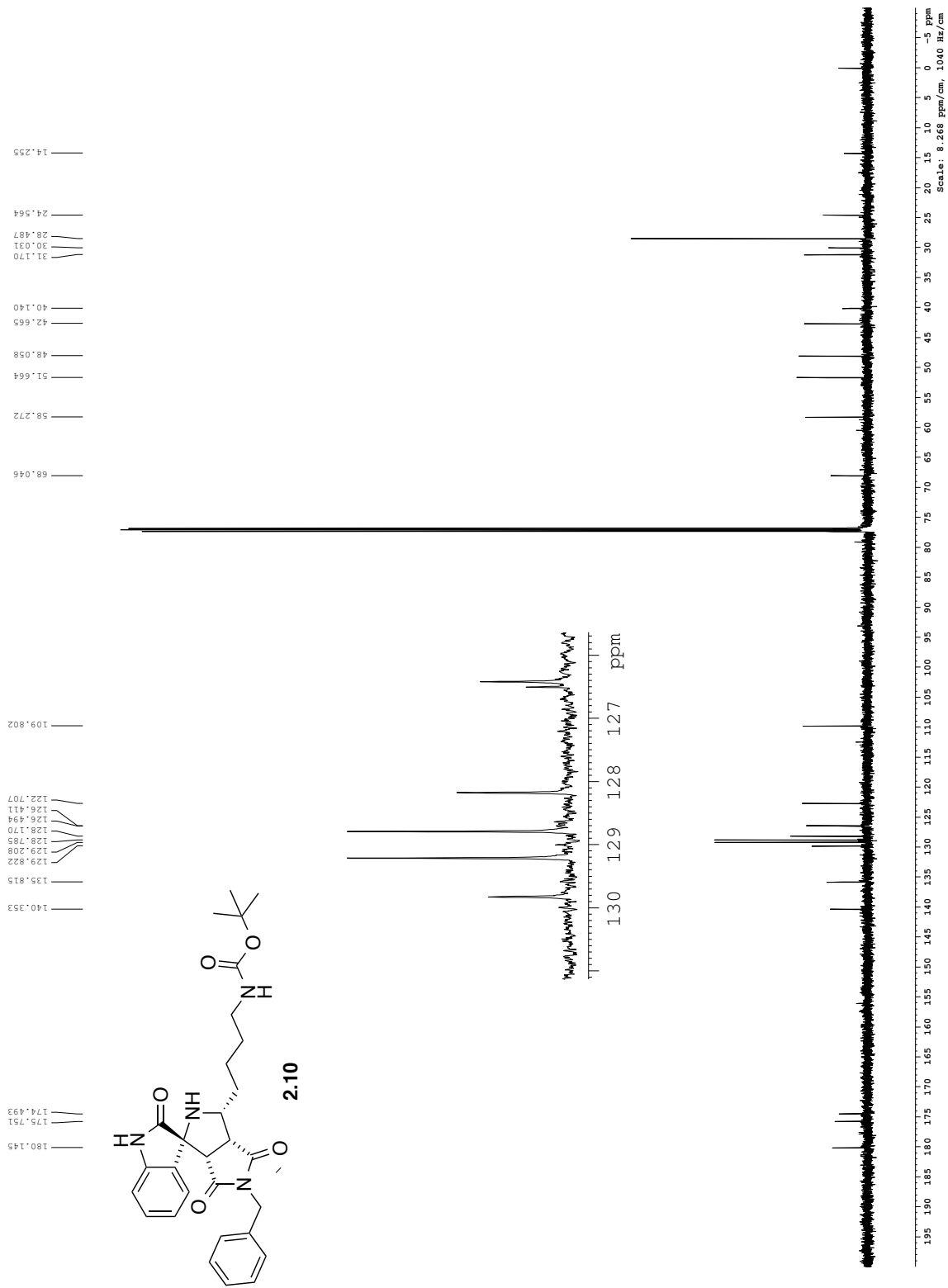


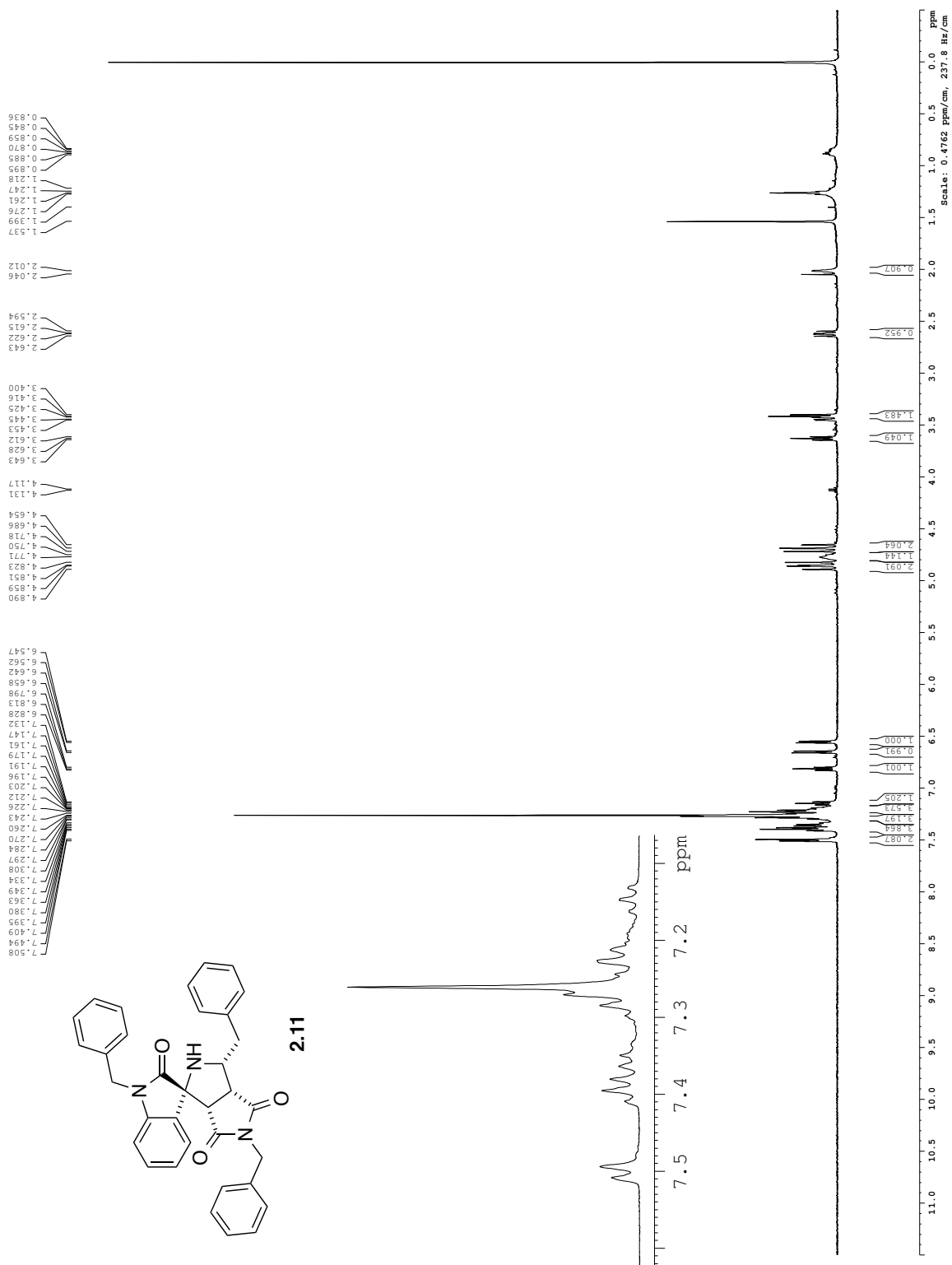


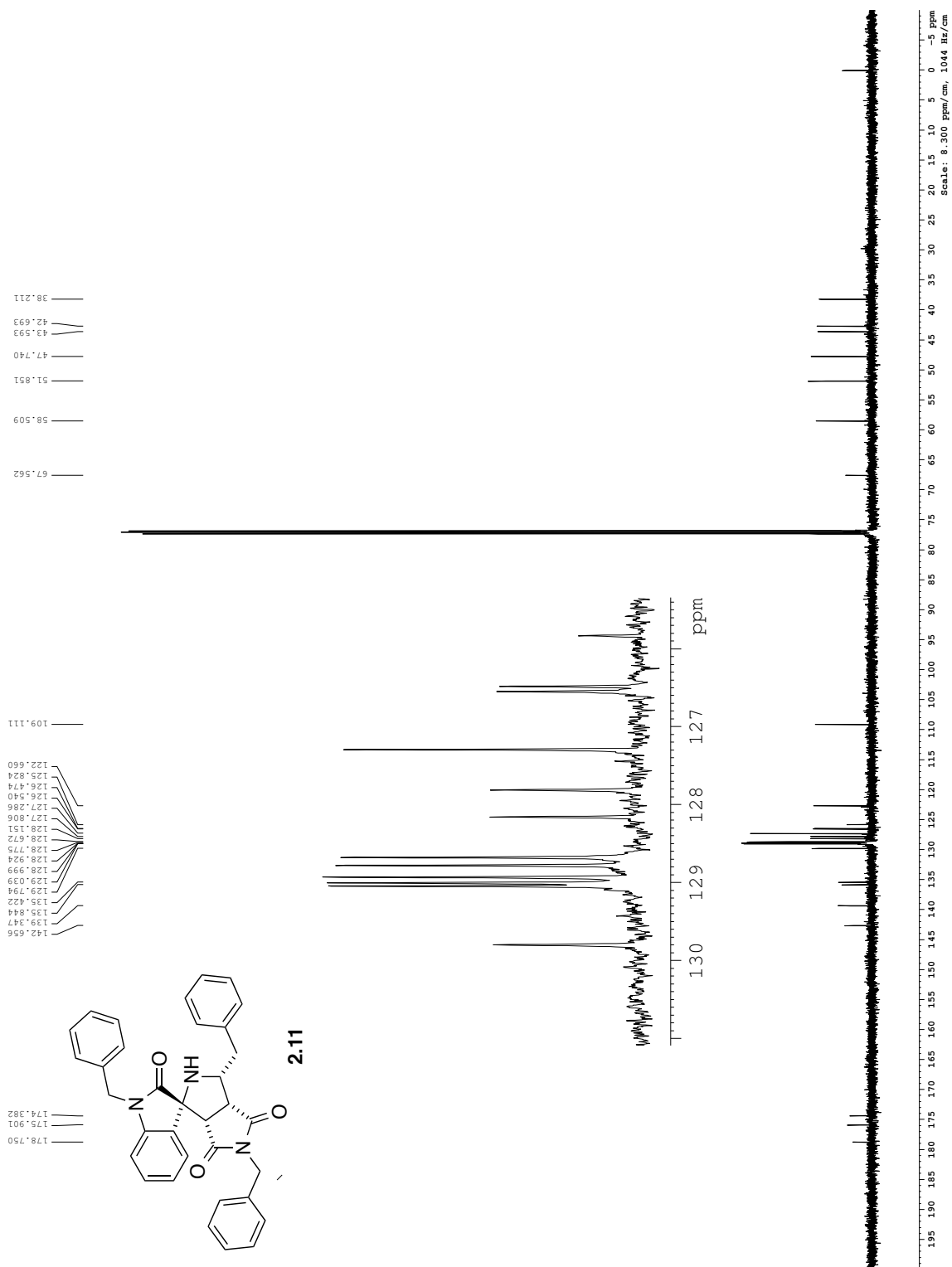


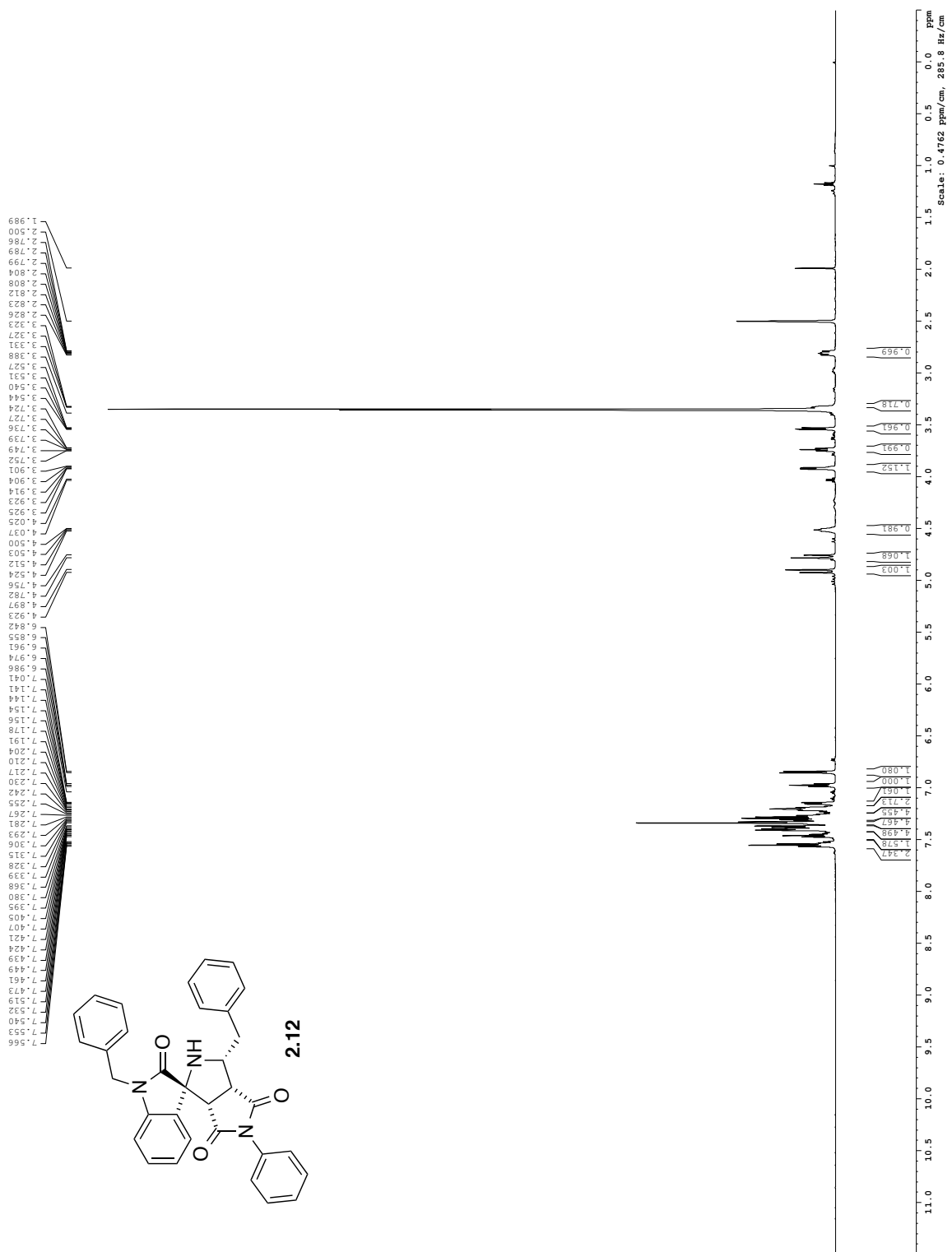


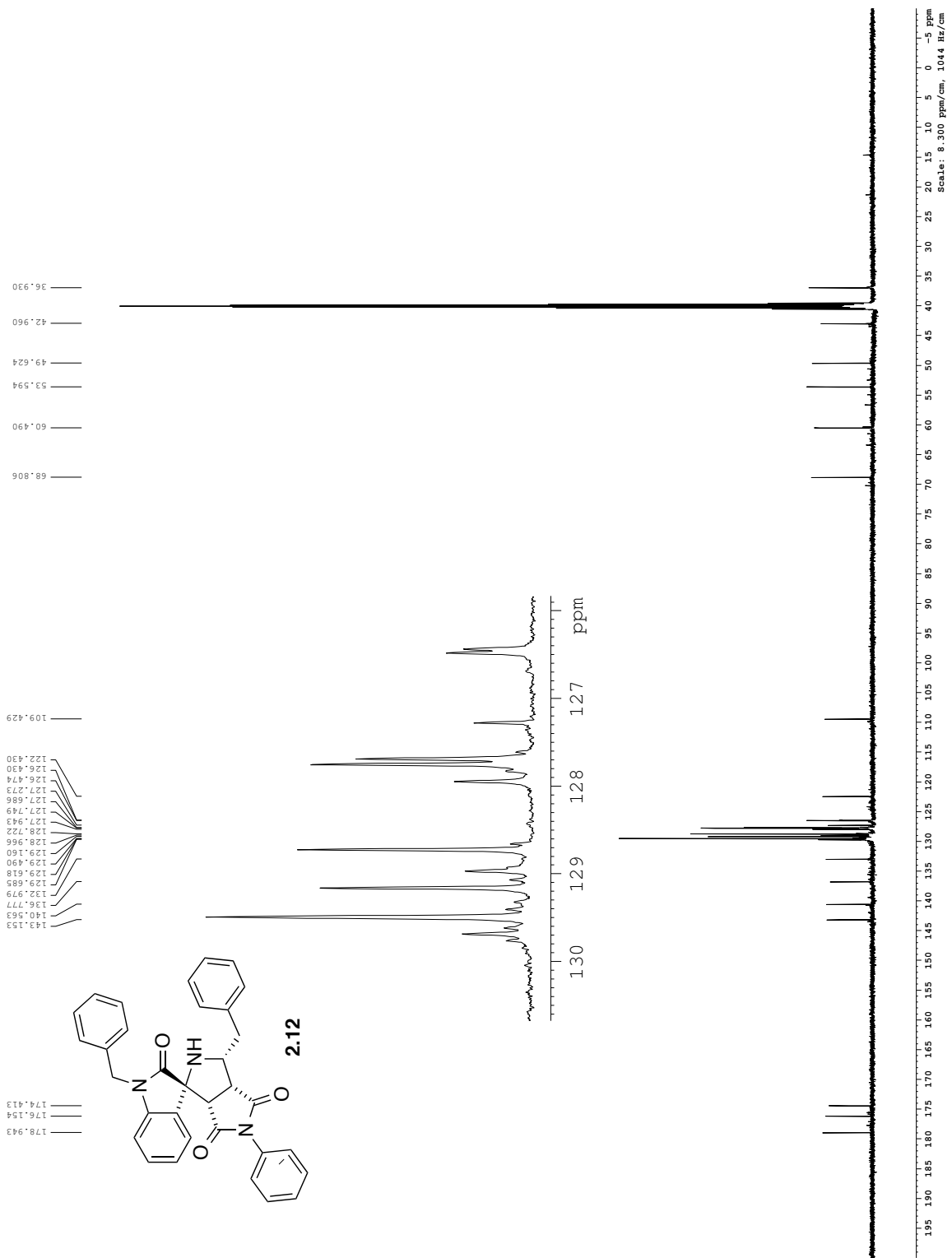


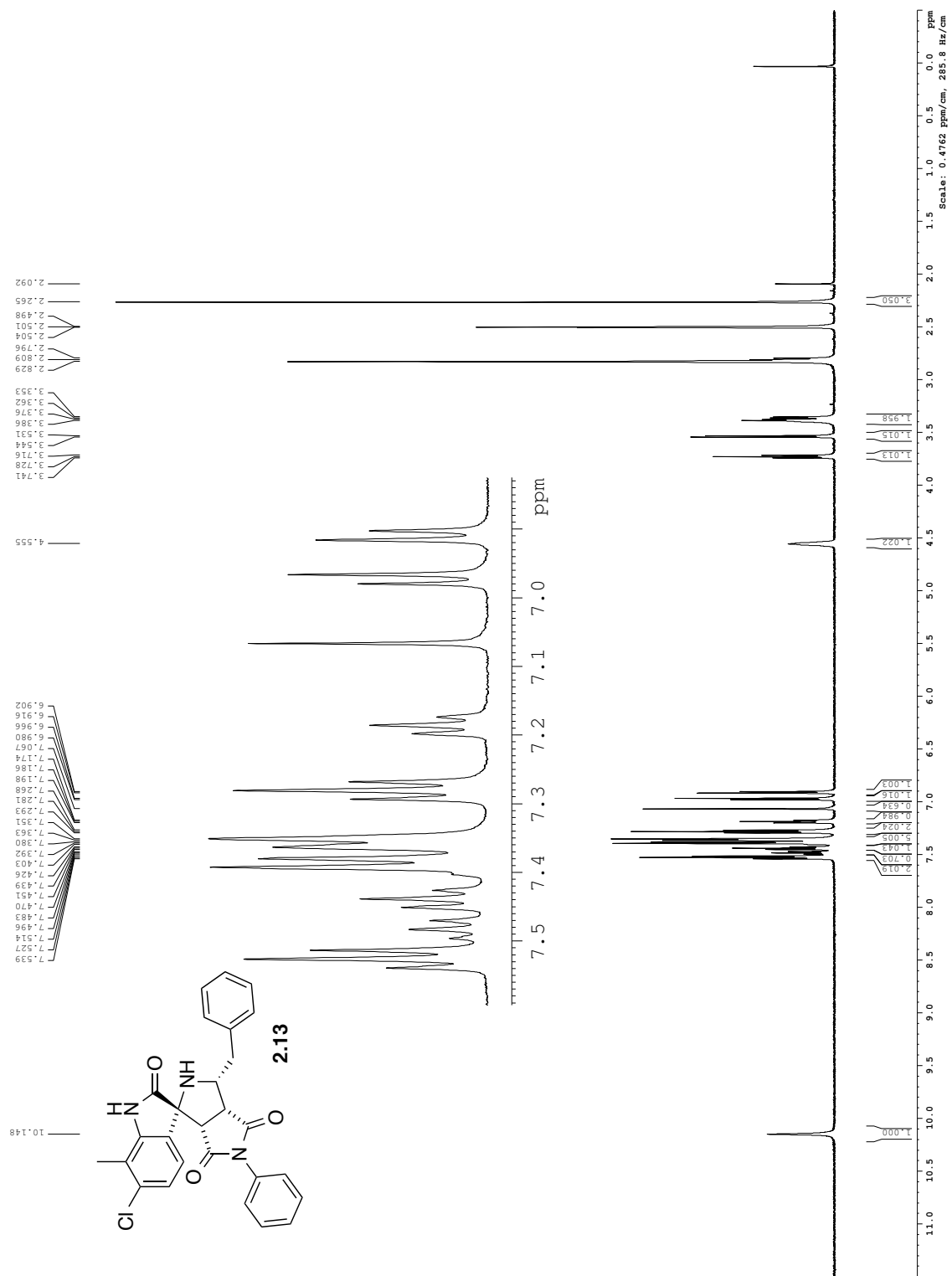


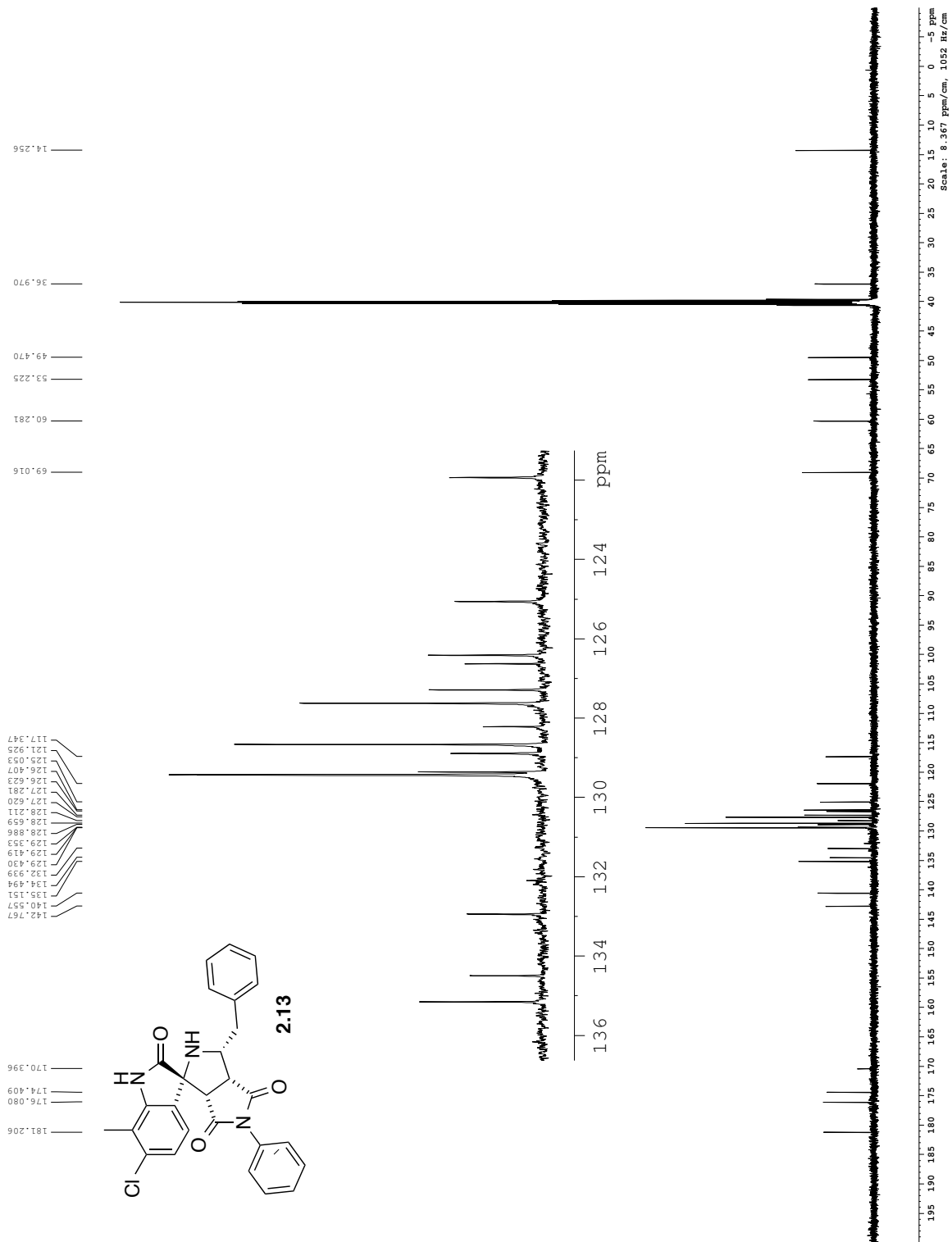


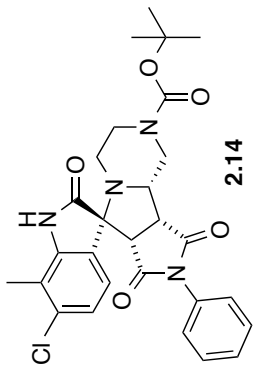
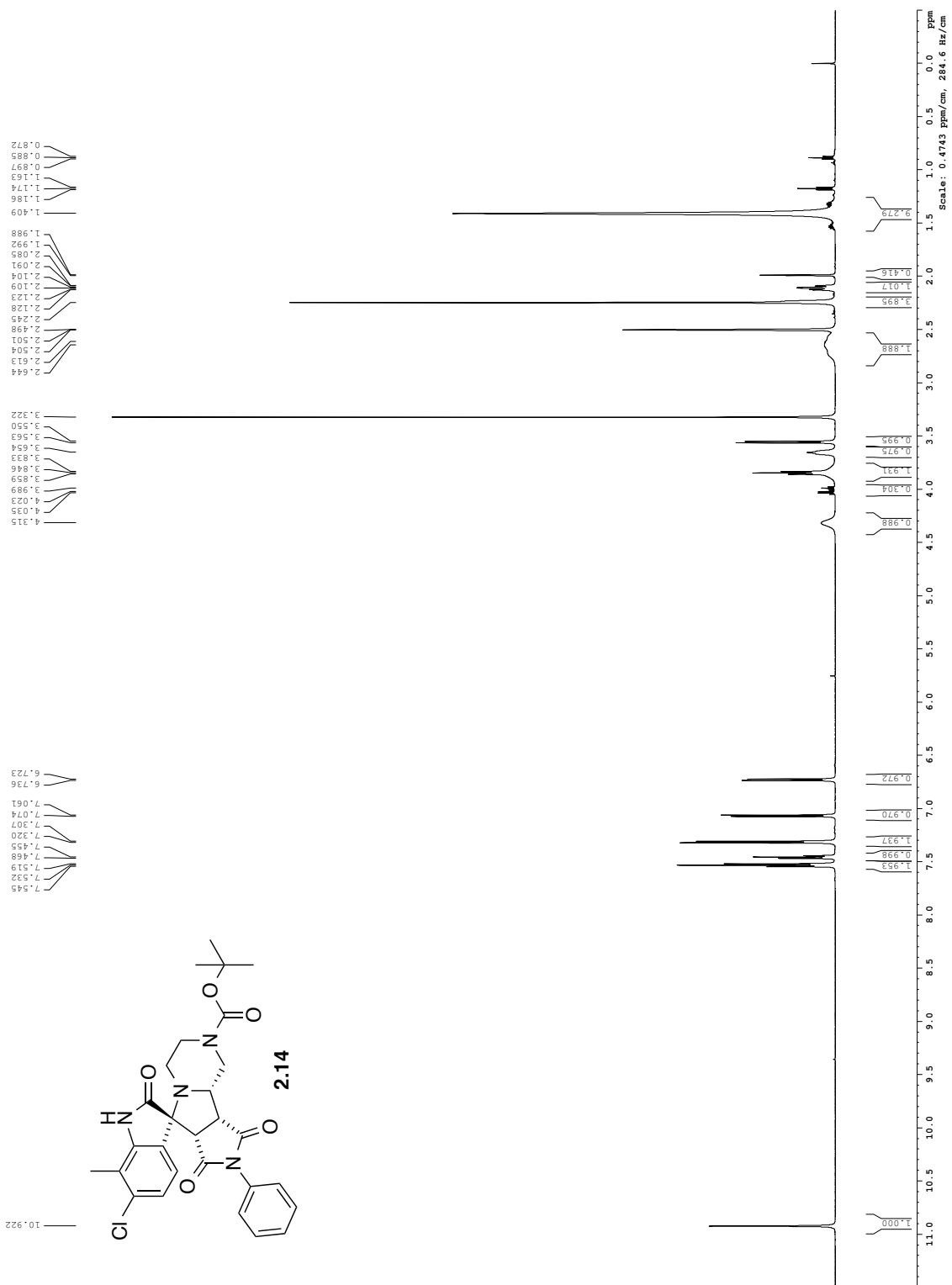


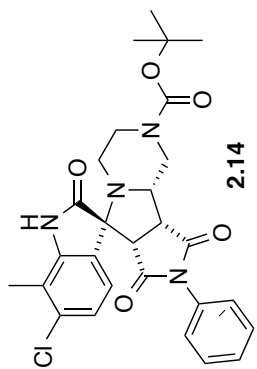
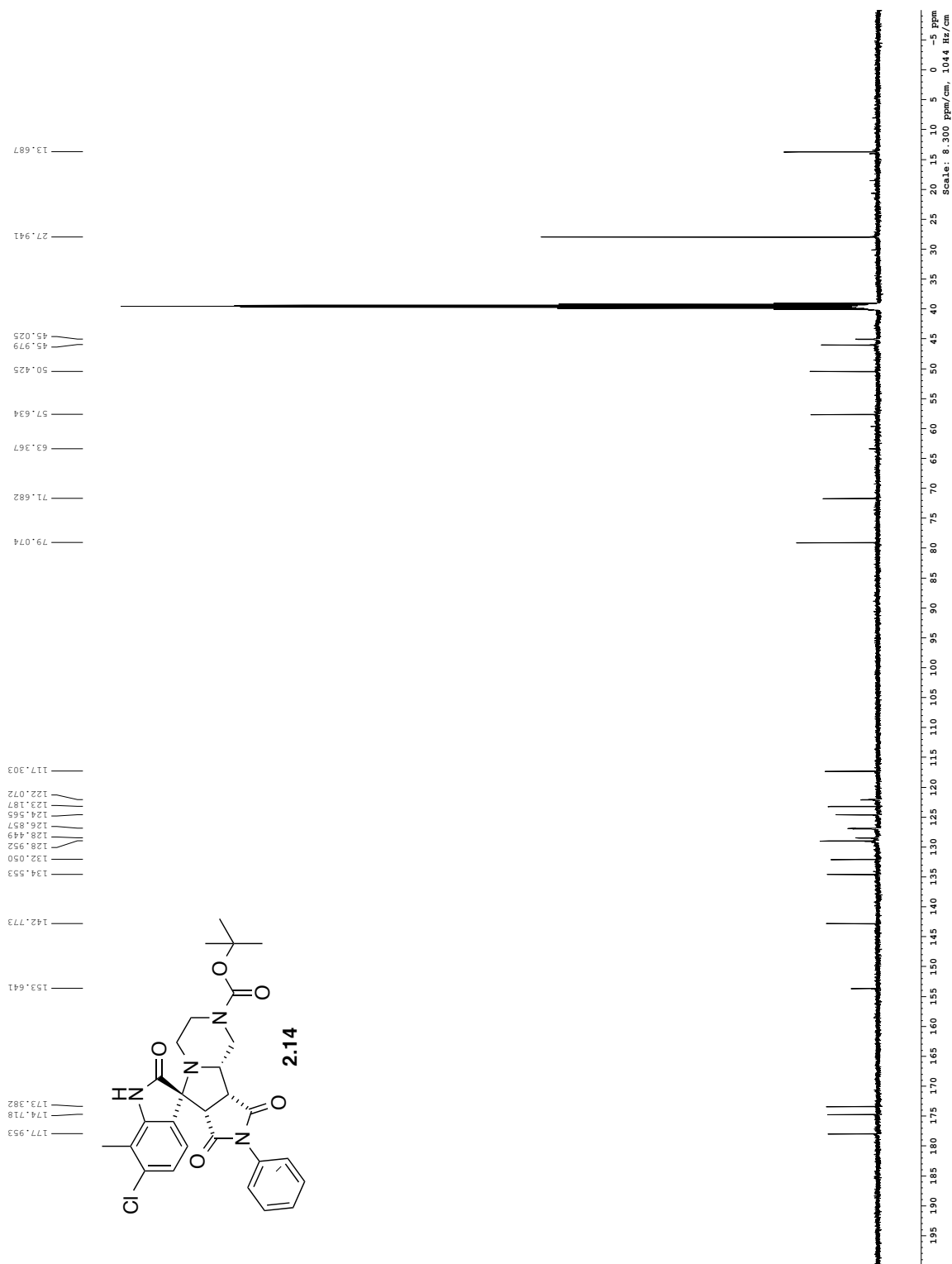


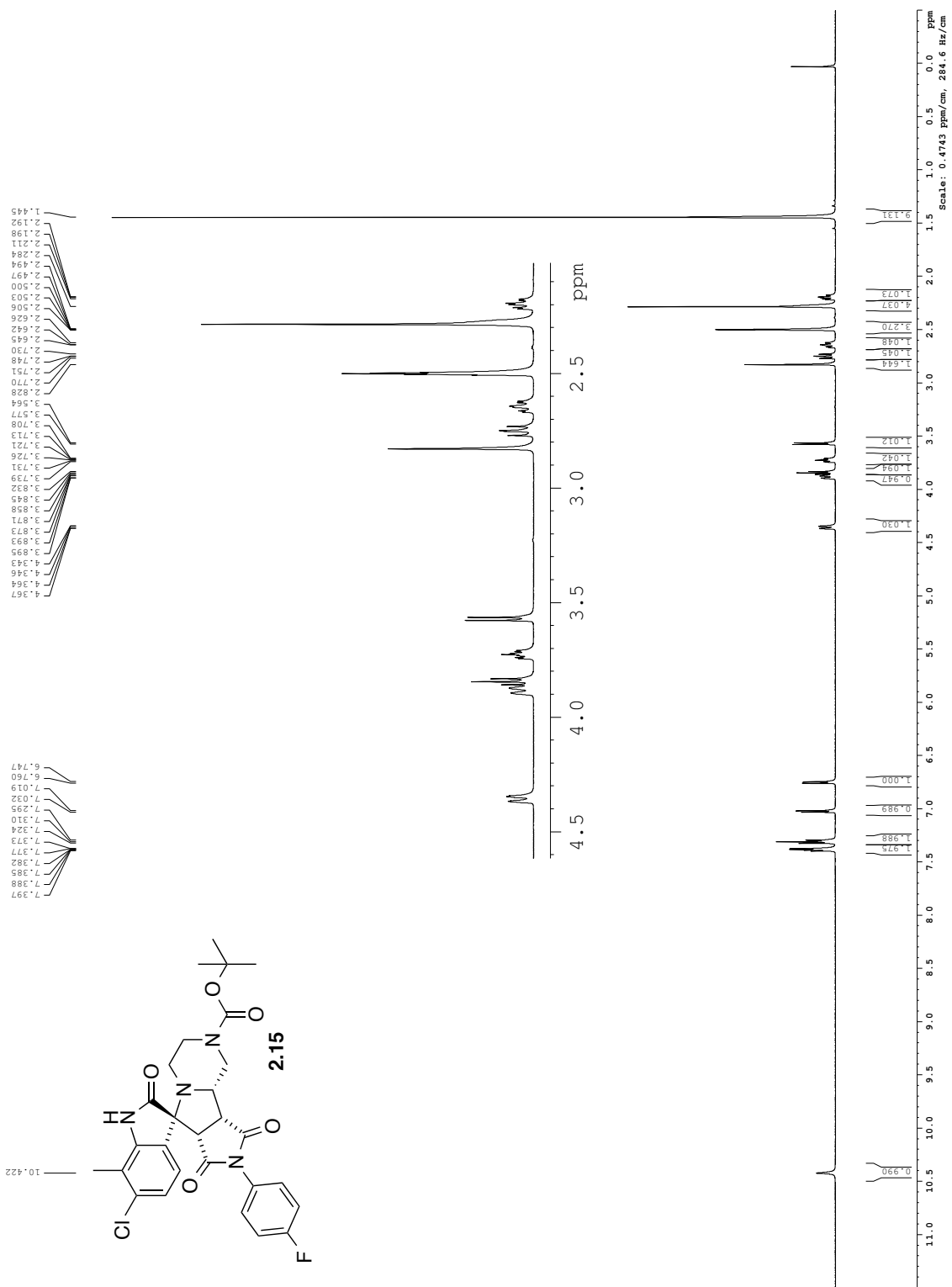


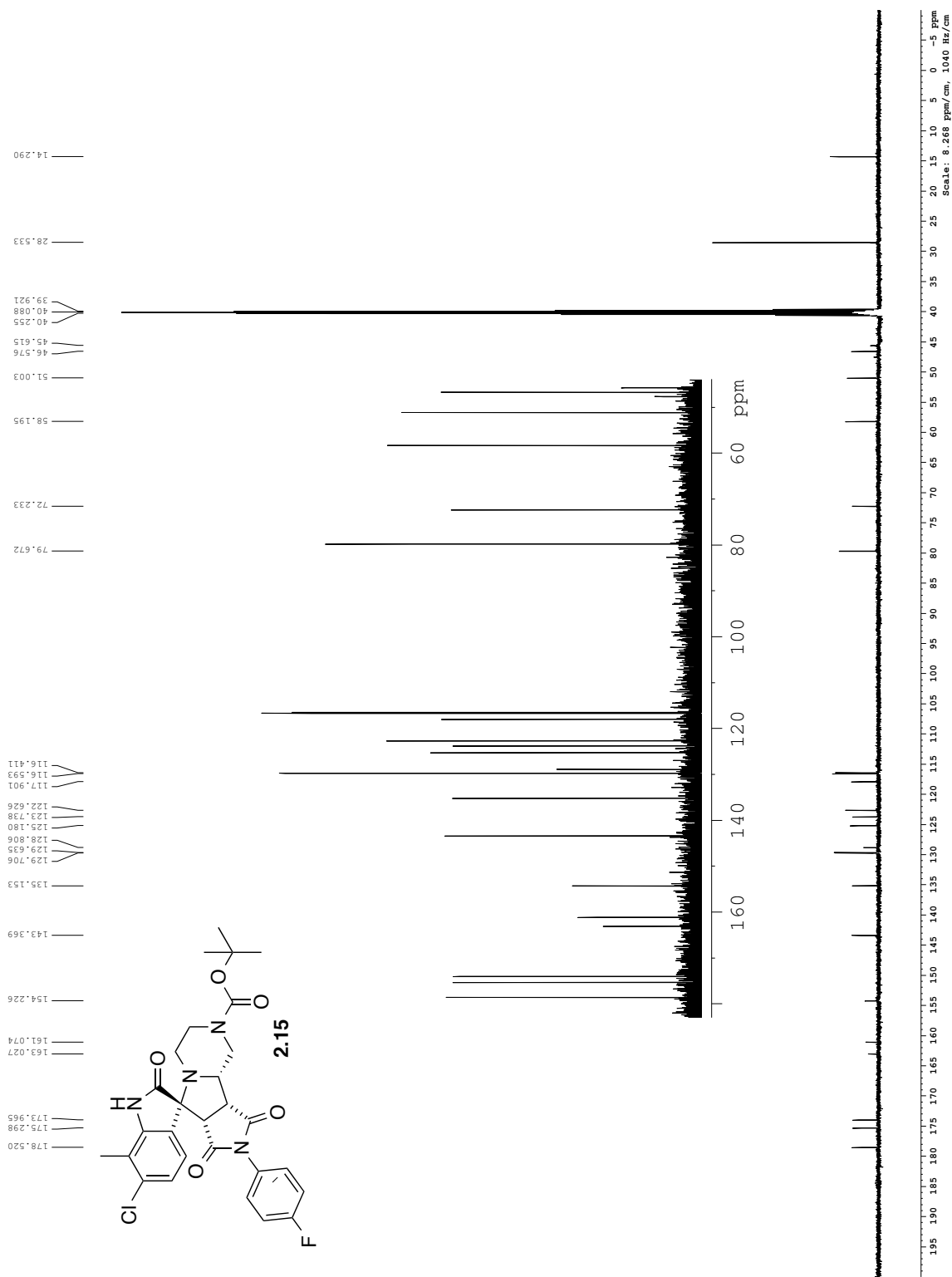


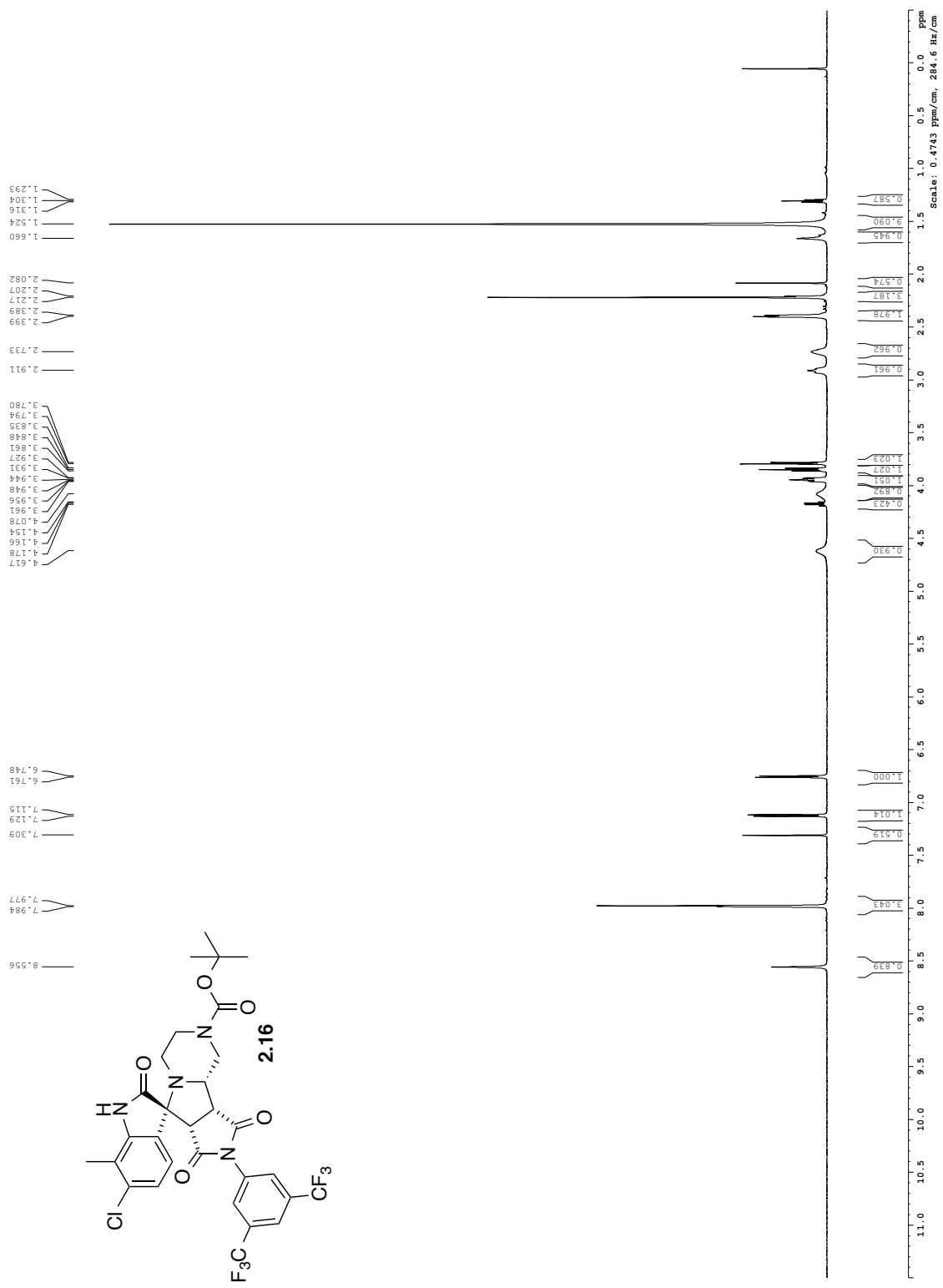


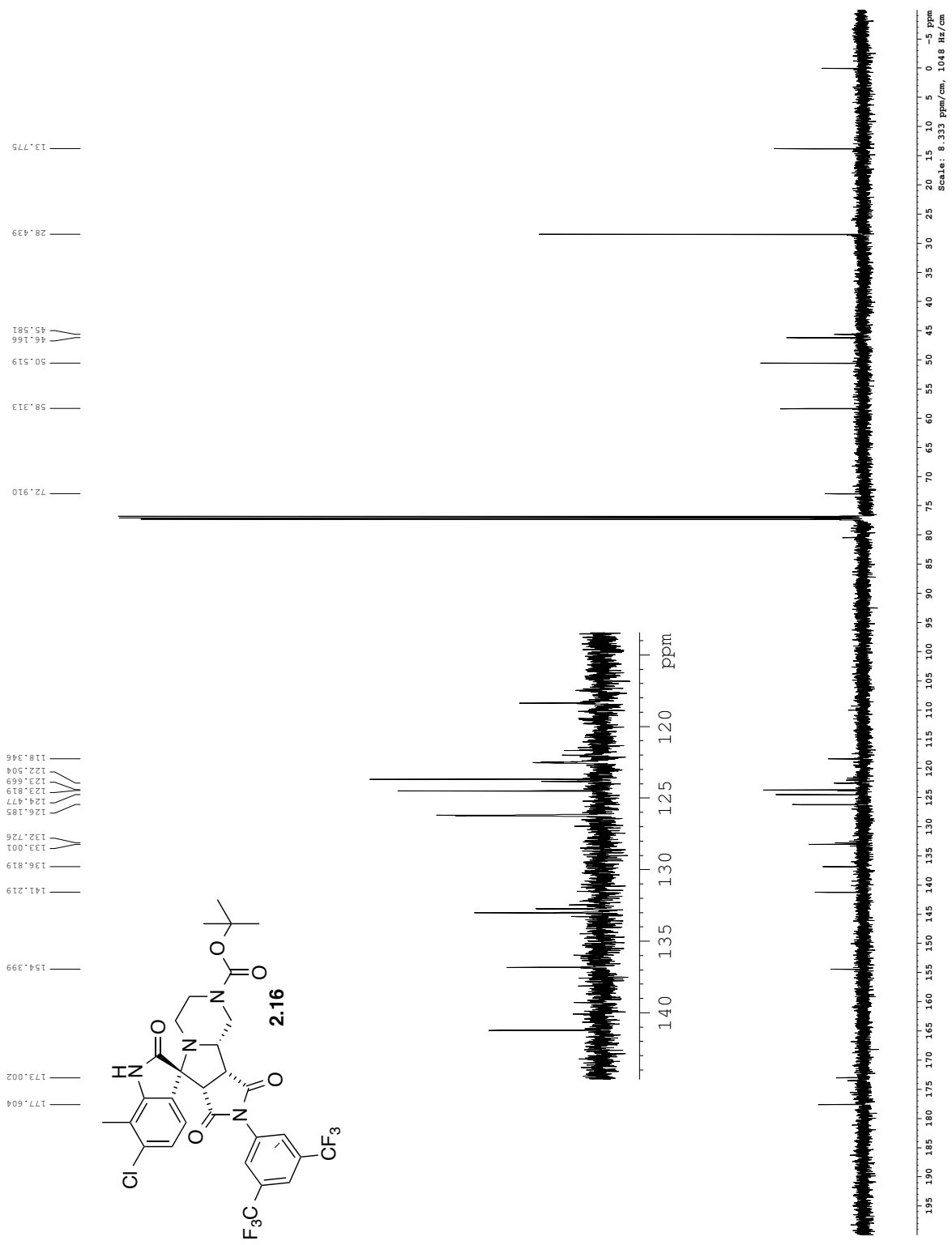


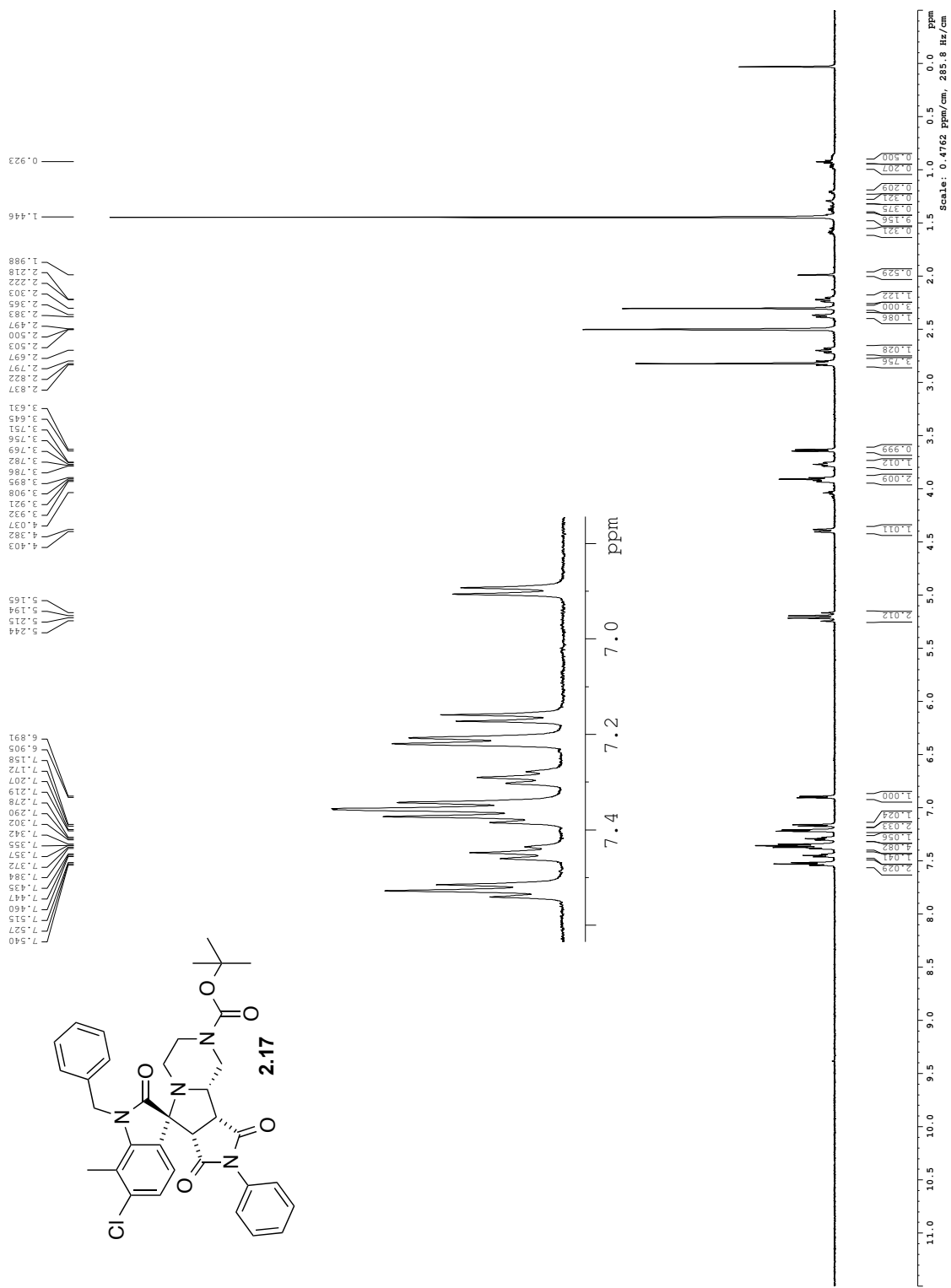


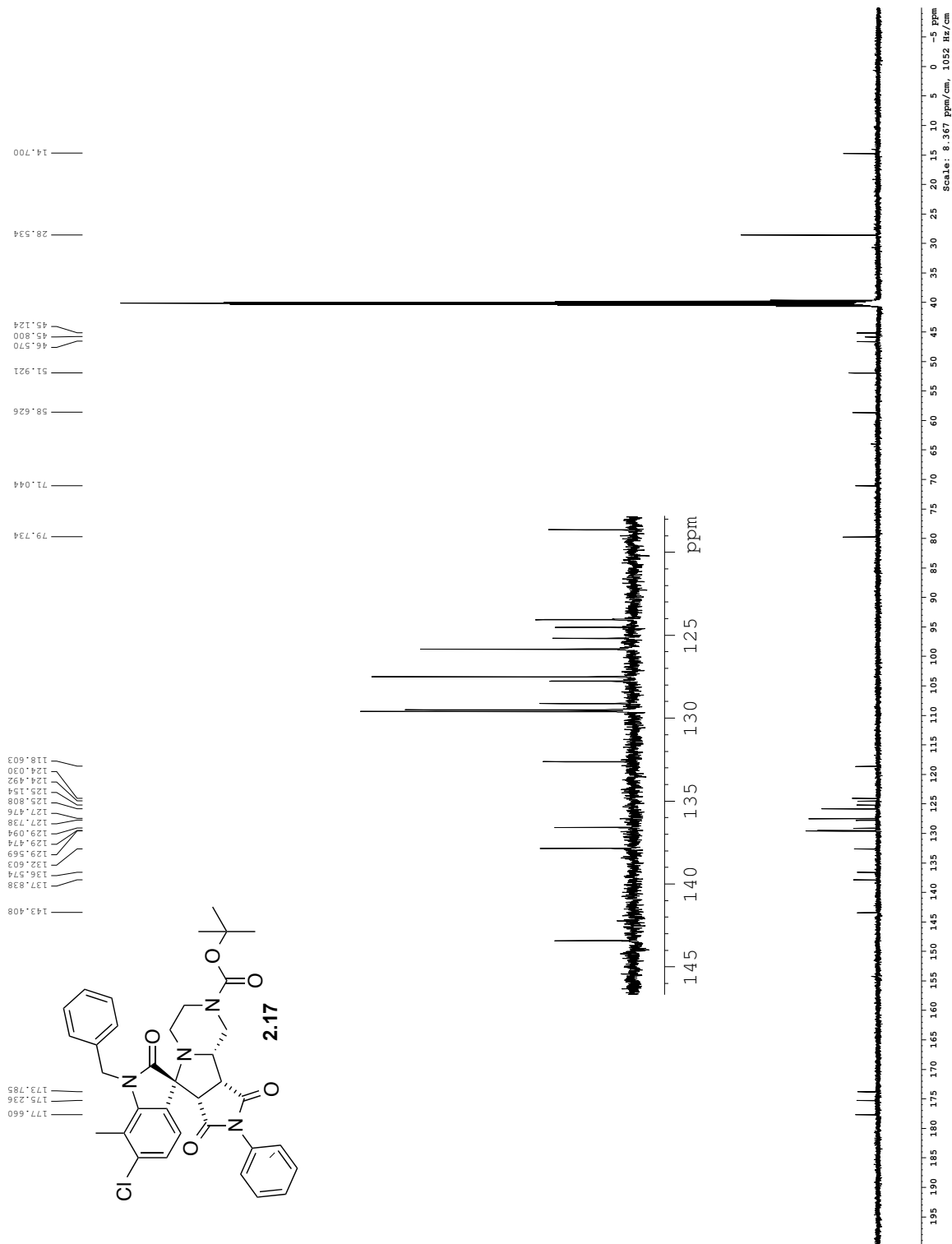


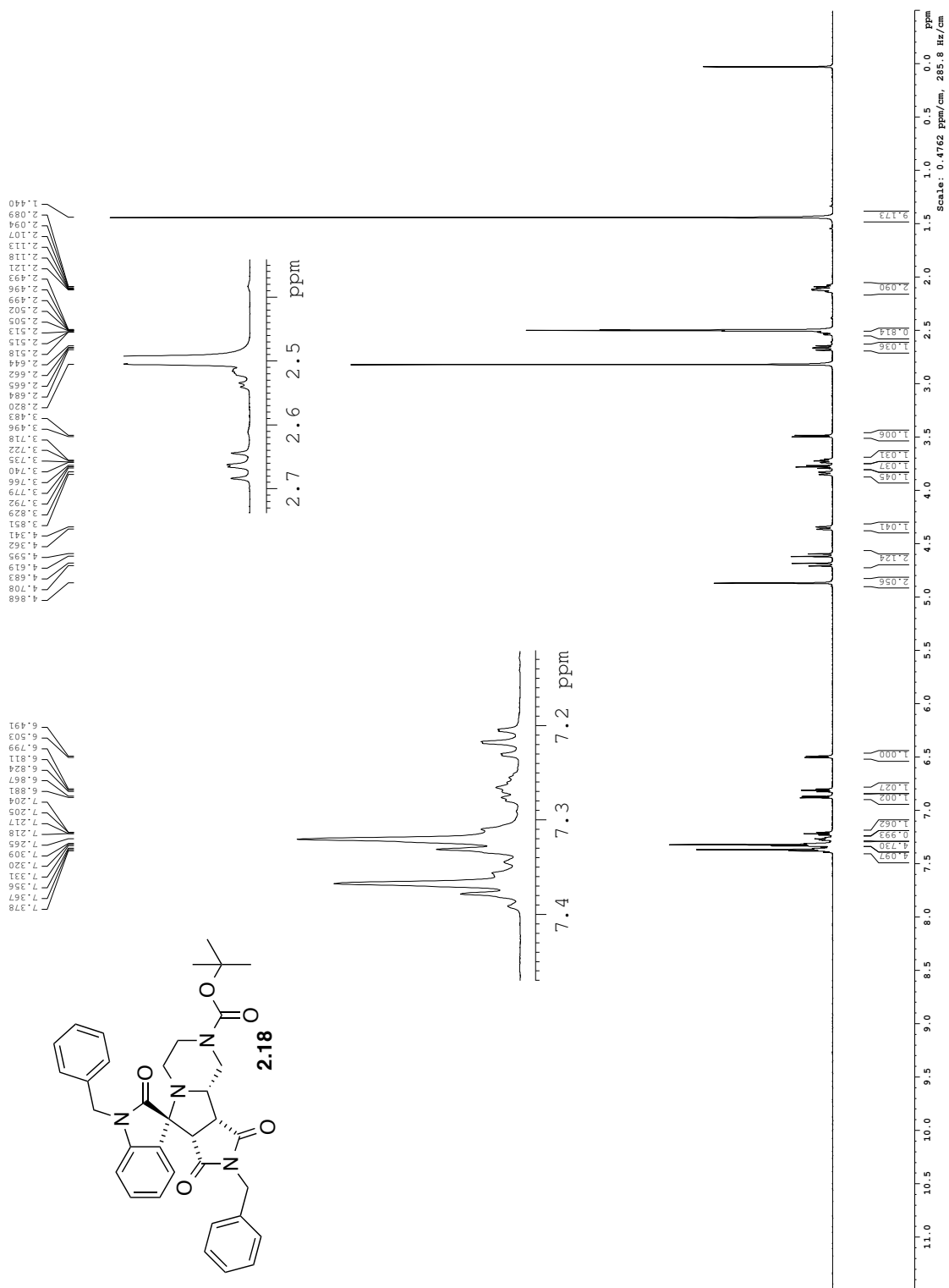


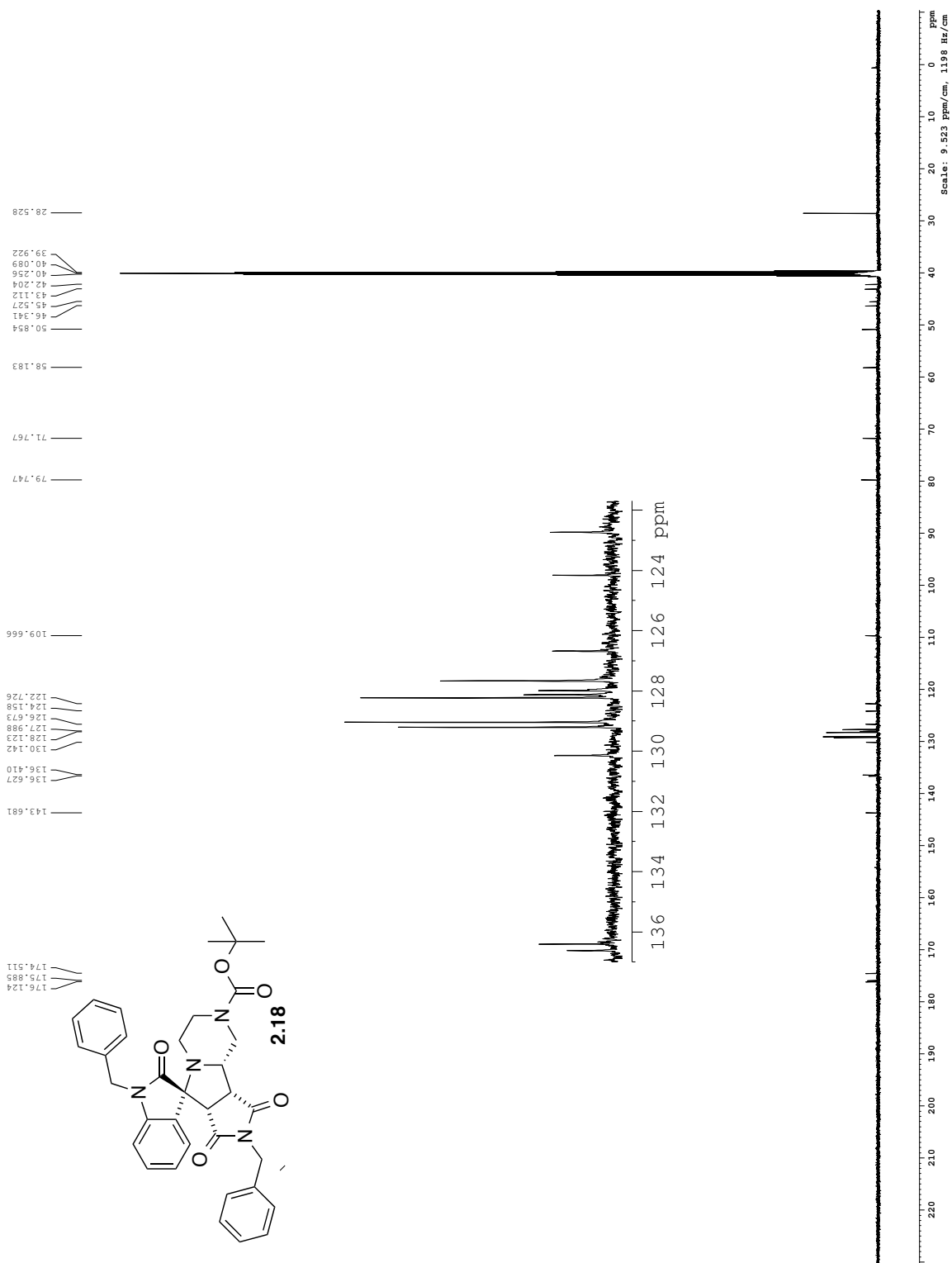


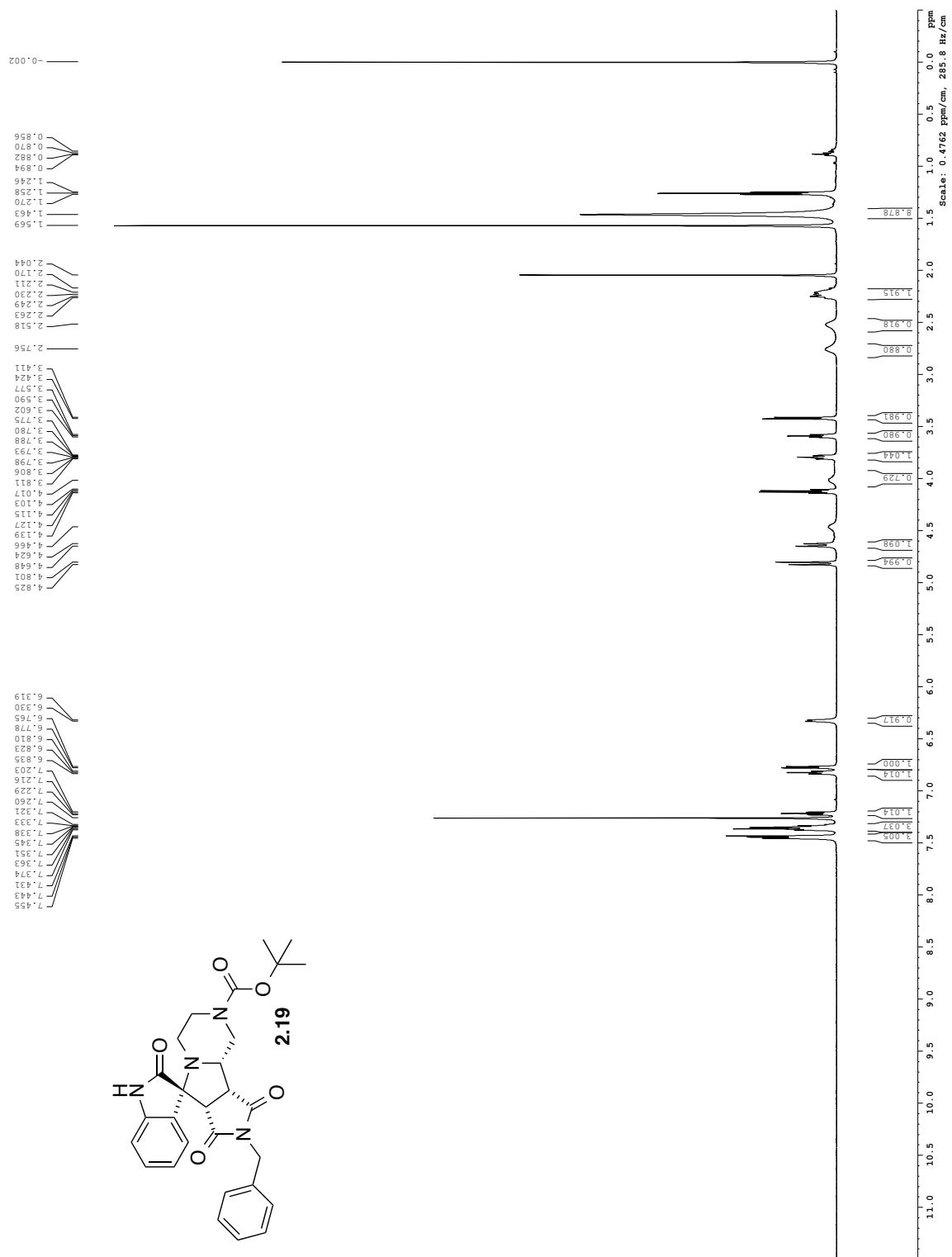


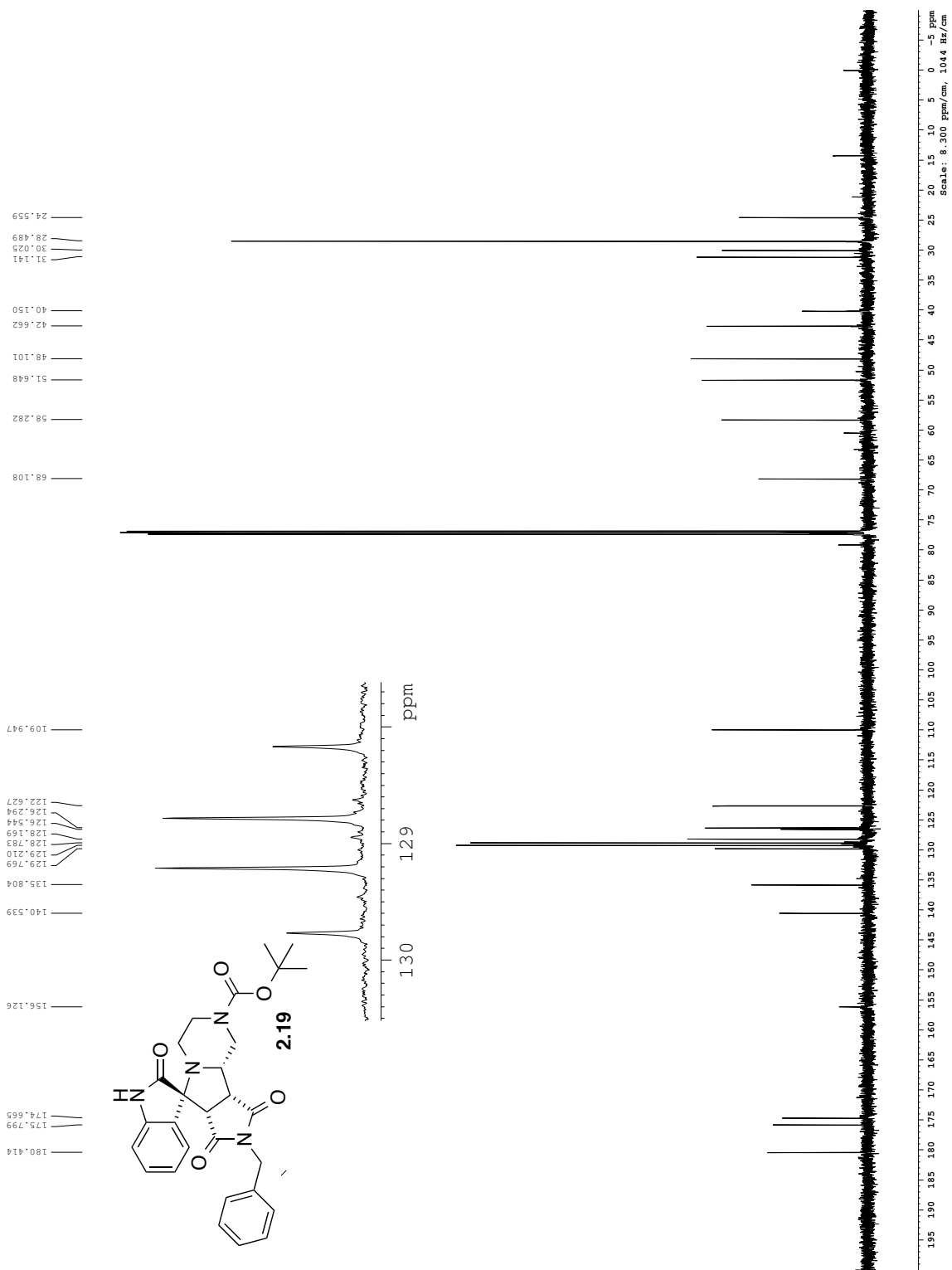


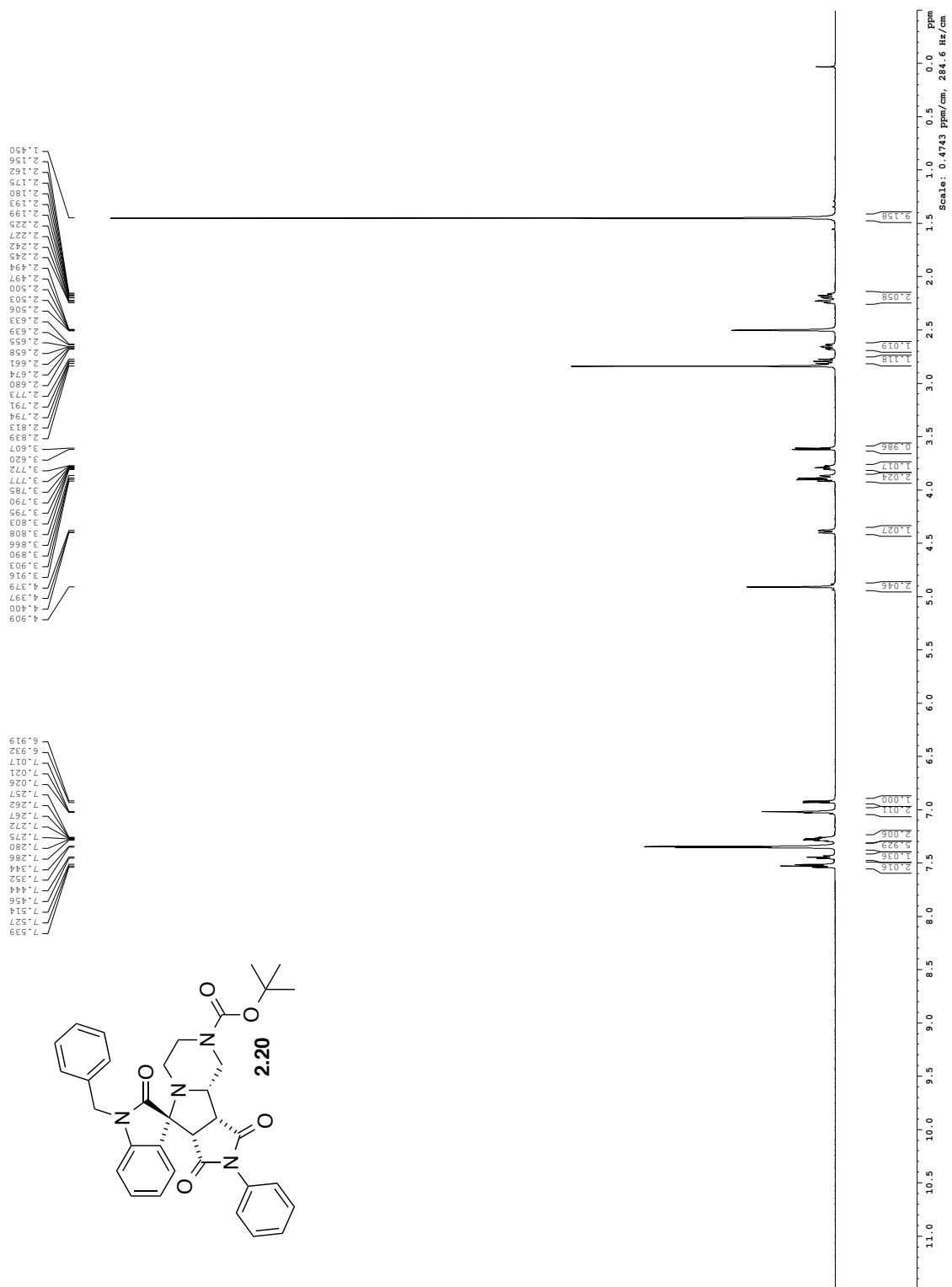


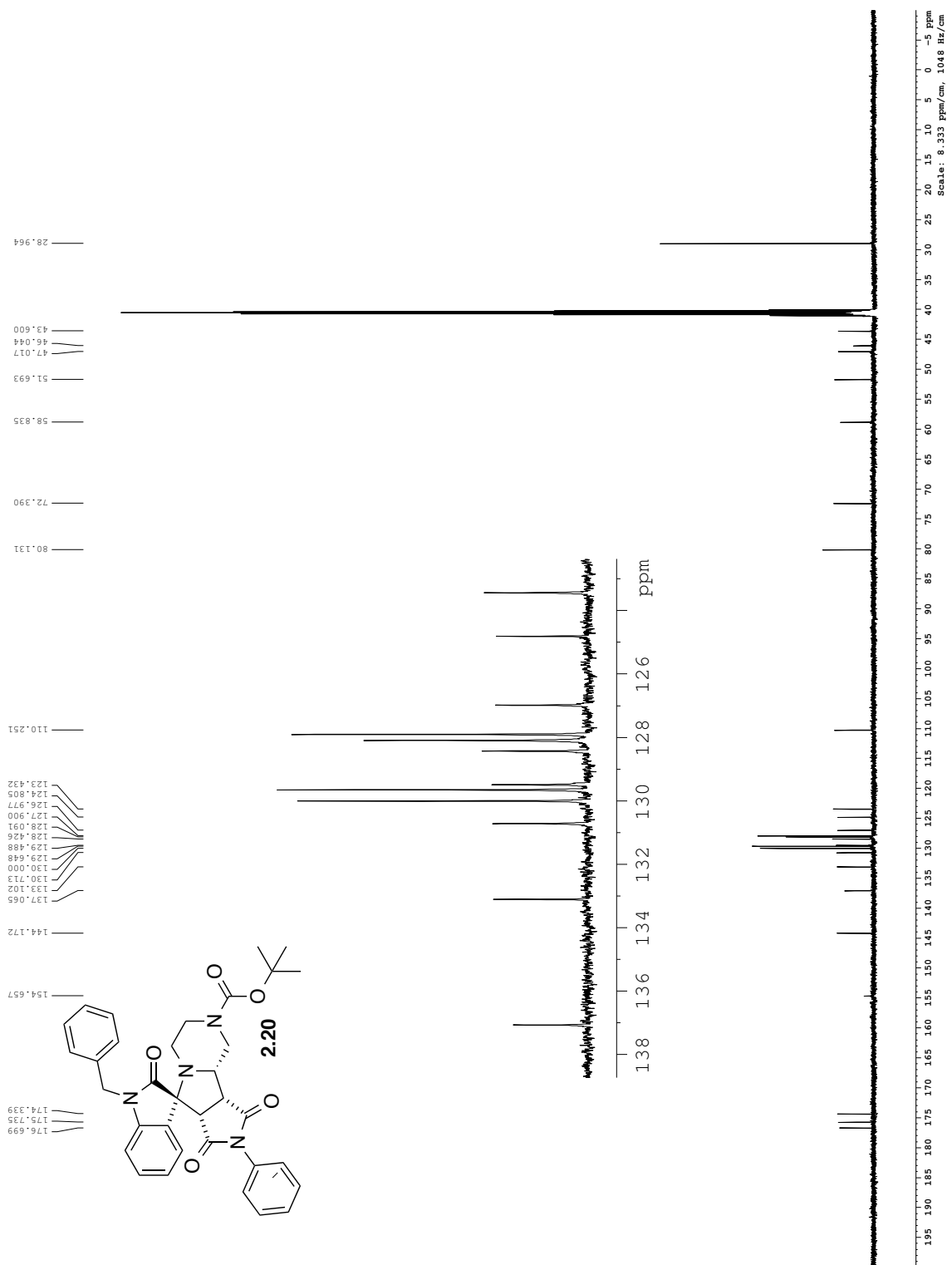


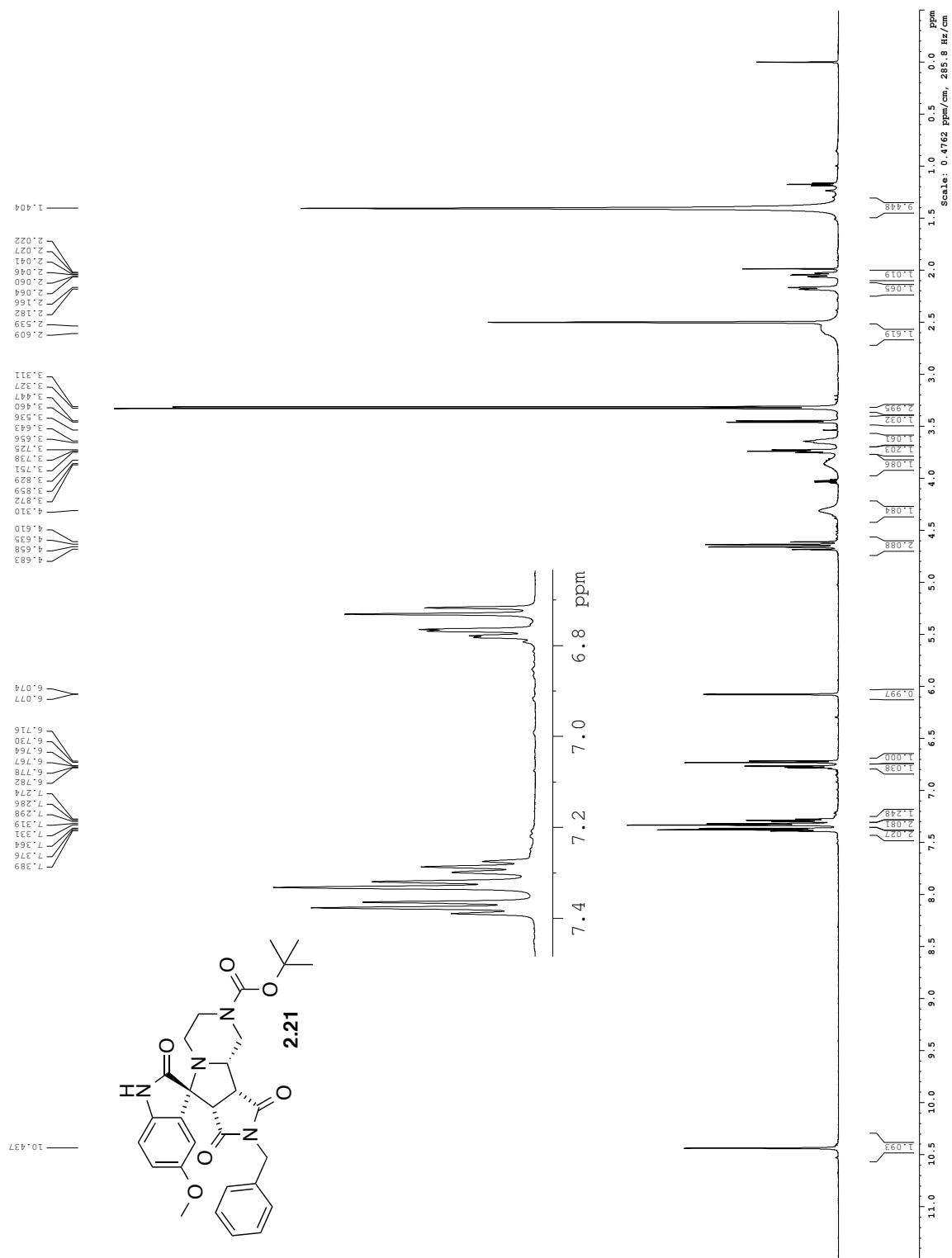


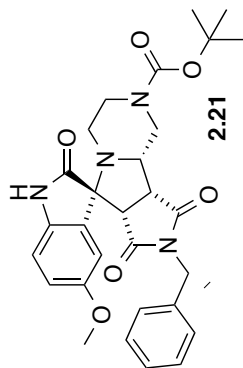
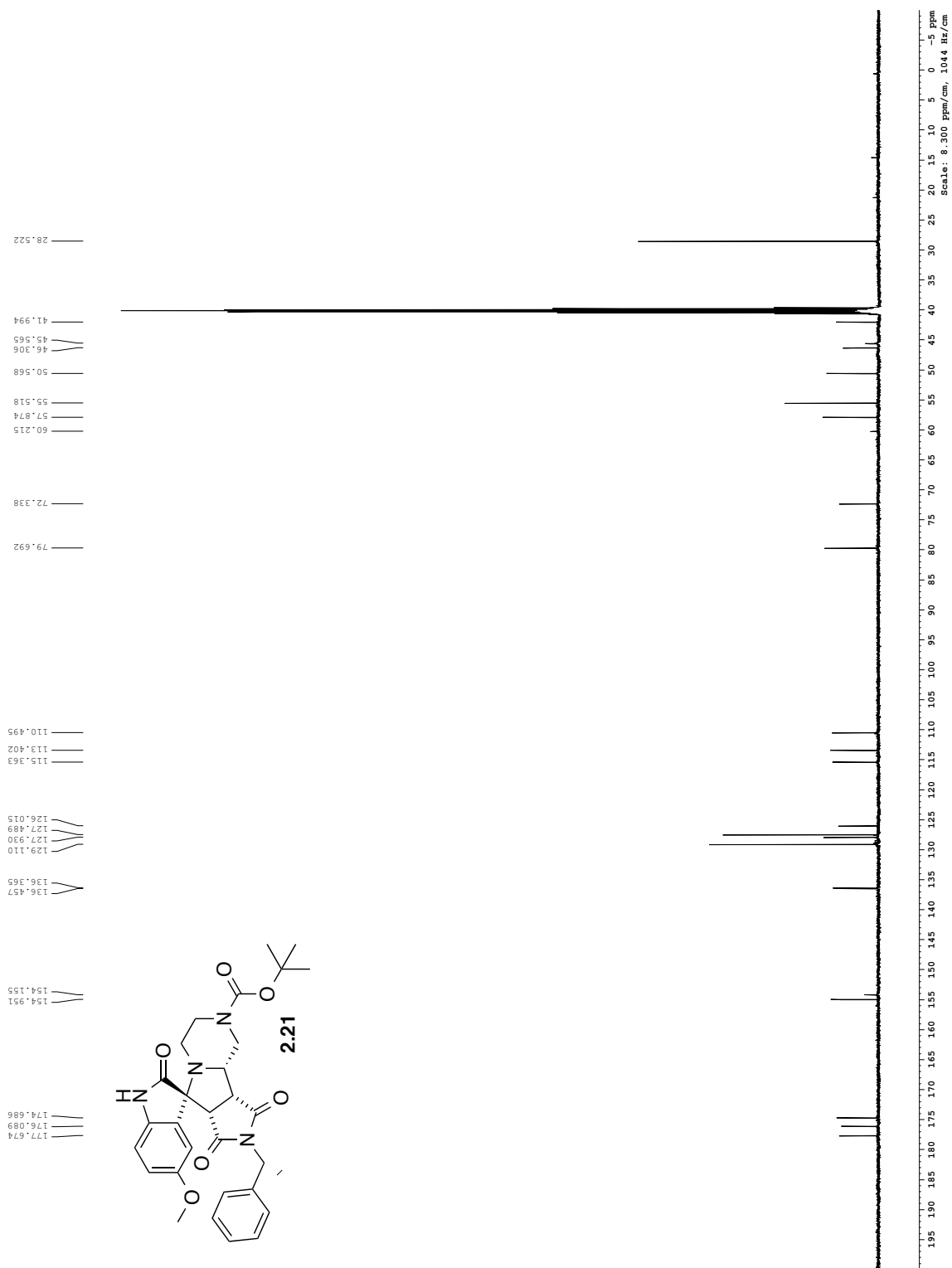


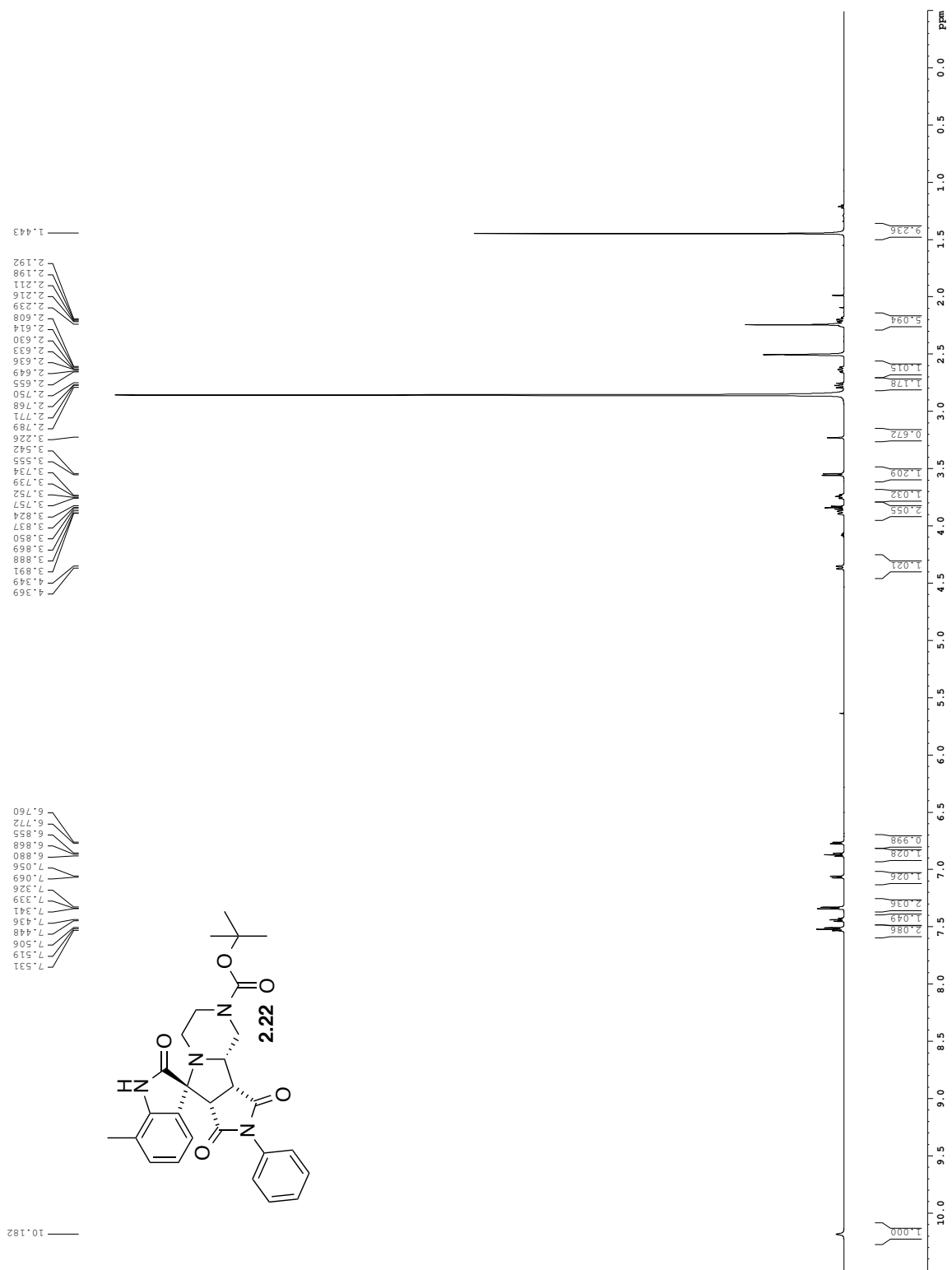


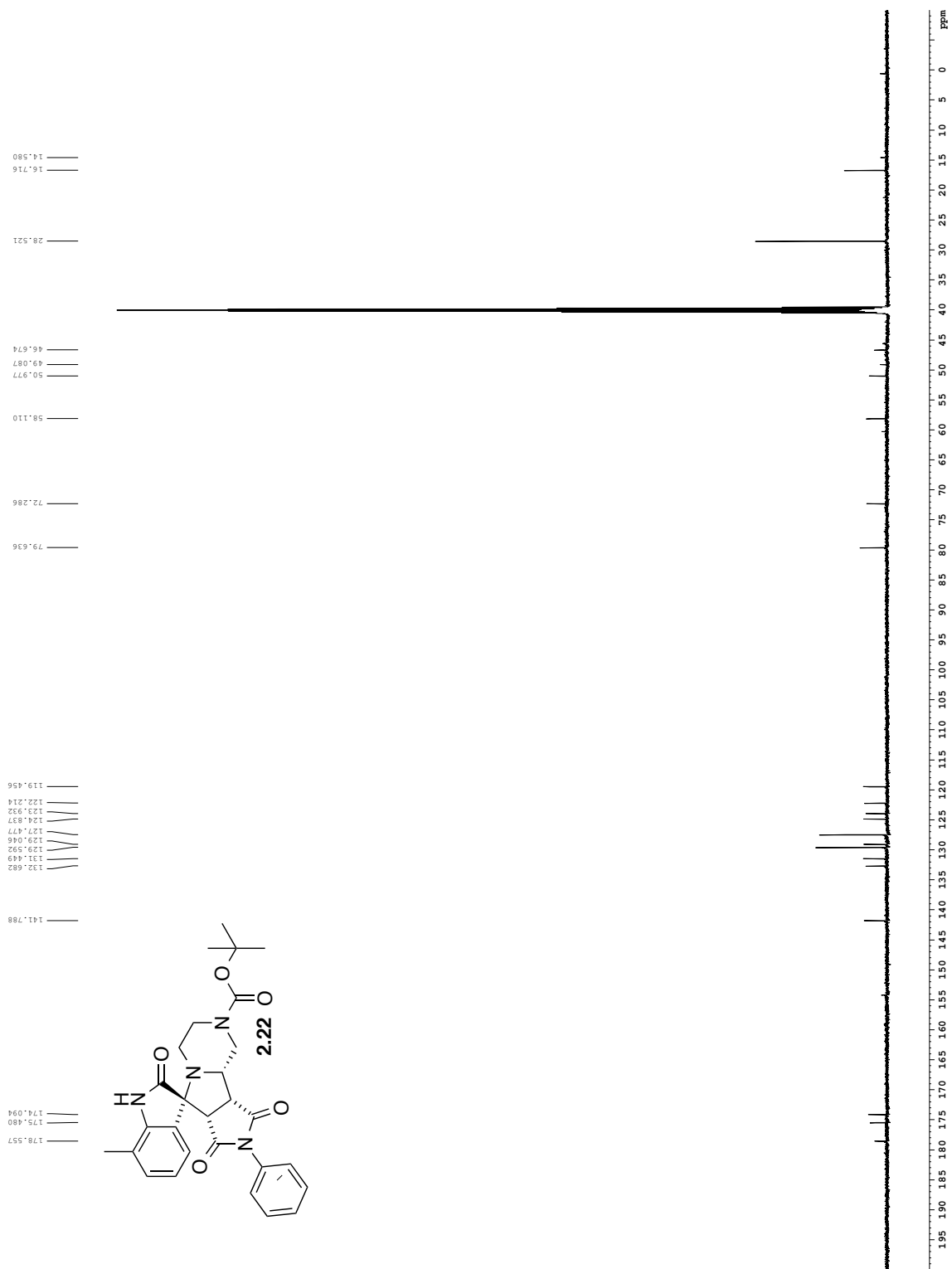


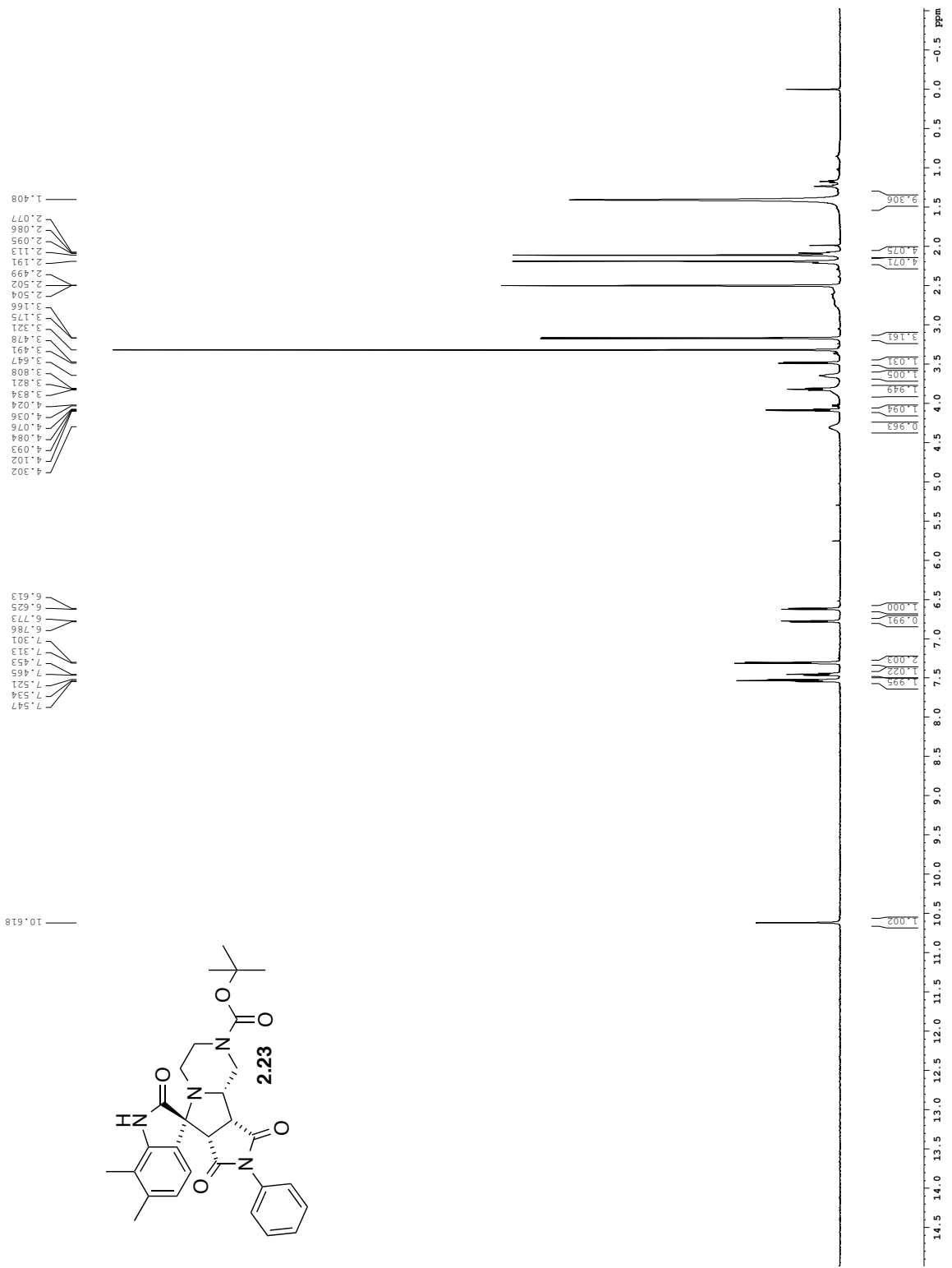


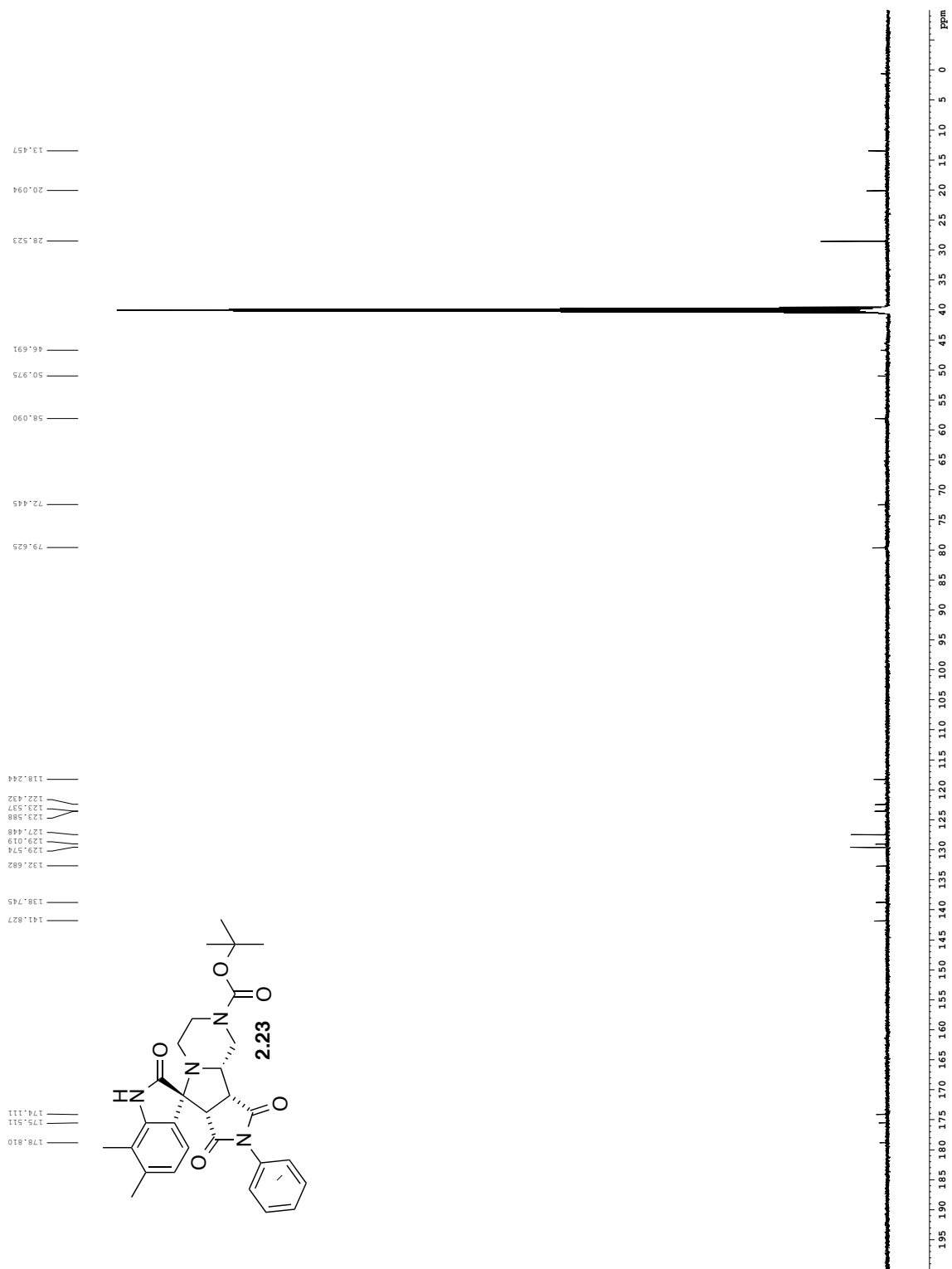


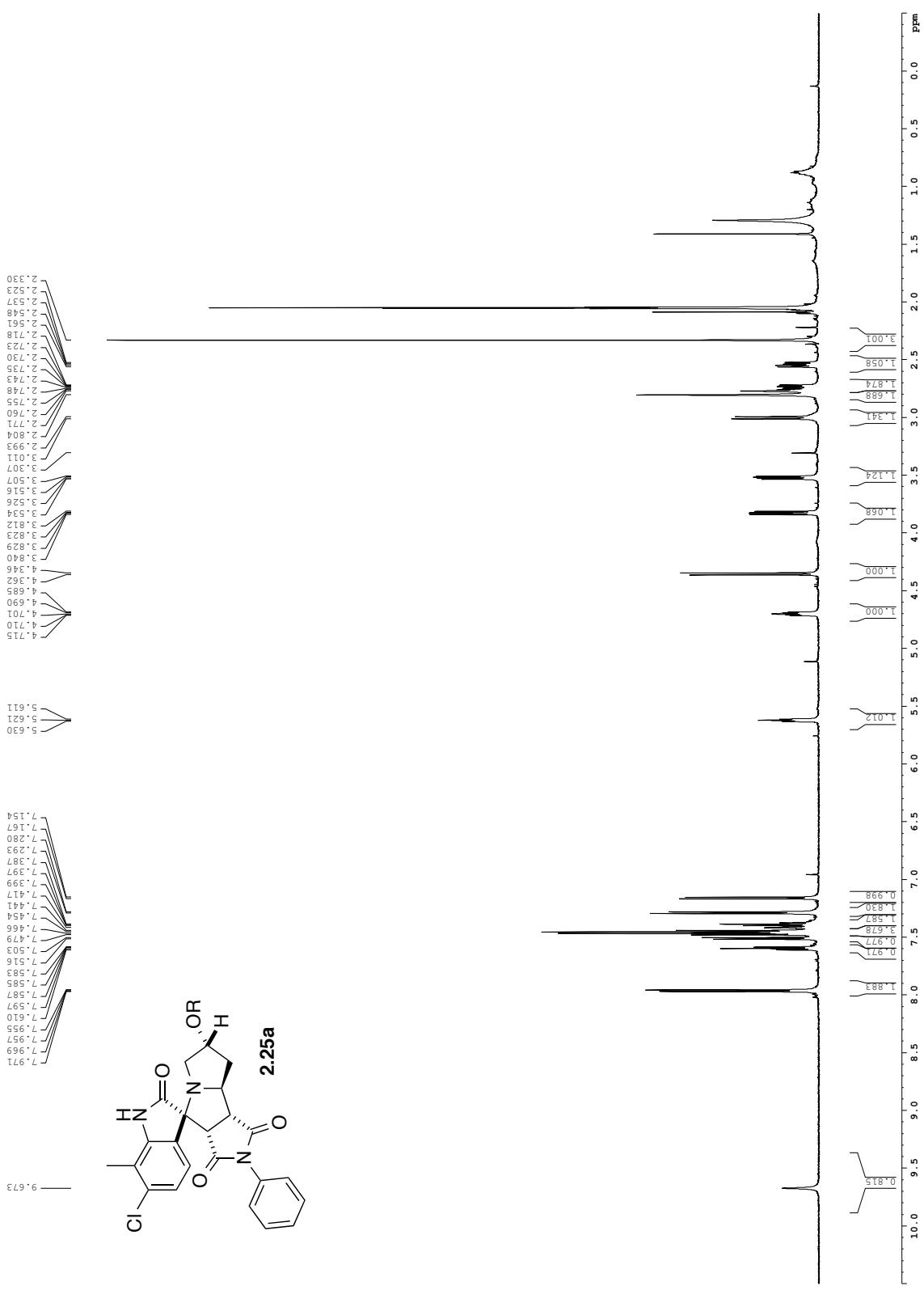


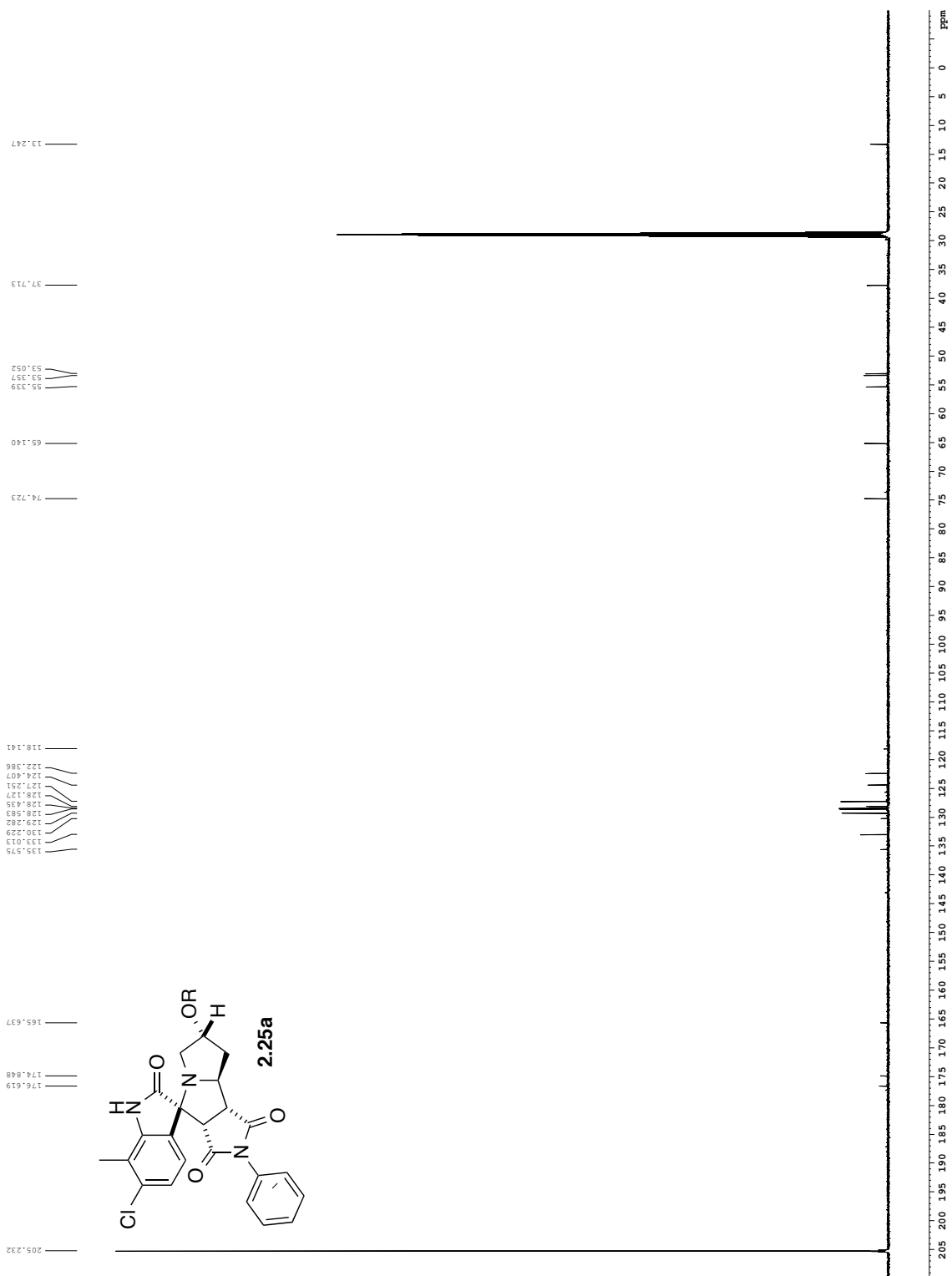


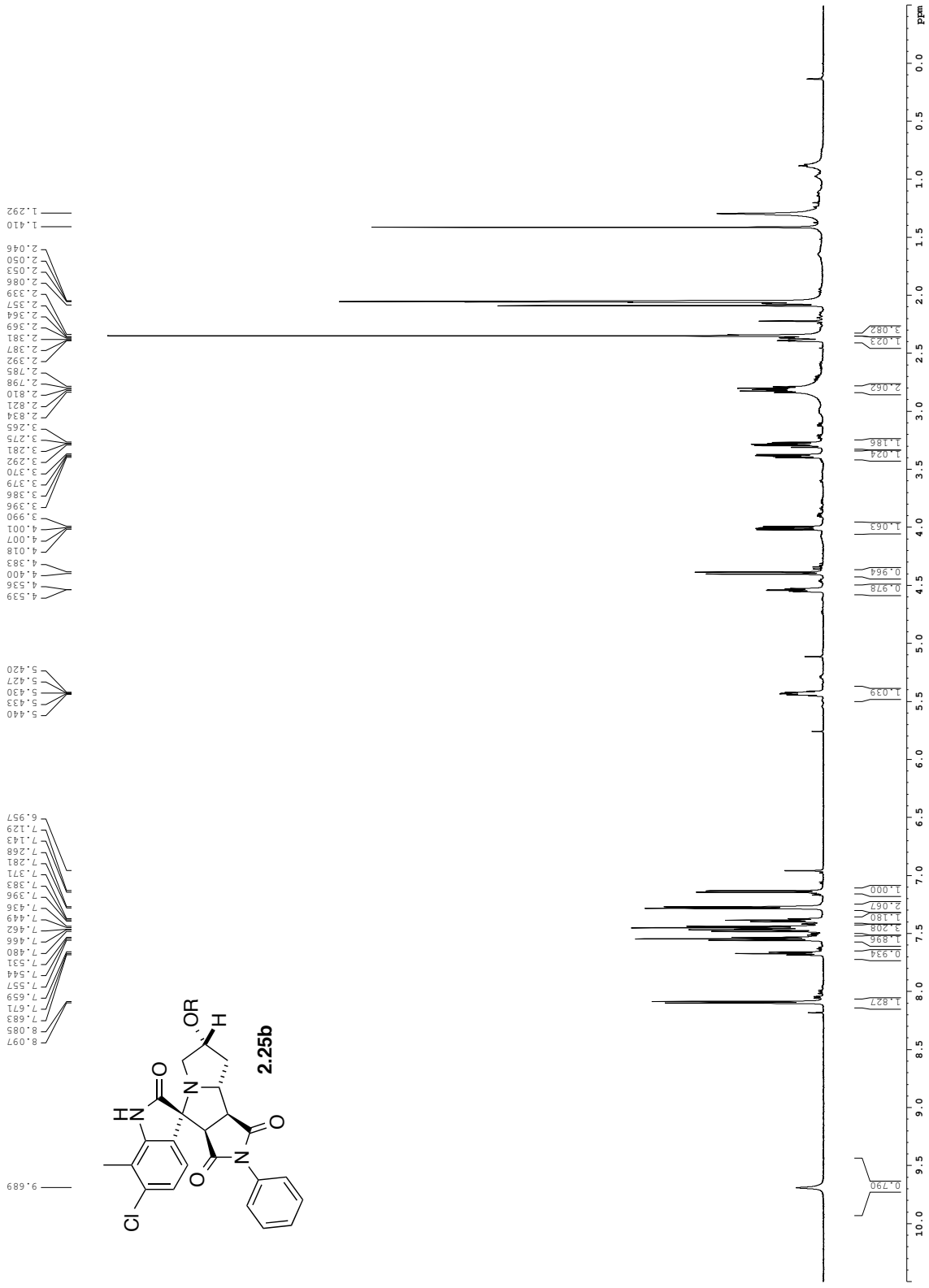


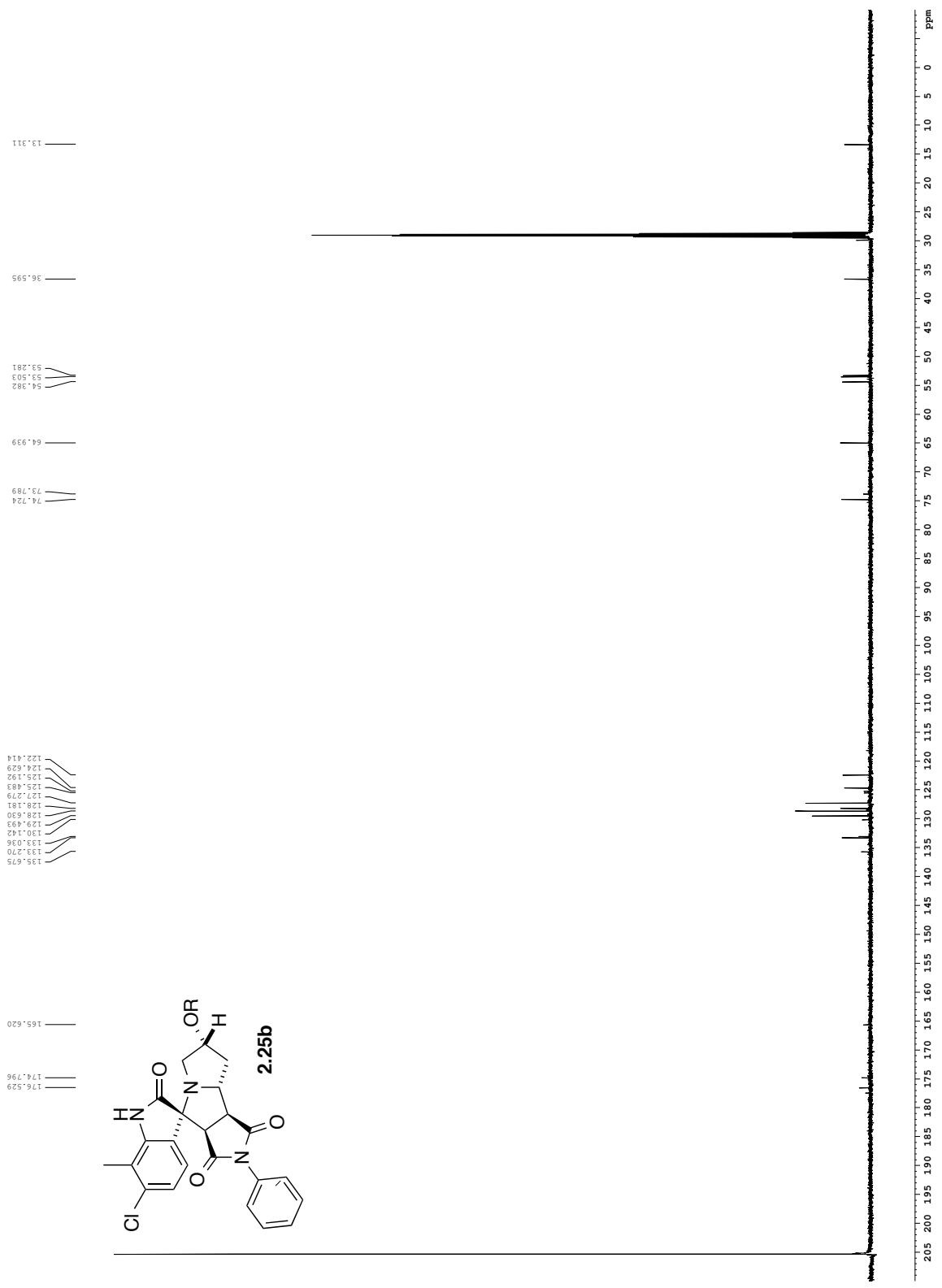


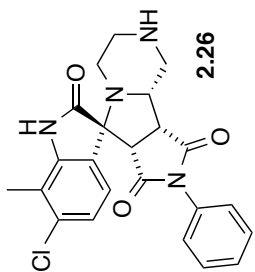
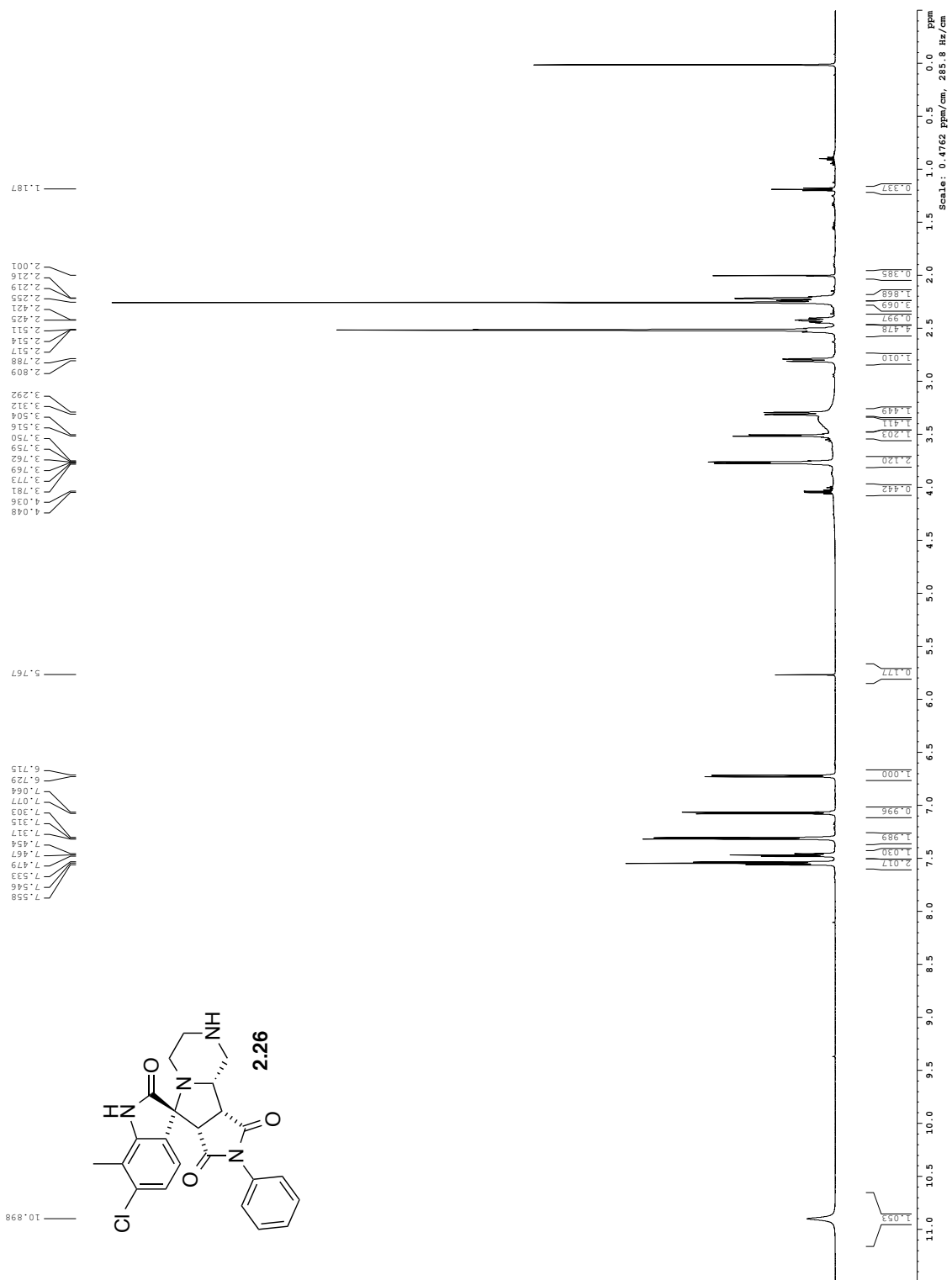


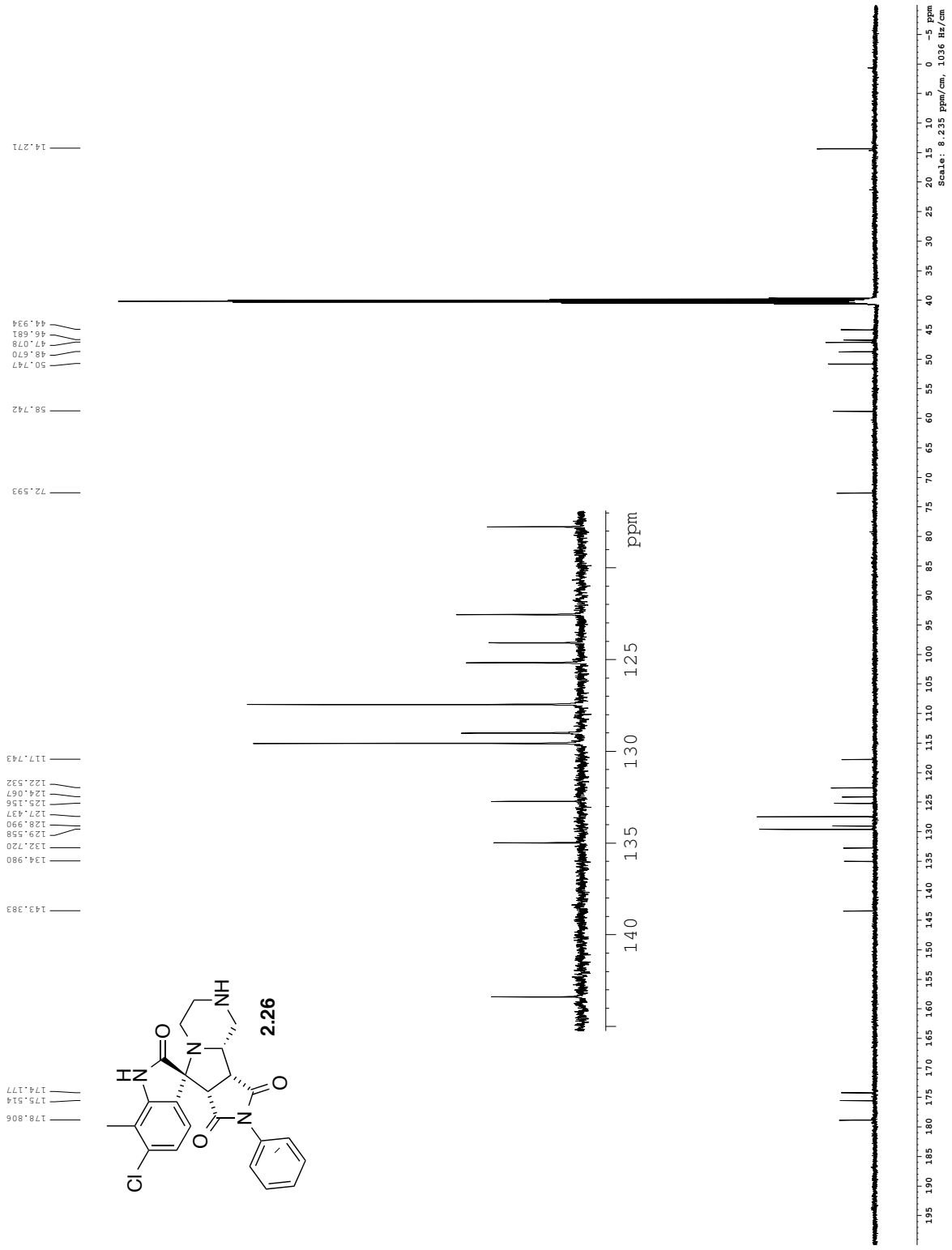


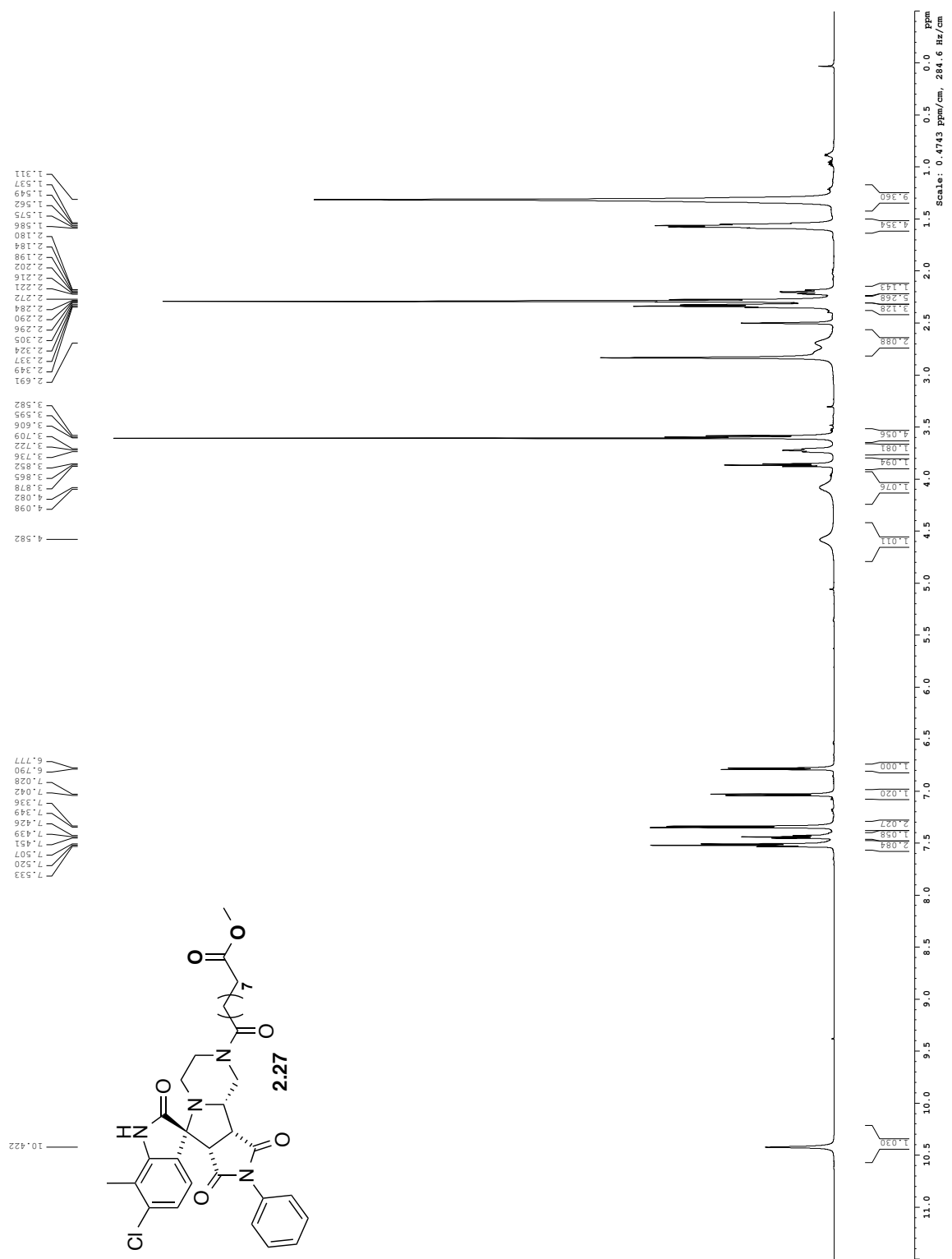


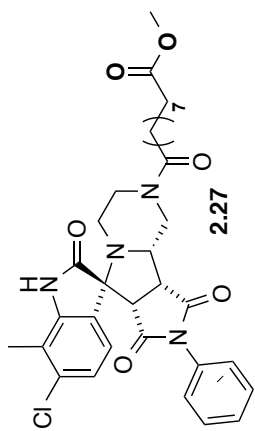
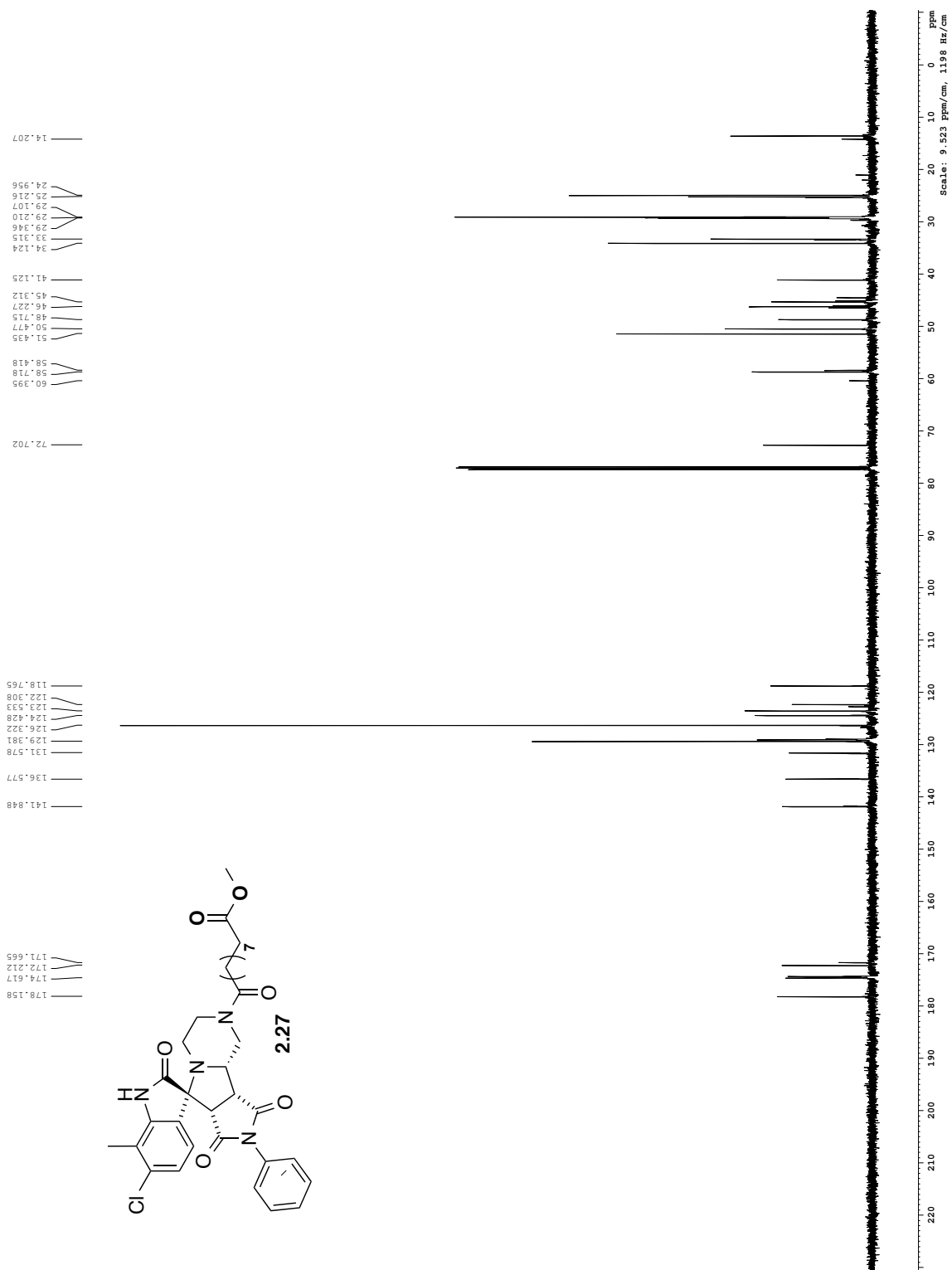


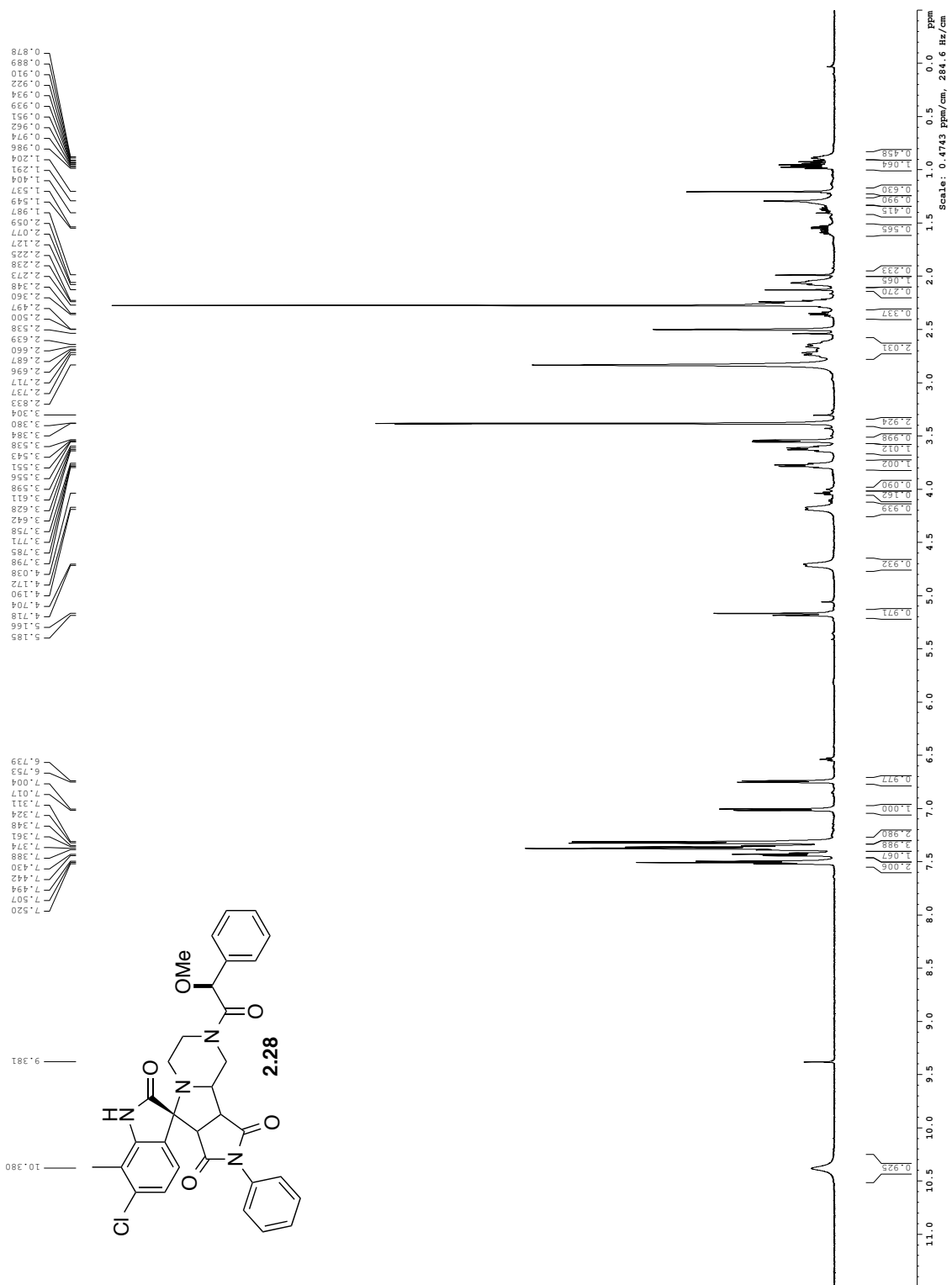


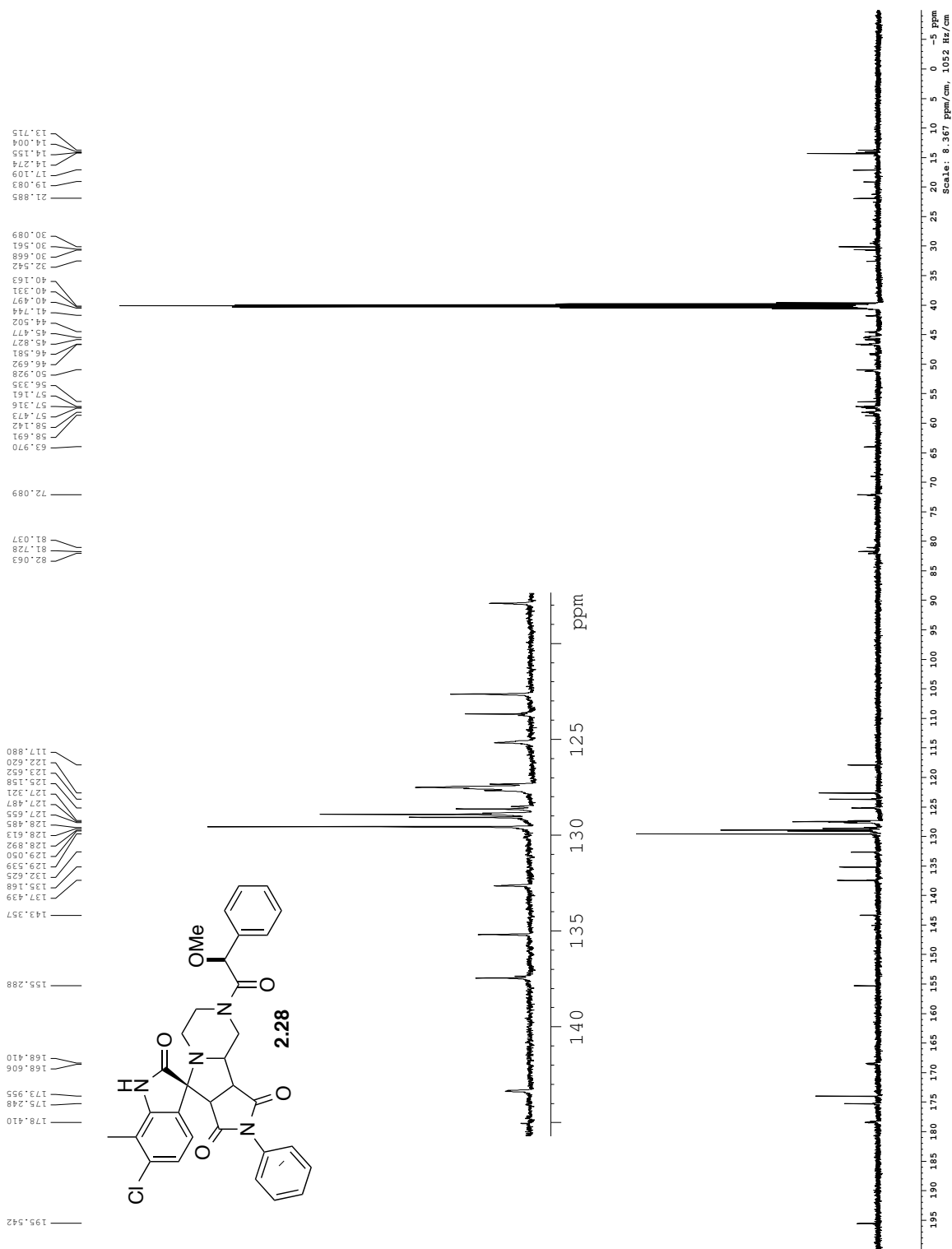


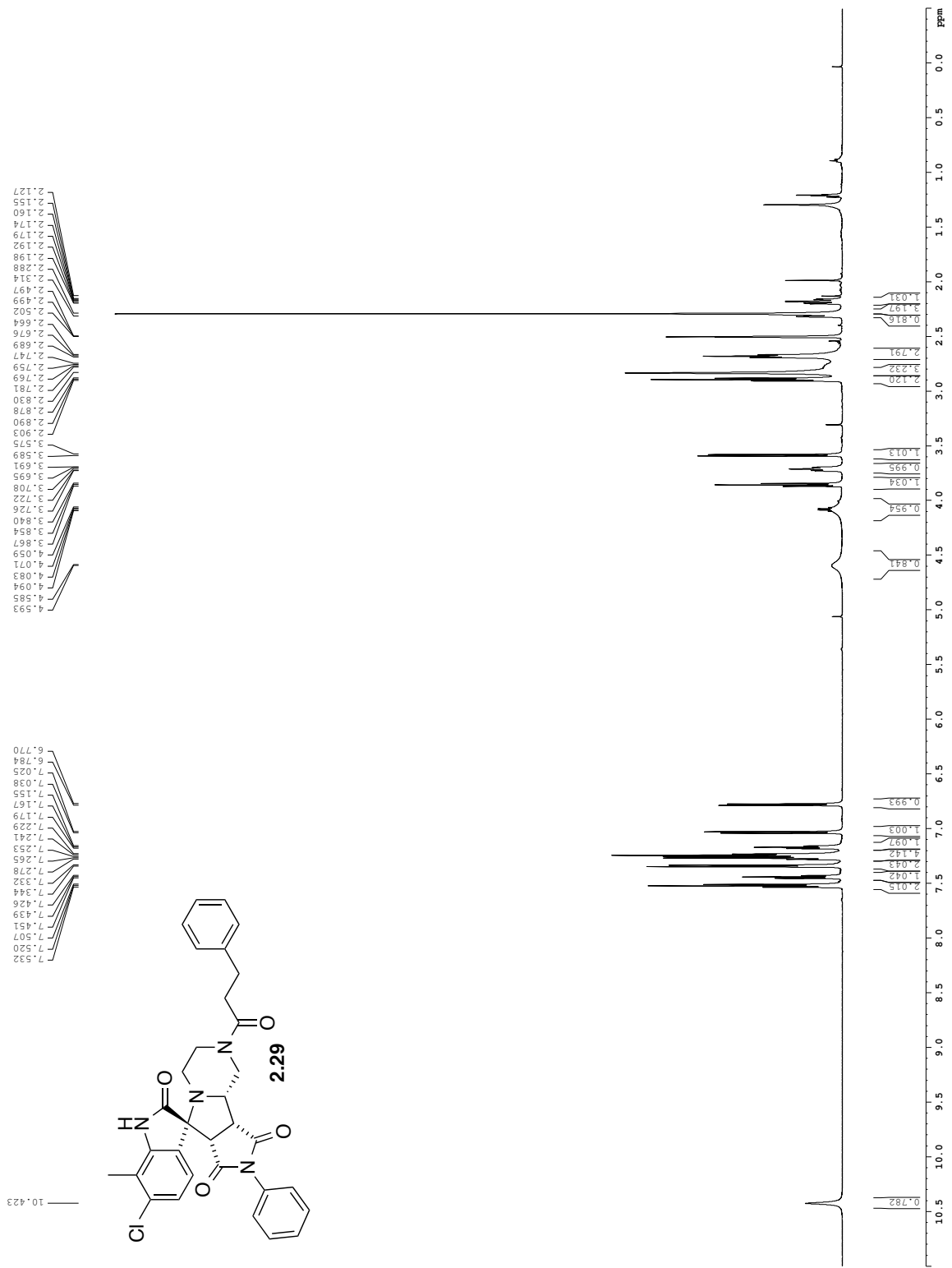


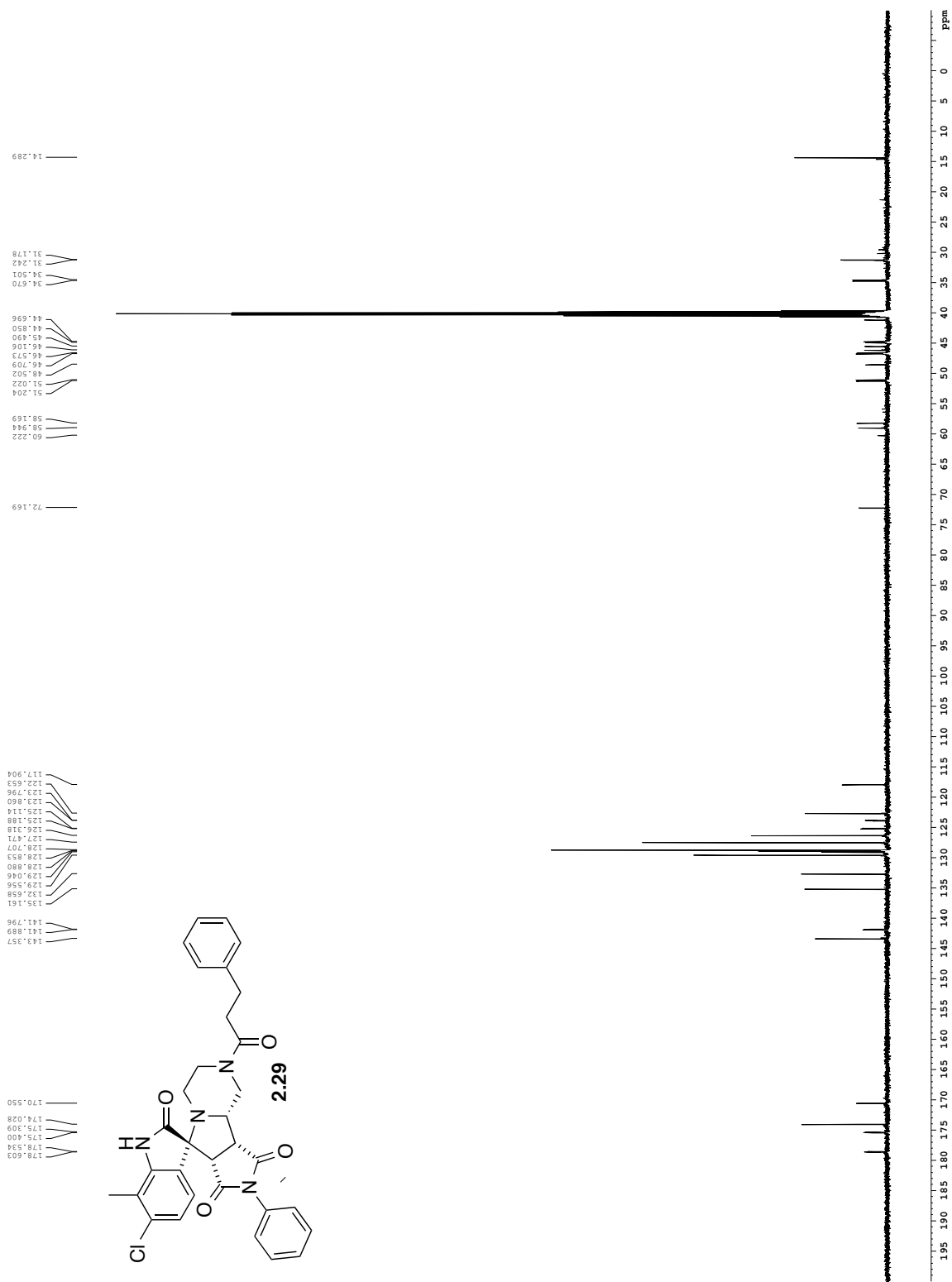


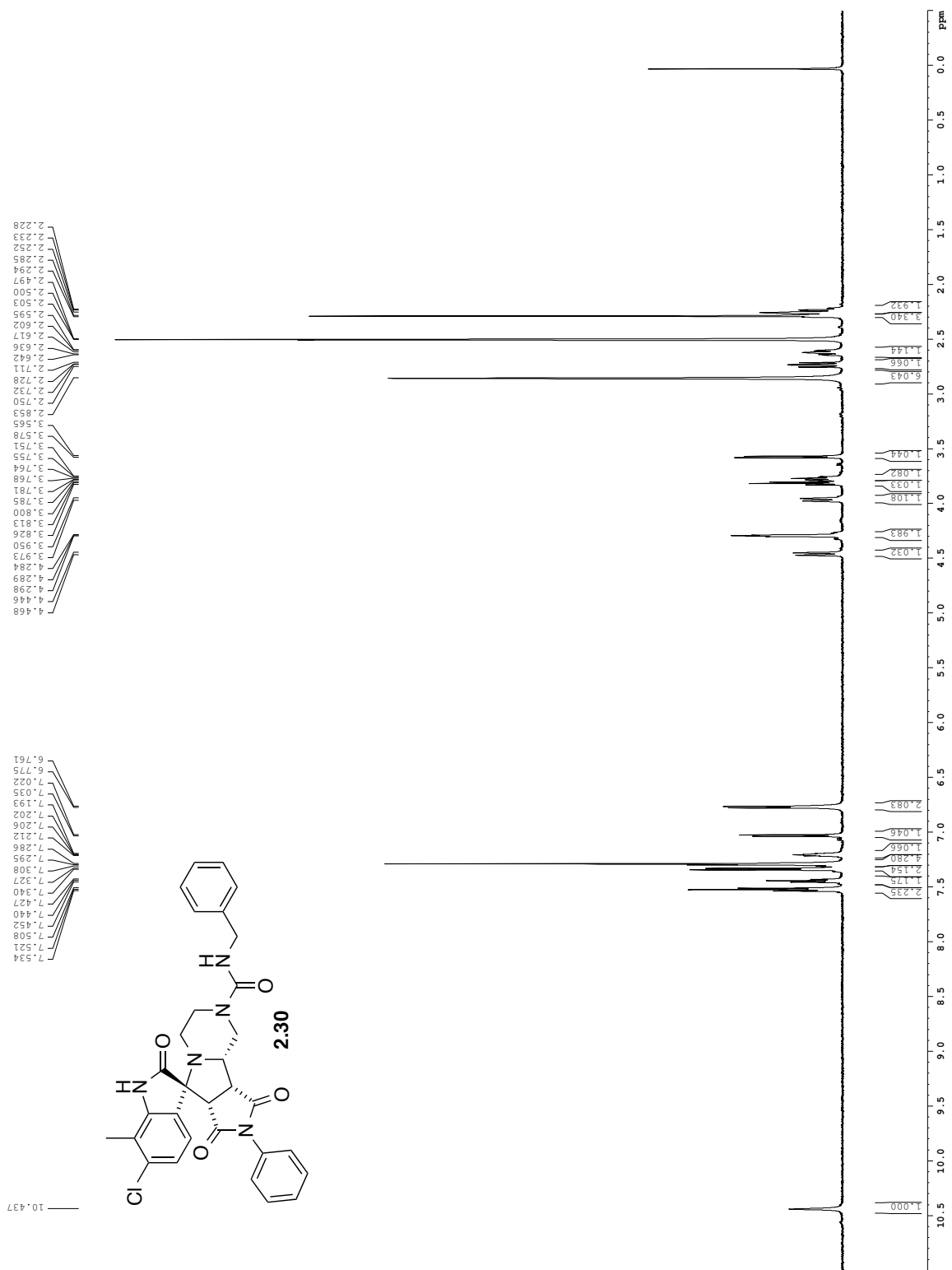


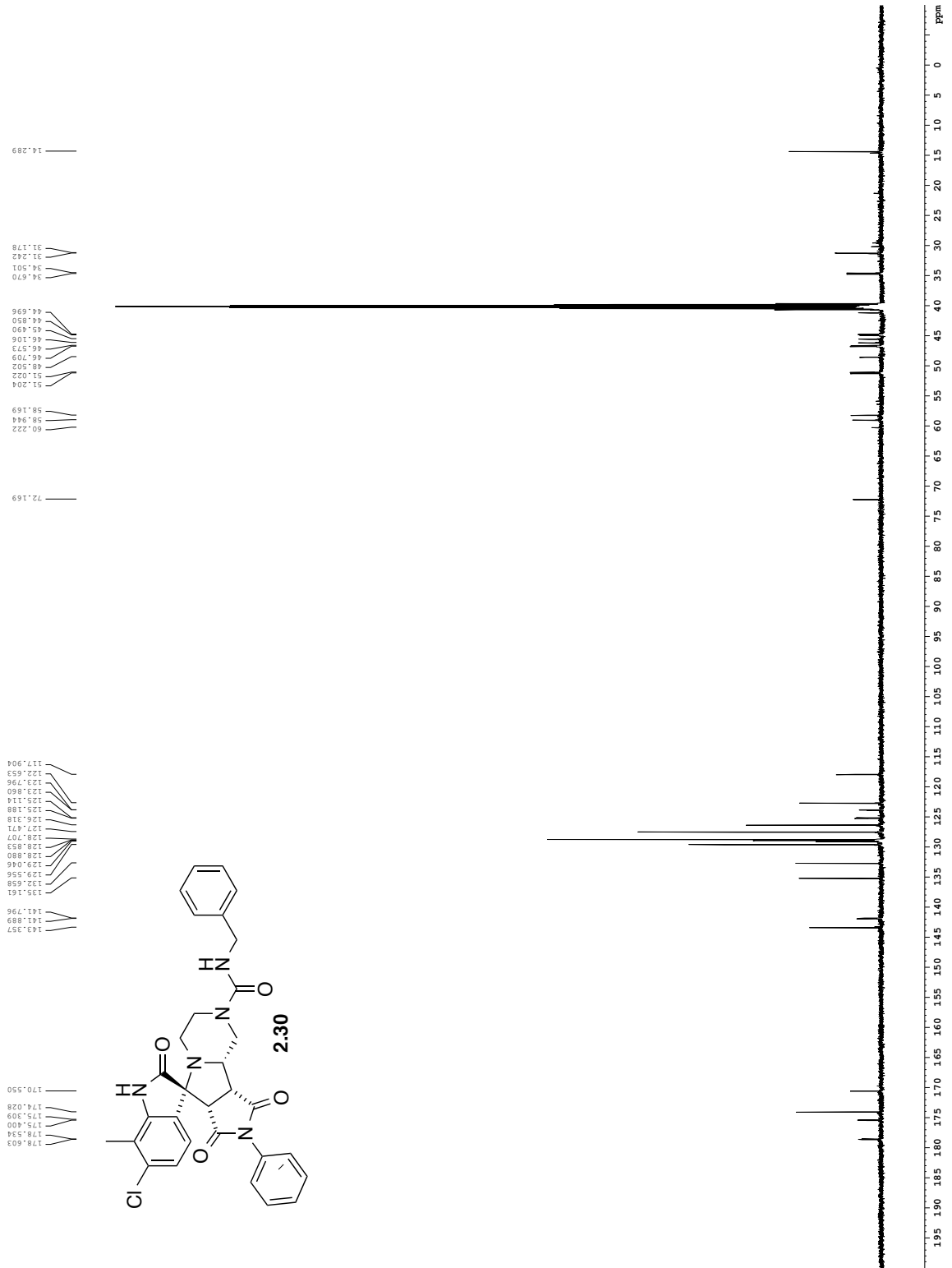


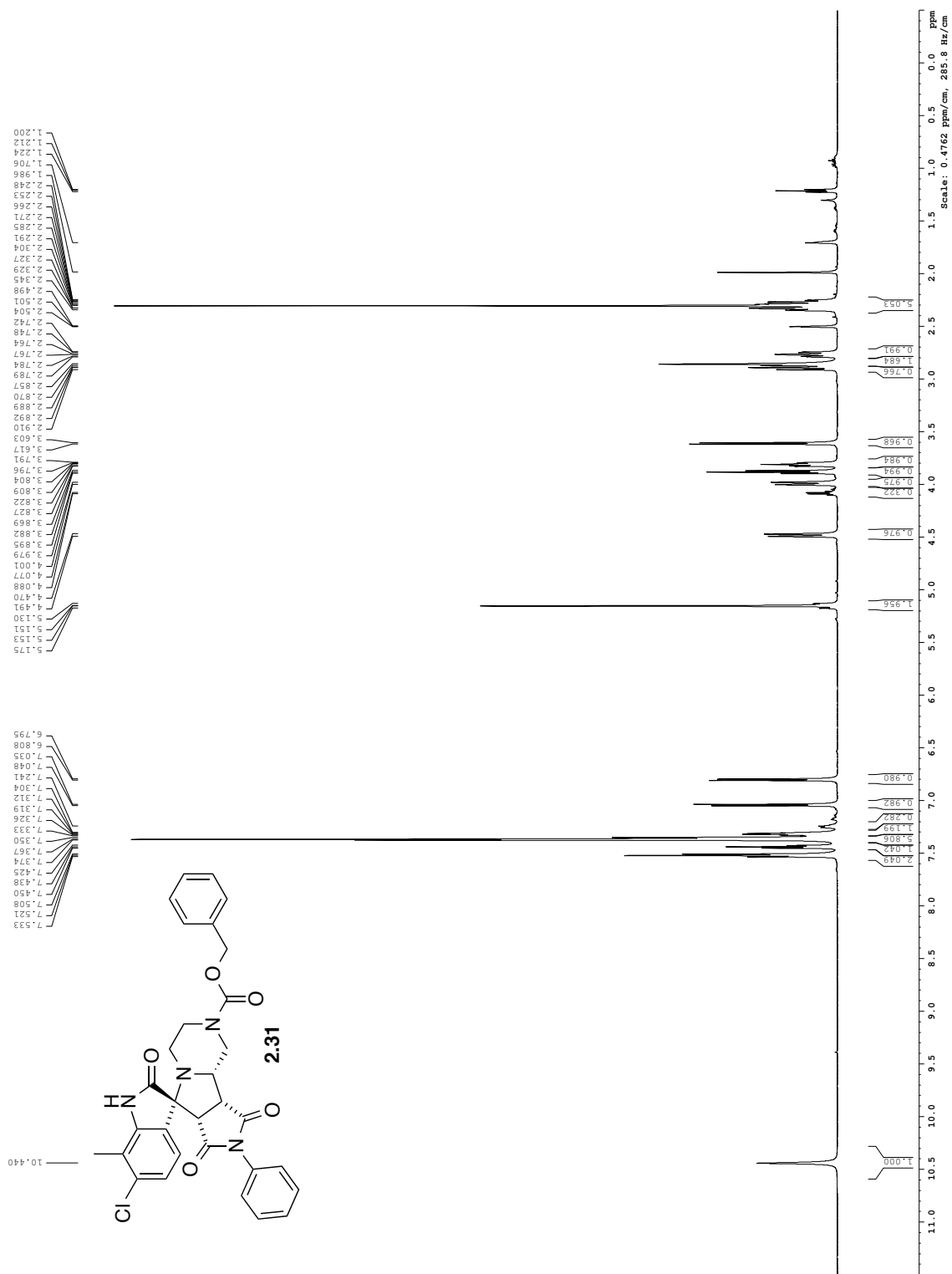


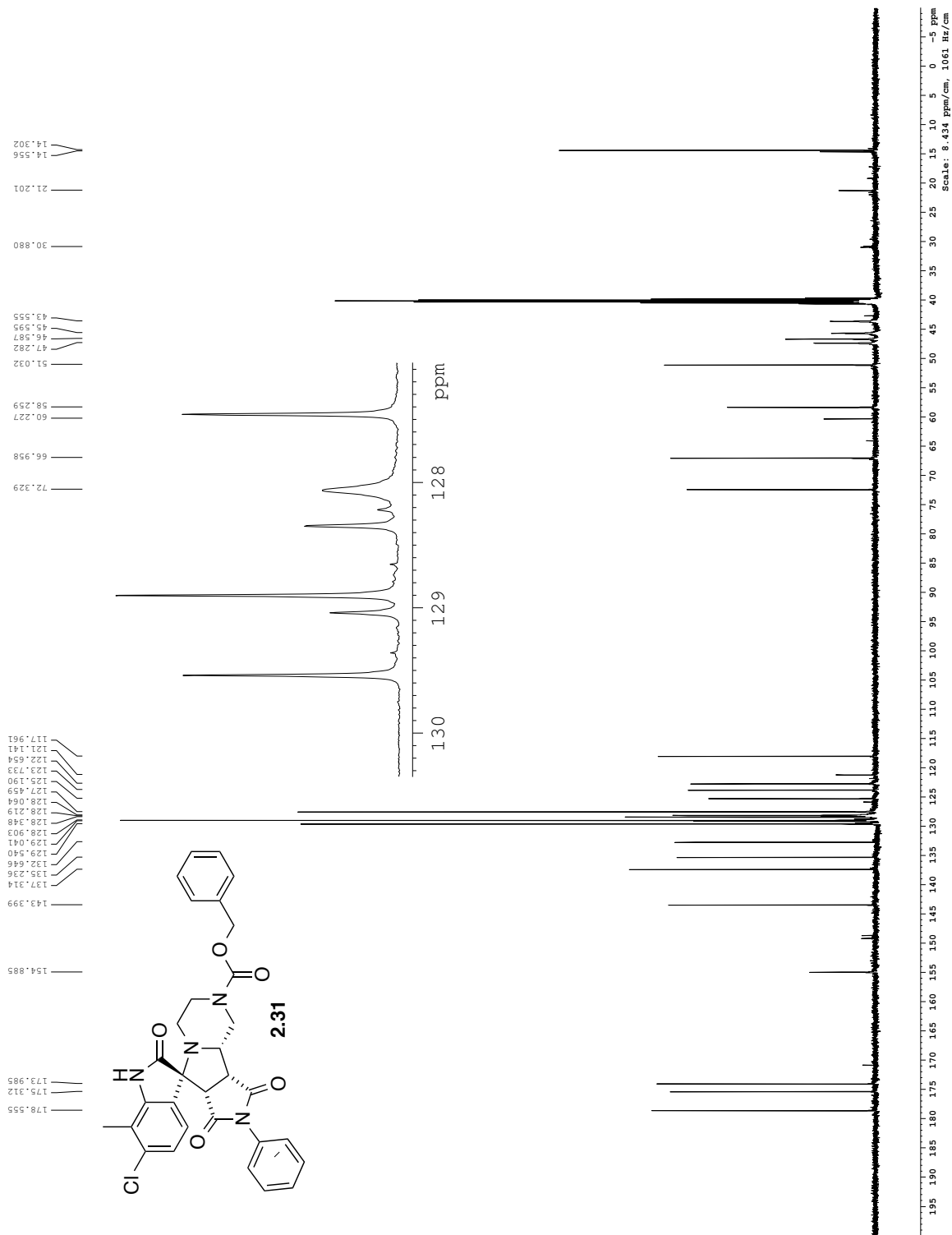


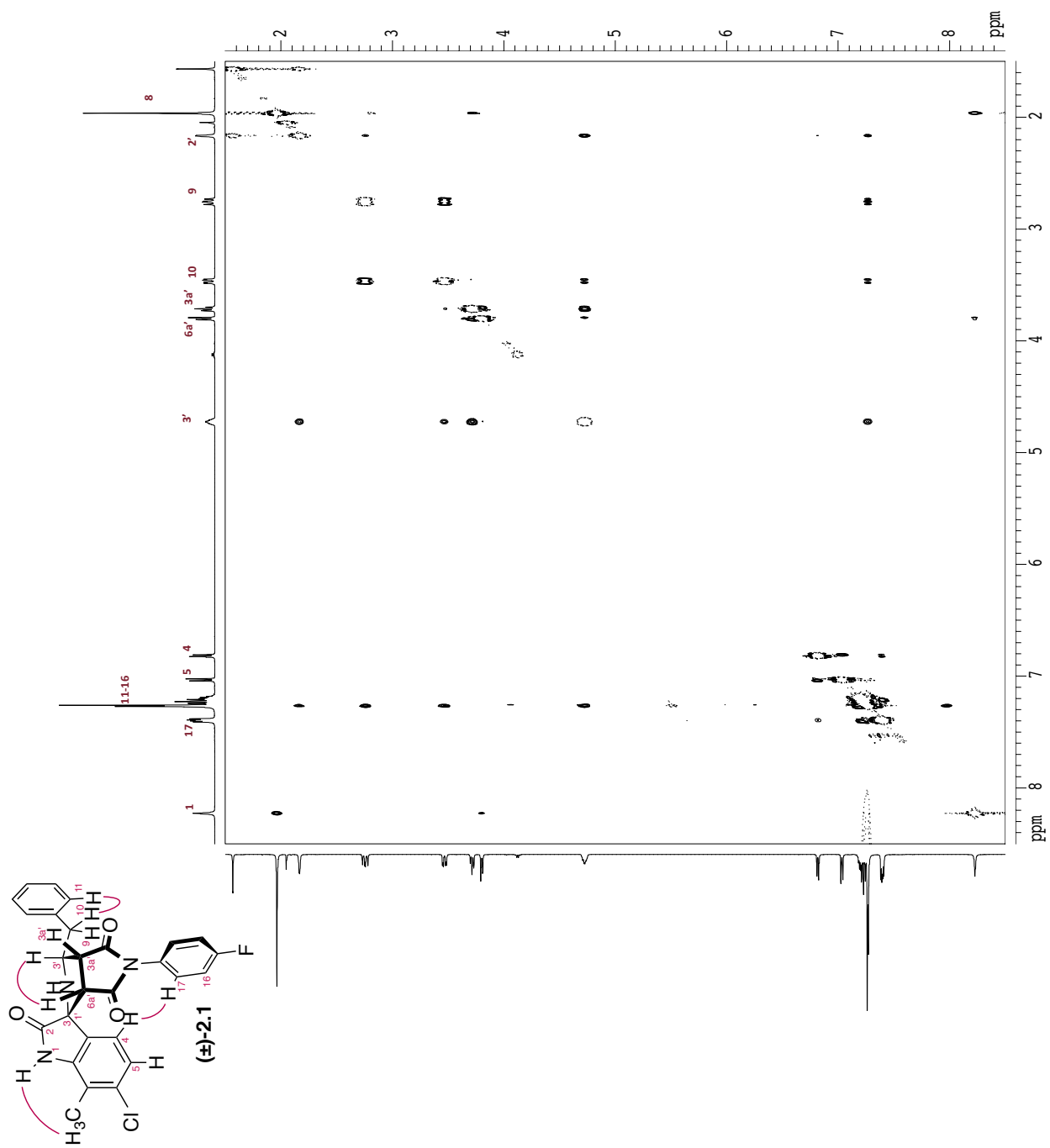


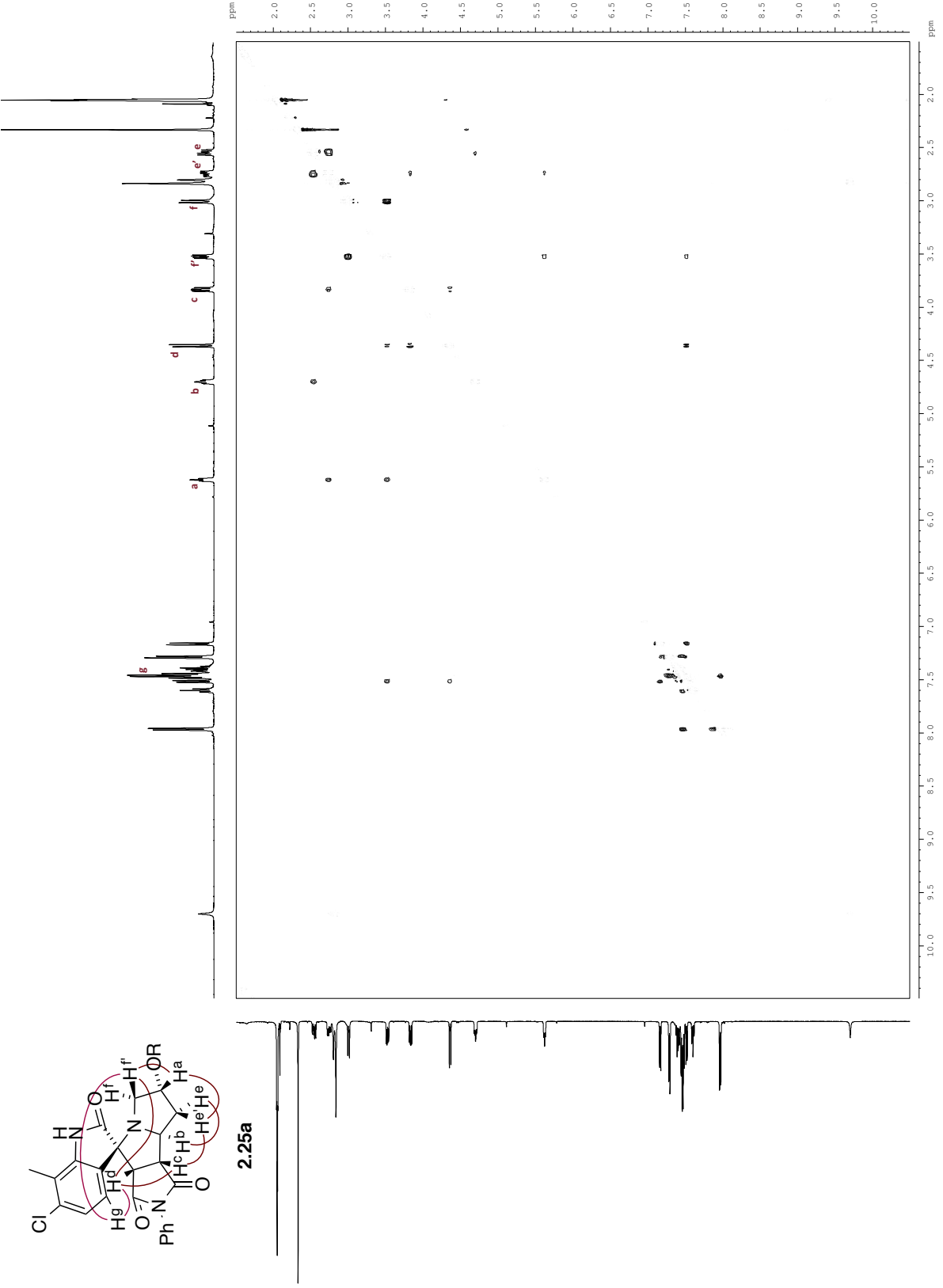


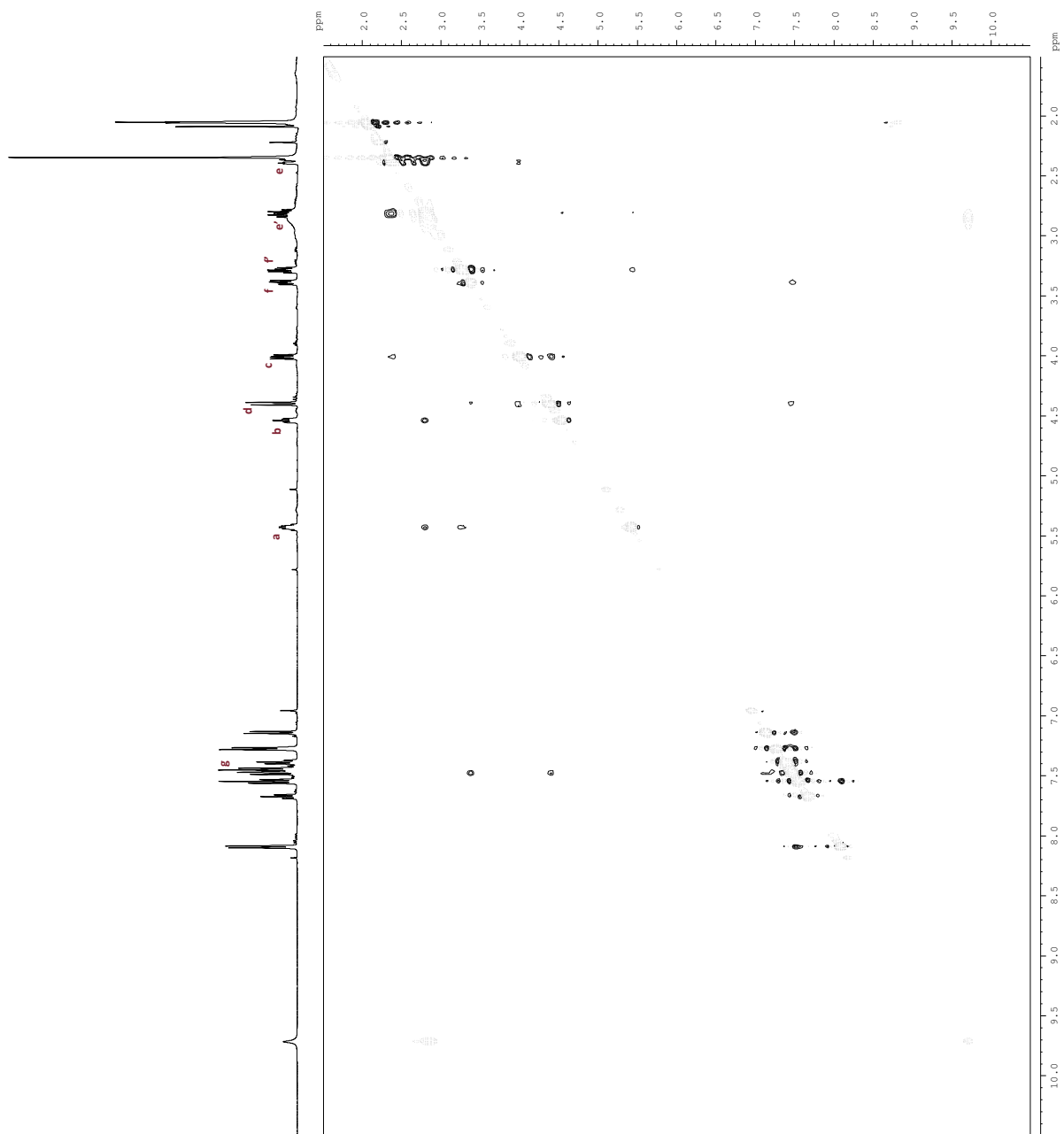
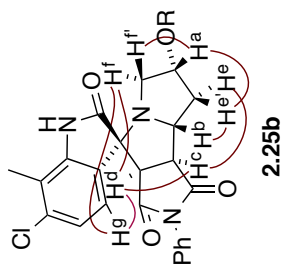


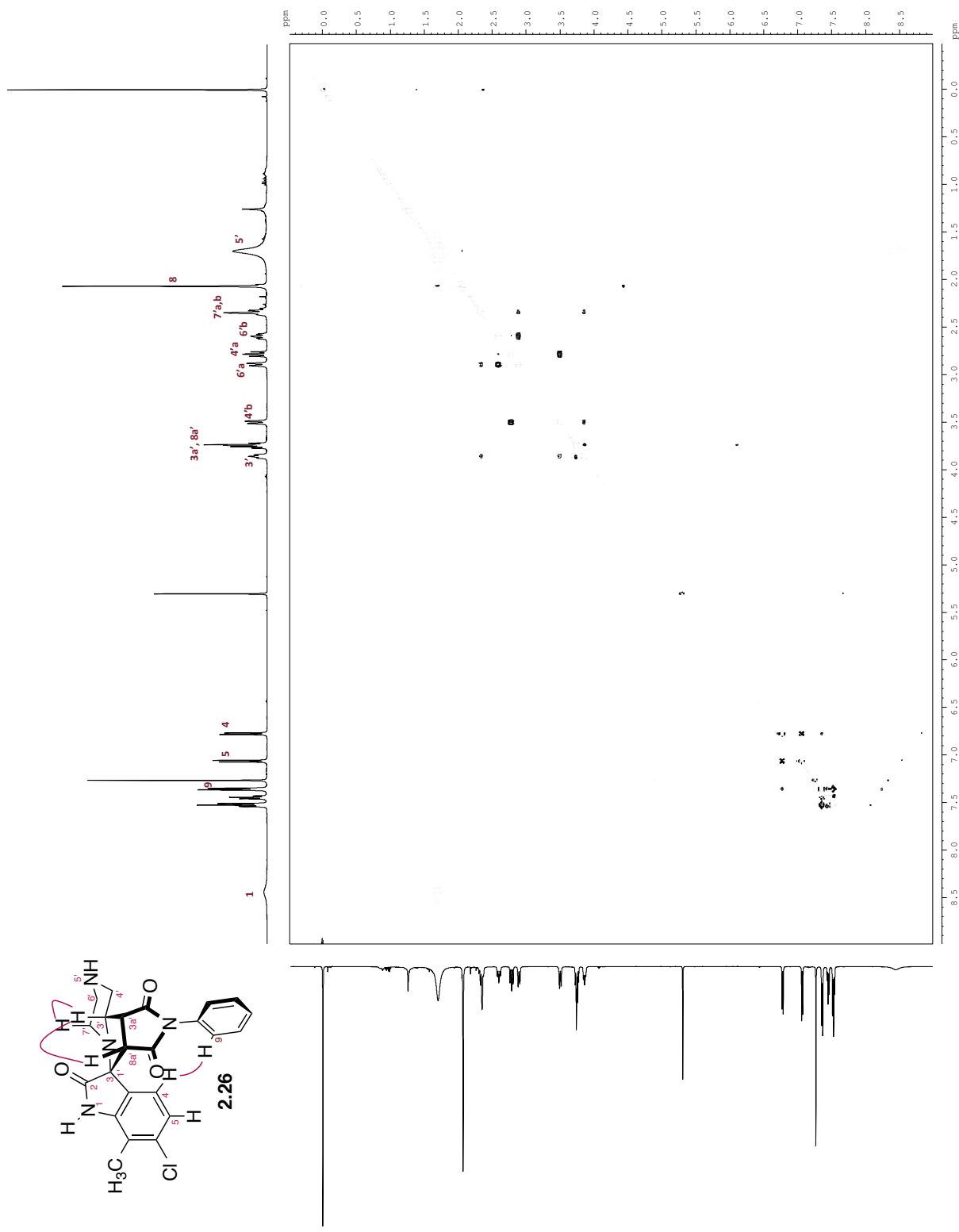


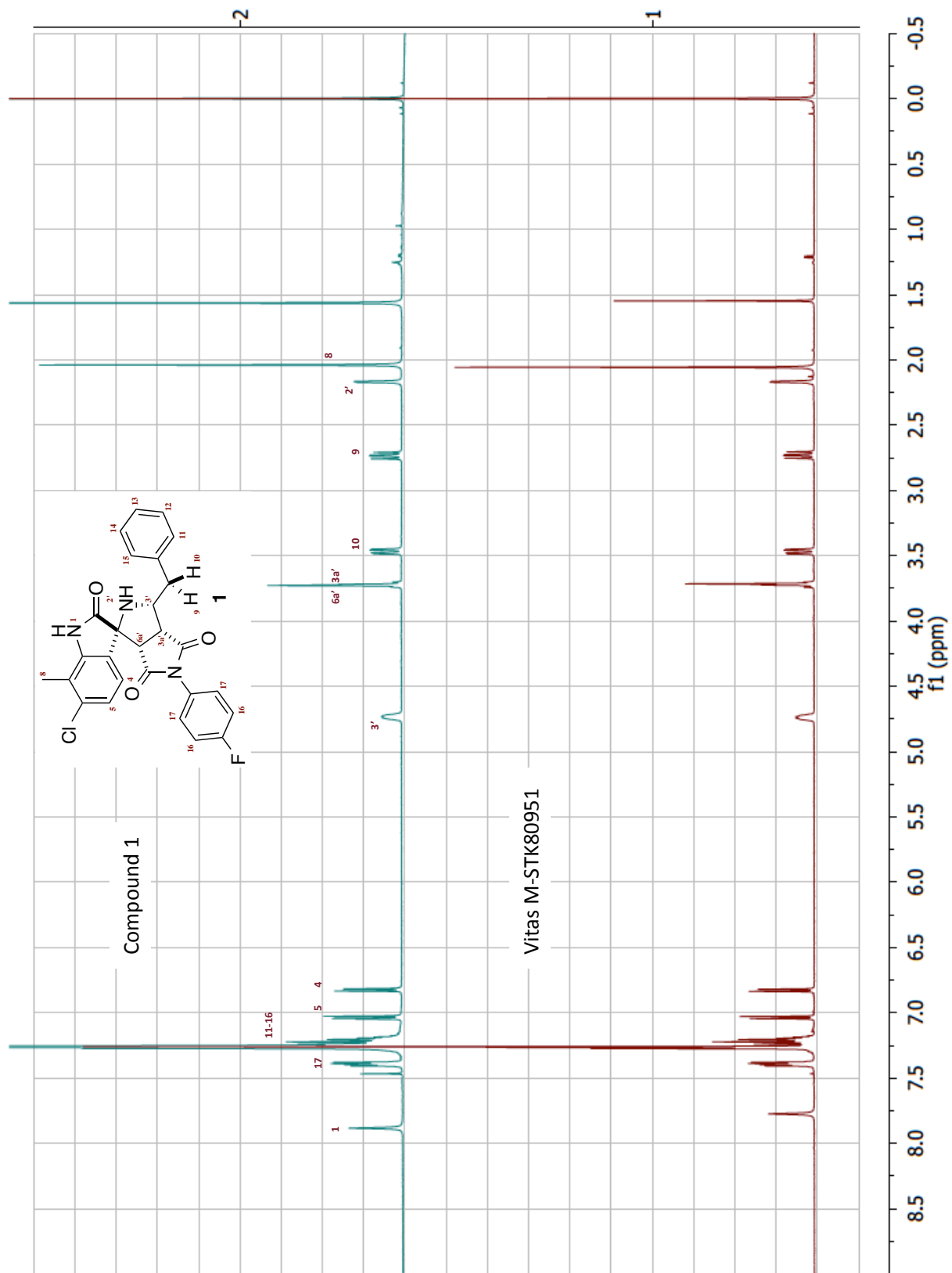


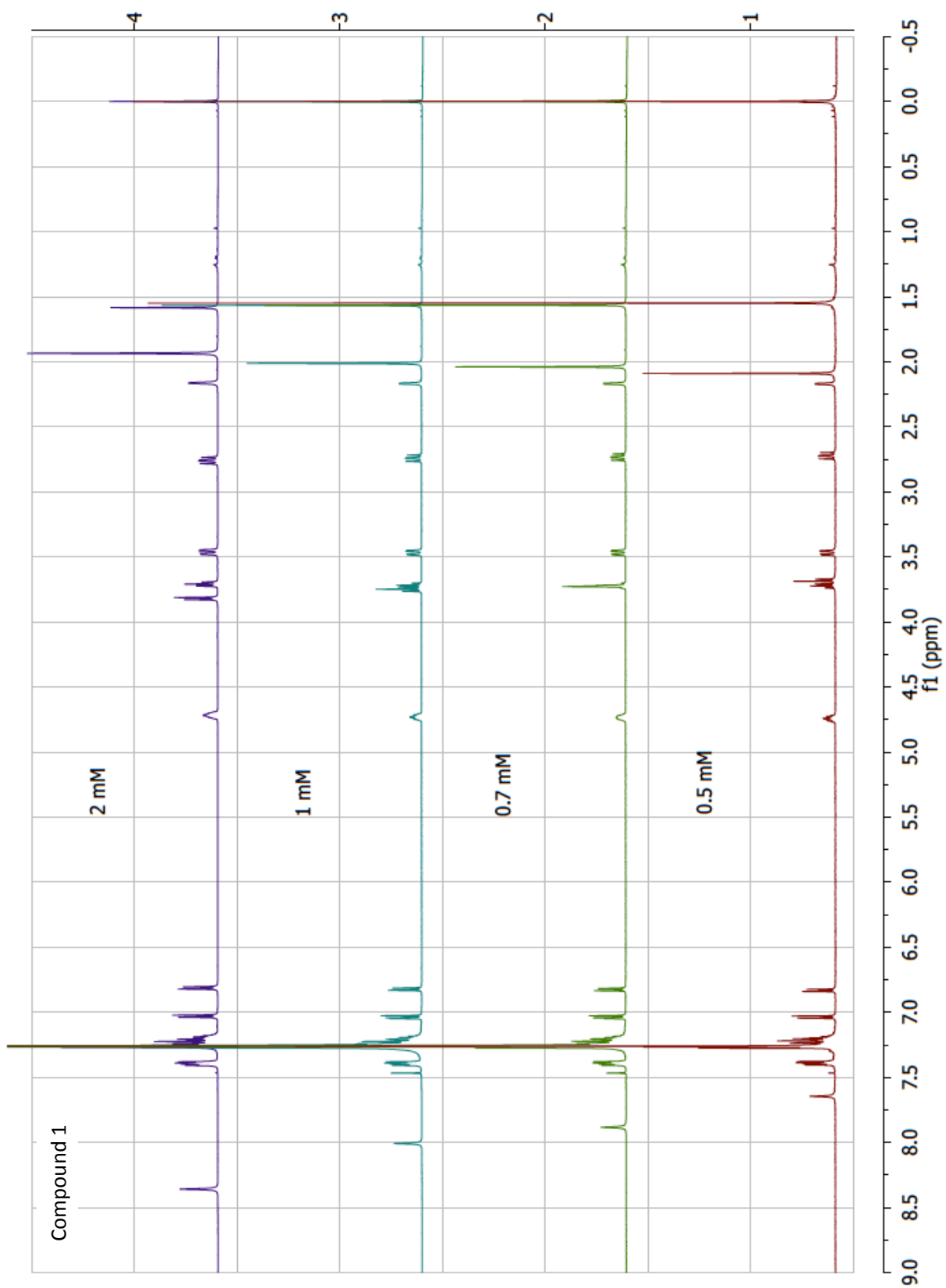




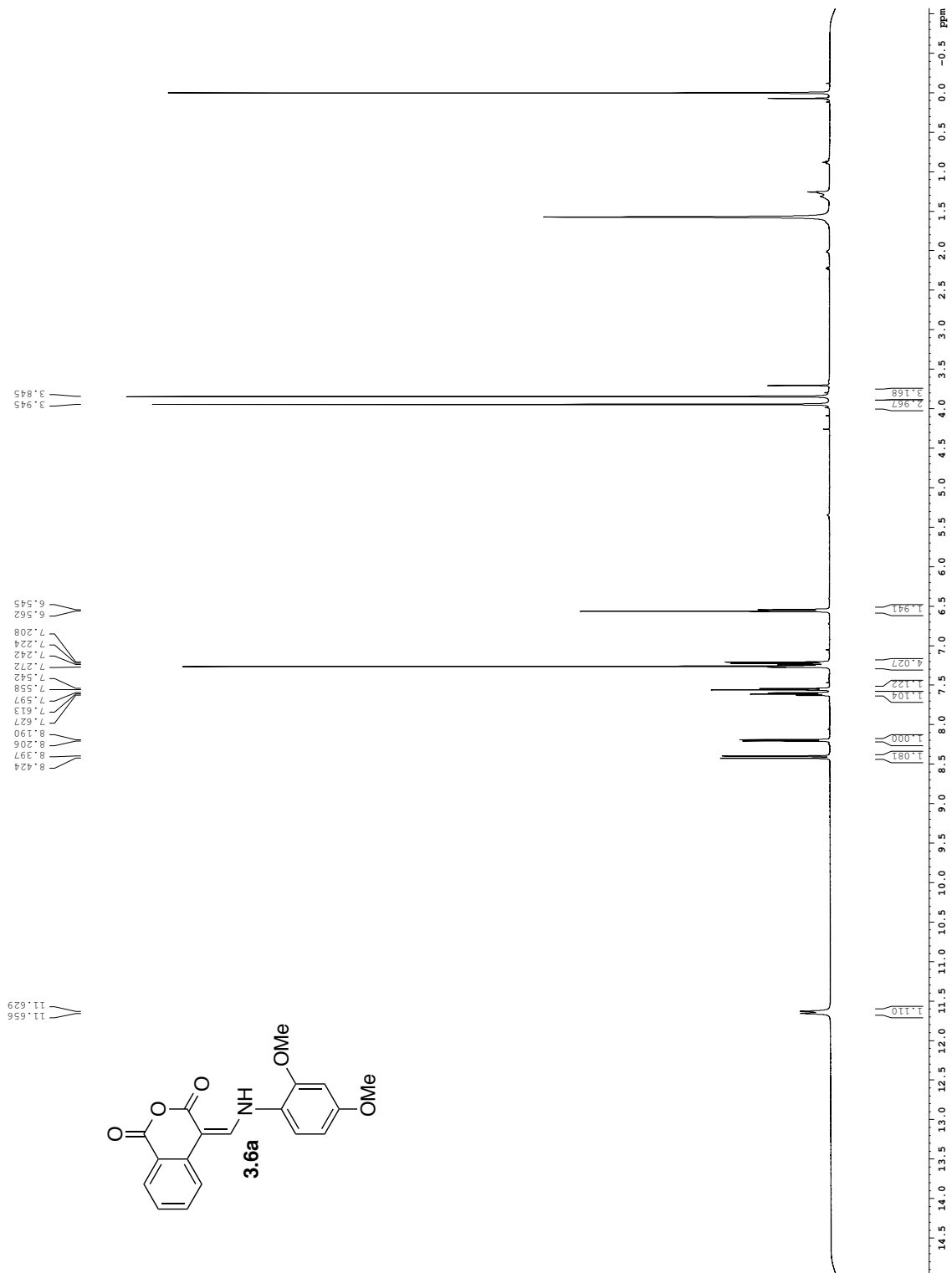


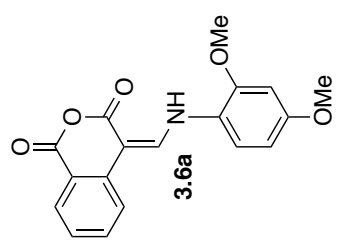
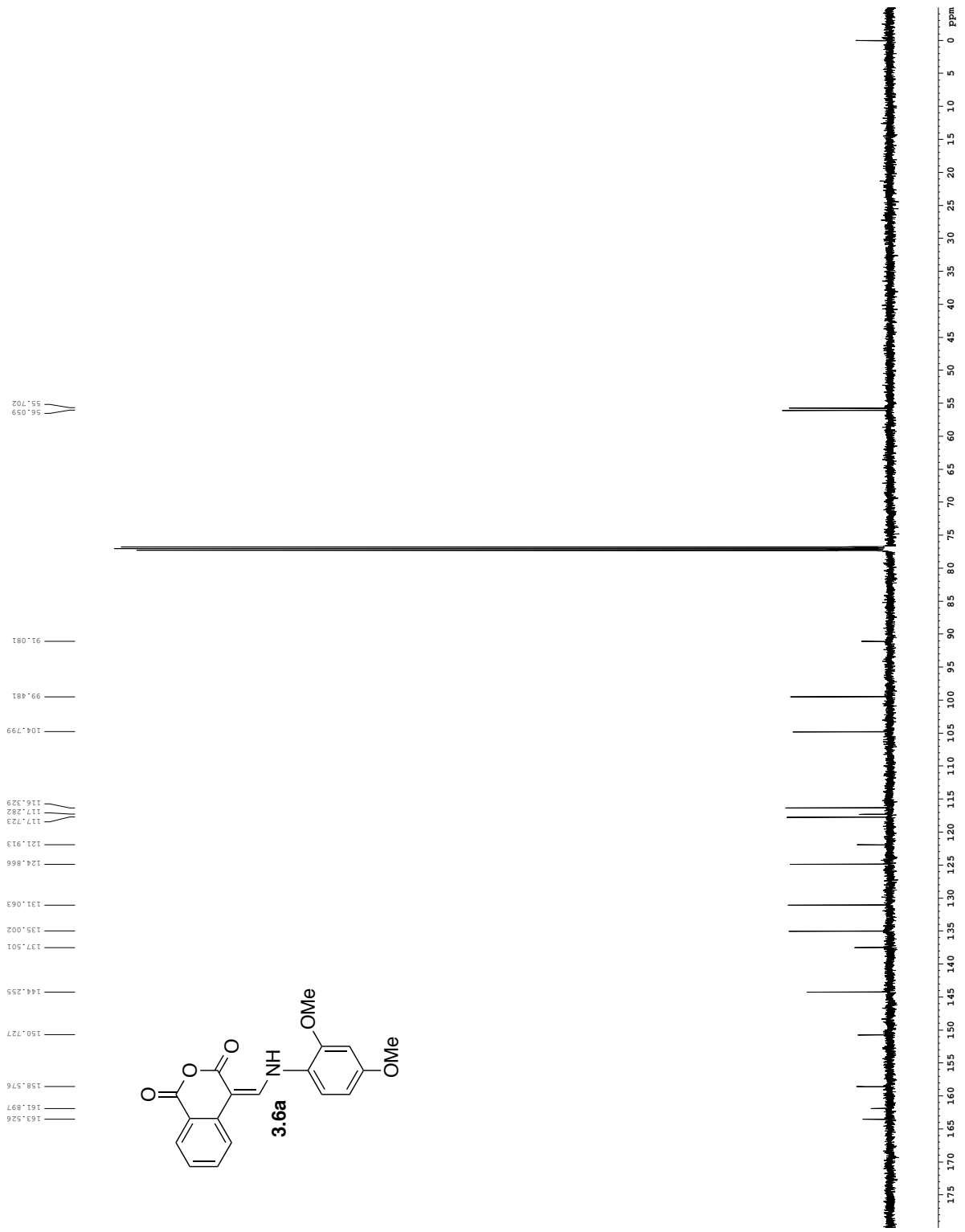


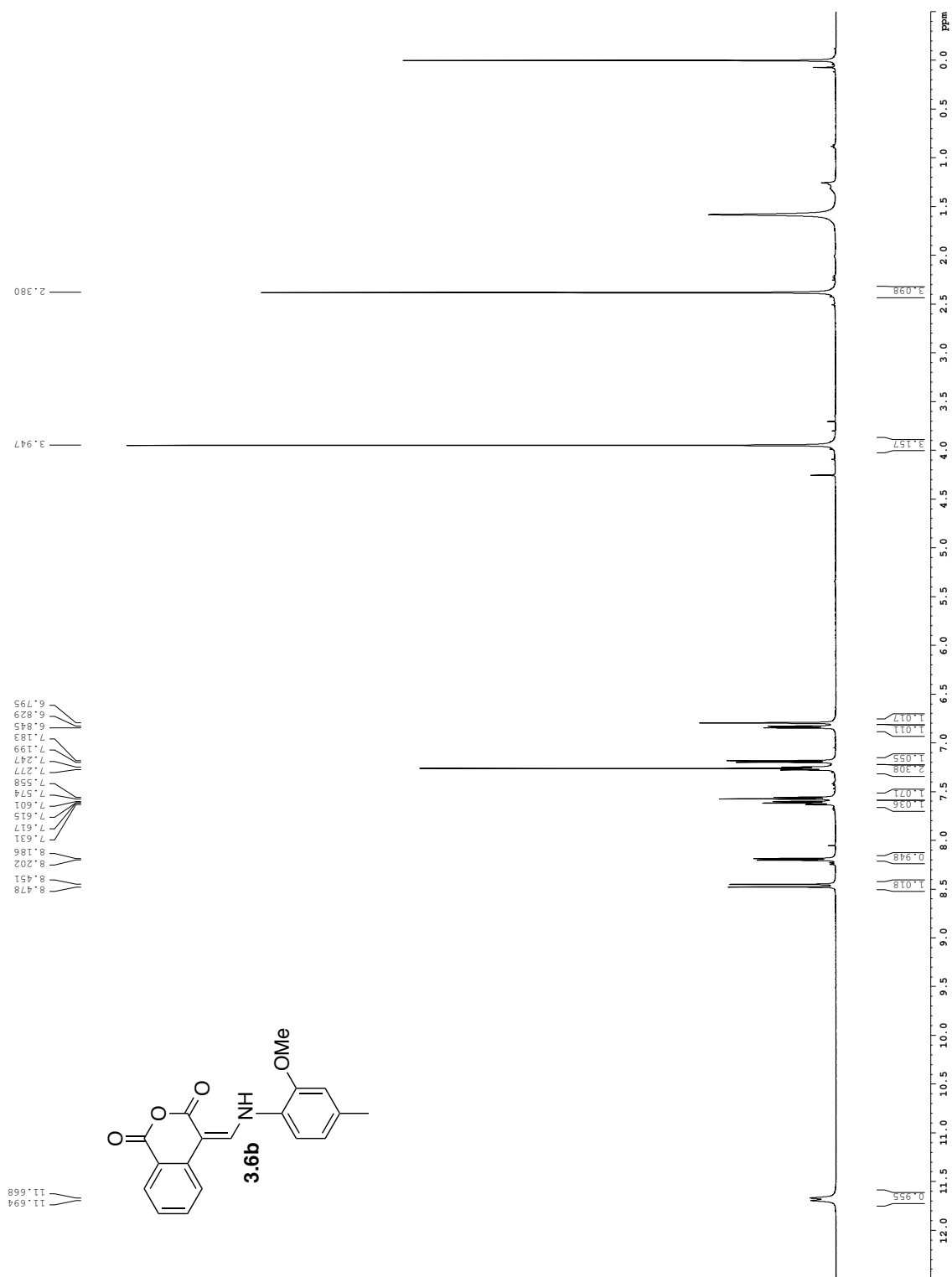


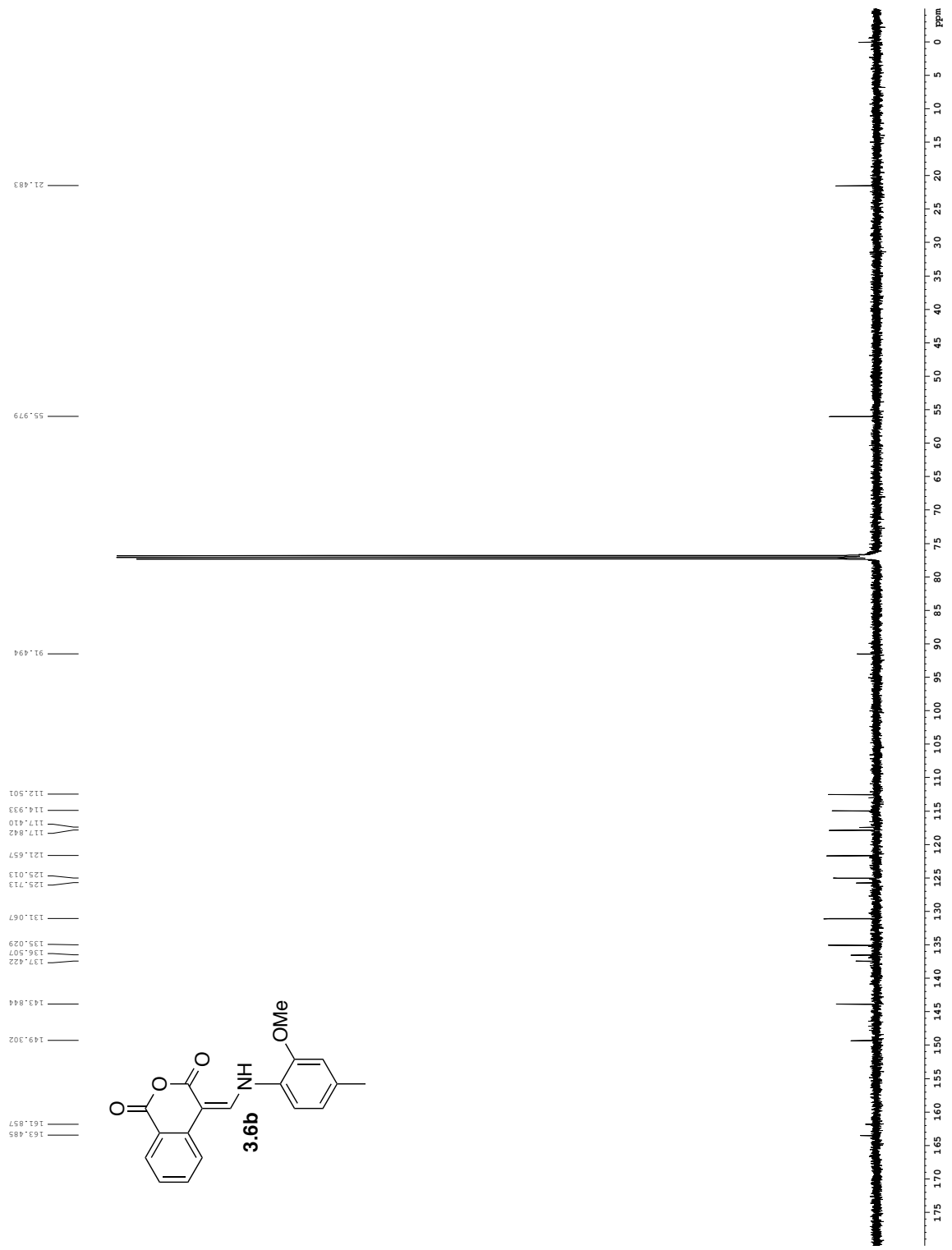


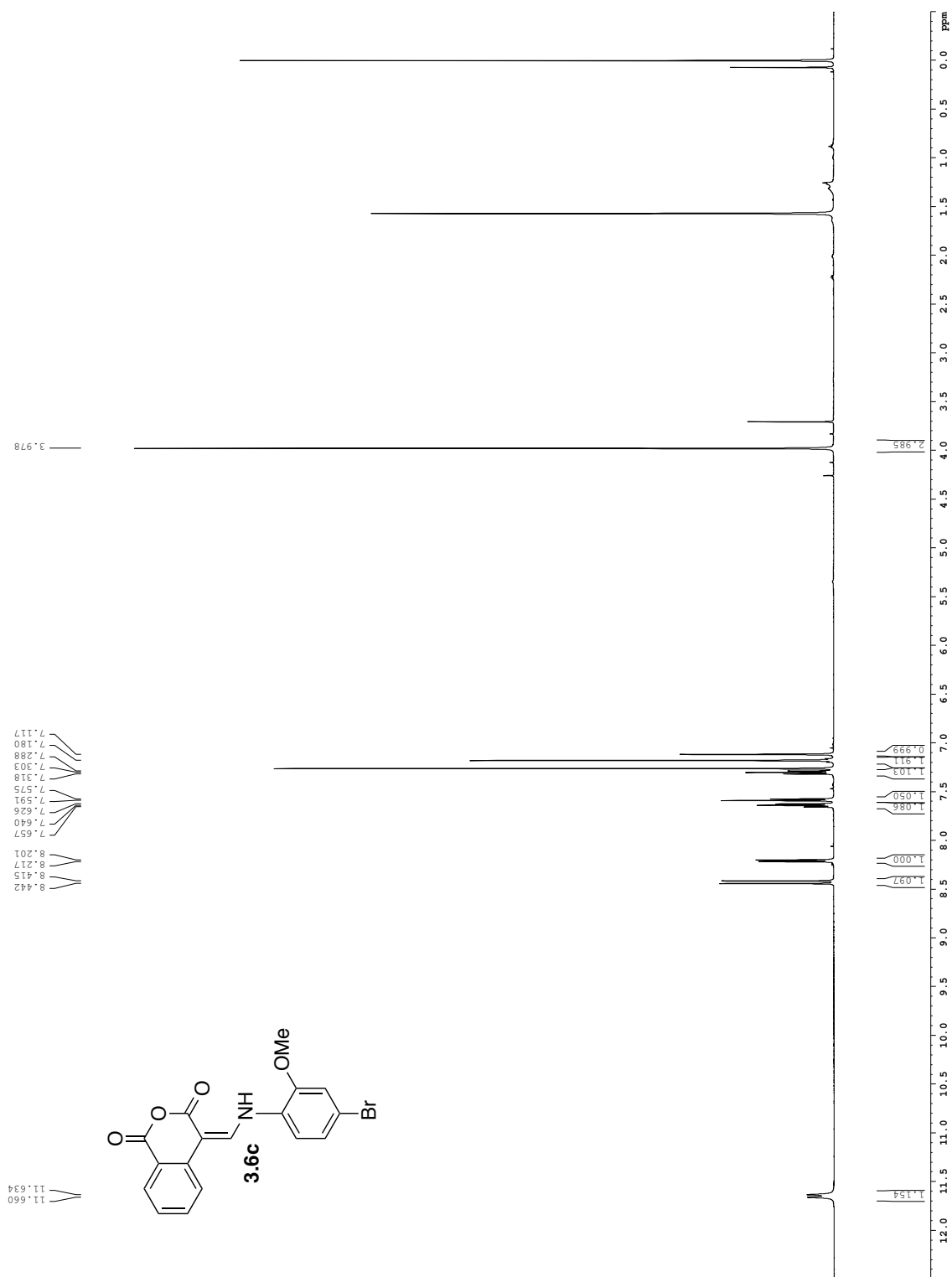
Appendix C: Chapter 3 – NMR Spectra

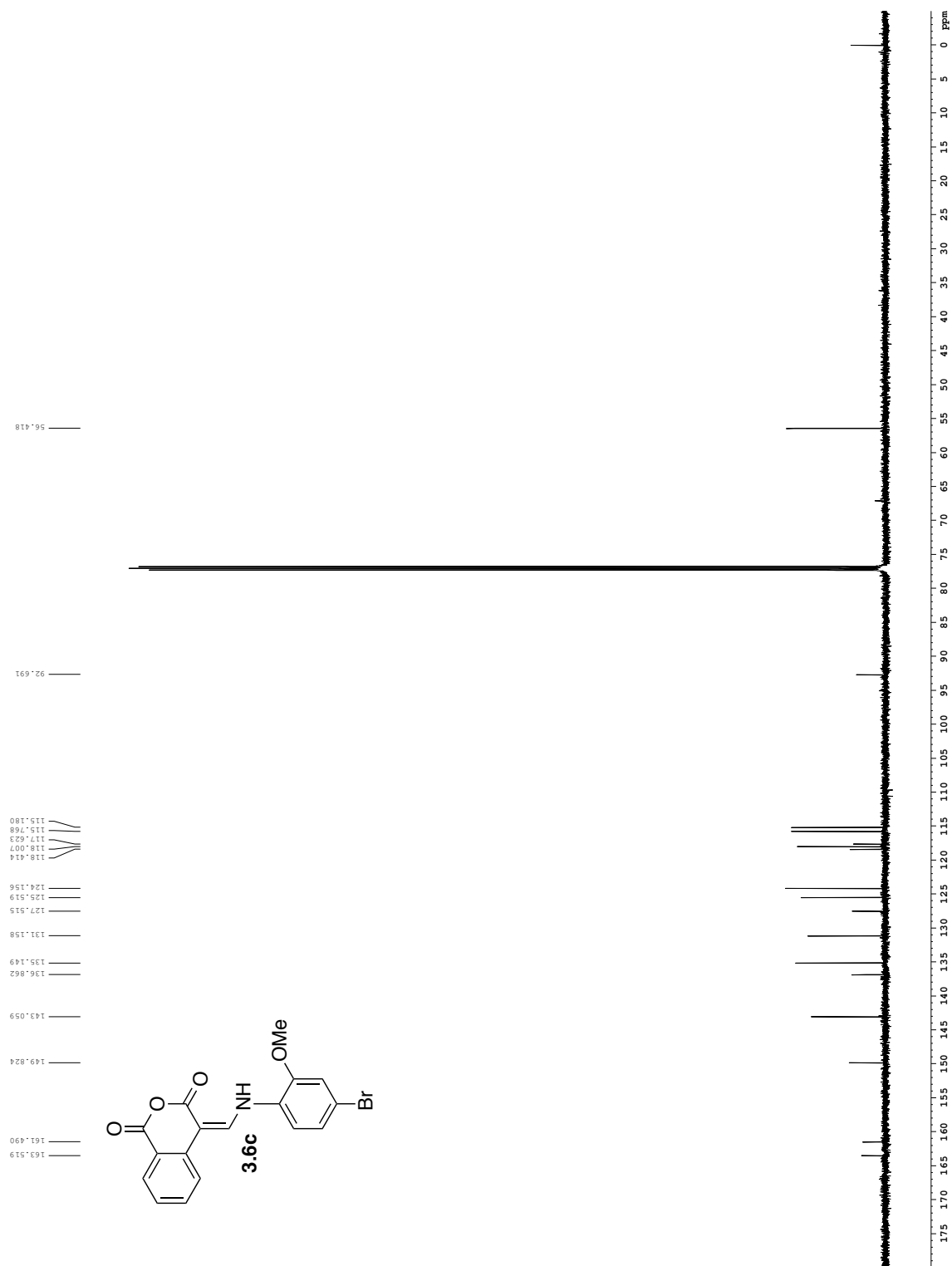


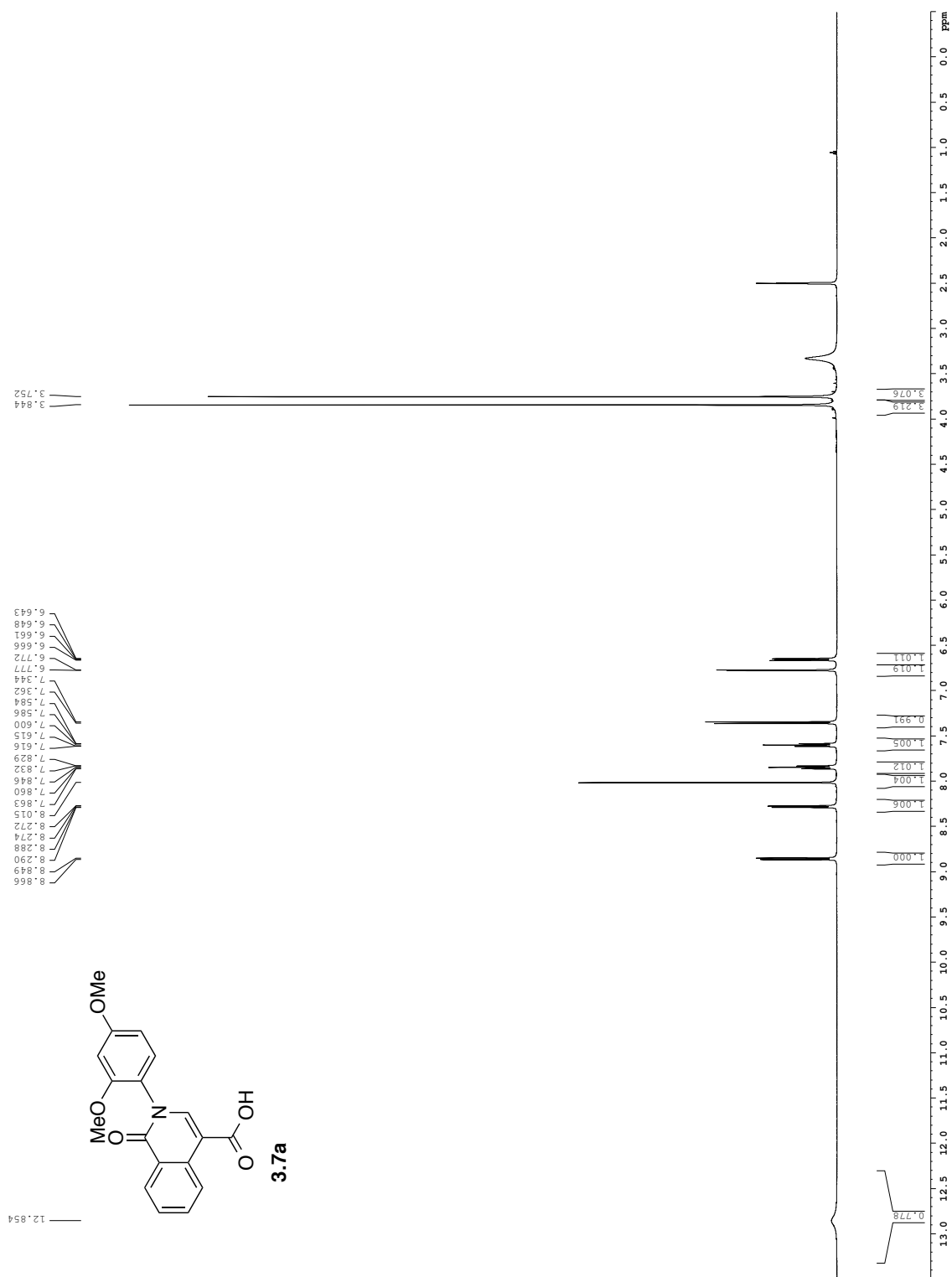


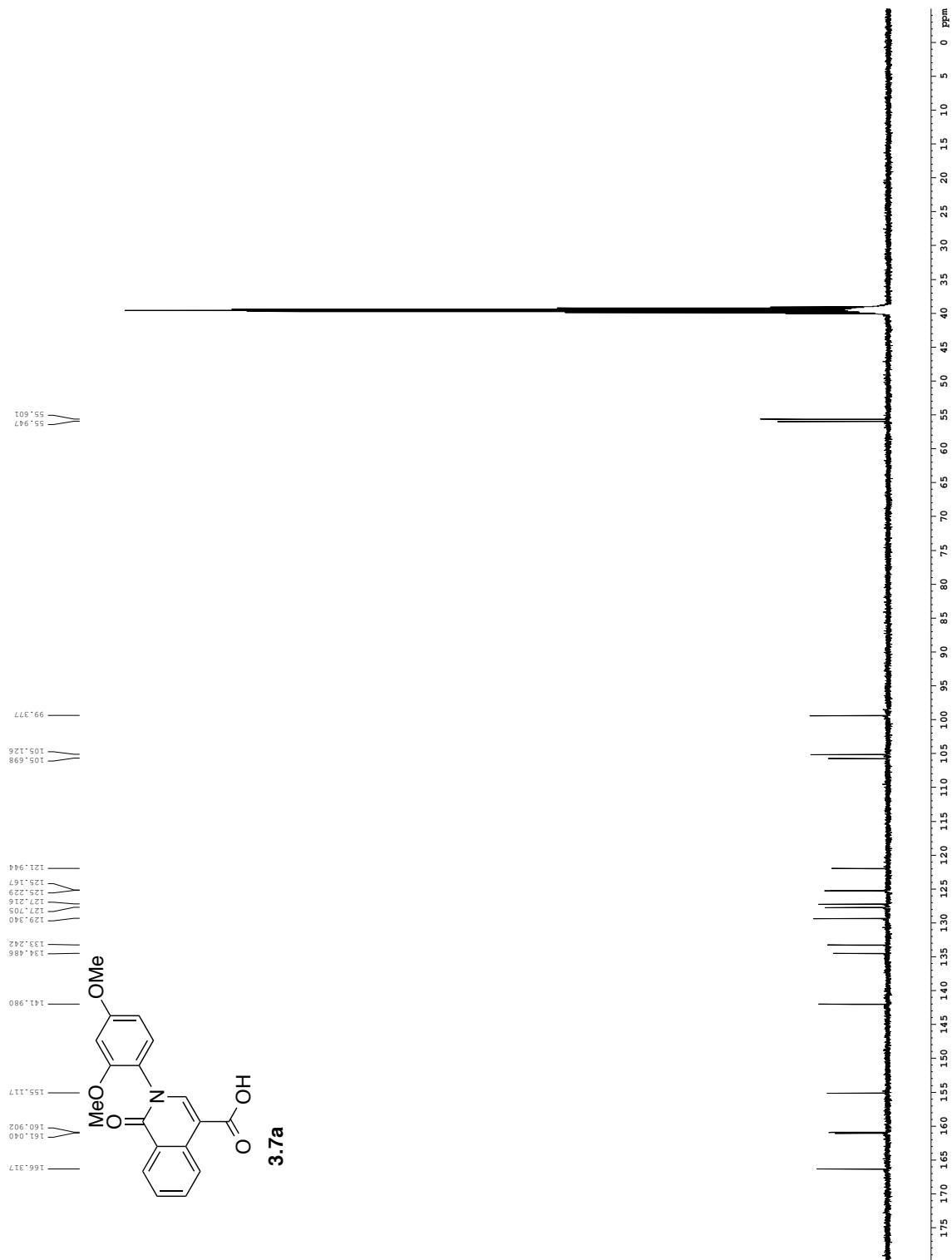


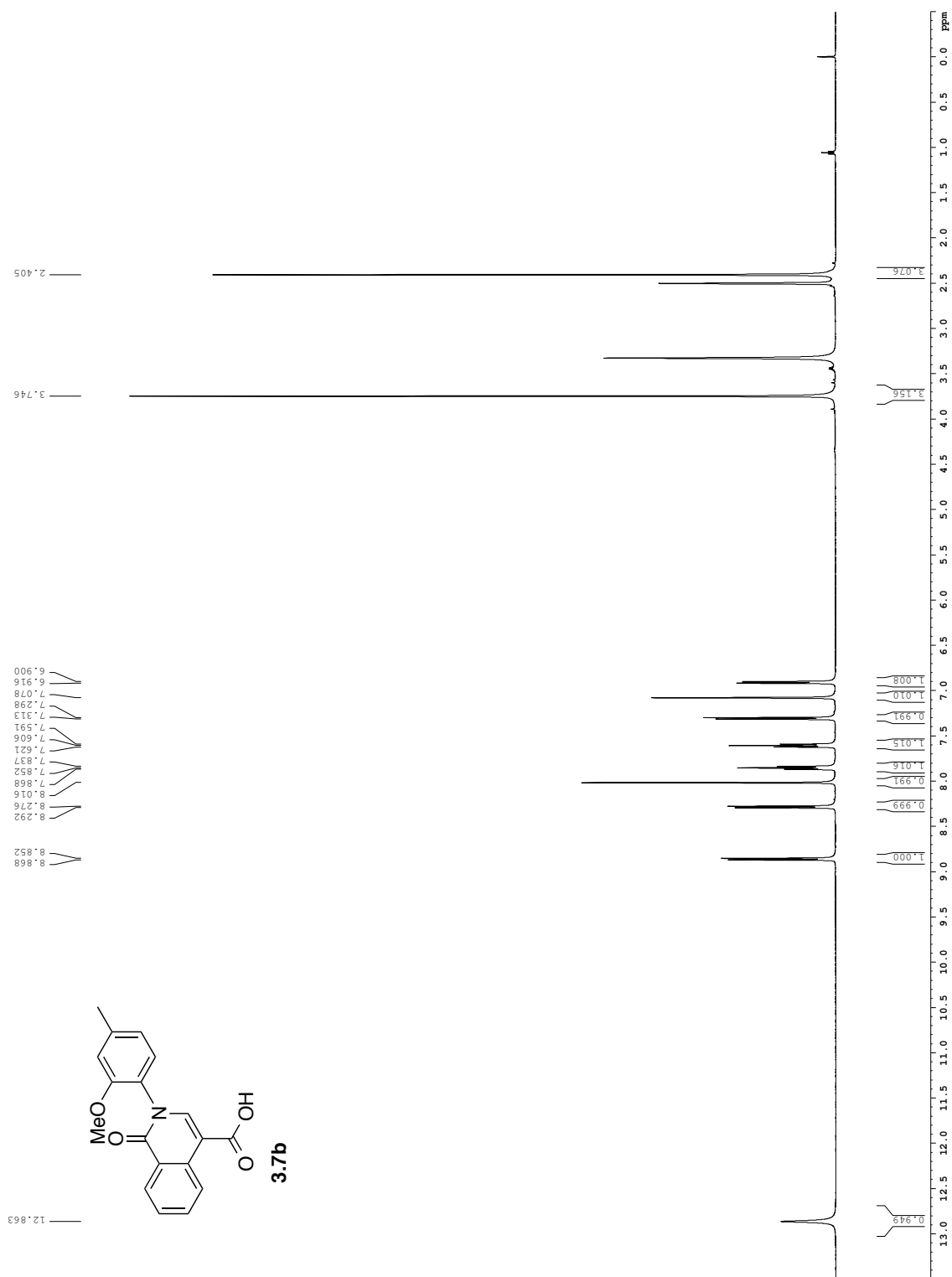


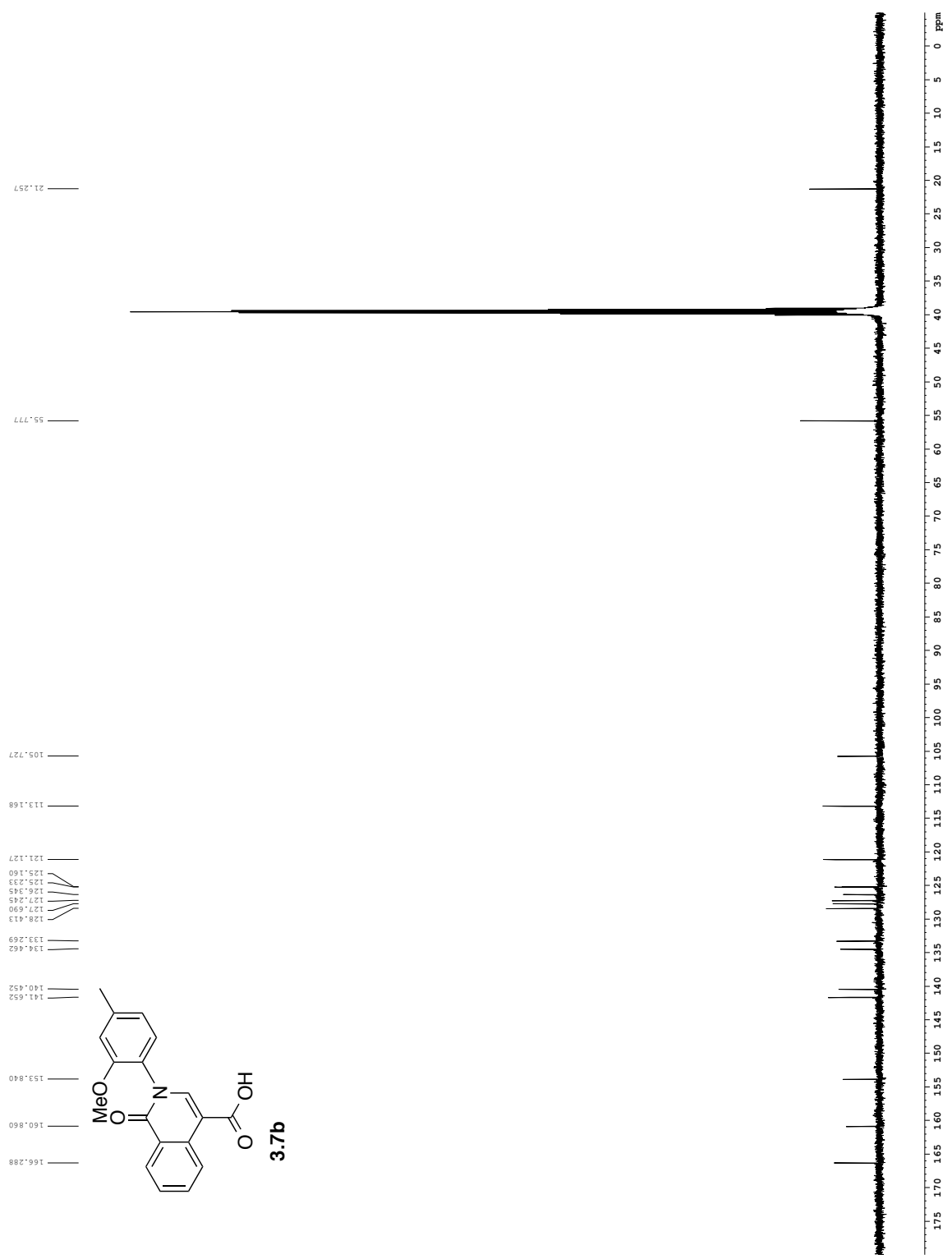


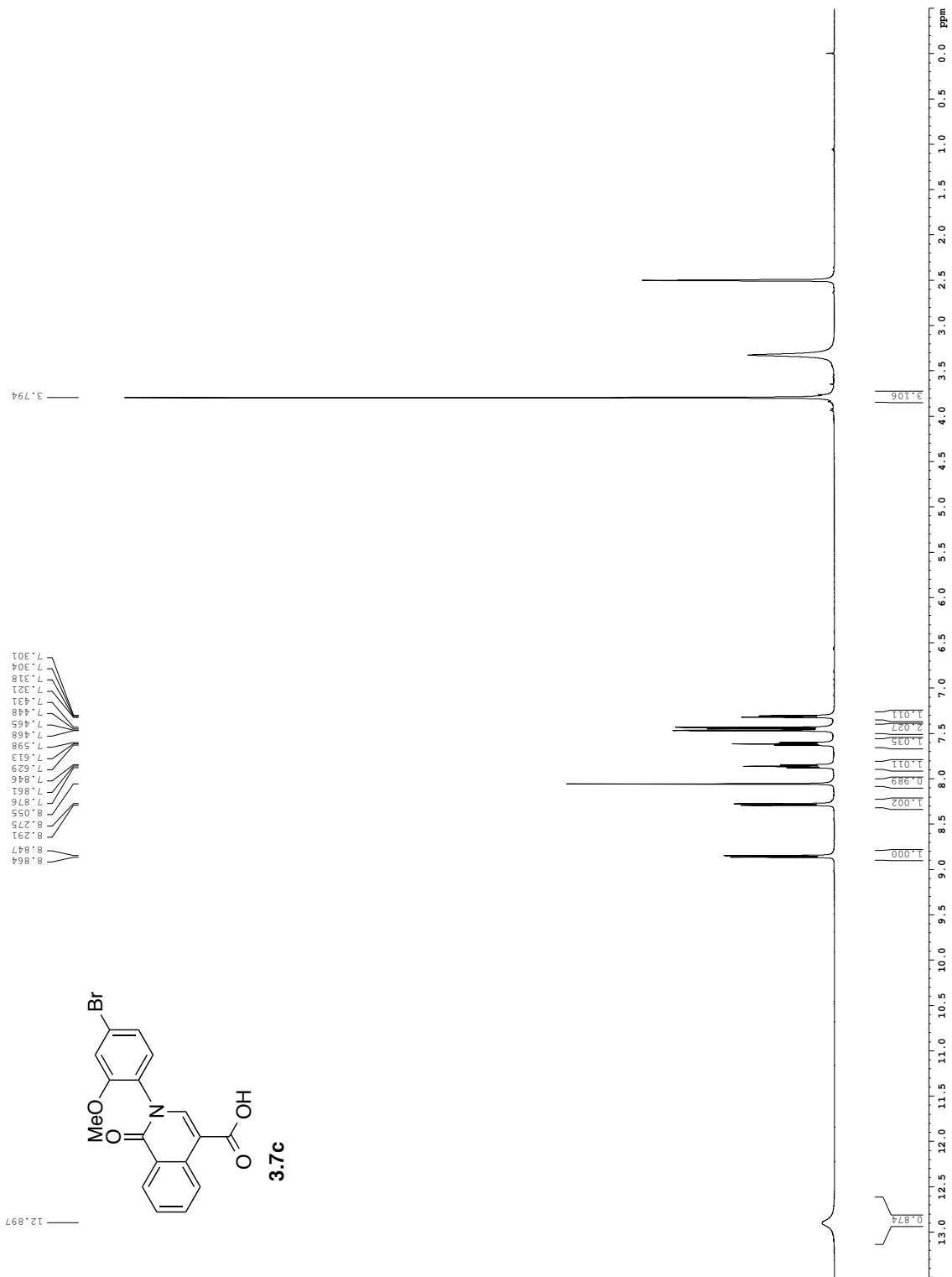


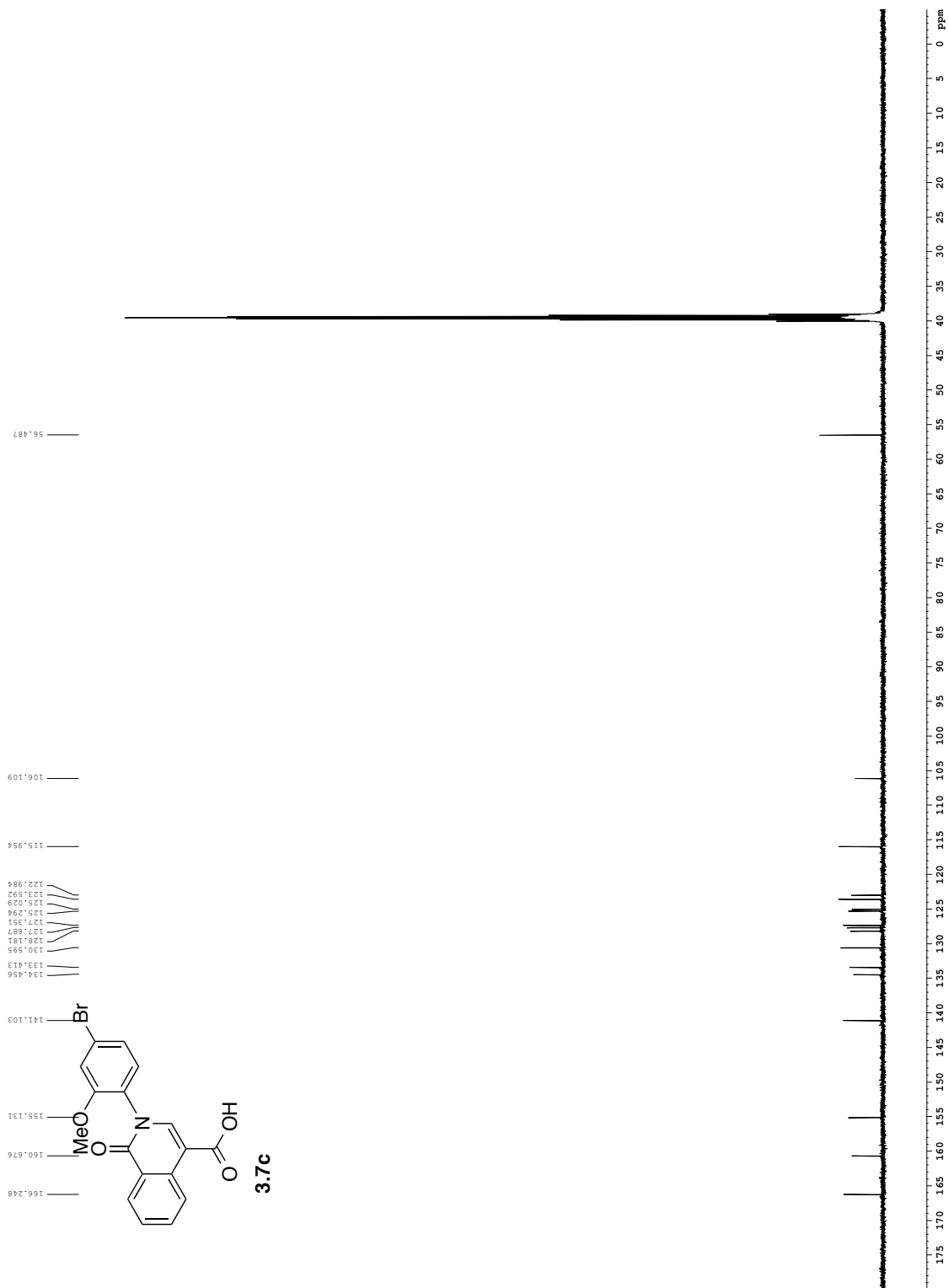


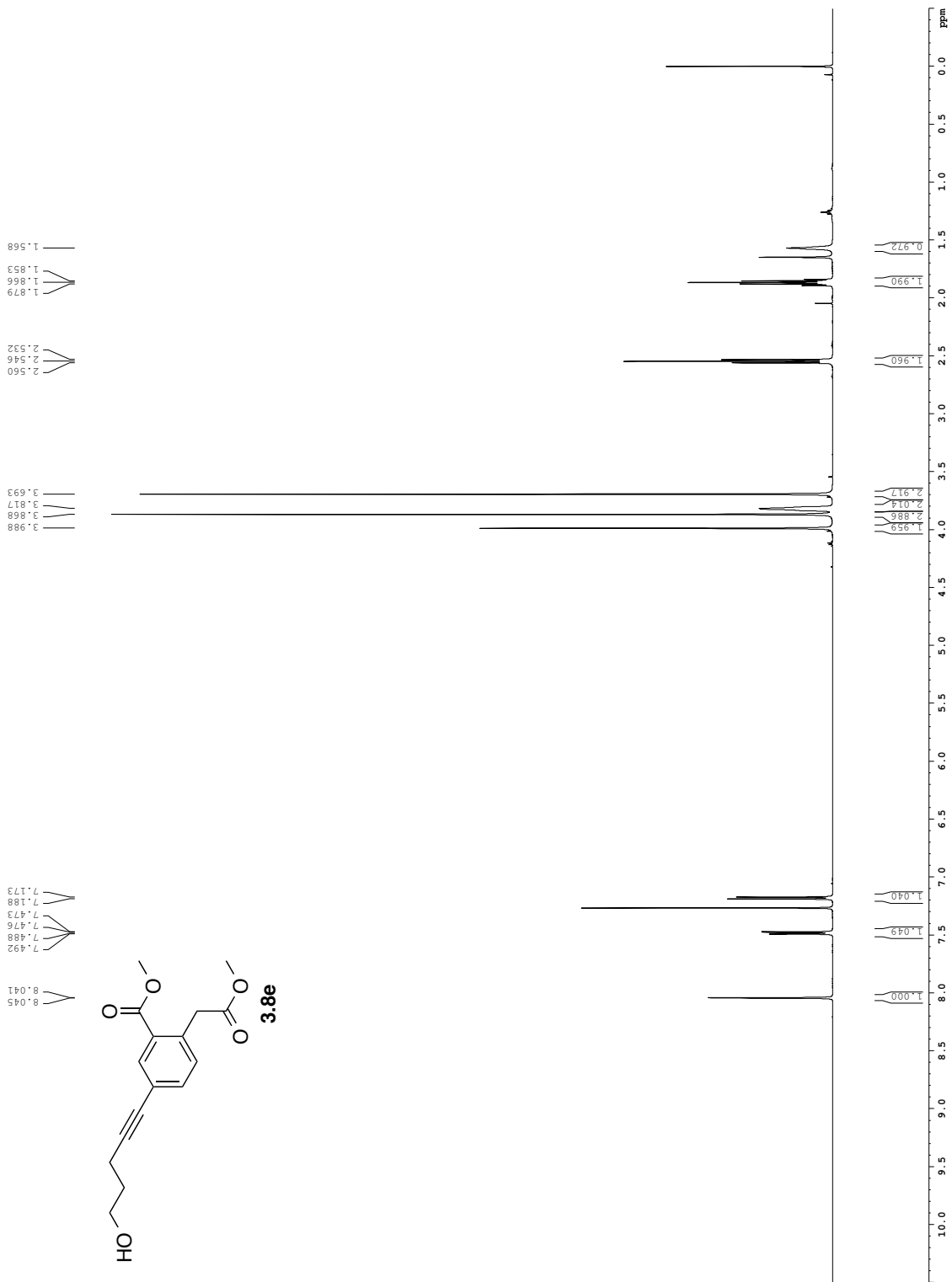


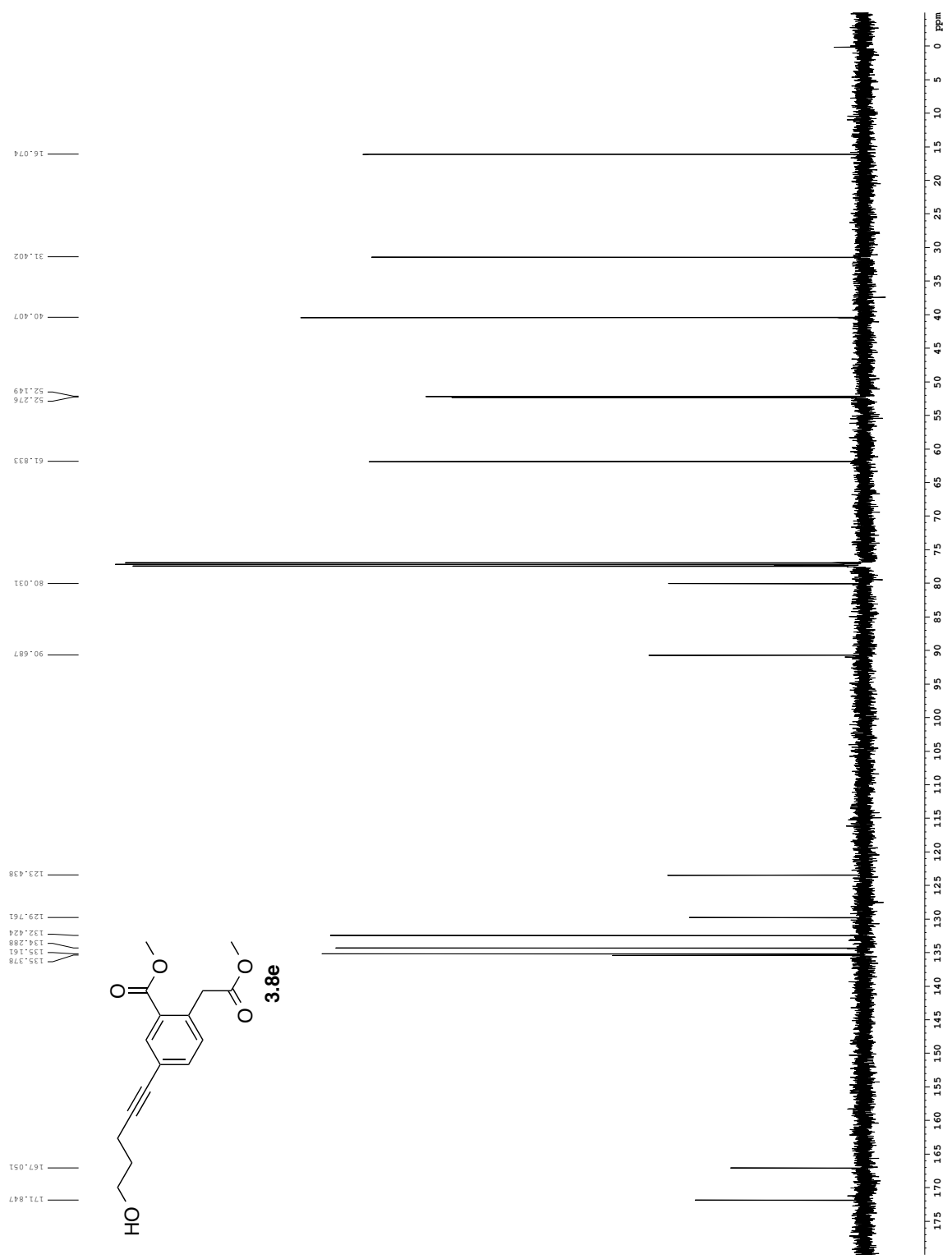


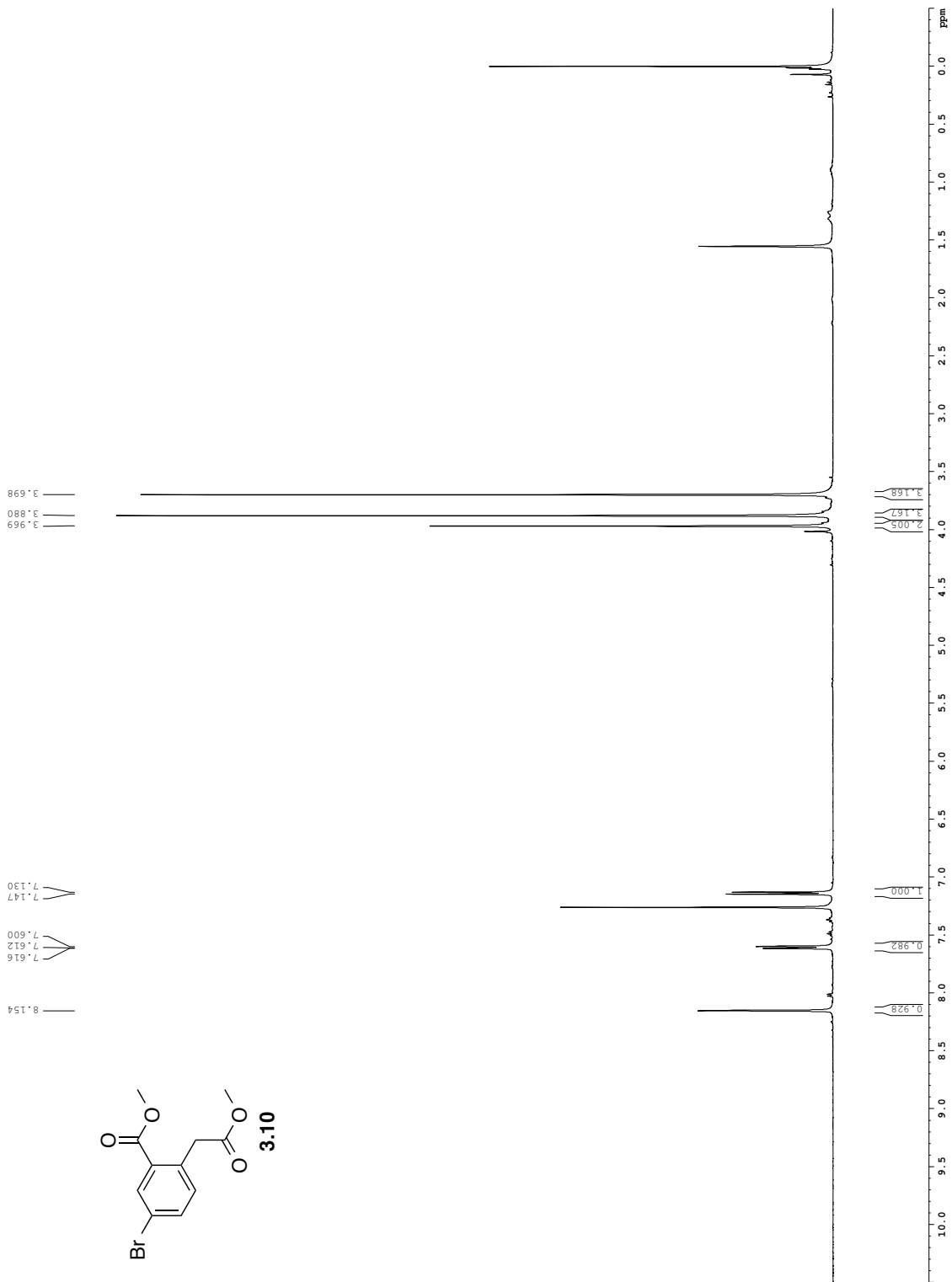
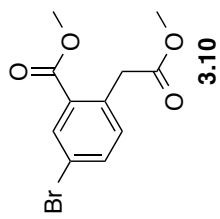


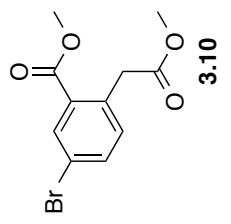
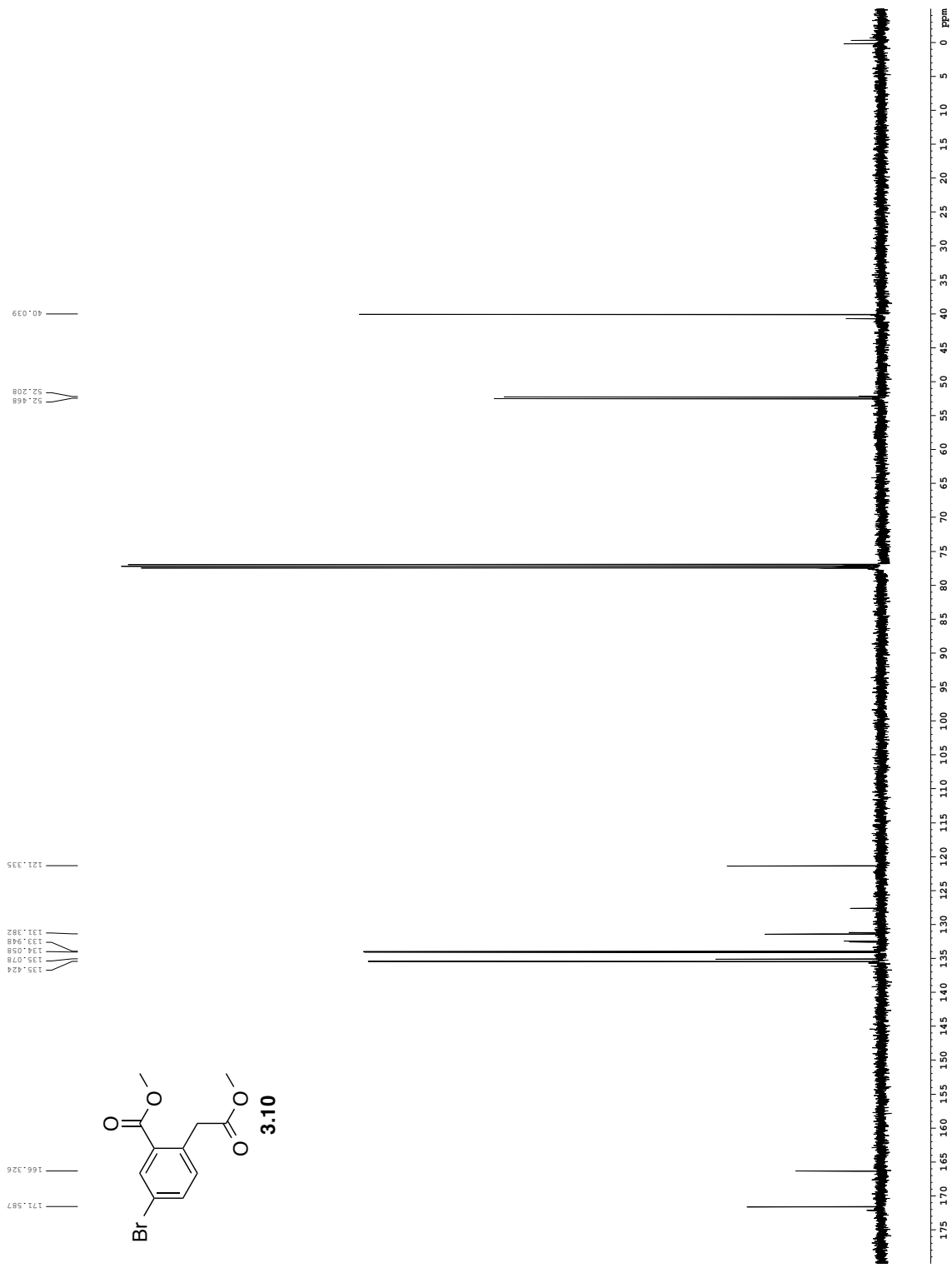


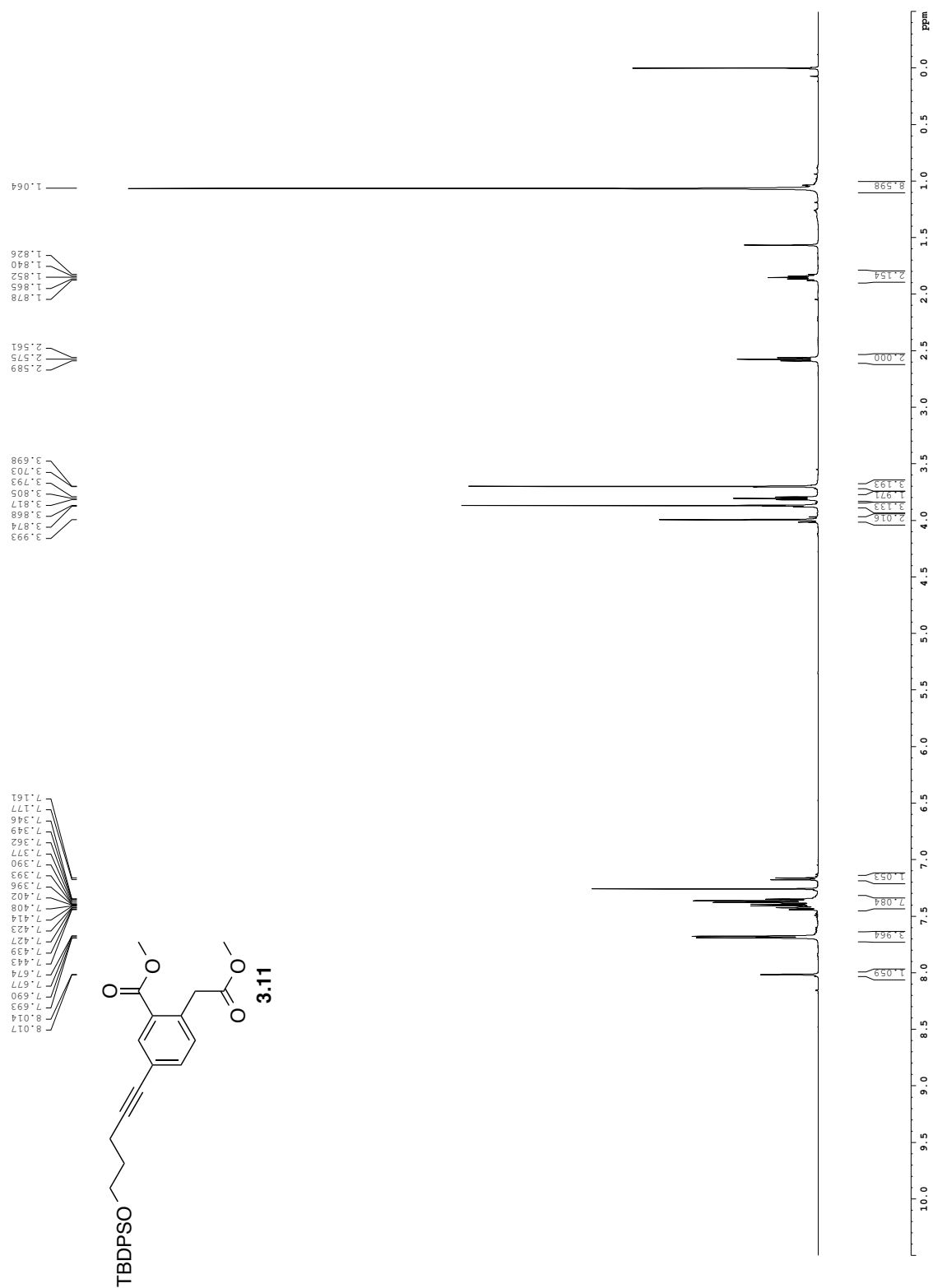


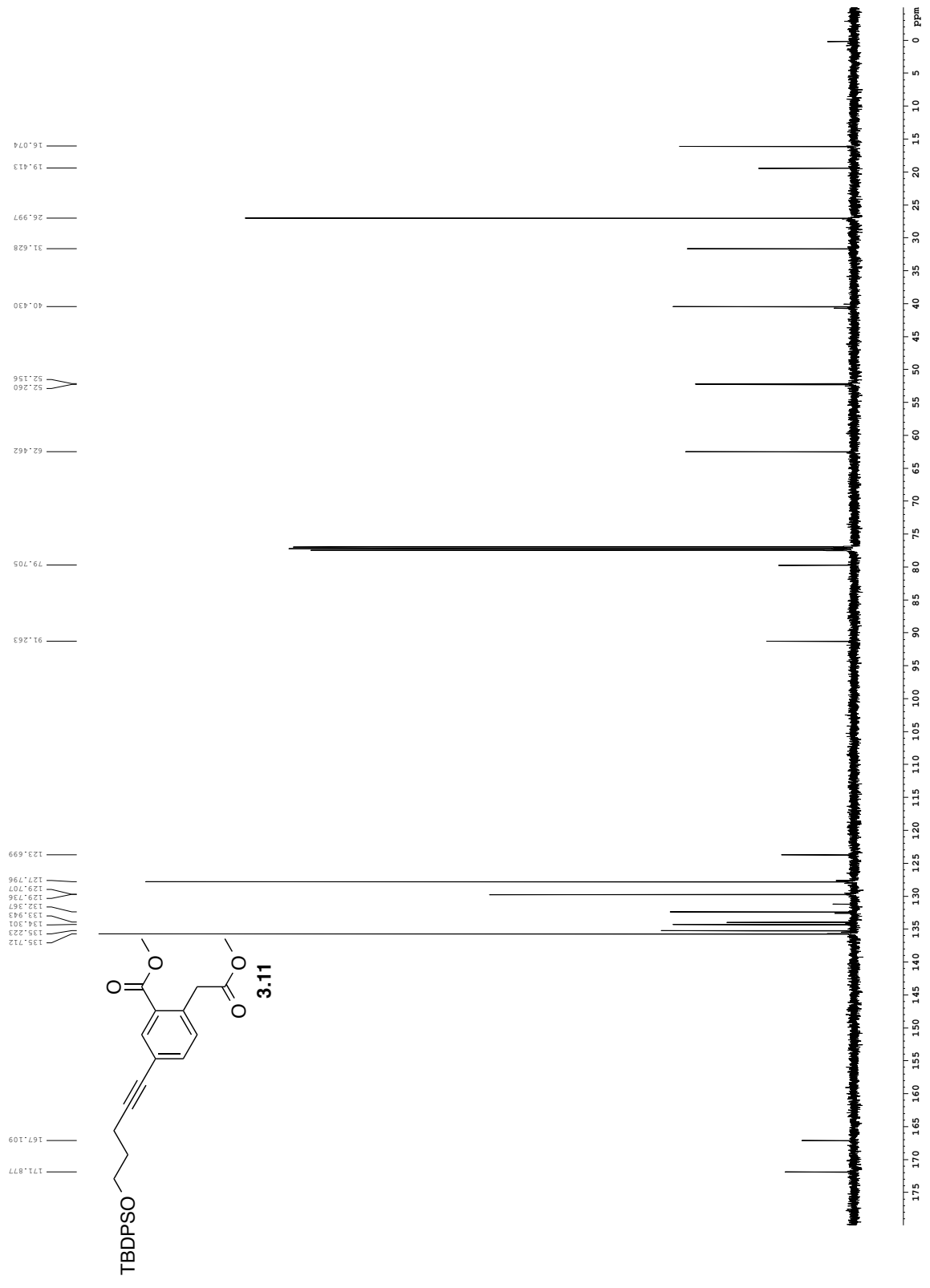


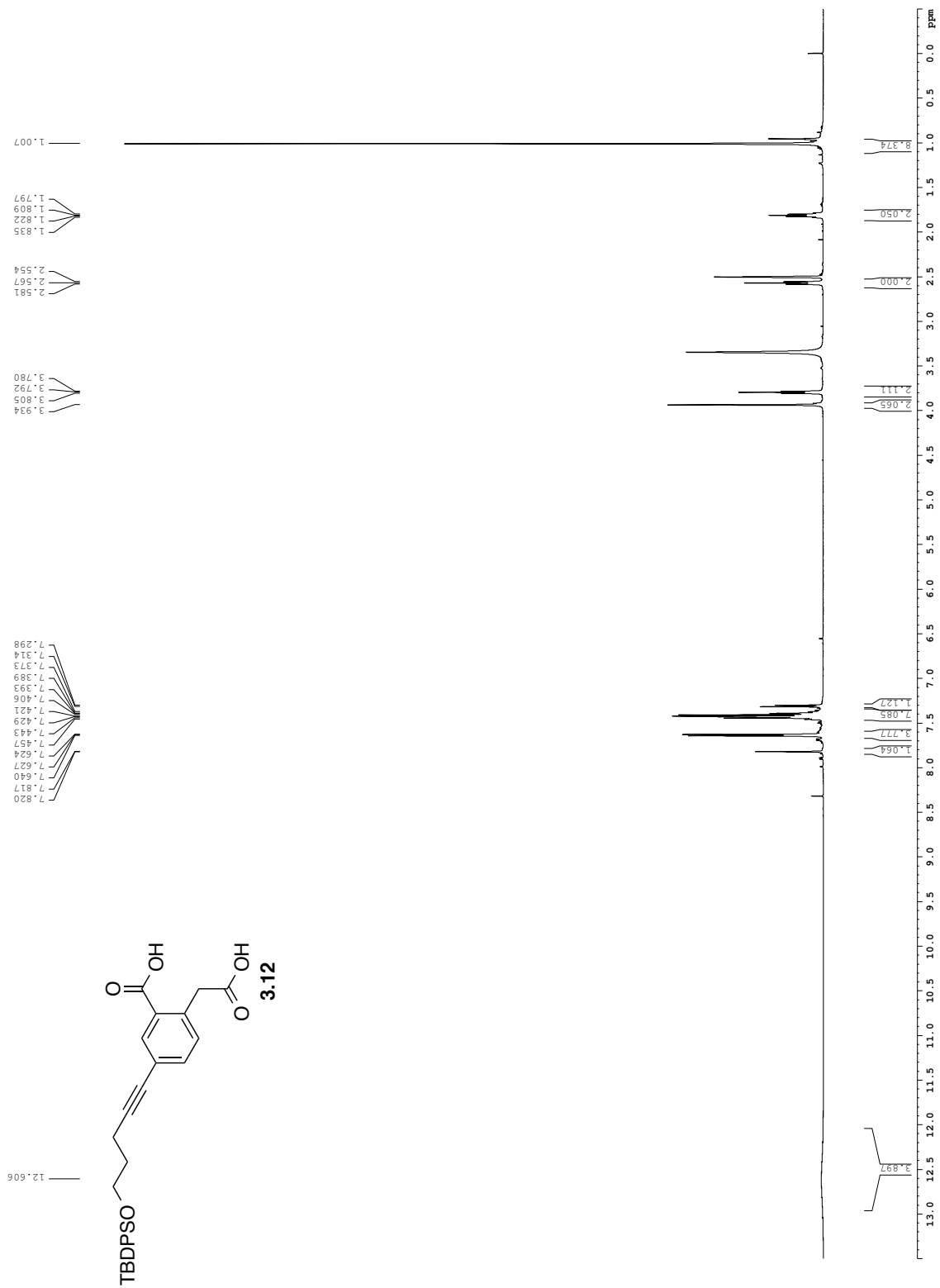


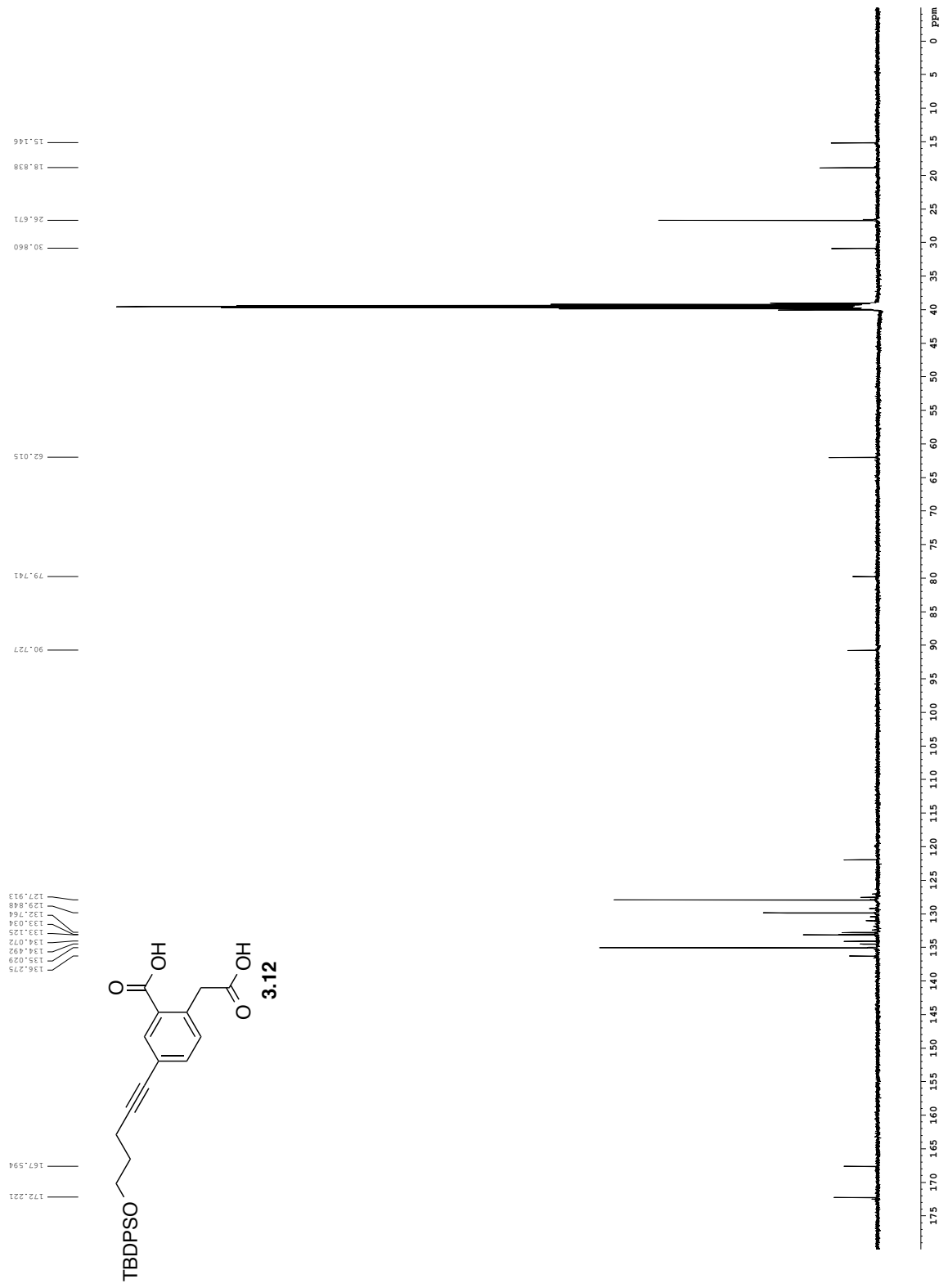


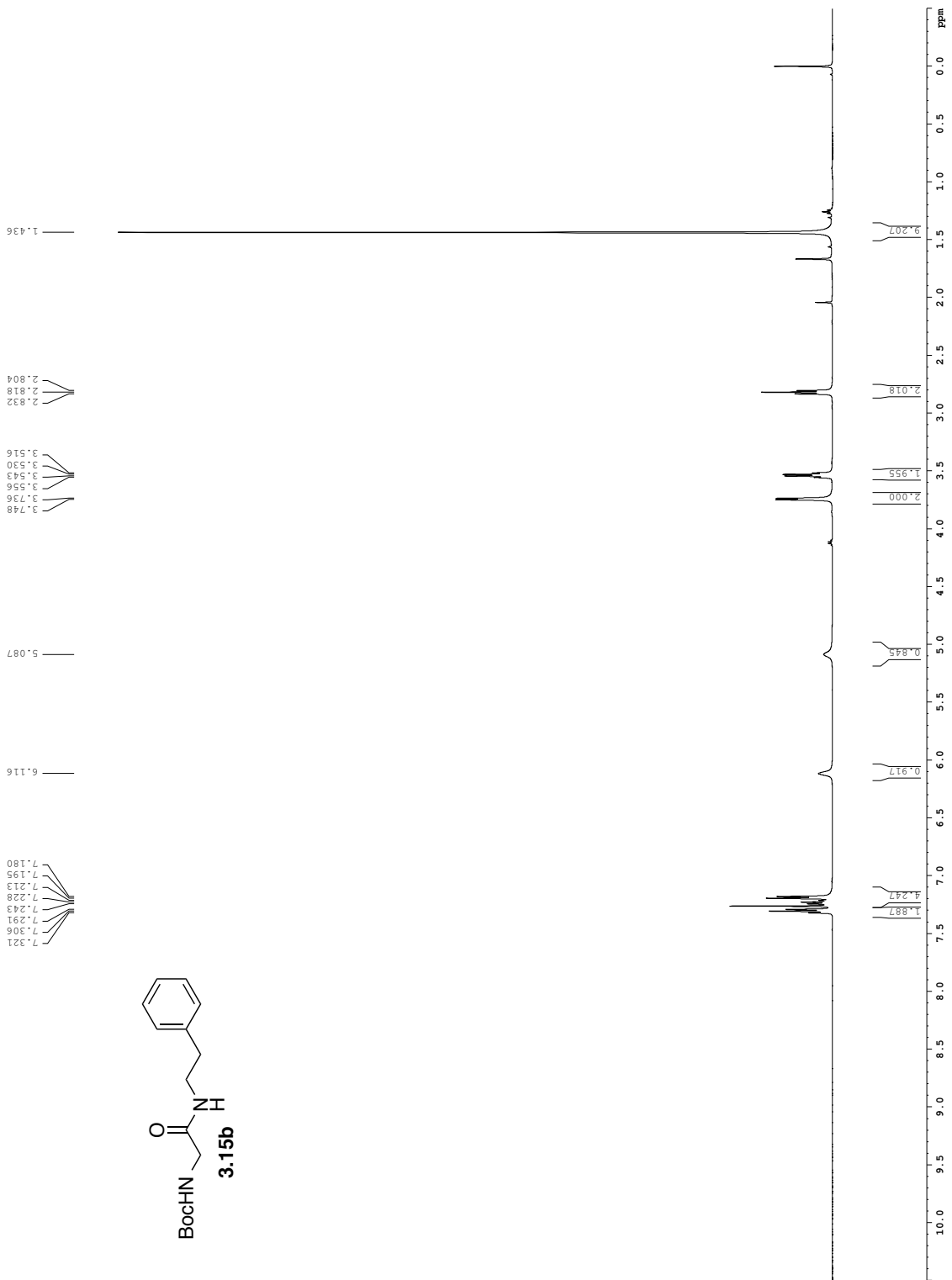


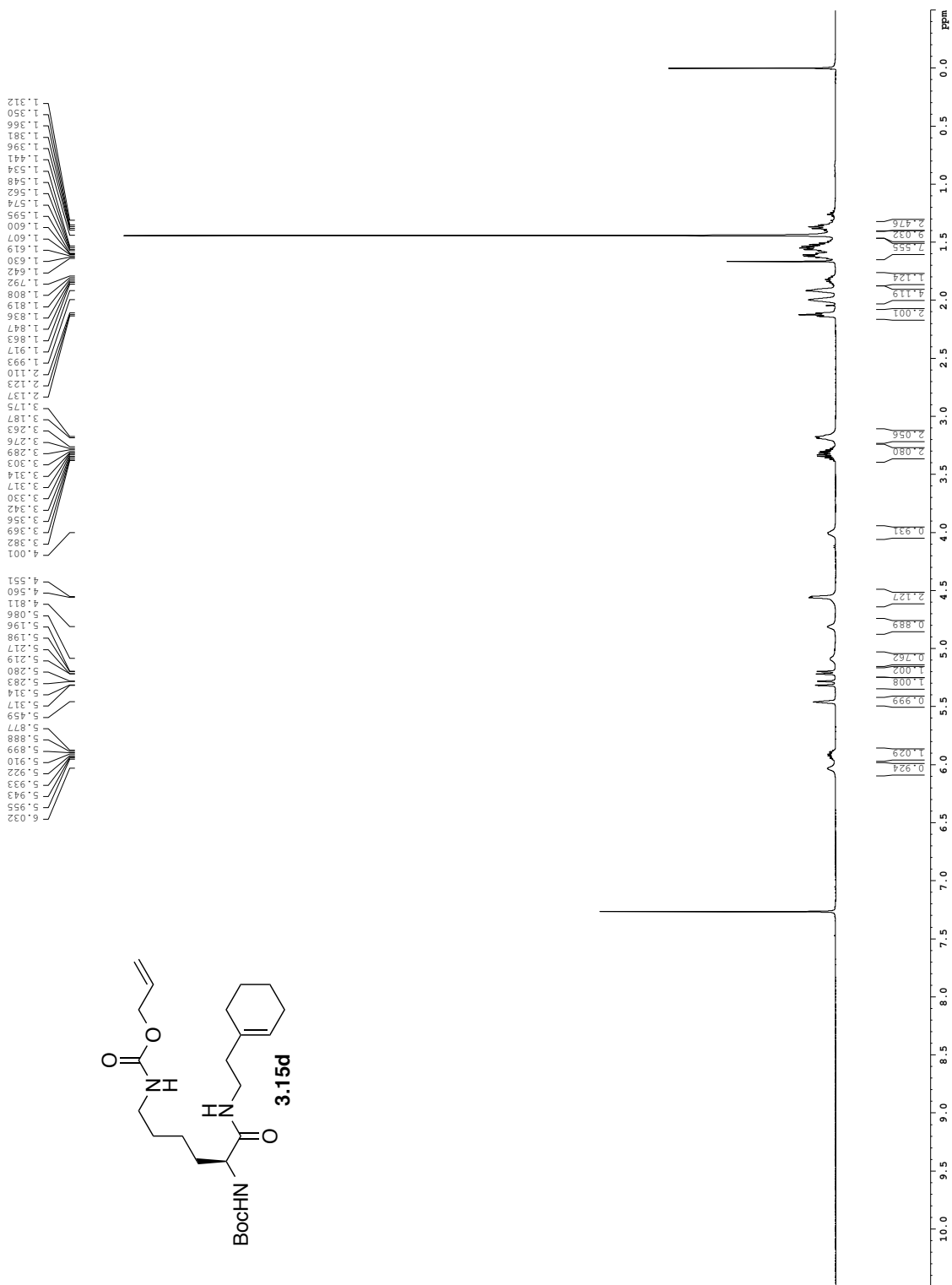
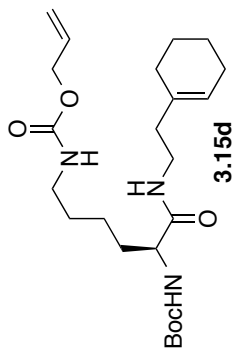


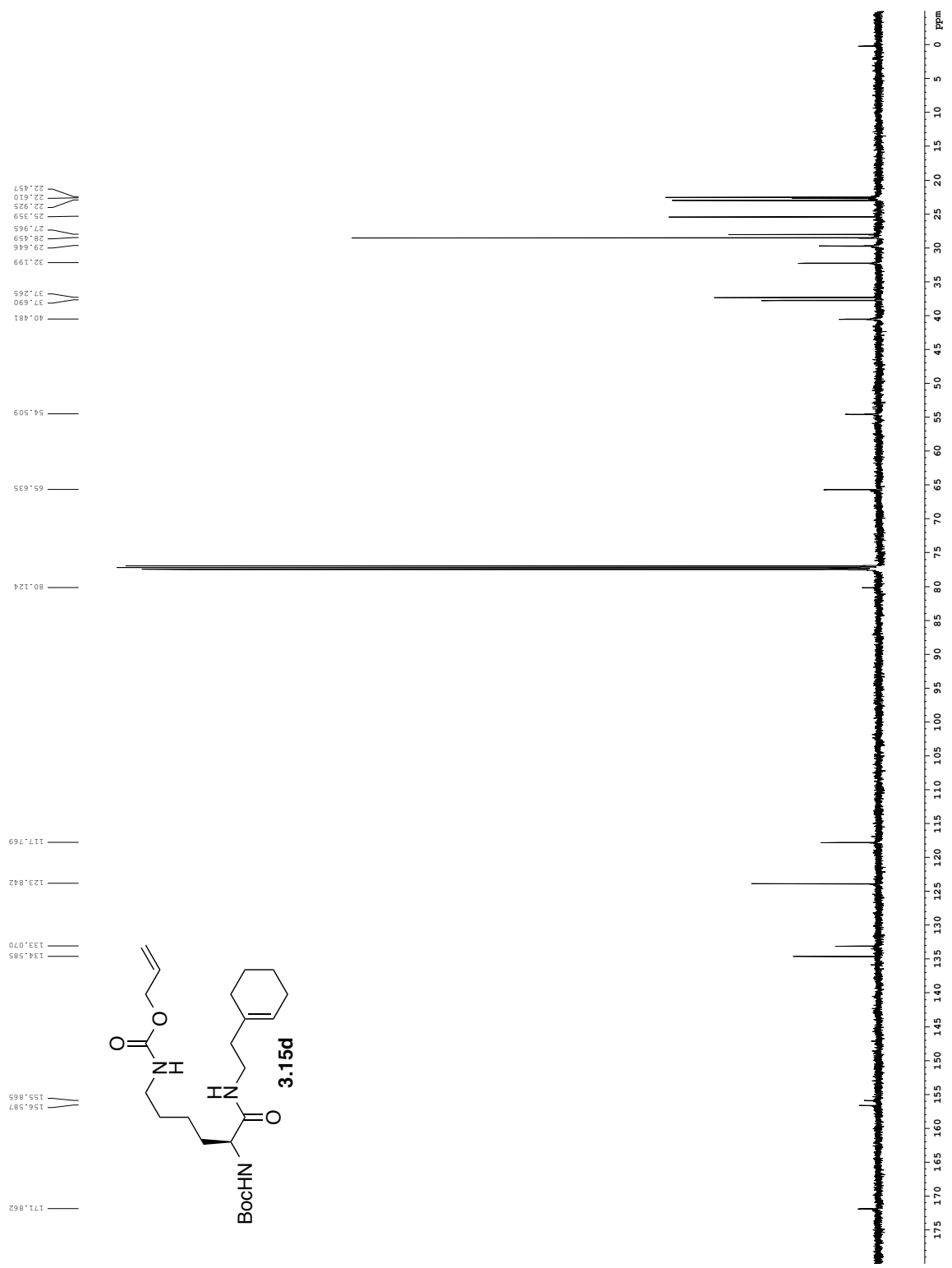


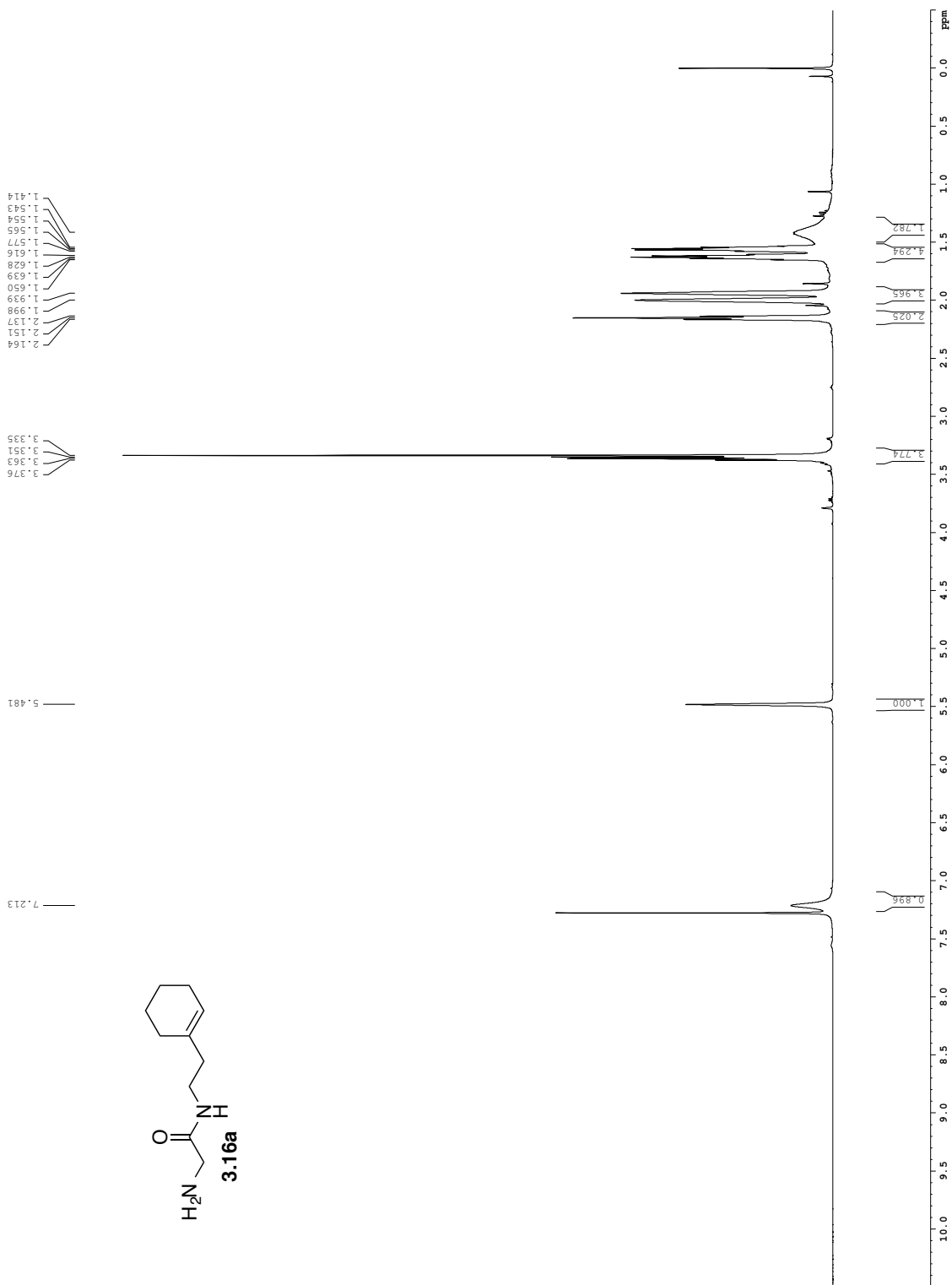
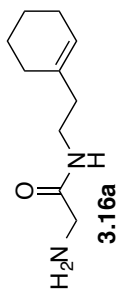


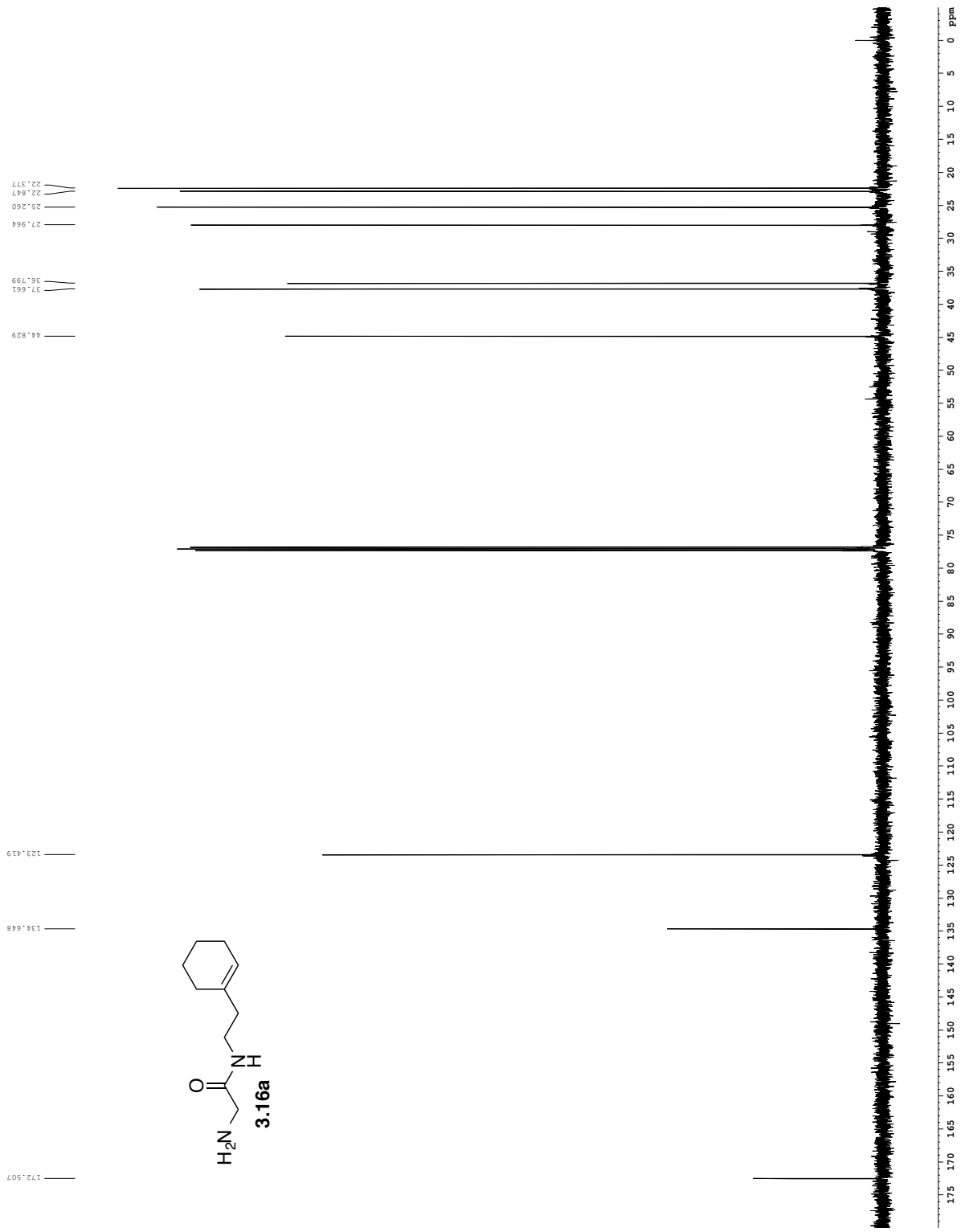


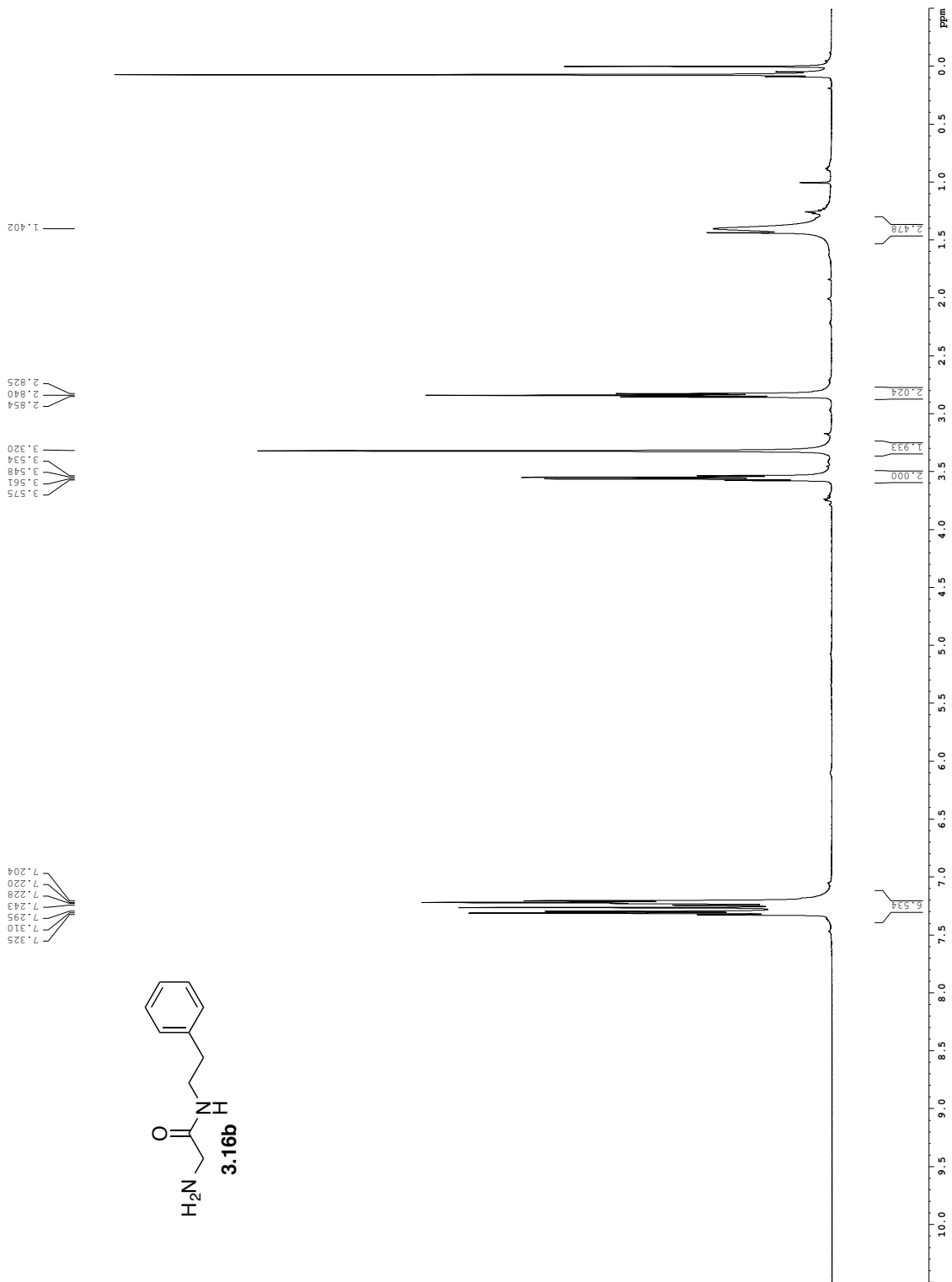
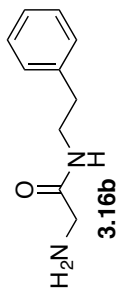


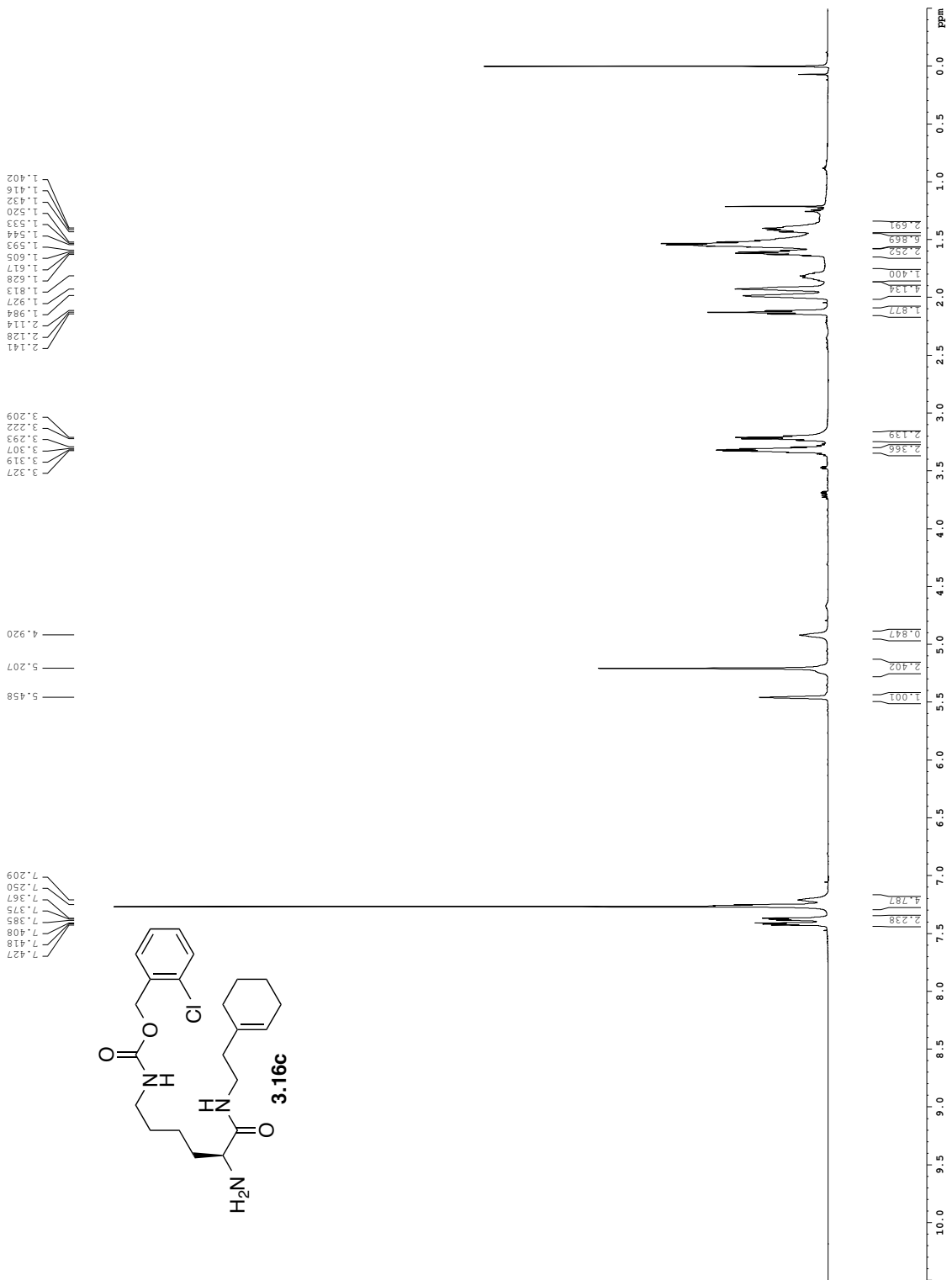


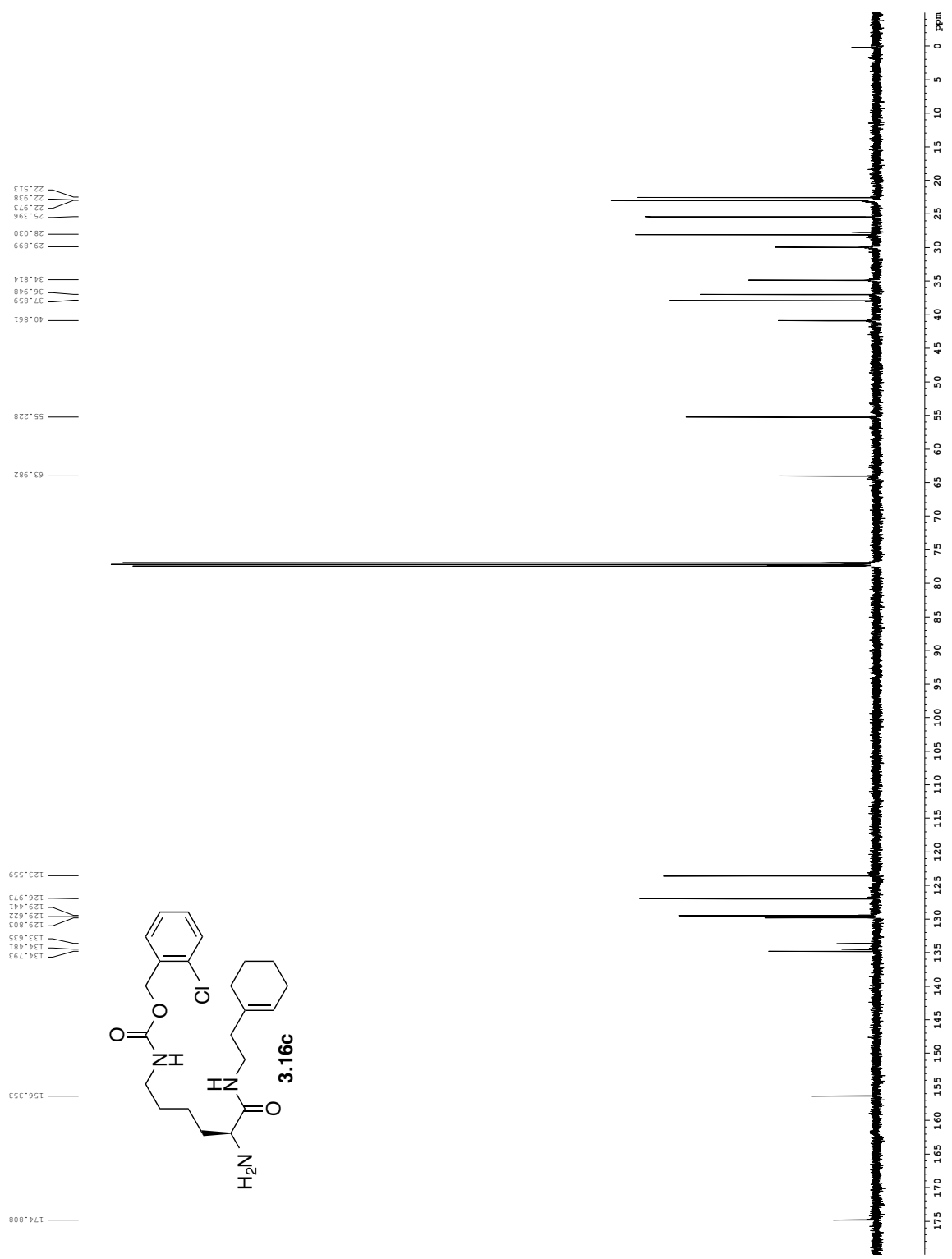


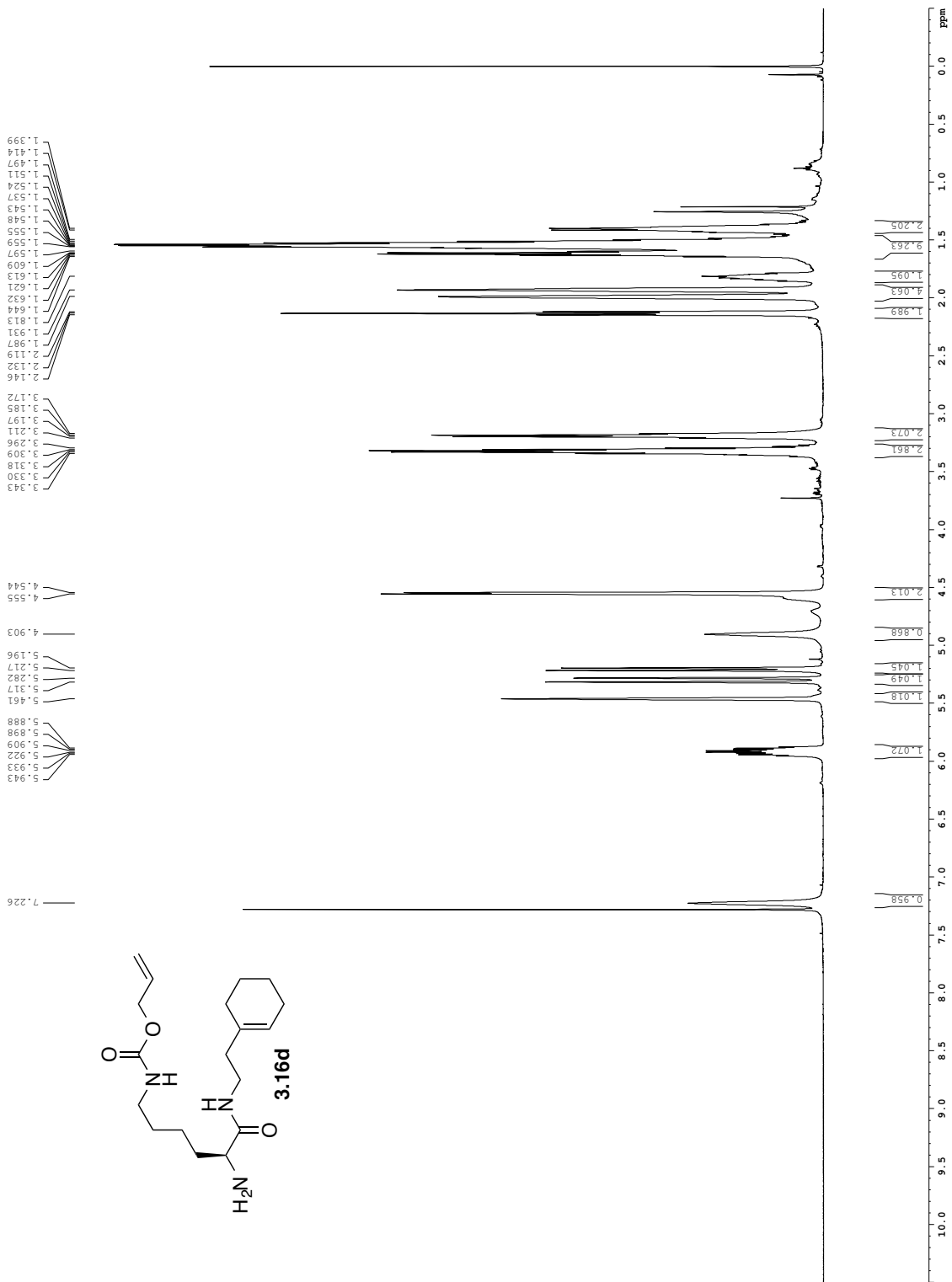


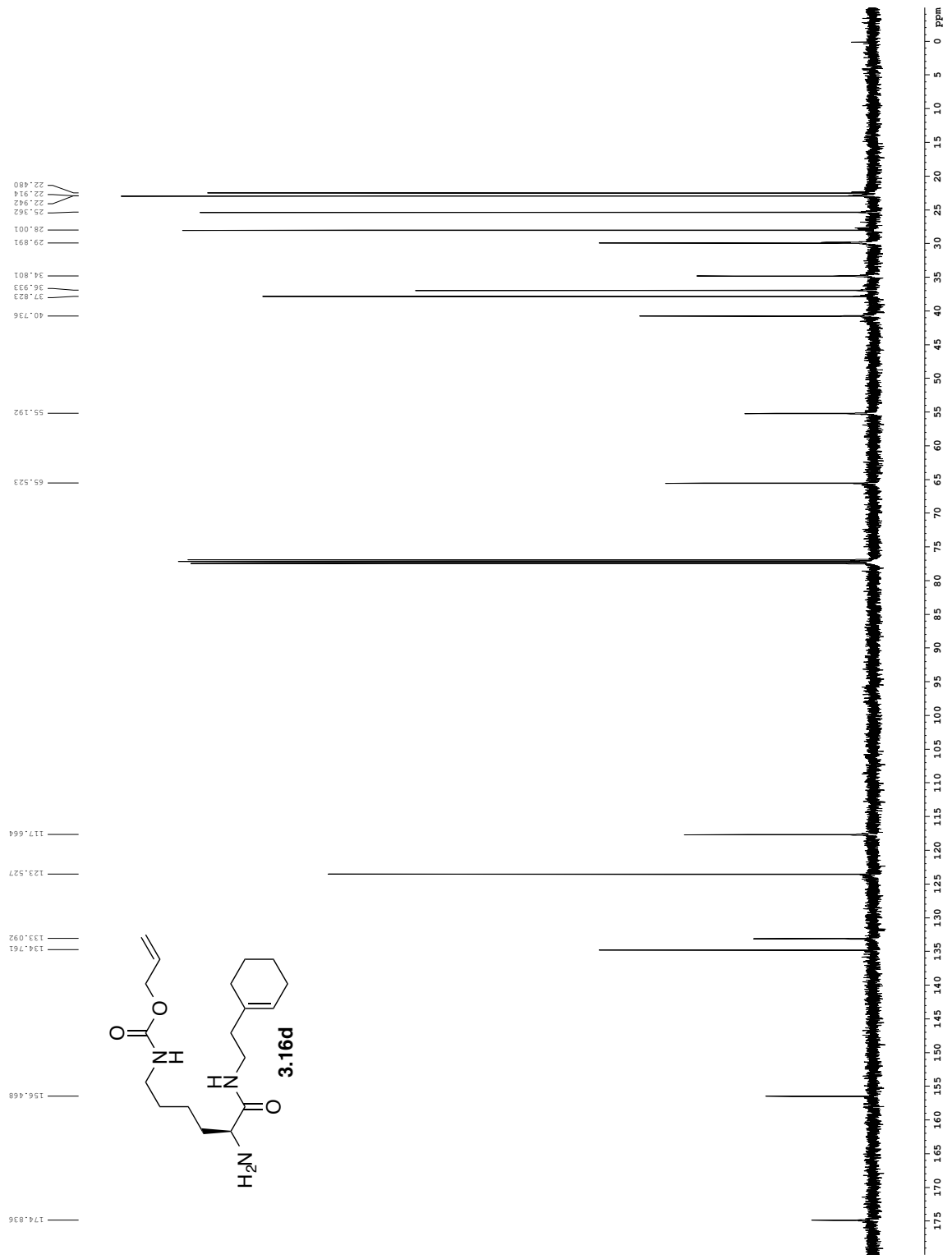


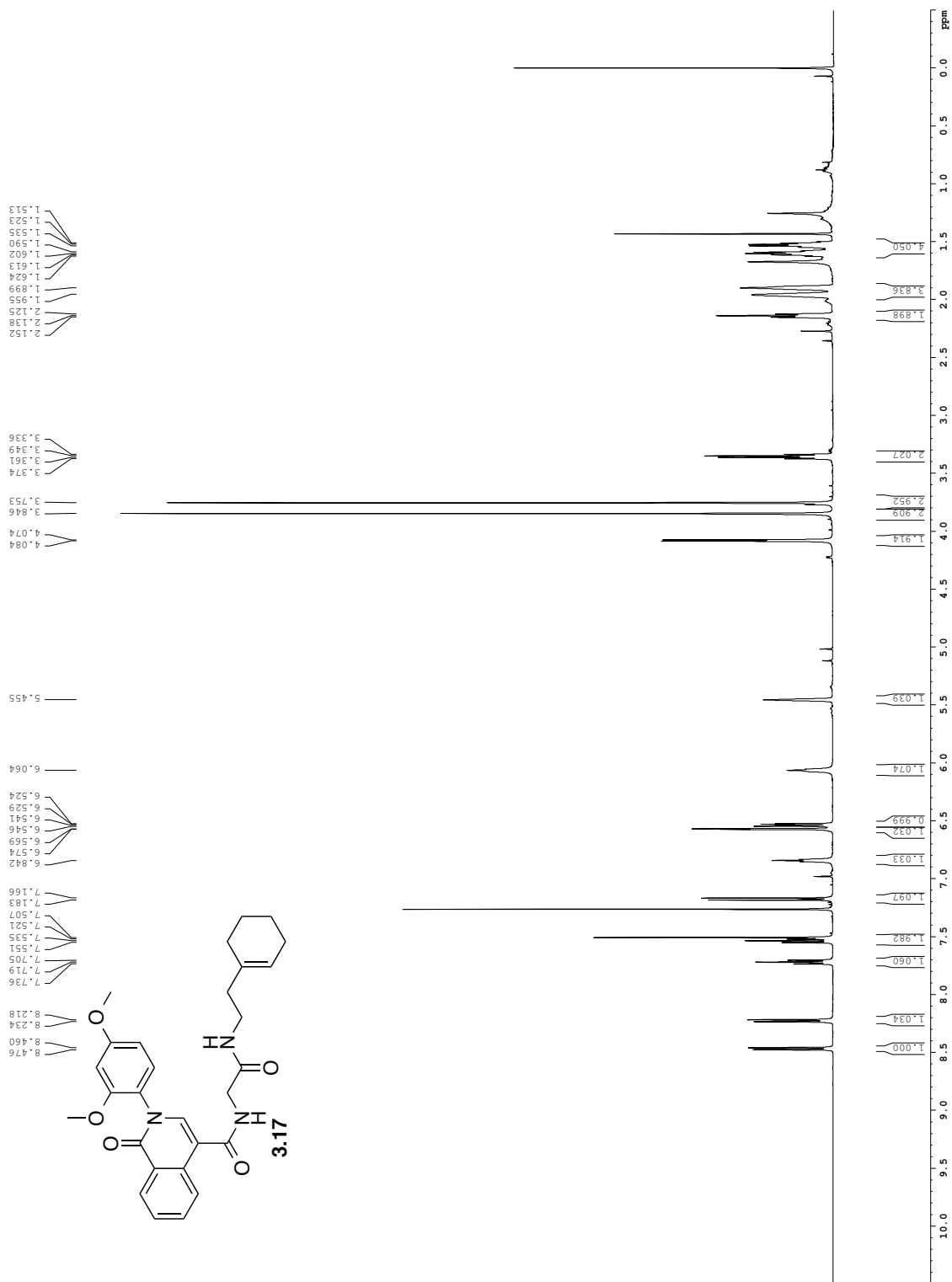


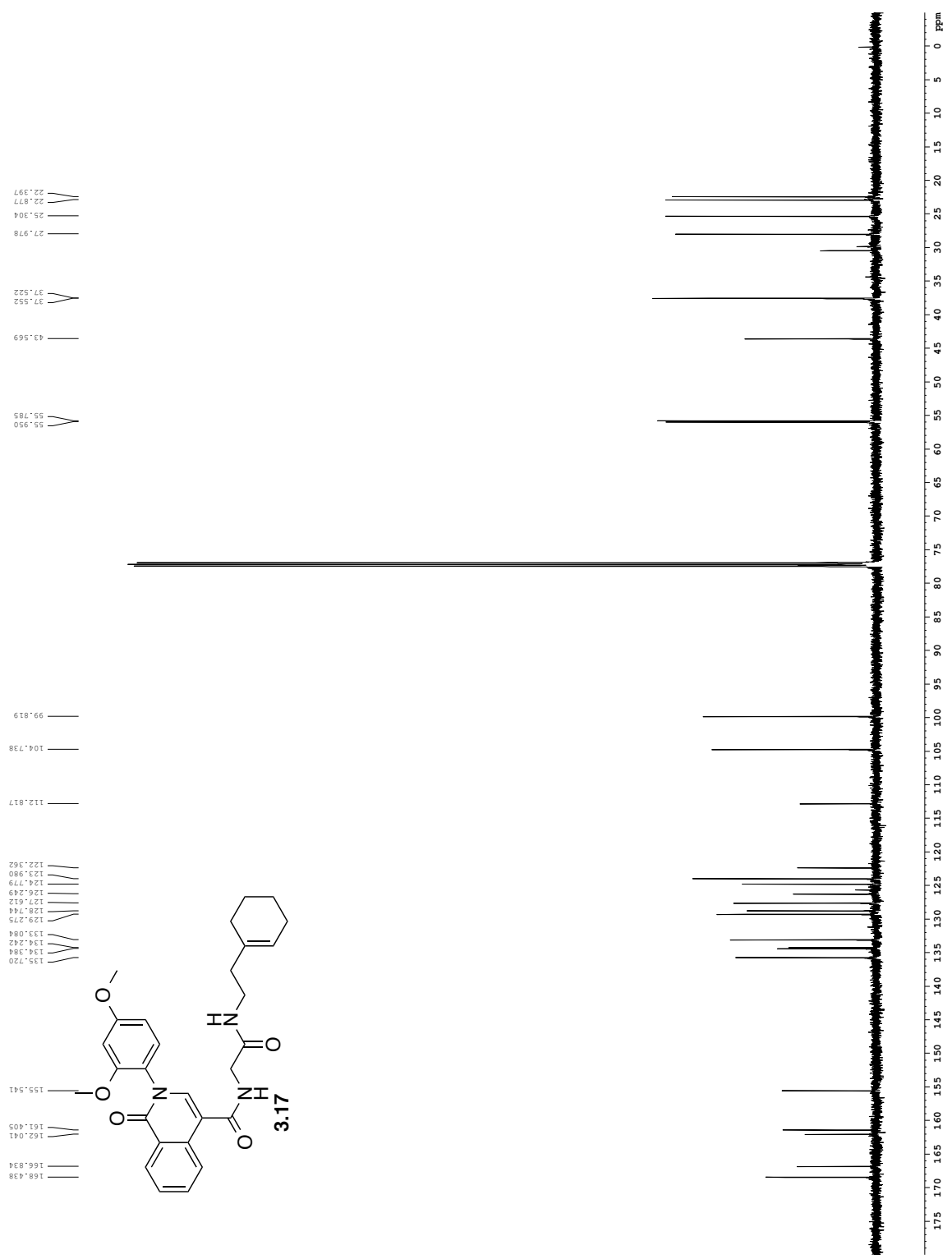


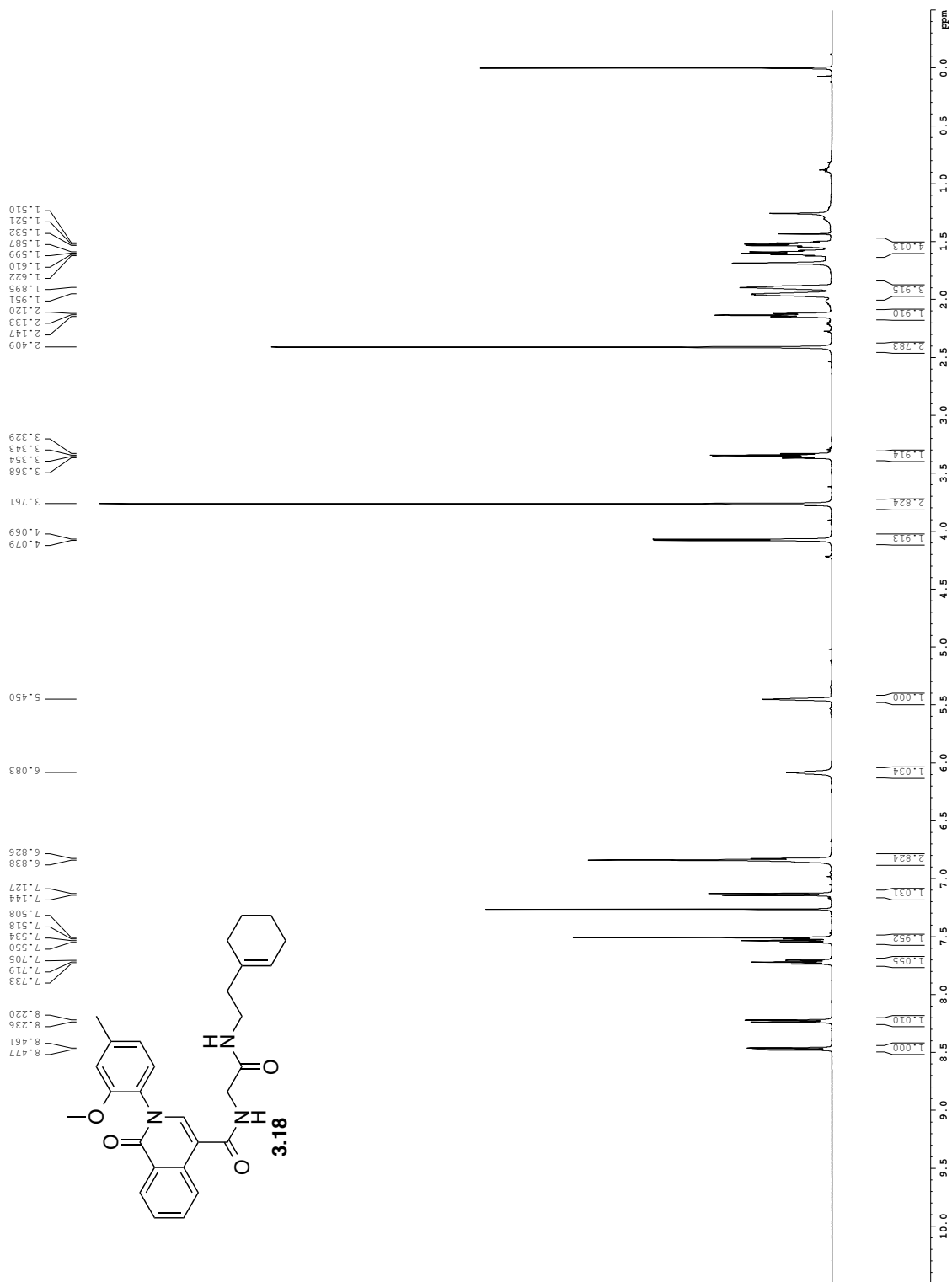


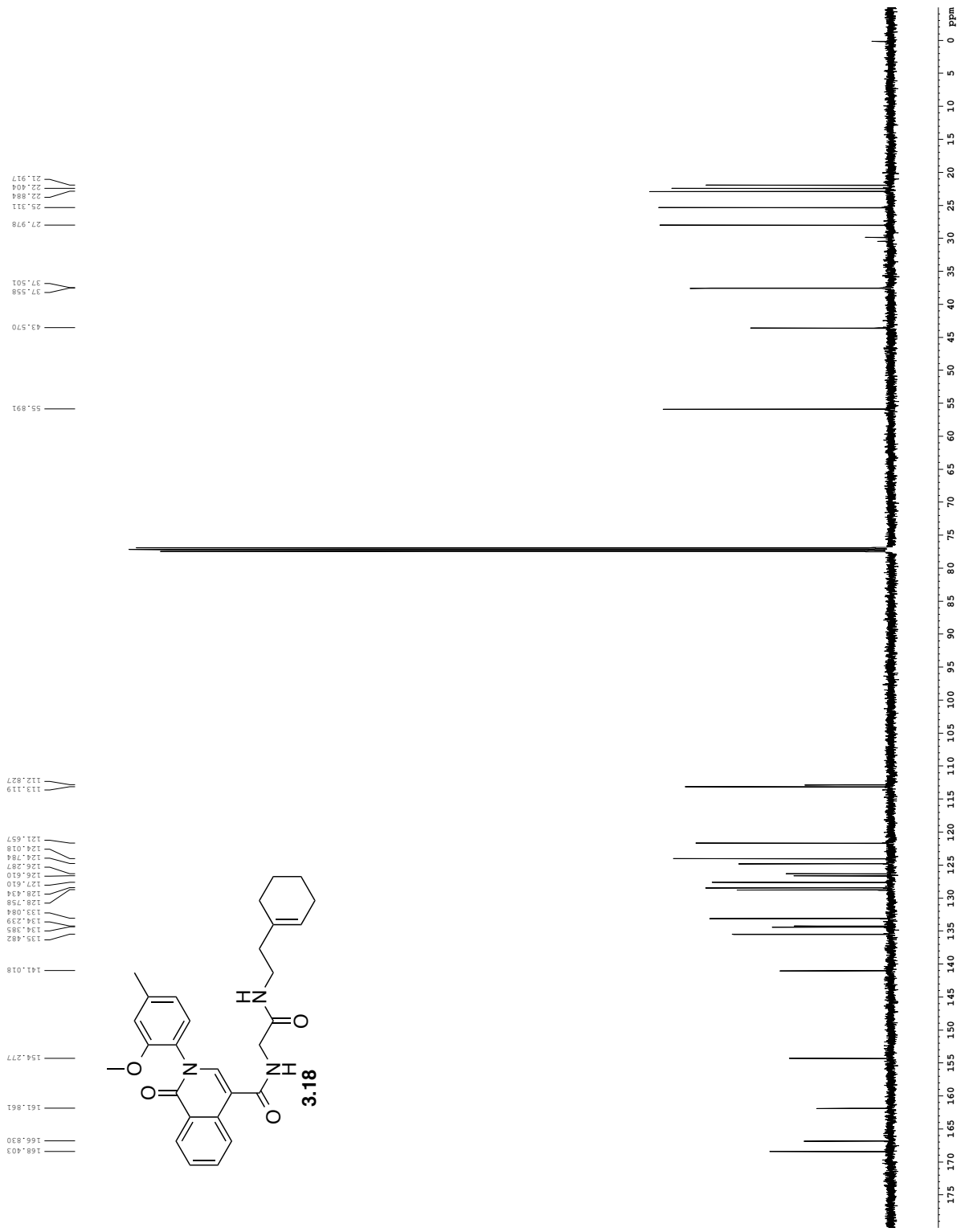


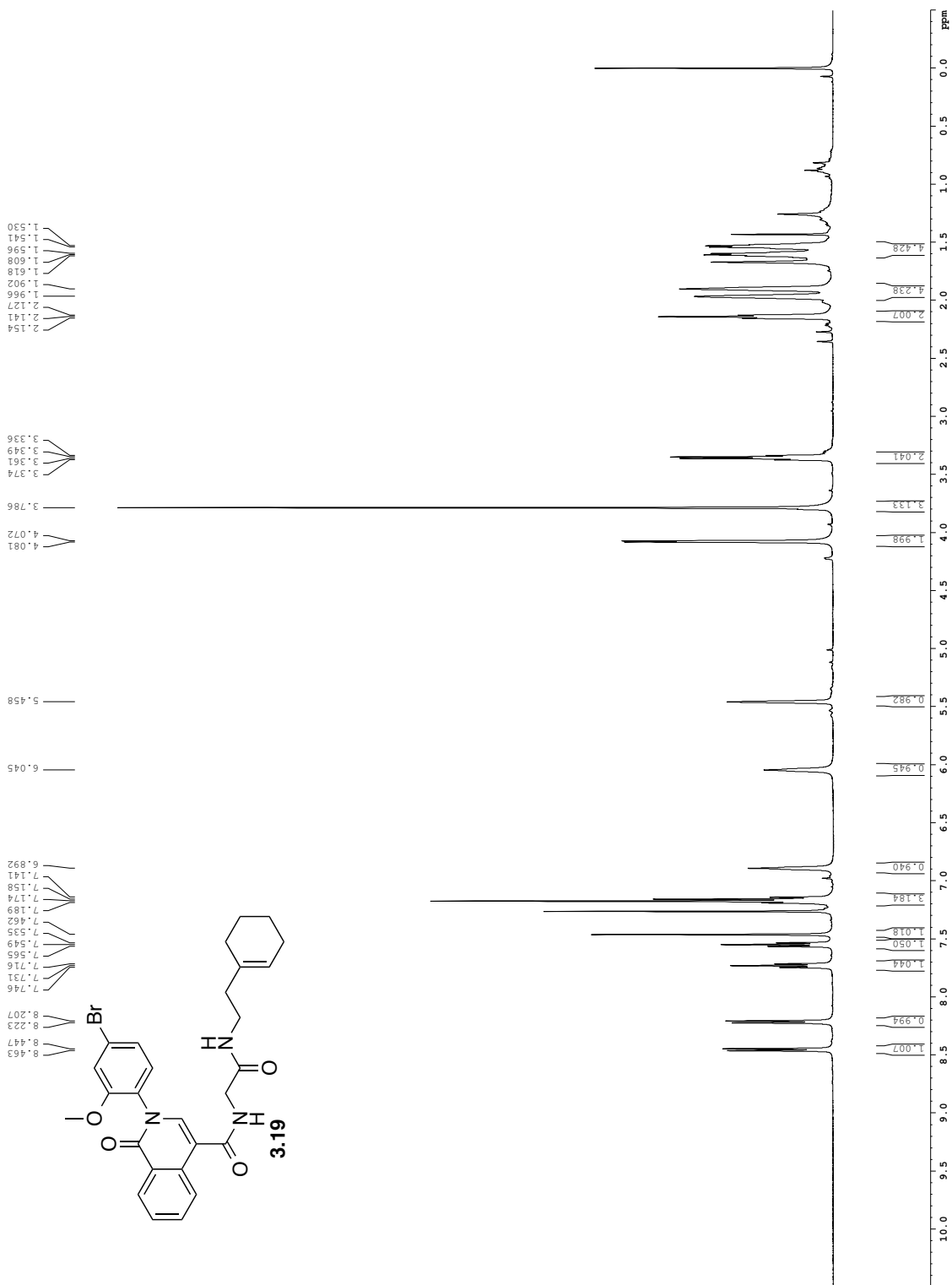


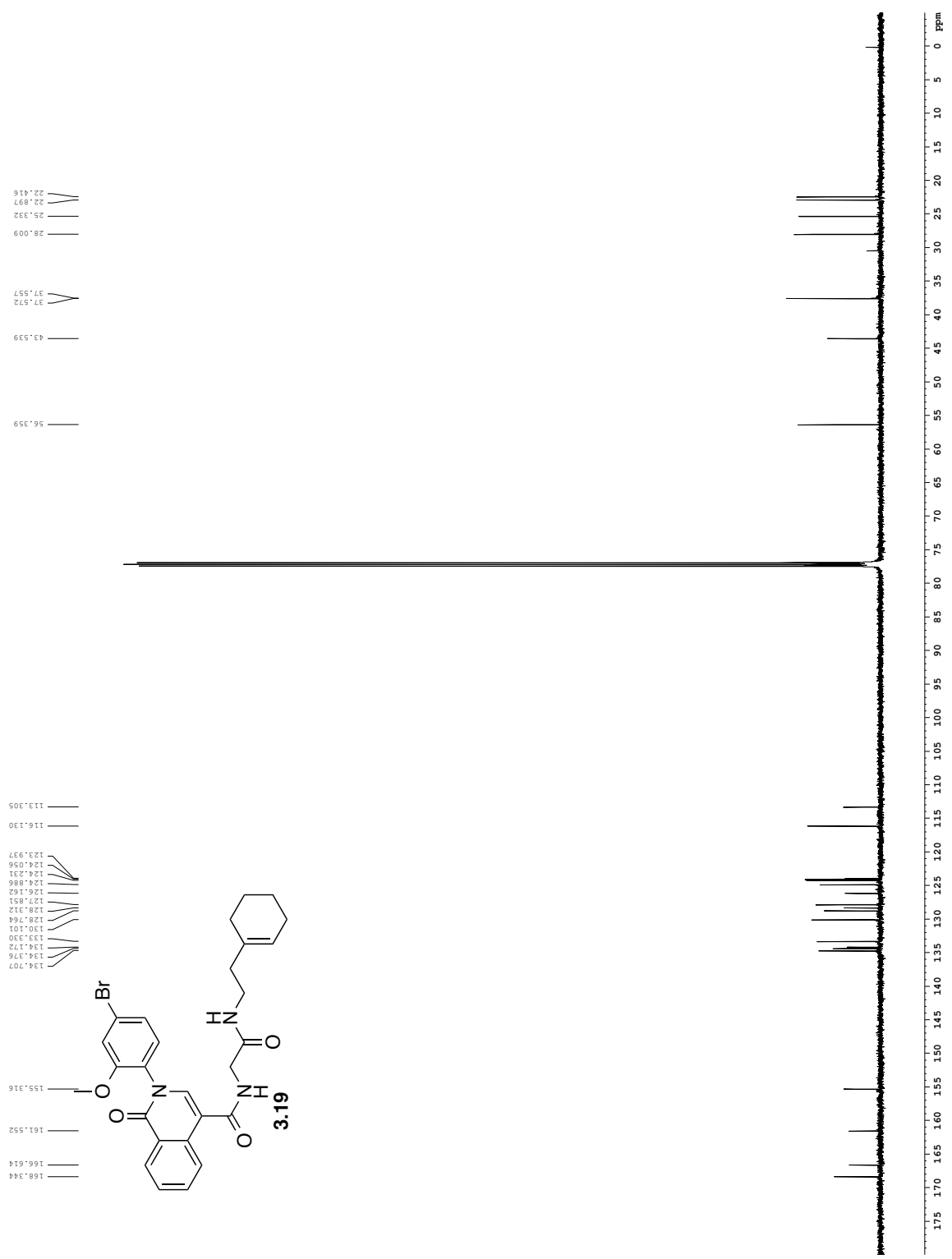


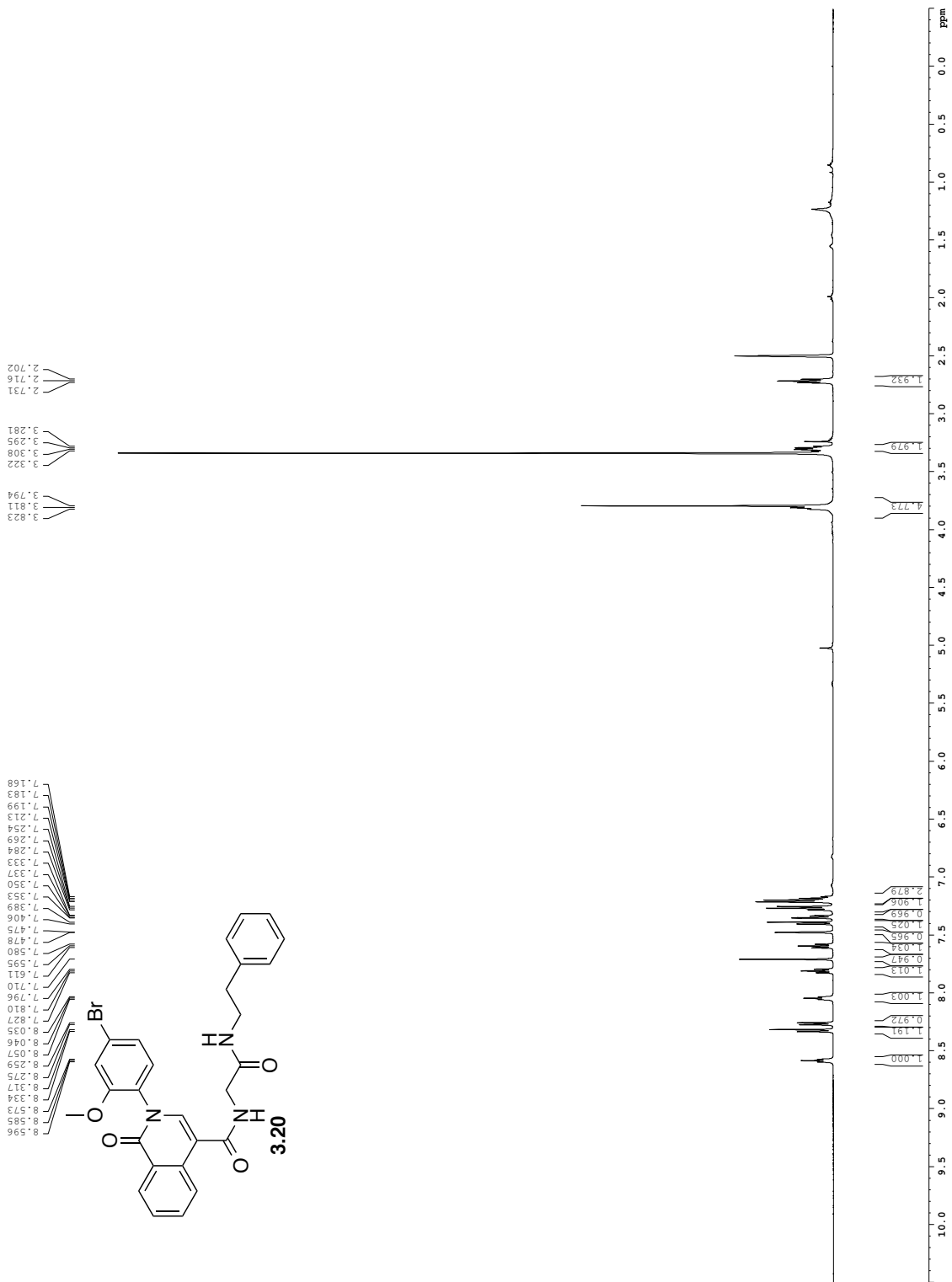


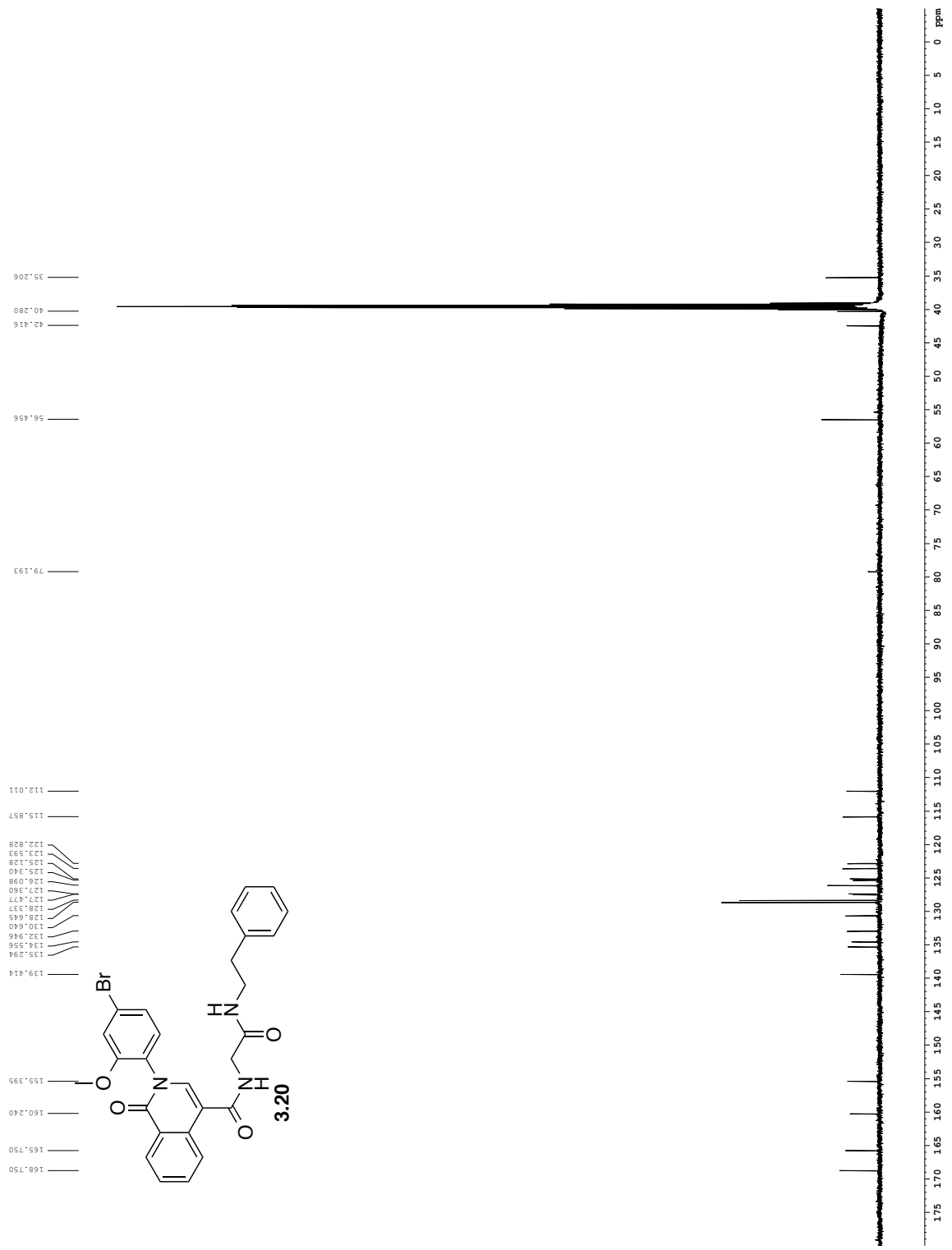


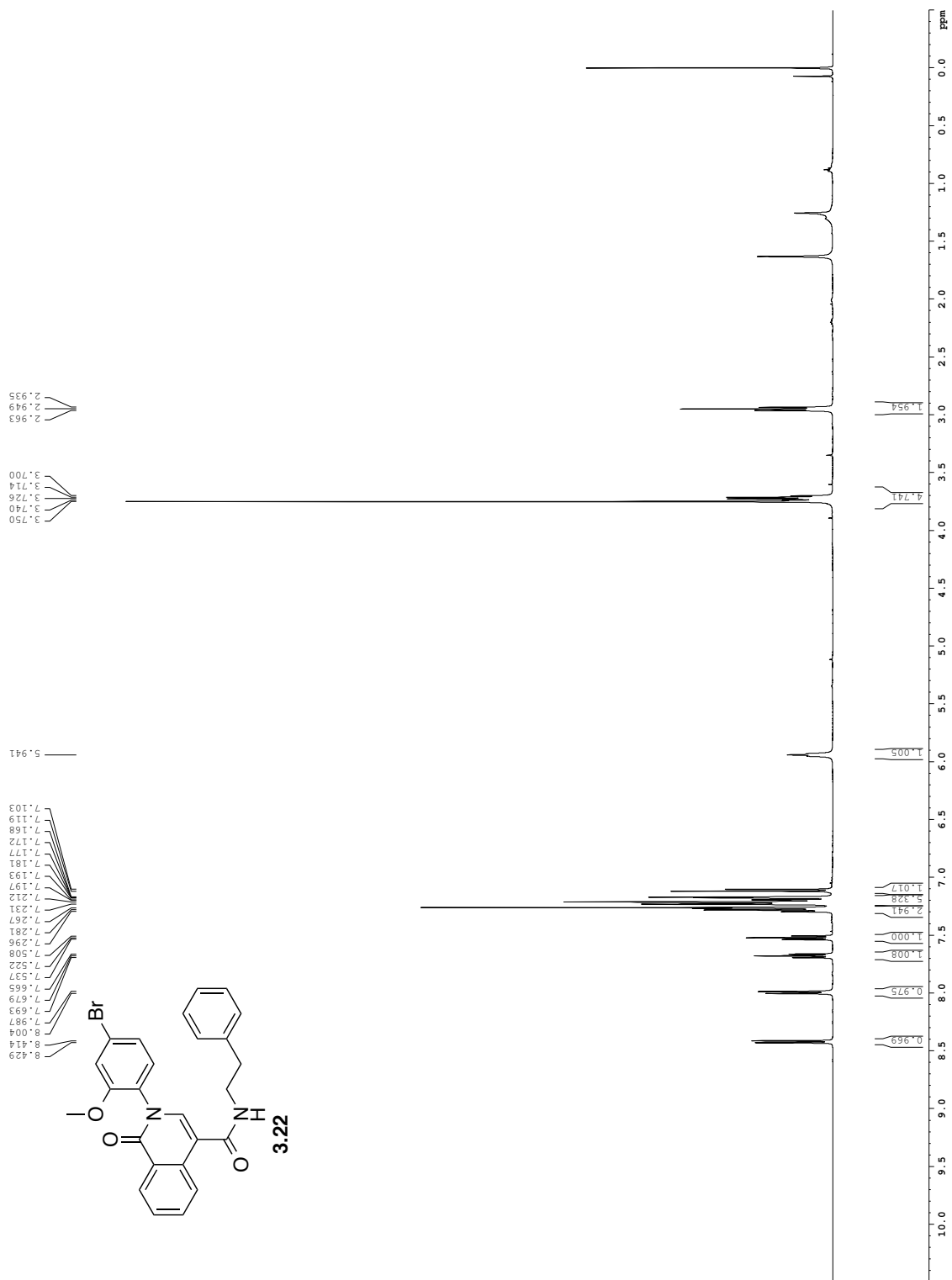


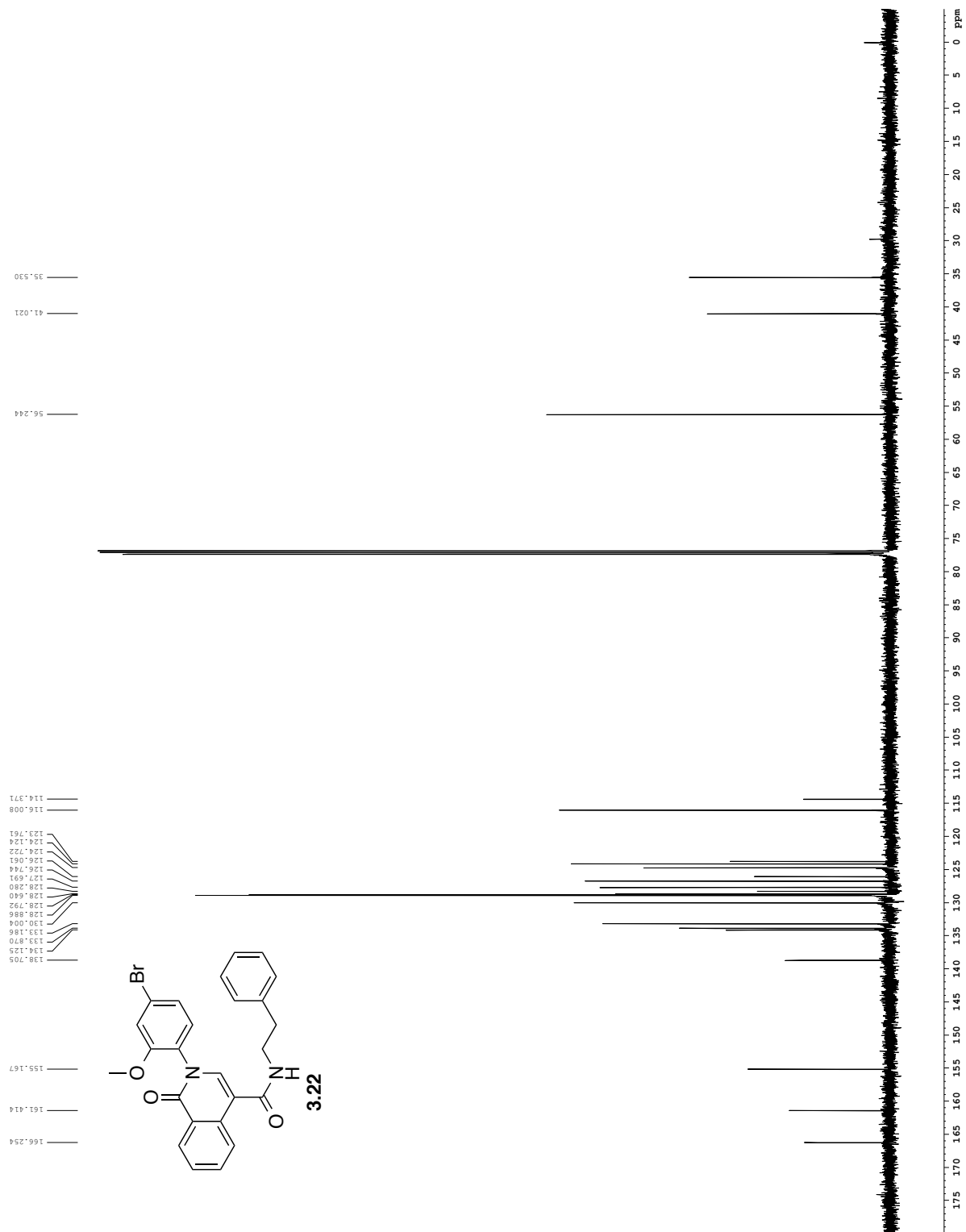


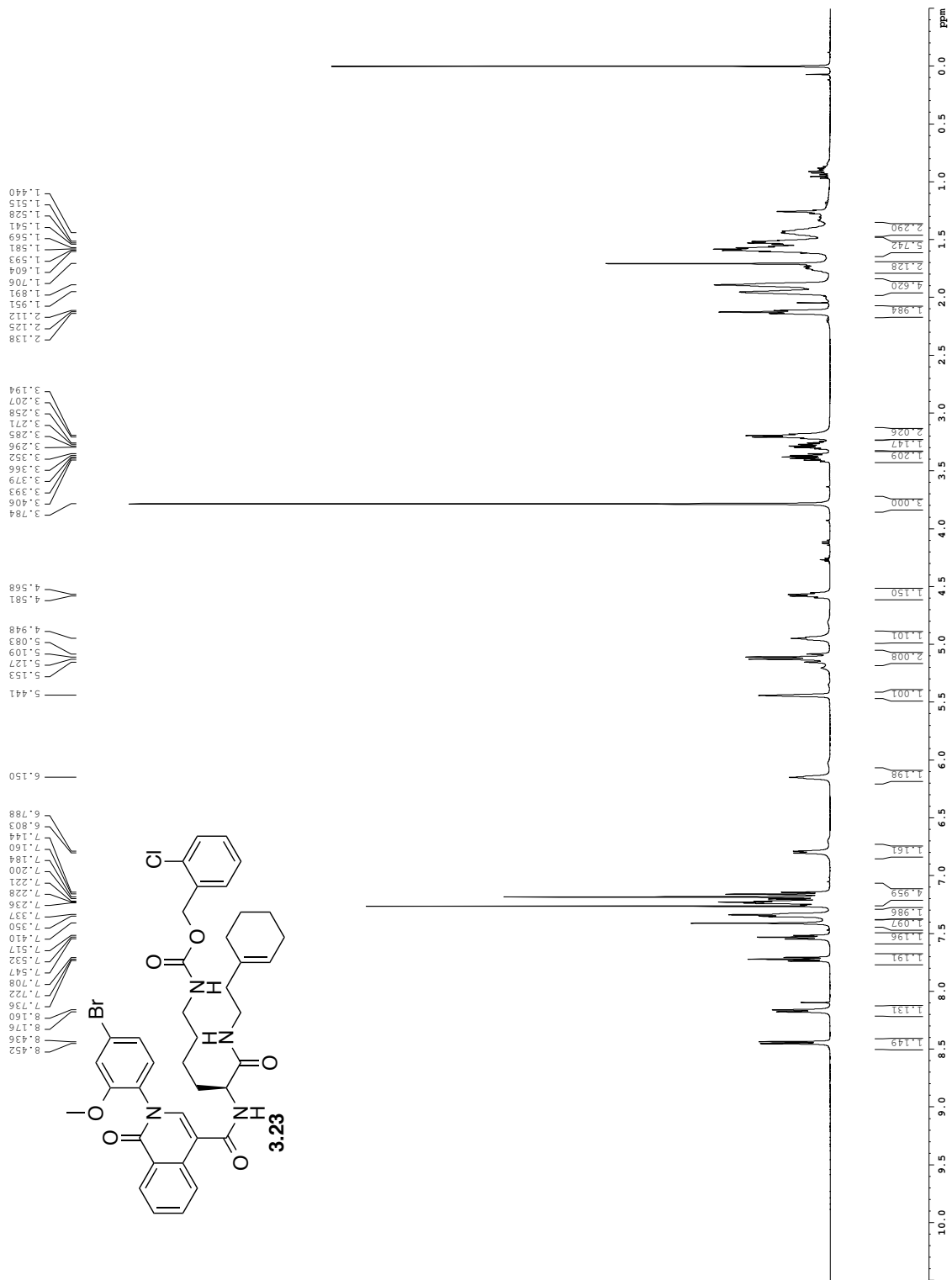


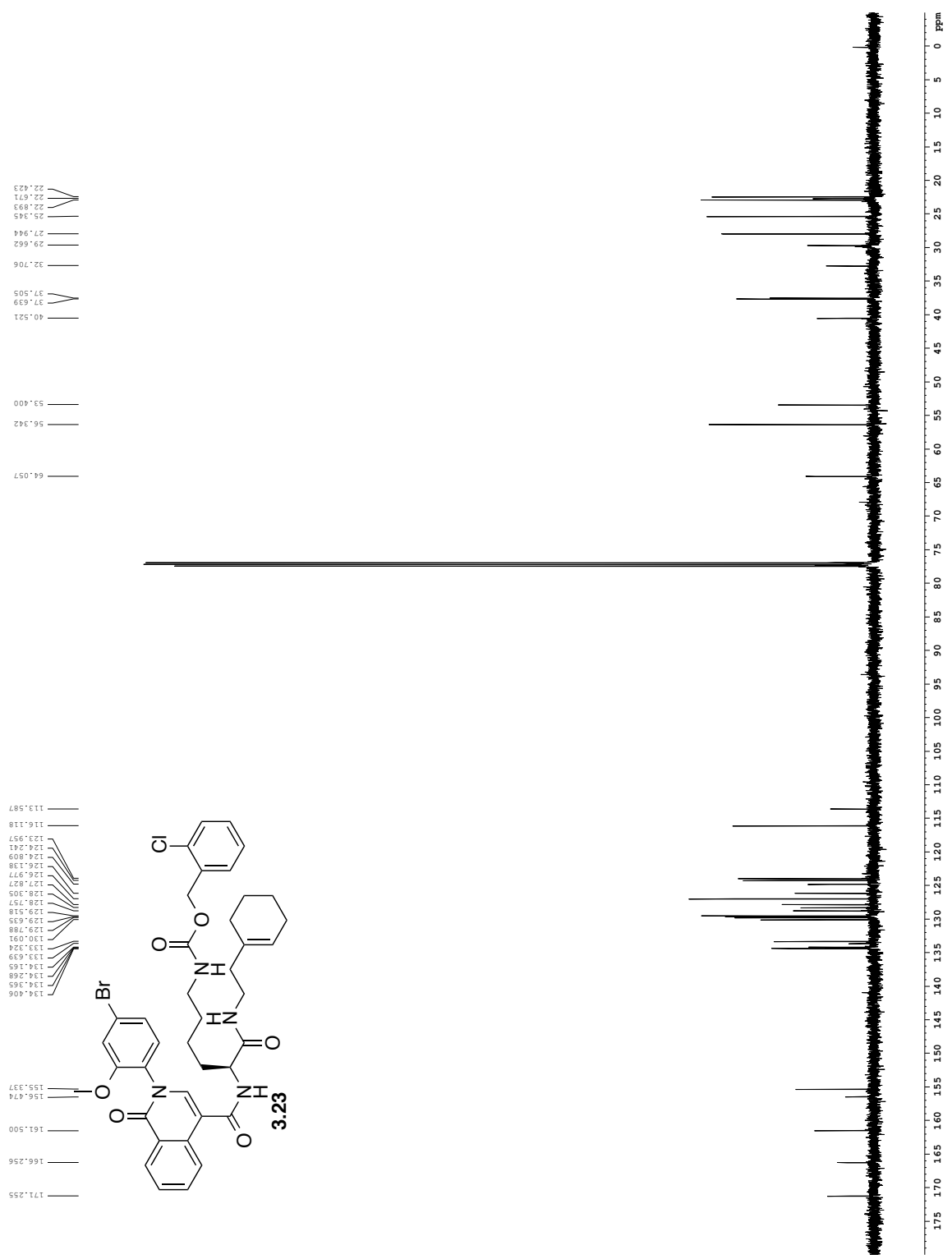


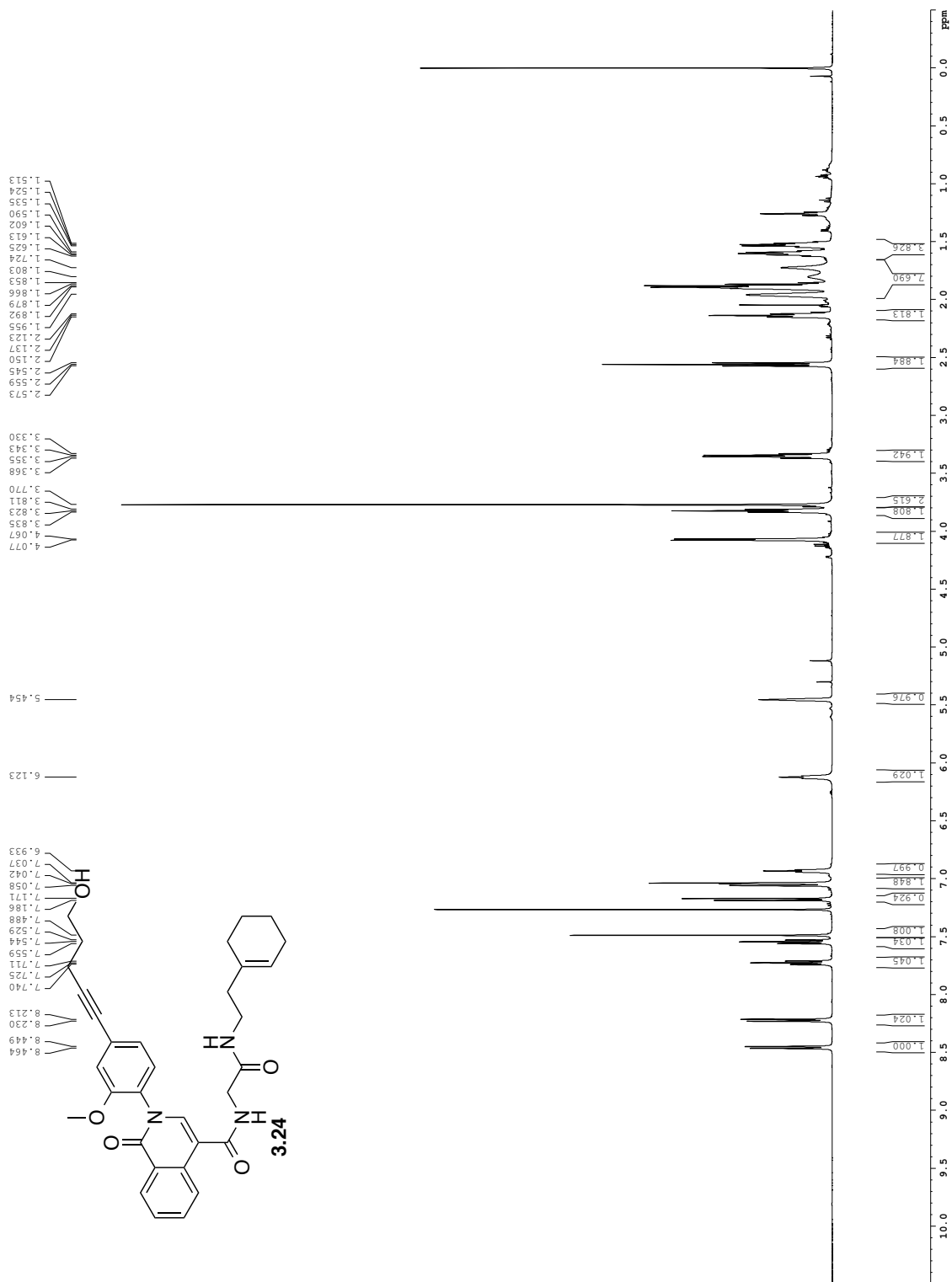


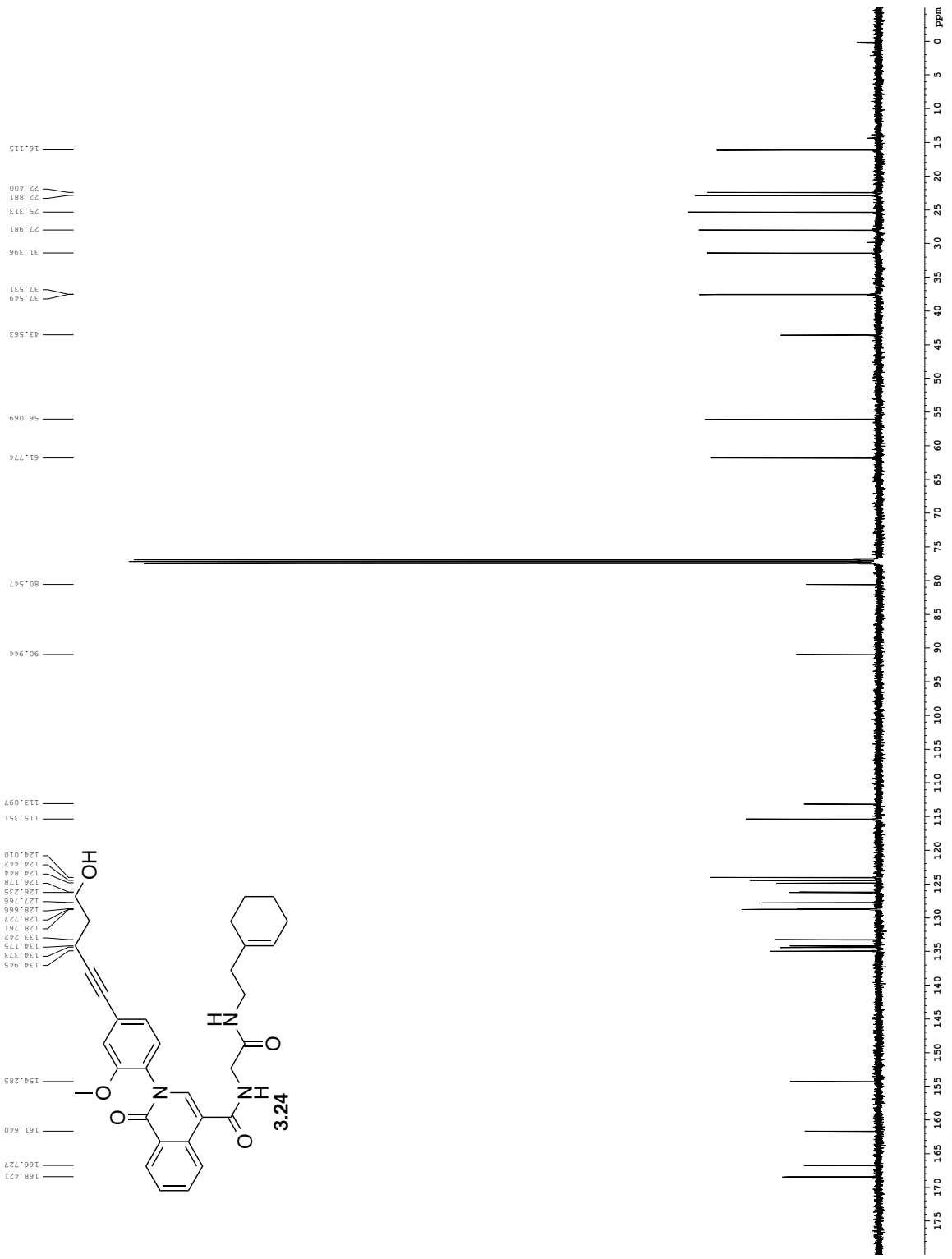


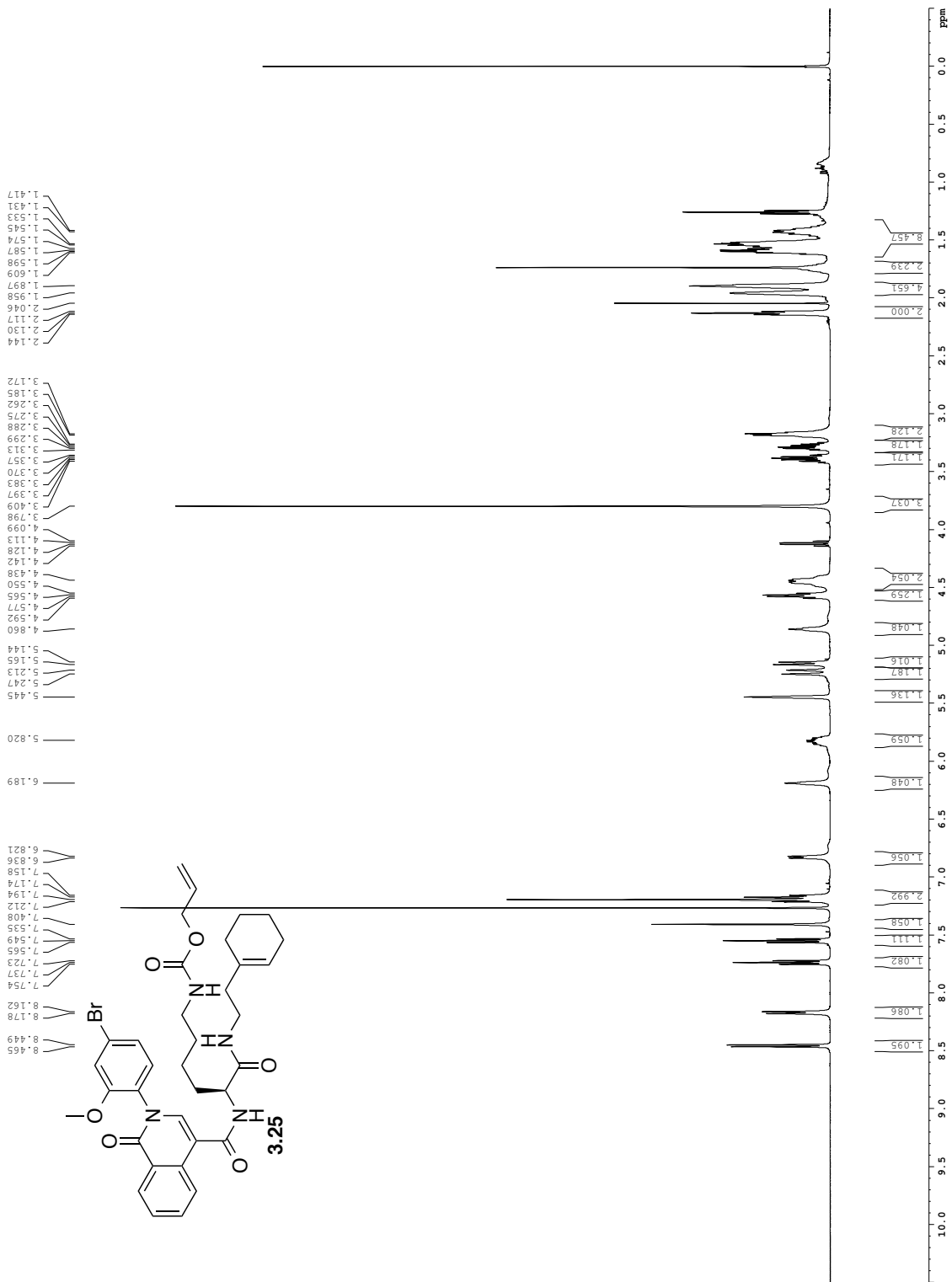


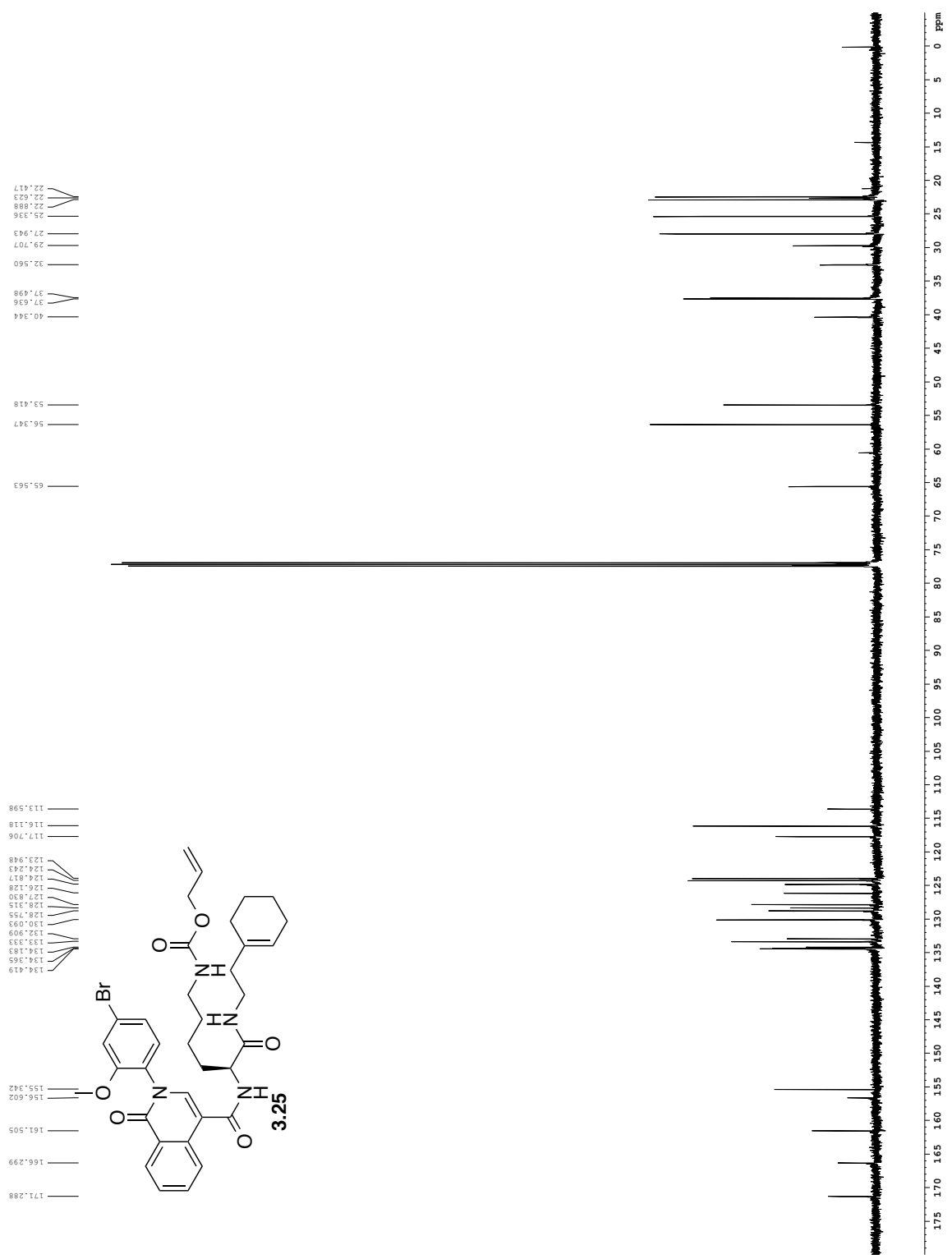


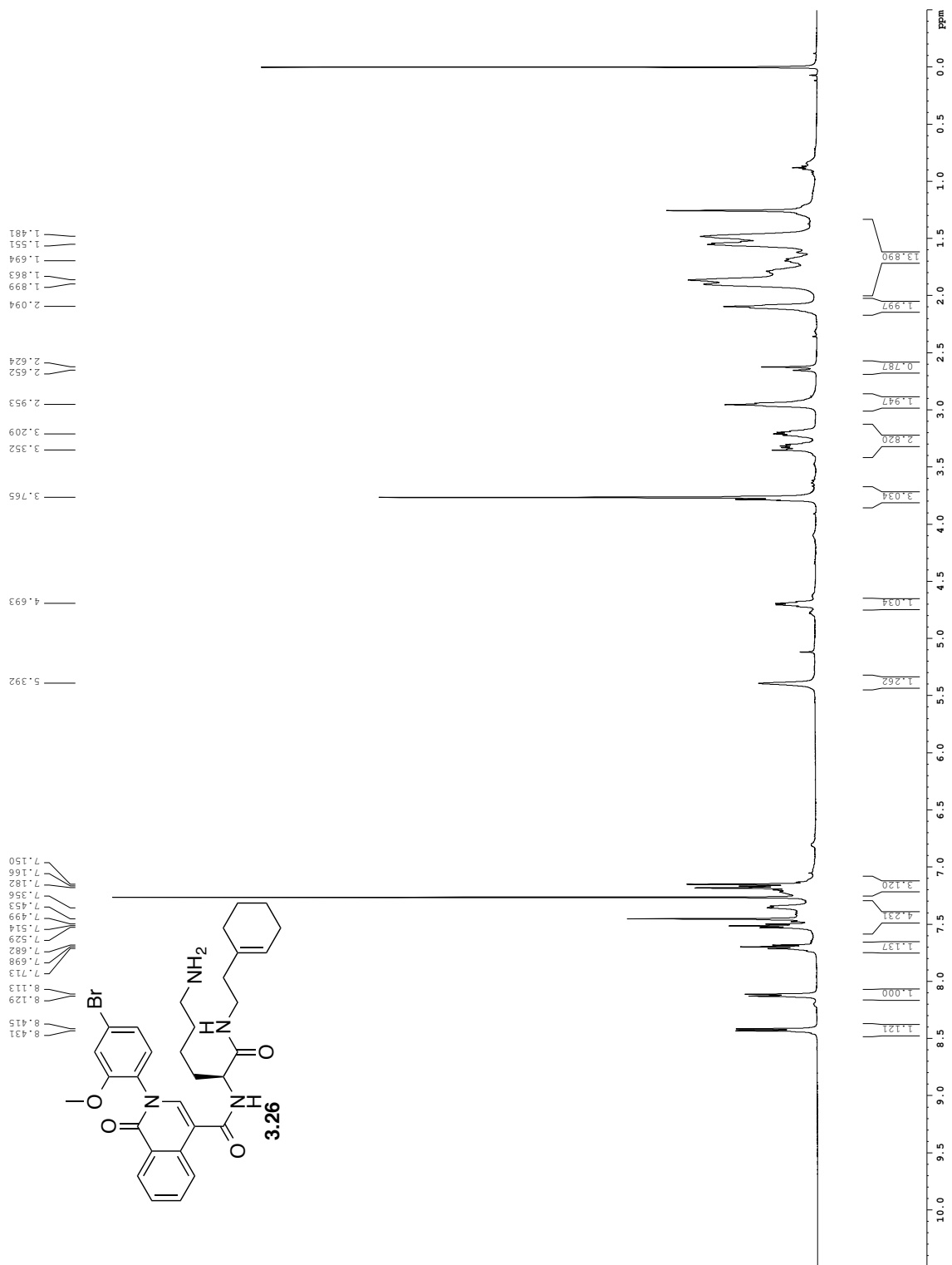


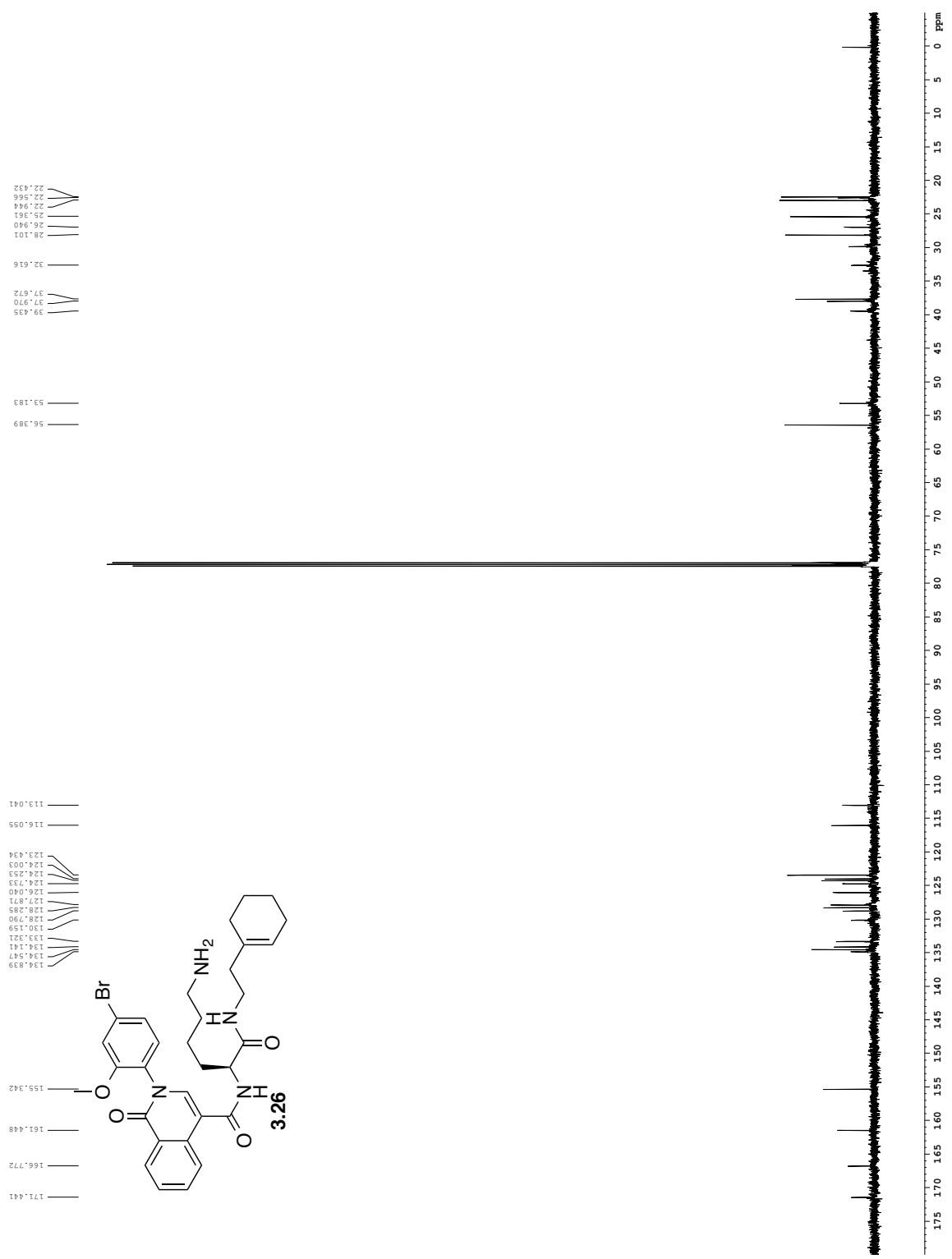


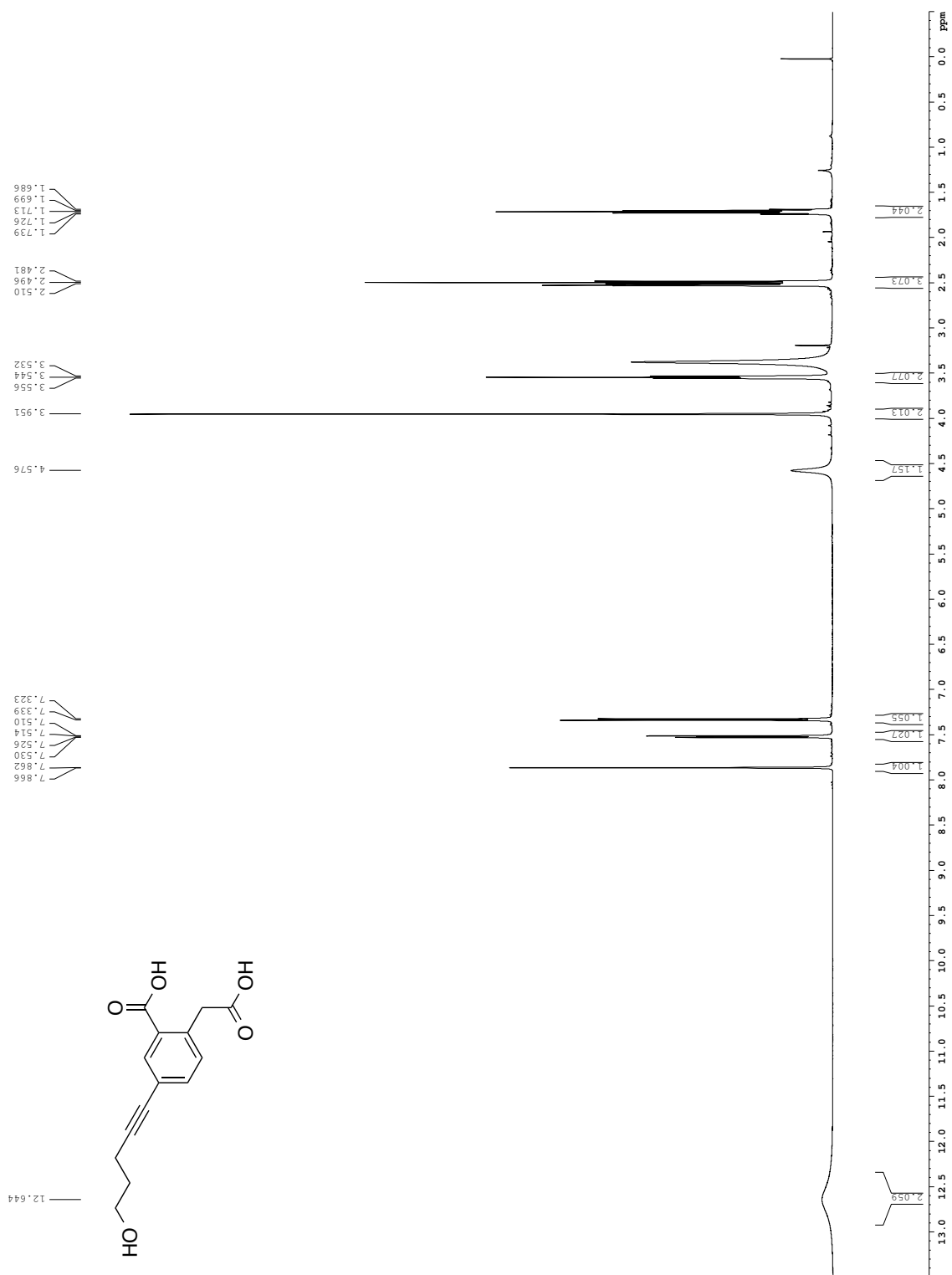


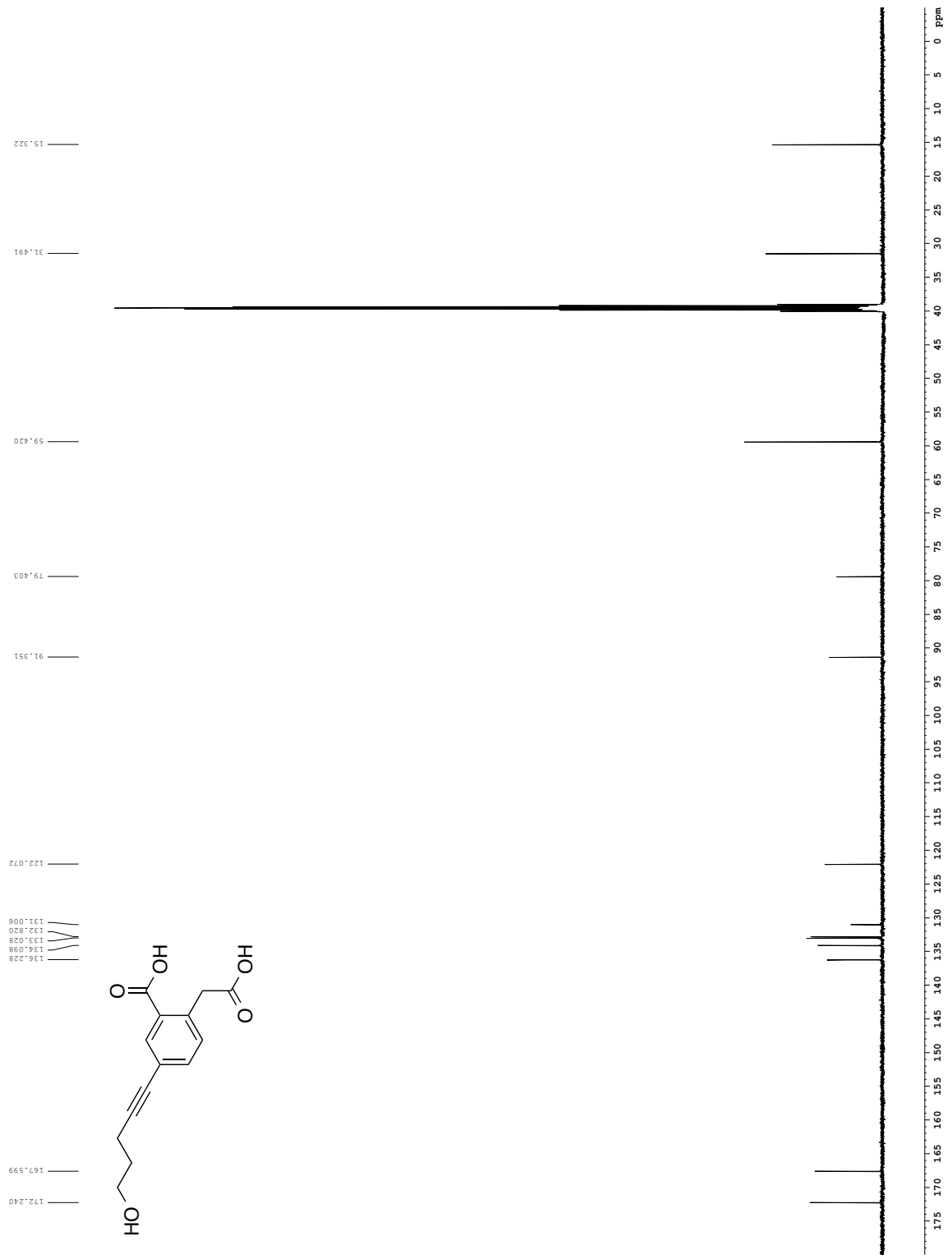


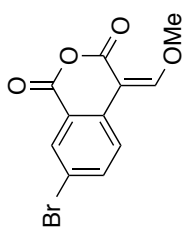






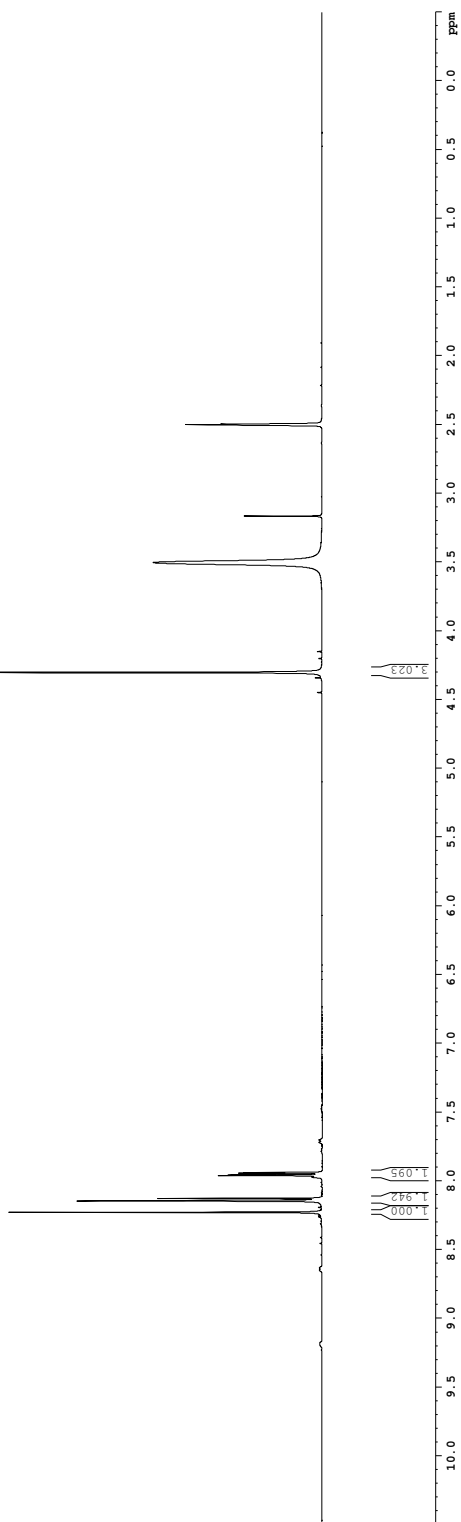


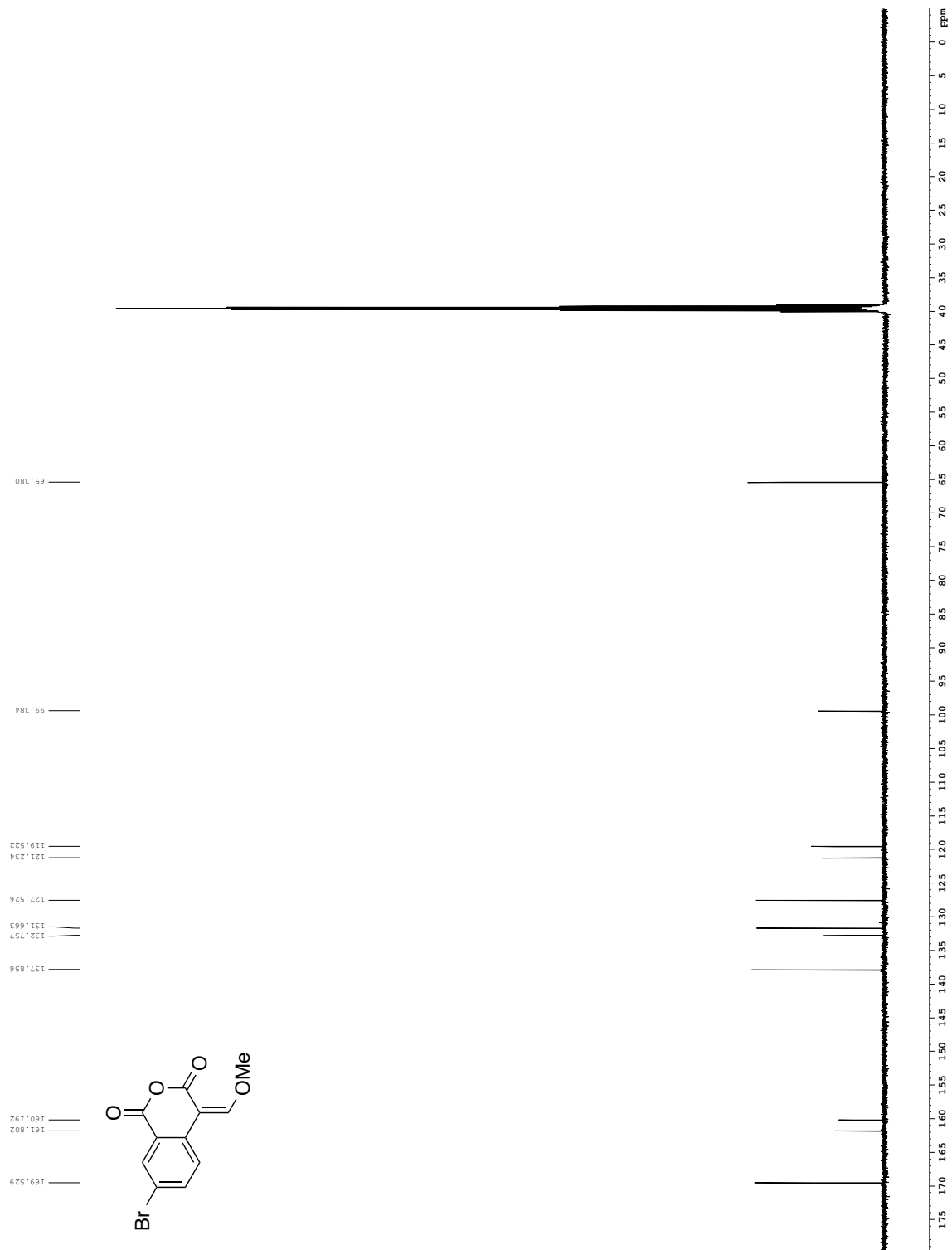


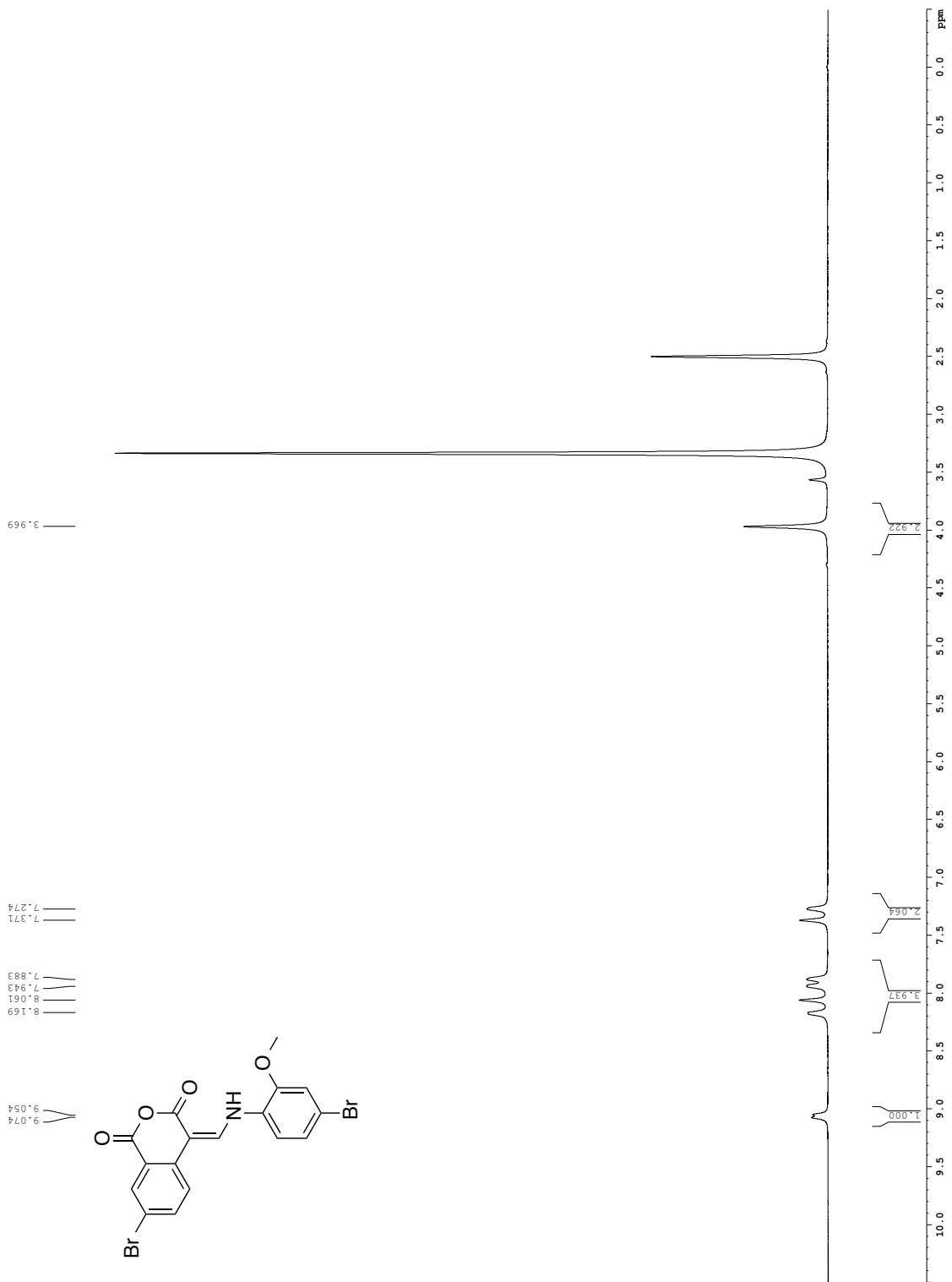


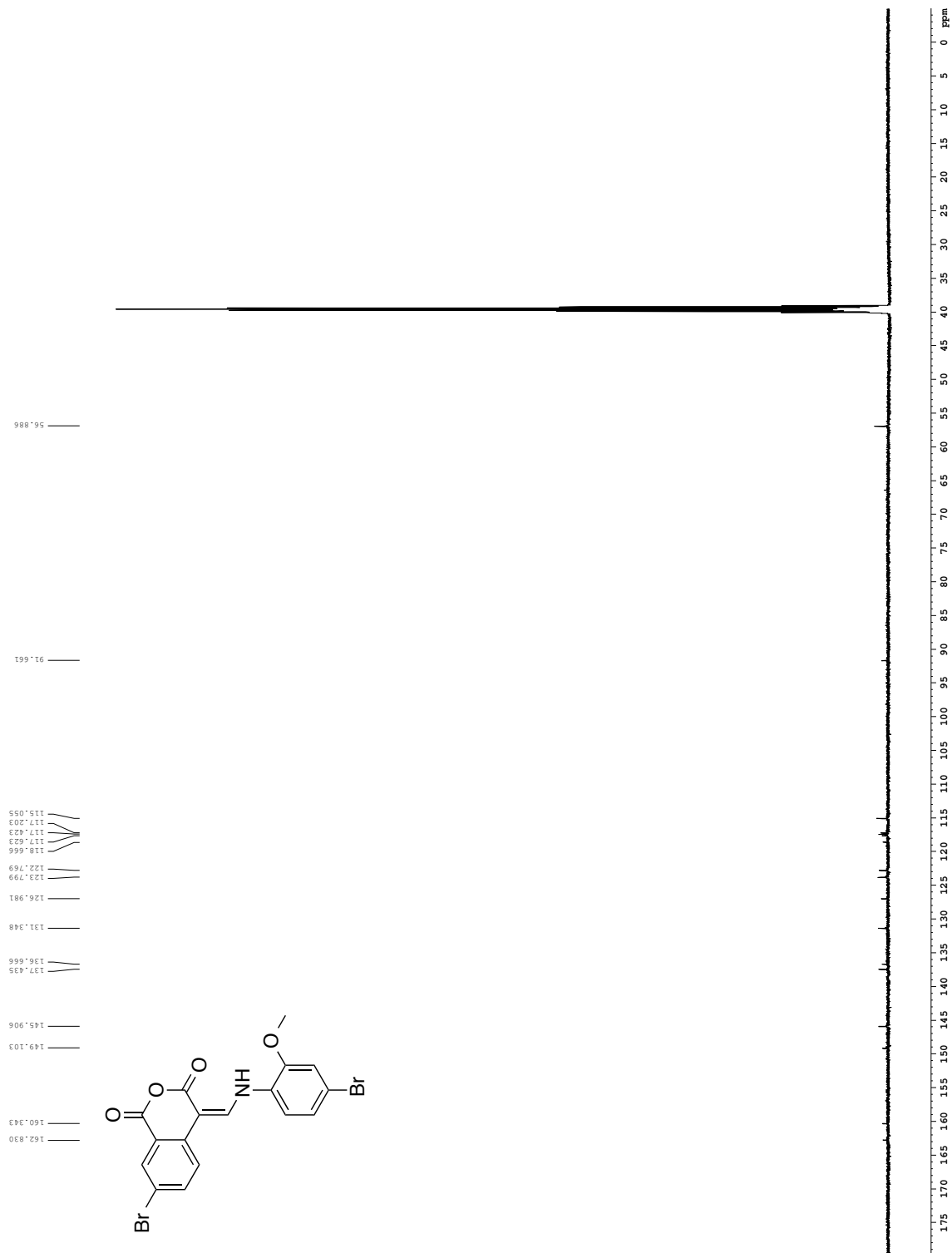
8.229
8.147
8.143
8.128
7.962
7.957
7.945
7.940

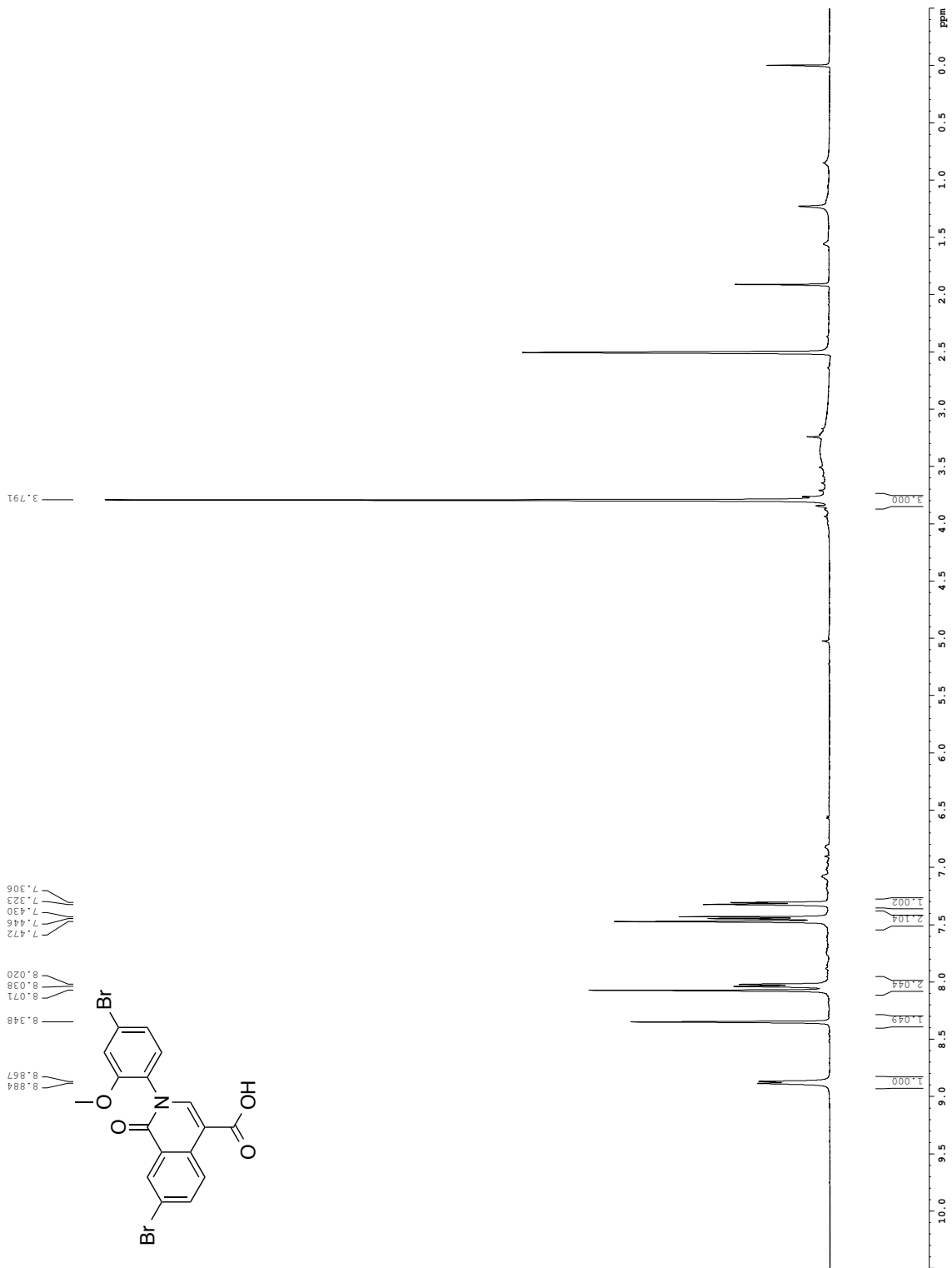
4.303

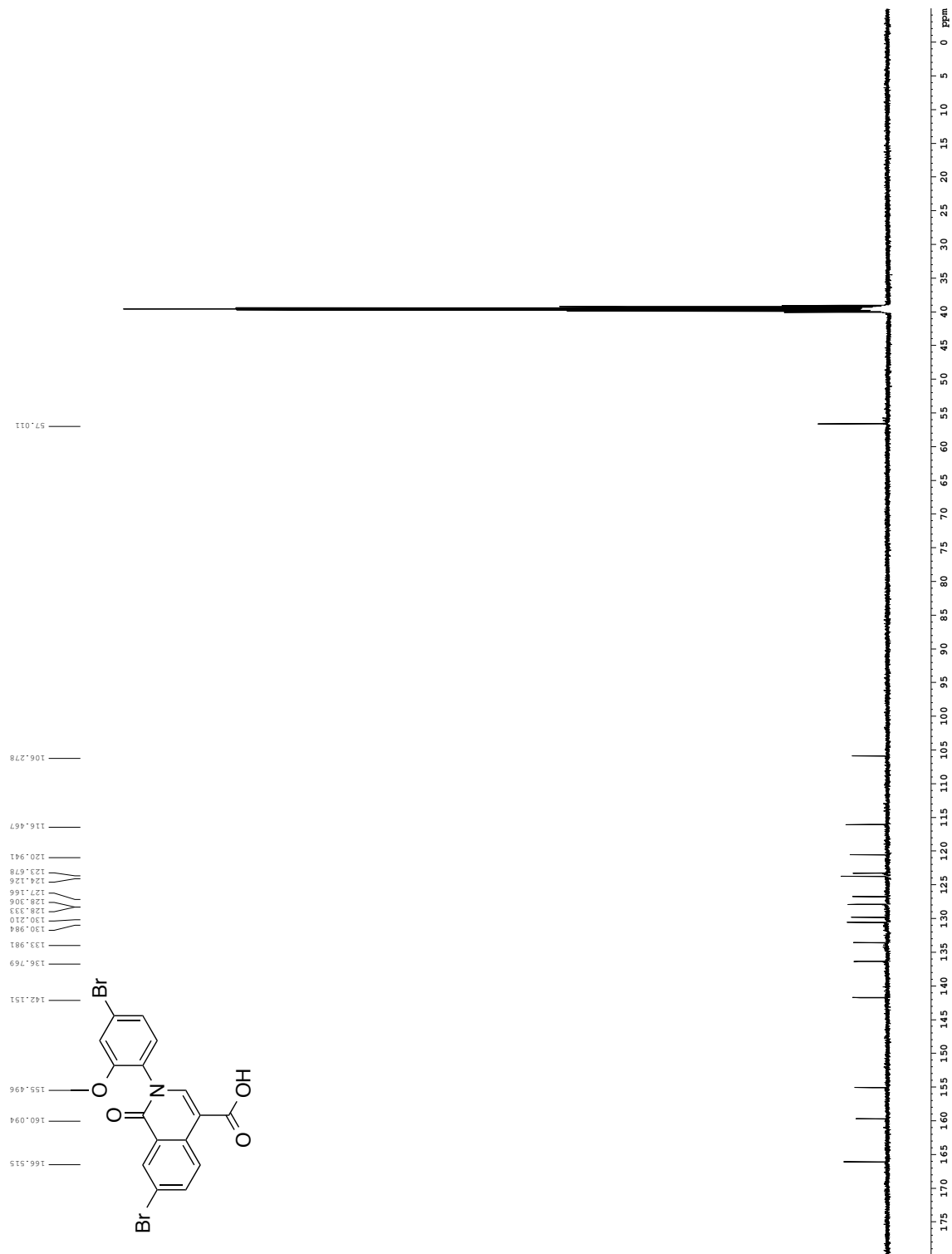


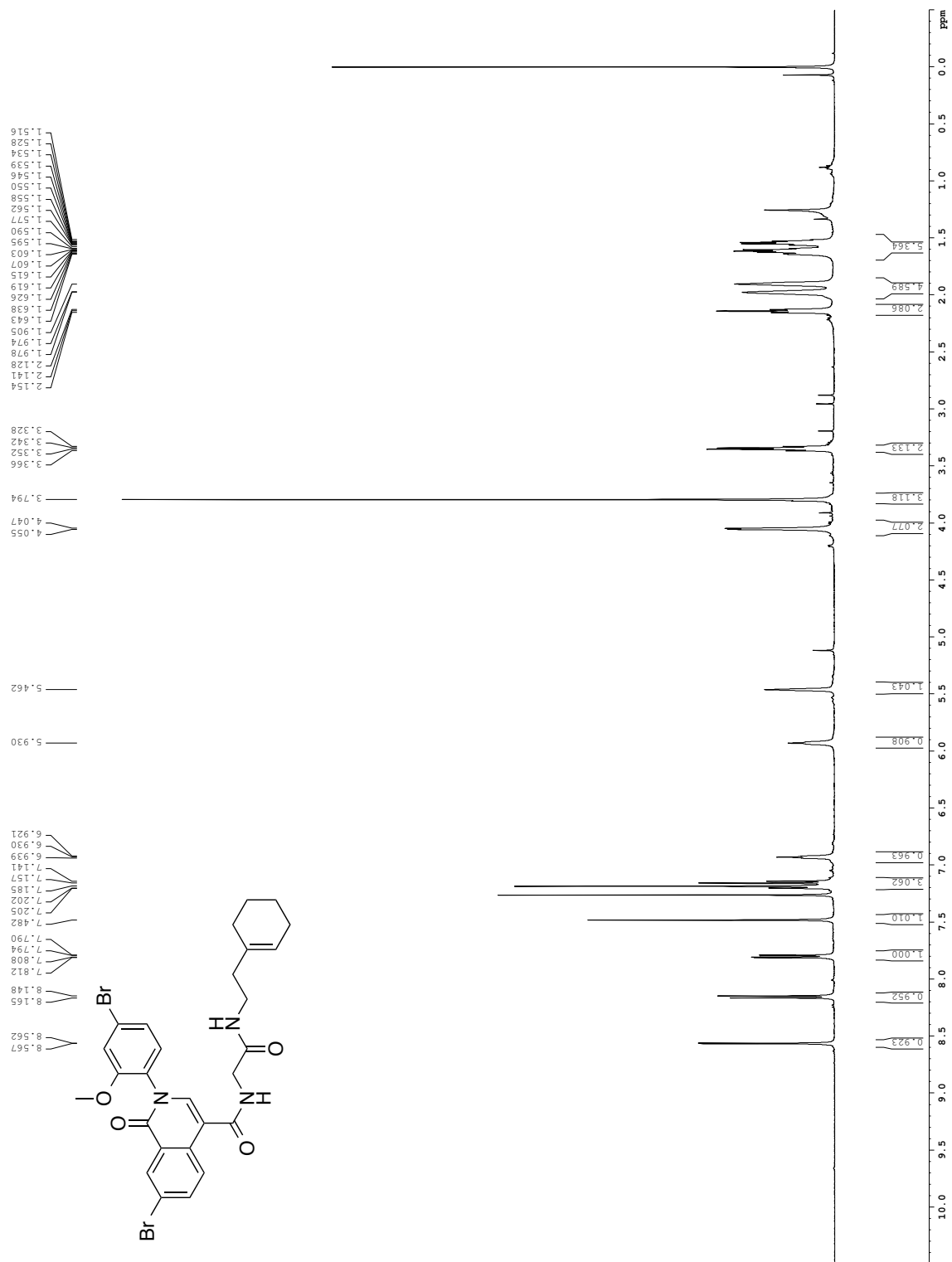


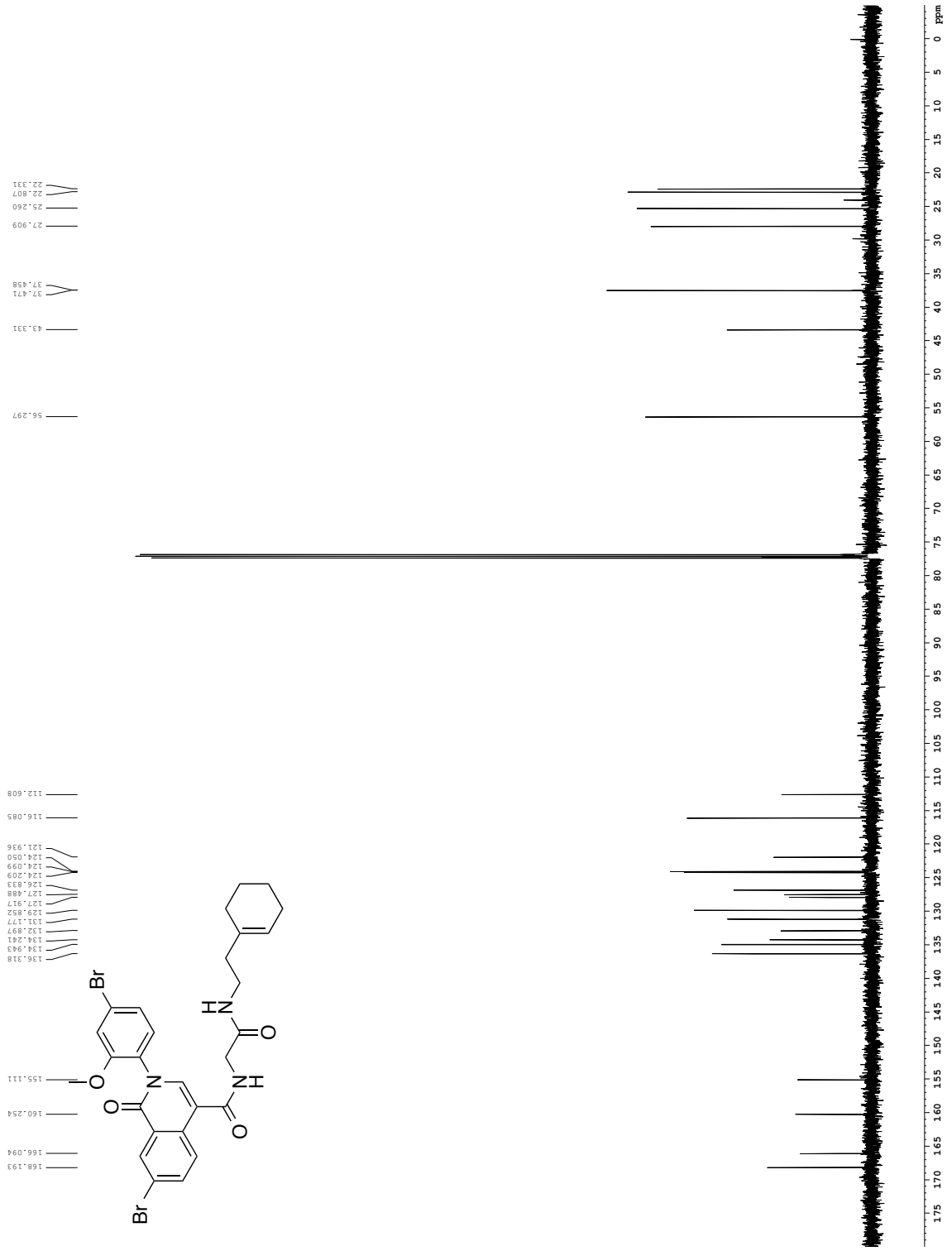


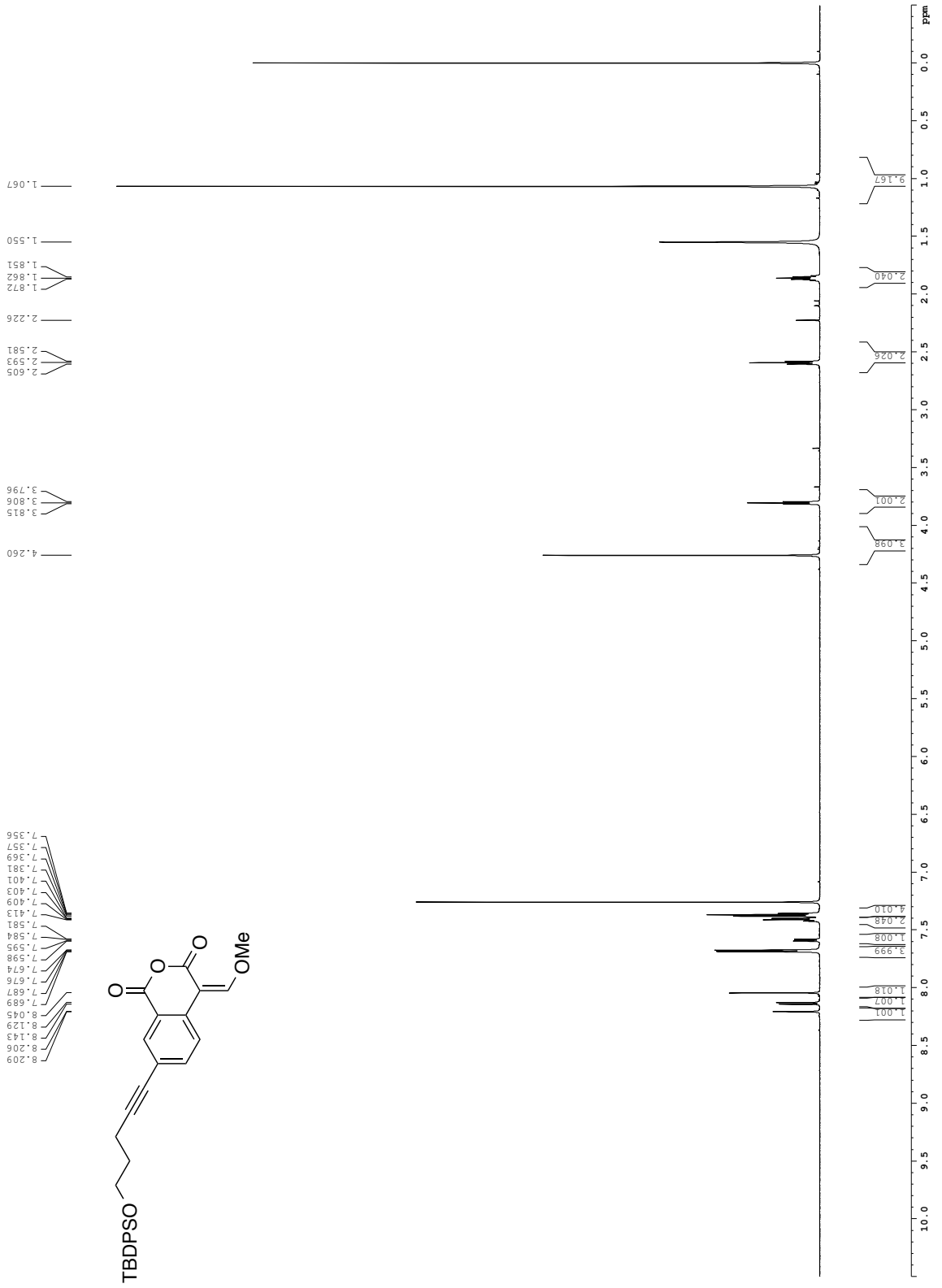


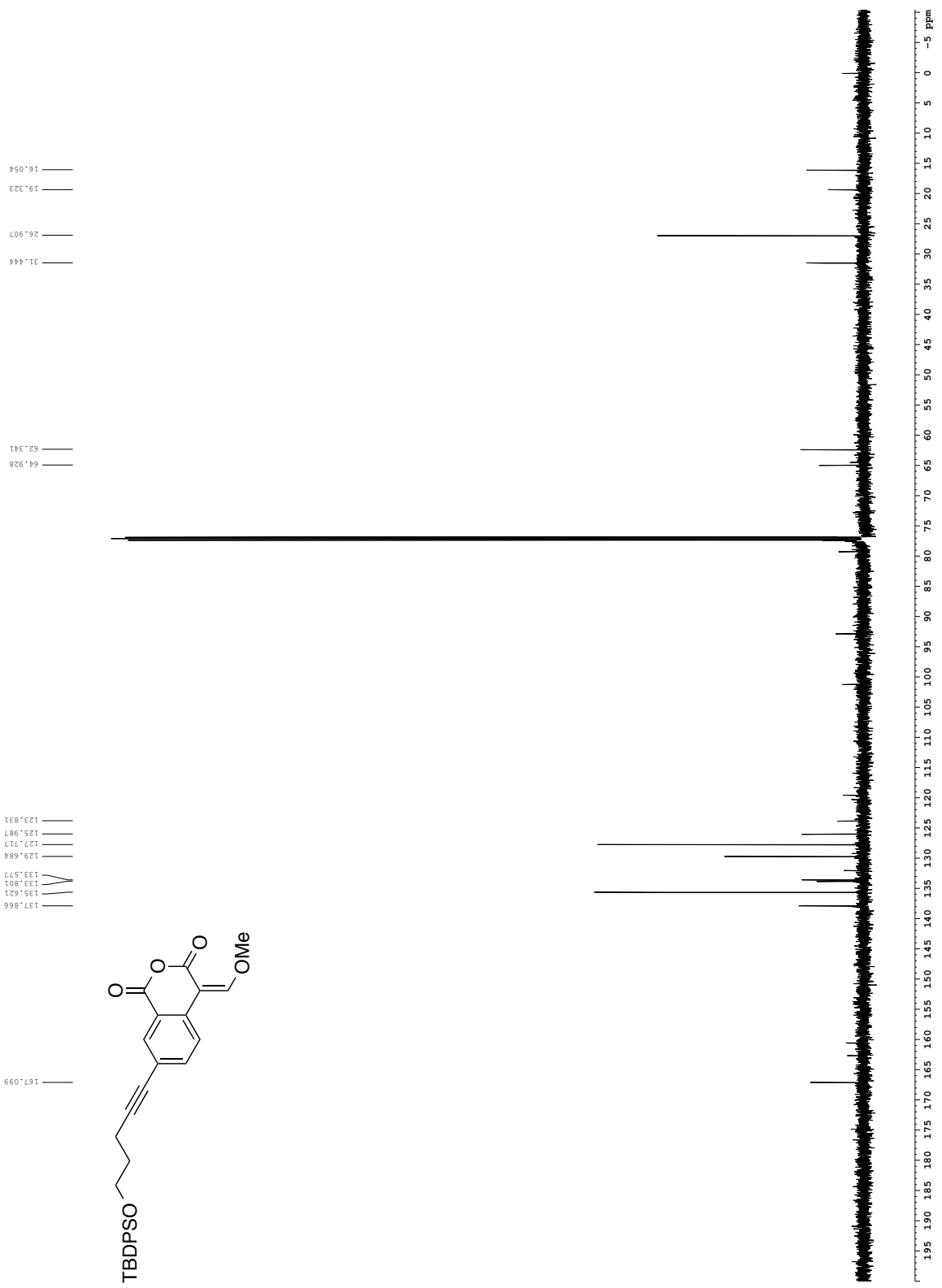


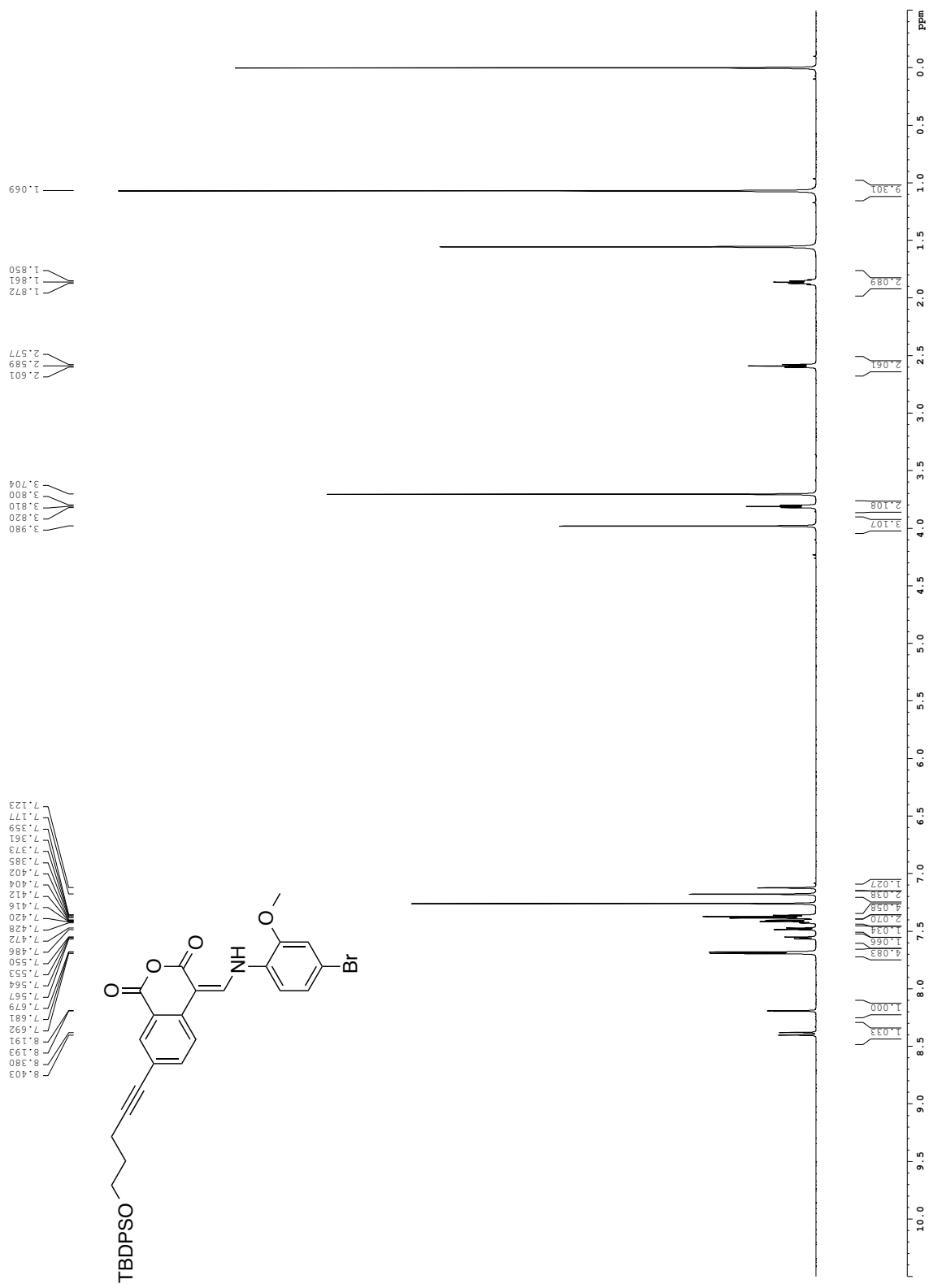


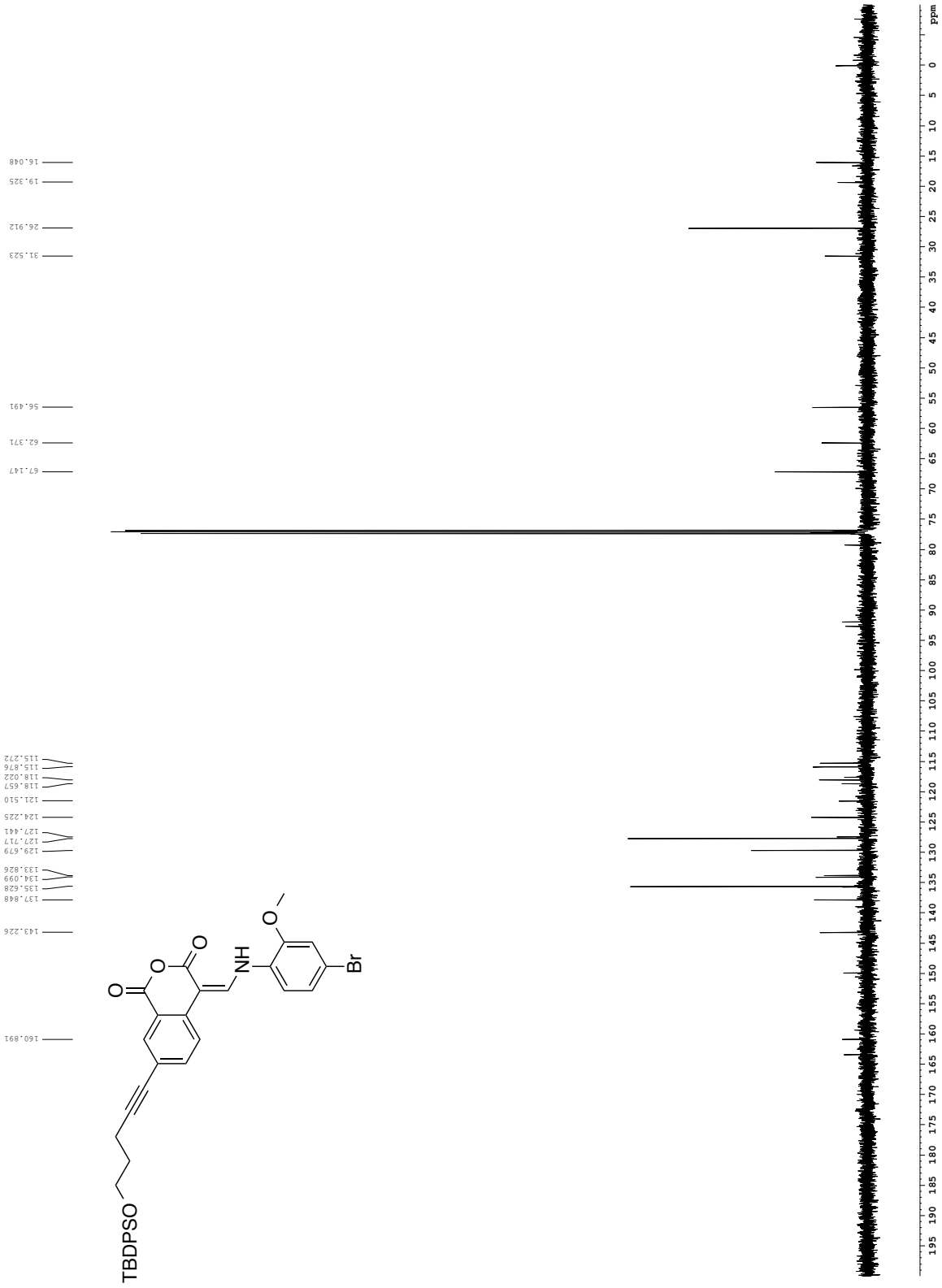


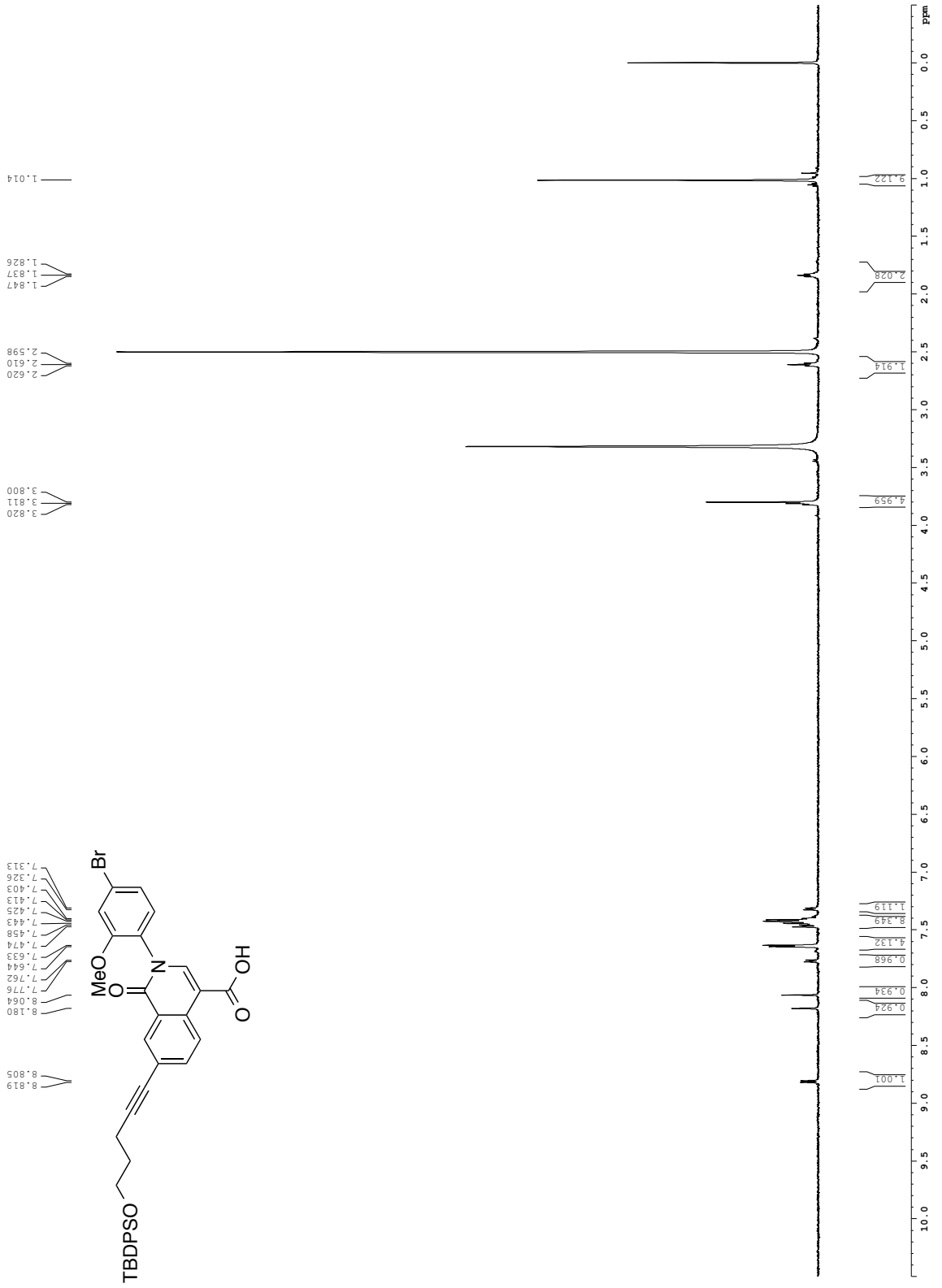


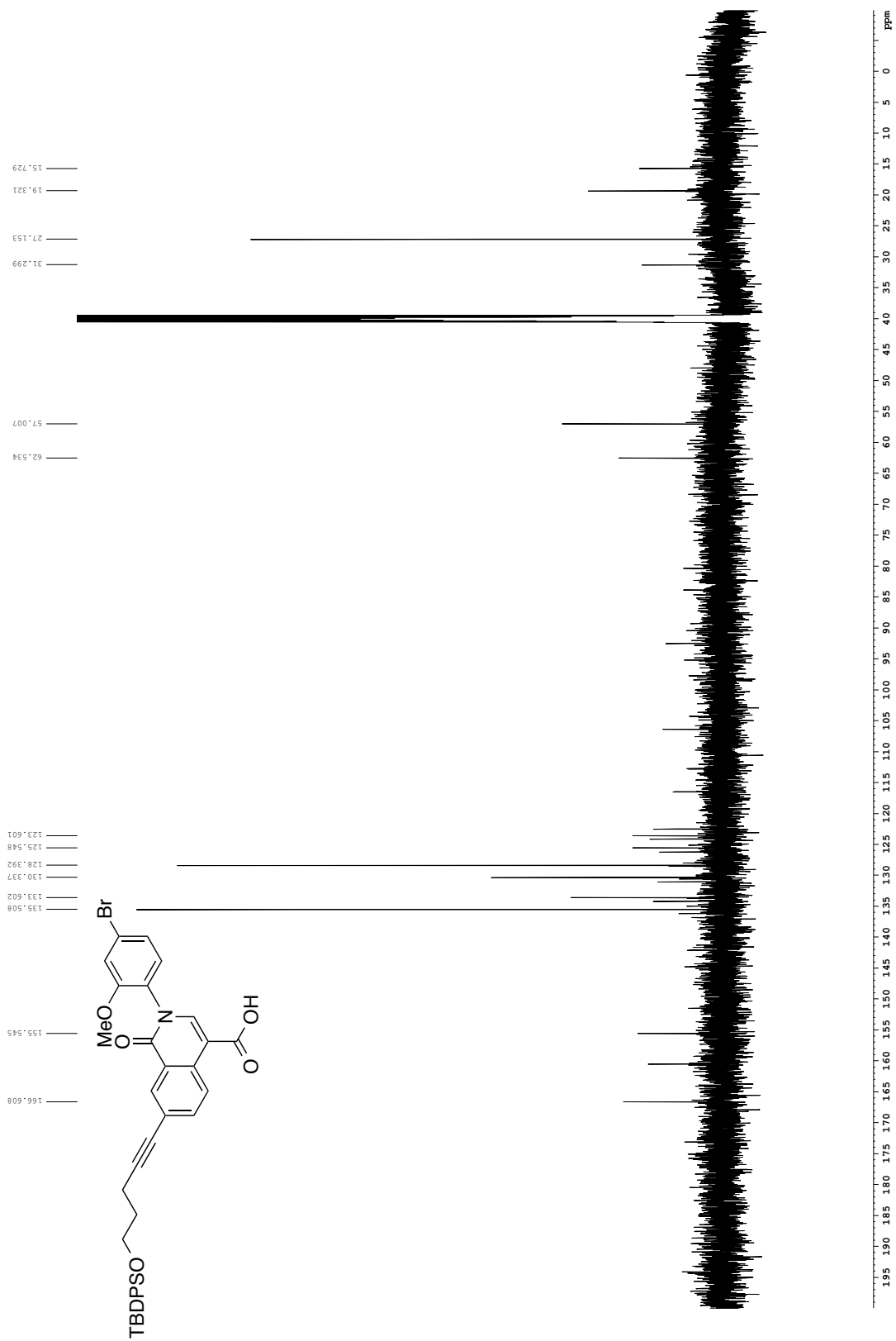


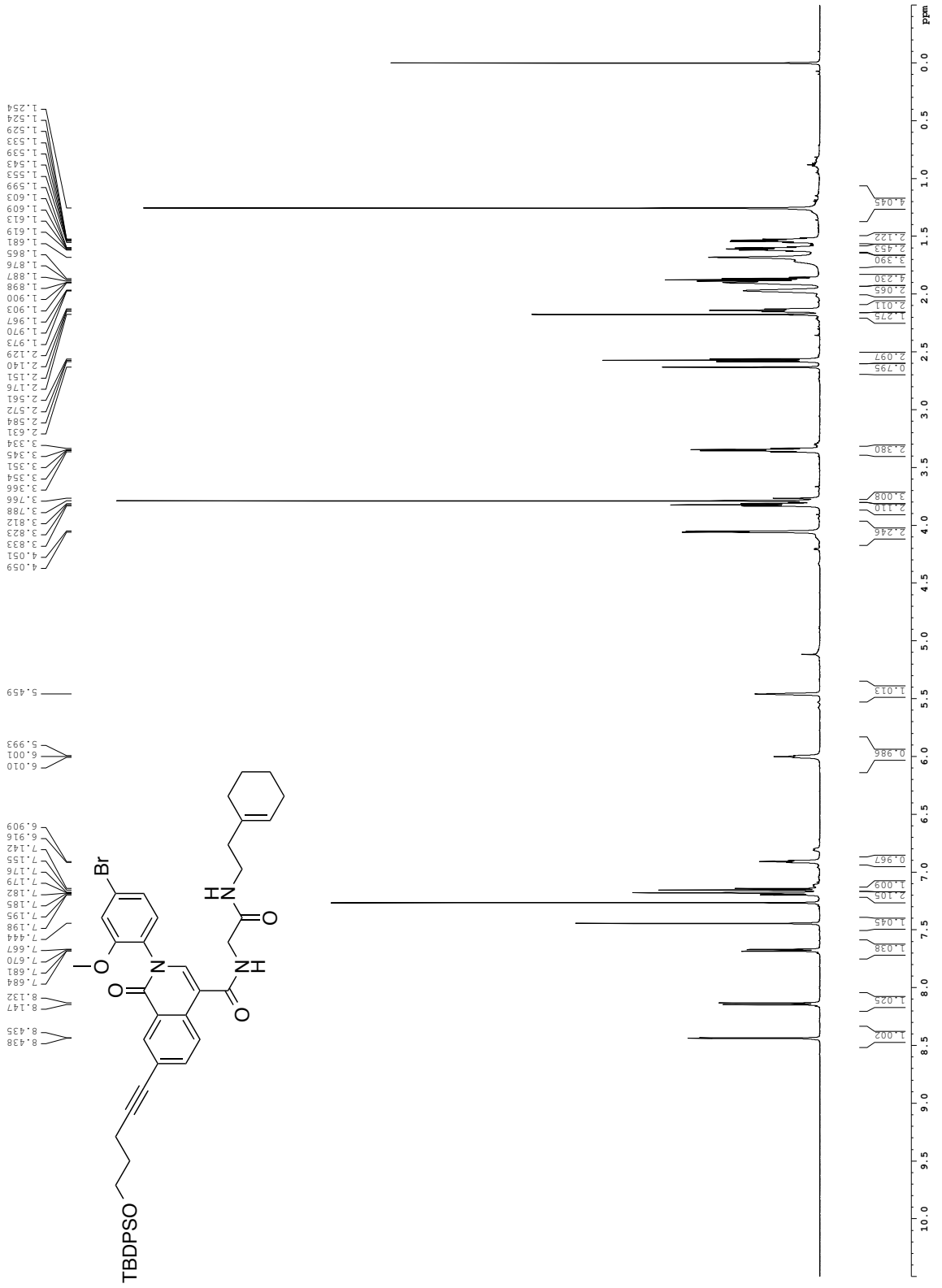


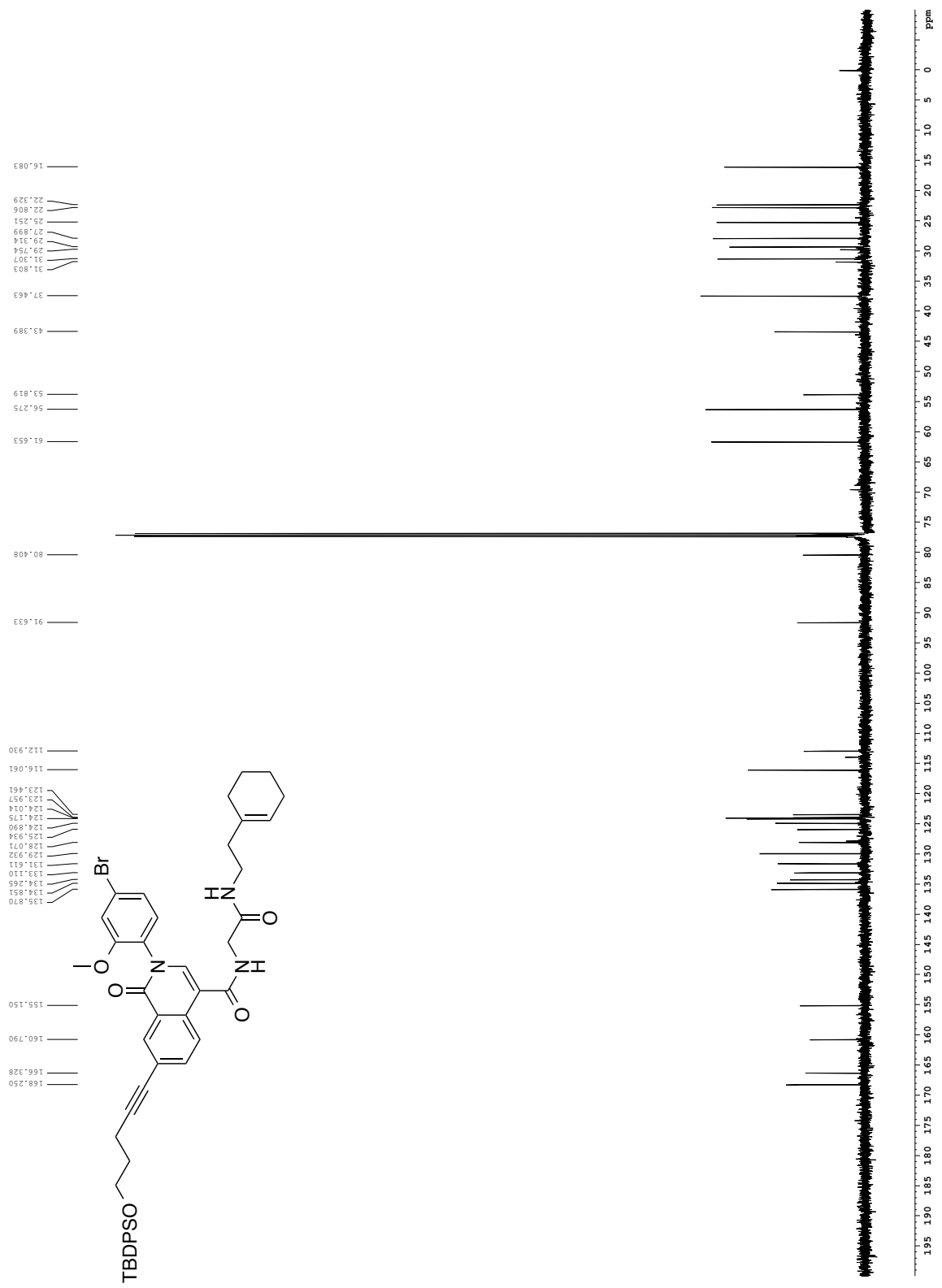




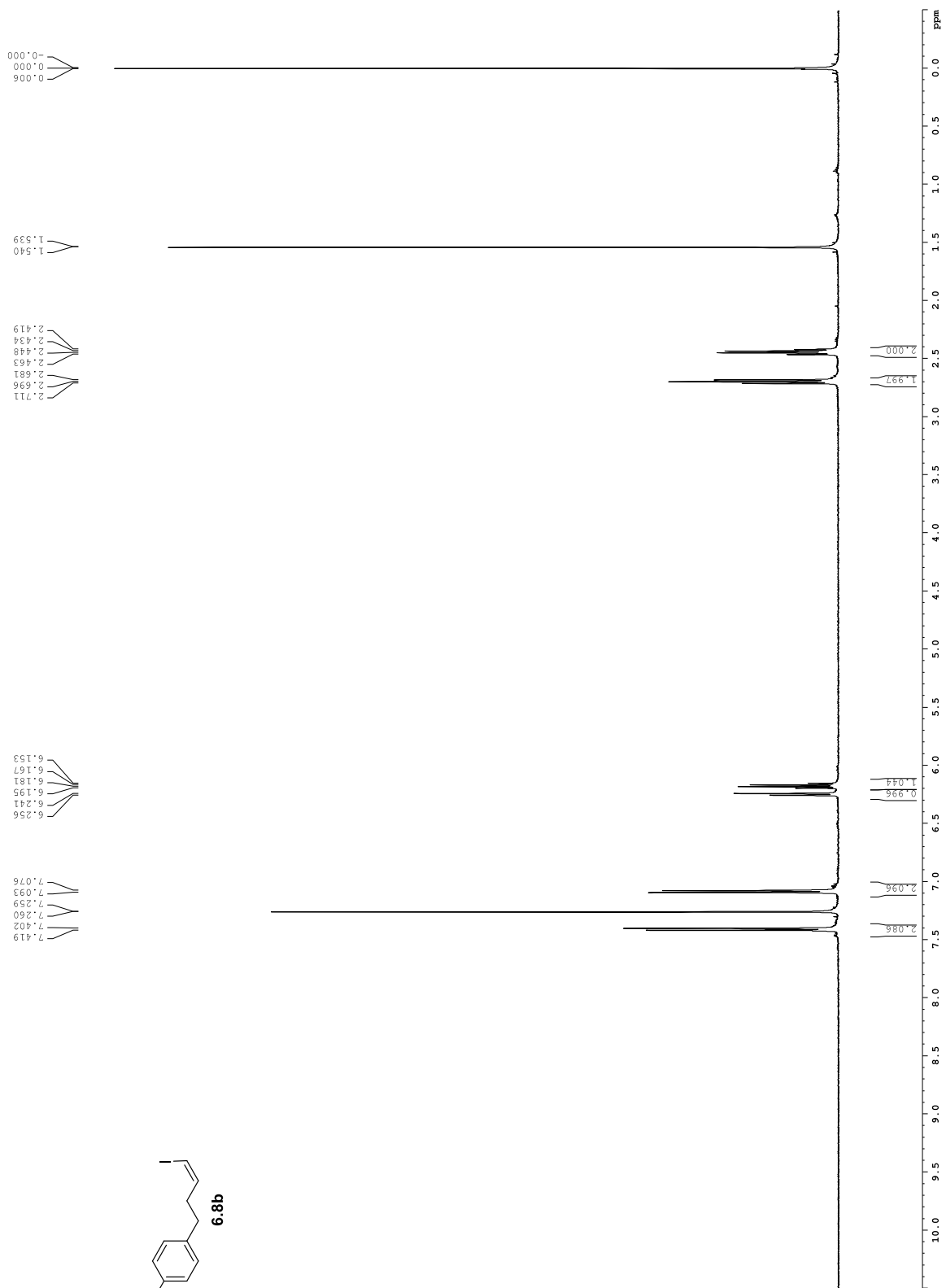


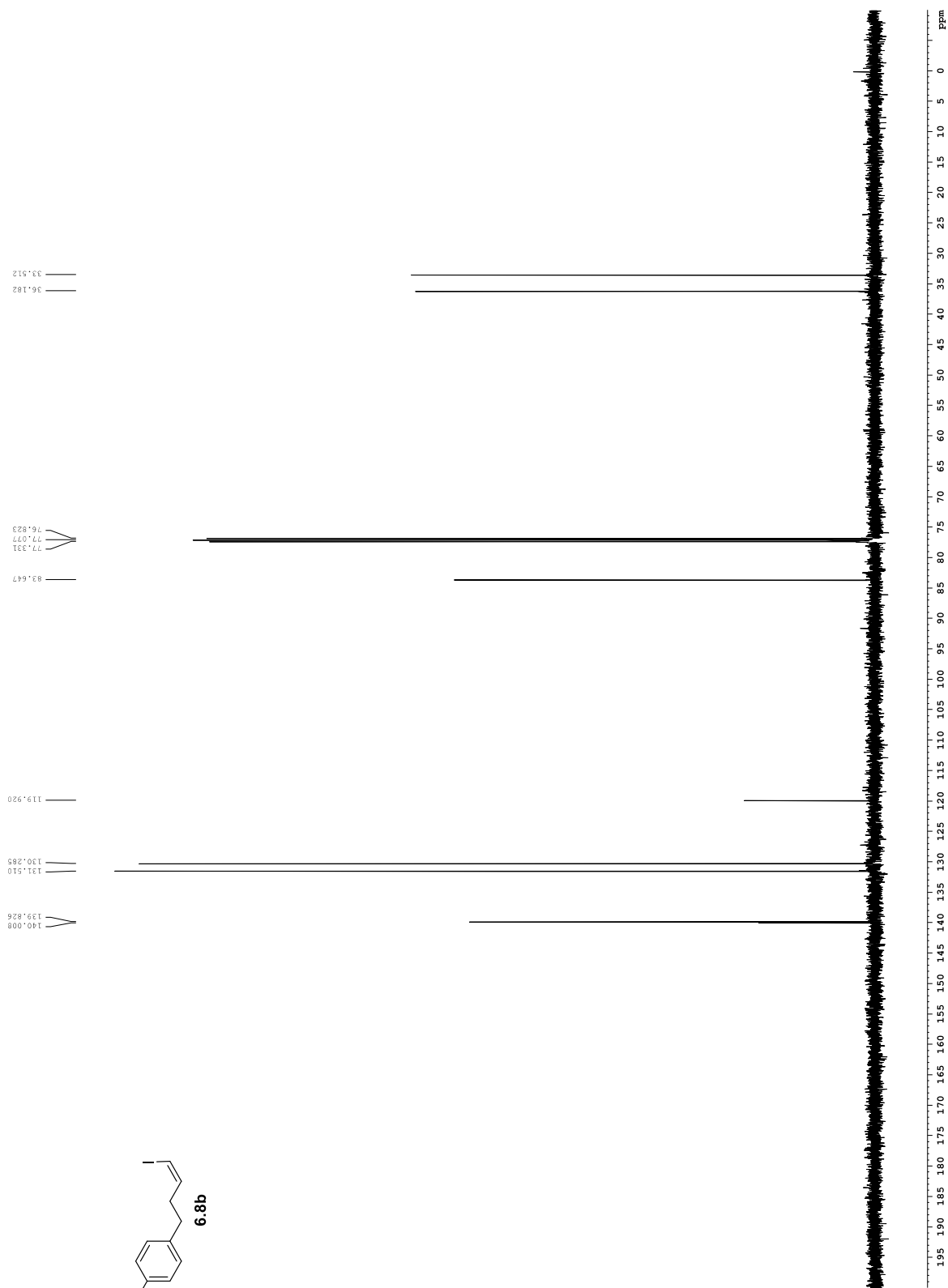
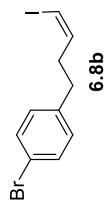


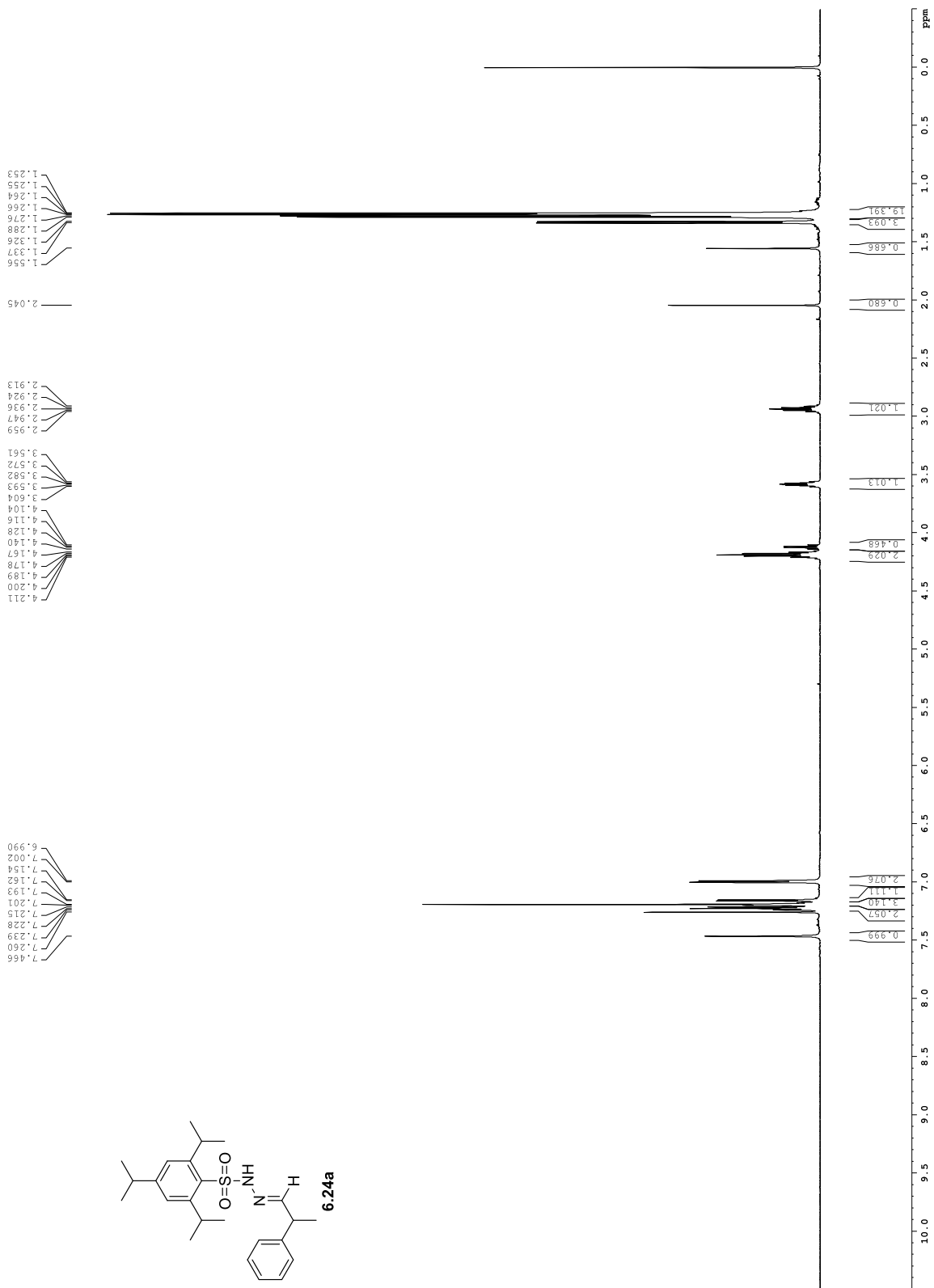
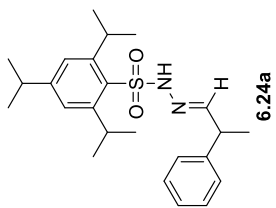


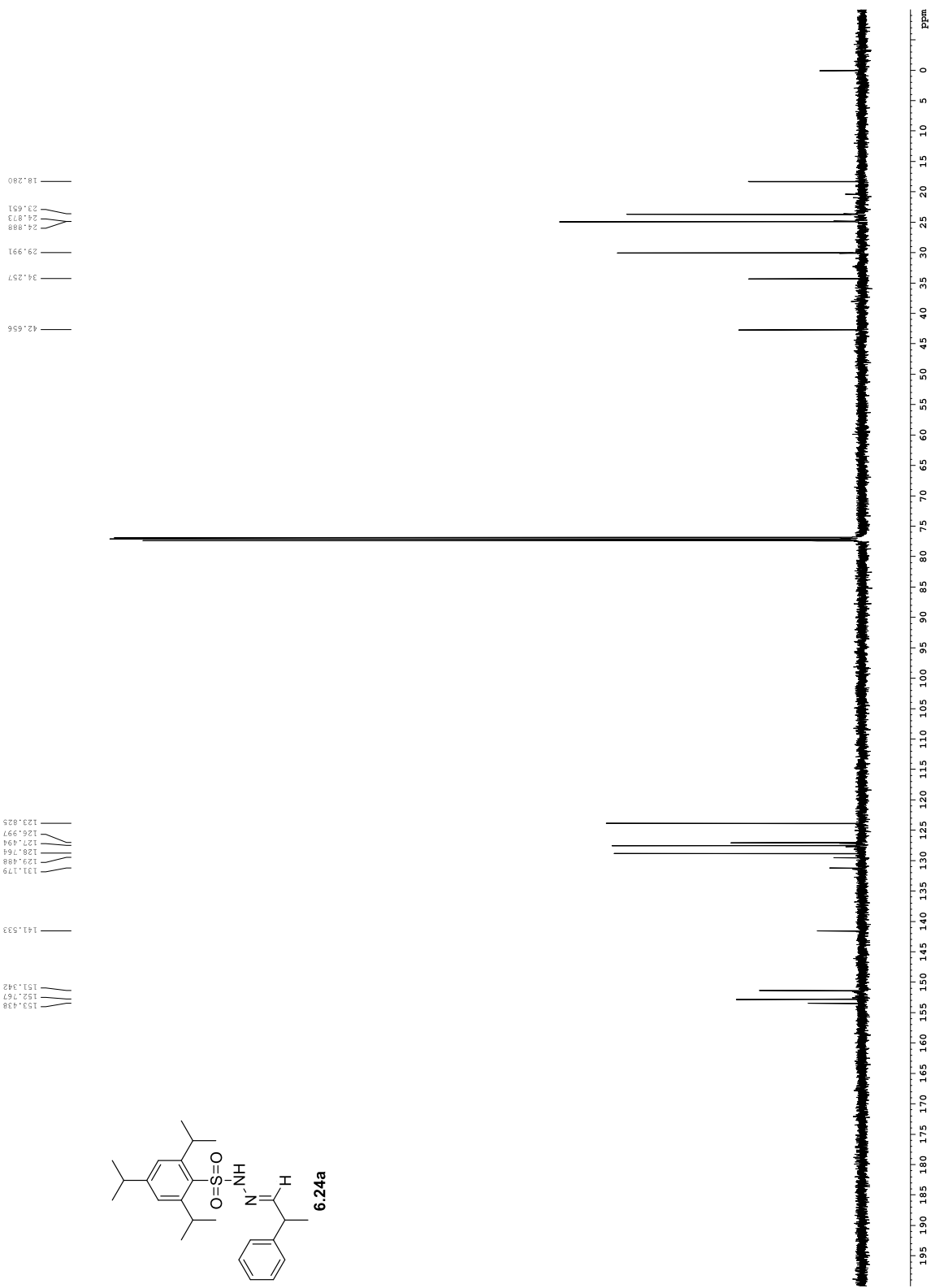
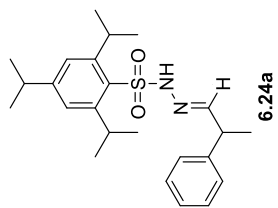


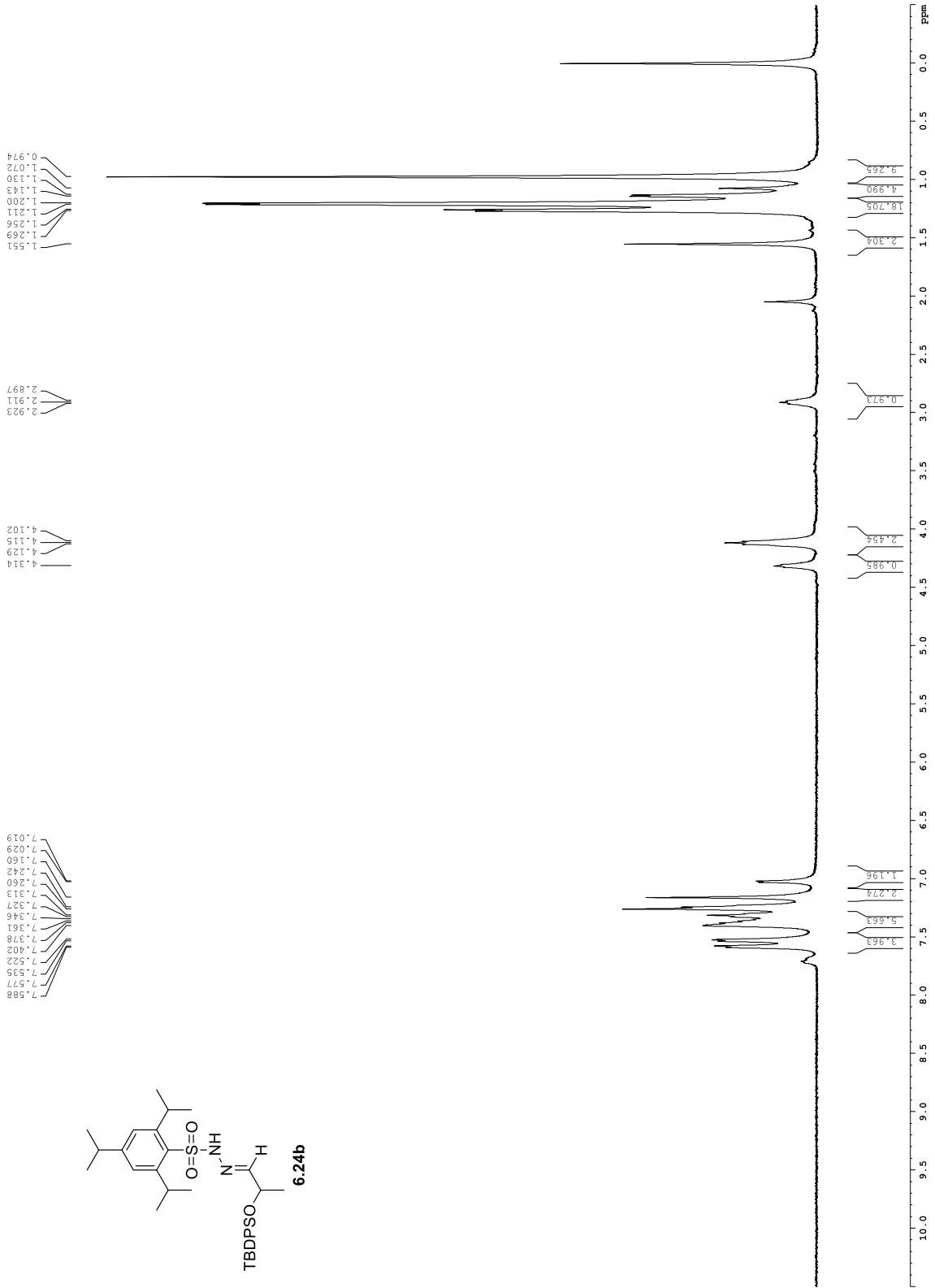
Appendix D: Chapter 6 – NMR Spectra

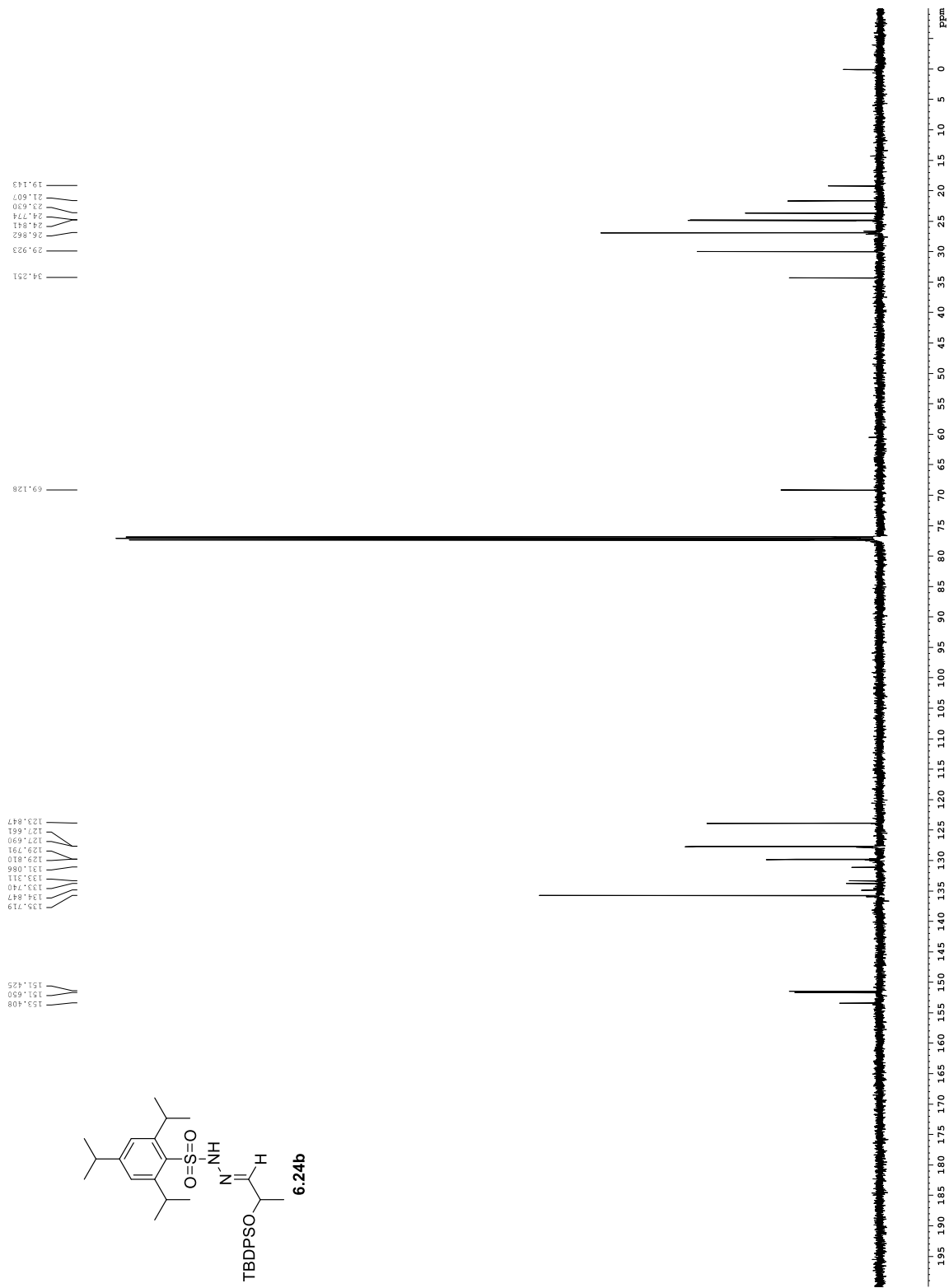
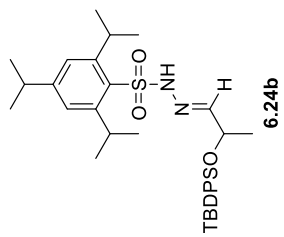


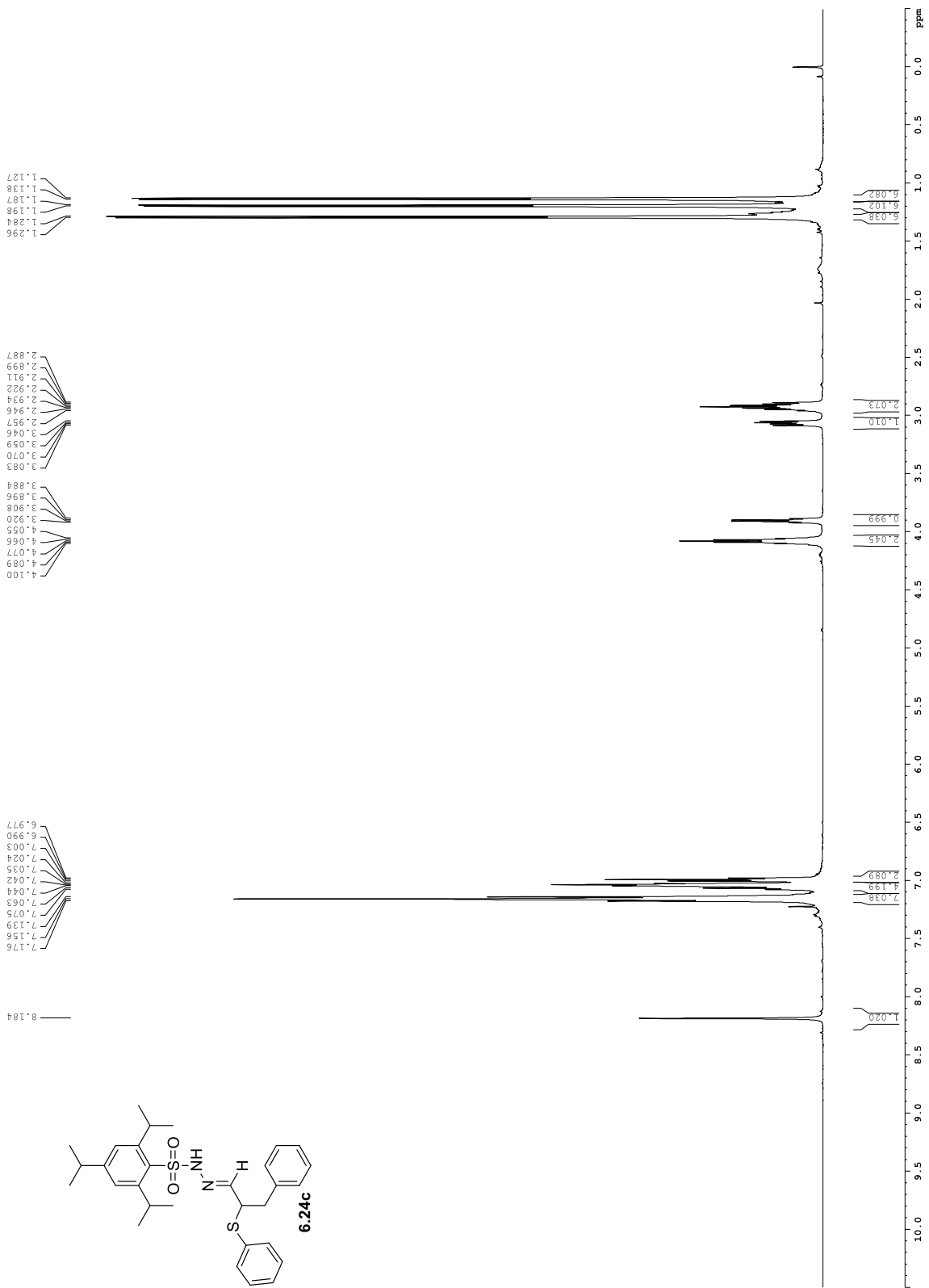


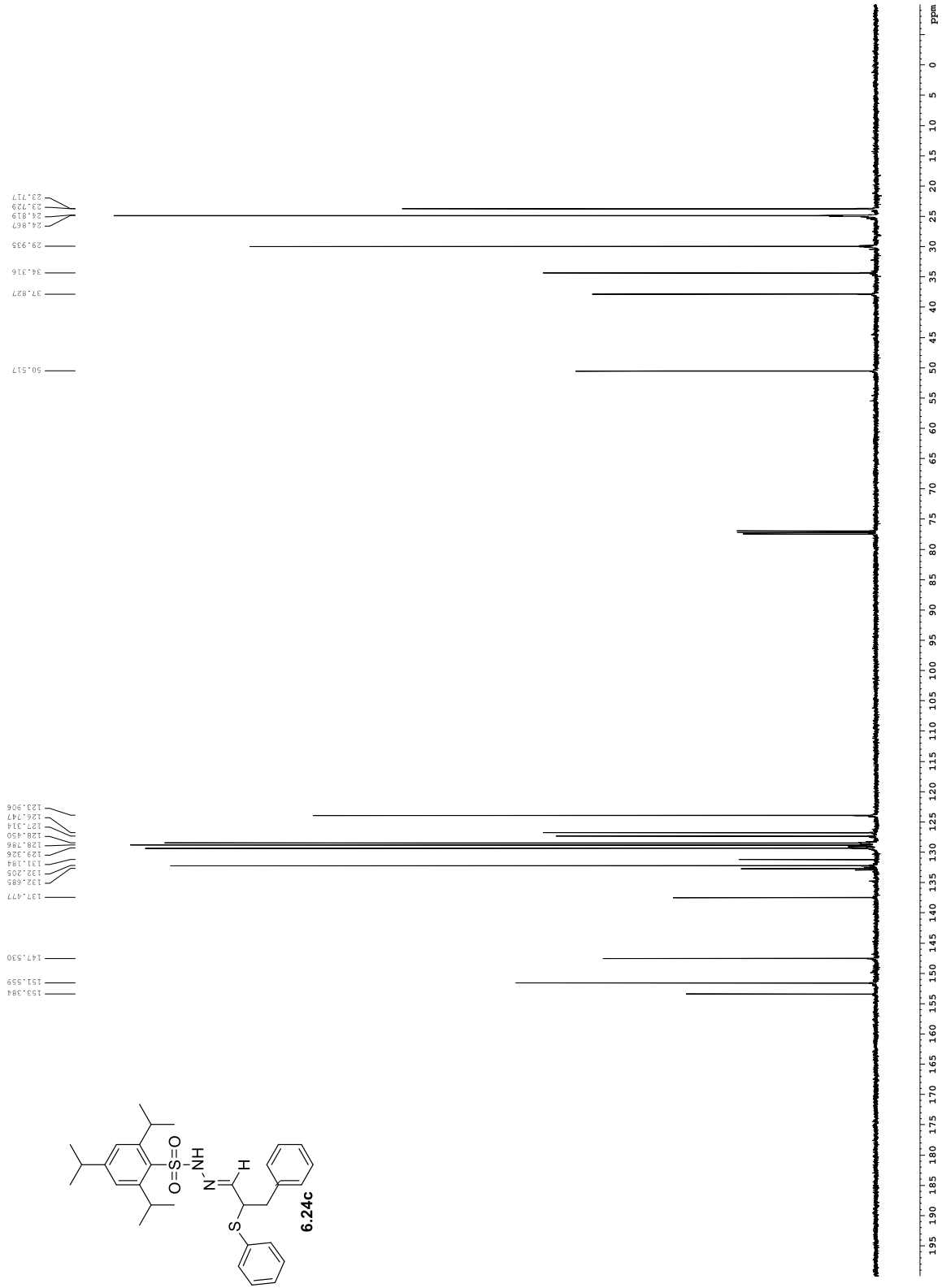


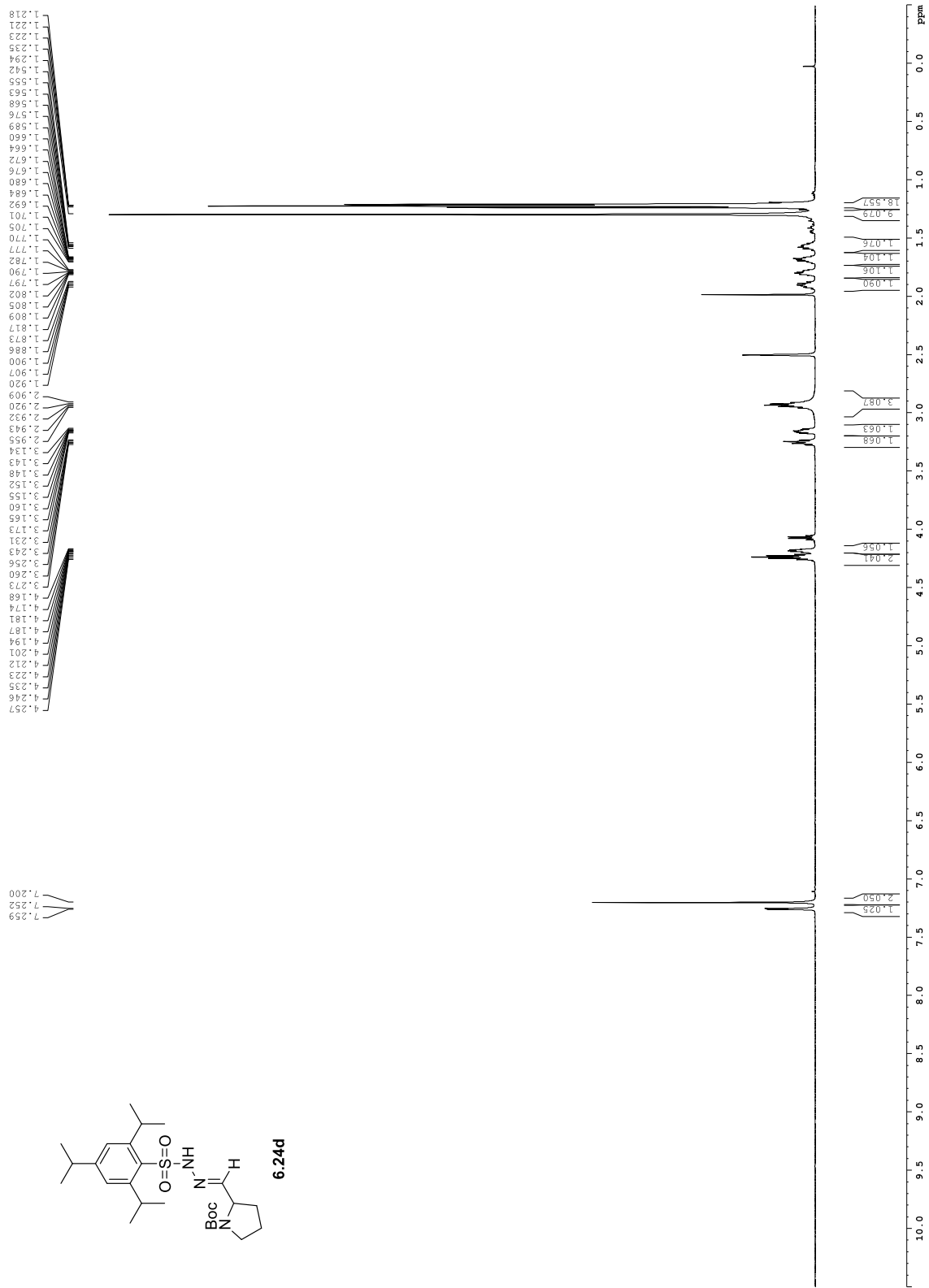


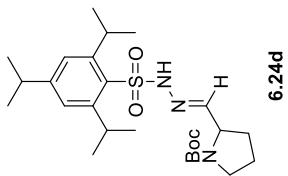








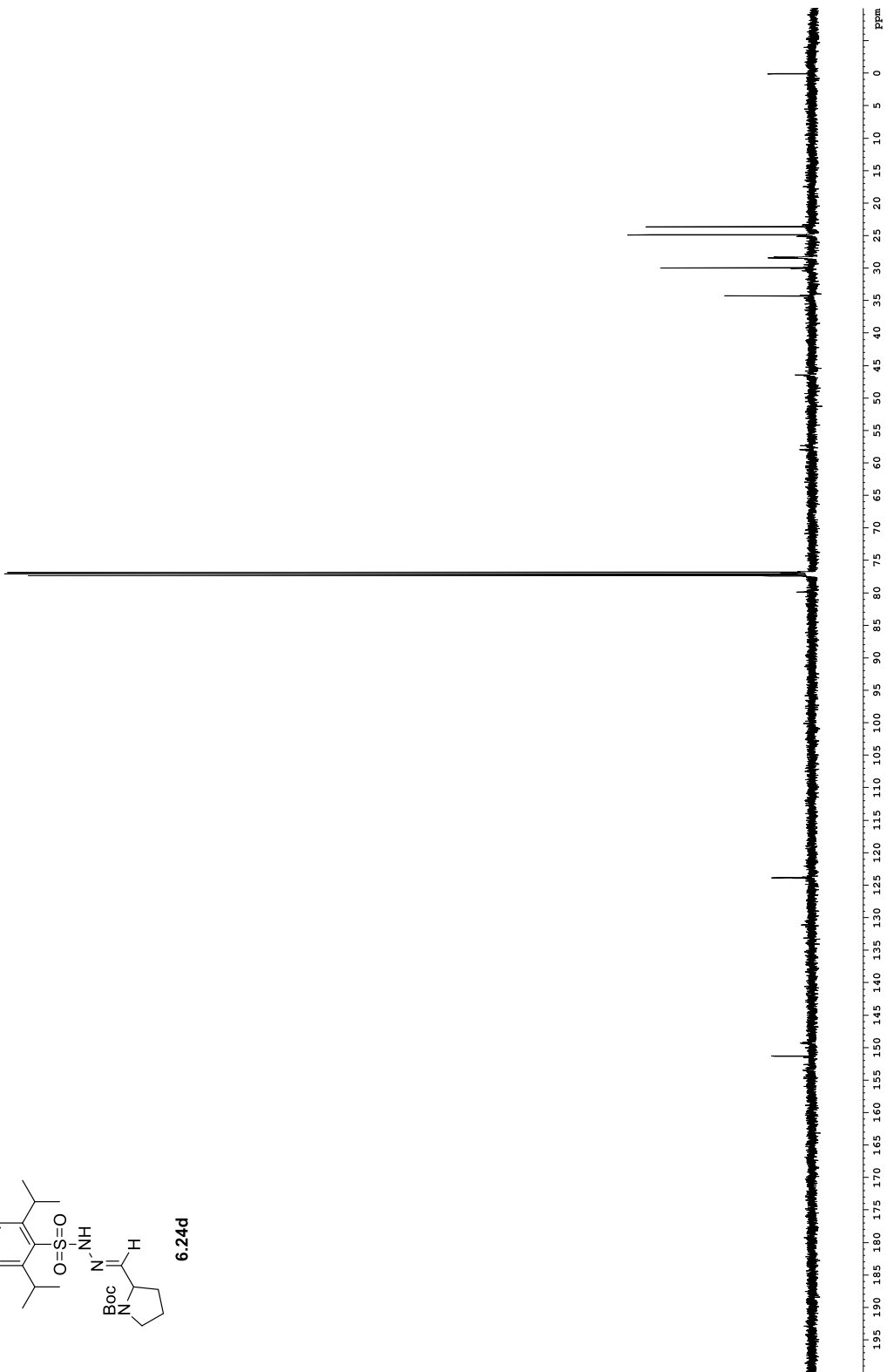


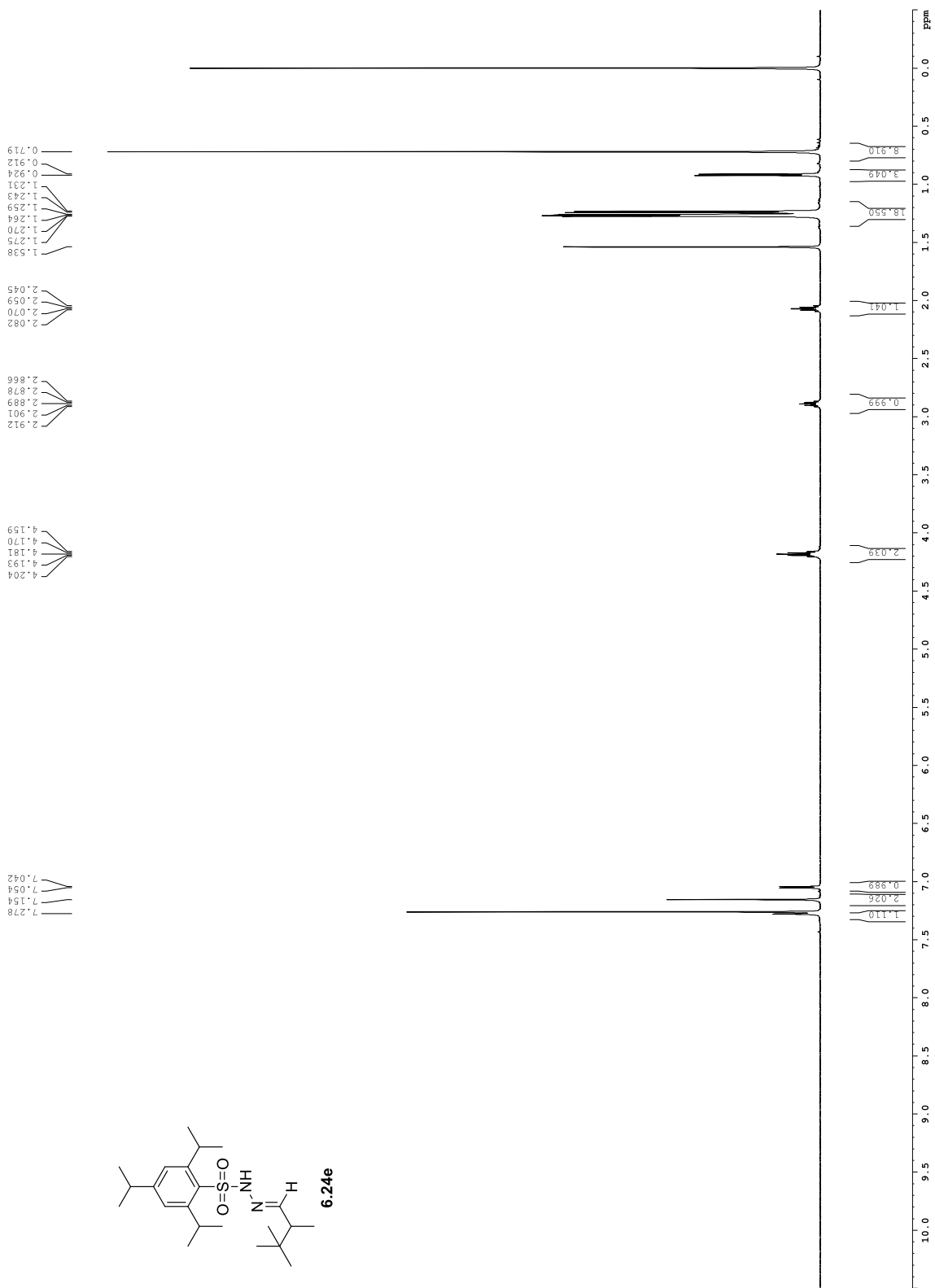
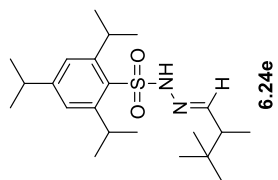


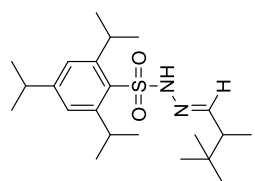
34.251
29.938
28.420
28.300
24.883
24.826
23.627

123.852

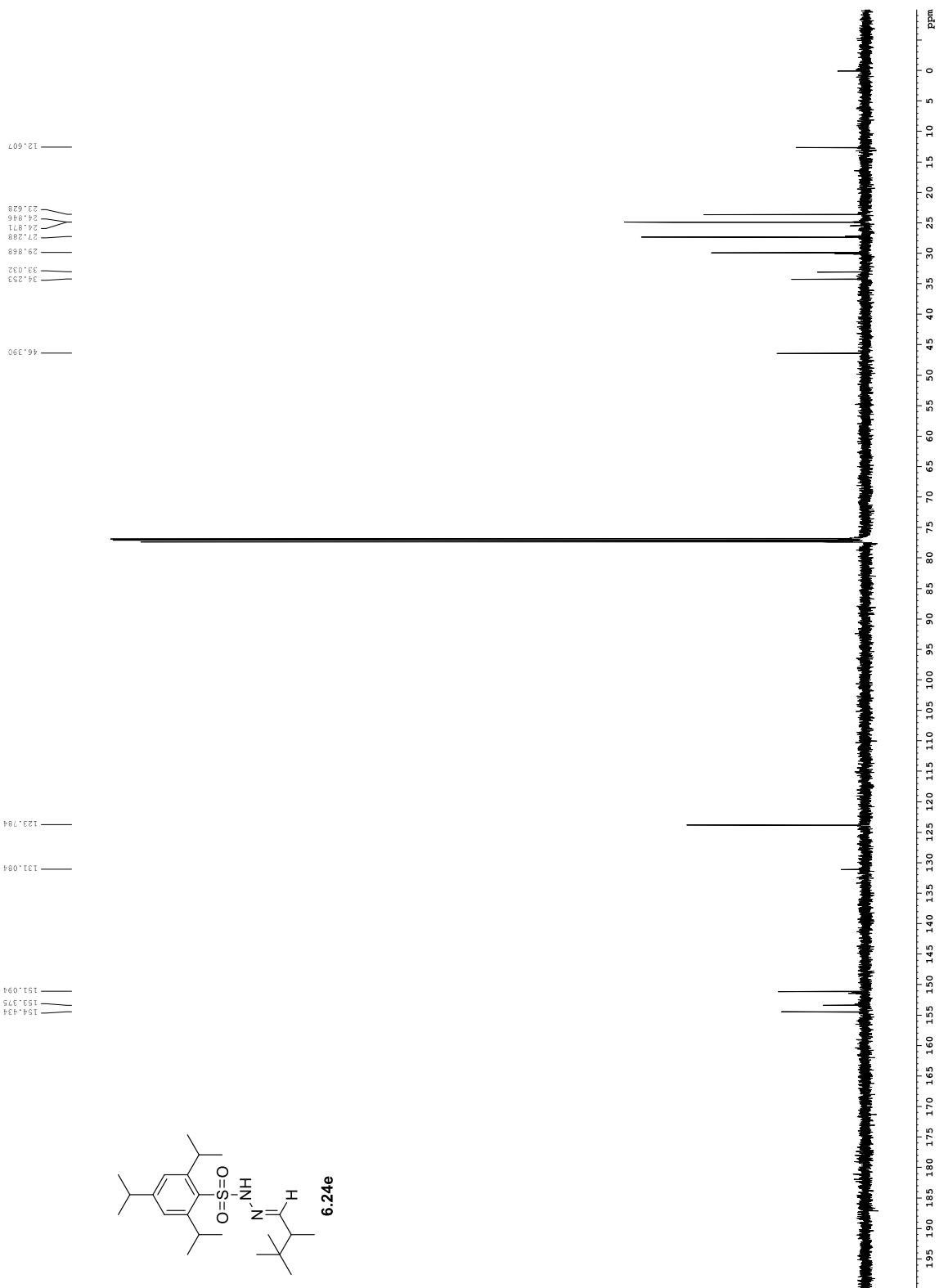
151.295

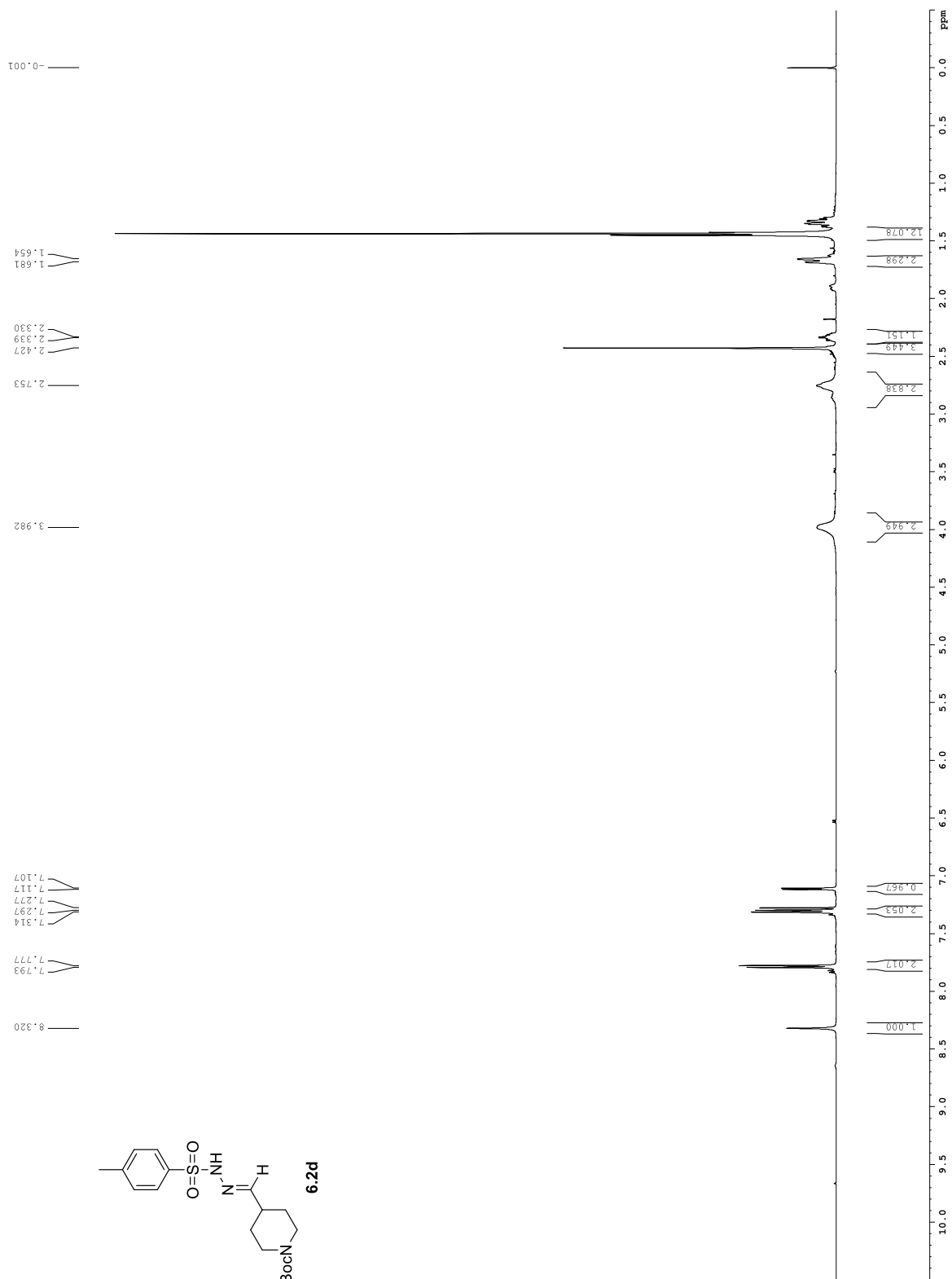


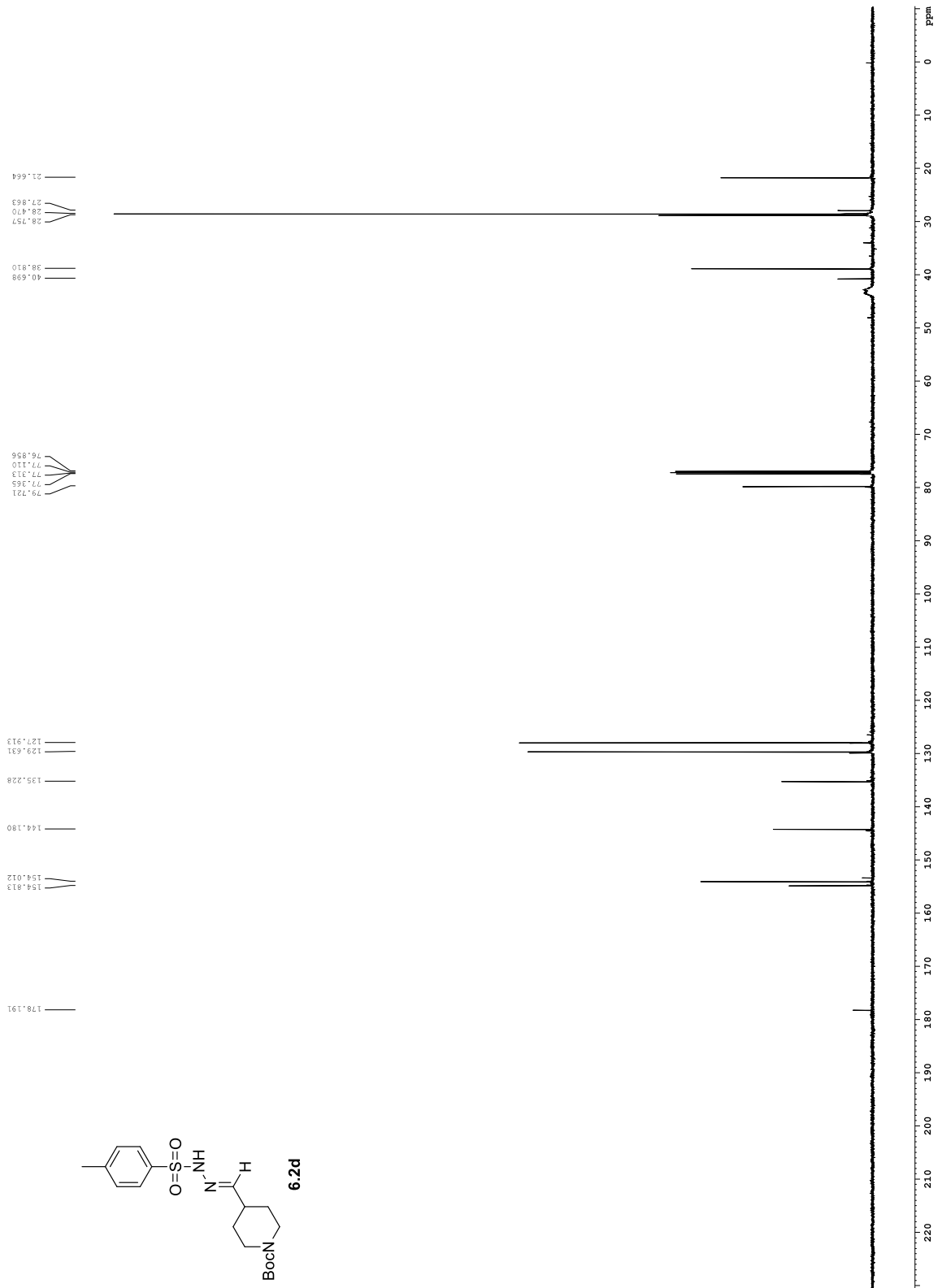
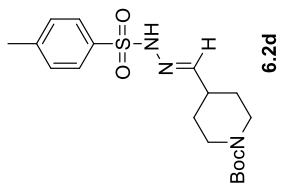


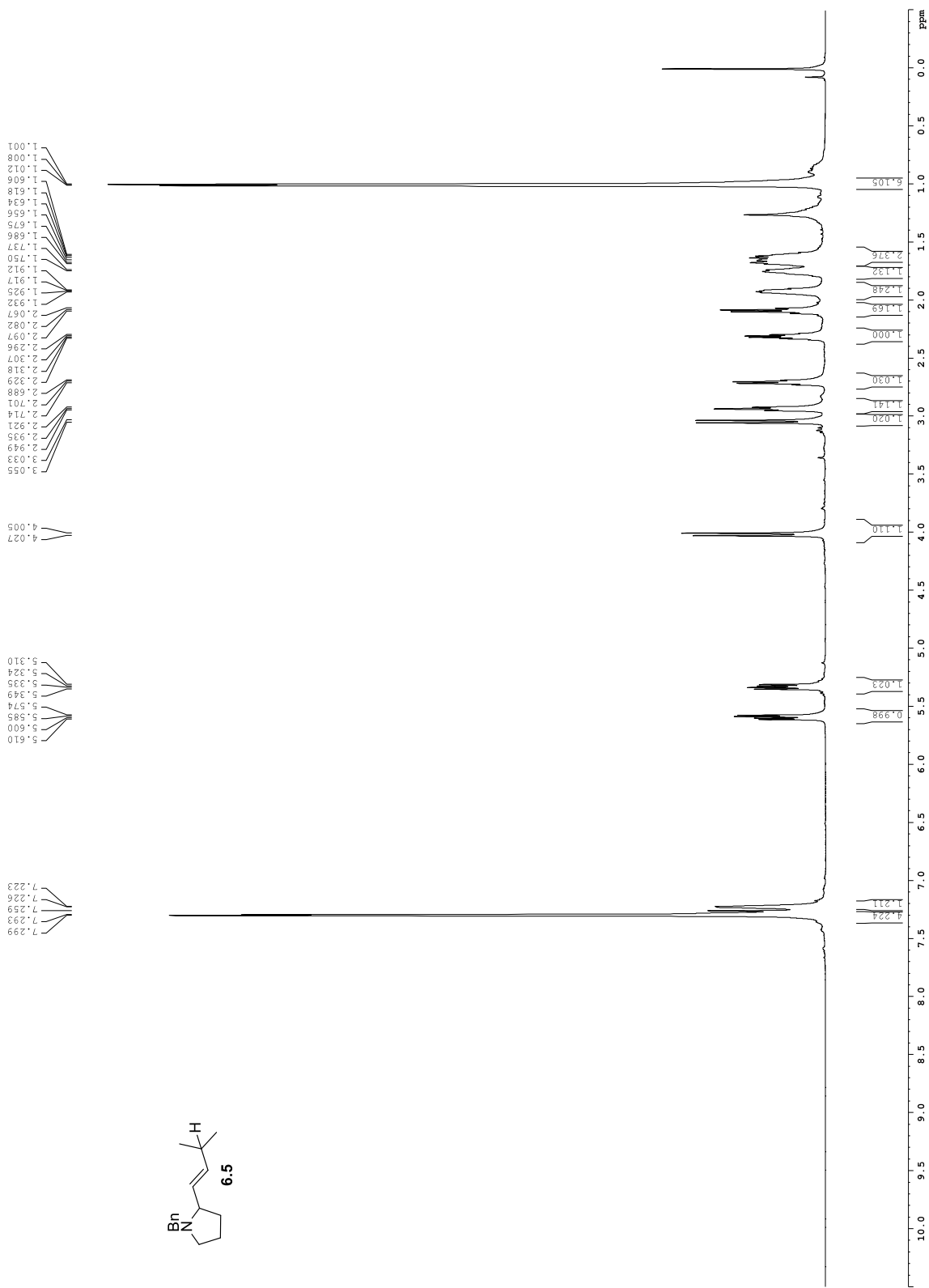
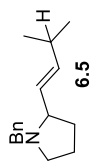


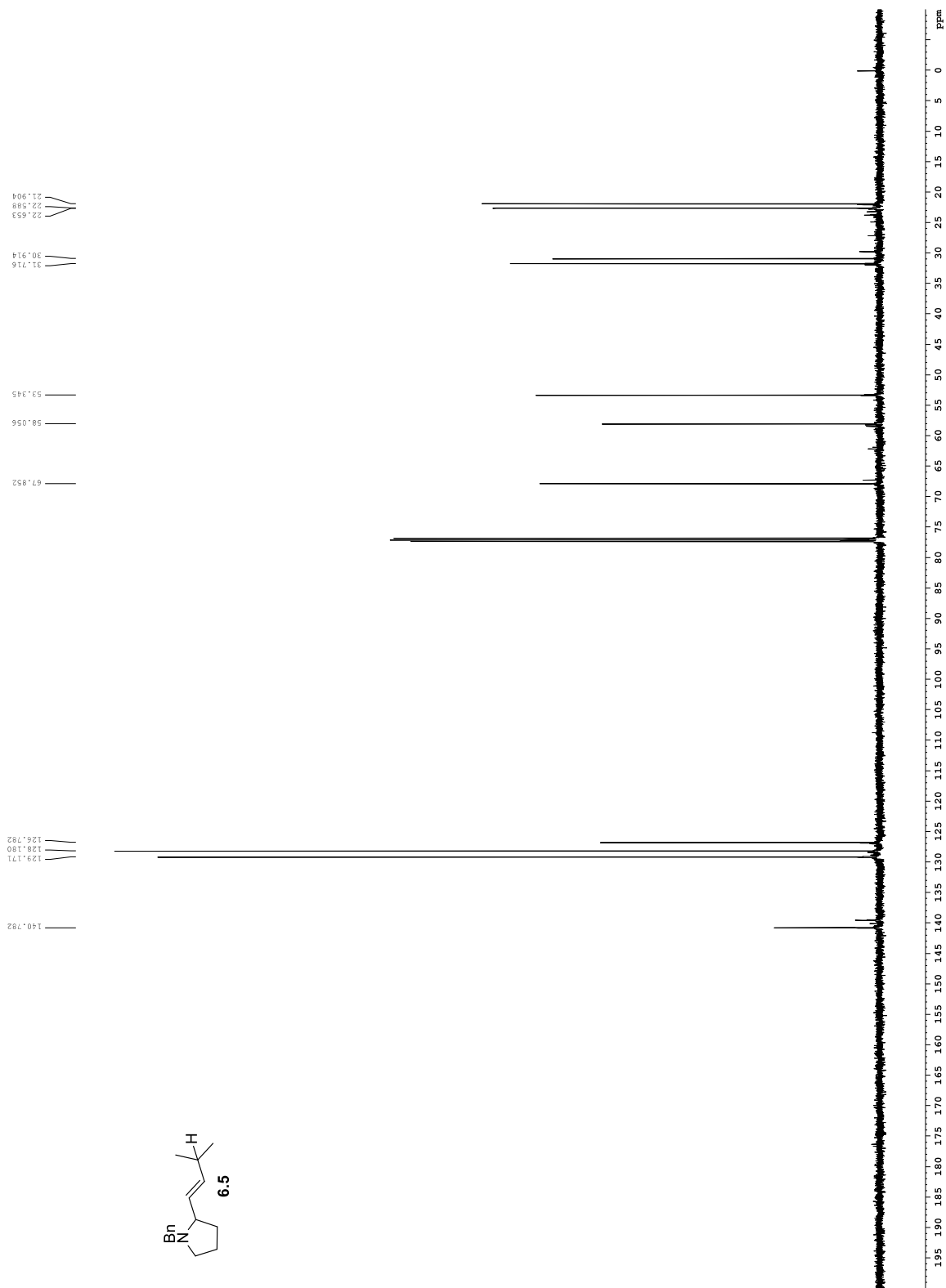
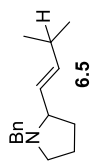
6.24e

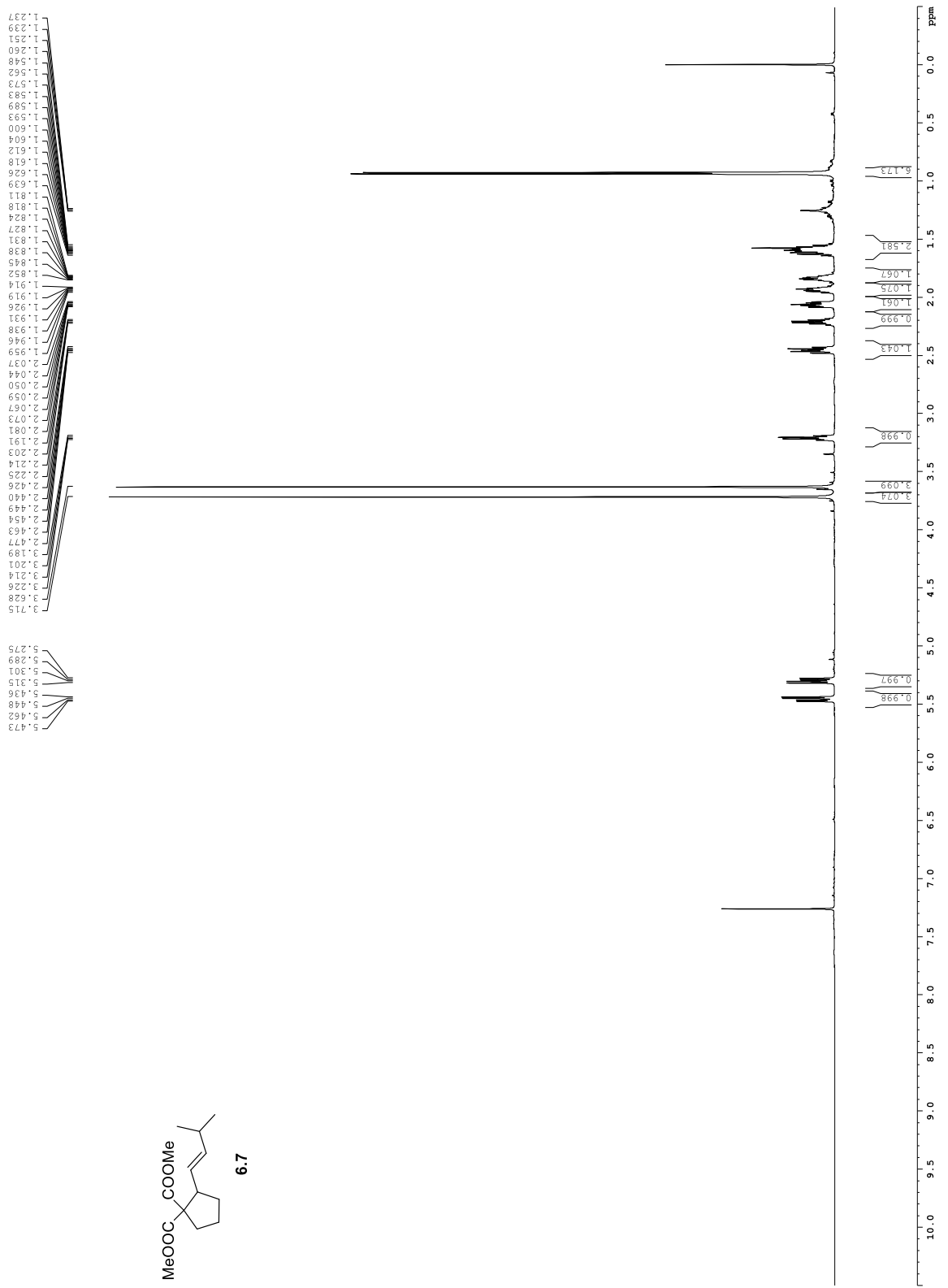
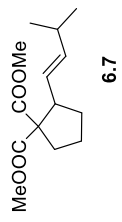


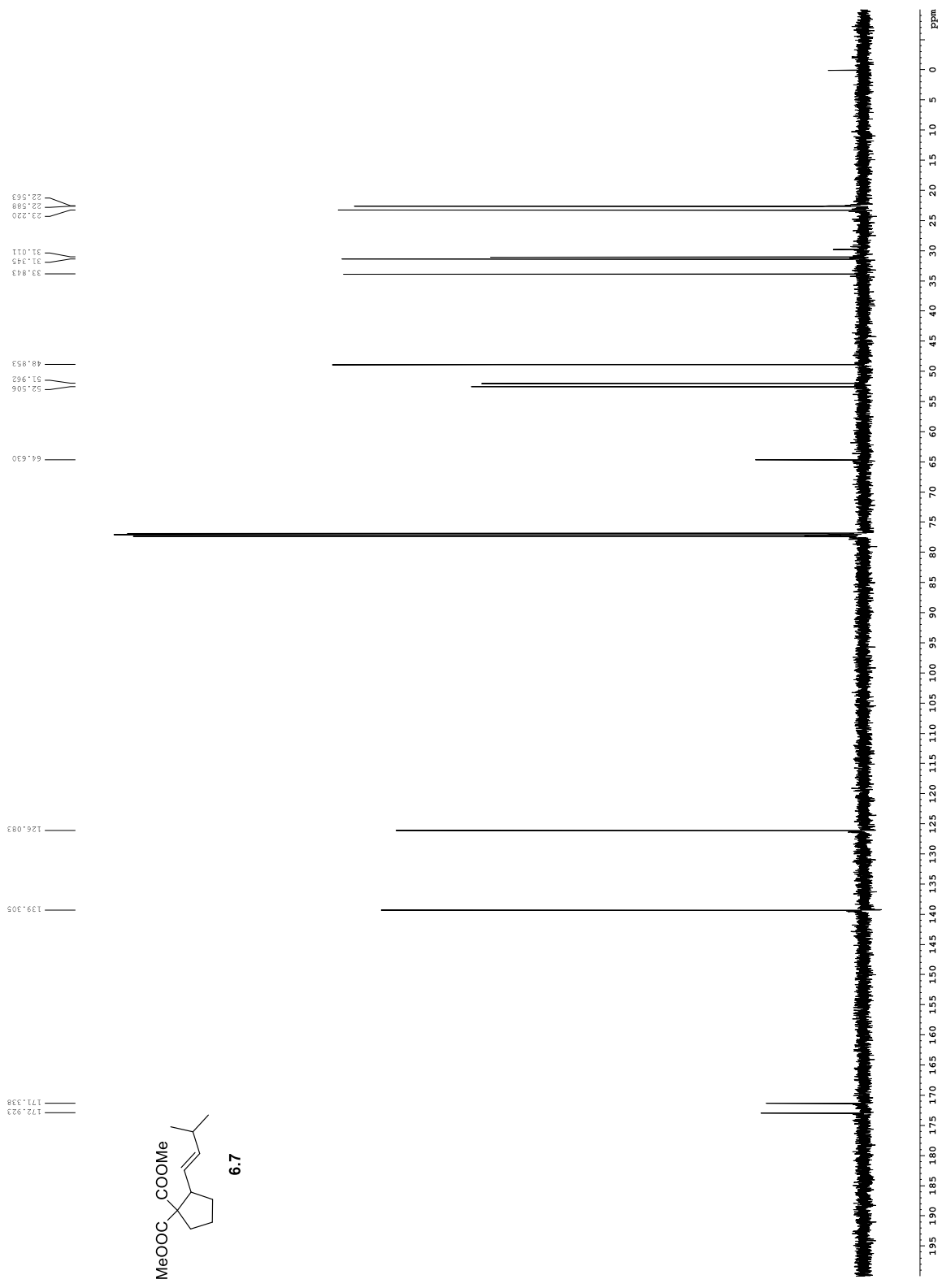


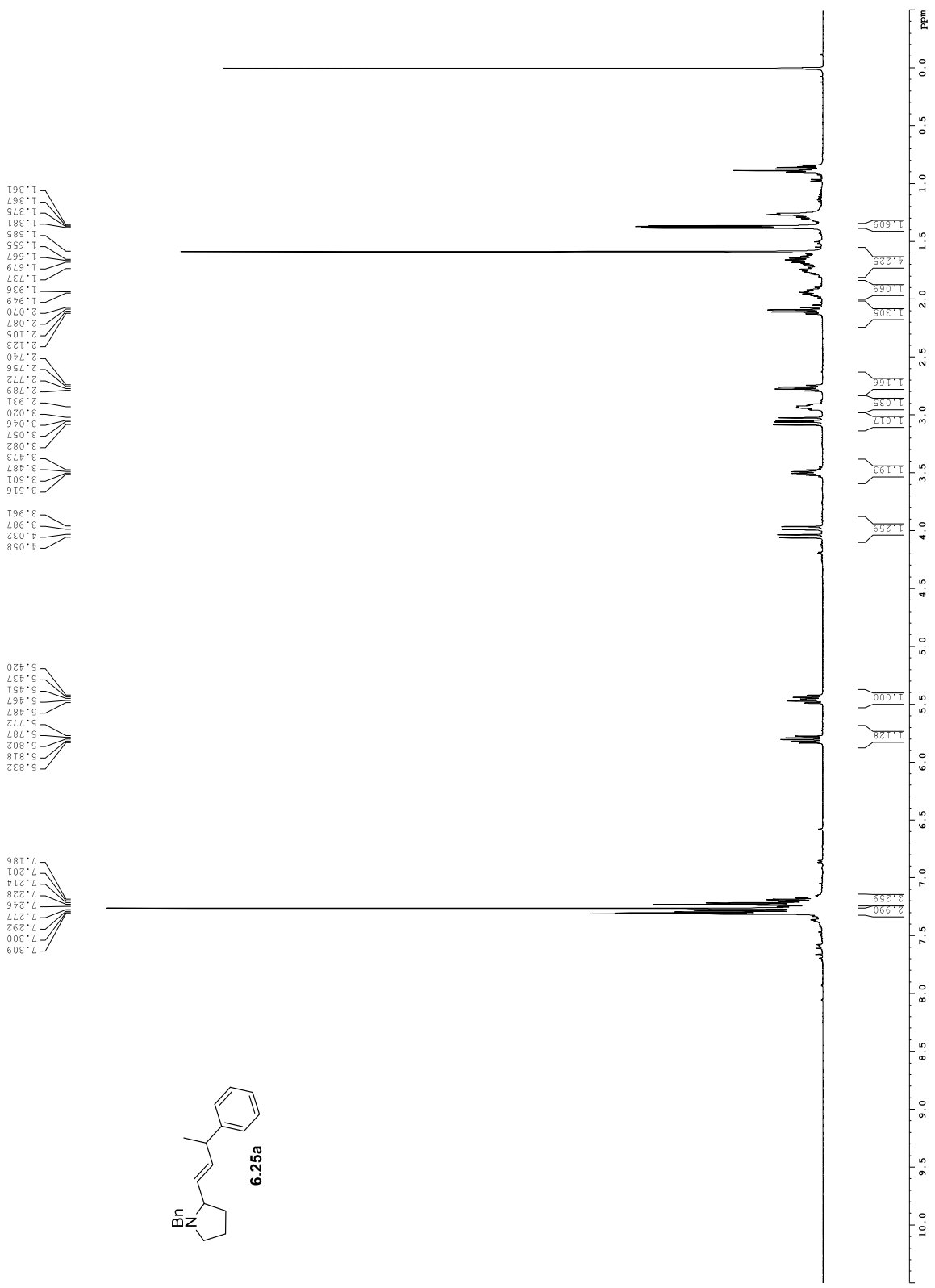
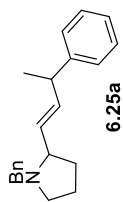


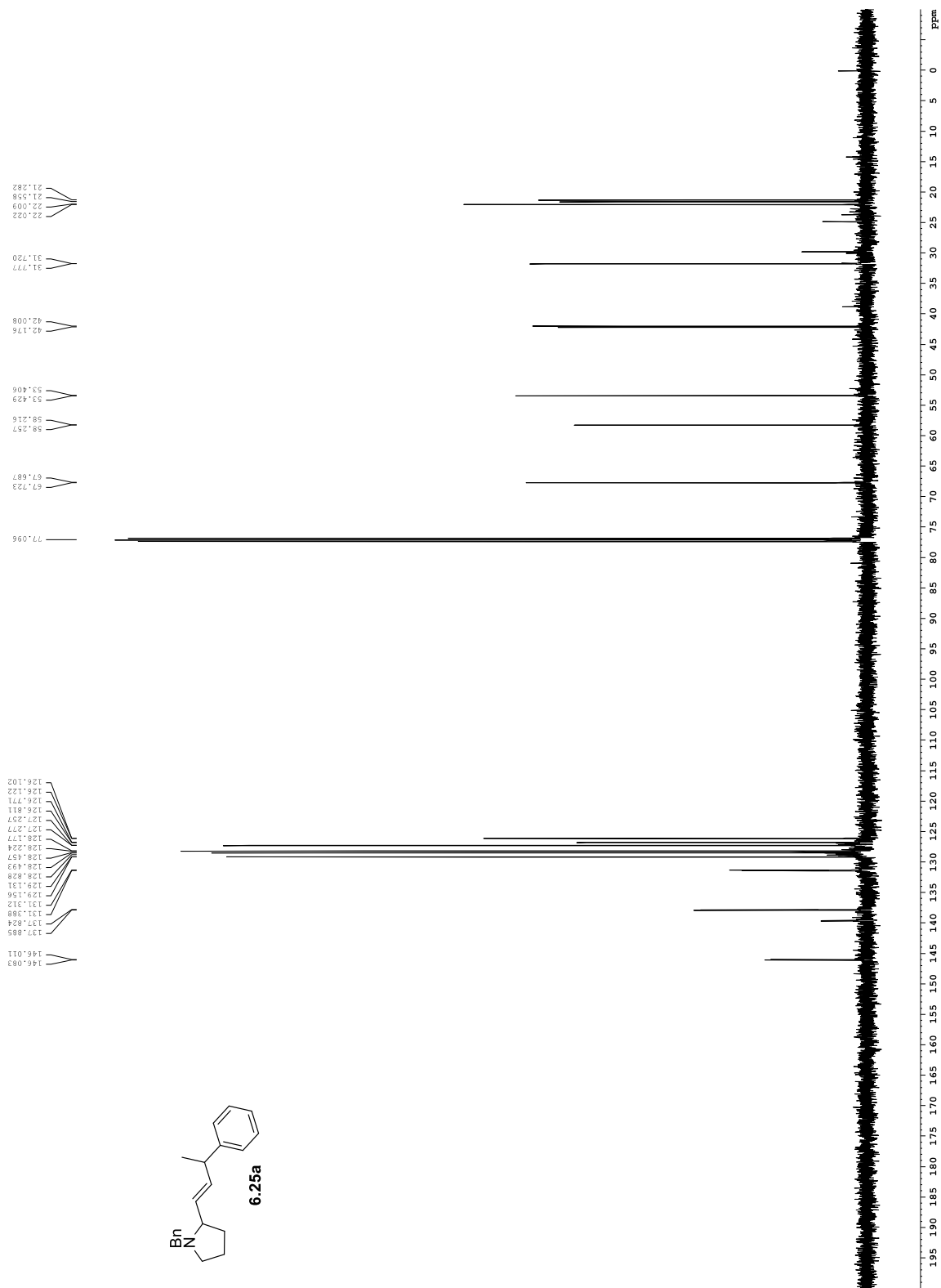
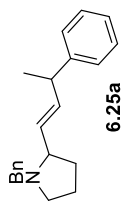


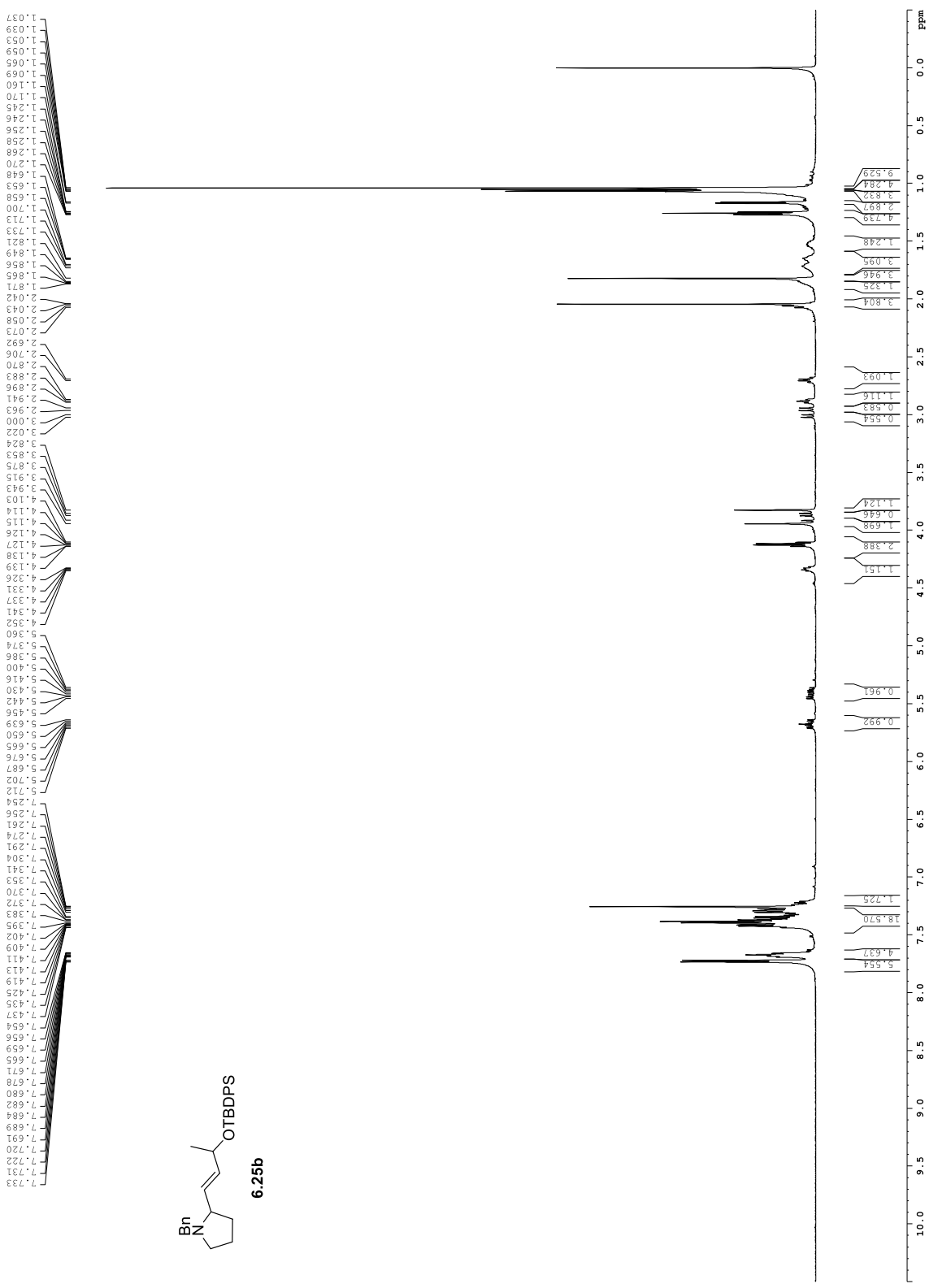


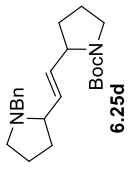
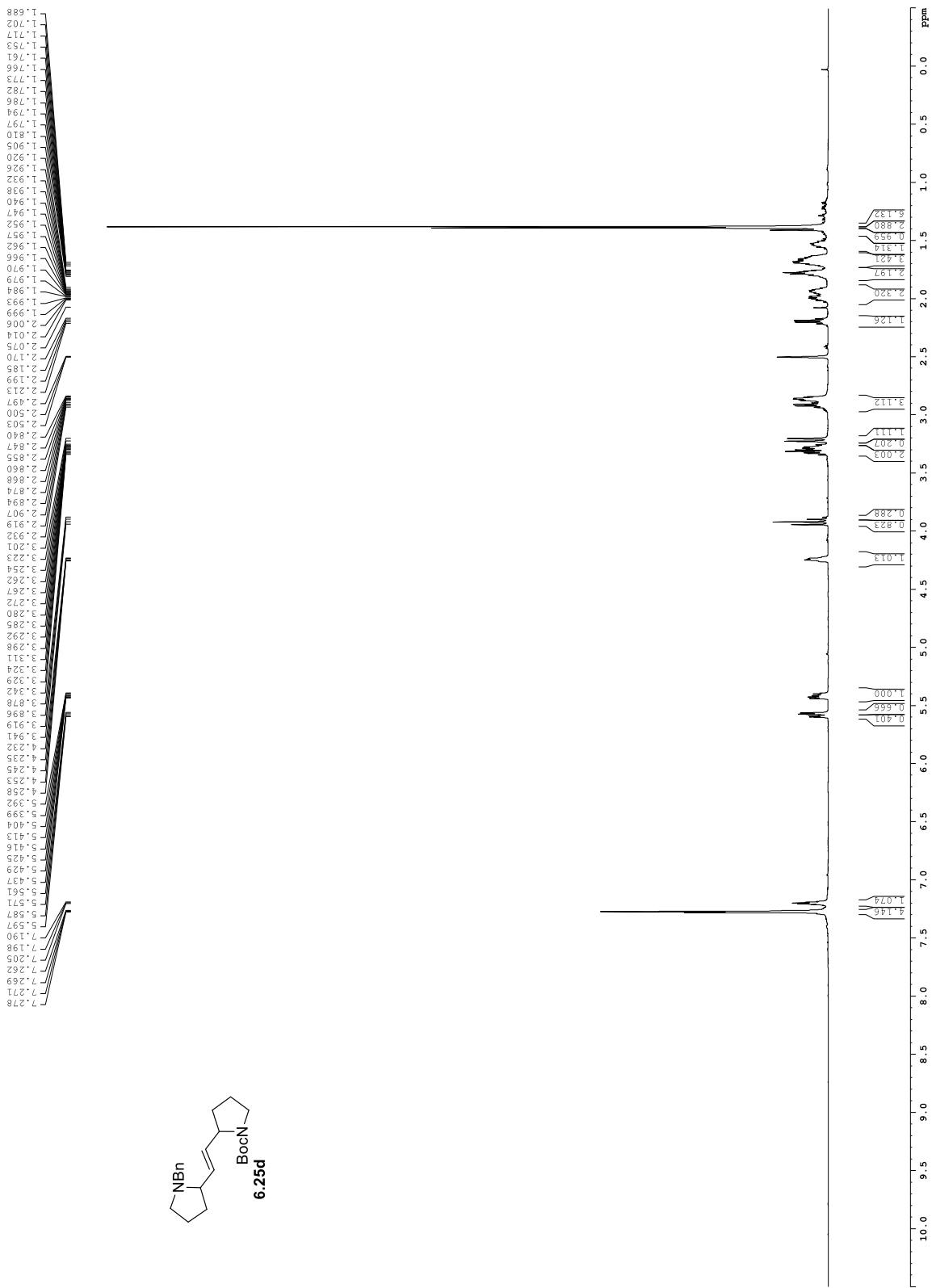


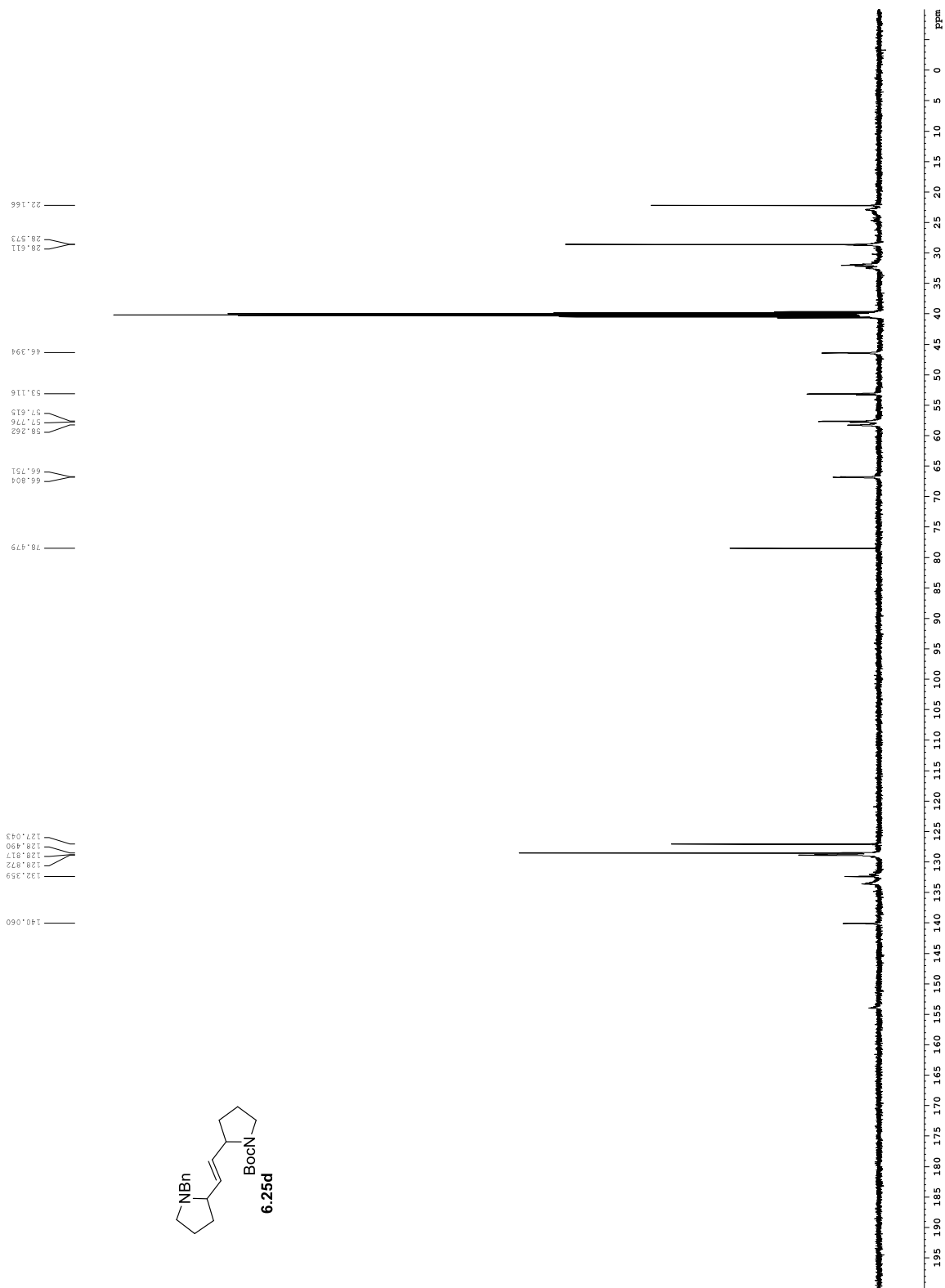
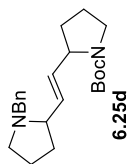


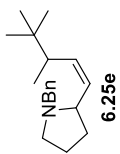
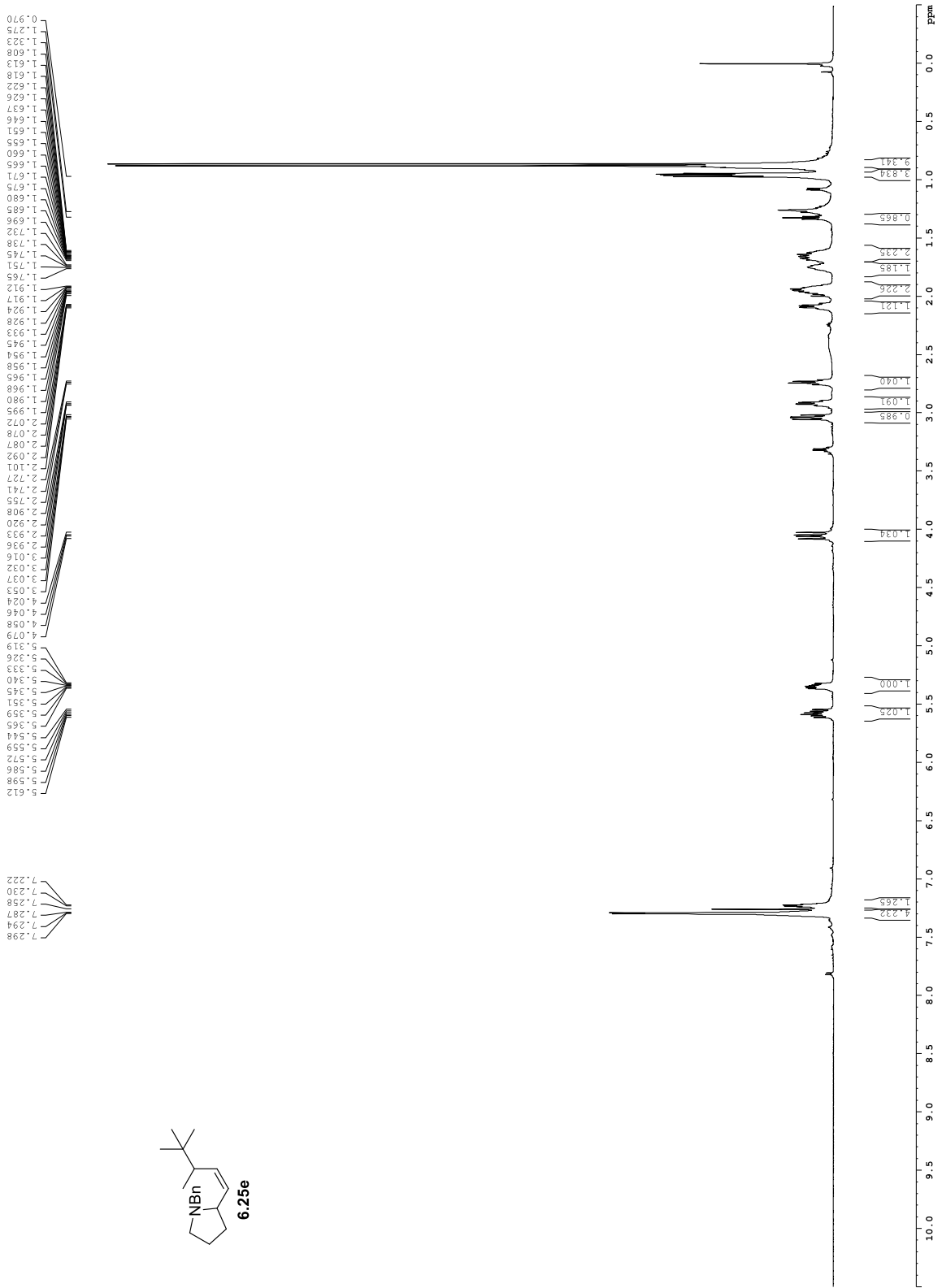


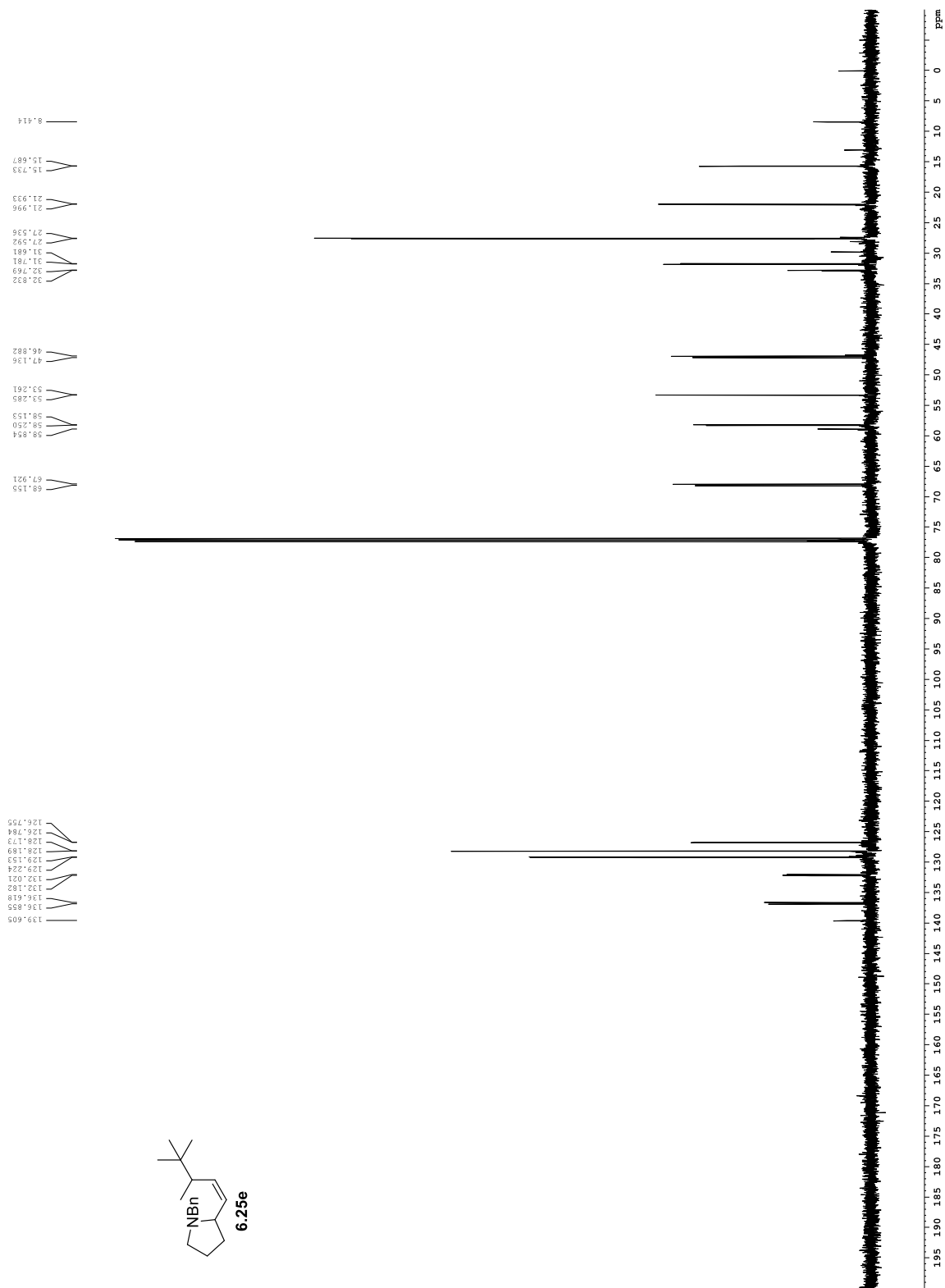
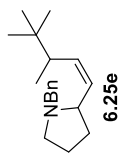


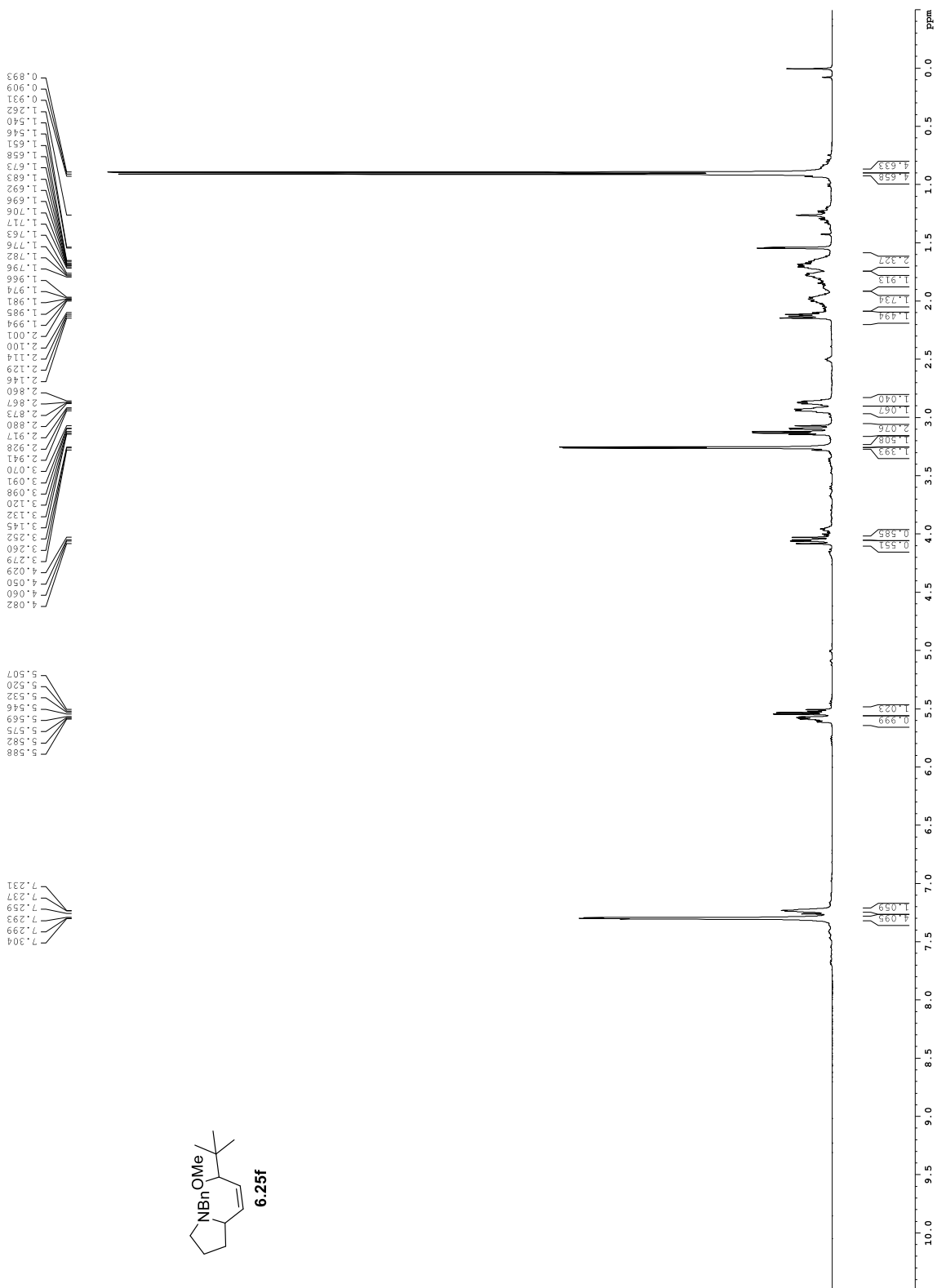
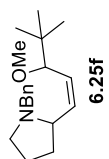


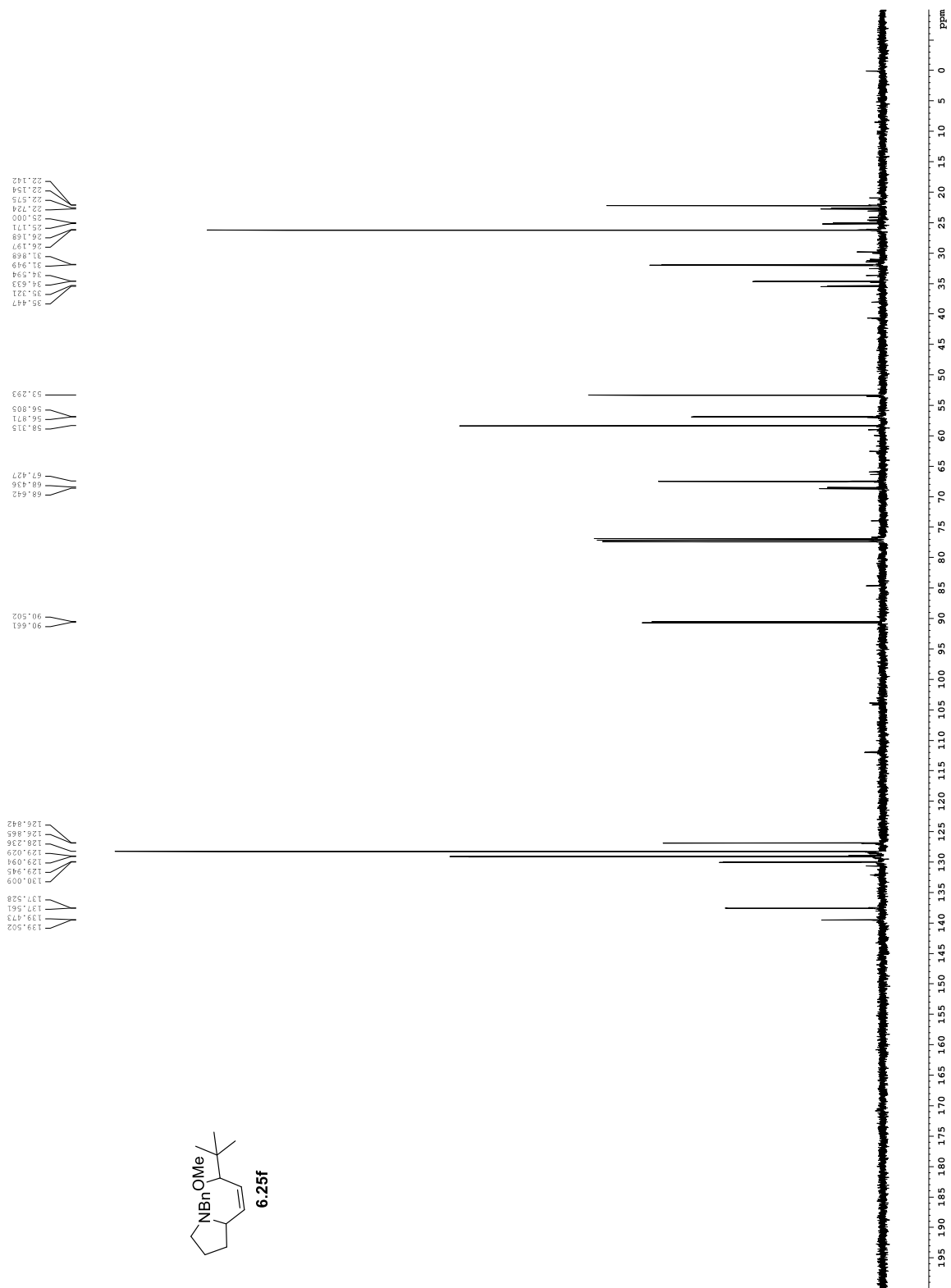
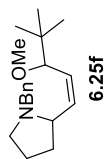


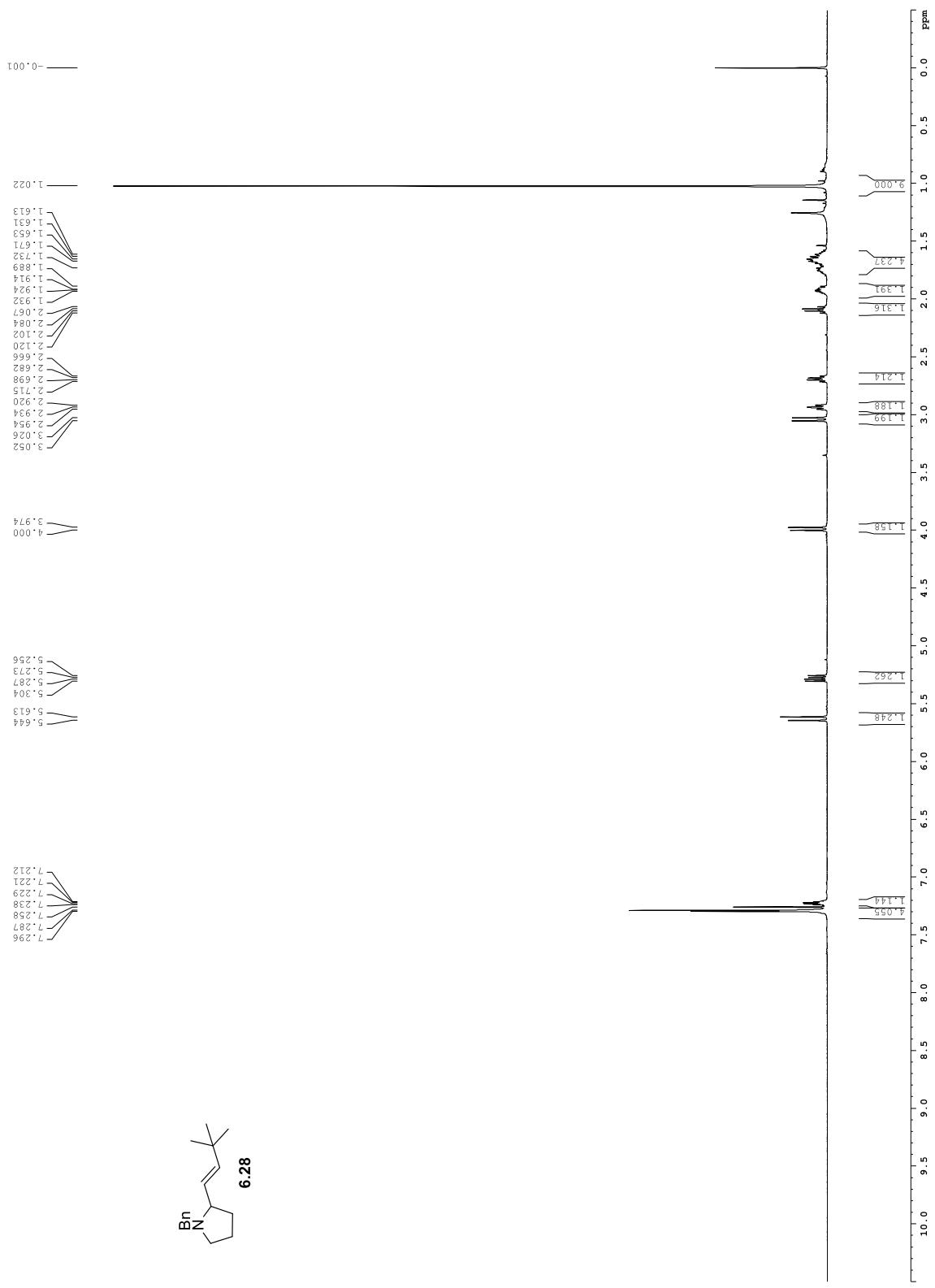
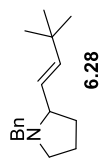


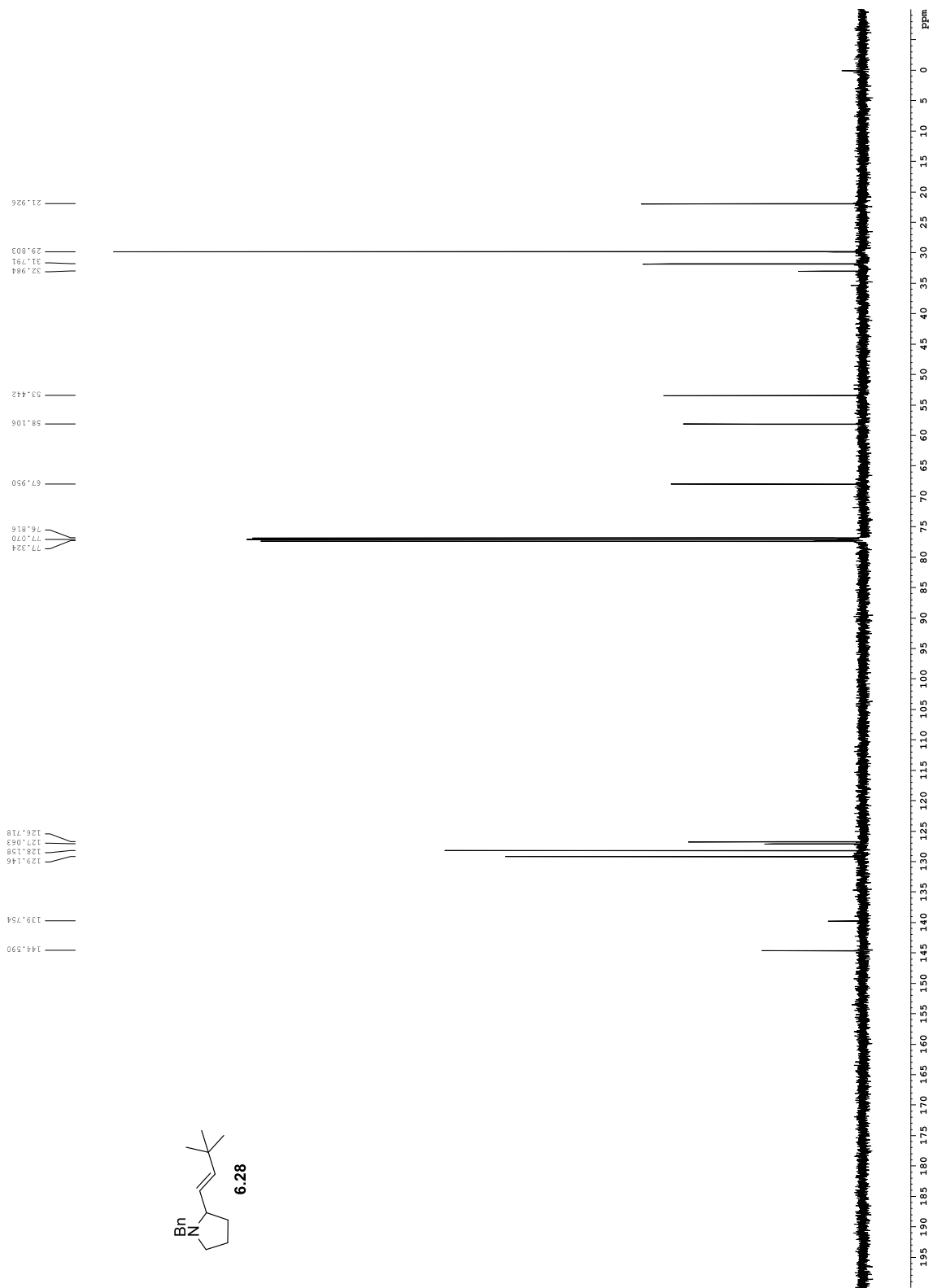
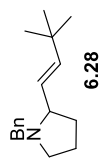


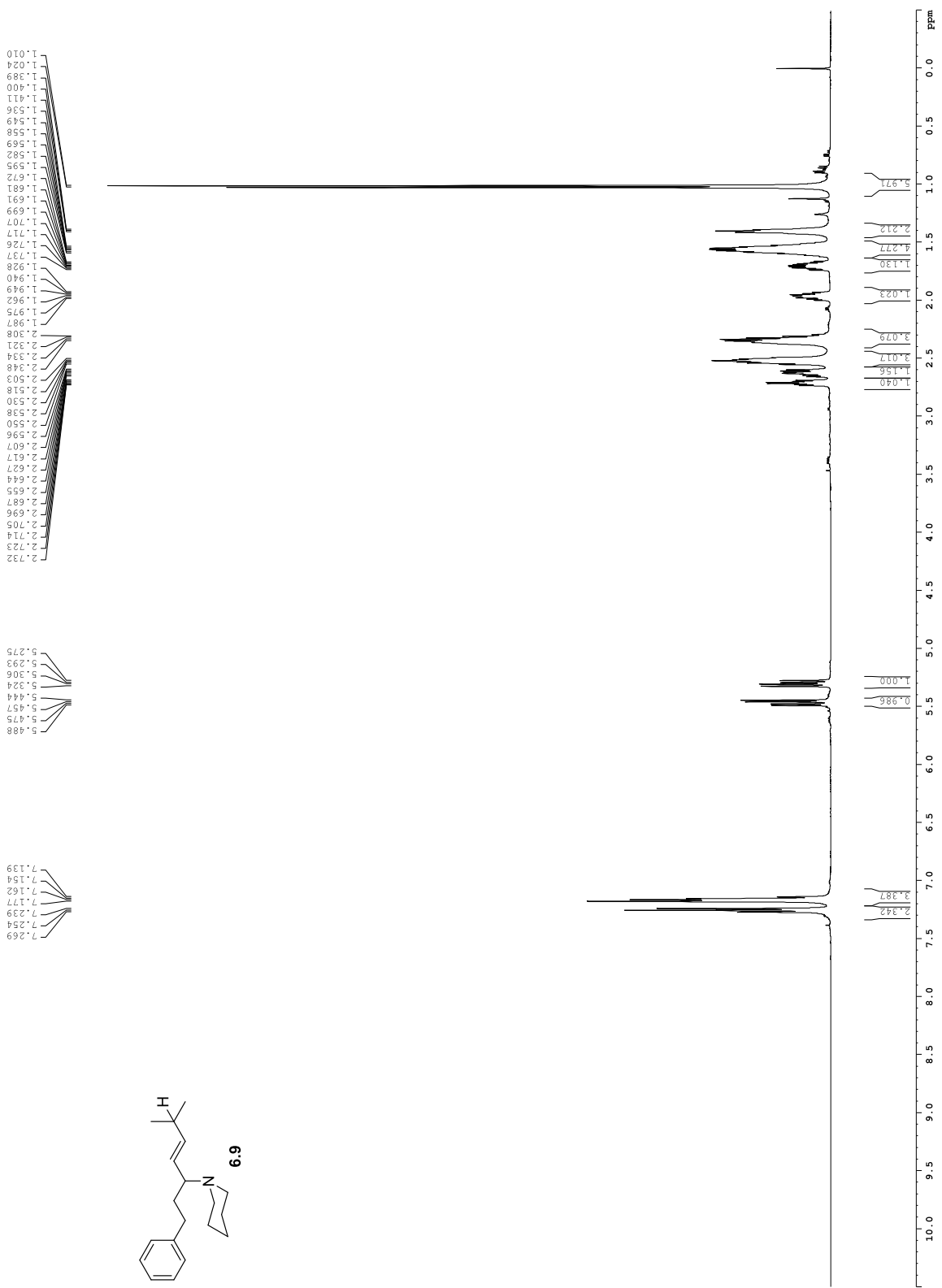


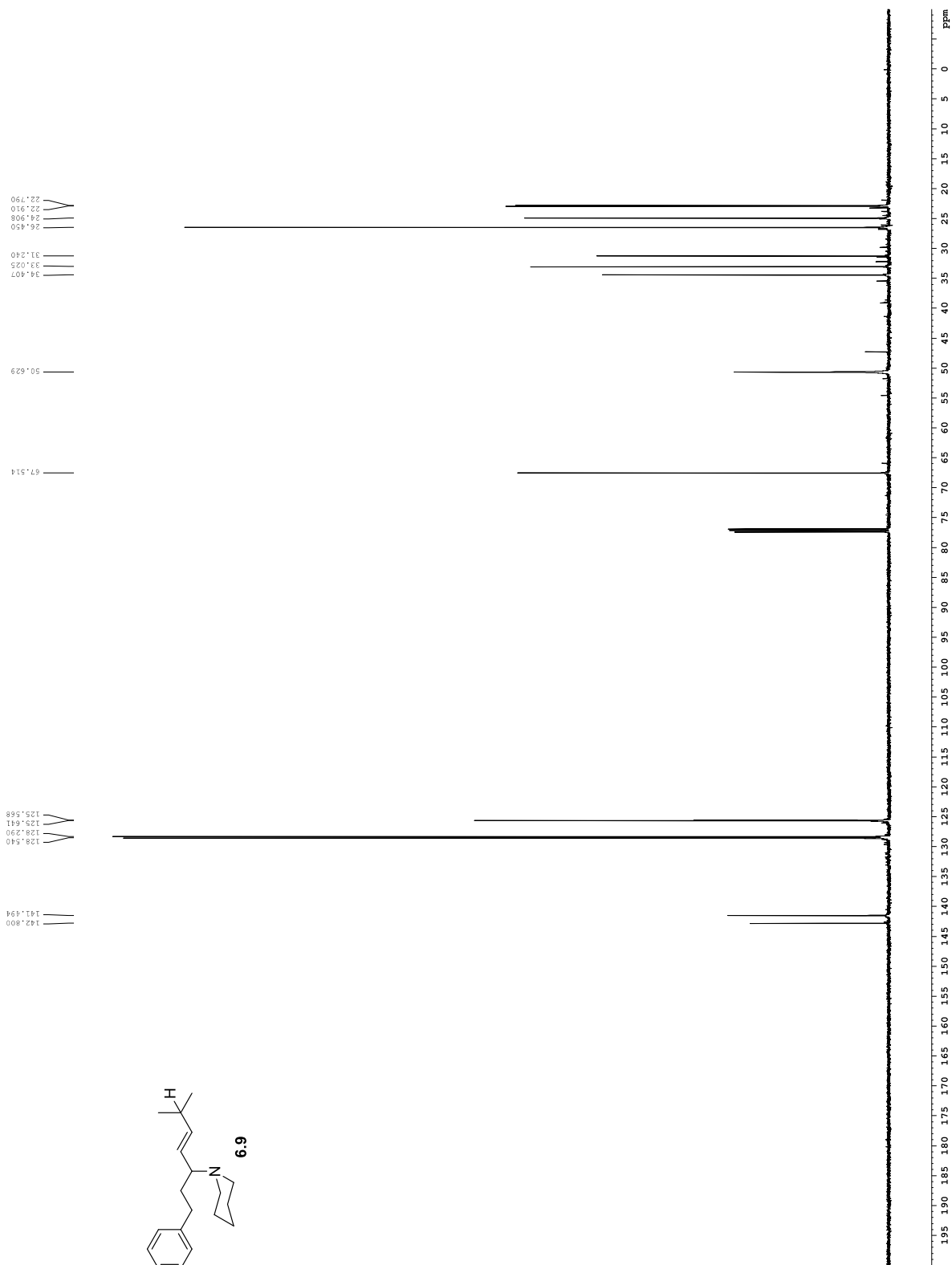


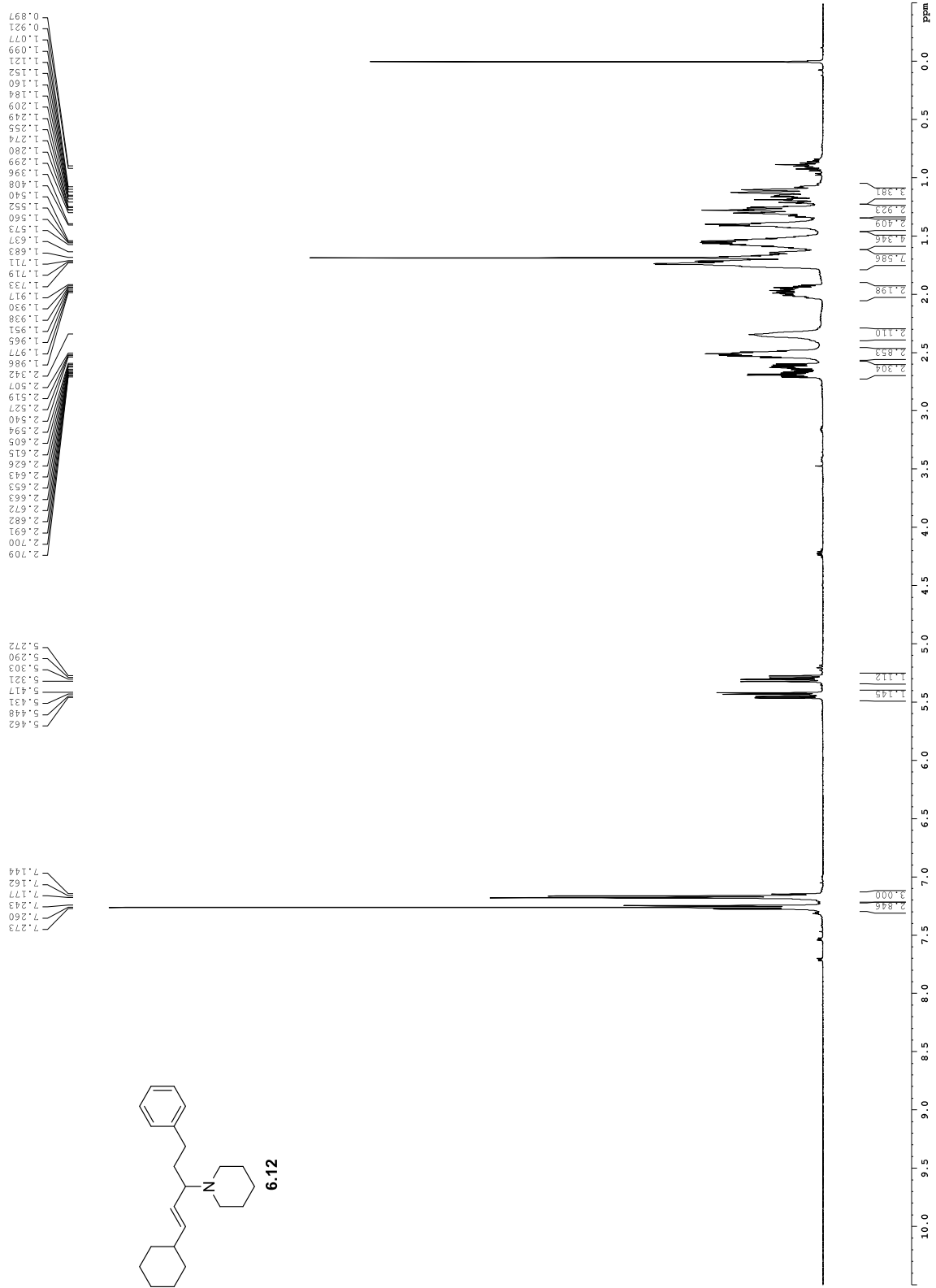


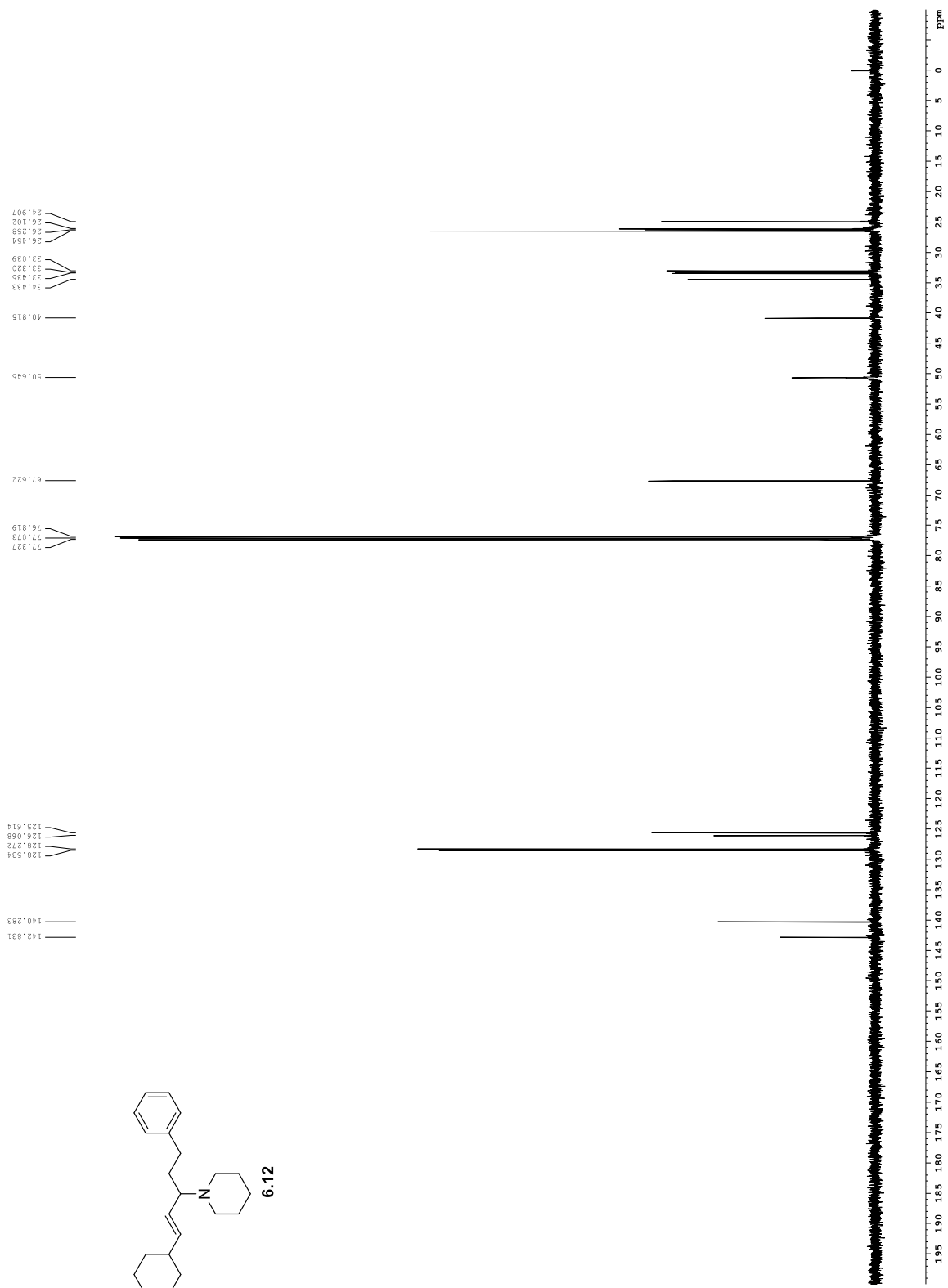
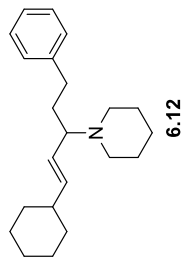


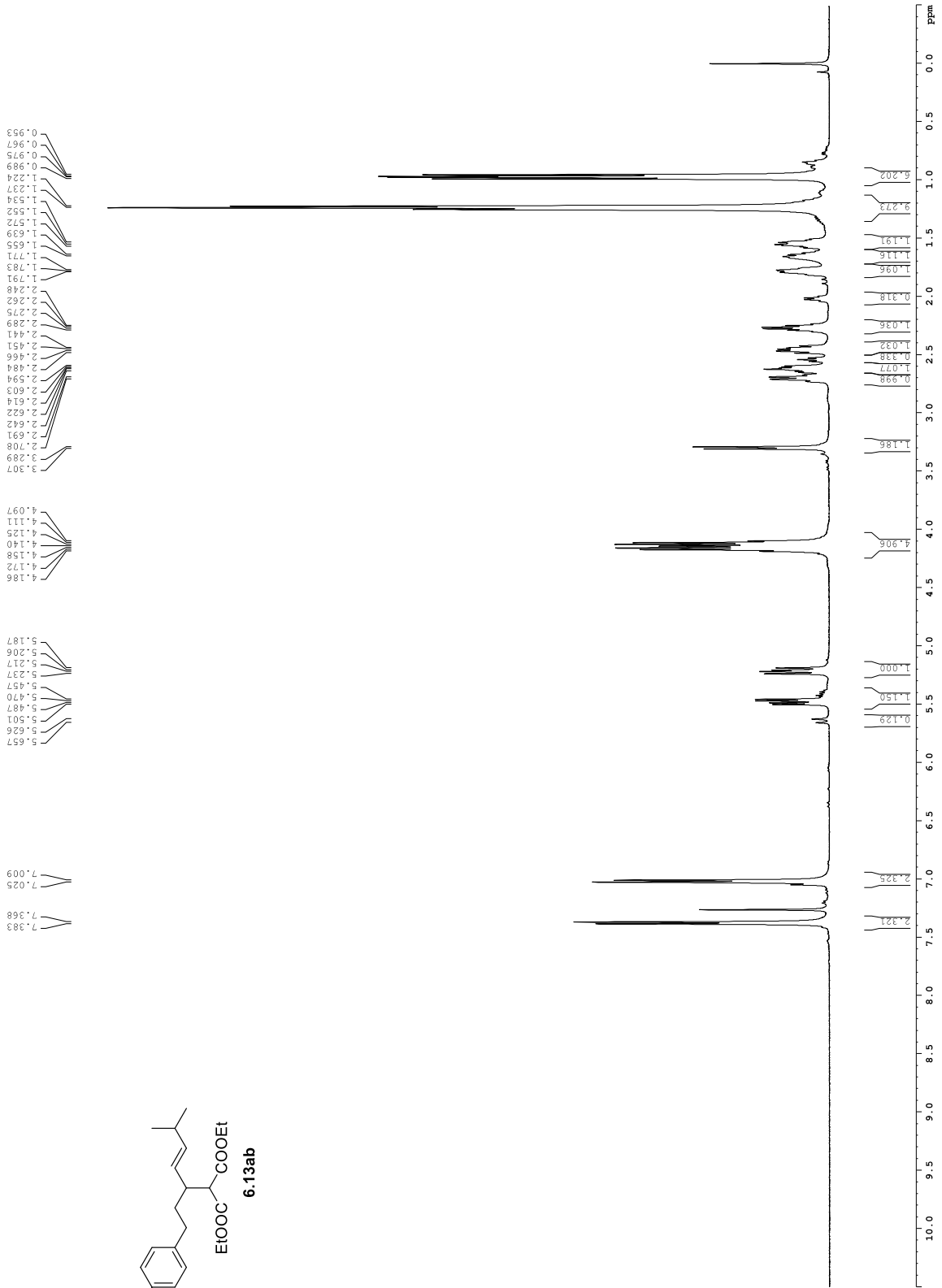
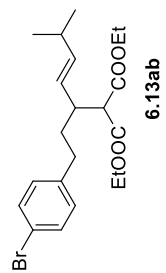


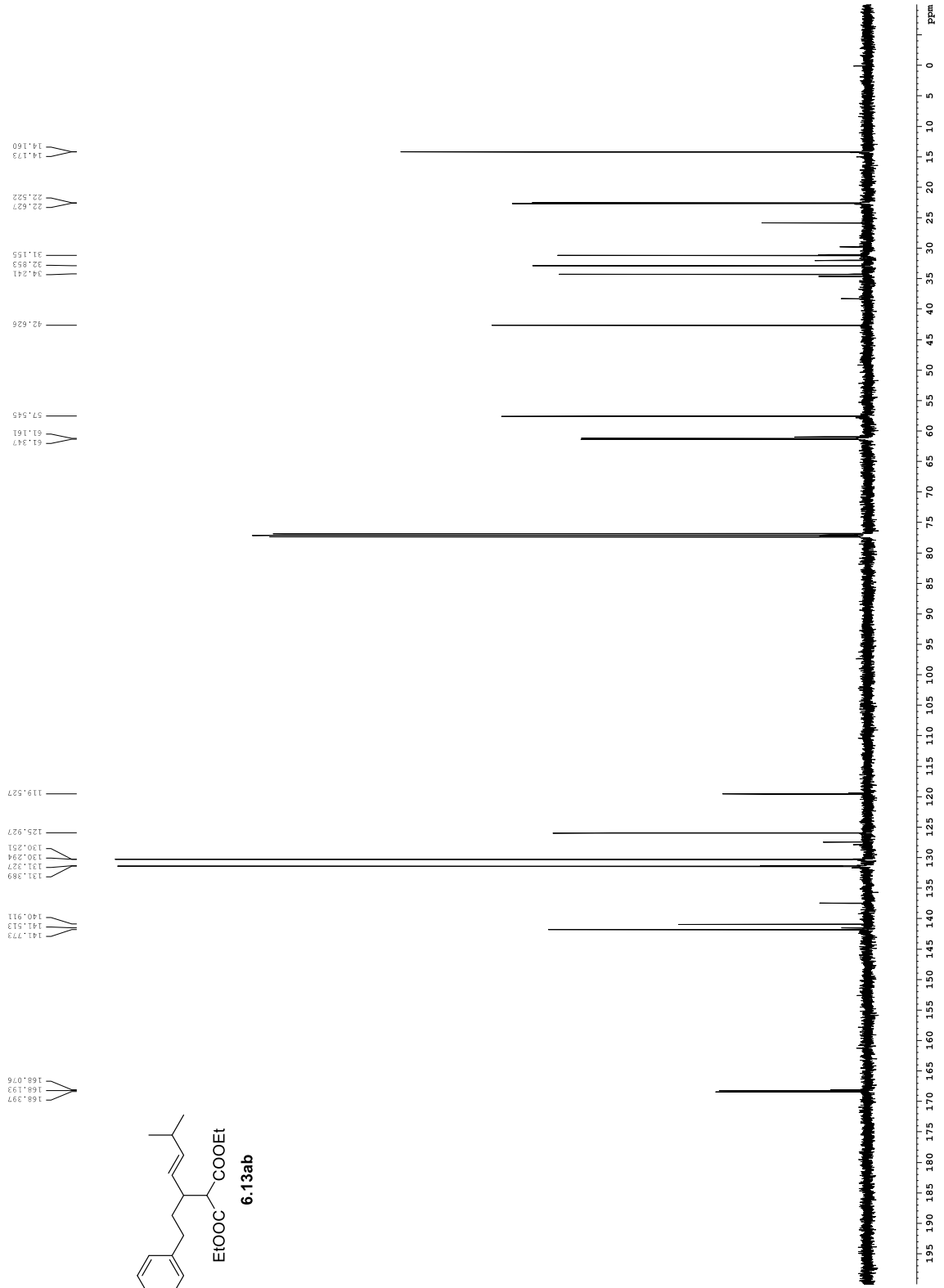


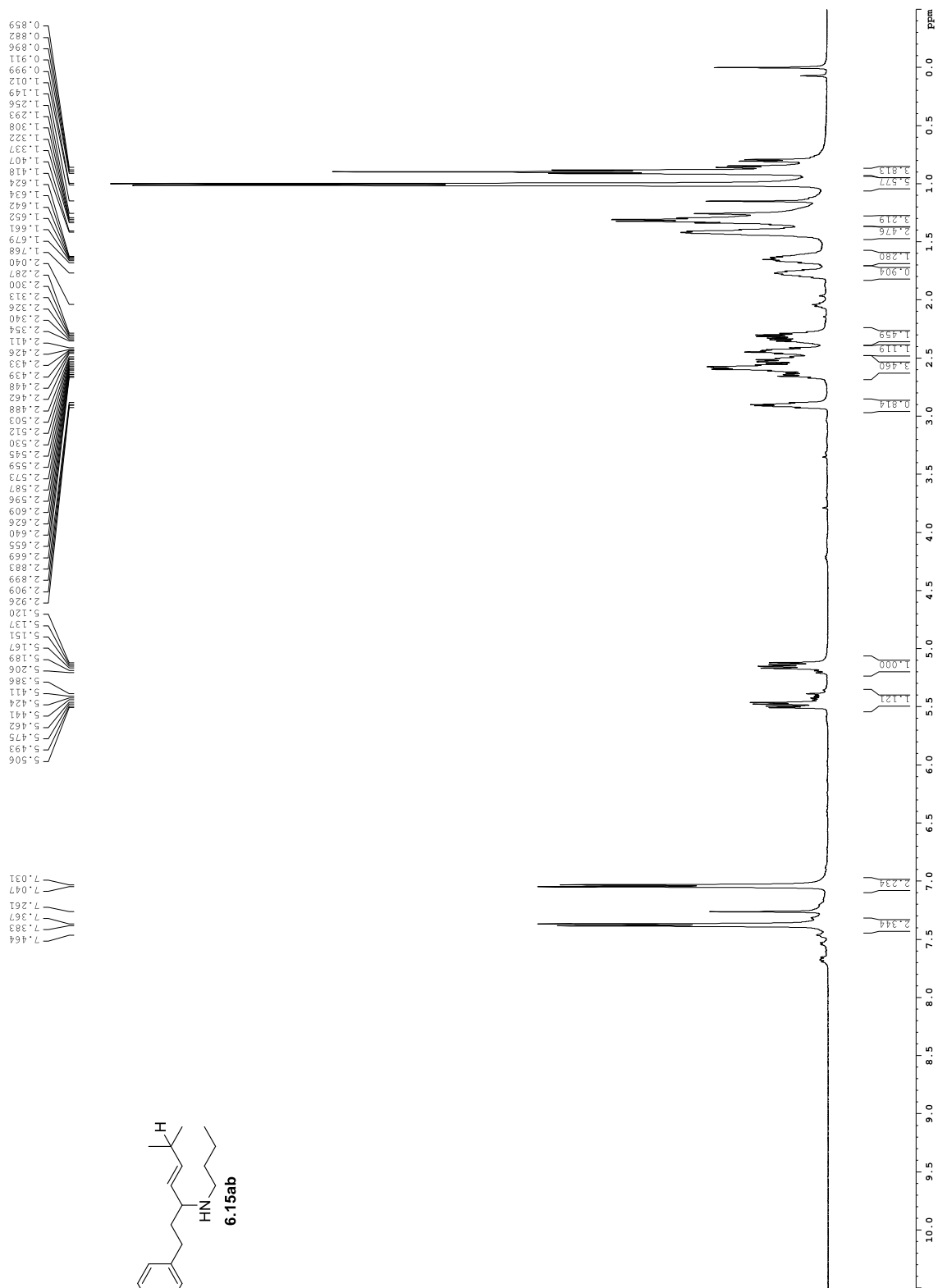
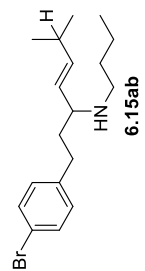


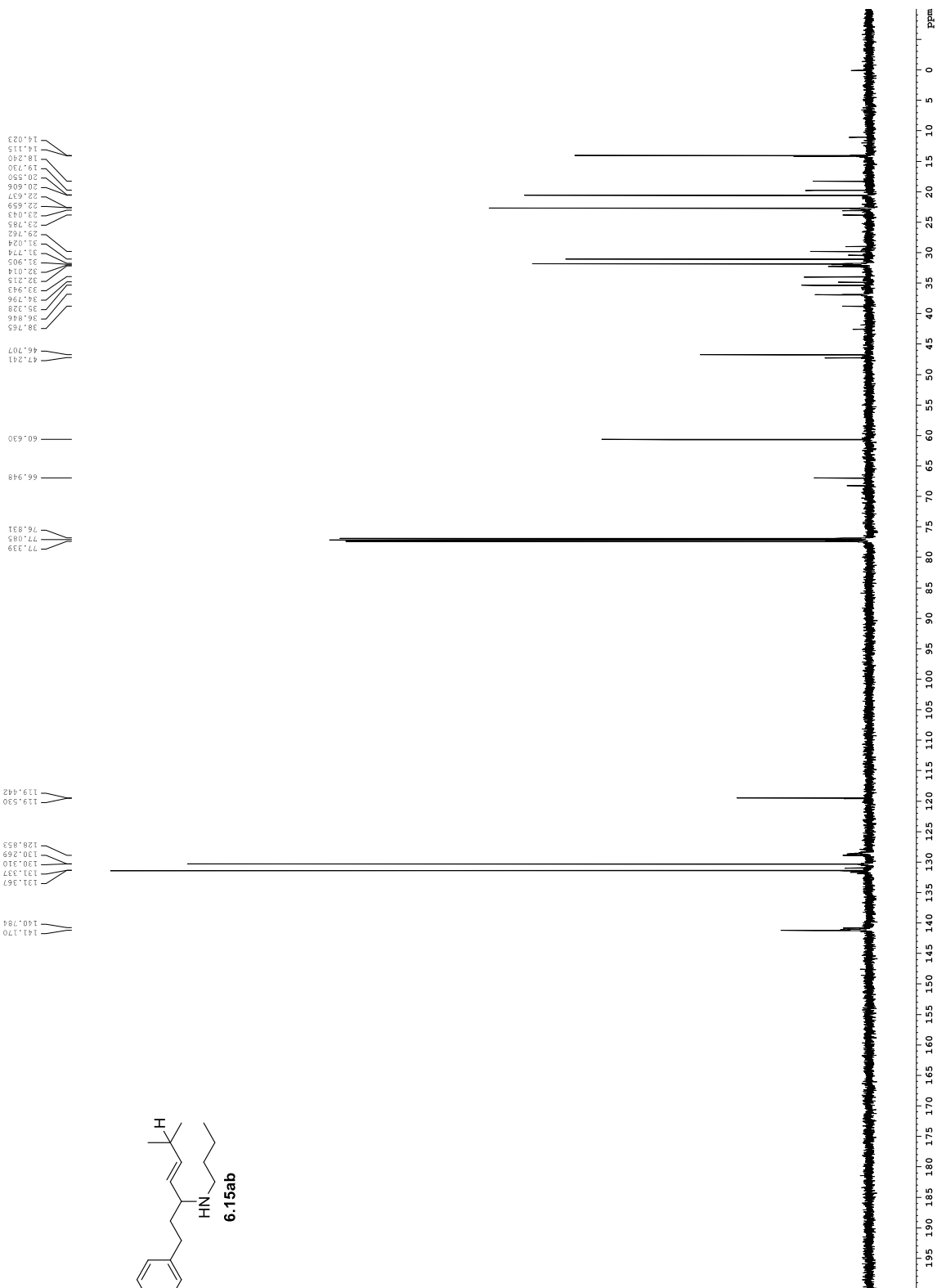
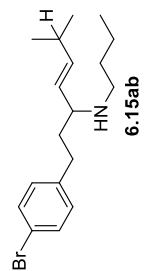


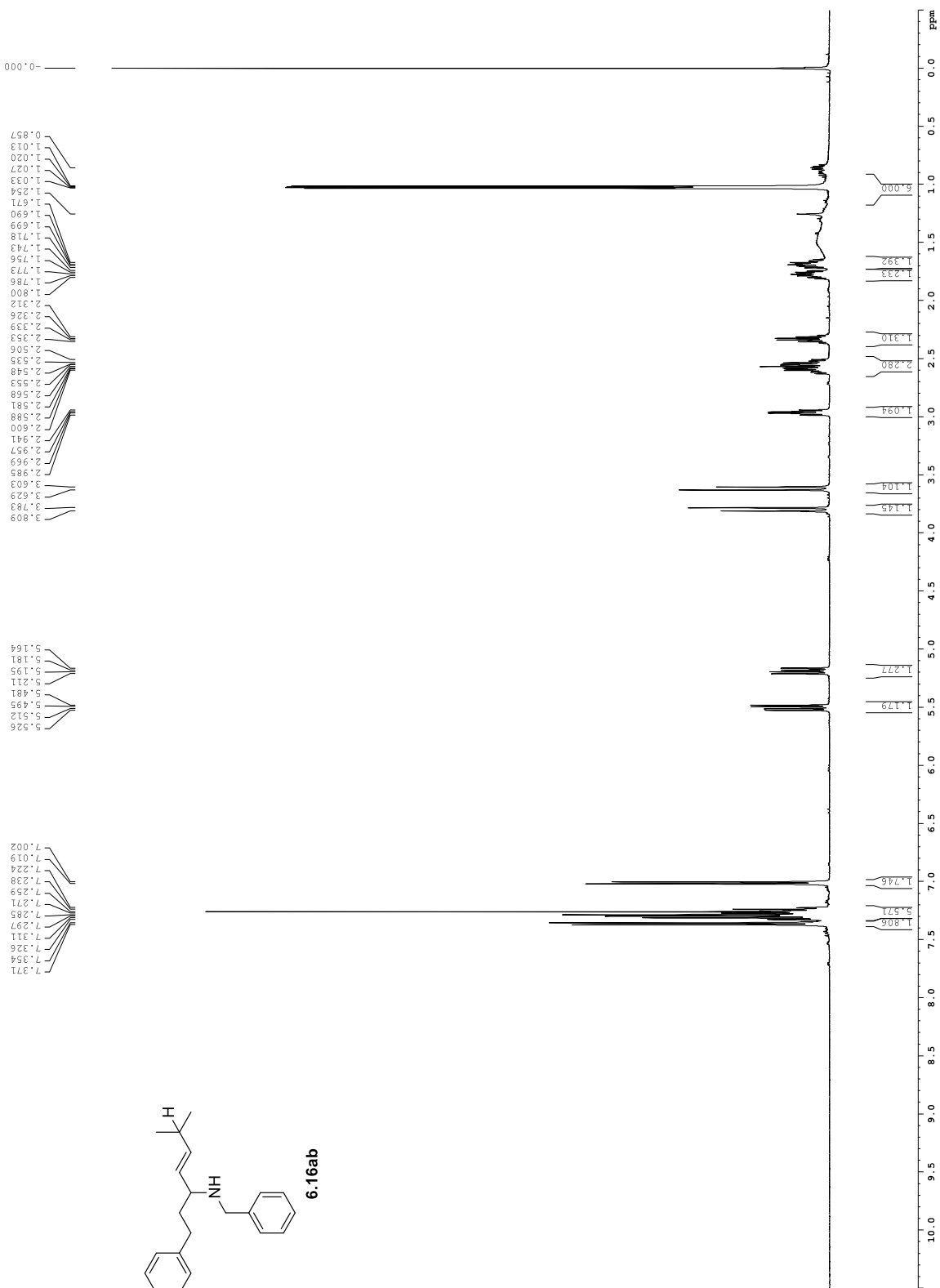
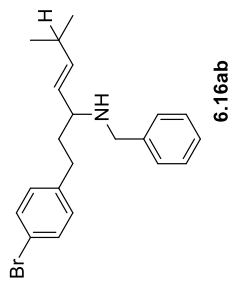


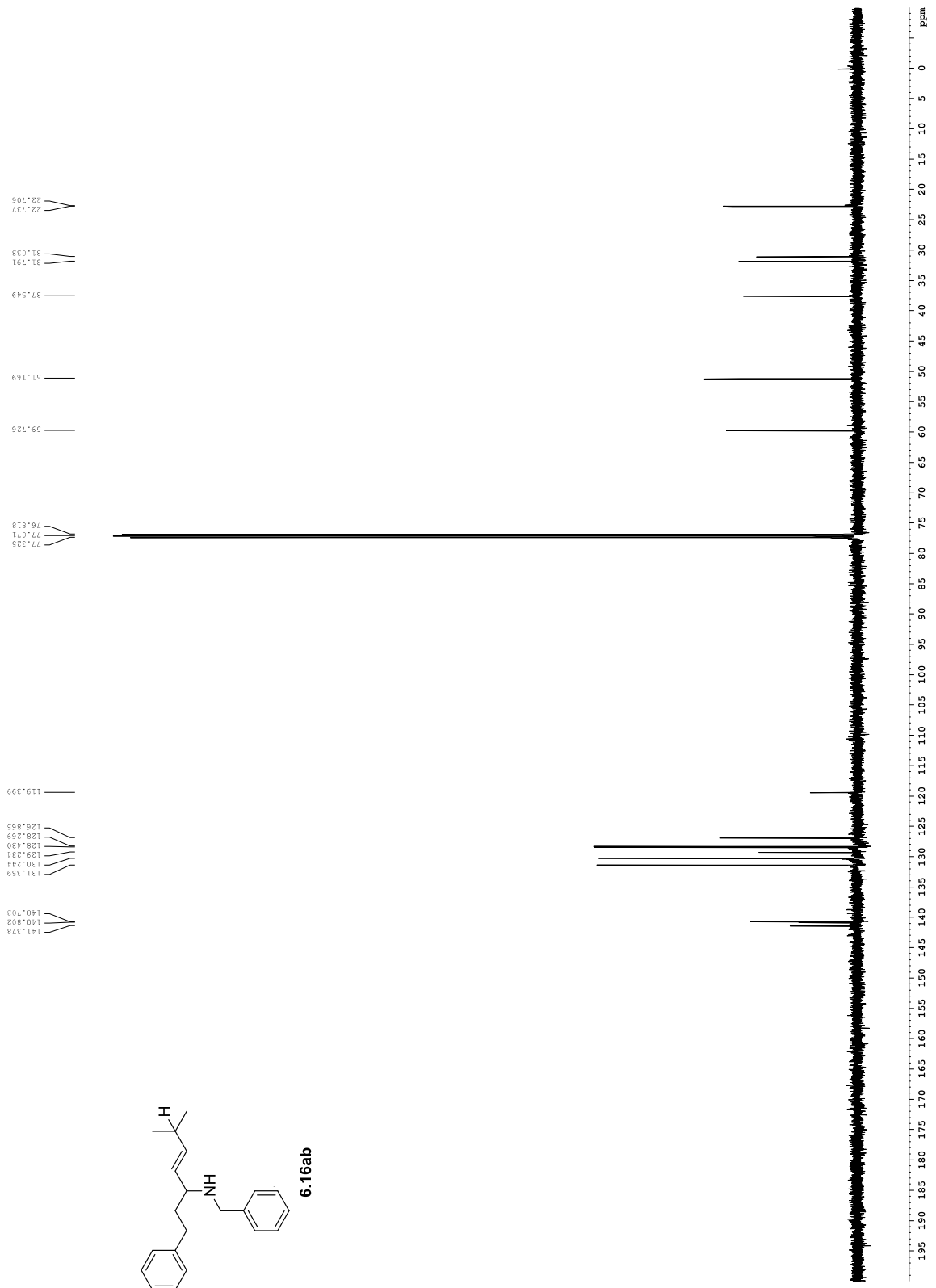
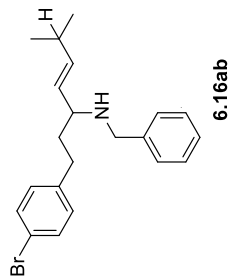


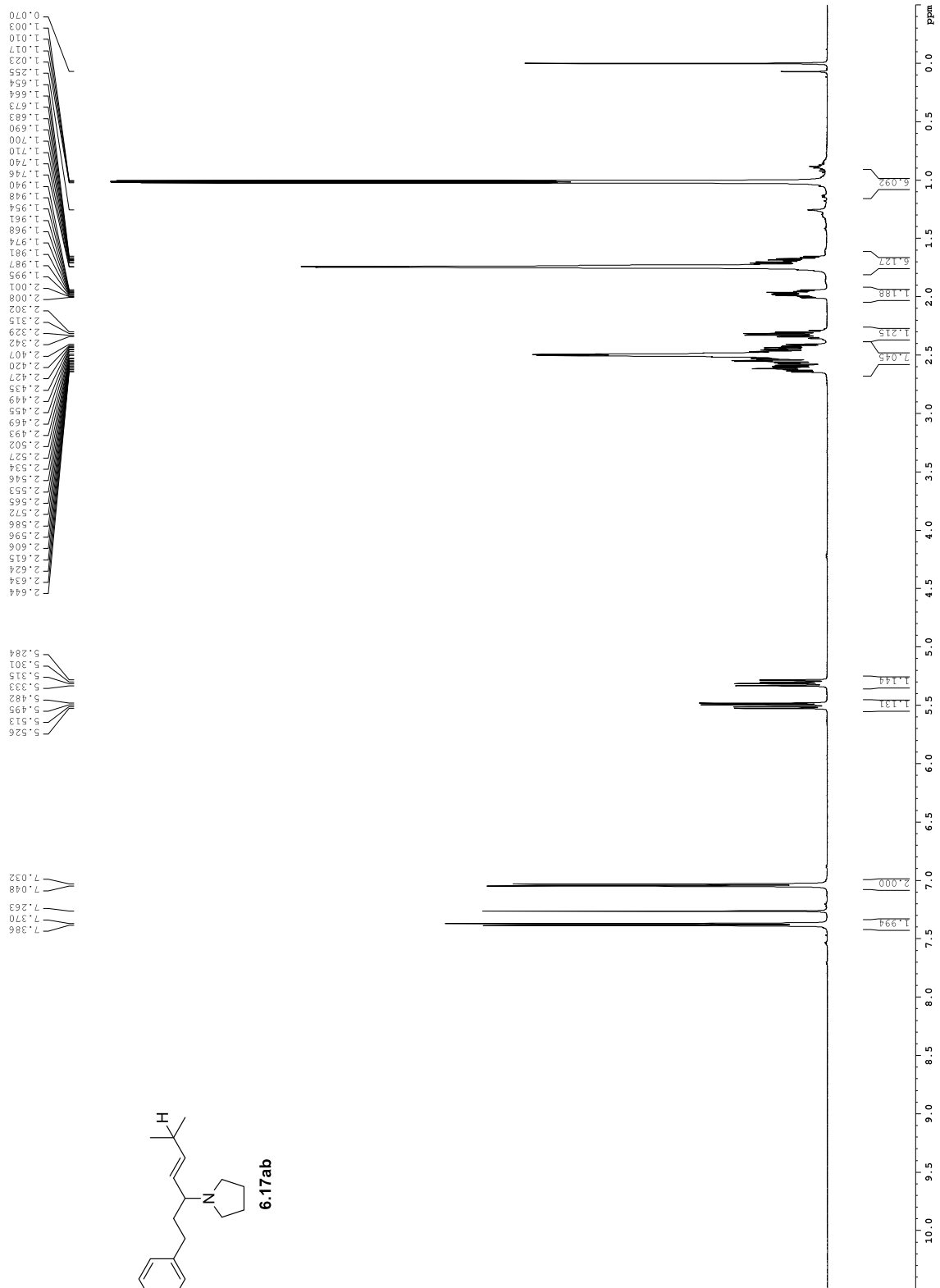


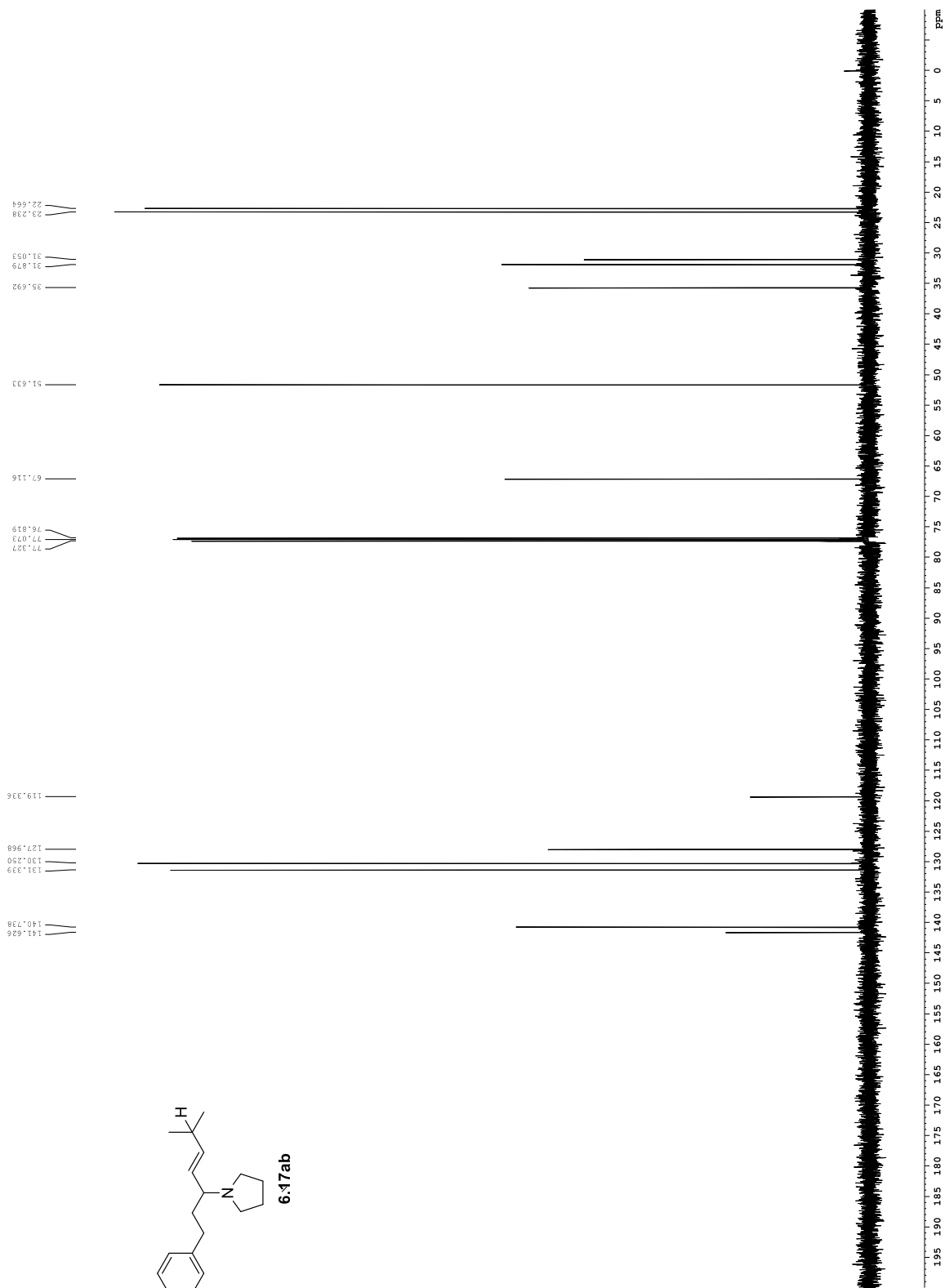
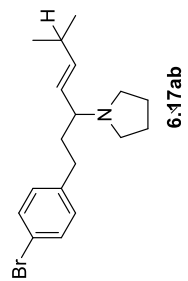


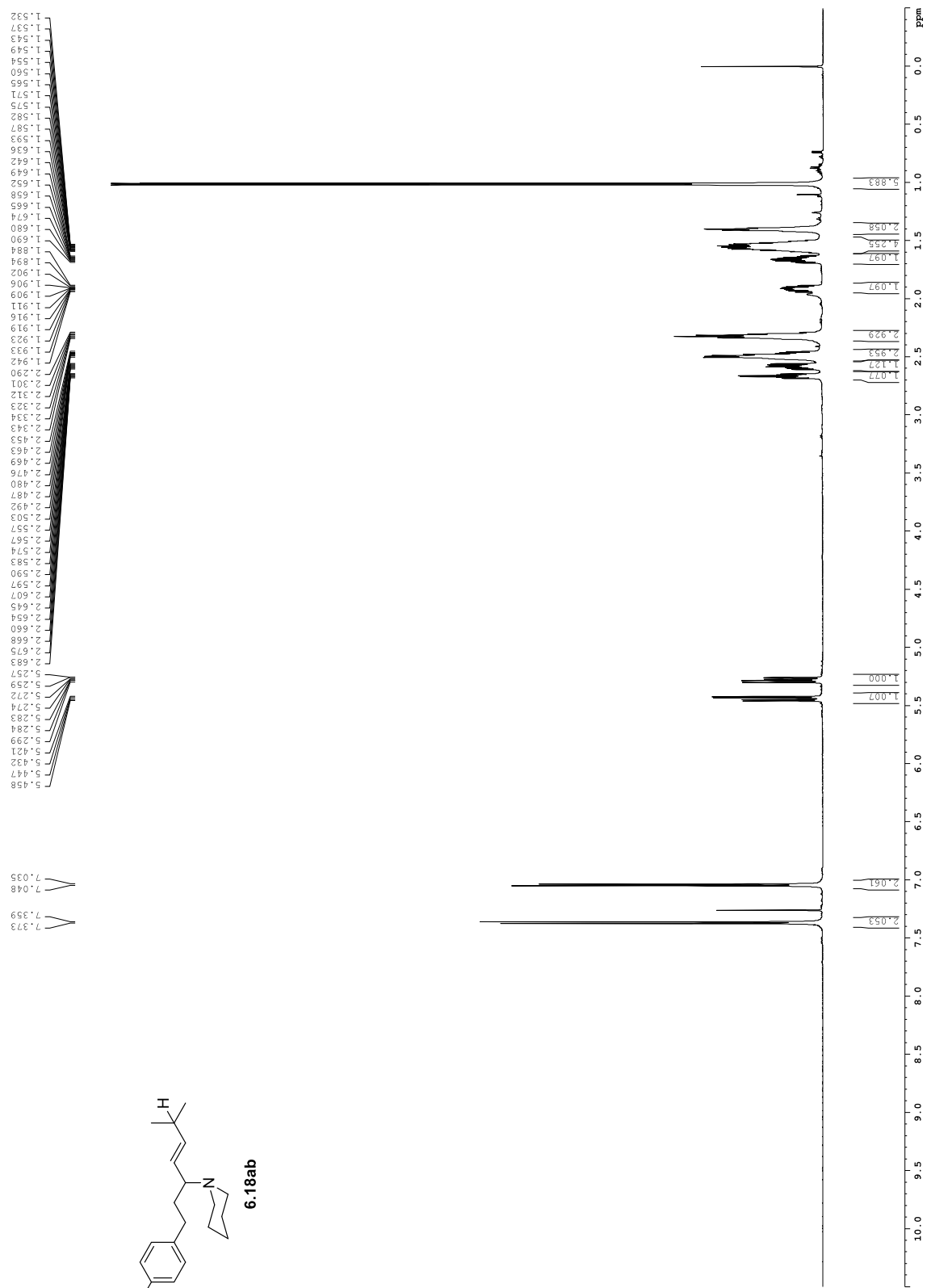
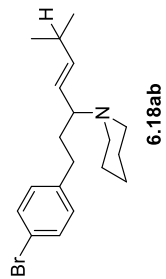


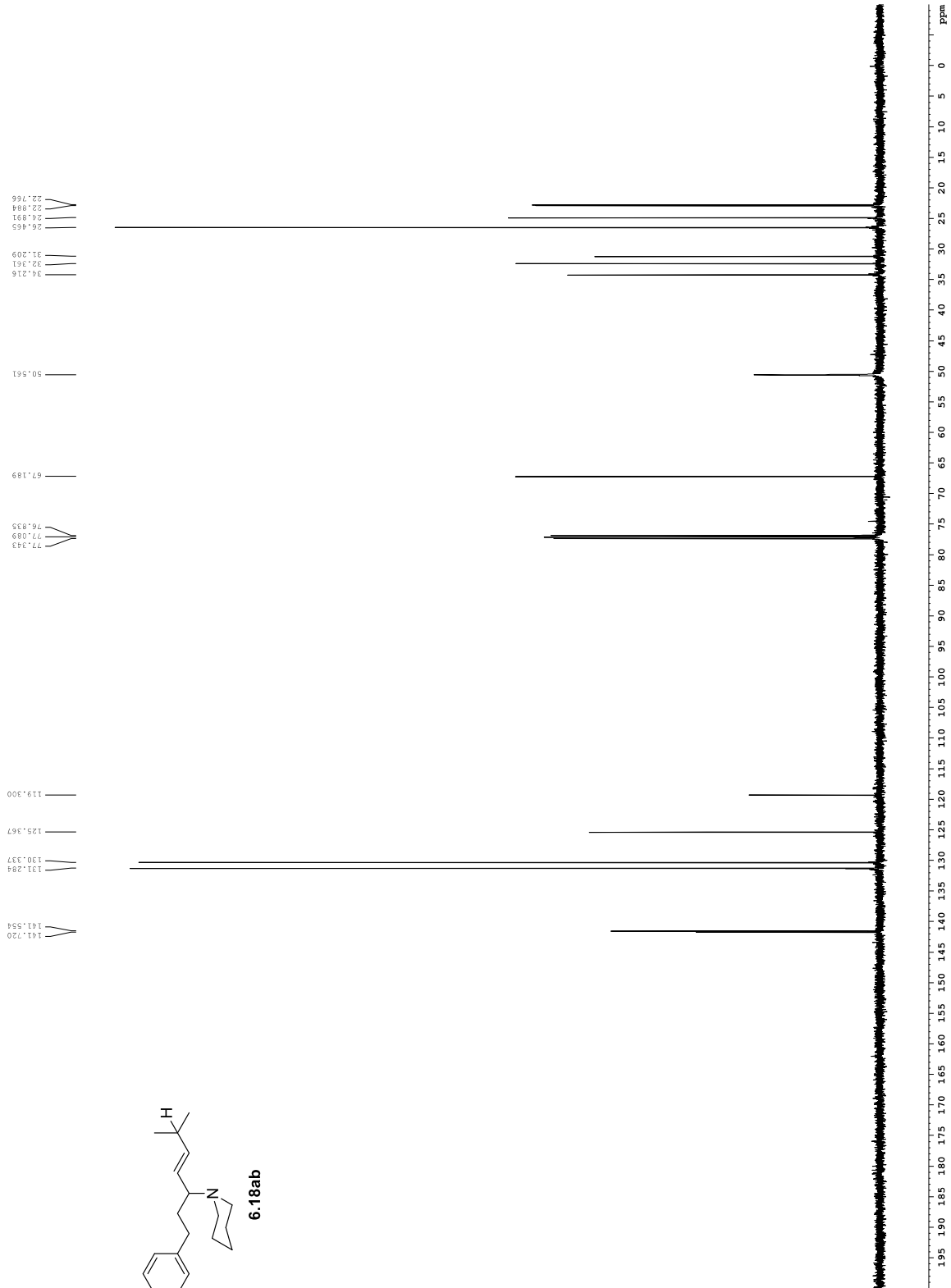
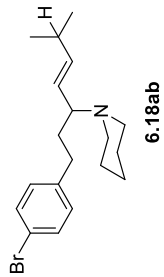


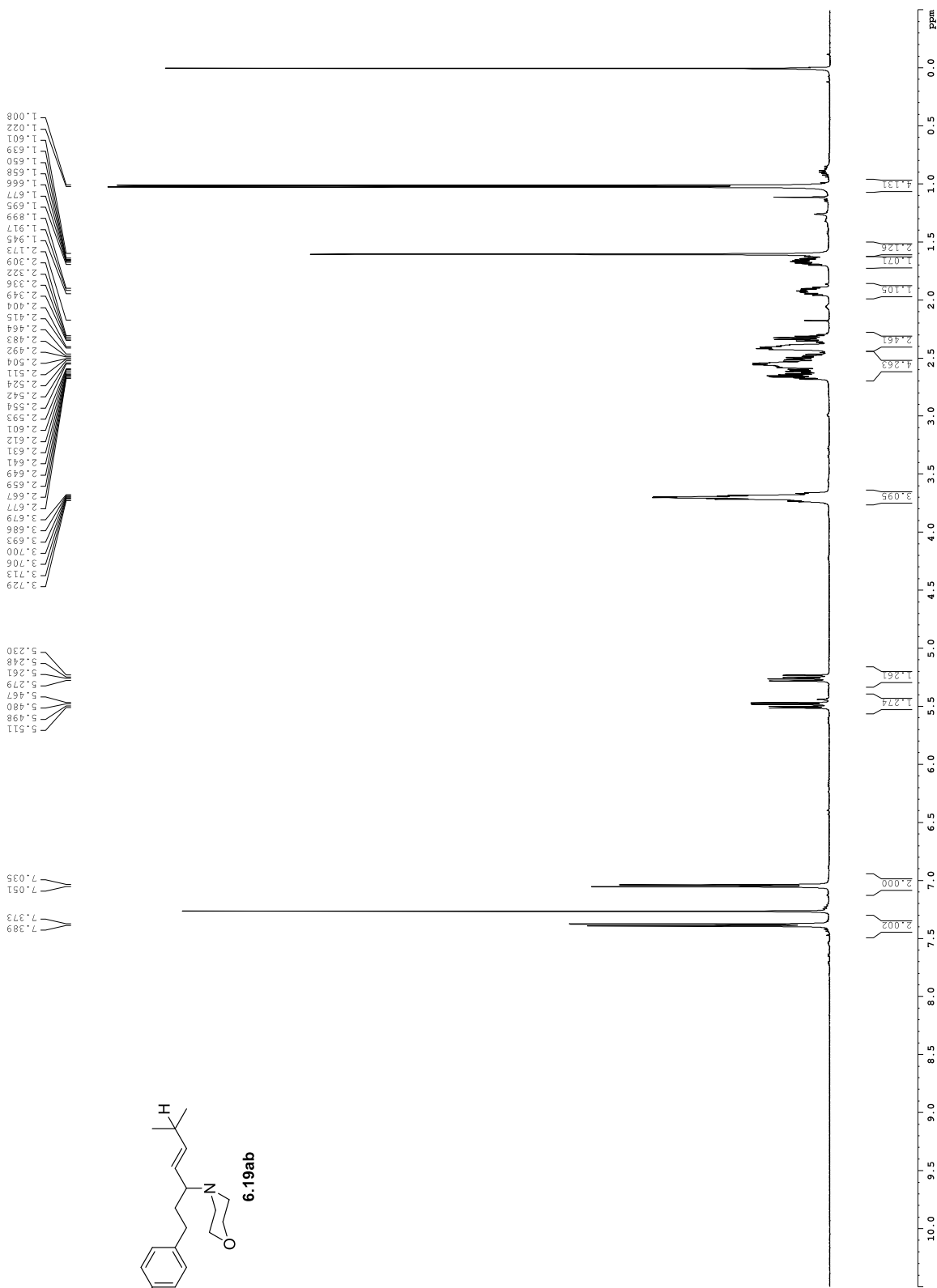
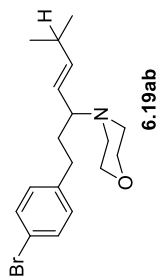


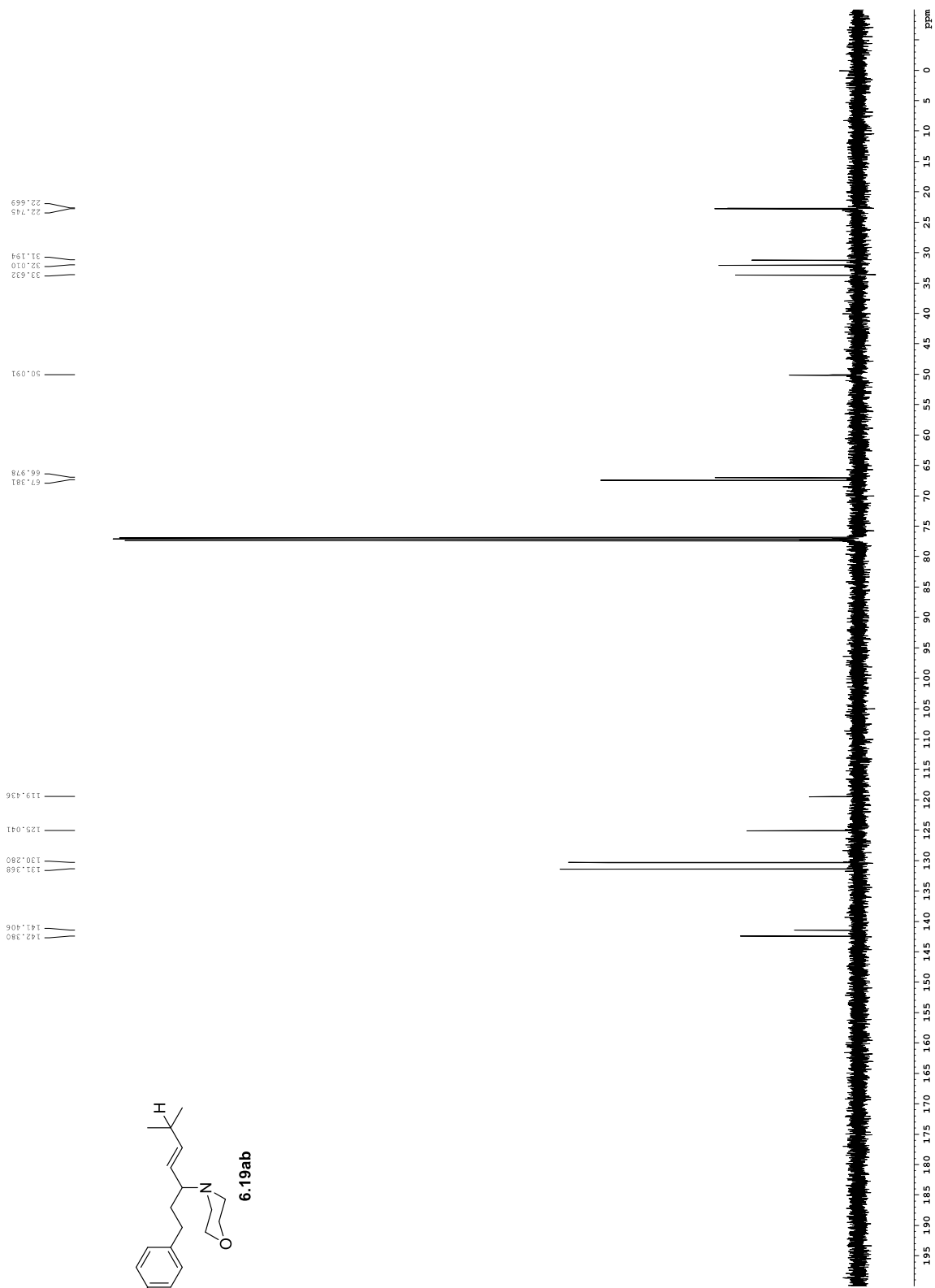
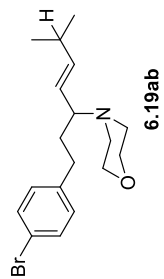


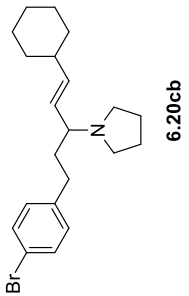
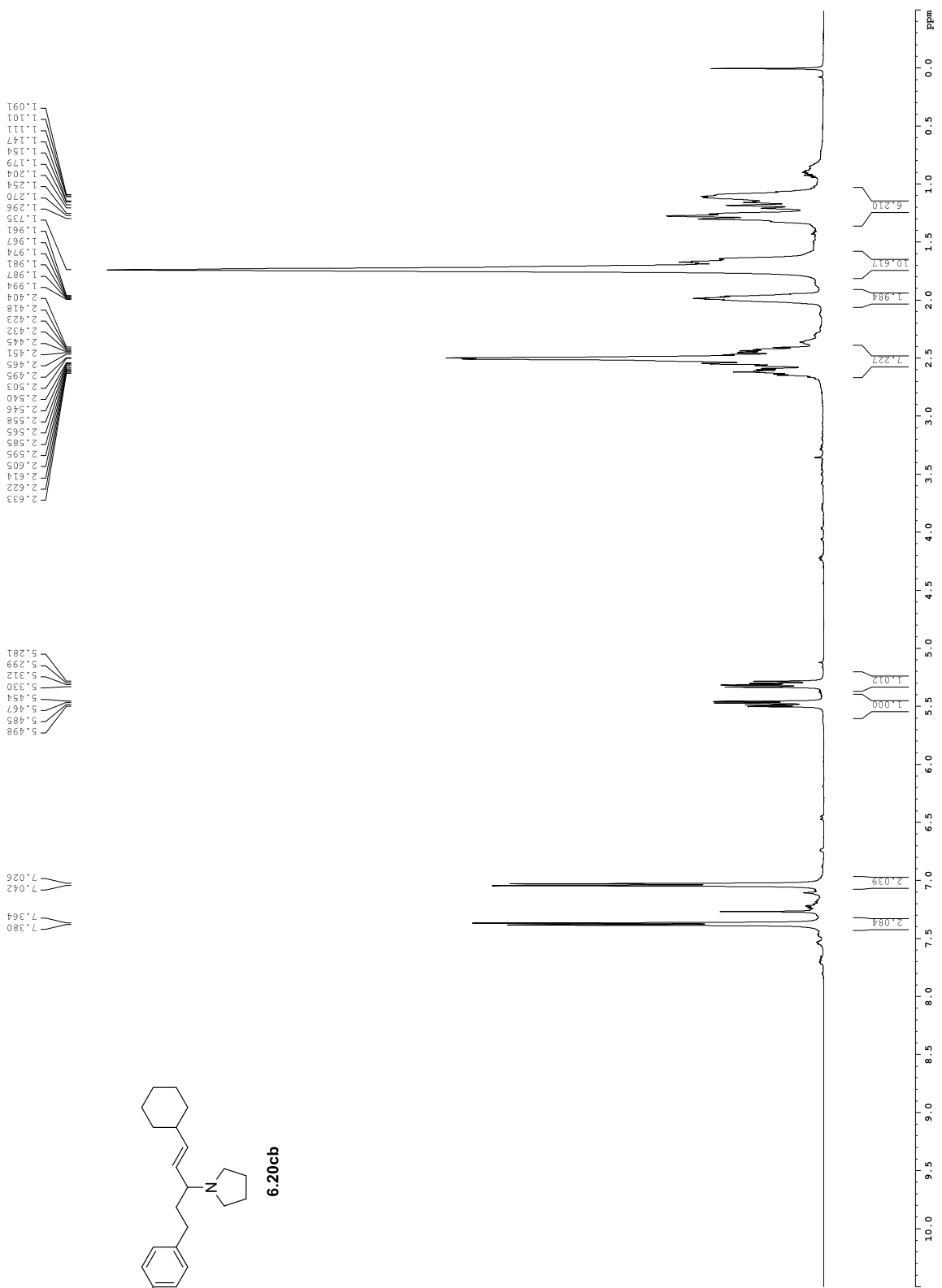


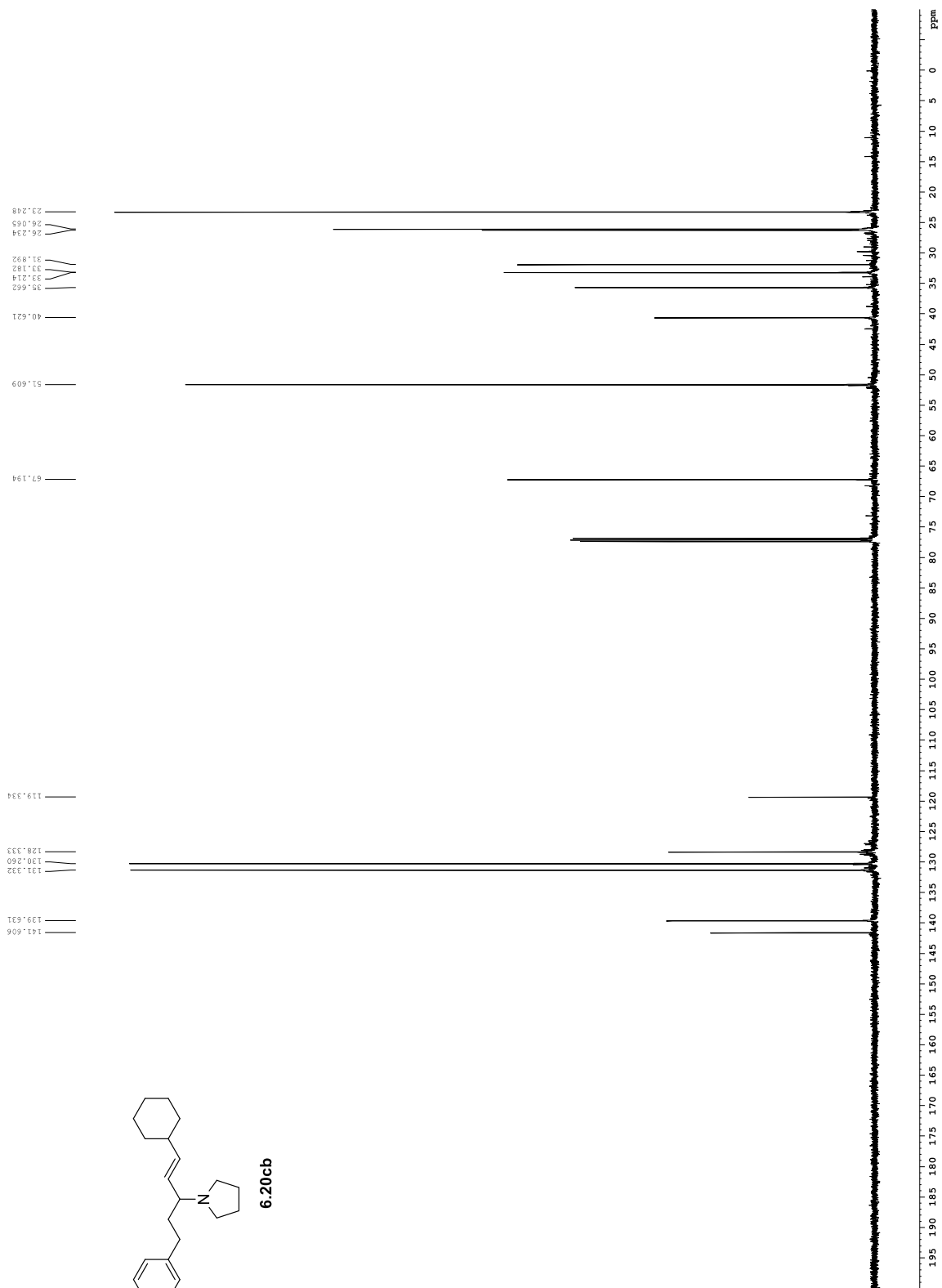
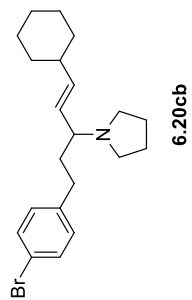


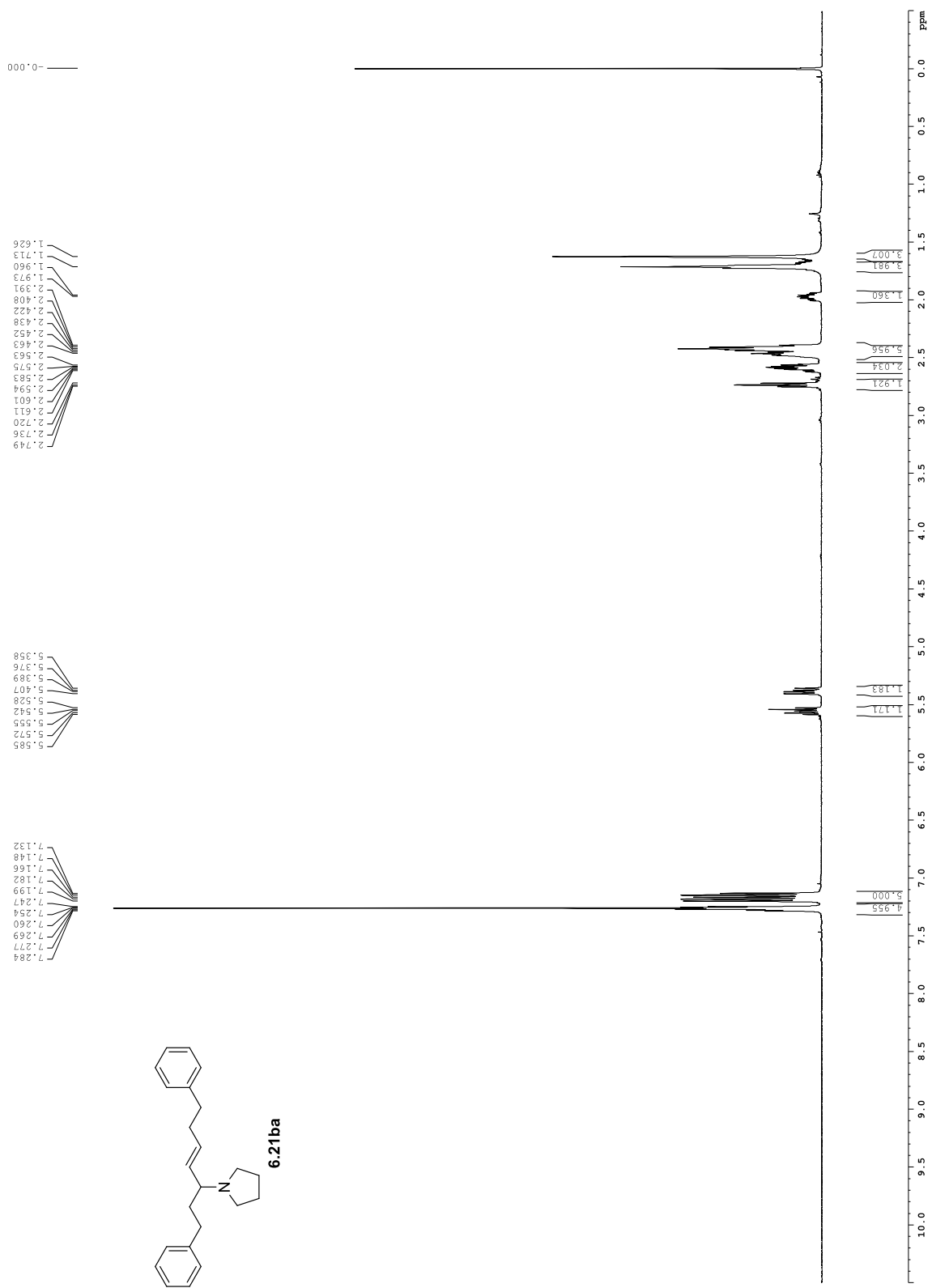


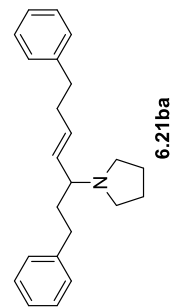
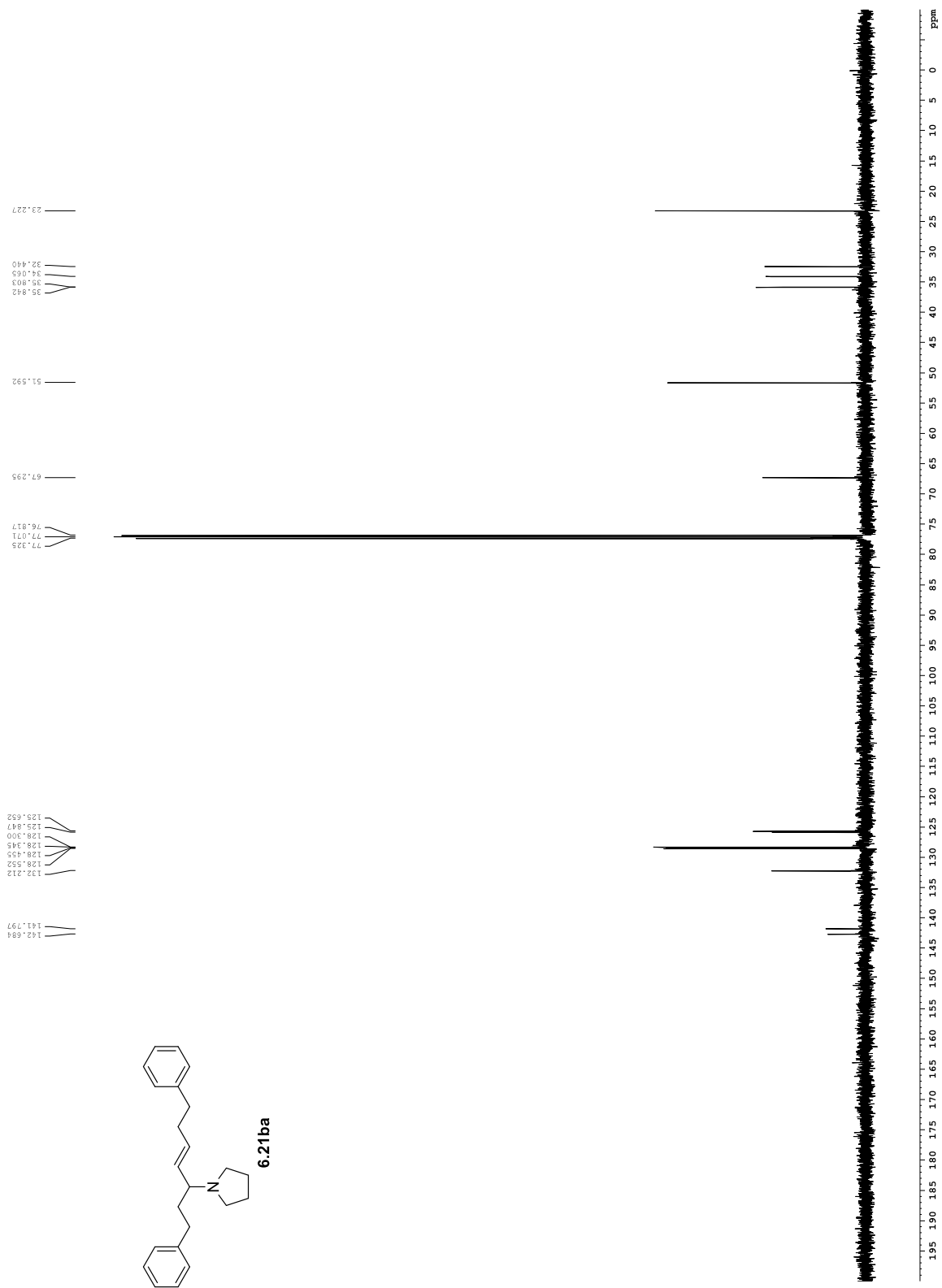


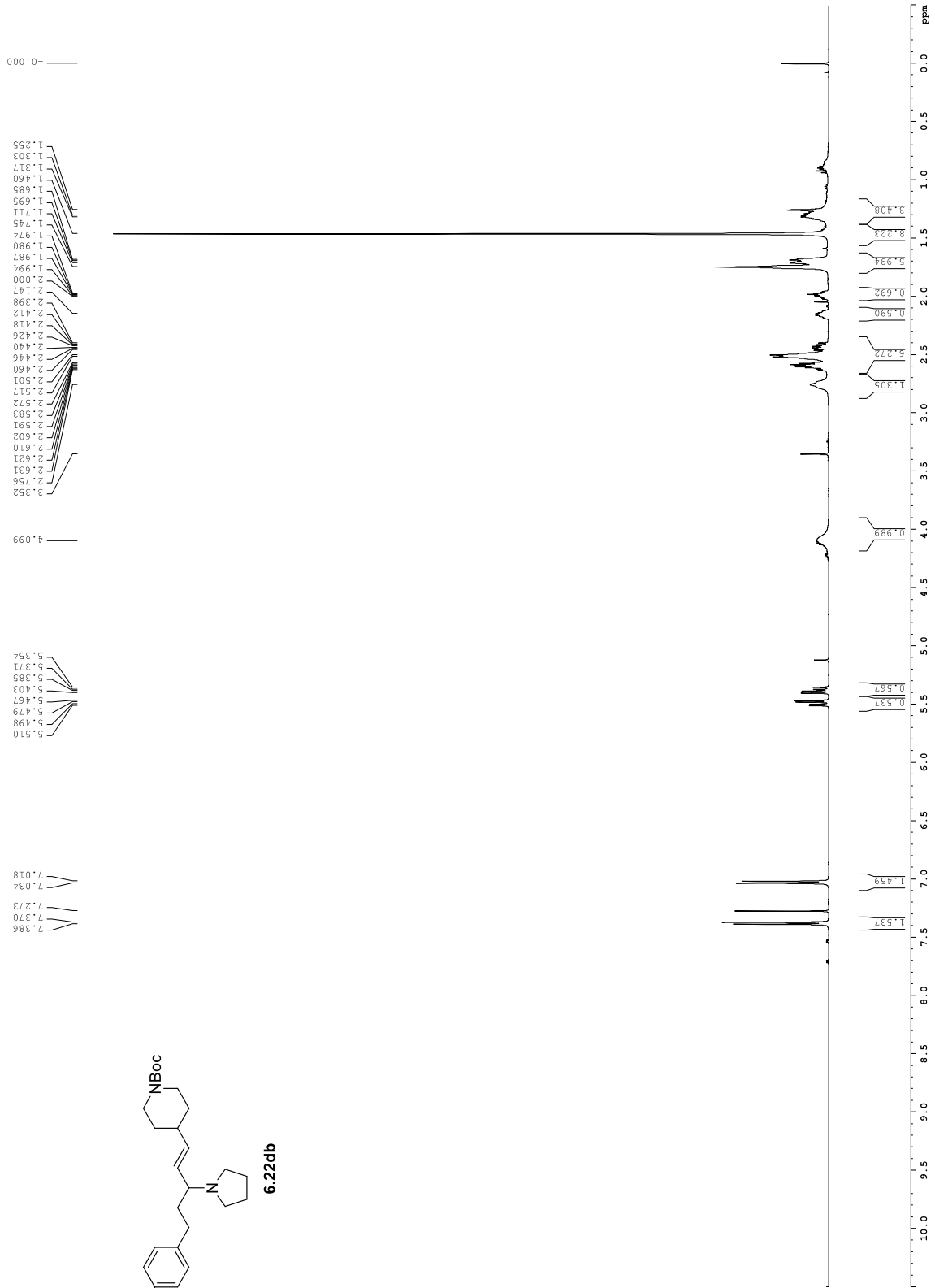
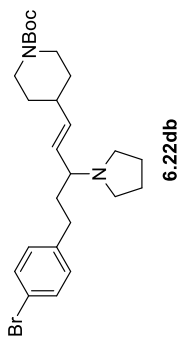


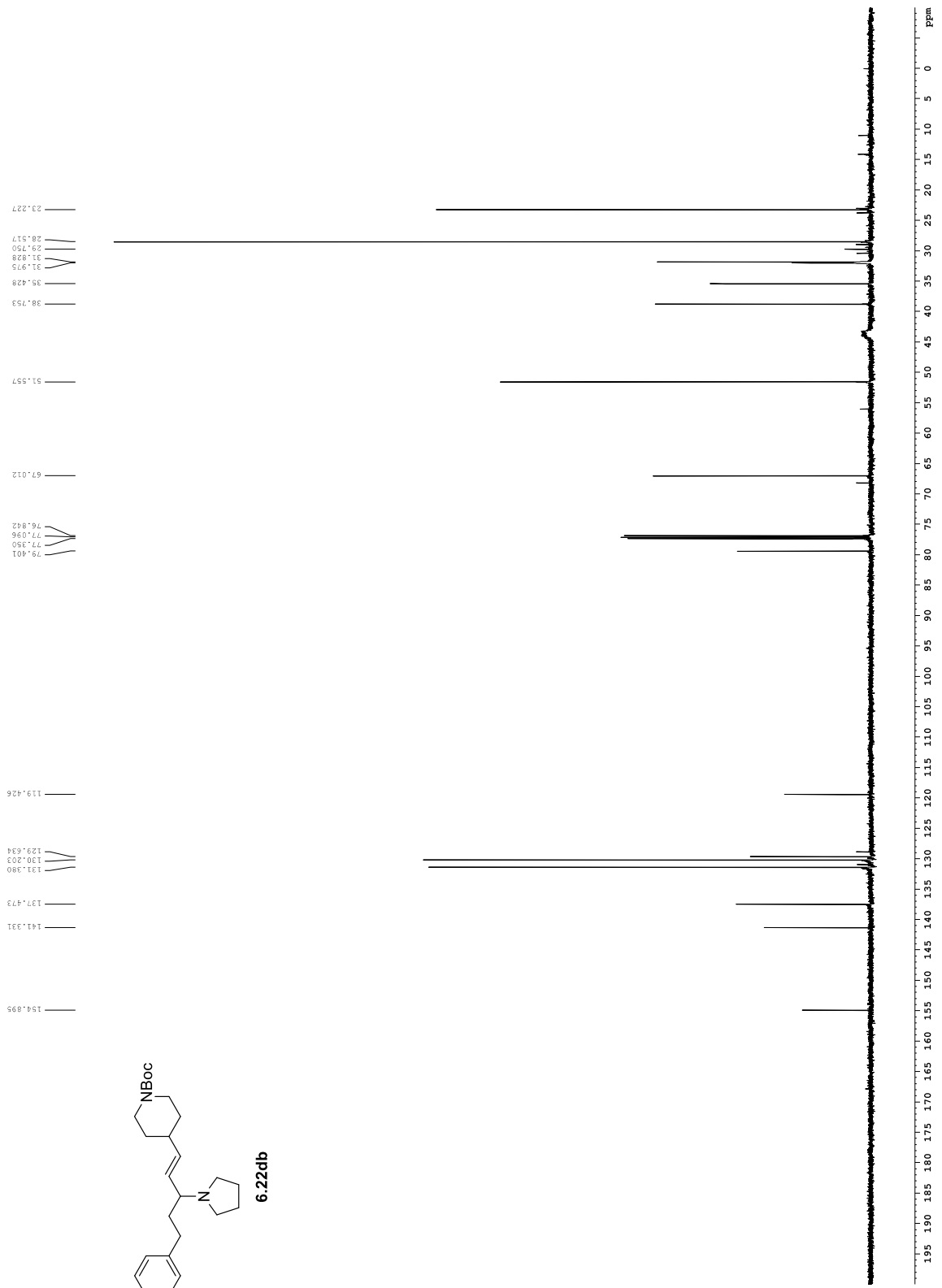
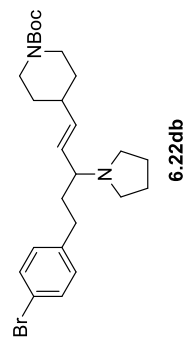




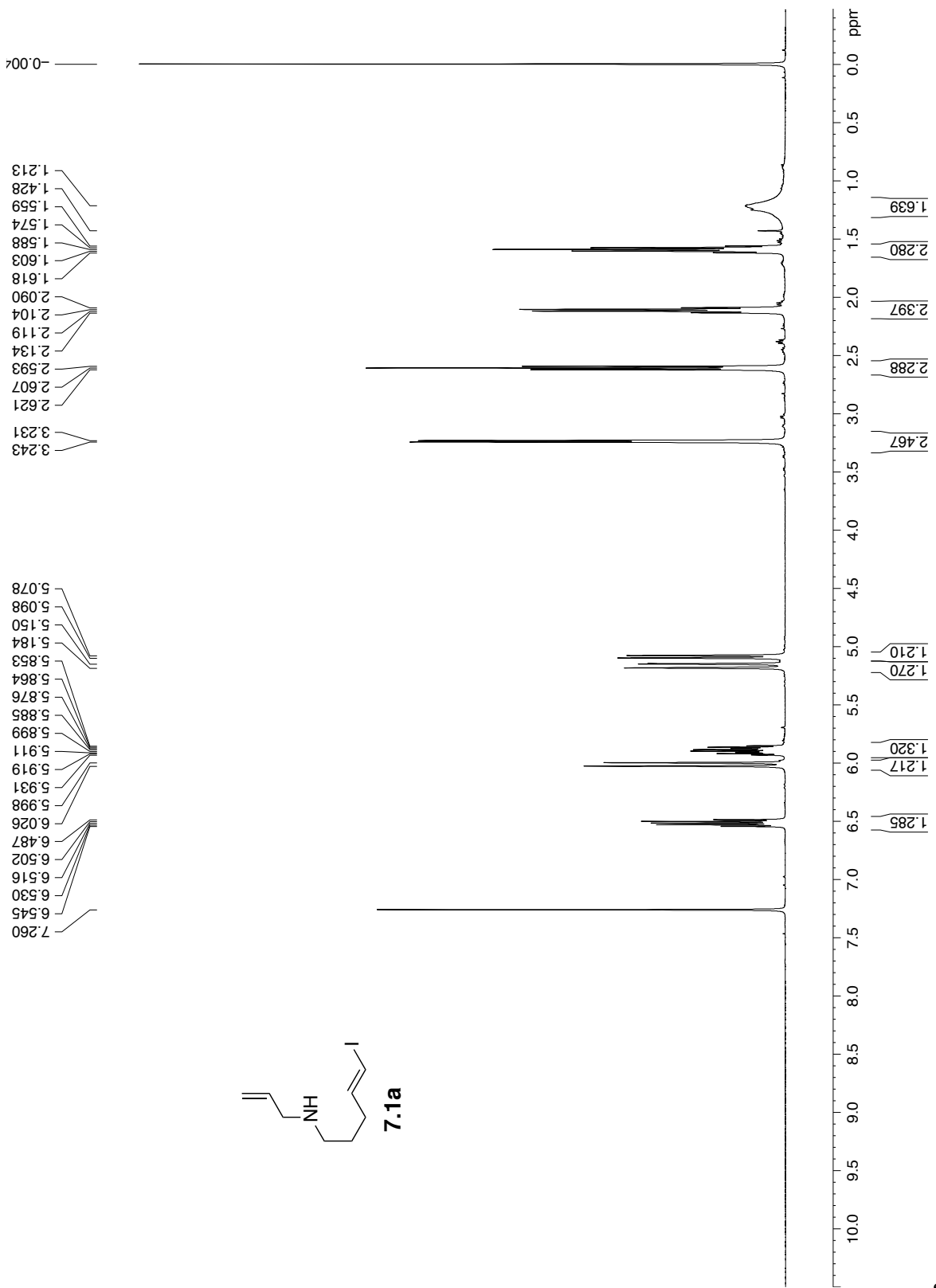


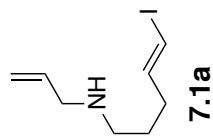
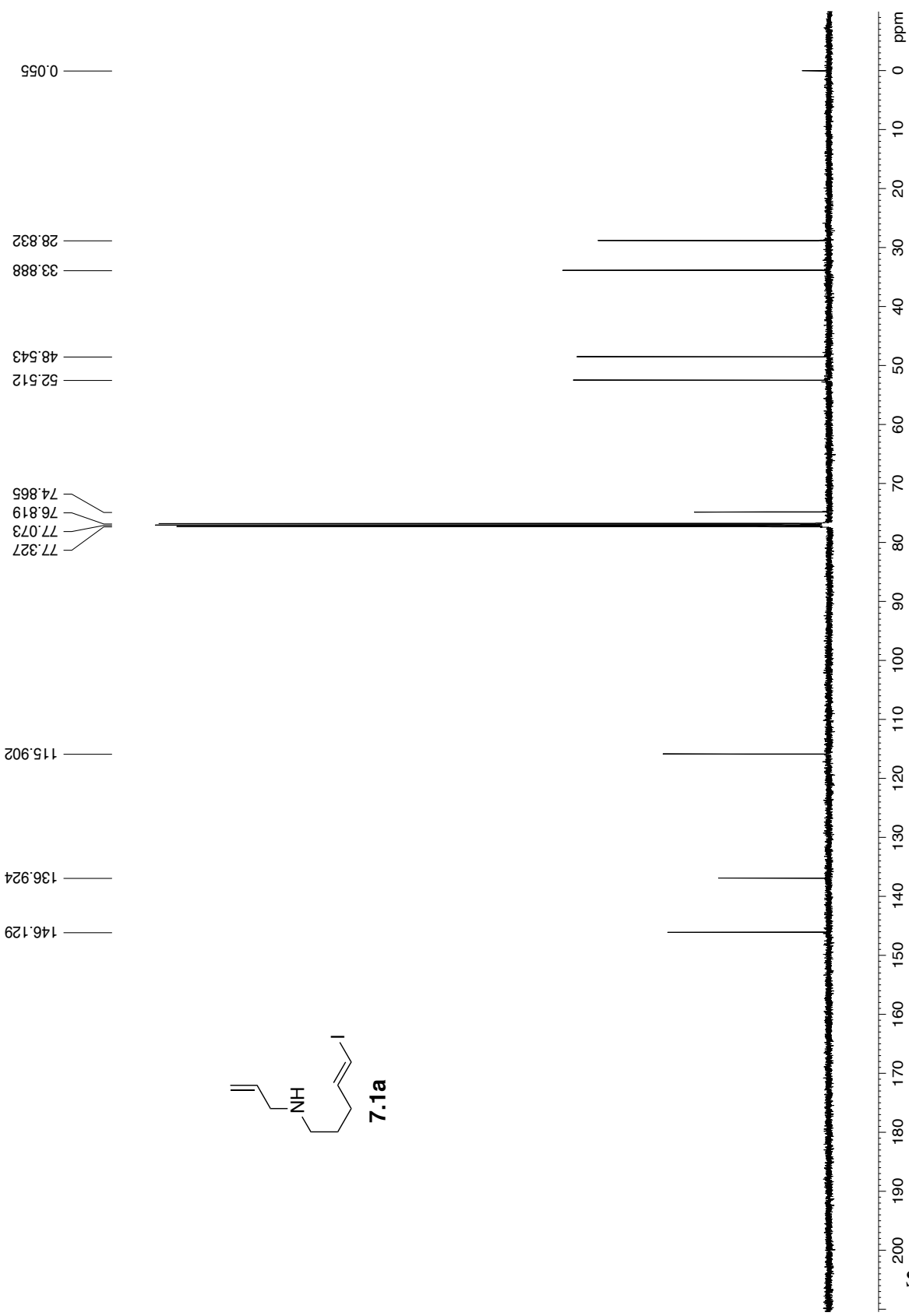




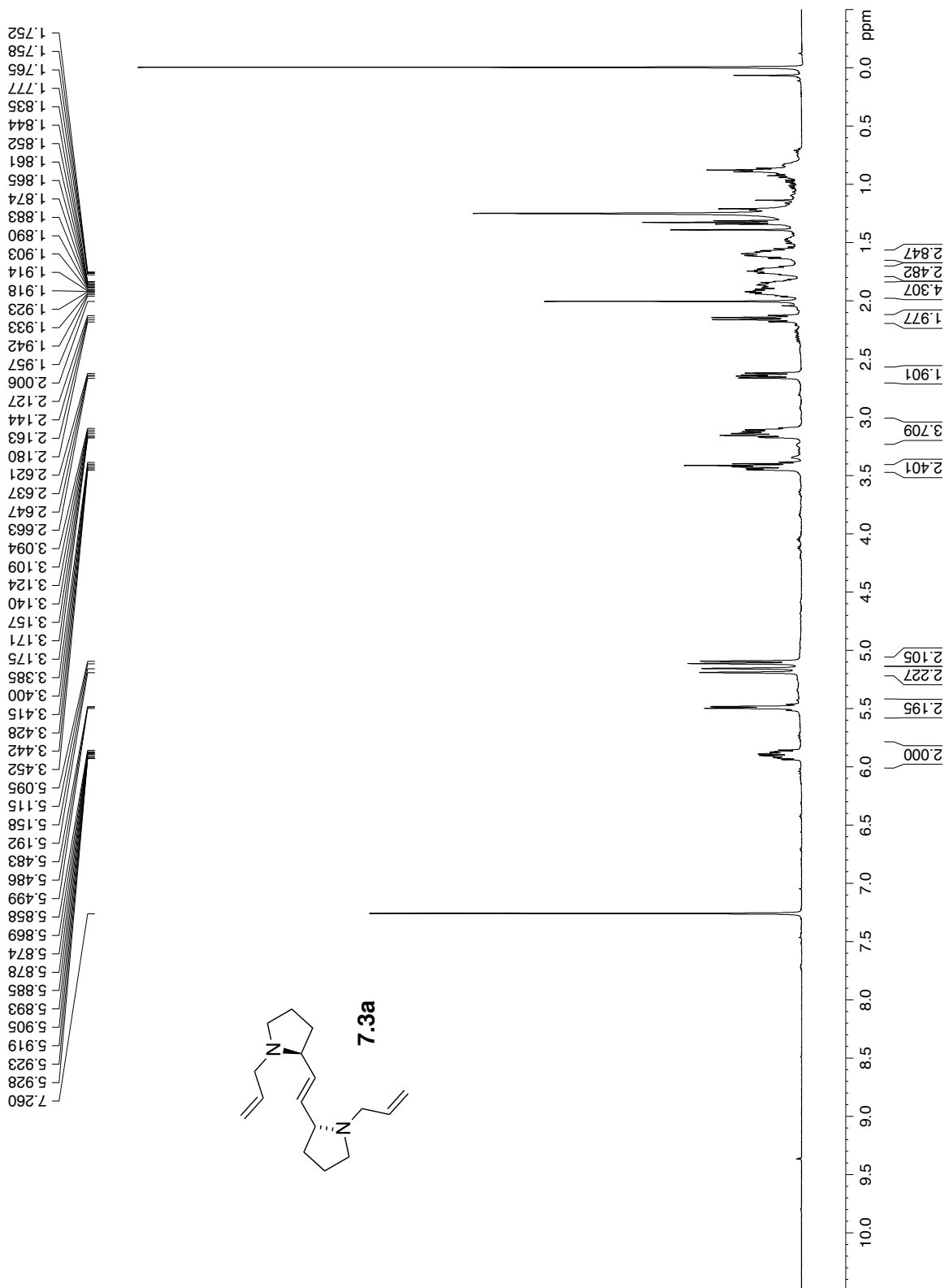


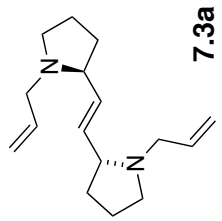
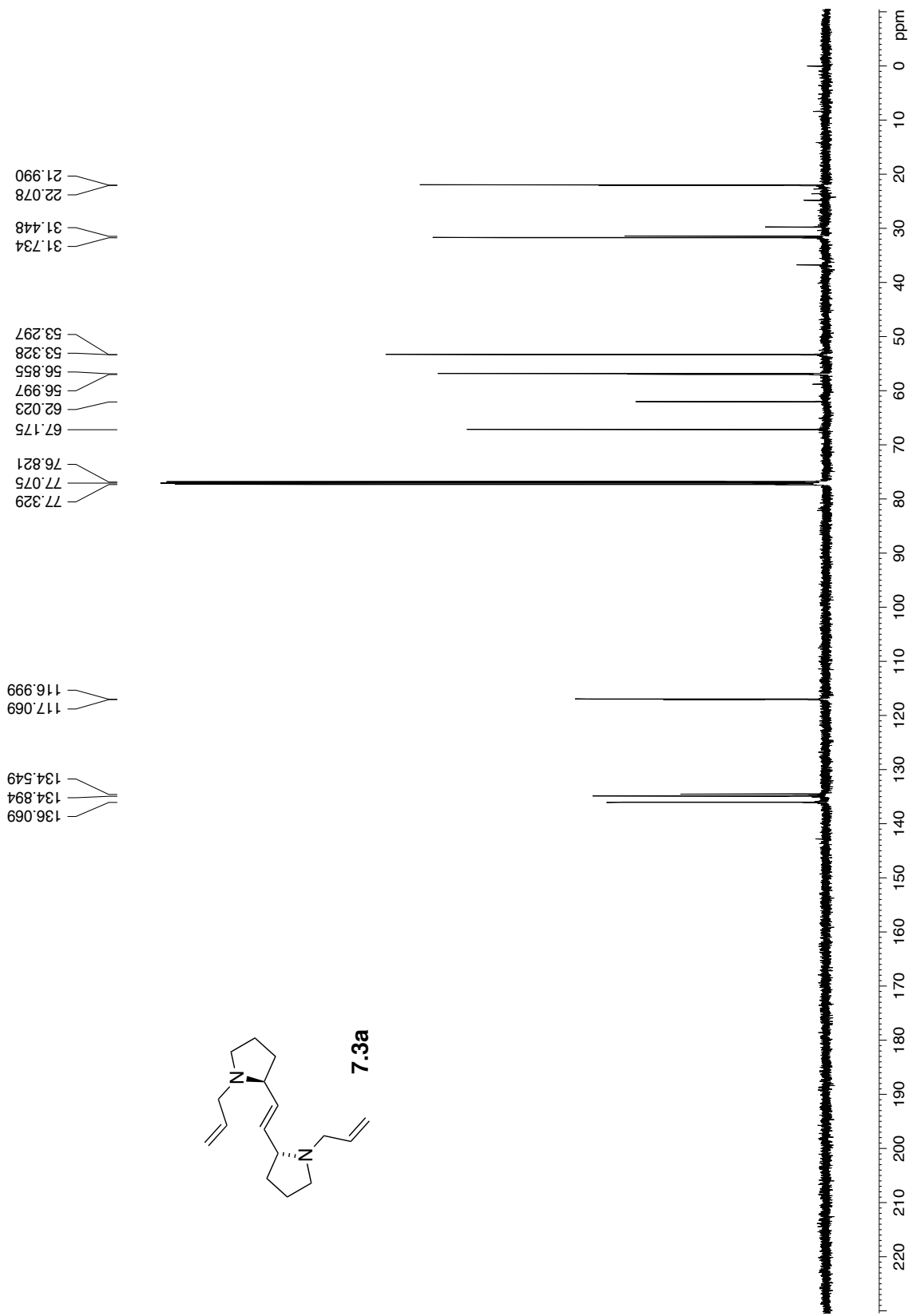
Appendix E: Chapter 7 – NMR Spectra

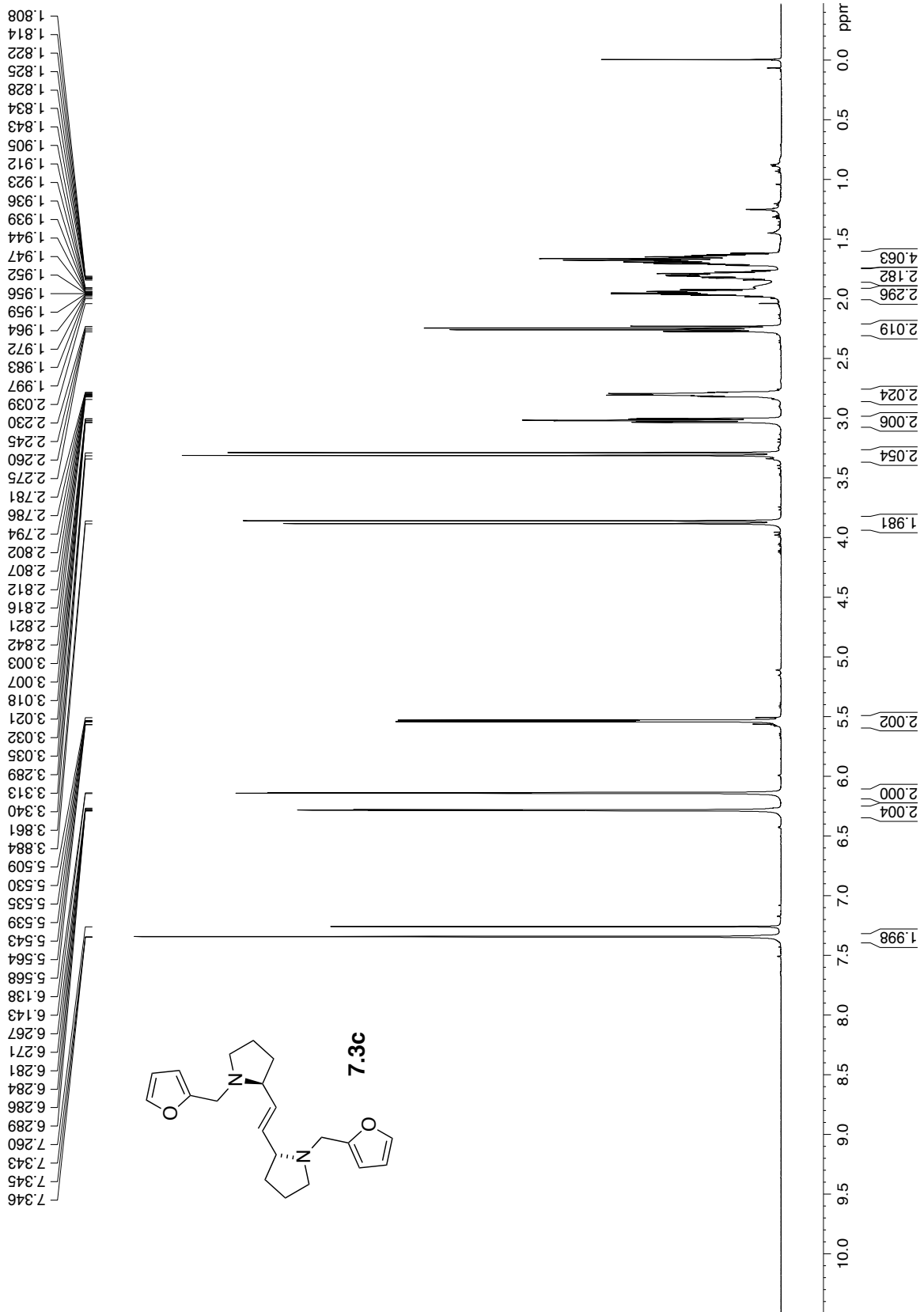




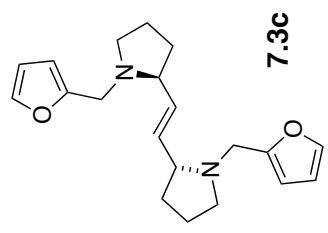
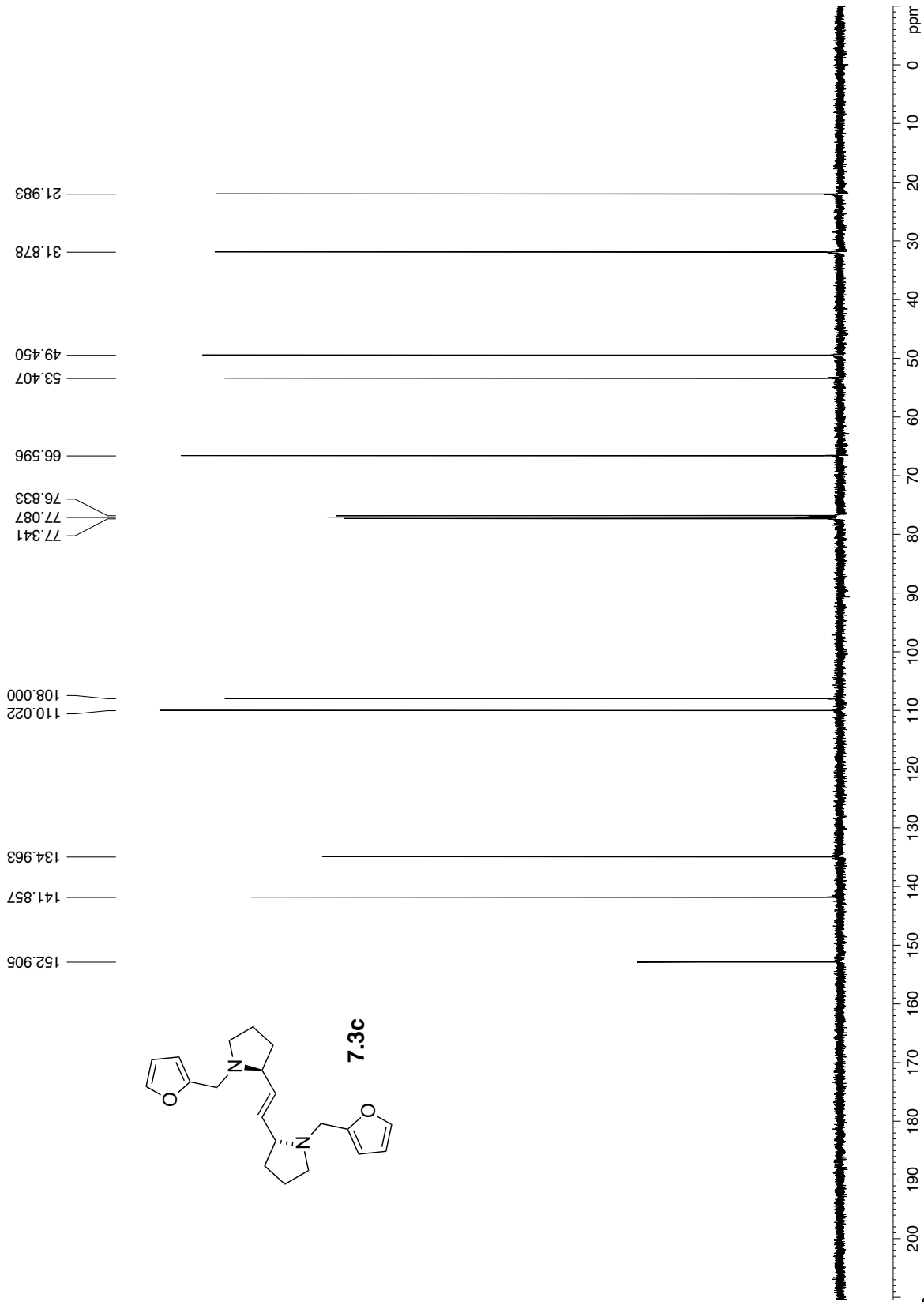
S11

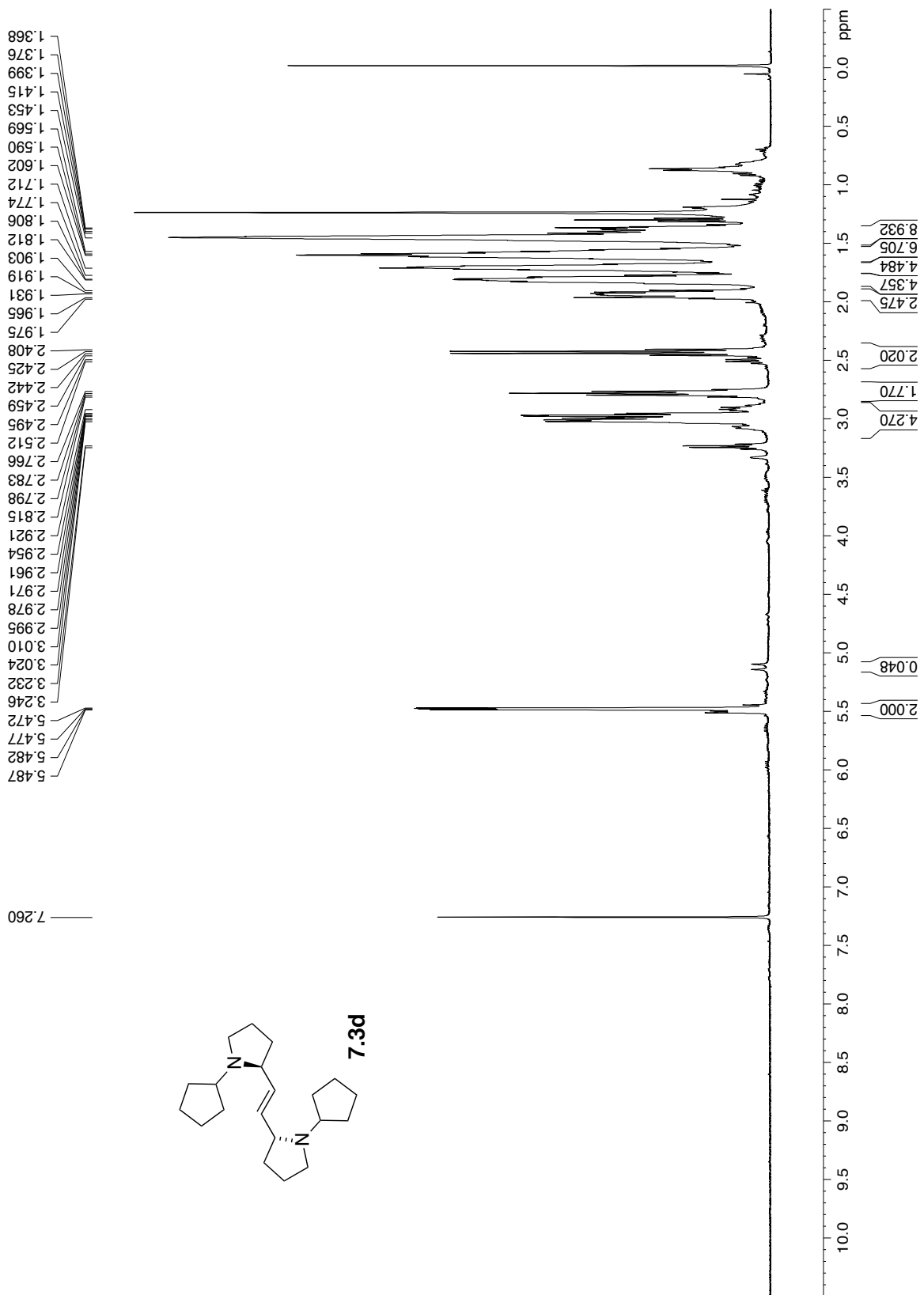




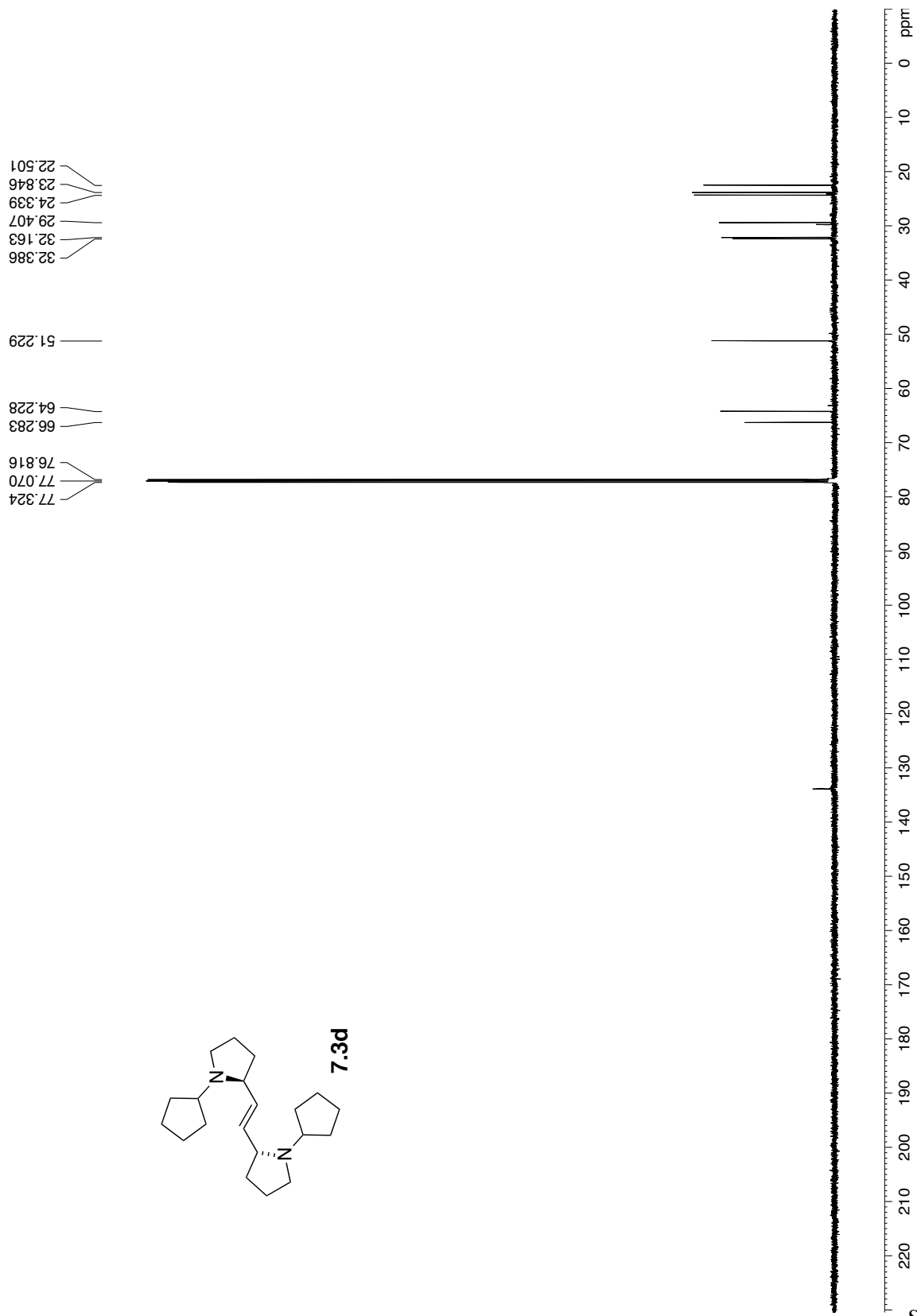
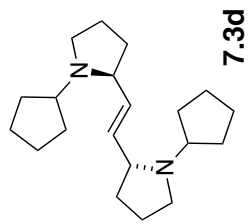


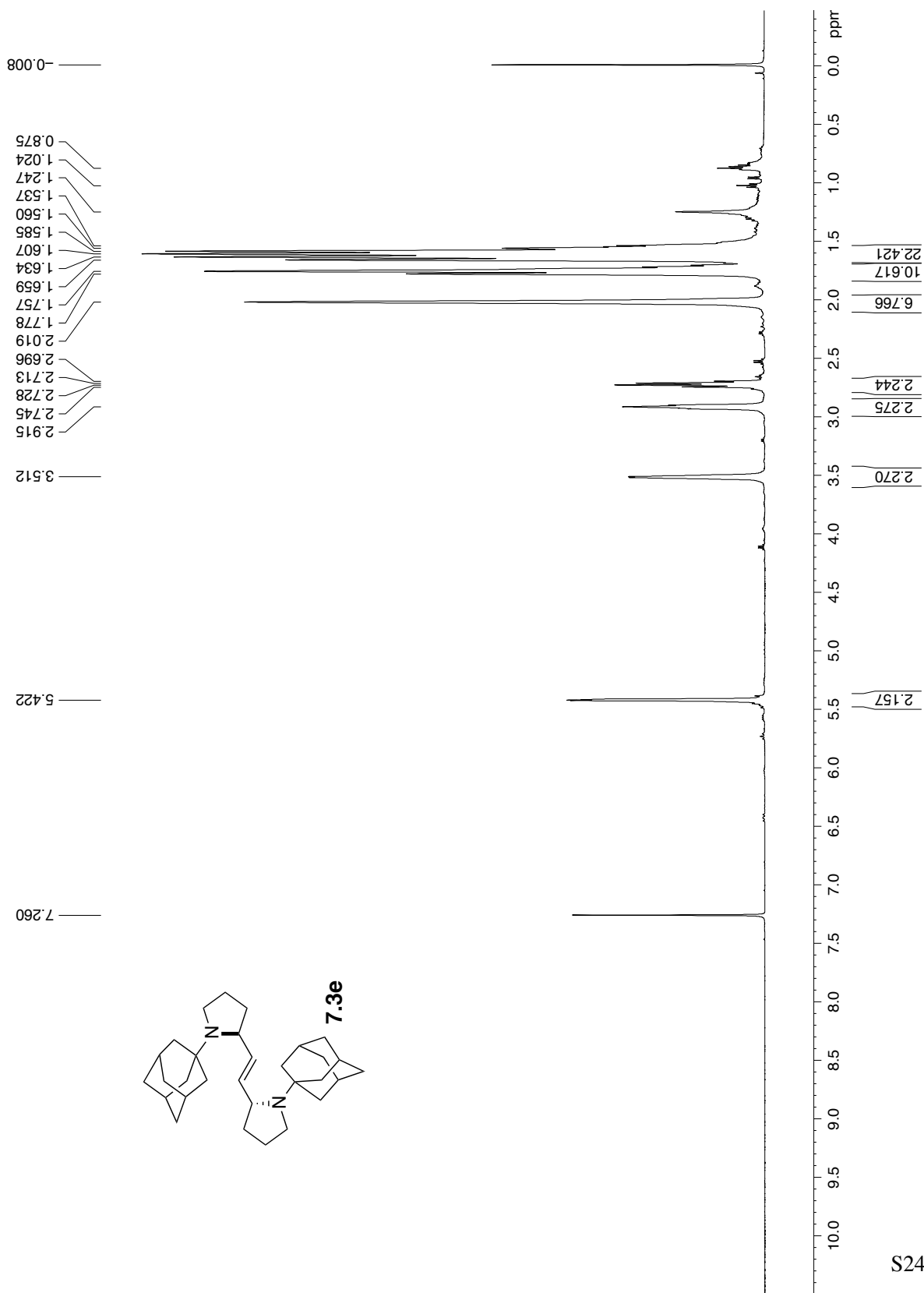
S20

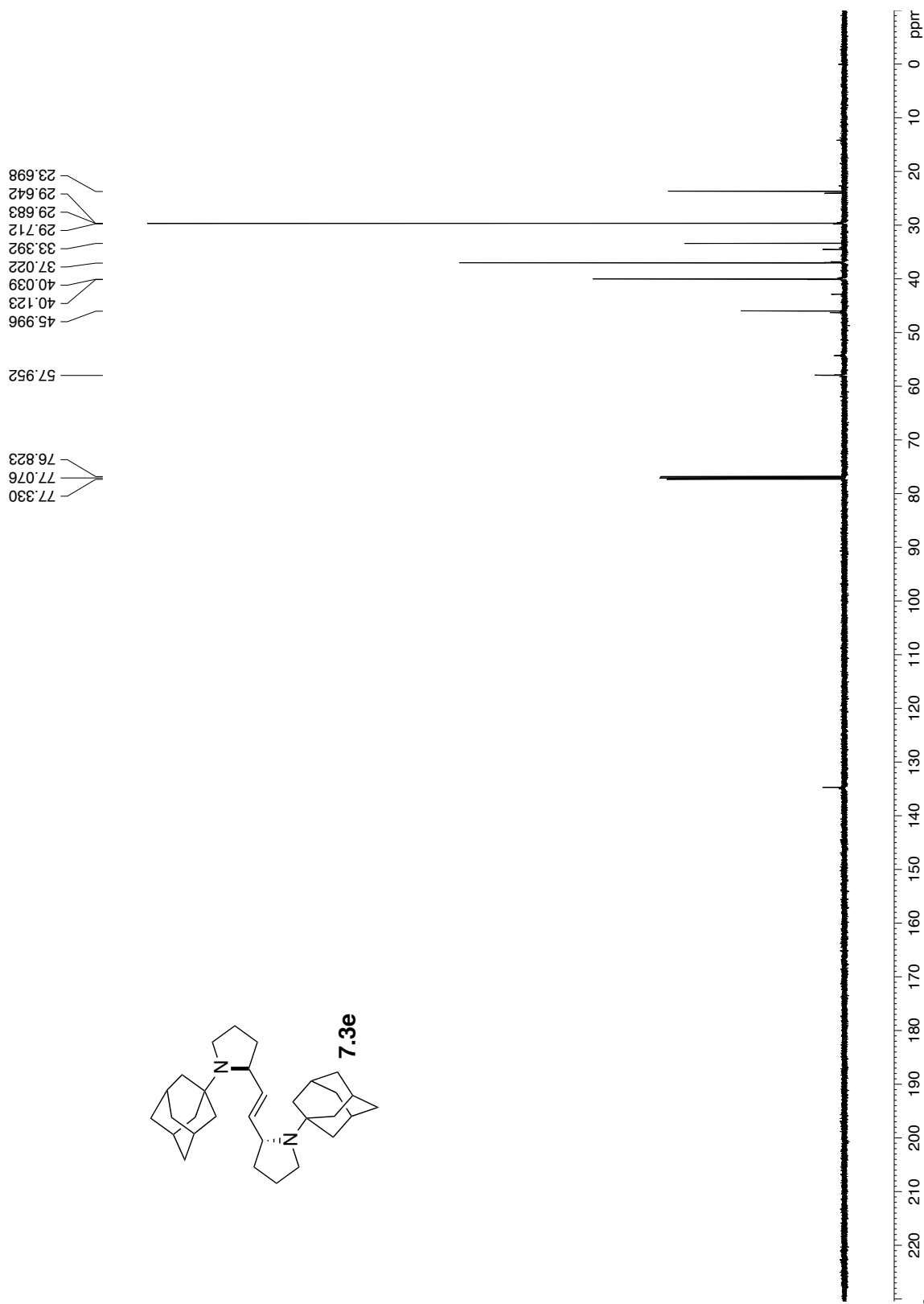
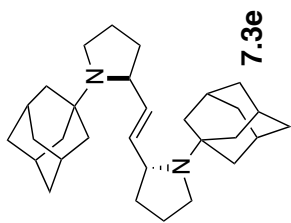




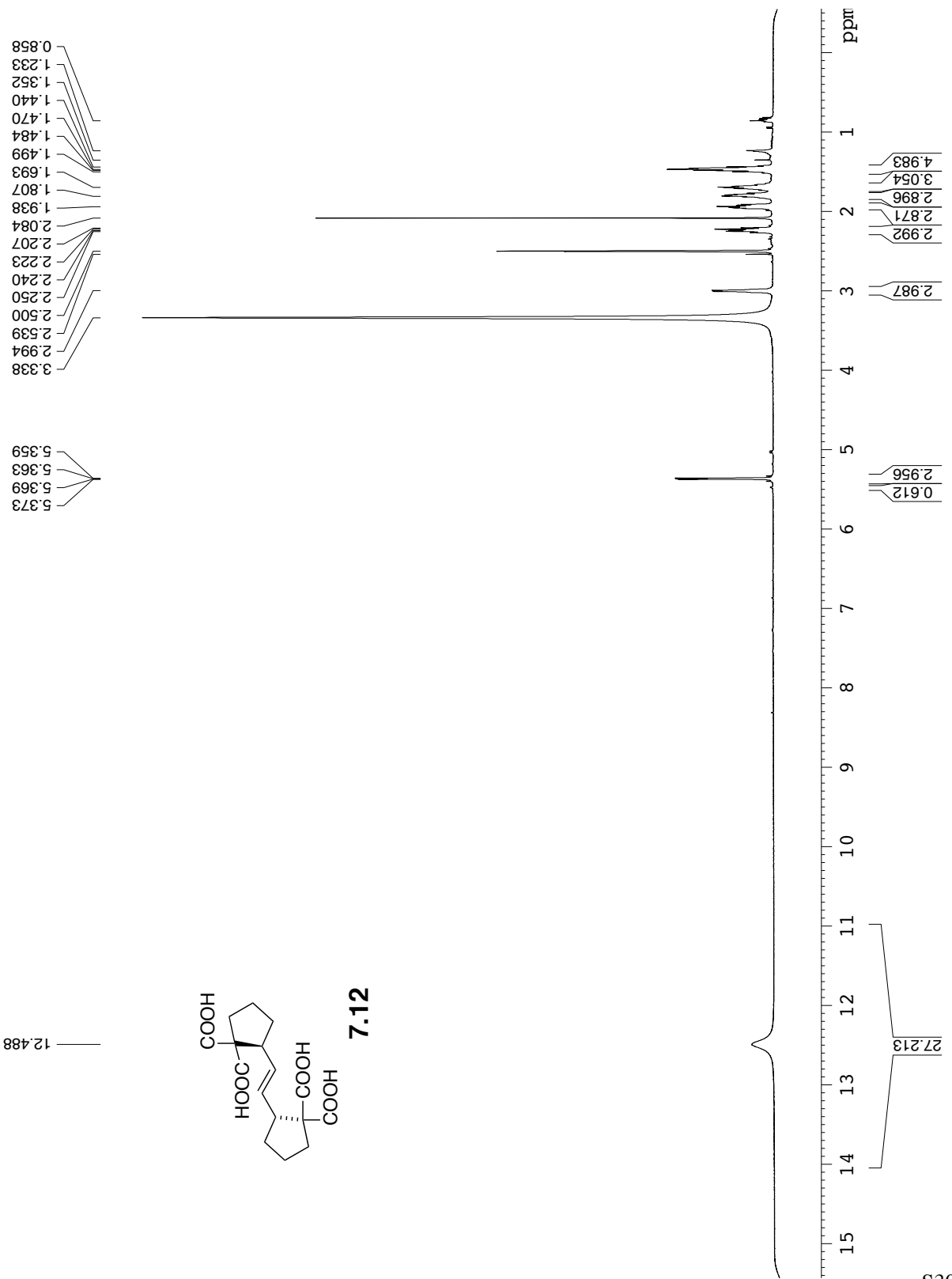
S22



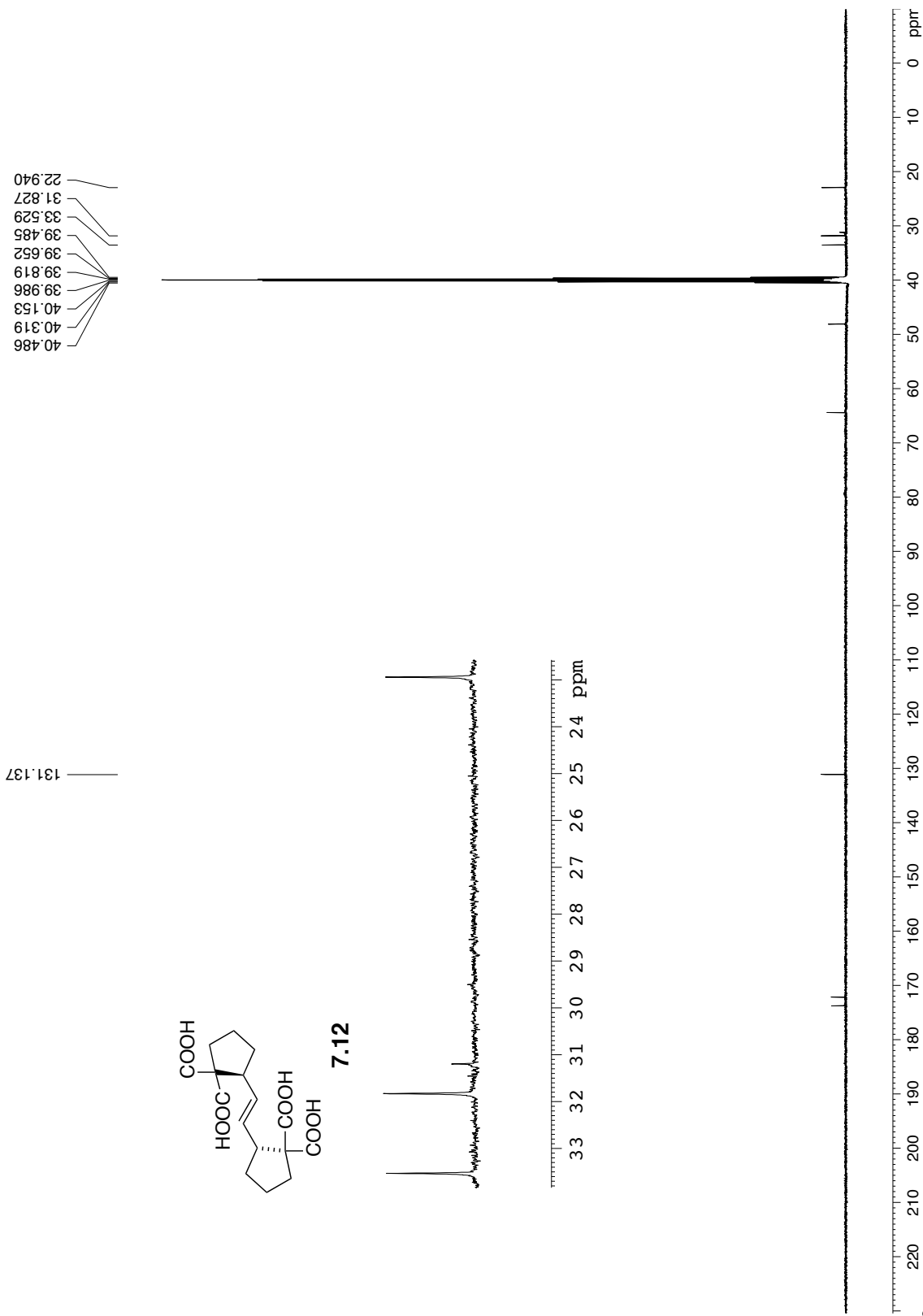




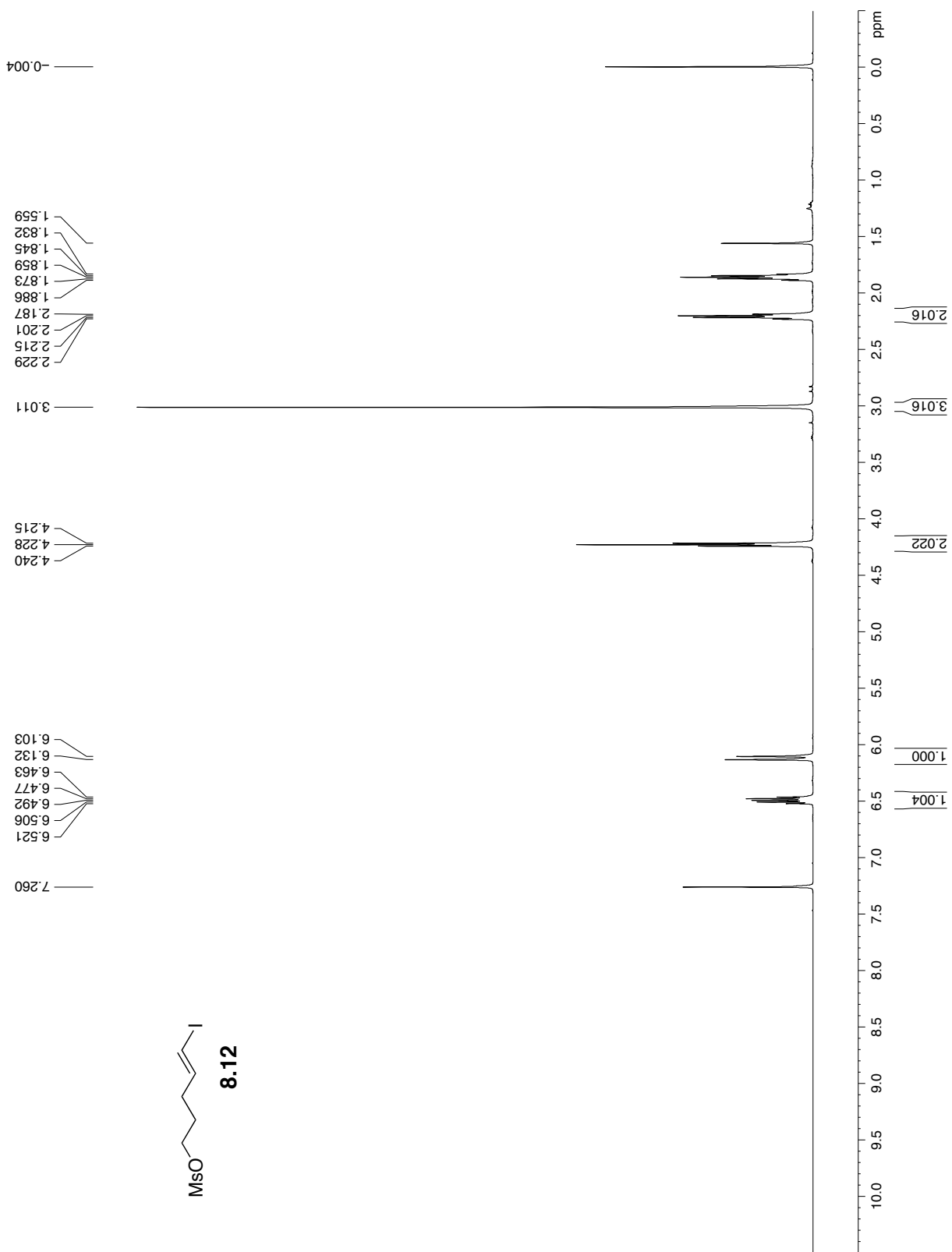
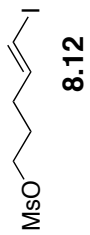
S25



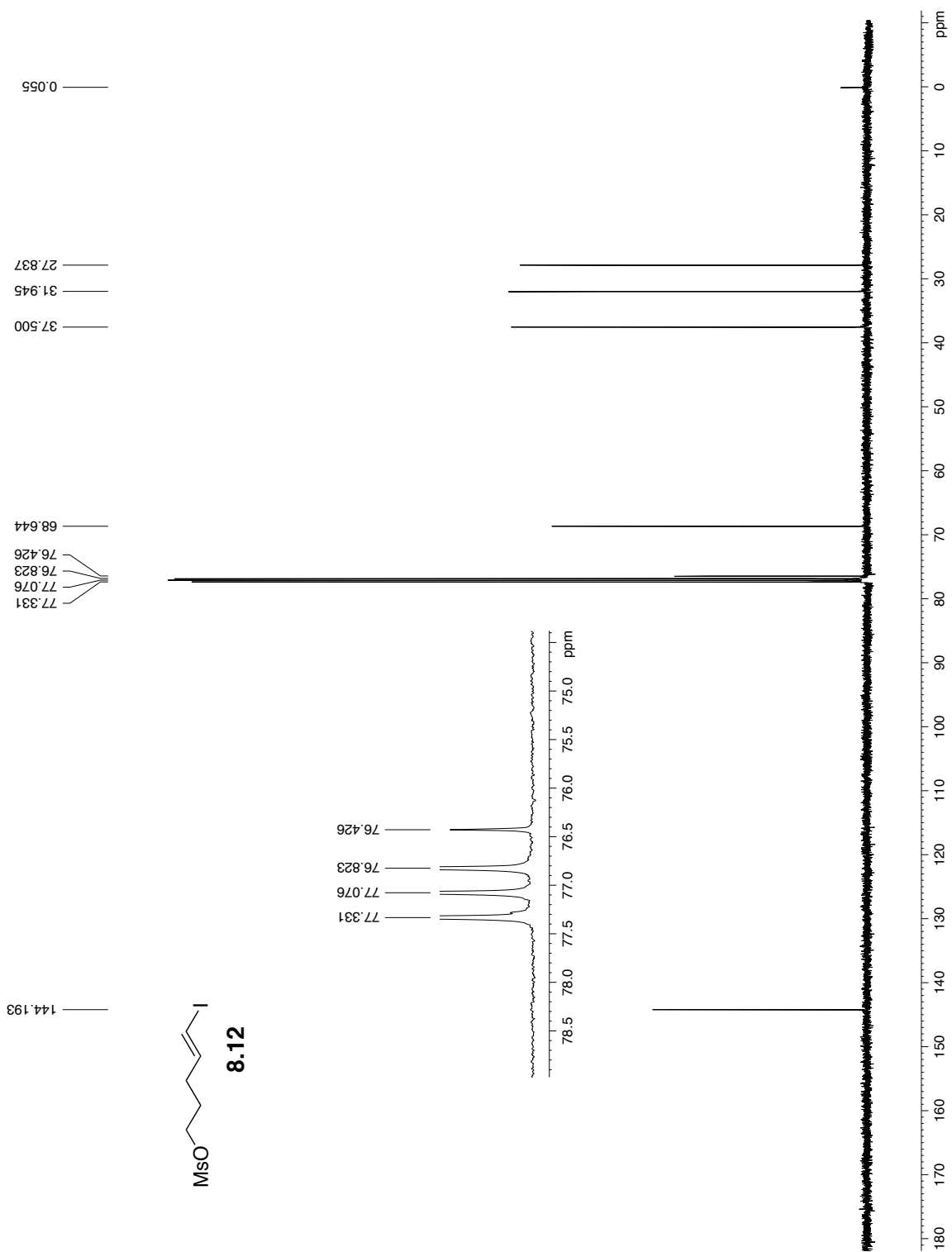
S30

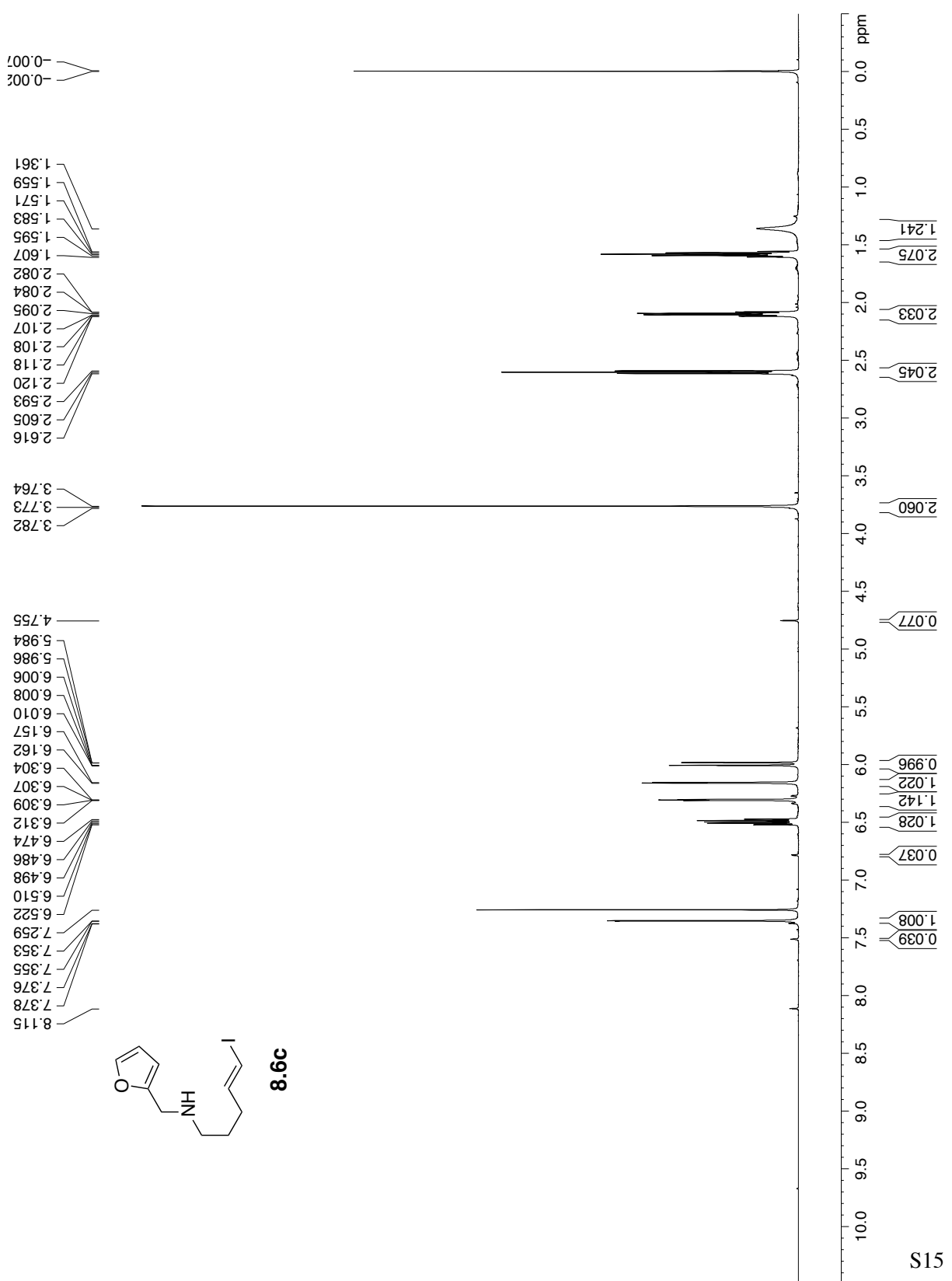


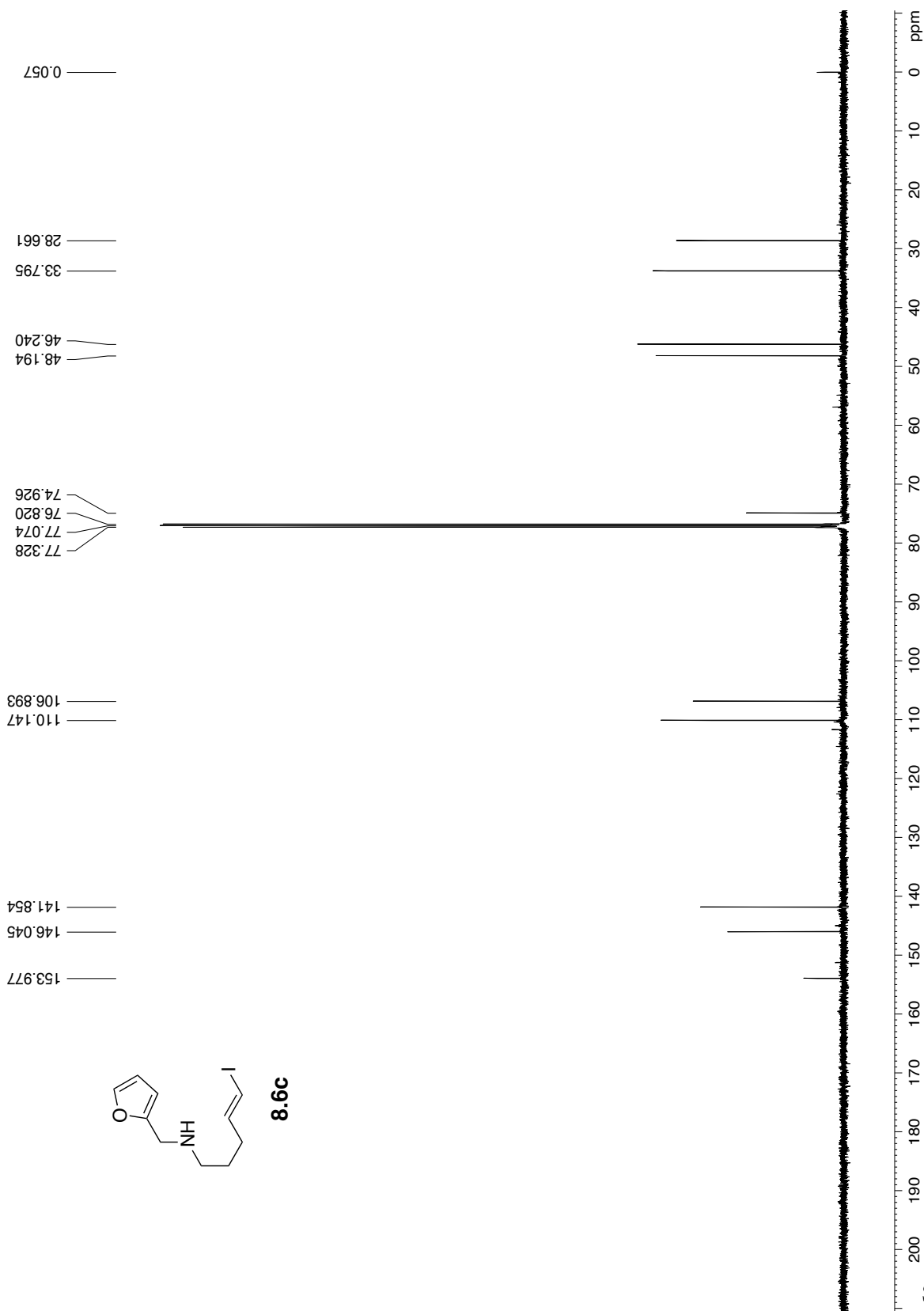
Appendix F: Chapter 8 – NMR Spectra



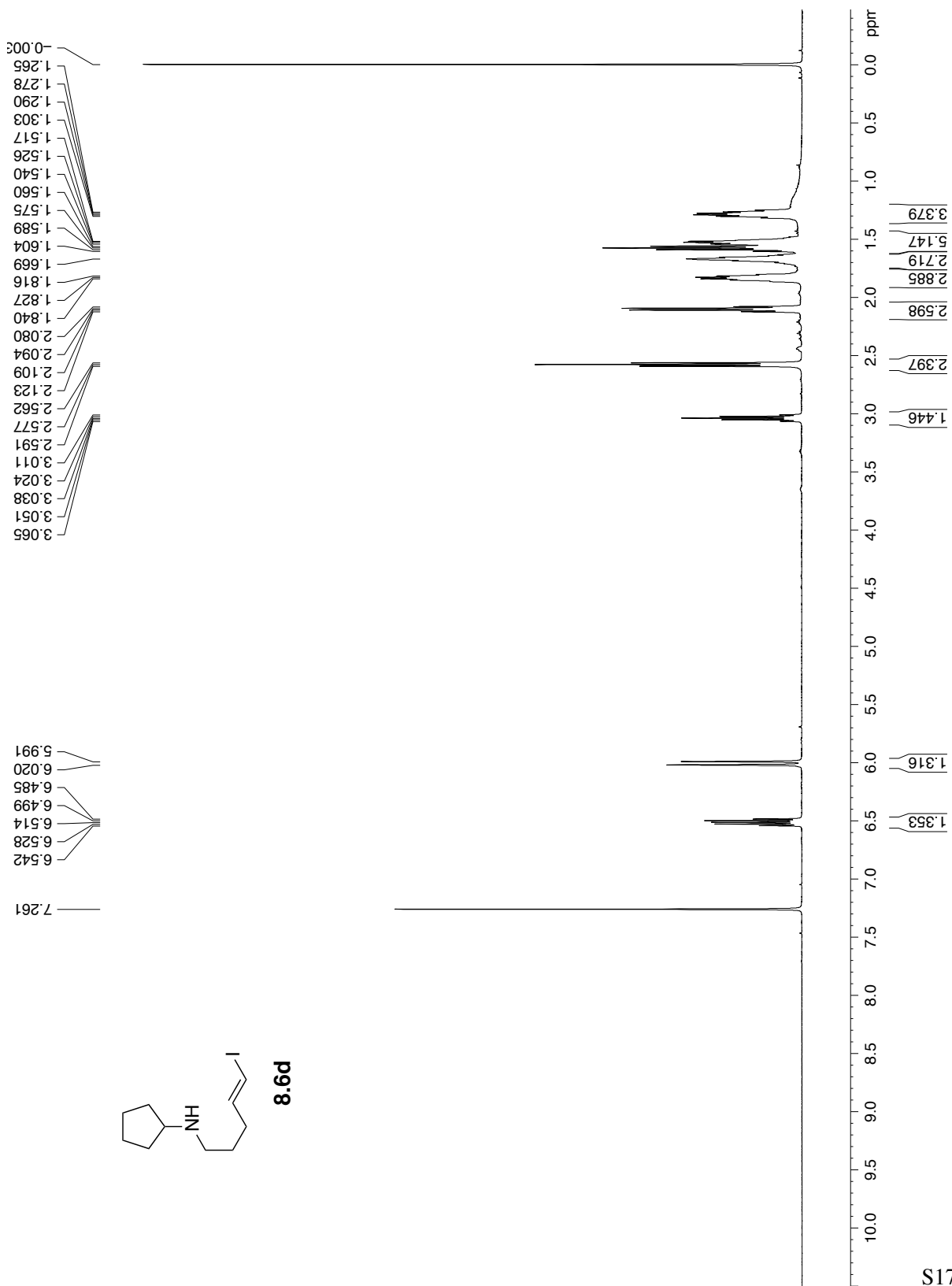
S11

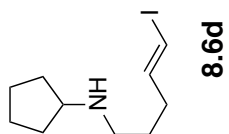
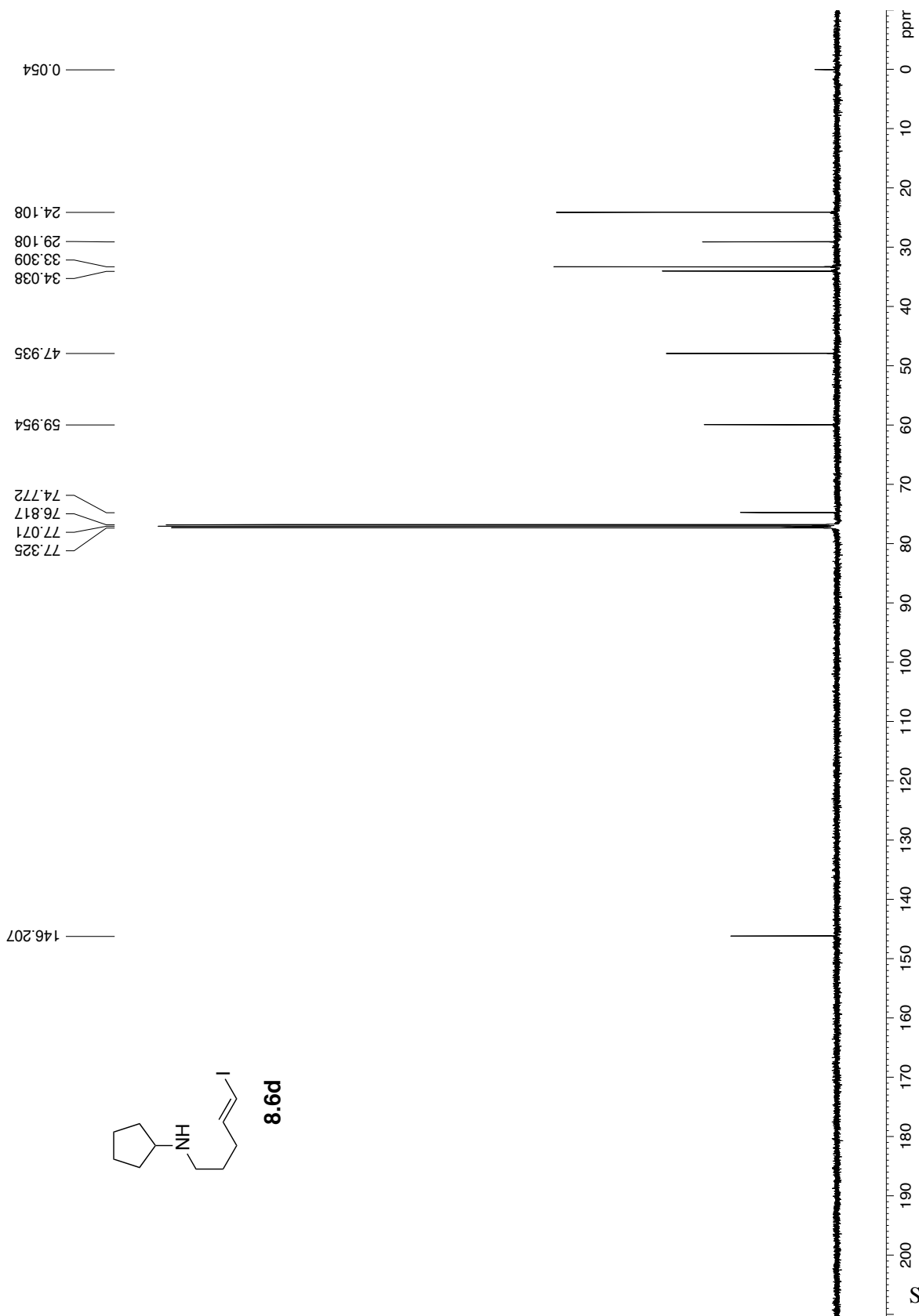


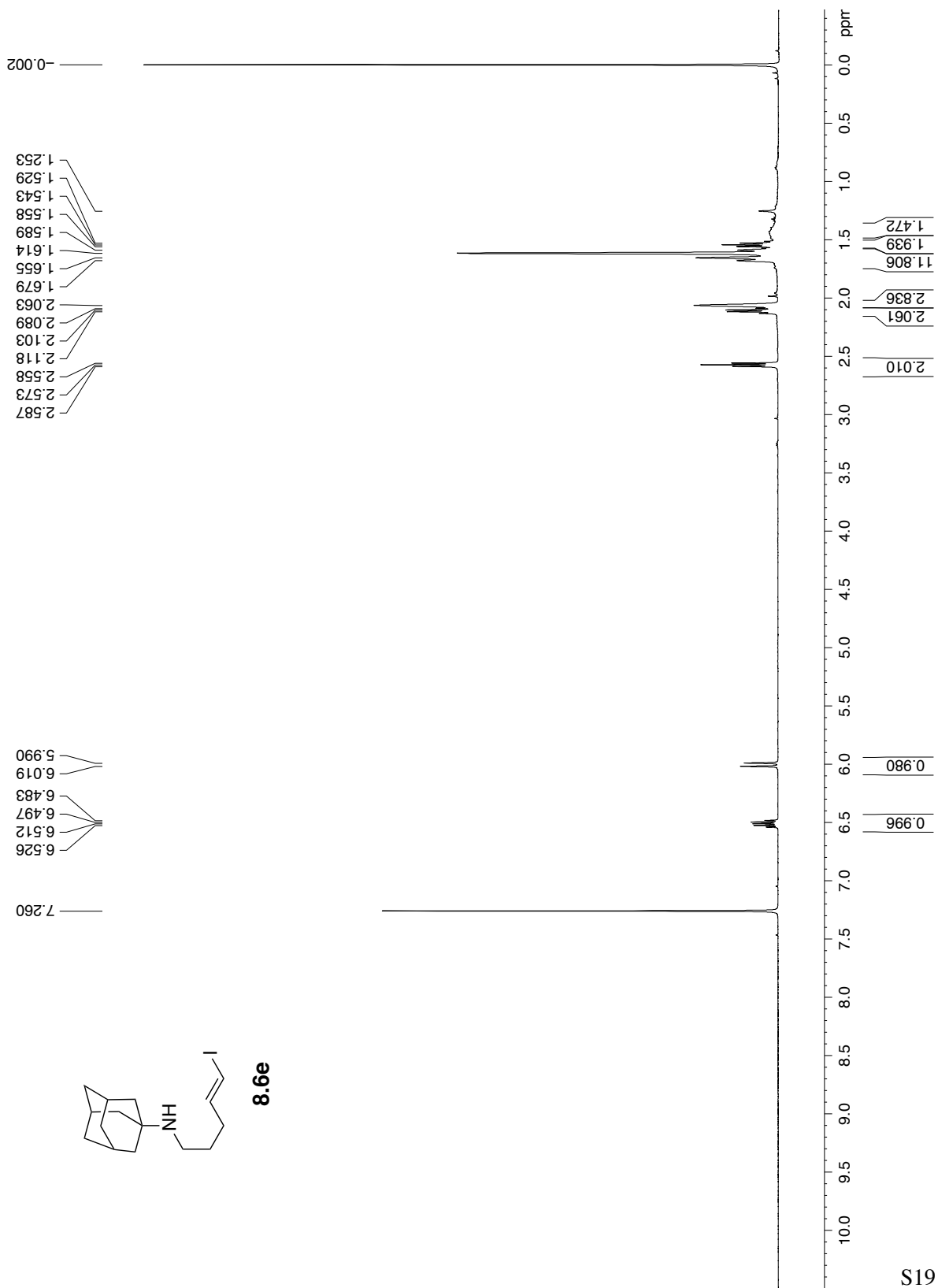


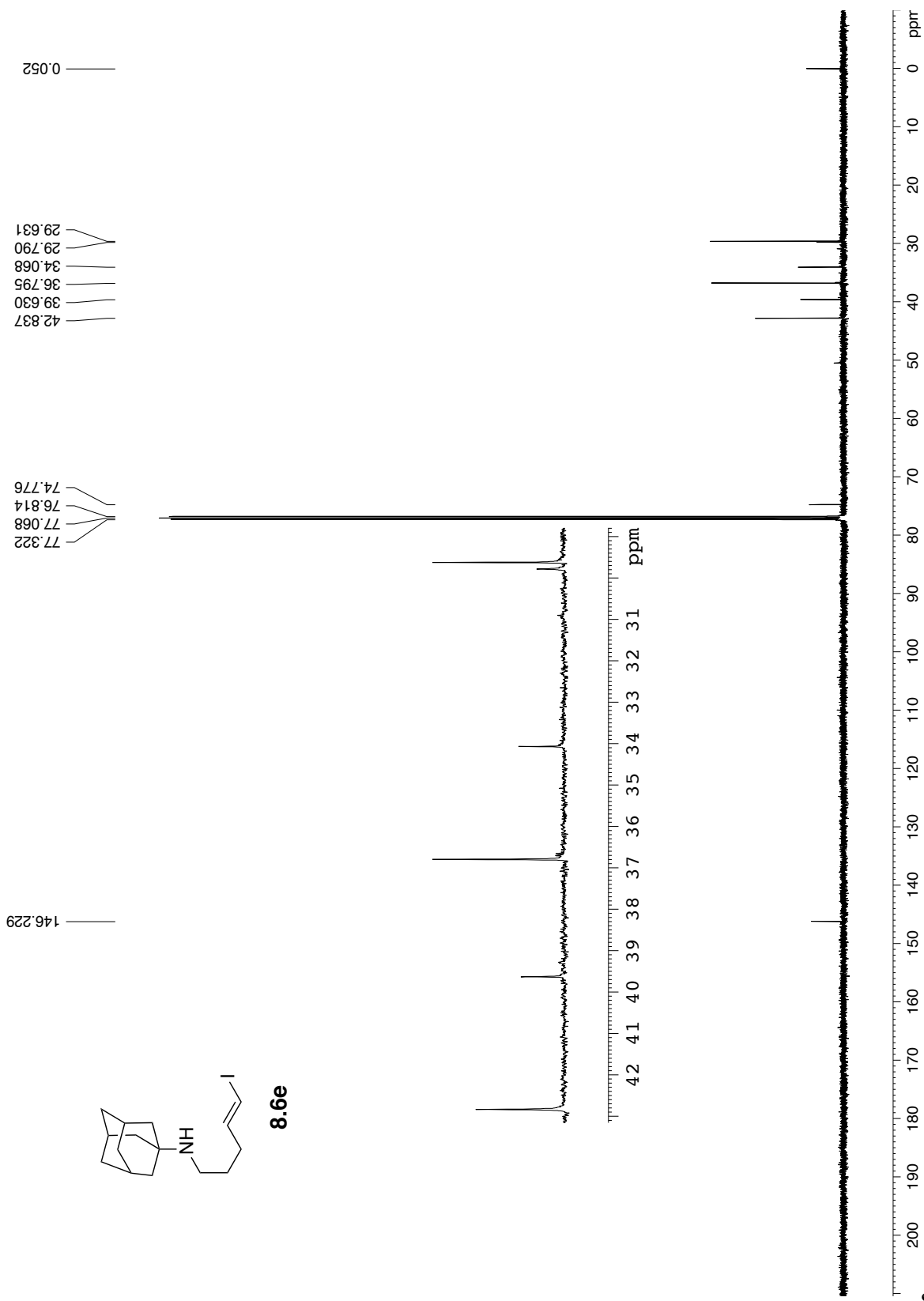


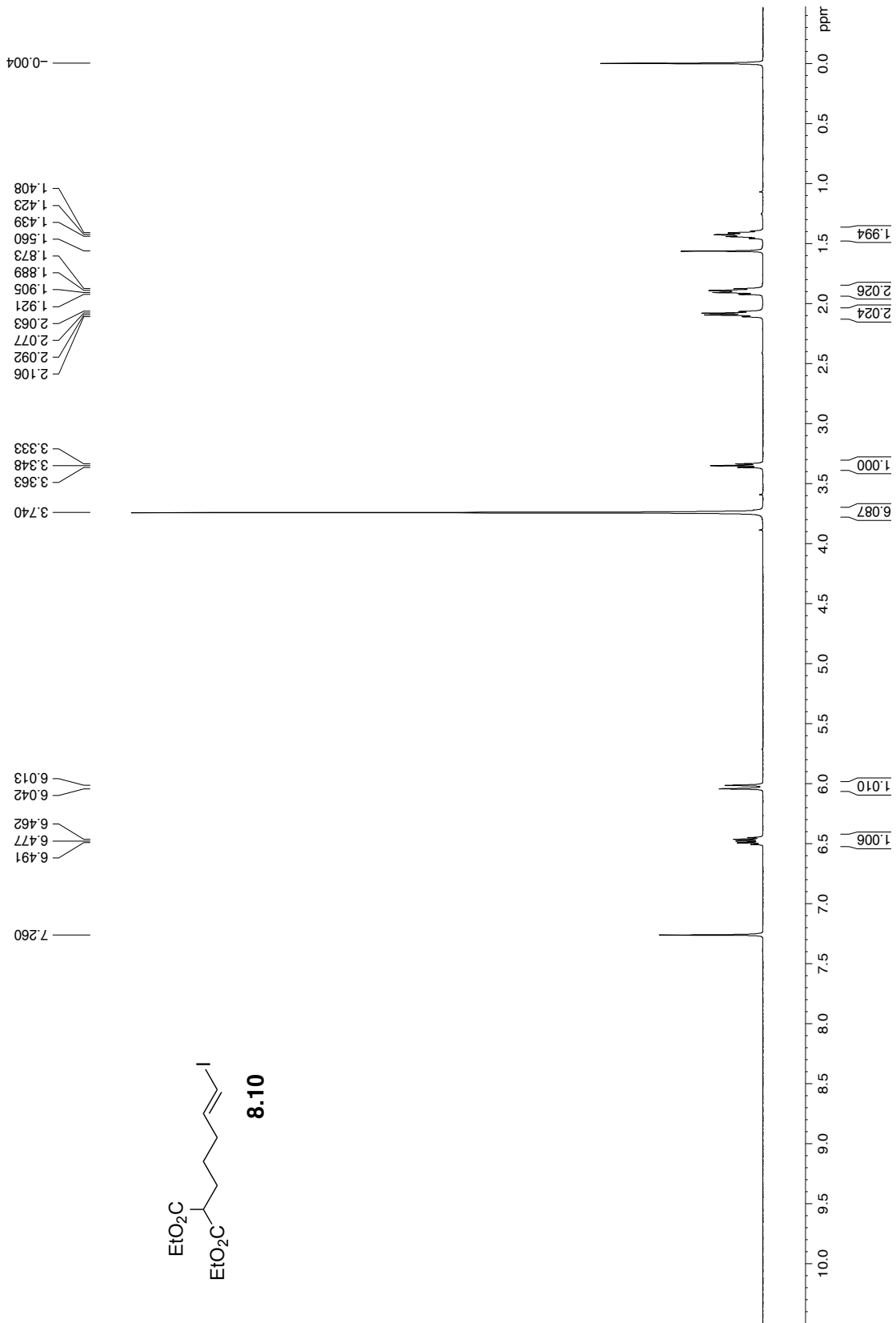
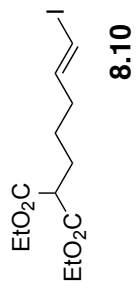
S16



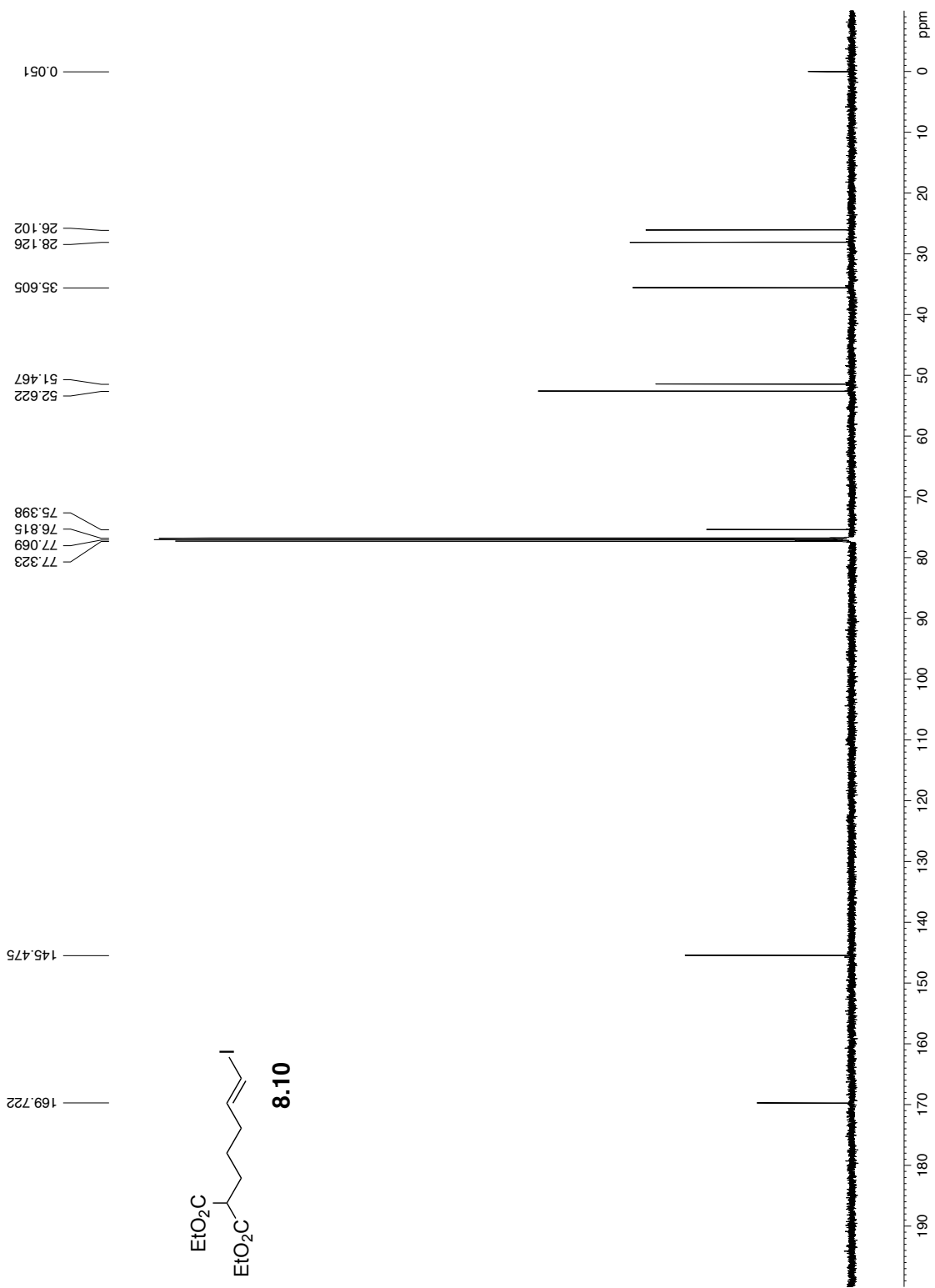


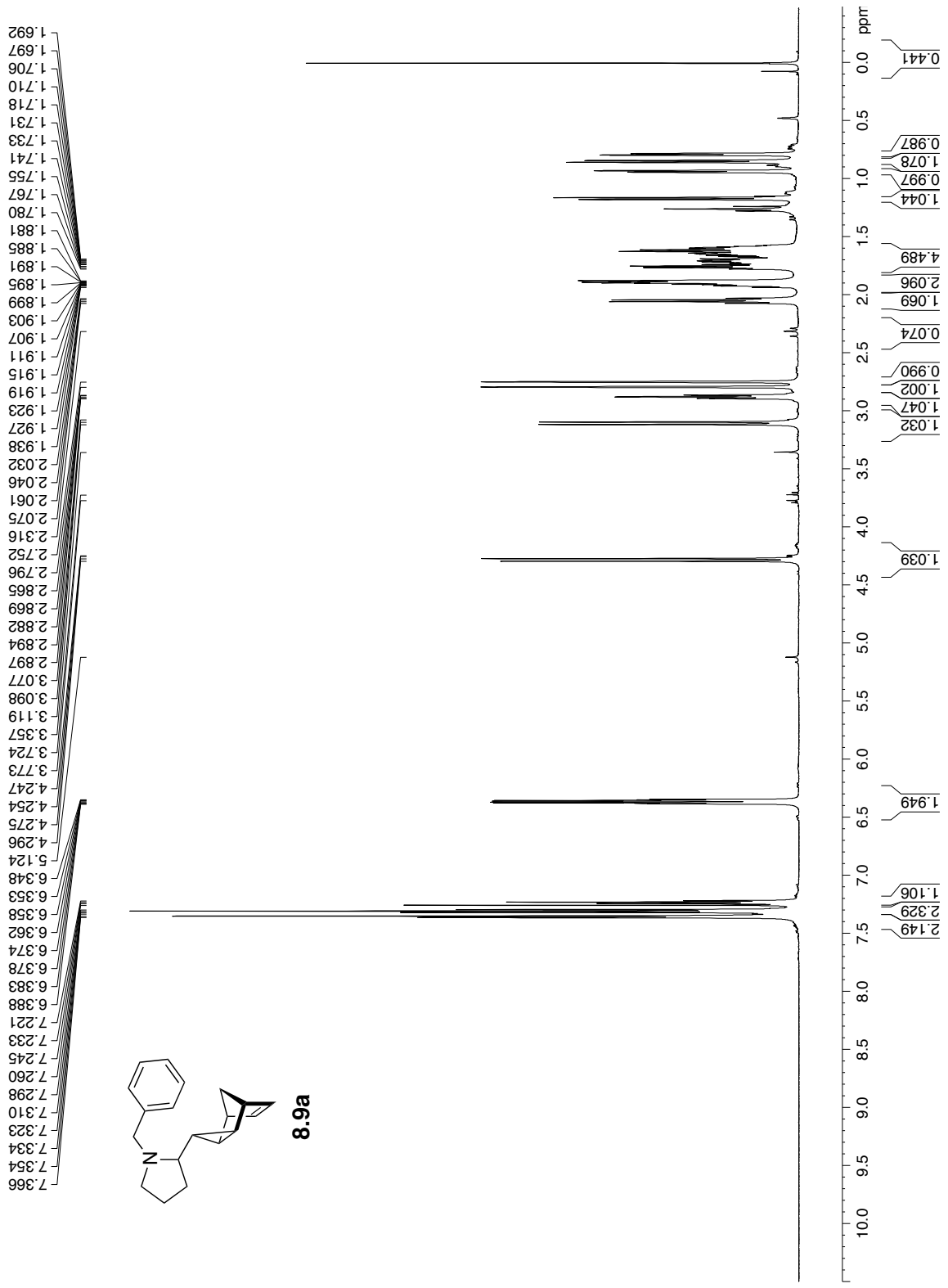






S21



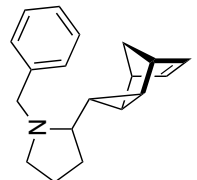



```

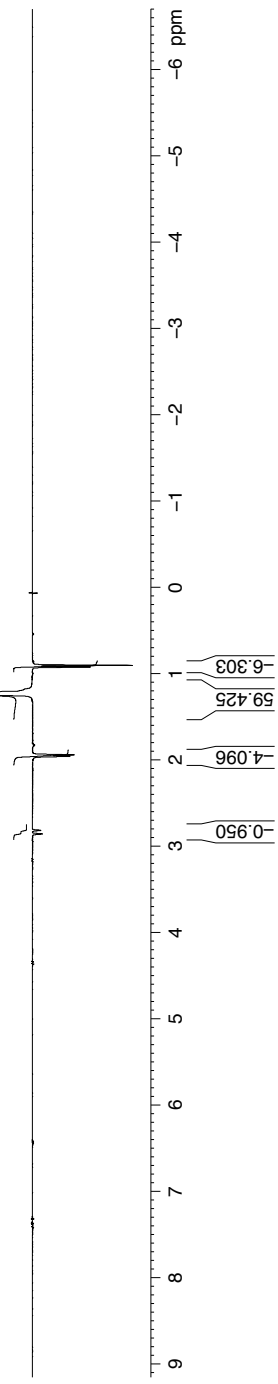
Current Data Parameters
USER      AK-IV-280_Noe
NAME      AK-IV-280_Noe
PROCNO    1
=====
F2 - Acquisition Parameters
Date_     20130403
Time      11:00:00
INSTRUM   spect
PROBHD    5 mm cryo500
PULPROG   zgpg30
TD        65536
SFO       500.131350
AQ        0.3376500
RG        62.00
DE        6.00
TE        120.0
FIDRES    0.3376500
AQRES     0.3376500
DETECTOR  cryo
NS        56
DS        4
SOLVENT   CDCl3
SRH        8012.820
F1RES     0.332266
RG1       143.7
DE1       6.00
TE1       120.0
D8        0.5000000
D81       0.5000000
d21       0.3376500
d22       0.1639969
P4        45.00
=====
NUC1      1H
=====
P1        7.50
P2        30.00
P3        30.00
P4        30.00
P12       4000.00
P13       4000.00
P14       4000.00
P15       500.230
P16       61.60
SFO1      500.131350
SFO2      61.60
SFO3      61.60
SFO4      61.60
SFO5      61.60
SFO6      61.60
SFO7      61.60
SFO8      61.60
SFO9      61.60
SFO10     61.60
SFO11     61.60
SFO12     61.60
SFO13     61.60
SFO14     61.60
SFO15     61.60
SFO16     61.60
=====
===== GRADIENT CHANNEL =====
GPRM1     sine,100
GPRM2     sine,100
GPRM3     sine,100
GPRM4     sine,100
GPRM5     sine,100
GPRM6     sine,100
GPRM7     sine,100
GPRM8     sine,100
GPRM9     sine,100
GPRM10    sine,100
GPRM11    sine,100
GPRM12    sine,100
GPRM13    sine,100
GPRM14    sine,100
GPRM15    sine,100
GPRM16    sine,100
=====
F2 - Processing parameters
SF        500.1313500
AQ        0.3376500
RG        62.00
DE        6.00
TE        120.0
D8        0.5000000
D81       0.5000000
d21       0.3376500
d22       0.1639969
P4        45.00
PC        1.00

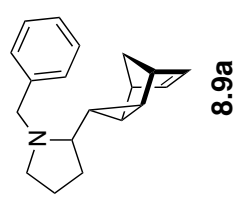
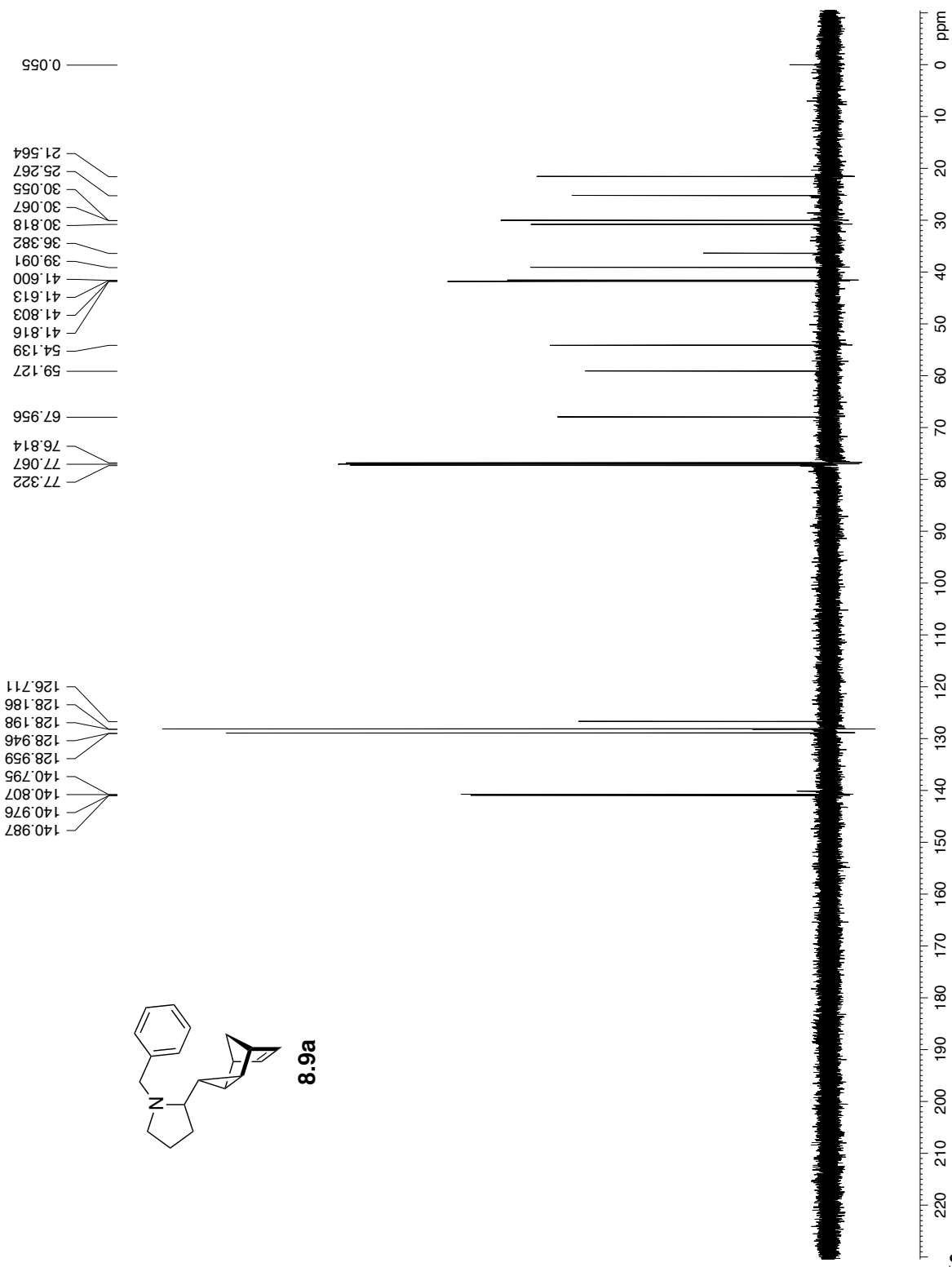
```

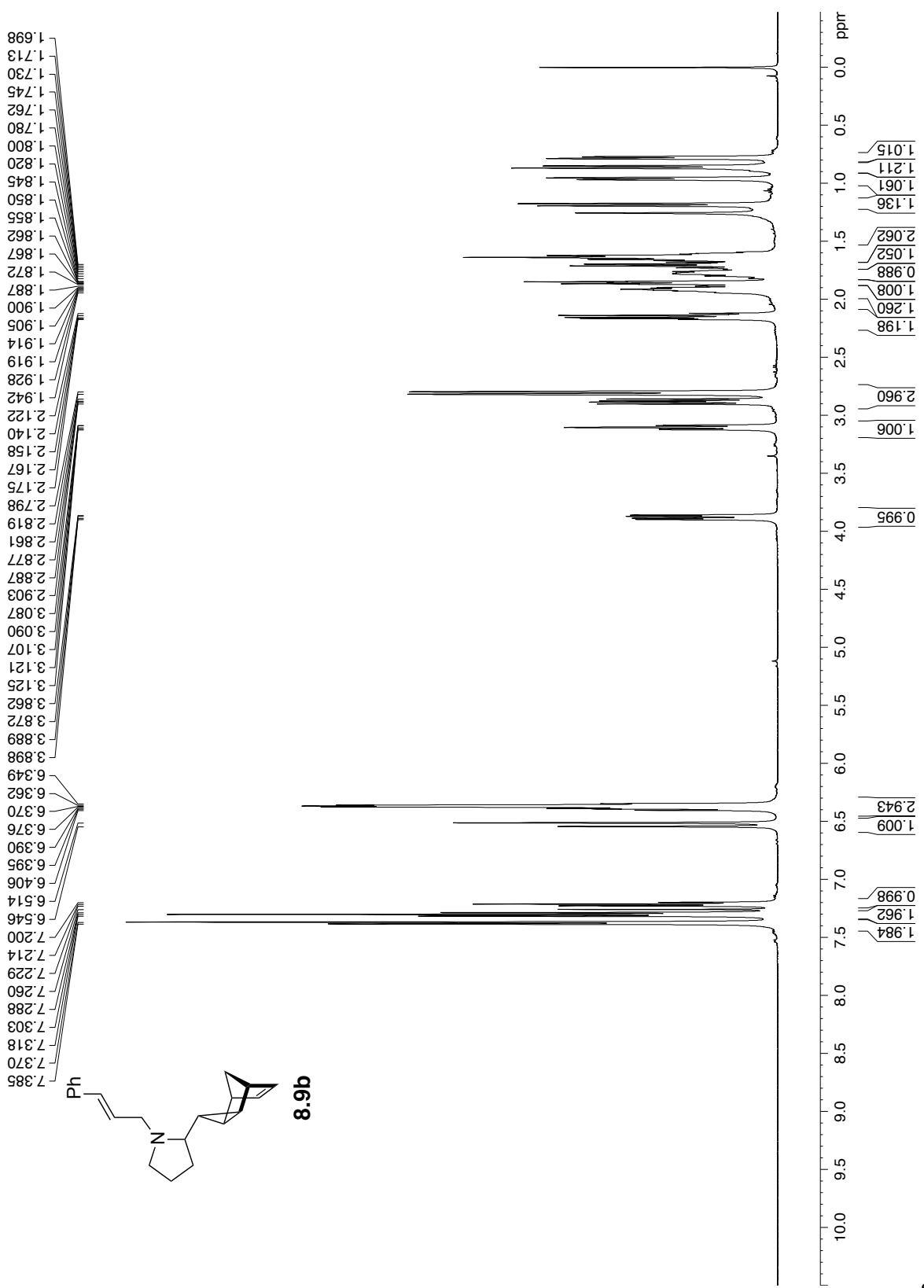
1.245
1.226
1.214
0.067
0.066
0.066

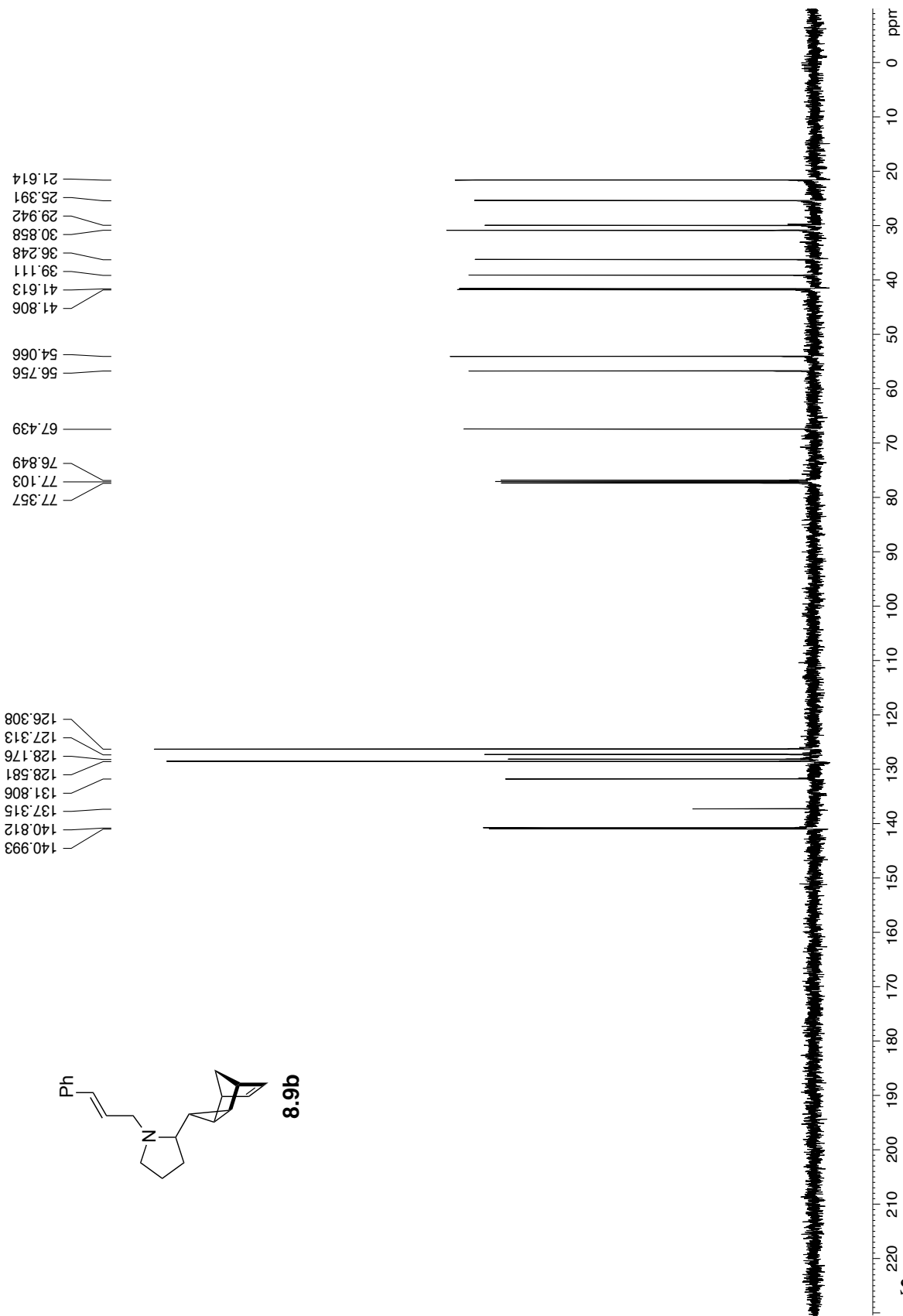


8.9a

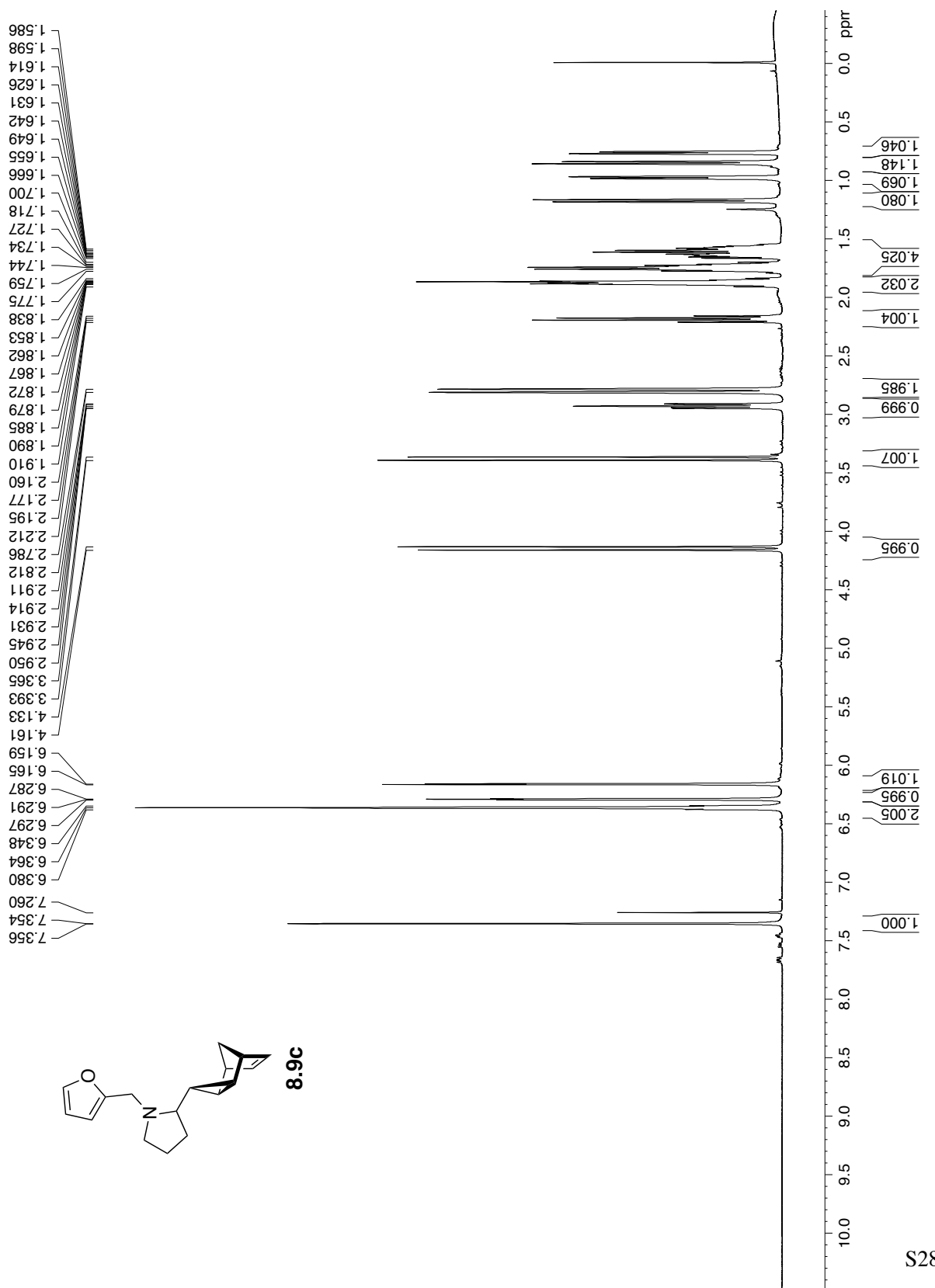


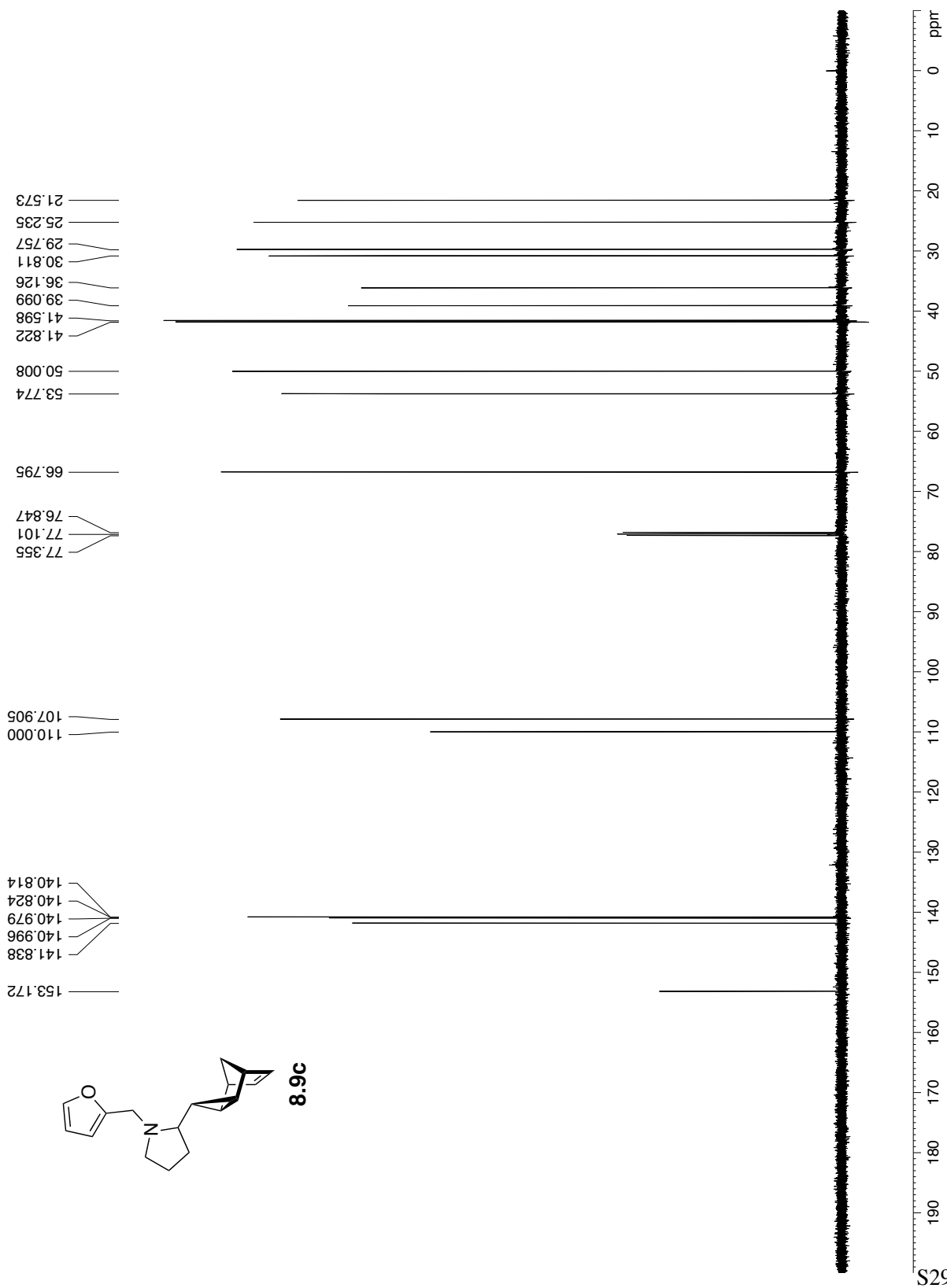


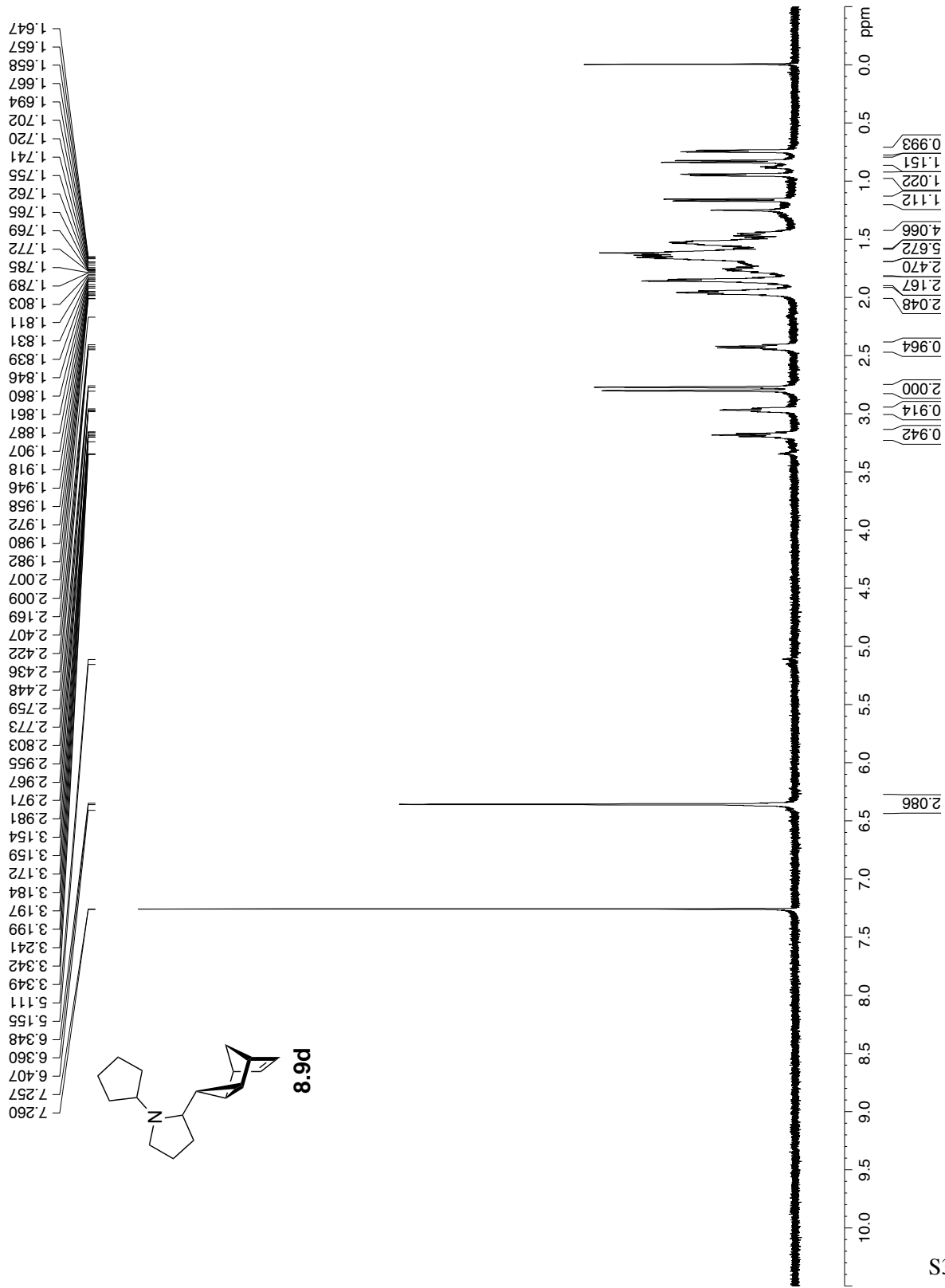




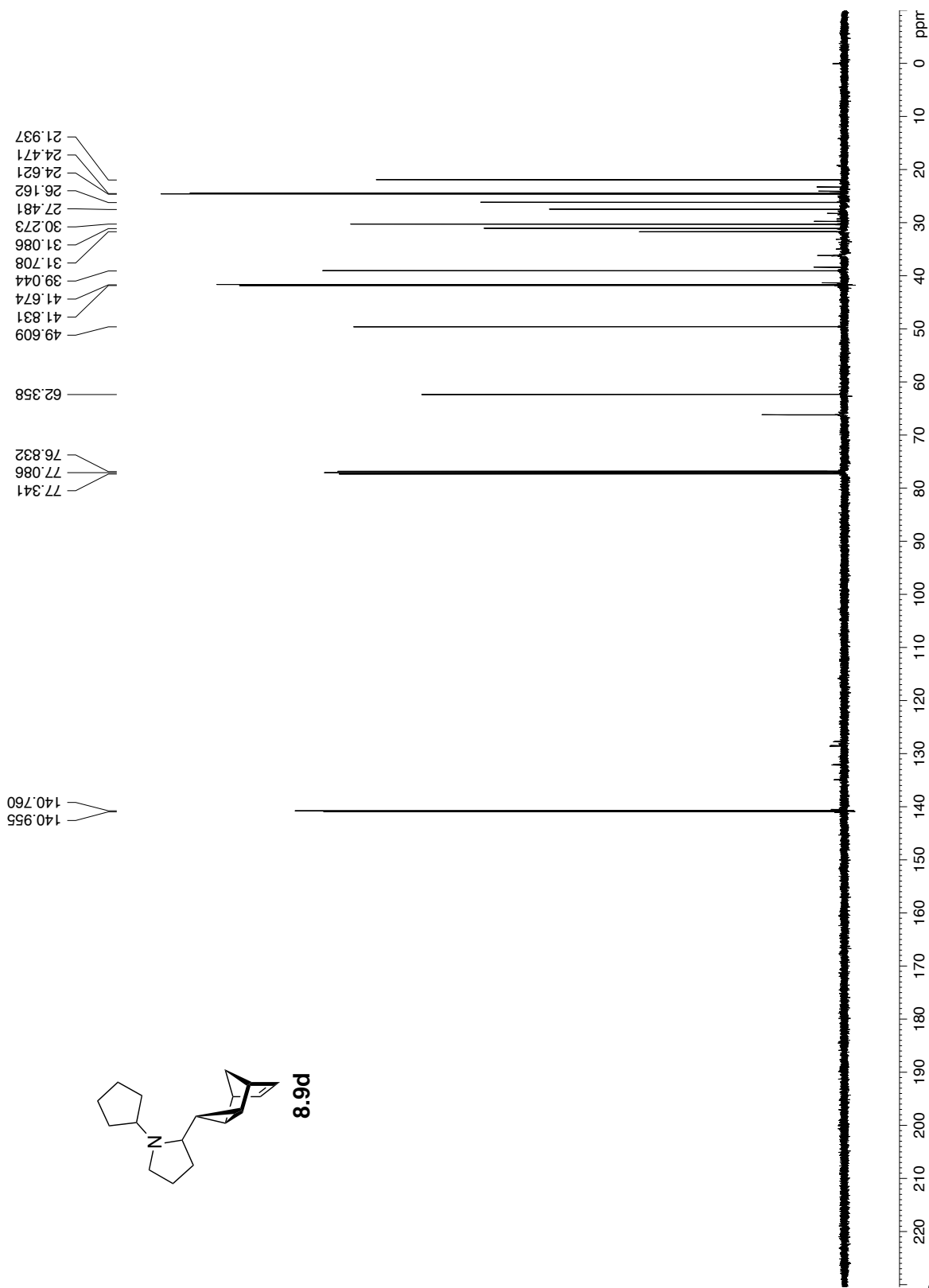
S27



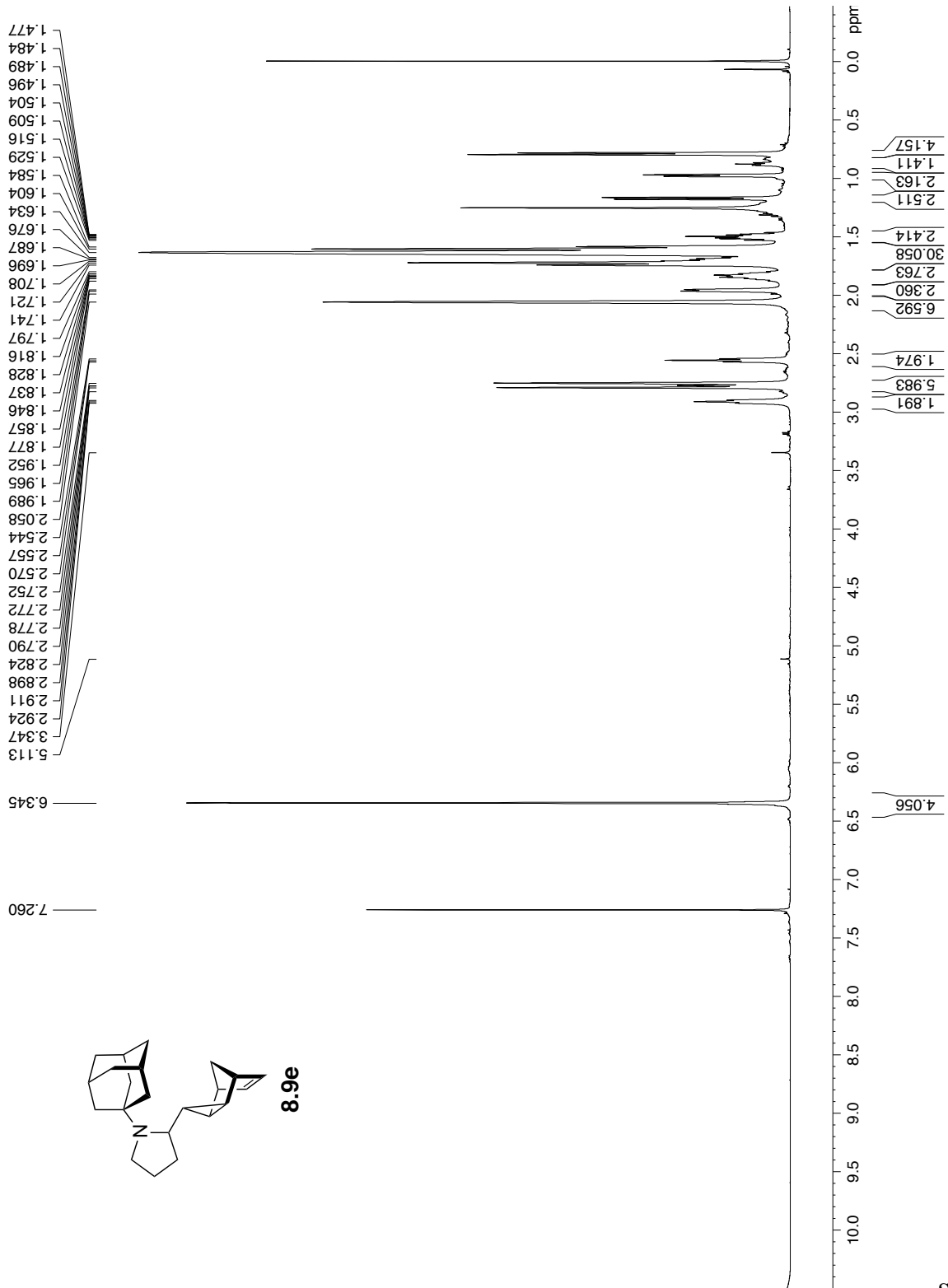




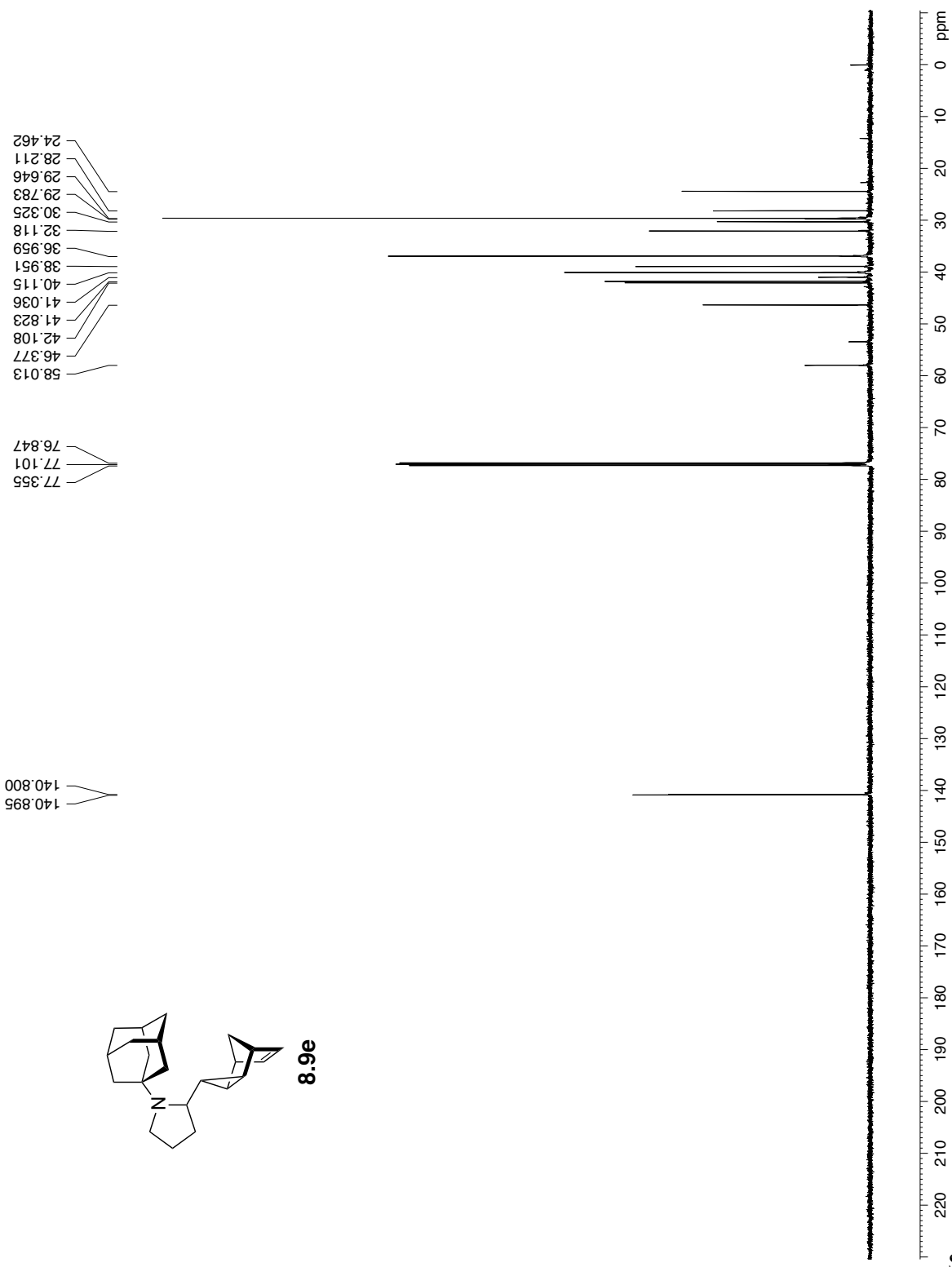
S30

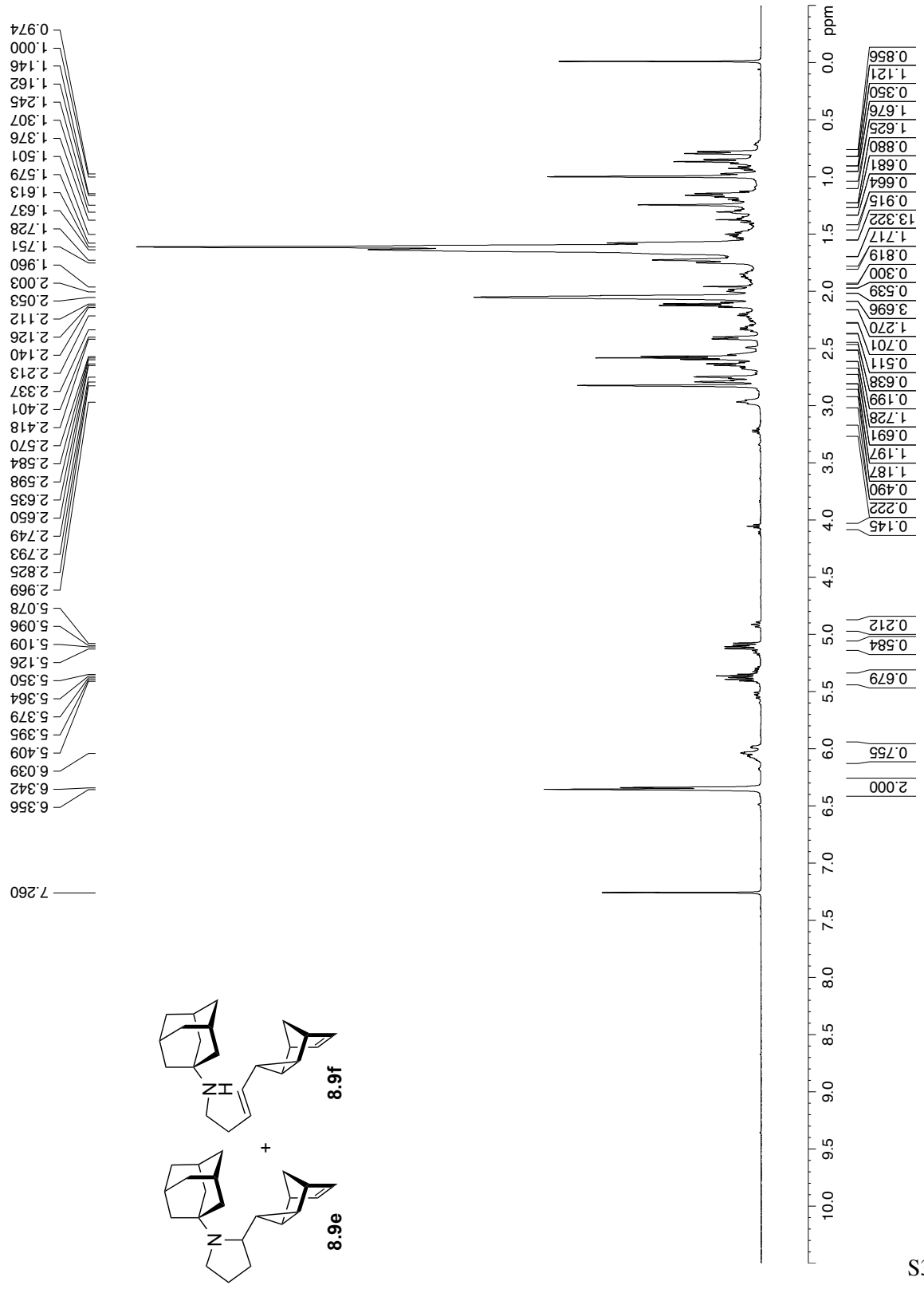


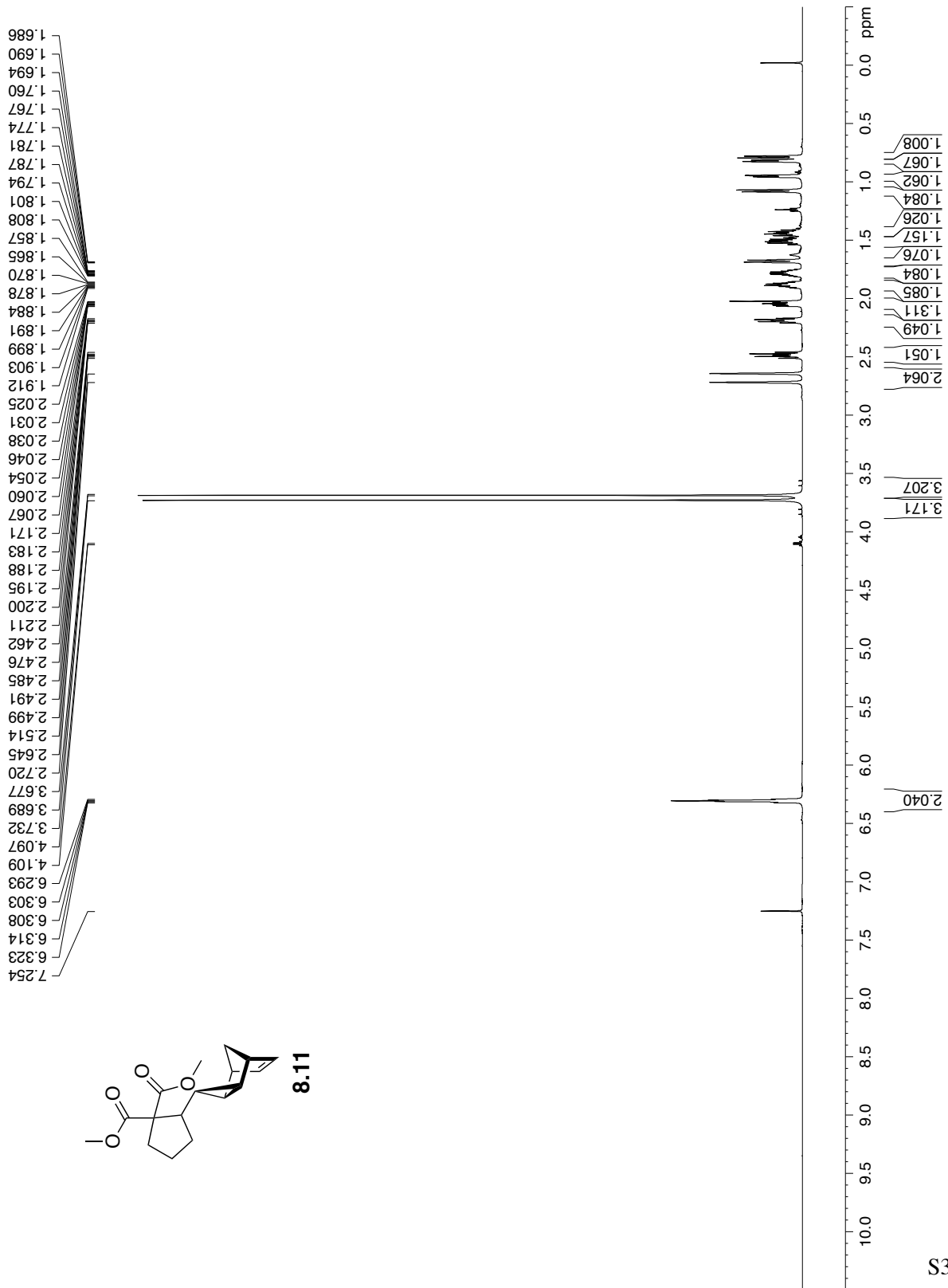
S31

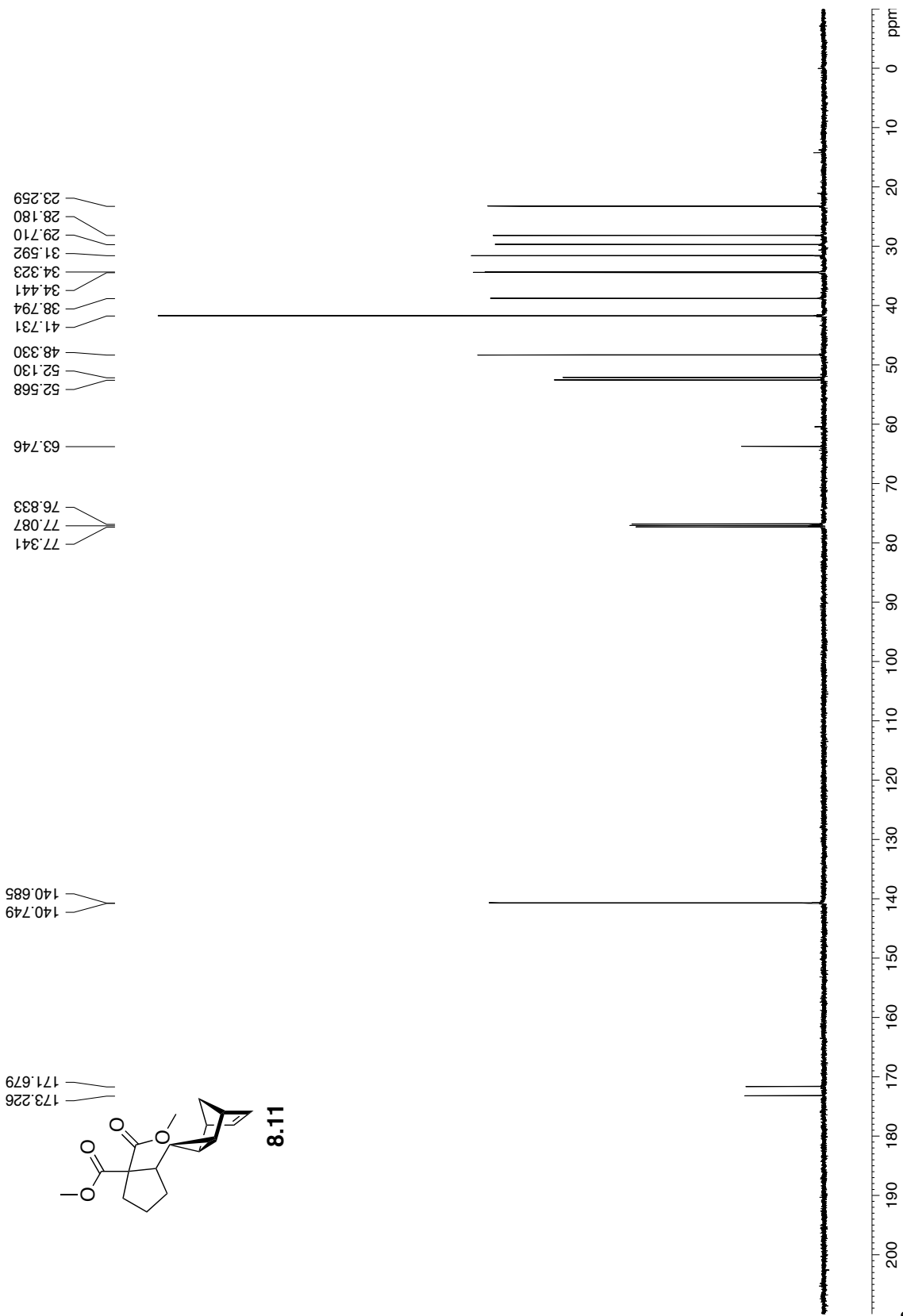


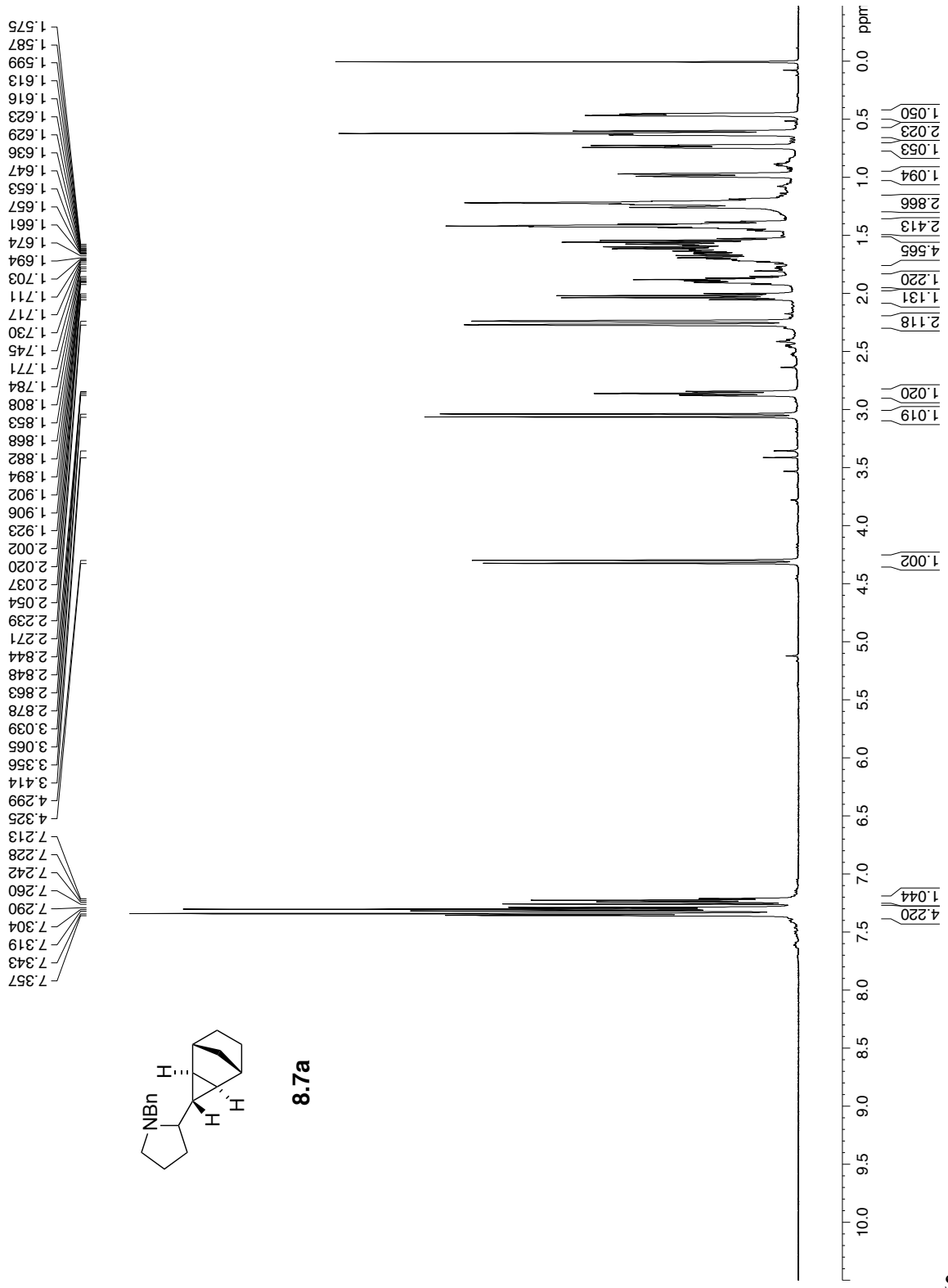
S32

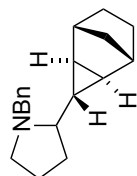












8.7a

